NAC-LWT

Legal Weight Truck Cask System

SAFETY ANALYSIS REPORT

Volume 3 of 3

NON-PROPRIETARY VERSION

Docket No. 71-9225

NAC INTERNATIONAL

LIST OF EFFECTIVE PAGES

LIST OF EFFECTIVE PAGES (Continued)

LIST OF EFFECTIVE PAGES (Continued)

Table of Contents

Table of Contents (continued)

Note: See separate Section 6.6 for Appendices to this chapter.

List of Figures

List of Figures (continued)

List of Figures (continued)

List of Figures (continued)

Note: See separate Section 6.6 for Appendices to this chapter, along with the List of Figures for
the Appendices.

List of Tables

List of Tables (continued)

List of Tables (continued)

List of Tables (continued)

List of Tables (continued)

List of Tables (continued)

List of Tables (continued)

List of Tables (continued)

List of Tables (continued)

List of Tables (continued)

6   CRITICALITY EVALUATION

The NAC-LWT cask is designed to transport either 1 pressurized water reactor (PWR) assembly; up to 25 intact PWR or BWR rods in a rod holder or fuel assembly lattice; up to 25 PWR or BWR fuel rods with a maximum of 14 of the rods classified as damaged in a rod holder; up to 16 PWR UO_2 or MOX rods in a rod holder; 2 boiling water reactor (BWR) assemblies; 15 sound metallic fuel rods; 6 failed metallic fuel rods; up to 42 high enriched uranium (HEU), medium enriched uranium (MEU) or low enriched uranium (LEU) Materials Test Reactor (MTR) fuel elements, or DIDO fuel assemblies; up to 140 TRIGA fuel elements; two packages of General Atomics Irradiated Fuel Material (GA IFM); up to 560 TRIGA fuel cluster rods; 1 consolidation canister with up to 300 TPBARs (including up to 2 damaged TPBARs); up to 700 PULSTAR fuel elements; up to 42 spiral fuel assemblies; up to 42 MOATA plate bundles; up to 800 SLOWPOKE rods; up to 18 NRU or NRX fuel assemblies; or 4 HEUNL containers. This chapter illustrates that all packages meet the requirements of parts 71.55, 71.59 and 71.71 of 10 CFR 71.

In accordance with the requirements of 10 CFR 71.59 (b), the NAC-LWT cask is assigned a Criticality Safety Index (CSI) for criticality control for the authorized contents as follows:

Approved Contents	CSI
PWR fuel assemblies	100
BWR fuel assemblies	5.0
MTR fuel elements	0.0
Metallic fuel rods	0.0
TRIGA fuel elements (in poisoned TRIGA fuel baskets)	0.0
TRIGA fuel elements (in nonpoisoned TRIGA fuel baskets)	12.5
TRIGA fuel cluster rods	0.0
High burnup PWR (UO_2 or MOX) rods*	0.0
High burnup BWR rods*	0.0
DIDO fuel elements	12.5
General Atomic Irradiated Fuel Material (GA IFM)	0.0
TPBARS and segmented TPBARS	0.0
Intact (uncanned) PULSTAR fuel	0.0
Canned PULSTAR fuel	33.4
ANSTO fuel (spiral and/or MOATA)	0.0
Solid irradiated hardware	0.0
ANSTO-DIDO fuel combination	0.0
SLOWPOKE fuel rods (undamaged or damaged)	0.0
NRU and NRX	100
HEUNL containers	0.0

* up to 14 damaged rods

6.1   Discussion and Results

Analyses are performed on the NAC-LWT cask for one PWR assembly and two BWR assemblies. Both PWR and BWR packages are examined for normal transport conditions and hypothetical accident conditions. The hypothetical accident conditions are modeled with the fuel at its most reactive credible configuration. The design of the cask and the fuel basket is such that, under all conditions, the highest neutron multiplication factor with correction for bias and uncertainty is less than 0.95. Analyses to demonstrate conformance to this criterion include (1) no dissolved boron in the neutron shield tank, thus improving the shield tank neutron reflection, (2) no structural material present in the assembly, and (3) no dissolved boron in the cask cavity or surrounding loading or storage area. No credit is included for burnup or for the buildup of fission product neutron poisons.

Analyses are performed for the NAC-LWT cask with the most limiting single PWR assembly and also for the most limiting BWR assemblies. Sections 6.3.1 and 6.3.2 present the methods (CSAS25) and KENO-Va models used in the analysis for each of these respective fuel assemblies. Sections 6.4.1 and 6.4.2 present the criticality analysis results for the PWR and BWR fuel assemblies, respectively. The maximum PWR fuel enrichment is set at 3.7 wt % ^{235}U, but it was found that certain PWR fuel assemblies were required to be limited to a maximum uranium enrichment of 3.5 wt % ^{235}U. Thus, two design-basis PWR assemblies were consequently selected. Namely, a design basis case with the uranium enrichment limited to 3.7 wt % ^{235}U and a second design basis case for those assemblies with the uranium enrichment limited to 3.5 wt % ^{235}U.

Analyses are performed on the NAC-LWT with fuel baskets designed to transport up to 42 MTR research reactor fuel elements. Shipment of MTR loose fuel plates is evaluated inside an MTR plate canister. Section 6.3.2 presents the methods (CSAS25) and KENO-Va models used in the analysis. Section 6.4.3 presents the criticality analysis results of the NAC-LWT loaded with MTR fuel. Section 6.5.2 presents the validation of CSAS25 for use in criticality evaluations of MTR fuel. Criticality of the NAC-LWT cask with the most limiting MTR fuel assembly type and basket configuration is evaluated. The fuel assemblies are assumed to be unburned. An infinite array of casks of infinite axial extent is analyzed. The cask/basket configuration is examined for normal transport and accident conditions. Both normal and accident conditions consider variation in moderator density inside and outside the cask as well as the spacing between casks. Reactivity penalties for mechanical perturbations are also considered. The results show that the k_{eff} of an infinite array of NAC-LWT casks with the most limiting MTR fuel and at optimum interspersed moderation is always below 0.95 including the method bias, method uncertainty, Monte Carlo uncertainty and penalties due to mechanical perturbations.

Analyses are performed on the NAC-LWT with up to 25 PWR or BWR fuel rods of 5.0 wt % ^{235}U initial enrichment. Separate evaluations are performed for a payload consisting of only intact rods in a rod holder, a payload including up to 14 damaged rods in a rod holder, and rods in a fuel assembly lattice. Section 6.3.3 presents the methods (CSAS25) and KENO-Va model used in the rod holder or fuel assembly lattice analyses. Section 6.4.4 presents the criticality analysis results of the NAC-LWT loaded with up to 25 PWR or BWR fuel rods in either a rod holder or a fuel assembly lattice. The system reactivity of the NAC-LWT with up to 25 PWR or BWR fuel rods in intact (rod holder or lattice) or damaged configurations is evaluated as a function of rod pitch. Damaged fuel evaluations include the removal of clad and fuel and moderator mixture studies. The fuel is assumed to be fresh, i.e., no burnup credit. An infinite array of casks is analyzed. Variation of moderator density inside and outside the cask also is considered. The results show that the k_{eff} of an infinite array of NAC-LWT casks at optimum fuel rod pitch and at optimum interspersed moderation is significantly below 0.95 including the method bias, method uncertainty and Monte Carlo uncertainty.

Poisoned and nonpoisoned basket configurations of the NAC-LWT cask are evaluated for TRIGA fuel elements with up to 70 wt % ^{235}U initial enrichment and TRIGA fuel cluster rods with up to 93.3 wt % ^{235}U initial enrichment. The placement of sealed canisters in the top and bottom baskets of the cask is also evaluated to permit the transport of failed TRIGA fuel. Section 6.3.4 presents the methods (CSAS25) and the models used in the analyses. Section 6.4.5 presents the criticality analysis results for the NAC-LWT cask loaded with TRIGA fuel elements, while Section 6.4.6 presents the results for TRIGA fuel cluster rods. The fuel is assumed to be fresh (unirradiated) and the effects of burnable absorbers are conservatively ignored. An infinite array of casks is analyzed. Variation of moderator density inside and outside the cask is considered. Variation of geometrical configurations are also analyzed, including the tolerances of the TRIGA basket materials and fuel element positioning, to determine the most reactive configuration. The results show that the k_{eff} of an array of NAC-LWT casks with TRIGA fuel at optimum fuel element pitch, geometrical configuration, and optimum moderation is always below 0.95, including corrections for bias and uncertainty. An infinite cask array is evaluated for the poisoned and nonpoisoned TRIGA cluster rod baskets and the poisoned TRIGA fuel element basket, while a finite cask array is applied to the nonpoisoned TRIGA fuel element evaluations.

Analyses are performed on the NAC-LWT with fuel baskets designed to transport up to 42 DIDO fuel assemblies. Section 6.1.1 presents the methods (CSAS25) and KENO-VA models used in the analysis. Section 6.4.7 presents the criticality analysis results of the NAC-LWT loaded with DIDO fuel. Section 6.5.2 presents the validation of CSAS25 for use in criticality evaluations of DIDO fuel. Criticality of the NAC-LWT cask with the most limiting DIDO fuel assembly type

(HEU) and basket configuration is evaluated. The fuel elements are assumed to be unburned. An infinite array of casks of infinite axial extent is analyzed. The cask/basket configuration is examined for normal transport and accident conditions. Variations in moderator density inside and outside the cask are evaluated. Reactivity penalties for mechanical perturbations are also considered. The results show that the bias adjusted k_{eff} of an infinite array of NAC-LWT casks with the most limiting DIDO fuel under accident conditions at optimum interspersed moderation (void) is above 0.95. Limiting the accident array to a maximum of eight casks results in a k_{eff} below 0.95, including the method bias, method uncertainty, Monte Carlo uncertainty, and penalties due to mechanical perturbations.

Analyses are performed of the NAC-LWT with a fuel basket designed to transport two Fuel Handling Units (packages) of General Atomics (GA) Irradiated Fuel Material (IFM). The first IFM package is composed of Reduced-Enrichment Research and Test Reactor (RERTR) type TRIGA fuel and the second is composed of High-Temperature Gas-cooled Reactor (HTGR) type fuel. Each set of IFM is packaged into stainless steel weld-encapsulated primary and secondary enclosures. Section 6.3.8 presents the methods (CSAS25) and KENO-Va models used in the analyses. Section 6.4.8 presents the criticality analysis results of the two GA IFM packages in the NAC-LWT. Section 6.1.1 presents the validation of CSAS25 for use in criticality evaluations of TRIGA fuel, which is deemed relevant for the GA IFM as discussed in Section 6.4.8. Criticality of the NAC-LWT cask with GA IFM is evaluated using pre-irradiation material compositions. No credit is taken for the basket structure axially or radially, and an infinite array of casks of infinite axial extent is analyzed. Variations in moderator density inside and outside the cask are evaluated, as well as the partial flooding of the IFM packages. The results show that the bias adjusted k_{eff} of an infinite array of NAC-LWT casks under accident conditions at optimum internal and interstitial moderation is less than 0.95, including corrections for bias and uncertainty. Maximum reactivity is obtained with flooded IFM packages, a void NAC-LWT cavity, and a void exterior.

The metallic fuel rods are not analyzed because the metallic fuel is at natural enrichment, and cannot become critical without the presence of heavy water (Paxton).

Criticality evaluations for the NAC-LWT loaded with TPBARs (Tritium Producing Burnable Absorber Rods) are not required because the TPBARs do not contain fissile material and, therefore, cannot form a critical configuration.

Analyses are performed of the NAC-LWT with a stack of four 28 MTR 7-element modules with a PULSTAR fuel element payload. PULSTAR fuel assemblies are comprised of a 5×5 rectangular fuel element array surrounded by a Zircaloy box with aluminum upper and lower fittings. The fuel elements are Zircaloy-clad UO_2 pellets conservatively evaluated at an

enrichment of 6.5 wt % ^{235}U. PULSTAR fuel assemblies may be loaded directly into the module cells. Individual intact PULSTAR fuel elements may be loaded into either a 4×4 fuel rod insert, or one of two PULSTAR cans. The can loadings are only permissible in the top and base modules. Damaged PULSTAR fuel elements or debris must be loaded into either of the cans. Section 6.3.7 presents the methods (CSAS25) and KENO-Va models used in the analyses. Section 6.4.9 presents the criticality analyses results of the various permissible loading configurations. Section 6.5.1 presents the validation of CSAS25 for use in criticality evaluations of PWR and BWR fuel, which is deemed relevant for PULSTAR fuel as discussed in Section 6.4.9. Criticality is evaluated using pre-irradiation material compositions. The basket structure axial and radial extents are explicitly modeled in a cask of finite axial extent. Cask arrays analyzed are dependent on the payload of either intact fuel or a mixed loading of intact fuel and canned elements. Variations in moderator density inside and outside the cask are evaluated, as well as the preferential flooding of the cans. The results show that the bias adjusted k_{eff} under accident conditions at optimum internal and interstitial moderation is less than 0.95, including corrections for bias and uncertainty. Maximum reactivity is obtained for a preferentially flooded cask containing two modules baskets of intact fuel assemblies and two modules of cans (each can contains 25 damaged fuel elements). Preferential flooding in this case is a void NAC-LWT cavity, flooded fuel cans, and a void cask exterior (including a void neutron shield).

Analyses are performed on the NAC-LWT with ANSTO fuel baskets designed to transport up to 42 spiral fuel assemblies, 42 MOATA plate bundles, or a combination of spiral assembly baskets and plate bundle baskets. Section 6.3.8 presents the methods (CSAS25) and KENO-VA models used in the analysis. Section 6.4.10 presents the criticality analysis results of the NAC-LWT loaded with spiral fuel assemblies or plate bundles. Section 6.5.2 presents the validation of CSAS25 for use in criticality evaluations of the ANSTO basket. Criticality of the NAC-LWT cask with the most limiting fuel characteristics and basket configuration is evaluated. The fuel elements are assumed to be unburned. An infinite array of casks in both the radial and axial extent is analyzed. The cask/basket configuration is examined for normal transport and accident conditions. Variations in moderator density inside and outside the cask are evaluated. Reactivity penalties for mechanical perturbations are also considered. The results show that the bias adjusted k_{eff} of an infinite array of NAC-LWT casks with the most-limiting ANSTO basket payload under normal and accident conditions at optimum interspersed moderation (void) is below 0.95.

Analyses are performed on the NAC-LWT with up to 16 PWR (UO$_2$ or MOX) fuel rods. UO$_2$ fuel rods are permitted with up to 5.0 wt % ^{235}U initial enrichment. Mixed oxide (MOX) rods are evaluated up to 7 wt % fissile plutonium (^{239}Pu + ^{241}Pu). The payload consists of undamaged

fuel rods (i.e., no gross fuel failure, hairline cracks or pinholes are allowed). All evaluation detail, including input, method, analysis results and critical benchmarks, are included in Section 6.7.1. Included are the fuel rod geometry and material description, the MCNP model used in the rod holder analyses, and the criticality analysis results of the NAC-LWT loaded with up to 16 PWR rods (fueled with either UO_2 or MOX material). The system reactivity of the NAC-LWT with up to 16 undamged PWR rods is evaluated as a function of rod pitch. The fuel is assumed to be fresh, i.e., no burnup credit. An infinite array of casks is analyzed. Variation of moderator density inside and outside the cask is considered. Also included in the analysis are preferential flooding evaluations of the canister that contains the rod array. The results show that the bias adjusted k_{eff} of an infinite array of NAC-LWT casks at optimum fuel rod pitch and at optimum interspersed moderation is significantly below the upper safety limit (USL) for MOX and UO_2 criticality benchmarks.

Analyses are performed on the NAC-LWT with five DIDO baskets containing DIDO elements and an ANSTO top basket module containing DIDO or ANSTO fuel elements. ANSTO basket contents have been evaluated with an aluminum damaged fuel can (DFC). Section 6.3.10 presents the methods (CSAS25) and KENO-VA models used in the analysis. Section 6.4.11 presents the criticality analysis results of the NAC-LWT cask loaded with the combined payload. Criticality of the NAC-LWT cask with the most limiting fuel characteristics and basket configuration is evaluated. The fuel elements are assumed to be unburned. An infinite array of casks in both the radial and axial extent is analyzed. The results of the analysis show that the bias adjusted k_{eff} of an infinite array of NAC-LWT casks with the most-limiting DIDO/ANSTO basket payload under normal and accident conditions at optimum interspersed moderation (void) is below 0.95.

Analyses are performed on the NAC-LWT with up to 800 SLOWPOKE rods. SLOWPOKE fuel rods are permitted with up to 95.0 wt % ^{235}U initial enrichment. The payload consists of undamaged and/or damaged fuel. All evaluation details, including input, method, and analysis results, are included in Section 6.7.2. The criticality benchmark (defined here) analysis for this material is shown in Section 6.5.5. Included in Section 6.7.2 are the fuel rod geometry and material description, the MCNP model used in the canister, and the criticality analysis results of the NAC-LWT loaded with up to 800 SLOWPOKE rods. The fuel is assumed to be fresh, i.e., no burnup credit. An infinite array of casks is analyzed. Variation of moderator density inside and outside the cask is considered. Also included in the analysis are preferential flooding evaluations of the canister that contains the rod array. The results show that the bias adjusted k_{eff} of an infinite array of NAC-LWT casks at optimum fuel rod pitch and at optimum interspersed moderation is significantly below the upper safety limit (USL).

Analyses are performed on the NAC-LWT with 18 NRU or NRX fuel assemblies. Section 6.7.3 presents the methods and MCNP 5 models used in the analyses. Section 6.7.3.3 also presents the

criticality analysis results of the NAC-LWT cask loaded with the NRU/NRX payload. Criticality of the NAC-LWT cask with the most reactive configuration is evaluated. The fuel assemblies are assumed to be unburned. A single cask is analyzed. The results of the analysis show that the k_{eff} + 2σ of the NAC-LWT cask with the most reactive NRU/NRX configuration under normal and accident conditions is below the upper safety limit (USL) for highly enriched uranium (HEU) fuel.

Analyses are performed on the NAC-LWT with 4 HEUNL containers. The HEUNL material is permitted with up to 7.40 g/L ^{235}U at a maximum ^{235}U enrichment of 93.4 wt%. The evaluated payload considers a bounding container volume of 64.3 L (17.0 gal). Due to void volume in the container that allows HEUNL thermal expansion, actual container capacity is less. All evaluation detail, including input, method, and analysis results are included in Section 6.7.4. The criticality benchmark for this material is provided in Section 6.5.7. Criticality of the NAC-LWT cask with the most reactive configuration is evaluated. Considered in the most reactive configuration is the uranyl nitrate (other nitrates separated) at optimal H/U. The results show that the bias adjusted k_{eff} of an infinite array of NAC-LWT casks with the most reactive HEUNL configuration under normal and accident conditions is below the upper safety limit (USL) for highly enriched uranyl nitrates.

6.2   Package Fuel Loading

The NAC-LWT cask can safely transport 1 PWR assembly, up to 25 intact PWR or BWR rods in a rod holder or fuel assembly lattice, up to 25 PWR or BWR rods with up to 14 of the fuel rods classified as damaged in a rod holder, 2 BWR assemblies, 15 sound metallic fuel rods, 6 failed metallic fuel rods, up to 42 MTR fuel elements, up to 140 TRIGA fuel elements, up to 560 TRIGA fuel cluster rods, up to 42 DIDO fuel assemblies, two General Atomics Irradiated Fuel Material packages, up to 300 TPBARs (of which two can be damaged), up to 700 PULSTAR fuel elements, up to 42 spiral fuel assemblies, up to 42 MOATA plate bundles, up to 800 SLOWPOKE rods, or up to 18 AECL NRU or NRX fuel assemblies. The characteristics for payloads containing fissile material are presented in the following sections. Fresh fuel is conservative because the fuel becomes less reactive as burnup increases. Burnable poisons, such as the gadolinium rods sometimes used in BWR assemblies, are ignored for conservatism.

TPBARs are stainless steel clad rods containing $LiAlO_2$ absorber pellets and nickel-plated Zircaloy getter tube or nickel-plated zirconium (NPZ) alloy spacer tubes with no absorber pellets. The TPBARs do not contain any fissile material.

6.2.1   PWR Fuel Assemblies

Table 6.2.1-1 and Table 6.2.1-2 contain the geometry data for the PWR assemblies. Relevant dimensions are in three categories: Fuel Rod, Guide Tube and Instrument Tube. Fuel rod data includes the number of fuel rods, pitch, diameter, clad thickness, clad material, pellet diameter and active fuel length. The guide tube and instrument tube geometry sections include the number of tubes, tube diameter, tube thickness and tube material.

Table 6.2.1-1   B&W, CE and Westinghouse PWR Fuel Assembly Data

Fuel Type/ Parameter	B&W 15x15 Mark B4	B&W 17x17 Mark C	CE 14x14	CE 16x16 SYS 80	West 14x14 Std	West 14x14 OFA	West 15x15	West 17x17	West 17x17 OFA
Fuel Rod Data									
# Rods	208	264	176	236	179	179	204	264	264
Pin Pitch (in)	0.568	0.502	0.58	0.506	0.556	0.556	0.563	0.496	0.496
Rod Dia. (in)	0.43	0.379	0.44	0.382	0.422	0.4	0.422	0.374	0.36
Clad Thick. (in)	0.0265	0.024	0.028	0.025	0.0225	0.0243	0.0242	0.0225	0.0225
Clad Mat.	Zirc	Zirc	Zirc	Zirc	Zirc	Zirc	Zirc	Zirc	Zirc
Pellet Dia. (in)	0.3686	0.3232	0.3765	0.325	0.3674	0.3444	0.3659	0.3225	0.3088
Act. Length (in)	144	143	137	150	145.2	144	144	144	144
Guide Tube Data									
# Tubes	16	24	5	5	16	N/A	16	24	24
Tube Dia. (in)	0.53	0.465	1.15	0.98	0.539	N/A	0.545	0.482	0.482
Tube Thick. (in)	0.016	0.0175	0.04	0.035	0.034	N/A	0.015	0.016	0.016
Tube Mat.	Zirc	Zirc	Zirc	Zirc	Zirc	Zirc	Zirc	Zirc	Zirc
Instrument Tube Data									
# Inst. Tubes	1	1	0	0	1	N/A	1	1	1
Tube Dia. (in)	0.493	0.42	------	------	0.539	N/A	0.545	0.482	0.482
Tube Thick. (in)	0.026	0.015	------	------	0.034	N/A	0.015	0.016	0.016
Tube Mat.	Zirc	Zirc	------	------	Zirc	N/A	Zirc	Zirc	Zirc

N/A – Not Available. Westinghouse 14×14 standard data used in analysis.

Table 6.2.1-2   Exxon/ANF PWR Fuel Assembly Data

Fuel Type/ Parameter	Ex/ANF 14×14 WE	Ex/ANF 15×15 WE	Ex/ANF 17×17 WE	Ex/ANF 14×14 CE
Fuel Rod Data				
# Rods	179	204	264	176
Pin Pitch (in)	0.556	0.563	0.496	0.58
Rod Dia. (in)	0.424	0.424	0.36	0.44
Clad Thick. (in)	0.03	0.03	0.025	0.031
Clad Mat.	Zirc	Zirc	Zirc	Zirc
Pellet Dia. (in)	0.3505	0.3565	0.303	0.37
Act. Length (in)	142	144	144	134
Guide Tube Data				
# Tubes	N/A	20	24	4
Tube Dia. (in)	N/A	0.544	0.48	1.115
Tube Thick. (in)	N/A	0.017	0.016	0.036
Tube Mat.	N/A	Zirc	Zirc	Zirc
Instrument Tube Data				
# Inst. Tubes	N/A	1	1	1
Tube Dia. (in)	N/A	0.544	0.48	1.115
Tube Thick. (in)	N/A	0.017	0.016	0.036
Tube Mat. (in)	N/A	Zirc	Zirc	Zirc

N/A – Not Available. Westinghouse 14×14 standard data used in analysis.

6.2.2   BWR Fuel Assemblies

Table 6.2.2-1 through Table 6.2.3-3 contains the geometry data for the BWR assemblies. Relevant dimensions are in three categories: Fuel Rod, Water Rod and Channel. Fuel rod data includes the number of fuel rods, pitch, clad inner radius, clad outer radius, clad material, pellet radius and active fuel length. The water rod and channel geometry sections include the number of water rods, rod radii, rod and channel thickness and material.

Table 6.2.2-1 GE BWR Fuel Assembly Data

Parameter	GE 7×7	GE 8×8-1	GE 8×8-2	GE 8×8-4		GE 9×9
Fuel Rod						
Pellet Rad. (cm)	0.6058	0.5283	0.5207	0.5200	0.5200	0.4775
Clad Inner Rad. (cm)	0.6210	0.5398	0.5321	0.5350	0.5350	0.4890
Clad Outer Rad. (cm)	0.7150	0.6261	0.6134	0.6150	0.6150	0.5600
Clad Material	Zircaloy	Zircaloy	Zircaloy	Zircaloy	Zircaloy	Zircaloy
Pitch / 2 (cm)	0.9373	0.8128	0.8128	0.8100	0.8100	0.7190
Zircaloy Water Rod						
Inner Rad. (cm)	-------	0.5398	0.6744	0.5370	1.5000	1.1800
Outer Rad. (cm)	-------	0.6261	0.7506	0.6150	1.6000	1.2500
Zircaloy Channel 80 Mil						
Inner Dim. (cm)	±6.7031	±6.7031	±6.7031	±6.7500	±6.7900	±6.8000
Outer Dim. (cm)	±6.9063	±6.9063	±6.9063	±6.9500	±6.9500	±7.0000
Thickness (cm)	0.2032	0.2032	0.2032	0.2000	0.1600	0.2000
Zircaloy Channel 100 Mil						
Inner Dim. (cm)	N/A	±6.7031	±6.7031	N/A	N/A	N/A
Outer Dim. (cm)	N/A	±6.9571	±6.9571	N/A	N/A	N/A
Thickness (cm)	N/A	0.2540	0.2540	N/A	N/A	N/A
Zircaloy Channel 120 Mil						
Inner Dim. (cm)	N/A	±6.7031	N/A	N/A	N/A	N/A
Outer Dim. (cm)	N/A	±7.0079	N/A	N/A	N/A	N/A
Thickness (cm)	N/A	0.3048	N/A	N/A	N/A	N/A

N/A – Not Applicable. See Table 6.2.2-3 for combinations of fuel/channel.

Table 6.2.2-2 Exxon BWR Fuel Assembly Data

Parameter	Exxon 7×7	Exxon 8×8-1	Exxon 8×8-2	Exxon 9×9
Fuel Rod				
Pellet Rad. (cm)	0.6223	0.5137	0.5137	0.4528
Clad Inner Rad. (cm)	0.6325	0.5232	0.5232	0.4623
Clad Outer Rad. (cm)	0.7239	0.6147	0.6147	0.5385
Clad Material	Zircaloy	Zircaloy	Zircaloy	Zircaloy
Pitch / 2 (cm)	0.9373	0.8141	0.8141	0.7264
Zircaloy Channel <=80 Mil				
Inner Width (cm)	6.7031	6.7031	6.7031	6.8000

Table 6.2.2-3   BWR Fuel Assembly Data

Assembly Type	Number Rods		Channel Thickness	Active Fuel Length (in)
	Fuel	Water		
Exxon 9x9	79	2	80 Mil	150
Exxon 9x9	79	2	2mm	150
Exxon 9x9	74	2	2mm	150
GE 8x8	62	2	80 Mil	150
GE 8x8	62	2	100 Mil	150
GE 9x9	74	2	80 Mil	150
GE 7x7	49	0	80 Mil	146
Exxon 8x8-2	62	2	80 Mil	150
GE 8x8	60	4	2mm	150
GE 9x9	79	2	2mm	150
Exxon 8x8-1	63	1	80 Mil	145.2
GE 9x9	79	2	80 Mil	150
Exxon 7x7	49	0	80 Mil	144
GE 8x8	63	1	120 Mil	146
GE 8x8	63	1	100 Mil	146
GE 8x8	63	1	80 Mil	146

6.2.3   MTR Fuel Elements

The NAC-LWT MTR basket designs can transport up to 42 MTR research reactor fuel elements. This configuration consists of seven fuel elements placed radially in each of four, five or six axial fuel basket segments. The analysis provided herein is bounding for all MTR element loading configurations.

An MTR fuel element comprises fuel plates held in a parallel arrangement by thick aluminum slotted side plates. The number of fuel plates range from 10 to 23 per element. The fuel plates have a fuel meat composed of either U_3O_8-Al, U-Al or USi-Al. The listed fuel enrichment ranges up to slightly greater than 93 wt% ^{235}U. Thus, initial criticality analysis is performed at a nominal 93 wt% ^{235}U with a reactivity penalty of ± 1 wt% ^{235}U applied to allow for enrichment variation up to 94 wt% and with a reactivity penalty of ± 5 grams per element to allow for loading variation up to 355 grams per element. Figure 6.2.3-1 shows a cross-sectional view of the design basis MTR fuel element. The various design basis HEU, LEU and MEU MTR fuel characteristics are shown in Table 6.2.3-1, Table 6.2.3-2 and Table 6.2.3-3, respectively. The High Flux Beam Reactor (HFBR) is modeled in the criticality analysis as the design basis MTR fuel element design, and is shown in Figure 6.2.3-1. The listed fuel dimensions are extended to arrive at bounding fuel configurations in Section 6.4.3.

The bounding fuel dimensions provide for loading MTR fuel elements containing up to a maximum ^{235}U content of 460 grams (20 grams per plate in 23 plates), and LEU specific loads up to 736 grams ^{235}U (32 grams per plate in 23 plates). Total ^{235}U content of the fuel elements modeled in the criticality evaluations may exceed that used in the Chapter 5 shielding analysis. For cases containing a lower fissile material content in the shielding evaluations, the lower value represents the cask payload limit.

MTR fuel plates can also be transported. The loose plates are placed inside an MTR plate canister prior to placement into the NAC-LWT MTR basket. The number of fuel plates in each canister is restricted to that of an equivalent MTR fuel element.

Figure 6.2.3-1   Design Basis HFBR MTR Fuel Element
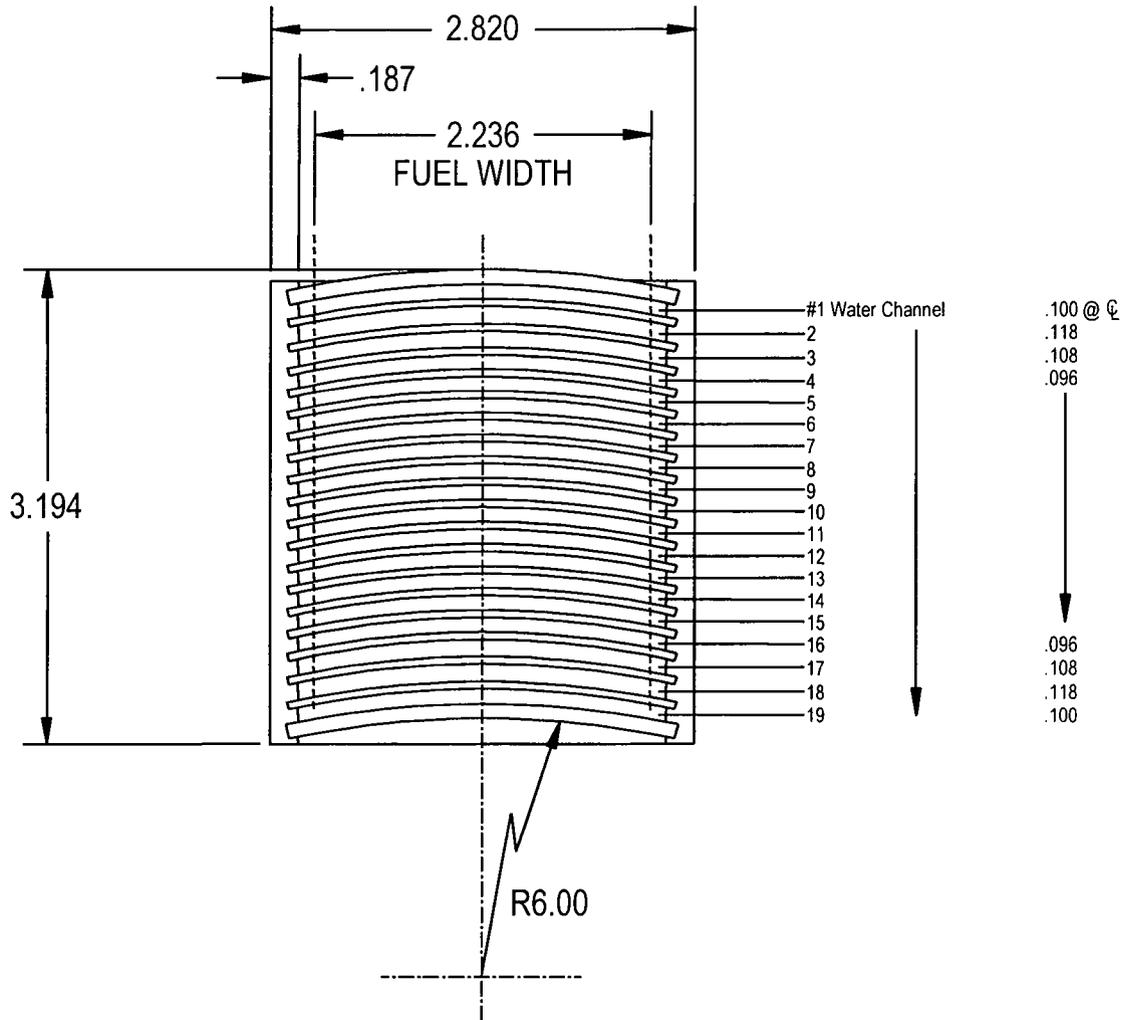
(18) INNER FUEL PLATES, 23 3/4" LONG, .050" THICK
FUEL ALLOY CORE 22 3/4 LONG, .021 THICK
CLADDING .0145" THICK. TOTAL U^{235} CONTENT – 351 g
OUTER ALUMINUM PLATES .100" THICK

Table 6.2.3-1   Characteristics of Design Basis HEU MTR Fuels

Reactor1/ Fuel Parameters	HFBR	ORR #1	ORR #2	OWR	BSR	NISTR3	THOR
Element Length (cm)	145.4	97.5	97.5	108.31	94.3	34	100.3
Element Width (cm)	7.2	7.6	7.6	7.7	7.6	7.6	7.6
Element Depth (cm)	8.2	8.0	8.0	8.4	8.4	8.3	7.7
Side Plate Thickness (cm)	0.475	0.475	0.475	0.475	0.475	0.475	0.51
No. of Plates	18+2 Al	19	19	19	19	17+2 Al	10
Plate Thickness (cm)	0.127	0.127	0.127	0.127	0.129	0.127	0.251
Active Fuel Length (cm)	57.8	60.0	60.0	61.2	59.8	28.0	60.0
Active Fuel Width (cm)	5.72	6.35	6.35	6.47	6.3	6.35	6.0
Active Fuel Thickness (cm)	0.053	0.051	0.051	0.051	0.051	0.051	0.175
Clad Thickness (cm)	0.037	0.038	0.038	0.038	0.038	0.038	0.038
Water Channel Thickness (cm)	0.244[2]	0.295	0.295	0.295	0.295	0.295	0.51
Fuel Composition	U_3O_8-Al	U-Al	U_3O_8-Al	U_3O_8-Al	U-Al[4]	U_3O_8-Al	U-Al
Wt% ^{235}U (nominal)[5]	93	93	93	93	93	93	93
^{235}U per Fuel Element (grams)	351	202	285	232	223	181.05	140
^{235}U per Plate (grams)	19.5	10.6	15	12.21	11.7	10.65	14
U Density (g U/cm^3)	1.197	0.59	0.83	0.60	0.66	1.25	0.23
U in Fuel Composition (wt%)	30	20	25	25	20	30	8

Notes:
1. Reactors:
   HFBR – High Flux Beam Reactor, Brookhaven USA
   ORR – Oak Ridge Research Reactor, Oak Ridge USA
   OWR – Omega West Reactor, Los Alamos USA
   BSR – Bulk Shielding Reactor, Oak Ridge USA
   NISTR – National Institute of Standards Test Reactor, Washington D.C. USA
   THOR – Tsing Hua Open-Pool Reactor, Hsinchu, Taiwan
2. Variable outer plate spacing.
3. Fuel element cut in half. Two half-sections are loaded into each basket cell.
4. Two plates in some fuel elements contain U_3O_8.
5. Maximum 94 wt % enrichment analyzed in Section 6.4.3.4 for conservatism.

Table 6.2.3-1 Characteristics of Design Basis HEU MTR Fuels (continued)

Reactor1/ Fuel Parameters	GRR #1 (NUKEM)	GRR #2 (US Nuc)	GRR #3 (CERCA)	ASTRA	SAPFIR #1	SAPFIR #2	PRR
Element Length (cm)	95.0	95.0	95.0	87.3	87.3	87.3	100.3
Element Width (cm)	7.6	7.6	7.6	7.6	7.6	7.6	7.6
Element Depth (cm)	8.0	8.0	8.0	8.0	8.0	8.0	7.6
Side Plate Thickness (cm)	0.45	0.45	0.45	0.45	0.45	0.45	0.47
No. of Plates	19	18	18	23	23	23	18
Plate Thickness (cm)	0.127	0.127	0.152	0.127	0.127	0.127	0.152
Active Fuel Length (cm)	60.	60.	60.	62.5	62.5	62.5	62.2
Active Fuel Width (cm)	6.3	6.3	6.3	6.28	6.28	6.28	6.12
Active Fuel Thickness (cm)	0.051	0.051	0.050	0.051	0.051	0.051	0.1016
Clad Thickness (cm)	0.038	0.038	0.051	0.038	0.038	0.038	0.0254
Water Channel Thickness (cm)	0.295	0.315	0.290	0.223	0.223	0.223	0.279
Fuel Composition	U-Al	U-Al	U-Al	U-Al	U-Al	U_3Si_2-Al	U-Al
Wt% ^{235}U (nominal)	93	93	93	93	90	93	94
^{235}U per Fuel Element (grams)	180.5	187.2	180.9	281	281	281	247
^{235}U per Plate (grams)	9.5	10.4	10.05	12.2	12.2	12.2	13.7
U Density (g U/cm^3)	0.53	0.58	0.57	0.66	0.68	0.66	0.378
U in Fuel Composition (wt%)	20	20	20	20	20	20	12.5

Notes:
1. Reactors:
   GRR – Greek Research Reactor, Greece
   ASTRA – Adapter Schwimmbecken Tank Reaktor, Austria
   SAPFIR – Research Reactor, Switzerland
   PRR – Philippine Research Reactor, Philippines

Table 6.2.3-1 Characteristics of Design Basis HEU MTR Fuels (continued)

Reactor1/ Fuel Parameters	PRR (Mod)	CNEA #1	CNEA #2	CNEA (Hybrid)
Element Length (cm)	100.3	88.0	88.0	88.0
Element Width (cm)	7.6	7.62	7.6	7.62
Element Depth (cm)	8.03	8.4	8.4	8.4
Side Plate Thickness (cm)	0.47	0.52	0.49	0.49
No. of Plates	19	19	19	19
Plate Thickness (cm)	0.1496	0.130 ± 0.015	0.140 (+0.05, -0.02)	0.108
Active Fuel Length (cm)	62.2	61.5 ± 1.0	61.5 ± 1.0	60.5
Active Fuel Width (cm)	6.12	6.0 ± 0.13	5.9 (+0.05, -0.0)	6.15
Active Fuel Thickness (cm)	0.1016	0.052 ± 0.003	0.056 ± 0.003	0.060
Clad Thickness (cm)	0.024	0.039	0.042 ± 0.006	0.024
Water Channel Thickness (cm)	0.279	0.312 ± 0.015	0.302 (+0.05, -0.02)	0.334
Fuel Composition	U-Al	U-Al	U-Al	U-Al
Wt% ^{235}U (nominal)	94	90 ± 1	90 ± 1	91
^{235}U per Fuel Element (grams)	262	148.2 ± 5.7	200.1 ± 10.1	218.5
^{235}U per Plate (grams)	13.7	7.8 ± 0.3	10.53 ± 0.53	11.5
U Density (g U/cm³)	0.378	0.452 (+0.071, -0.061)	0.576 (+0.081, -0.075)	0.566
U in Fuel Composition (wt%)	12.5	$15.0\% \pm 0.6\%$	$18.3\% \pm 0.9\%$	20.5%
Fuel Meat Al Alloy Weight (g)	102.02	49.1	52.3	49.0

Notes:

1. Reactors:

PRR (Mod) – NAC modified PRR fuel element – 19 plates and reduced clad thickness (0.024 cm).

CNEA – Comision Nacional De Energia Atomica.

CNEA (Hybrid) – NAC modified CNEA element containing maximum reactivity dimensions from the two CNEA plate/element types.

Table 6.2.3-2   Characteristics of Design Basis LEU MTR Fuel

Reactor1/ Fuel Parameters	BSR	ZPRL	THOR	RSG-GAS	IEA-R1
Element Length (cm)	97.5	100.3	100.3	N/A	N/A
Element Width (cm)	7.8	7.7	7.62	7.7	7.7
Element Depth (cm)	8.4	7.7	7.73	7.7	7.7
Side Plate Thickness (cm)	0.475	0.477	0.510	0.477	0.477
Number of Plates	19	10	10	21	18
Plate Thickness (cm)	0.127	0.251	0.251	0.130	0.150
Active Fuel Length (cm)	60	60	60	60	60
Active Fuel Width (cm)	6.35	6	6	6.275	6
Active Fuel Thickness (cm)	0.051	0.175	0.175	0.064	0.084
Clad Thickness (cm)	0.038	0.038	0.038	0.033	0.033
Water Channel Thickness (cm)	0.295	0.5356	0.510	0.2724	0.3138
Fuel Composition	U_3Si_2-Al	U-Al	U-Al	U_3O_8-Al	U-Al
Weight Percent ^{235}U (wt %)	19.75	20	20	19.75	20
^{235}U per Fuel Element (grams)	340	210	210	271	180
^{235}U per Plate (grams)	17.9	21	21	13	10
U Density (grams U/cm^3)	4.66	0.64	0.64	3	1.8
U in Fuel Composition (wt %)	74	40	40	57	40

Notes:
1. Reactors:
   BSR – Bulk Shielding Reactor, ORNL
   ZPRL – ZPRL Research Reactor Facility, Taiwan
   THOR – Tsing Hua Open-Pool Reactor, Hsinchu, Taiwan
   RSG-GAS – National Center for Research and Technology, Serpong, Indonesia
   IEA-R1 – IEA-R1 Facility, Brazil

Table 6.2.3-3   Characteristics of Design Basis MEU MTR Fuel

Reactor1/ Fuel Parameters	ASTRA	MEUG
Element Length (cm)	68.65 (cut)	--- [2]
Element Width (cm)	7.61	7.61
Element Depth (cm)	8.05	8.05
Side Plate Thickness (cm)	0.45	0.45
Number of Plates	23	23
Plate Thickness (cm)	0.127	0.127
Active Fuel Length (cm)	60.0	60.0
Active Fuel Width (cm)	6.275	6.275
Active Fuel Thickness (cm)	0.051	0.053
Clad Thickness (cm)	0.038/0049	0.037
Water Channel Thickness (cm)	0.221[3]	0.221[3]
Fuel Composition	UAl_x-Al	UAl_x-Al[4]
Weight Percent ^{235}U (wt %)	45%	20%-80%
^{235}U per Fuel Element (grams)	320	333.5
^{235}U per Plate (grams)	13.9	14.5
U Density (grams U/cm^3)	1.63	0.91-2.08
U in Fuel Composition (wt %)	63	38-87

Notes:

1. Reactors:
   ASTRA – Adaptierter Schwimmbecken Tank Reactor Austria
   MEUG – Modified ASTRA MEU fuel element parameters
2. Not required for infinite length criticality evaluation.
3. Channel thickness was not included in reference information.
   Indicated channel thickness is the result of assuming a constant
   channel between all plates and one-half the channel beyond the outer
   plates.
4. Based on a constant fuel mass and material thickness, the fuel
   material composition (ex. U_3O_8, UAl_x, USi_2) will not have a
   significant impact on the reactivity of the system.

6.2.4 PWR and BWR Rods in a Rod Holder or Fuel Assembly Lattice

The NAC-LWT cask may transport up to 25 intact PWR or BWR fuel rods in a fuel rod holder or fuel assembly lattice. Up to 14 of 25 PWR or BWR fuel rods in a fuel rod holder may be classified as damaged.

6.2.4.1 Intact PWR or BWR Rods in a Rod Holder or Fuel Assembly Lattice

To bound all PWR and BWR rods that may be transported in the NAC-LWT cask, rods with a maximum enrichment of 5.0 wt % ^{235}U were analyzed. Characteristics of the design basis PWR rods are presented in Table 6.2.1-1 and Table 6.2.1-2. Characteristics of the design basis BWR rods are presented in Table 6.2.2-1, Table 6.2.2-2 and Table 6.2.2-3. Given an infinite length rod and an enrichment of 5.0 wt % ^{235}U as the basis for this analysis, the most reactive PWR and BWR rod has the greatest fissile mass, i.e. the rod with the largest pellet radius. Therefore, the rod used in the CE 14×14 assembly was chosen as the most reactive PWR fuel rod and the rod used in the Exxon 7×7 assembly was chosen as the most reactive BWR fuel rod. A maximum of 25 PWR or BWR rods were used in the analysis.

6.2.4.2 Damaged PWR or BWR Rods in a Rod Holder

The evaluation of the damaged fuel rods uses the bounding fuel characteristics for the intact fuel rod condition as described in Section 6.2.4.1, but assumes that up to 14 of the fuel rods are classified as damaged. Fuel transported in this configuration must be in a fuel rod holder. The fuel rod used in the CE 14×14 assembly was chosen as the most reactive PWR fuel rod, and the rod used in the Exxon 7×7 assembly was chosen as the most reactive BWR fuel rod.

6.2.5   TRIGA Fuel Elements

The NAC-LWT TRIGA non-poisoned and poisoned basket designs can transport up to 140 TRIGA fuel elements. These configurations contain sets of up to 4 intact TRIGA fuel elements. Each set of elements is placed in the cells of the five TRIGA basket modules. In the non-poisoned configuration, the central cell of each module is blocked to prohibit the placement of fuel elements in that location. The NAC-LWT TRIGA basket design can also accommodate sets of four follower control rod (FFCR) elements per cell in the top module. The TRIGA base and top basket modules can accommodate screened failed fuel cans or sealed failed fuel cans for TRIGA failed fuel or fuel debris. The screened failed fuel can is able to hold up to four intact TRIGA fuel elements. The sealed failed fuel can is limited to the equivalent content of two TRIGA fuel elements.

Figure 6.2.5-1 and Figure 6.2.5-2 show typical TRIGA aluminum and stainless steel clad fuel elements, respectively (Tomsio). The various design basis TRIGA fuel element characteristics are shown in Table 6.2.5-1 and Table 6.2.5-2. The TRIGA fuel matrix is a solid uranium-zirconium-hydride metal alloy in which the zirconium-hydride moderator is homogeneously combined with the enriched uranium into pellets. Uranium enrichment in the TRIGA fuel elements is typically either nominal 20 wt % or 70 wt % with test fuel element enrichment up to 93 wt %. The fuel pellets are loaded into cylindrical rods approximately 1.5 inches in diameter and 30 inches long. Sections of graphite are placed above and below the active fuel section of the TRIGA fuel elements. TRIGA fuel elements can be aluminum clad or stainless steel clad. The FFCR TRIGA fuel element is 45 inches long and has a 15 inch U-ZrH active fuel region with a slightly smaller diameter than 1.5 inches, a 15-inch boron carbide upper section and 6 inch void lower section.

As shown in Figure 6.4.5-1, the design basis TRIGA fuel element type for criticality evaluations is the stainless steel clad element with the FLIP composition enriched to 70 wt % ^{235}U (HEU) and with 137 grams ^{235}U per element. This fuel element design bounds all the other standard TRIGA fuel elements under consideration, including the stainless steel clad FLIP LEU-II fuel element enriched to 20 wt% ^{235}U and with 169 grams ^{235}U per element. The FFCR elements are also bounded by the design basis TRIGA fuel element.

Analysis in Section 6.4.5 addressess TRIGA fuel elements with fissile material mass and enrichment fabrication tolerances slightly above the initial design basis element values, and test elements with substantially higher fissile material mass and/or enrichments.

Figure 6.2.5-1   Aluminum Clad TRIGA Fuel Element
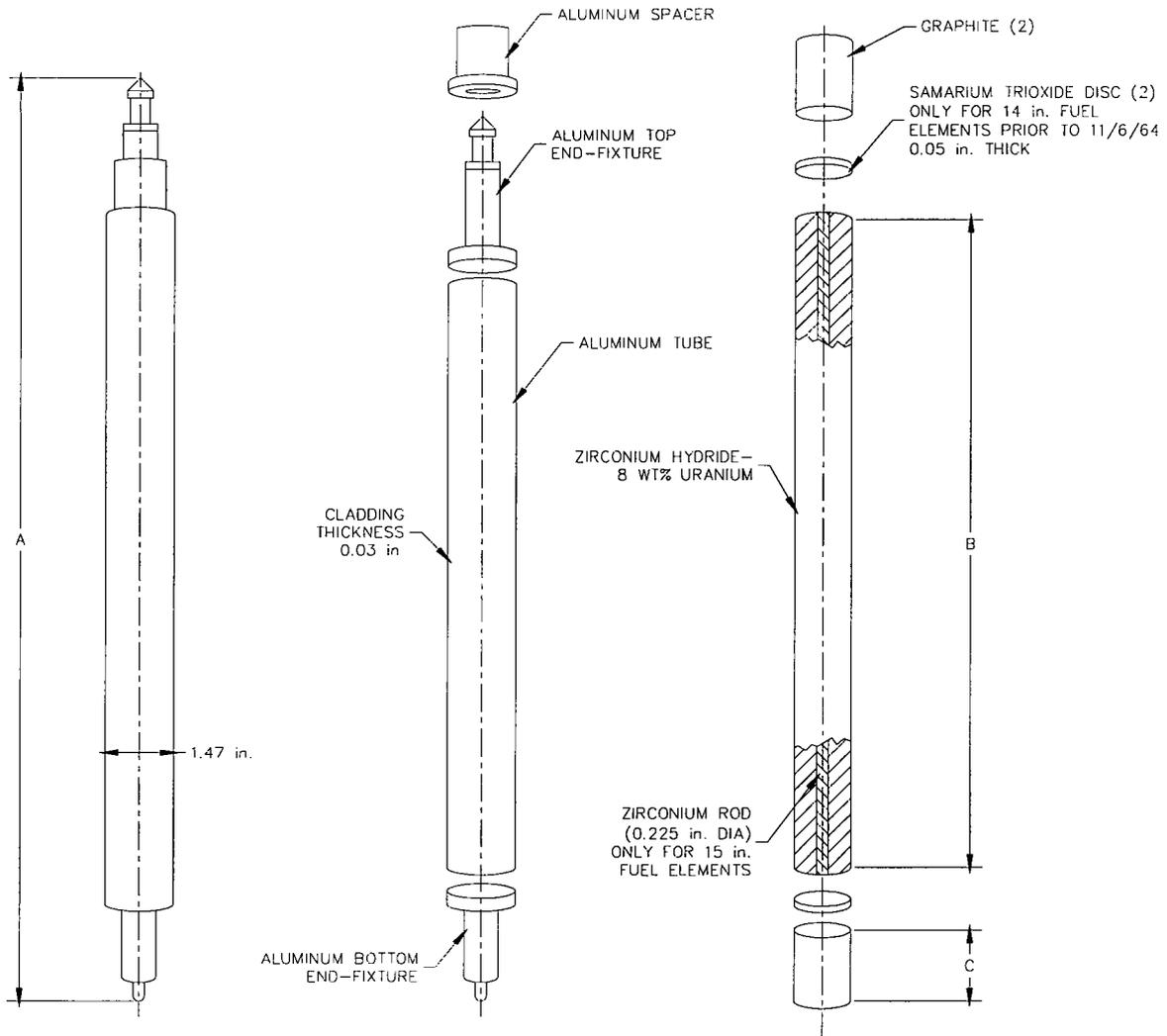
TRIGA Fuel Type	A (in.)	B (in.)	C (in.)
Original - 14 in.	28.37	14.0	3.95
Original - 15 in.	28.3	15.0	3.53

Figure 6.2.5-2   Stainless Steel Clad TRIGA Fuel Element

NOTE:
APPLICABLE DIMENSIONS "A–D"
AND FITTING TYPES ARE LISTED
ON TABLE 3–2.

STAINLESS STEEL
TOP END FITTING
TYPE I–A

GRAPHITE
(2)

SAMARIUM TRIOXIDE
DISC (2) ONLY
FOR FUEL ELEMENTS
PRIOR TO 11/6/64

STAINLESS
STEEL TUBE

CLADDING
THICKNESS
0.02 in.

URANIUM
ZIRCONIUM
HYDRIDE
(3)*

15 in.

A

D

B

ZIRCONIUM
ROD
(0.225 in. DIA)

0.05 in. THICK

MOLYBDENUM DISC
0.031 in. **

*ACPR FUEL ELEMENT CONSIST OF
ONE 15 in. FUEL ROD
** NOT INCLUDED IN
FUEL ELEMENTS PRIOR TO
4/15/71 AND IN ACPR
FUEL ELEMENTS

STAINLESS STEEL
BOTTOM END FITTING
TYPE I–A

APPLIES FOR DRAWINGS:
T13S210D210
T0S210D210
T4S210D105
T5A210D210

TRIGA Fuel Type	A (in.)	B (in.)	C (in.)	D(in.)
Standard - streamline	29.68	1.478	2.56(2)	1.435
Standard - plain	28.9	1.478	3.42	1.435
ACPR(1)	28.89	1.478	3.45	1.40

(1) Annular Core Pulse Reactor
(2) Lower graphite is 3.72 inches

Table 6.2.5-1   Characteristics of Design Basis TRIGA Fuels Elements

Element Type	Al Clad	ACPR(1)	Steel Clad	Fuel Follower Standard Control Rod(6)
Element Diameter (in.)	1.47	1.478	1.478	1.355
Element Length(in.)	28.4[2] 28.3[3]	28.89	29.7[4] 28.9[5]	45
Active Length (in.)	14[2] 15[3]	15	15	15
Graphite Reflector (in.)	3.53	3.45	2.56, 3.72[4] 3.42 [5]	-
Graphite Diameter	1.41	1.40	1.435	-
Reflector (2) Mass (g)	450	450	450	-
End Fitting Mass (g)	140	530	530	290
Clad Material	Al	SS304	SS304	SS304
Clad Thickness (in.)	0.03	0.02	0.02	0.02
Clad Mass (g)	140	270	270	462
Fuel Material	U-ZrH	U-ZrH	U-ZrH	U-ZrH
Pellet Diameter (in.)	1.41	1.40	1.435	1.311[7]
Central Hole (in.)	0.25	0.25	0.25	0.25
Filling Rod Mat'l	Zirc	Zirc	Zirc	Zirc
Filling Rod Dia. (in.)	0.225	0.225	0.225	0.225

Notes:
1. Annular Core Pulse Reactor.
2. Al clad fuel with 14-inch active fuel has no central hole with Zircaloy rod.
3. Al clad fuel 15-inch active fuel has a central hole with Zircaloy rod.
4. Steel clad standard streamline fuel has 2.56 and 3.72-inch upper and lower graphite reflectors.
5. Steel clad standard plain fuel has 3.42-inch upper and lower graphite reflectors.
6. Fuel follower control rod has an uppermost 6.5-inch air void section, a 15-inch boron carbide upper section, a 15-inch UZrH fuel section, and 5.88-inch lower void section.
7. Fuel meat diameter.

Table 6.2.5-2   Characteristics of Design Basis TRIGA Fuels – Fuel Compositions

Element Type	Al Clad	Steel Clad					Fuel Follower Control Rod		
		ACPR	Stand.	FLIP[1]	FLIP LEU-I	FLIP LEU-II	Stand.	FLIP LEU-I	ACPR
U in Fuel (max. wt%)	8.5	12.5	12	8.5	20	31	8.5	8.5	12.5
^{238}U- Mass (g)	164	224	164	59	403	676	150	387	224
^{235}U in U (wt%)	20	20	20	70	20	20	20	20	20
^{235}U-Mass (g)	41	56	41	137	101	169	38	97	56
H to Zr Ratio	1.0	1.7	1 - 1.7	1.6	1.6	1.6	1.6	1.6	1.7
Zr Mass (g)	2300	1962	2300	2060	1988	1886	2004	1908	1962

[1] FLIP – Fuel Life Improvement Program

Note:

Variation in fuel characteristics from the indicated values is evaluated in Section 6.4.5.

6.2.6   TRIGA Fuel Cluster Rods

The NAC-LWT TRIGA non-poisoned and poisoned basket designs can transport up to 560 TRIGA fuel cluster rods. These configurations contain sets of up to 16 intact TRIGA fuel cluster rods within an insert. Each set of elements is placed in the cells of the five TRIGA basket modules. In the non-poisoned configuration, the central cell of each module is blocked to prohibit the placement of fuel elements in that location. The NAC-LWT TRIGA basket design can also accommodate sets of four follower control rod (FFCR) elements per cell in the top module. The TRIGA base and top basket modules can accommodate sealed failed fuel cans containing failed TRIGA fuel cluster rods or debris. The sealed failed fuel can is limited to the equivalent content of six TRIGA fuel cluster rods.

Figure 6.2.6-1 shows details of typical TRIGA fuel cluster rods (Tomsio). The design-basis TRIGA fuel cluster rod characteristics are shown in Table 6.2.6-1 and Table 6.2.6-2. The TRIGA fuel matrix is a solid uranium-zirconium-hydride metal alloy in which the zirconium-hydride moderator is homogeneously combined with the enriched uranium into pellets. Uranium enrichment in the HEU TRIGA fuel cluster rods is 93.3 wt % ^{235}U. LEU TRIGA cluster rods contain a uranium enrichment of 20 wt % ^{235}U. The fuel pellets are loaded into cylindrical rods approximately 0.5 inch in diameter and 30 inches long. TRIGA cluster rods are clad with Incoloy 800 material.

Figure 6.2.6-1   TRIGA Fuel Cluster Rod Details

TRIGA *FUEL CLUSTER*

Security-Related Information
Figure Withheld Under 10 CFR 2.390

Table 6.2.6-1   Characteristics of TRIGA Fuel Cluster Rods

Element Type	TRIGA Fuel Cluster Rod
Element Diameter (in.)	0.542
Element Length (in.)	30.13
Active Length (in.)	22
End Fitting Mass (g)	121
Clad Material	Incoloy 800
Clad Thickness (in.)	0.016
Clad Mass (g)	210
Fuel Material	U-ZrH
Pellet Diameter (in.)	0.51

Table 6.2.6-2   Characteristics of TRIGA Fuel Cluster Rods – Fuel Compositions

Parameter	HEU Value	LEU Value
U in Fuel (wt%)	10.2	45
235U in U Mass (wt%)	93.3	20
235U Mass (g)	42	54
H to Zr Ratio[1]	1.6	1.6
Zr Mass (g)	380	--[2]

---

[1] Specifications allow for a maximum H to Zr ratio of 1.7.

[2] Zirconium mass is calculated in the analysis section based on the uranium percentage in the fuel meat. Range of the as-fabricated fuel meat is 43 to 47 wt % uranium.

6.2.7   Metallic Fuel Rods

The design characteristics of the metallic fuel rods are shown in Table 6.2.7-1. As stated in Section 6.1, no criticality analyses are performed for these contents because naturally enriched uranium cannot become critical in light water.

Table 6.2.7-1   Characteristics of Design-Basis Metallic Fuel Rods

Parameter	Metallic
Assembly Rod Array	N/A
Assembly Weight, lbs	1,805 (15 rods)
Fuel Rod Length, in	120.5
Active Fuel Length, in	120.0
Number of Fuel Rods/Assembly	N/A
Fuel Rod Diameter, in	1.36
Cladding Material	Al
Cladding Thickness, in	0.080
Pellet Diameter, in	1.36
Fuel Cell Pitch, in	N/A
Pellet Material	Uranium metal
Theoretical Density percent	100
Maximum Initial Enrichment wt % ^{235}U	Natural
Design-basis Burnup, MWd/MTU	1,600
Weight of Uranium, kg/assembly	54.5
Weight of UO_2, kg/assembly	N/A

6.2.8   DIDO Fuel Assemblies

The NAC-LWT DIDO fuel basket module design can transport up to 42 DIDO research reactor fuel assemblies in six fuel basket modules. This configuration consists of seven fuel assemblies per basket, one placed in a center tube and one in each of six peripheral tubes. The analysis provided herein is bounding for all DIDO fuel assembly loading configurations.

A DIDO fuel assembly is comprised of four annular fuel elements that may be crimped at a common point after the assembly is cut to size. The fuel elements have a fuel meat composed of either U_3O_8-Al, U_3Si_2-Al, or U_3Si_2 in an aluminum matrix dispersing material. While data available did not indicate U-Al mixture, it will be enveloped by the evaluation shown in Section 6.4.7. Highly enriched, medium enriched and low enriched assemblies are available at maximum enrichments of 93 wt % ^{235}U, 45 wt % ^{235}U and 20 wt % ^{235}U, respectively. HEU fuel assemblies are conservatively evaluated at 94 wt % ^{235}U. Figure 6.2.8-1 shows a view of the DIDO fuel assembly. Nominal characteristics for the DIDO fuel assemblies are shown in Table 6.2.8-1. Uranium weight percent in the fuel composition is indicated as 57.5, 33.7, and 18.4 weight percent for the HEU, MEU and LEU fuel, respectively. The listed fuel dimensions are extended by the tolerances shown in Table 6.2.8-2 to arrive at bounding fuel configurations in Section 6.4.3.

Figure 6.2.8-1   DIDO Fuel Assembly
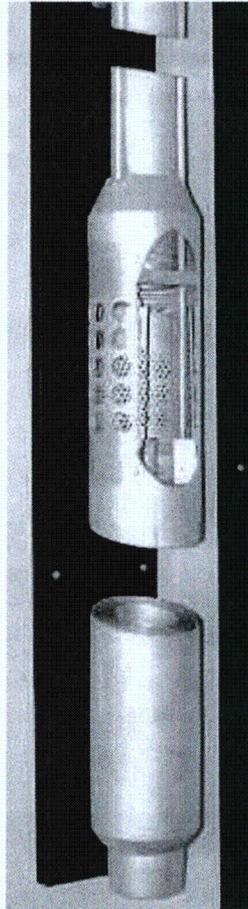
Table 6.2.8-1   Characteristics of DIDO Fuel Assemblies

Fuel Parameters	Units	U3Si2-Al	U3Si2	U3O8
Tube 1 outer diameter	[cm]	6.395	6.38	6.38
Tube 1 ^{235}U	[g]	36.0	35.67	35.67
Tube 2 outer diameter	[cm]	7.375	7.36	7.36
Tube 2 ^{235}U	[g]	42.0	41.88	41.88
Tube 3 outer diameter	[cm]	8.355	8.34	8.34
Tube 3 ^{235}U	[g]	48.0	48.09	48.09
Tube 4 outer diameter	[cm]	9.335	9.32	9.32
Tube 4 ^{235}U	[g]	54.0	54.36	54.36
Clad thickness	[cm]	0.048	0.0425	0.0425
Tube thickness	[cm]	0.146	0.15	0.15
Fuel meat thickness	[cm]	0.050	0.065	0.065
Active fuel length	[cm]	60.90	60.0	60.0
Total element length	[cm]	66.04	62.5	62.5
^{235}U per fuel assembly	[g]	180.0	180.0	180.0

Table 6.2.8-2   DIDO Fuel Assembly Tolerances

Description	Units	Value
Fuel Tube Diameter	[cm]	0.20
Plate Thickness	[cm]	0.02
Clad Thickness	[cm]	0.01
Fuel Cylinder Pitch	[cm]	0.02
Active Fuel Length	[cm]	1.25
Fuel Element Length	[cm]	1.00
235U per Fuel Assembly	[g]	10.00
U wt% in Fuel Composition		5

6.2.9 General Atomics Irradiated Fuel Material

The NAC-LWT General Atomics (GA) Irradiated Fuel Material (IFM) basket module is designed to transport two IFM packages, also referred to as Fuel Handling Units (FHUs). The module is placed in the top of the NAC-LWT cavity with a bottom spacer to facilitate unloading of the IFM packages.

The two GA IFM FHUs are intended for a single shipment in the NAC-LWT. The first IFM FHU contains a Reduced-Enrichment Research and Test Reactor (RERTR) type fuel and the second contains a High-Temperature Gas-cooled Reactor (HTGR) type fuel. Each FHU consists of stainless steel weld-encapsulated primary and secondary enclosures that contain the GA IFM.

The RERTR IFM is comprised of 20 irradiated TRIGA fuel elements; 13 of the elements are intact and the remaining seven have been previously sectioned for examination purposes. The component segments of each sectioned element have been collected into separate aluminum tubes with crimped ends. Since the TRIGA elements are loaded in both intact and sectioned configurations, two models of the TRIGA fuel are considered: 1) intact elements in a regular array, and 2) fuel homogenization within the confines of the RERTR primary enclosure. The latter model is used to demonstrate system subcriticality for a damaged package.

Parameters characterizing the RERTR/TRIGA fuel elements are shown in Table 6.2.9-1. Three distinct mass loadings of uranium were used in the 20 TRIGA elements: 20, 30 and 45 wt % U; the average mass of the fueled portion of these elements is 551 g with an enrichment of 19.7 wt % ^{235}U. The overall mass fractions of the 20 elements are given in Table 6.2.9-2 and the composition of the incoloy clad is given in Table 6.2.9-3. For a homogenized (damaged) fuel description, equivalent densities calculated for each of the RERTR/TRIGA elemental constituents are shown in Table 6.2.9-4. The volume inside the RERTR primary enclosure is 436 in^3 (7140 cm^3).

The HTGR IFM is comprised of fuel in four forms: fuel particles (kernels), fuel particles (coatings), fuel compacts (rods), and fuel pebbles. Fuel kernels are solid, spheridized, high-temperature sintered fully-densified, ceramic kernel substrate, composed of: UC_2, UCO, UO_2, $(Th,U)C_2$, or $(Th,U)O_2$. The as-manufactured enrichment of the HTGR fuel varies from ~10.0 to 93.15 wt % ^{235}U. Fuel coatings are solid, spheridized, isotropic, discrete multi-layered fuel particle coatings with chemical composition including pyrolitic-carbon (PyC) and silicon carbide (SiC). Fuel compacts are multi-coated ceramic fuel particles, bound in solid, cylindrical, injection-molded, high-temperature heat-treated compacts. The fuel compact matrix is composed of carbonized graphite shim, coke, and graphite powder. Fuel pebbles are multi-coated fuel particles, bound in solid, spherical injection-molded, high-temperature heat-treated

pebbles. The fully-cured binding matrix is composed of carbonized graphite shim, coke and graphite powder.

The HTGR material composition is provided for the entire IFM package as shown in Table 6.2.9-4. Based on the dimensions of the stainless steel cylinders encapsulating both the RERTR and HTGR material, shown in Table 6.2.9-5, equivalent densities calculated for each of the HTGR elemental constituents are also shown in Table 6.2.9-4. The volume inside the HTGR primary enclosure is 583 in^3 (9555 cm^3).

Table 6.2.9-1   GA IFM RERTR/TRIGA Fuel Parameters

Description	Unit	Value
Fuel OD	[cm]	1.3
Fuel Length	[cm]	56.0
Clad OD	[cm]	1.38
Clad Thickness	[cm]	0.041
Element Length	[cm]	76.0
Number of Elements		20
Enrichment	[wt % 235U]	19.7

Table 6.2.9-2   GA IFM RERTR/TRIGA Fuel Composition

Constituent	Mass Fraction [wt %]
Zr	62.42
U	35.77
H	1.08
Er	0.59
C	0.14

Table 6.2.9-3   GA IFM RERTR/TRIGA Clad Composition

Constituent	Mass Fraction [wt %]
Fe	40
Ni	35
Cr	25

Table 6.2.9-4   GA IFM Elemental Constituents

Fuel Type	Element	Mass [g]	Density [g/cc]
RERTR	Zr	6721.1	0.9413
	U	3850.66	0.5393
	H	116.02	0.0162
	Er	63.32	0.0089
	C	15.44	0.0022
	Fe	1704.5	0.2387
	NI	919.1	0.1287
	Cr	761.7	0.1067
	Mn	30.8	0.0043
	Mo	17.3	0.0024
	Total	14199.94	1.9888
HTGR	C	7075.55	0.7405
	Th	1956.87	0.2048
	Si	1408.37	0.1474
	U	204.81	0.0214
	O	22.40	0.0023
	Total	10668.00	1.1165

Table 6.2.9-5   GA IFM Primary and Secondary Enclosure Dimensions

Description	Value [in]
RERTR Primary Enclosure Interior Height	34.50
RERTR Primary Enclosure OD	4.25
RERTR Secondary Enclosure OD	4.75
RERTR Enclosure Wall Thickness	0.12
HTGR Primary Enclosure Interior Height	36.50
HTGR Primary Enclosure OD	4.75
HTGR Secondary Enclosure OD	5.25
HTGR Enclosure Wall Thickness	0.12

6.2.10   PULSTAR Fuel Elements

Four 28 MTR 7-element modules are stacked in the NAC-LWT cavity to accommodate PULSTAR fuel elements. PULSTAR fuel elements (rods) may be loaded as either loose rods or intact fuel assemblies. PULSTAR fuel elements are zirconium-alloy-clad UO_2 pellets with an analyzed enrichment of 6.5 wt % ^{235}U. PULSTAR fuel assemblies are a 5×5 rectangular array of elements surrounded by a zirconium alloy box with aluminum upper and lower fittings.

Possible loading configurations for PULSTAR fuel elements are listed below.

- intact assemblies loaded directly into any 28 MTR module cell
- up to 16 intact elements loaded in the 4×4 TRIGA fuel rod insert (rod insert is placed into a module cell),
- up to 25 intact or damaged (failed) elements and nonfuel components of fuel assemblies in the PULSTAR can, or (failed fuel or screened can)

Damaged fuel elements may include severe fuel damage, i.e., fuel debris.

PULSTAR fuel element and assembly characteristics are summarized in Table 6.2.10-1. A sketch of a PULSTAR fuel assembly is shown in Figure 6.2.10-1.

Figure 6.2.10-1   PULSTAR Fuel Assembly
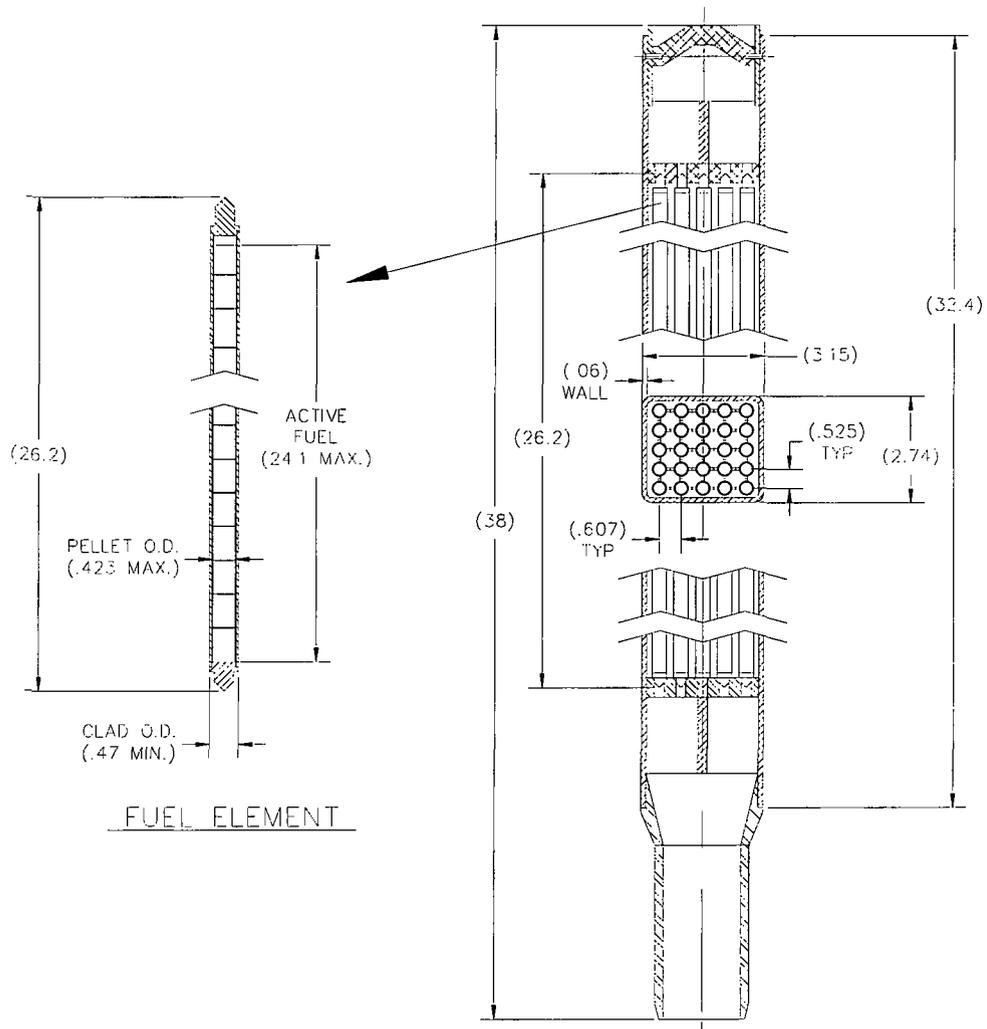
FUEL ELEMENT

Table 6.2.10-1   PULSTAR Fuel Characteristics

Description	Value [in]
Maximum Pellet Diameter (inch)	0.423
Minimum Clad Thickness (inch)	0.0185
Minimum Element (Rod) Diameter (inch)	0.470
Maximum Active Fuel Height (inch)	24.1
Fuel Element (Rod) Length (inch)	26.2
Rod Pitch (inch)	0.525 × 0.607
Assembly Length	38 inch
Box Width	2.745 × 3.155
Box Thickness	0.06
Maximum Enrichment (wt % 235U)	6.5
Maximum 235U Content per Element (g)	33
No of Element (Rods) per Assembly	25

6.2.11   Spiral Fuel Assemblies

The NAC-LWT ANSTO fuel basket module design can transport up to 42 spiral fuel assemblies in six fuel basket modules. This configuration consists of seven fuel assemblies per basket, one placed in a center fuel tube and one in each of six peripheral fuel tubes.

A spiral fuel assembly is comprised of 10 curved fuel plates in a spiral pattern located in the annulus formed by two concentric aluminum sleeves. The assembly top and bottom sections may be cropped outside the fuel region to allow the fuel assembly to fit within the basket cavity. The fuel elements have a fuel meat composed of U-Al alloy. Nominal enrichment for the assembly is 80 wt % ^{235}U enriched. The assemblies are evaluated up to 85 wt % ^{235}U enriched. Figure 6.2.11-1 shows a cross-section view of the spiral fuel assembly. Nominal characteristics for the spiral assemblies are shown in Table 6.2.11-1. The listed fuel dimensions are extended by the tolerances shown in Table 6.2.11-2 to arrive at bounding fuel configurations in Section 6.4.10.

Figure 6.2.11-1   Spiral Fuel Assembly Cross-Section Sketch

⌀10.16 (cm)   ⌀5.82 (cm)
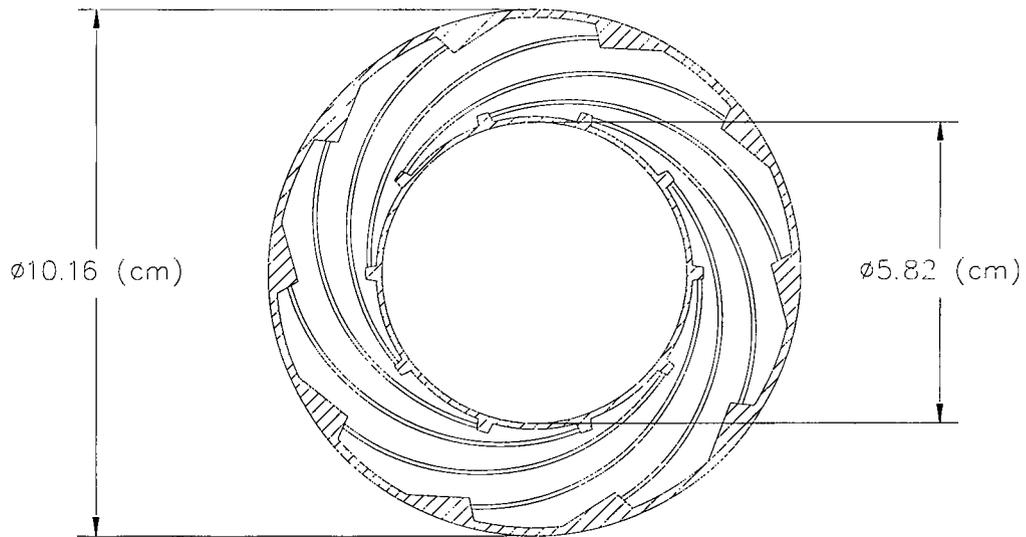
Table 6.2.11-1   Spiral Fuel Assemblies Characteristics

Fuel Parameters	Units	Value
Number of plates		10
Inner aluminum plate ID	[cm]	5.82
Inner aluminum plate OD	[cm]	6.045
Outer aluminum plate ID	[cm]	9.85
Outer aluminum plate OD	[cm]	10.16
Fuel length	[cm]	60.325
Active Fuel Width	[cm]	6.0
Active Fuel Thickness	[cm]	0.061
Plate Width	[cm]	7.33
Plate Thickness	[cm]	0.147
Total element length	[cm]	63.5
Fuel Material		U-Al
Clad Material		Al
Enrichment (wt % ^{235}U)		80%
Maximum ^{235}U per Assembly (nominal)	[g]	150.0
U wt % in Fuel Composition		38%
Mass of uranium (calculated)	[g]	176.5

Table 6.2.11-2   Spiral Fuel Assemblies Tolerances Applied

Fuel Parameters	Units	Value
Plate Thickness	[cm]	0.02
Clad Thickness	[cm]	0.020
Active Fuel Length	[cm]	1.25
Fuel Element Length	[cm]	1.00
^{235}U per Fuel Assembly	[g]	10.00
^{235}U wt % in U		5%
U wt % in Fuel Composition		20%

6.2.12   MOATA Plate Bundles

The NAC-LWT ANSTO fuel basket module design can transport up to 42 MOATA plate bundles in six fuel basket modules. This configuration consists of seven fuel assemblies per basket, one placed in a center fuel tube and one in each of six peripheral fuel tubes.

A plate bundle is comprised of a maximum 14 flat fuel plates sandwiched between two thick, nonfuel, aluminum side plates. The plates are pinned together at the top and bottom, outside the active fuel region, and the plates are separated by spacer disks. The fuel elements have a fuel meat composed of U-Al alloy. Nominal enrichment for the assembly is 90 wt % ^{235}U enriched. The assemblies are evaluated up to 92 wt % ^{235}U enriched. Figure 6.2.12-1 shows cross-section views of the plate bundle. Nominal characteristics for the plate bundle are shown in Table 6.2.12-1. The listed fuel dimensions are extended by the tolerances shown in Table 6.2.12-2 to arrive at bounding fuel configurations in Section 6.4.10.

Figure 6.2.12-1   MOATA Plate Bundle Sketch
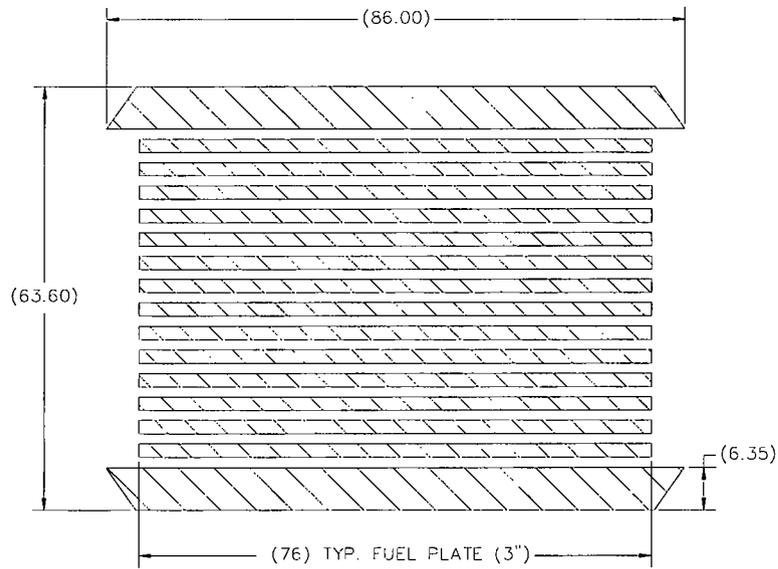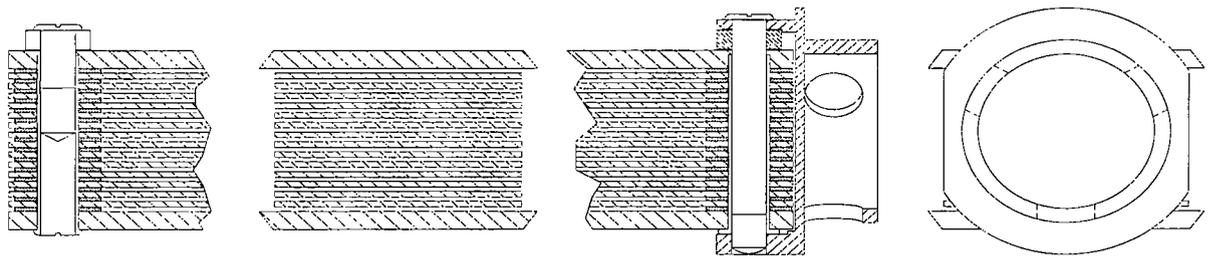
Table 6.2.12-1   MOATA Plate Bundle Characteristics

Fuel Parameters	Units	Value
Maximum Number of Plates		14
Plate Thickness	[cm]	0.2032
Plate Width		7.62
Total element length	[cm]	66.04
Clad thickness	[cm]	0.05
Fuel Meat Thickness (min)	[cm]	0.1032
Active Fuel Width	[cm]	6.985
Active Fuel Length	[cm]	58.42
Plate Spacer Thickness	[cm]	0.15
Side Plate Thickness	[cm]	0.635
Side Plate Width	[cm]	7.87[3]
Angle Cut-Back (degrees)		30
Fuel Composition		U-Al-alloy
Enrichment wt % ^{235}U		90%
Maximum ^{235}U per Plate (nominal)	[g]	22.0
U wt % in Fuel (Calculated)		18%
Mass of uranium - Calculated	[g]	23.9
Assembly Width (Y) – Calculated[2]	[cm]	7.87
Assembly Depth (X) - Calculated	[cm]	6.36

---

[3] Nominal width of "long side" is 8.60 cm. Listed value is "short side" to account for 30-degree chamfer.

[2] Assembly width and depth are calculated values based on the size of the plate stack-up. Circular plate bundle end-fittings and the "chamfered" side plates will minimize movement of fuel within the tube opening.

Table 6.2.12-2   MOATA Plate Bundle Tolerances Applied

Fuel Parameters	Units	Value
Plate Thickness	[cm]	0.00508
Plate Width	[cm]	0.0381
Fuel Element Length	[cm]	0.0381
Clad Thickness	[cm]	N/A
Active Fuel Width (calculated)[1]	[cm]	0.3175
Active Fuel Length	[cm]	1.27
Spacer Thickness	[cm]	0.03
Side Plate Thickness	[cm]	0.02
Side Plate Width	[cm]	0.02
235U per plate	[g]	0.30
Enrichment wt % 235U		2%
U wt % in Fuel Composition		10%

---

[1] Tolerance applied is one-half the difference between plate width and active fuel width.

6.3   Criticality Model Specifications

This section describes the models that are used in the criticality analyses for the NAC-LWT cask. The models presented are for cask loadings of one PWR assembly, two BWR assemblies, up to 42 HEU, MEU or LEU, MTR elements, up to 42 HEU, MEU or LEU DIDO assemblies, up to 140 TRIGA fuel elements, up to 560 TRIGA fuel cluster rods, two General Atomics Irradiated Fuel Material packages, 25 intact PWR or BWR rods in a rod holder or fuel assembly lattice, 25 PWR or BWR fuel rods with up to 14 of the fuel rods classified as damaged in a fuel rod holder, up to 700 PULSTAR fuel elements, up to 42 spiral fuel assemblies, or up to 42 MOATA plate bundles. The models are analyzed separately under normal operations and hypothetical accident conditions to ensure that all possible configurations are subcritical. The metallic fuel rods are not analyzed since this fuel is not enriched and cannot achieve criticality in light water.

6.3.1   PWR Fuel Assemblies

This section describes the methodology and the models used in the criticality analysis of the NAC-LWT cask with the design basis PWR assemblies. The methodology uses a 27 group neutron cross section library (27GROUPNDF4) and KENO-Va to determine the multiplication factor, k_{eff}, of the system. The models presented utilize configurations of the various PWR assemblies in the basket and the NAC-LWT cask.

The calculational methodology is the SCALE, CSAS25 criticality analysis sequence (Petrie). This sequence includes a material information processor (Landers), cross section and resonance treatment processing with the NITAWL code (Greene) and KENO-Va (Petrie) criticality analysis. The material information processor in the SCALE package calculates nuclide number densities for standard and non-standard compositions. The NITAWL code prepares a working library and performs resonance treatments on ^{235}U and ^{238}U. The KENO-Va code is used to model the PWR assemblies, basket and cask body of the NAC-LWT. KENO-Va uses Monte Carlo techniques to track neutrons through the geometry and determine the multiplication factor, k_{eff}, of the system. In these analyses, approximately 300 batches of 1000 neutrons per batch are tracked through the system.

6.3.1.1   Description of Calculational Models

Since it is planned to transport many types of PWR fuel assemblies in the NAC-LWT cask, a determination of the most limiting, i.e., highest k_{eff}, assembly must be made for criticality purposes. KENO-Va models of the assemblies in Table 6.2.1-1 and Table 6.2.1-2 are evaluated to determine the most limiting PWR assembly. This determination was first performed at a uranium enrichment of 3.7 wt % ^{235}U. The assembly with the highest reactivity, not exceeding

0.95 while accounting for bias statistical uncertainties, was then selected as the most limiting assembly for a uranium enrichment of 3.7 wt % ^{235}U. Those assemblies exceeding 0.95 were reexamined at a uranium enrichment of 3.5 wt % ^{235}U. A most limiting assembly was likewise selected for this uranium enrichment. The KENO-Va models developed to select the most limiting assemblies incorporate a single PWR fuel assembly in the fuel basket and the NAC-LWT cask as shown in Figure 6.3.1-1 and Figure 6.3.1-2. These KENO-Va models incorporate water at 1 gm/cc modeled between the fuel rods, in the basket holes surrounding the assemblies, in the neutron shield, and in the cask exterior. An active fuel length of 12 ft was utilized in constructing the KENO-Va PWR assembly models. The ends were reflected with water for the most reactive assembly analysis and with actual cask materials for the NCT and HAC moderator studies. The assemblies, the aluminum PWR basket, and the cask with radial shield regions are explicitly represented. There are no homogenizations of fuel, moderator or basket. In addition, water albedo boundary conditions were utilized as the boundary conditions for the cask exterior. The most limiting assembly analysis was performed with both a dry and a wet fuel pellet to clad gap.

The most limiting assembly models were analyzed to determine their most reactive configurations due to geometrical tolerances and mechanical perturbations. The models were analyzed under accident conditions with water at 1 gm/cc modeled between the fuel rods, in the basket holes surrounding the assemblies, in the neutron shield, and in the cask exterior. The most reactive configuration analysis incorporates the more reactive of the wet or dry gap configurations.

As shown in Section 6.4.1, the most limiting PWR fuel assemblies for 3.7 and 3.5 wt % ^{235}U enrichments were determined to be the Exxon ANF 15×15 and the Westinghouse 17×17 OFA fuel assemblies, respectively. The most reactive configurations are the nominal configuration for the Exxon ANF 15×15 assembly and the maximum basket opening for the Westinghouse 17×17 OFA assembly. The material properties used in the model are shown in Table 6.3.1-1.

These KENO-Va models of the most limiting assemblies in their most reactive configurations were then analyzed to determine the effects moderator variations in the cavity and outside the cask under normal conditions and inside the neutron shield tank under accident conditions. The k_{eff} results for single casks loaded with the most limiting design basis PWR assemblies for both 3.5 and 3.7 wt % ^{235}U are always below 0.95 including all biases and uncertainties.

6.3.1.2   Package Regional Densities

The composition densities (gm/cc) and nuclide number densities (atm/b-cm) calculated by the material information processor and used in the subsequent criticality analyses are shown in Table 6.3.1-1.

Figure 6.3.1-1   KENO-Va Model of the NAC-LWT Cask Model with PWR Basket and
15×15 PWR Assembly

(Dimensions in centimeters)
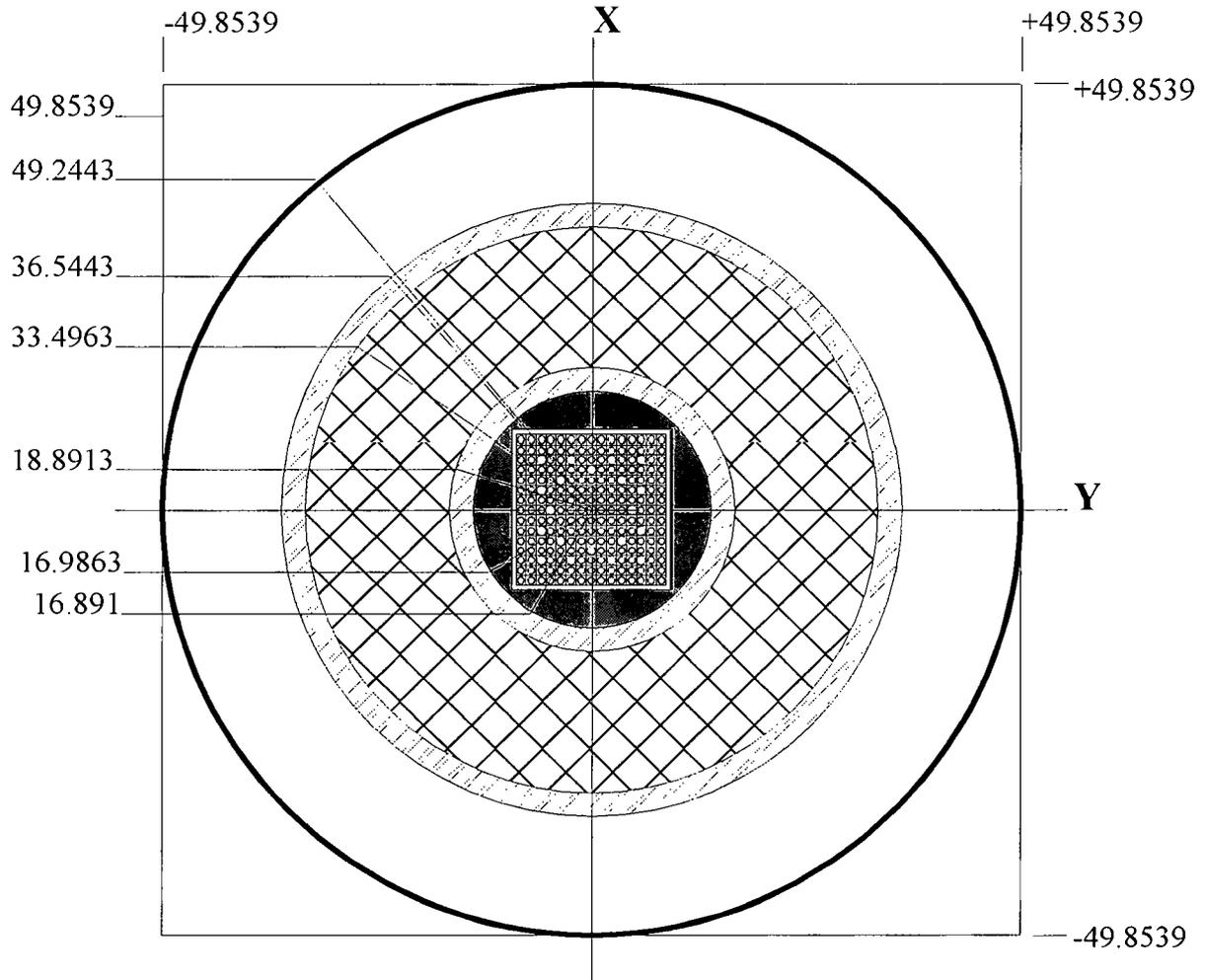
WATER   LEAD

STEEL   ALUMINUM

Figure 6.3.1-2   KENO-Va Model of the NAC-LWT Cask with PWR Basket and
                   Westinghouse 17×17 OFA Assembly

(Dimensions in centimeters)

☐ WATER   ☒ LEAD

▨ STEEL   ▢ ALUMINUM
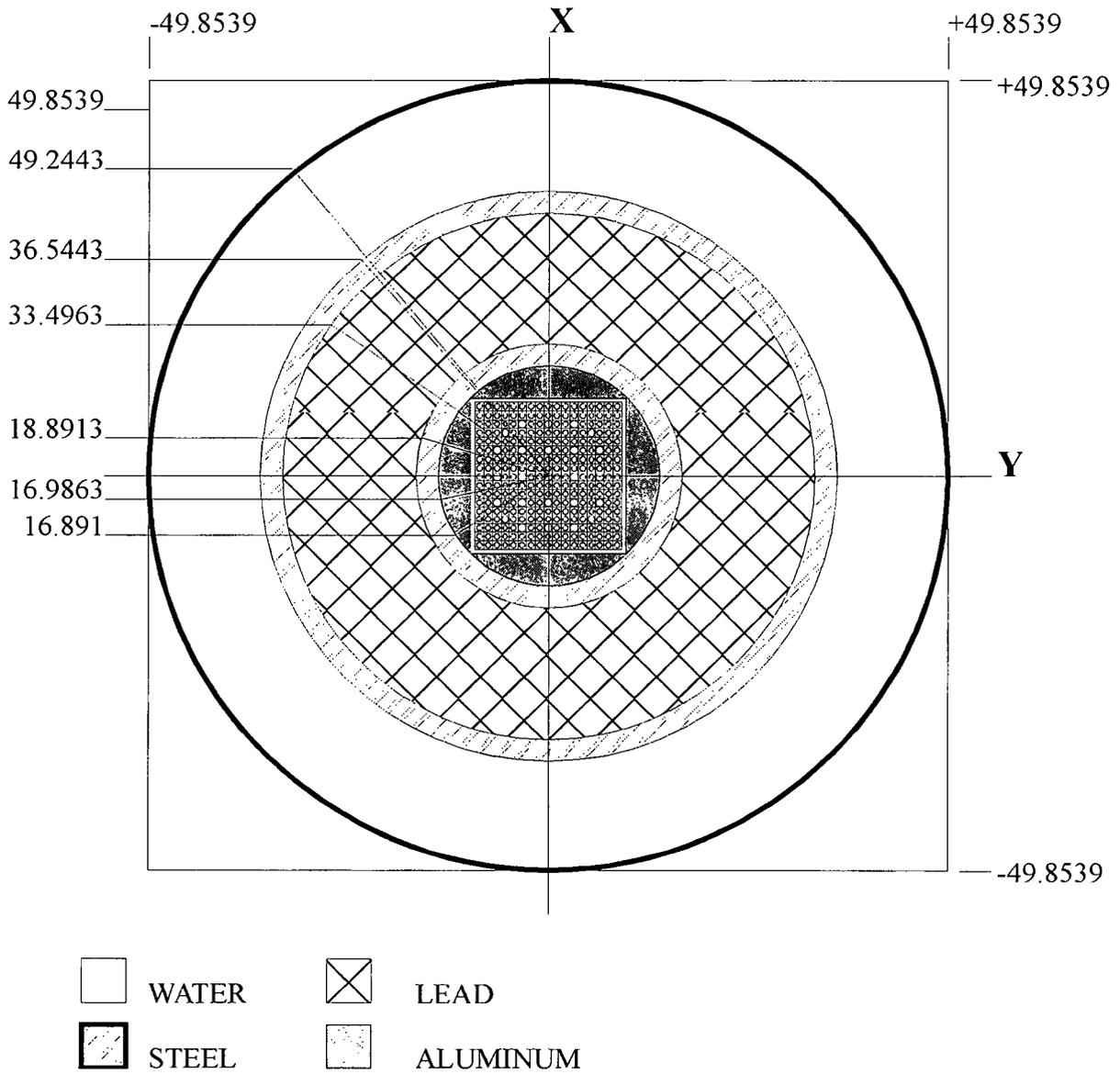
Table 6.3.1-1   Compositions and Number Densities Used in the Criticality Analysis of PWR Fuel Assemblies

Material	3.7% Enriched UO2	3.5% Enriched UO2	Zr	H2O	304 Stainless Steel	Pb	Al
Density, gm/cc	10.412	10.412	6.49	0.998	7.920	11.344	2.702
Nuclide	atm/b-cm						
^{235}U	8.701E-4	8.231E-4					
^{238}U	2.236E-2	2.241E-2					
Oxygen	4.646E-2	4.646E-2		3.338E-2			
Hydrogen				6.677E-2			
Zirconium			4.285E-2				
Iron					5.936E-2		
Chromium					1.743E-2		
Nickel					7.721E-3		
Manganese					1.736E-3		
Lead						3.297E-2	
Aluminum							6.031E-2

6.3.2   BWR Fuel Assemblies

This section describes the methodology and the models used in the criticality analysis of the NAC-LWT cask with the design basis BWR assemblies. The methodology uses a 27 group neutron cross section library (27GROUPNDF4) and KENO-Va to determine the multiplication factor, k_{eff}, of the system. The models presented utilize configurations of the various BWR assemblies in the basket and the NAC-LWT cask.

The calculation methodology is the SCALE, CSAS25 criticality analysis sequence (Petrie, June 1990). This sequence includes a material information processor (Landers), cross section and resonance treatment processing with the NITAWL code (Greene) and KENO-Va (Petrie, August 1990) criticality analysis. The material information processor in the SCALE package calculates nuclide number densities for standard and non-standard compositions. The NITAWL code prepares a working library and performs resonance treatments on ^{235}U and ^{238}U. The KENO-Va code is used to model the BWR assemblies, basket and cask body of the NAC-LWT. KENO-Va uses the Monte Carlo technique to track neutrons through the geometry and determine the multiplication factor, k_{eff}, of the system. In these analyses, approximately 300 batches of 1000 neutrons per batch are tracked through the system.

6.3.2.1   Description of Calculational Models

Since it is planned to transport different BWR assemblies in the NAC-LWT cask, a determination of the most limiting, i.e., higher k_{eff}, assembly must be made for criticality purposes. KENO-Va models of the assemblies in Table 6.2.2-1 and Table 6.2.2-2 are evaluated to determine the most limiting assembly. The KENO-Va models incorporate a mid-fuel slice of two identical BWR assemblies in the BWR basket and the NAC-LWT cask as shown in Figure 6.3.2-1. The most limiting assembly analysis is performed for accident conditions with water at 1 gm/cc modeled between the fuel rods and in the basket holes surrounding the assemblies. In addition, the neutron shield and cask exterior contain no water. The analysis is performed with these conditions with a dry and a wet clad gap. Reflecting boundary conditions are imposed on the sides, top and bottom of the KENO-Va CUBOID containing the loaded cask simulating an infinite array with no axial leakage. This produces the k_{eff} of an infinite array of BWR assemblies in the basket and cask. The most limiting assembly is the model that produces the highest k_{eff}. The most limiting assembly model is analyzed to determine its most reactive configuration due to geometric tolerances and mechanical perturbations. The model is analyzed for accident conditions with water at 1 gm/cc modeled between the fuel rods and in the basket holes surrounding the assemblies. In addition, the neutron shield and cask exterior contain no water. The most reactive configuration analysis incorporates the more reactive of the wet or dry gap configurations. The material properties used in the model are shown in Table 6.2.3-1.

A finite array KENO-Va model of the NAC-LWT cask with the design basis BWR fuel is developed from the KENO-Va model of the most limiting assembly in the most reactive configuration. As shown in Section 6.4.2, the Exxon 9×9 assembly with two water rods and an 80 mil channel (Ex 9×9-2/80) is the most limiting assembly and the nominal configuration is the most reactive configuration for the NAC-LWT cask with the two assembly BWR basket design. In the finite array model, the fuel assemblies, aluminum BWR basket, and the cask with radial shield regions are explicitly modeled. Twenty casks are placed on a triangular pitch in a KENO-Va region using the HOLE instruction. Finally, a CUBOID surrounds the array of casks. The KENO-Va model has an axial extent of ± 10 cm, but with reflecting boundary conditions imposed on top and bottom, the model is effectively infinite in axial extent. The water moderator is allowed to vary in the cavity and outside the cask under normal conditions and is allowed to vary inside the neutron shield tank under accident conditions. Cask center-to-center spacing is varied by adjusting the HOLE positions of the casks. The optimally moderated, most reactive configuration is then evaluated without the assembly channel to verify subcriticality in this arrangement. The k_{eff} results of this finite array model are always below 0.95, including all biases and uncertainties.

6.3.2.2   Package Regional Densities

The composition densities (gm/cc) and nuclide number densities (atm/b-cm) calculated by the material information processor and used in the subsequent criticality analyses are shown in Table 6.3.2-1.

Figure 6.3.2-1   KENO-Va Model of the NAC-LWT Cask Model with BWR Basket and 2
Exxon 9×9-2/80 Assemblies

(Dimensions in centimeters)
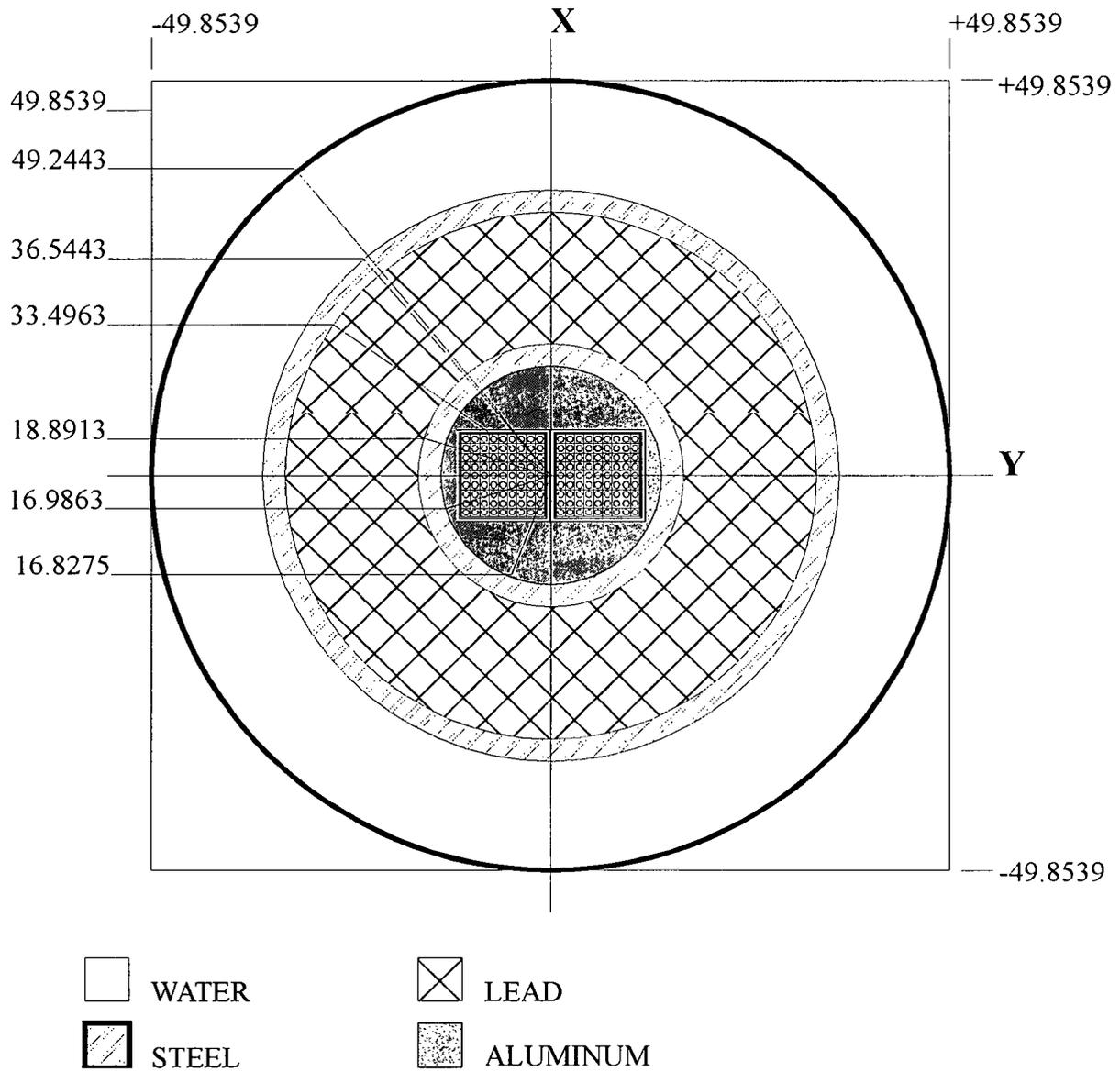
Table 6.3.2-1   Compositions and Number Densities Used in the Criticality Analysis of BWR Fuel Assemblies

Material	4.0% Enriched UO2	Zircaloy	H2O	304 Stainless Steel	Pb	Al
Density, gm/cc	10.412	6.56	0.9982	7.920	11.344	2.702
Nuclide	atm/b-cm					
^{235}U	9.406E-4					
^{238}U	2.229E-2					
Oxygen	4.646E-2		3.338E-2			
Hydrogen			6.677E-2			
Zircaloy		4.331E-2				
Iron				5.936E-2		
Chromium				1.743E-2		
Nickel				7.721E-3		
Manganese				1.736E-3		
Lead					3.297E-2	
Aluminum						6.031E-2

6.3.3   MTR Fuel Elements

6.3.3.1   Description of Calculational Models

Since it is planned to transport many types of MTR fuel elements in the NAC-LWT, a determination of the most limiting, i.e., higher k_{eff}, element must be made for criticality purposes. Primary candidates for the most limiting element from the MTR elements in Table 6.2.3-1 through Table 6.2.3-3 are selected for analysis. Limiting elements are primarily selected based on fissile material content. After establishing trends in reactivity versus the elements' physical characteristics, bounding element characteristics are defined.

Evaluations are performed with three distinct fuel element models. First stage evaluations compare reactivities between intact fuel element types in an infinite array of basket unit cells. The second phase of the evaluations employs a basket model representing a cross section of the cask at infinite height and is used to establish maximum reactivity basket configurations and moderator densities. Finally, the limiting fuel element parameters are defined by a three-dimensional cask model containing six baskets.

In the KENO-Va fuel/basket unit cell analysis, a unit cell of the fuel element and the basket is modeled. This includes the fuel element in a 3.44" × 3.44" (8.738 cm x 8.738 cm) opening surrounded by a 5/16" (0.7938 cm) web. Water at 1 gm/cc is modeled between the fuel plates and in the basket hole surrounding the fuel element as shown in Figure 6.3.3-1. Reflecting boundary conditions are imposed on the sides, top and bottom simulating an infinite array with no axial leakage. This produces the k_{eff} of an infinite array of fuel elements and basket cells without modeling the entire basket and cask.

The KENO-Va model of the NAC-LWT cask with the design basis MTR fuel is derived from a radial slice of the NAC-LWT at the active fuel region as shown in Figure 6.3.3-2. As described in Section 6.4.3.1, the HFBR fuel element is selected as the most limiting assembly for the seven element basket design. The KENO-Va model has an axial extent of ± 10 cm, but with reflecting boundary conditions imposed on top and bottom, the model is effectively infinite in axial extent. The fuel elements, steel basket and cask with radial shield regions are explicitly represented. There are no homogenizations of fuel, moderator or basket. A CUBOID surrounds the casks with reflecting boundary conditions imposed on the sides, top and bottom simulating an infinite array of infinite axial extent. Moderator (H_2O) is allowed to vary in the cavity and outside the cask under normal conditions and, also, is allowed to vary inside the neutron shield tank under accident conditions. Cask center-to-center spacing is varied by adjusting the X-Y spacing of the CUBOID surrounding the cask. The k_{eff} results of this infinite array model are always below 0.95 including all biases and uncertainties. Because the integrity of MTR fuel is not assured, the

fuel plates of an element may assume a more optimum configuration during accident conditions. Therefore, KENO-Va models of the NAC-LWT cask with MTR element plates optimally spaced within the limits of the basket opening are analyzed to verify that the HFBR element is the most limiting MTR element.

The full cask models are identical in cross section to the axially infinite cask models, but rather than axially reflecting an active fuel elevation section of a basket module, six basket modules are stacked into an array. The module chosen for stacking is the intermediate basket module. While axial extents differ from the bottom and top modules, the basket horizontal cross section is identical in all modules. Axial variations are associated with the stacking of the units, with all units containing the 0.5-inch thick base plate.

Figure 6.3.3-3 displays a side view of the intermediate module, with Figure 6.3.3-4 showing this basket module stacked six high inside the NAC-LWT. The cask bottom weldment and lid enclose the basket module array with its associated radial shielding. Reflecting boundary conditions on all sides simulate an infinite array of casks. This model neglects the impact limiters that would provide additional spacing between casks, and models the cask under accident conditions with the neutron shield voided.

As discussed in Section 6.4.3.10, the accident, optimum plate pitch configuration bounds the configuration of loose plates in the MTR plate canister. Therefore, no separate models are constructed for the loose plate evaluation.

For high fissile material payloads, the MTR basket may require partial loading. Figure 6.3.3-5 contains a basket layout with each potential loading position numbered to correlate the analysis in Section 6.4.3 to allowed loading locations. The model construction for partially loaded baskets is identical to that of the fully loaded basket with the exception of cask interior moderator material being assigned to the basket opening rather than an array of fuel plates and the side plates. The basket opening not occupied by a fuel element may be blocked to physically prevent loading of an element. The spacer consists of an aluminum tube, evaluated at an outer diameter of 3.25 inches and a 1/8-inch thickness, with a rectangular aluminum top plate. For baskets containing multiple fuel types, the SCALE material information processor input DAN and RES variables are provided for the fuel material not included in the LATTICECELL description. The Dancoff factors are extracted from LATTICECELL calculations of the single fuel type runs.

6.3.3.2   Package Regional Densities

The composition densities (gm/cc) and nuclide number densities (atm/b-cm) calculated by the SCALE material information processor for a range of elements evaluated in subsequent criticality analyses are shown in Table 6.3.3-1. Additional material densities may be obtained from the sample input/output files provided in Section 6.6.

Figure 6.3.3-1   KENO-Va Fuel/Basket Unit Cell Model for MTR Fuel

(Dimensions in Centimeters)
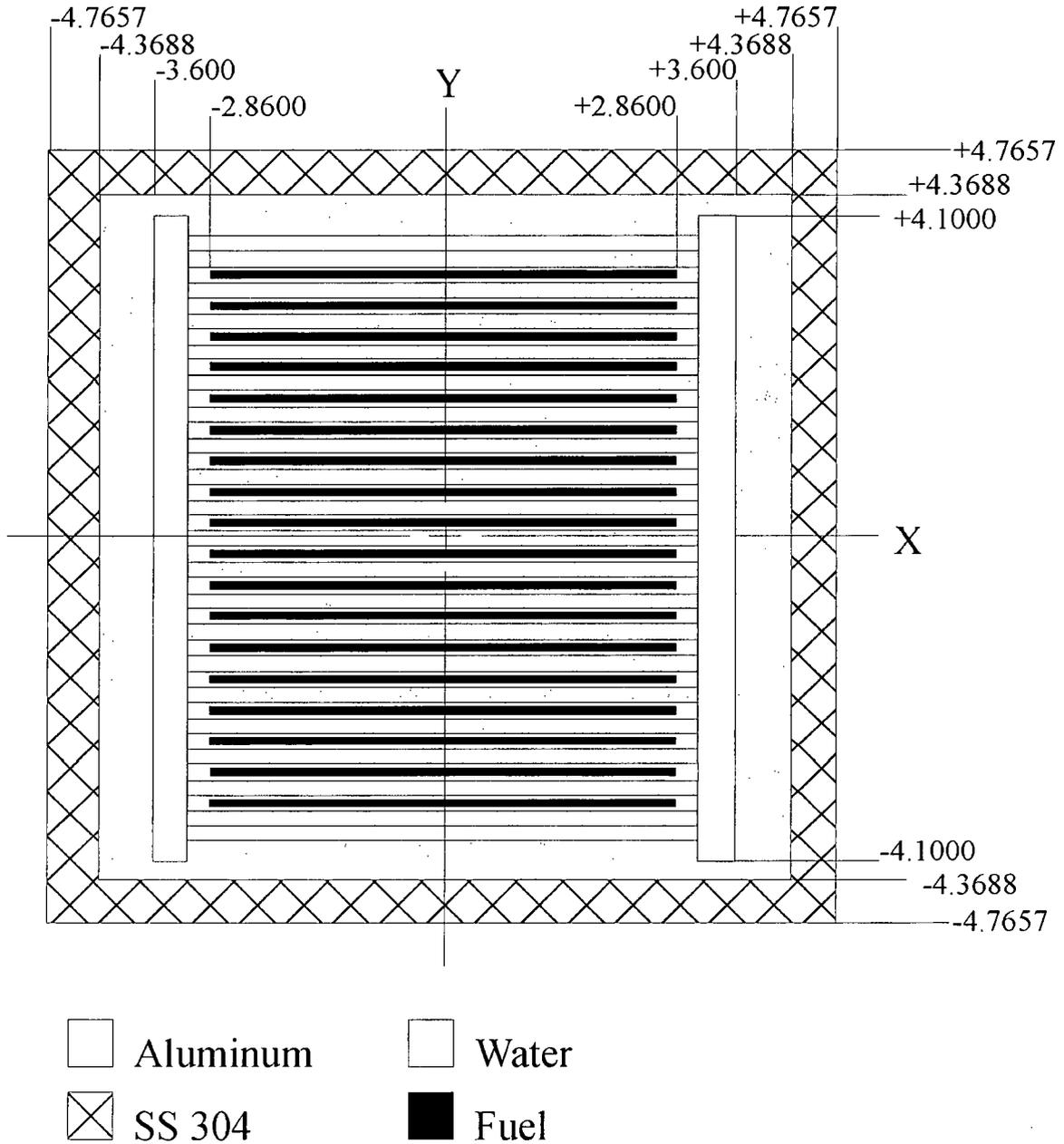
Figure 6.3.3-2   KENO-Va Model of NAC-LWT Cask with MTR Fuel
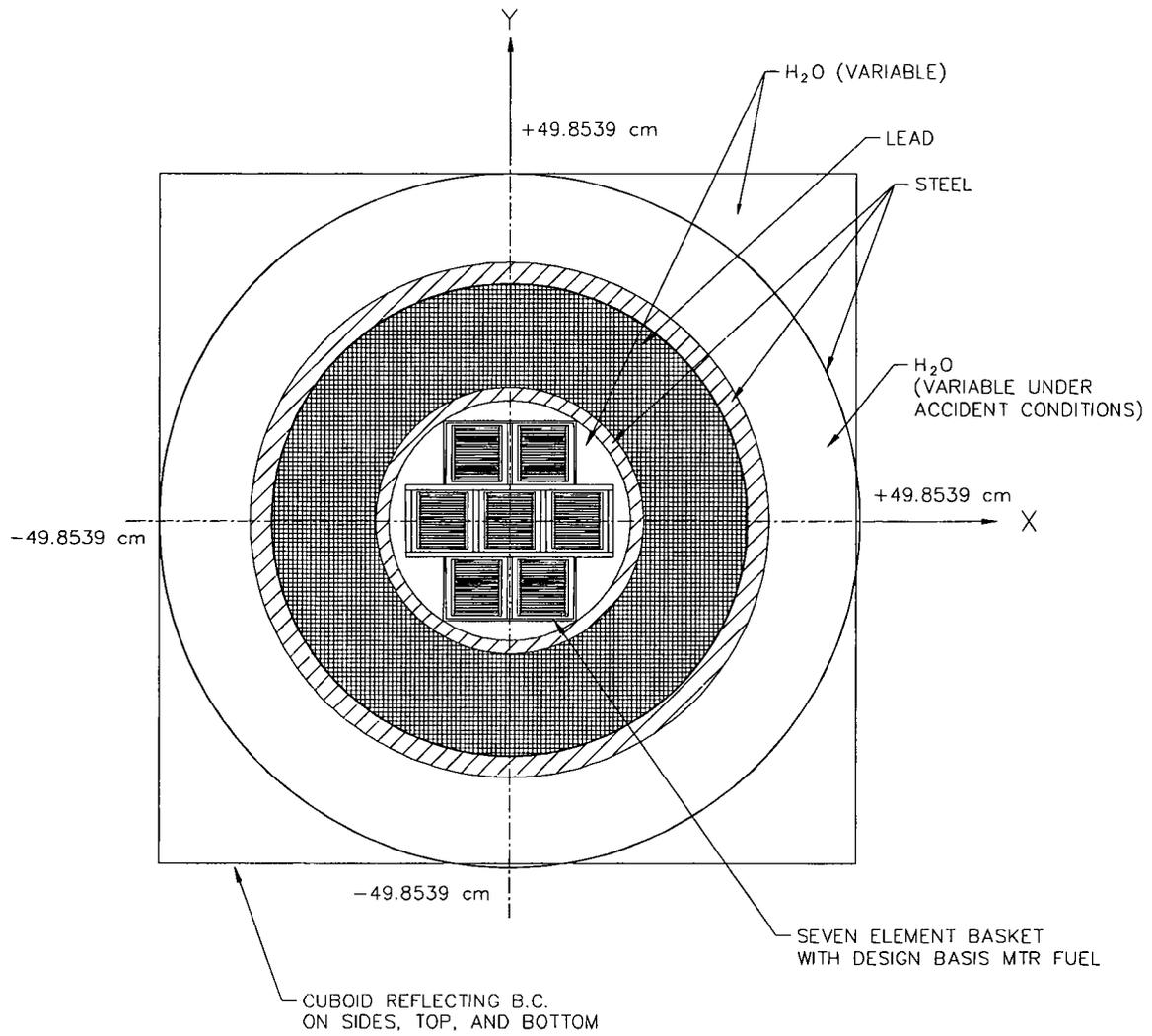
Figure 6.3.3-3   Intermediate MTR 42 Basket Module
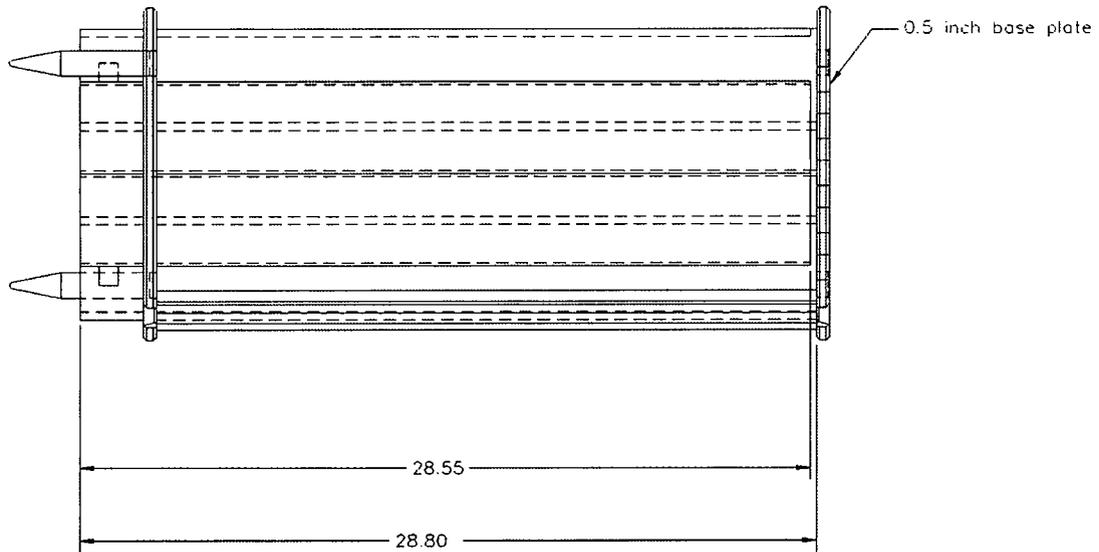
Figure 6.3.3-4   Full Length NAC-LWT Cask Model with 42 MTR Fuel Elements
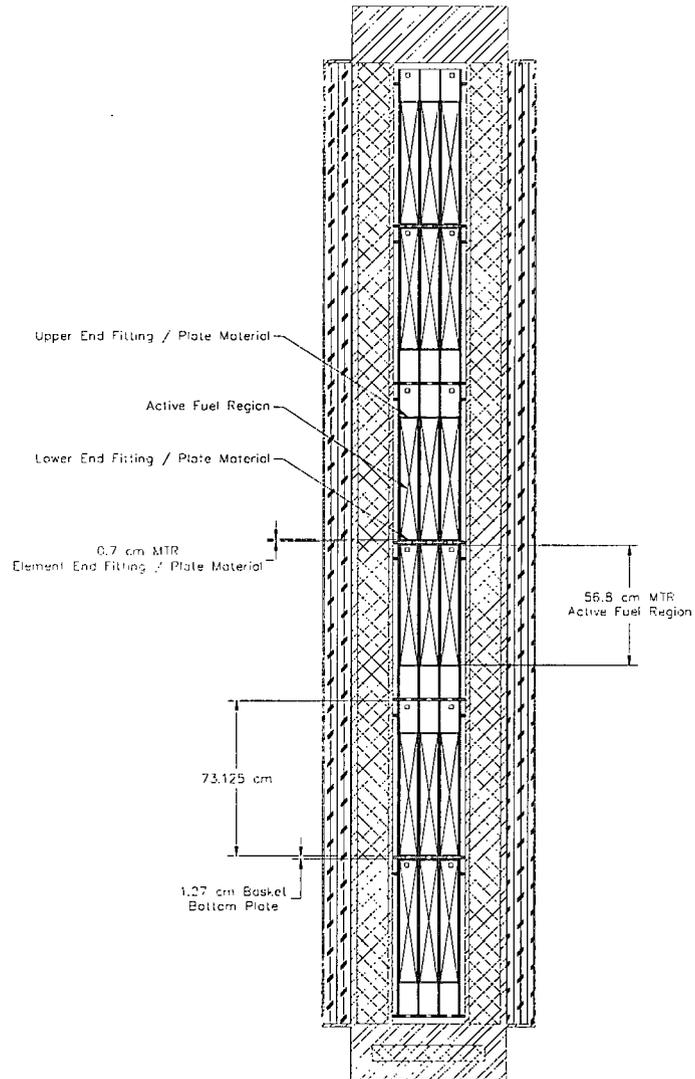
Figure 6.3.3-5   MTR Fuel Basket Module Loading Pattern
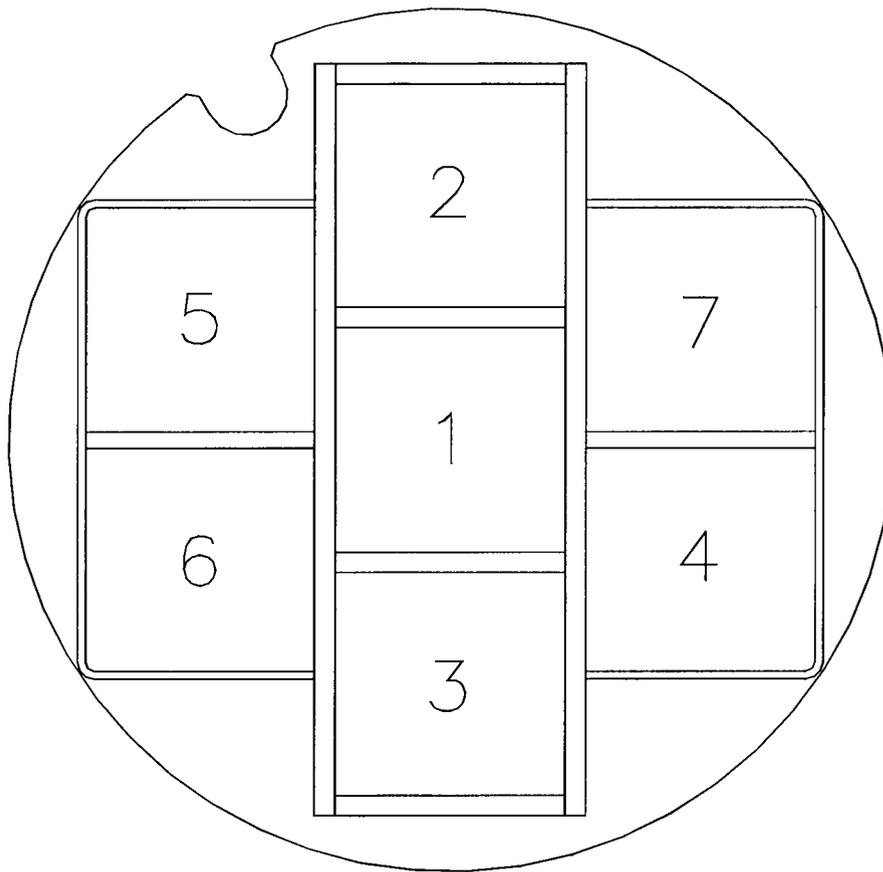
Table 6.3.3-1   Composition Densities Used in Criticality Analysis of MTR Fuel

Material	HFBR U3O8-Al	ORR U3O8-Al	GRR U-Al	IEA-R1 U-Al	THOR HEU UAl	THOR LEU U-Al	RSG-GAS U3O8-Al	BSR U3Si2	ZPRL U-Al
Density, gm/cc	3.99	3.32	2.90	4.10	2.90	4.10	4.80	5.01	4.10
Nuclide	atm/b-cm								
Uranium 235	2.852-3	1.978-3	1.382-3	8.493E-4	5.683E-4	8.542E-4	1.366E-3	2.358E-3	8.542E-4
Uranium 238	2.120-4	1.470-4	1.027-4	3.354E-3	4.12E-5	3.373E-3	5.480E-3	9.460E-3	3.373E-3
Silicon								7.505E-3	
Aluminum	5.630-2	5.222-2	5.178-2	5.502E-2	5.950E-2	5.499E-2	3.713E-2		5.499E-2
Oxygen	8.142-3	5.662-3					1.826E-2		

Material	RSG-GAS Clad	Al Clad	H2O	304 Stainless Steel	Pb	ASTRA[1] UAlx-A	MEUG UAlx-A 35 wt %	CNEA U-Al	PRR U-Al
Density, gm/cc	2.7	2.699	0.998	7.920	11.350	1.57	2.08	2.76	3.03
Nuclide	atm/b-cm								
Uranium 235						1.786E-3	1.862E-3	1.320E-3	9.113E-4
Uranium 238						2.205E-3	3.415E-3	1.289E-4	5.743E-5
Magnesium	9.916E-4								
Aluminum	5.892E-2	6.024E-2				5.303E-2	5.303E-2	4.900E-2	5.911E-2
Oxygen			6.675E-2						
Hydrogen			3.338E-2						
Iron				5.936E-2					
Chromium				1.743E-2					
Nickel				7.721E-3					
Manganese				1.736E-3					
Lead					3.299E-2				

[1] Based on 0.053 cm fuel meat width.

6.3.4   PWR and BWR Rods in a Rod Holder or Fuel Assembly Lattice

The NAC-LWT cask may transport up to 25 intact PWR or BWR fuel rods that are in a fuel rod holder or fuel assembly lattice. Up to 14 of 25 PWR or BWR fuel rods in a fuel rod holder may be classified as damaged.

Nonfuel-bearing irradiated guide tubes and water rods may be included in the rod holder. These components displace moderator space between fuel rods and reduce the maximum amount of fissile material in the cask. The model developed in this section, therefore, bounds the inclusion of nonfuel-bearing materials such as guide tubes and water rods in the NAC-LWT rod holder/insert.

6.3.4.1   Intact PWR or BWR Rods in a Rod Holder or Fuel Assembly Lattice

This section describes the methodology and the models used in the criticality analysis of the NAC-LWT with 25 design basis PWR or BWR rods in a rod holder or fuel assembly lattice. The methodology uses the CSAS25 criticality sequence from the SCALE 4.3 computer code package with the 27-group END/B-IV cross-section set. CSAS25 is the control sequence for the Material Information Processor (MIP), BONAMI, NITAWL-II and KENO-Va computer codes. The Material Information Processor generates number densities and prepares the geometry data for the resonance self shielding calculation. BONAMI and NITAWL-II calculate the resonance corrected cross sections in AMPX working format. KENO-Va uses the Monte Carlo technique to calculate the k_{eff} of a system. In these analyses, approximately 300 batches of 1000 neutrons per batch are tracked through the system.

Description of Calculational Models

The KENO-Va model of the NAC-LWT with 25 intact PWR or BWR fuel rods includes a triangular lattice formation of design basis rods centered in the cask cavity. No credit is taken for geometry control provided by either the rod holder or the fuel assembly lattice. The fuel rods, cask cavity and radial shields are explicitly modeled as shown in Figure 6.3.4-2. The KENO-Va model has two UNITs. UNIT 1 represents a PWR or BWR rod cell. It uses concentric CYLINDERs to model the fuel pellet, clad gap, and the cladding of the fuel rod. UNIT 2 is the GLOBAL UNIT containing CYLINDERs that model the cask, cavity, steel liners, and shields. There are 25 HOLEs placed in the cask cavity with X, Y, and Z coordinates that place rods in a triangular lattice position. The cask outer CYLINDER is surrounded by a CUBOID, and reflecting boundary conditions are imposed on the sides, top and bottom which simulates an infinite array of casks of infinite length. Adjusting the X-Y spacing of the

CUBOID surrounding the cask varies cask center-to-center spacing. The material properties used in the model are shown in Table 6.3.4-1.

To determine the optimum configuration, cask k_{eff} is studied as a function of fuel rod pitch within the cask cavity. This is done by changing the coordinates of the rod HOLEs. Twenty different pitch values that range from the most compact configuration to the most dispersed configuration are evaluated. Figure 6.3.4-1 shows a simplified view of the cask with three different configurations. The analysis is performed for accident conditions with water at 1 gm/cc modeled between the fuel rods, in the cask cavity surrounding the rods. In addition, the neutron shield and cask exterior contain no water. The analysis is performed with these conditions with a dry and a wet clad gap.

An infinite array KENO-Va model of the NAC-LWT cask with 25 PWR or BWR fuel rods at the optimum pitch is used to evaluate the reactivity of the cask. The water moderator is allowed to vary in the cavity and outside the cask under normal conditions and is allowed to vary inside the neutron shield tank under accident conditions. Cask center-to-center spacing is varied by adjusting the dimensions of the CUBOID surrounding the cask. The k_{eff} results of this infinite array model are always below 0.95 including all biases and uncertainties.

Package Regional Densities

The composition densities (gm/cc) and nuclide number densities (atm/b-cm) calculated by the material information processor and used in the subsequent criticality analyses are shown in Table 6.3.4-1.

6.3.4.2   Damaged PWR and BWR Rods in a Rod Holder

This section describes the methodology and the models used in the criticality analysis of the NAC-LWT with 25 PWR or BWR rods, up to 14 of which may be damaged. Although the NAC-LWT payload is limited to 14 damaged fuel rods in a 25-rod shipment, the analysis conservatively considers all 25 rods as failing during transport.

The methodology uses the CSAS25 criticality sequence from the SCALE 4.3 computer code package with the 27-group ENDF/B-IV cross-section set. CSAS25 is the control sequence for the Material Information Processor, BONAMI, NITAWL-II and KENO-Va computer codes. The Material Information Processor generates number densities and prepares the geometry data for the resonance self-shielding calculation. BONAMI and NITAWL-II calculate the resonance corrected cross-sections in AMPX working format. KENO-Va uses the Monte Carlo technique to calculate the k_{eff} of a system. In these analyses, approximately 300 batches of 1,000 neutrons per batch are tracked through the system.

Description of Calculational Models

Two calculational models were employed to evaluate the NAC-LWT system reactivity with damaged fuel rods.

The first model explicitly models unclad UO_2 rods in a triangular pitch. System reactivity is maximized by increasing the number of fuel rods while decreasing the rod diameter to conserve fuel area in the infinite height model (i.e., reflective boundary conditions are placed on the active fuel region). Fuel rod arrays of 25, 37 and 61 rods are considered. The latter two arrays are hexagonal with no lattice vacancies. For each of the three postulated rod arrays, the maximum reactivity pitch is determined for both PWR and BWR rods. System reactivity is determined using an axially infinite cask model in an infinite cask array. In establishing the trend of increasing reactivity with larger rod arrays, k_{eff} values for the explicit rod cases are calculated with full density water in the cask interior, exterior, and neutron shield. Void exterior and void neutron shield (accident) conditions are considered for the 61 rod array in addition to preferential flooding of the cask cavity. The maximum reactivity configuration for 61 rods (with an active fuel cross-sectional area equivalent to 25 intact rods) is shown in Figure 6.3.4-3. Fuel rod arrays with greater than 61 rods are not considered. As demonstrated in Section 0, increasing the number of fuel rods modeled increases the cross-sectional area of the most reactive lattice. The cross-sectional area required for the 61-rod array exceeds the area available in the interior of the rod holder and, therefore, represents a bounding, conservative configuration.

The second model considers a homogenized mixture of UO_2 and water with a square cross-section and finite axial height within the NAC-LWT fuel rod holder. The square cross-sectional area of the rod holder is conservatively based on the exterior width of the rod holder, 13.97 cm. Based on the maximum BWR pellet diameter and fuel length of 150 inches, the finite axial height of the fuel mixture is calculated based on various UO_2 volume fractions. The UO_2 volume fraction is varied until the maximum reactivity is determined. System reactivity is determined using an infinite cask array with a periodic reflection axial boundary condition. Given the limiting UO_2/water fuel material description, water moderation variations are considered in the cask cavity (outside the rod holder), the cask exterior, and the cask neutron shield. The neutron shield material definition is tied to the exterior moderator definition; a void exterior includes a void neutron shield. Thus, the accident condition of loss of neutron shielding is explicitly modeled when the exterior moderator is set to void. Figure 6.3.4-4 and Figure 6.3.4-5 give dimensions of the maximum reactivity homogenized mixture configuration of finite extent.

Package Regional Densities

The composition densities (gm/cc) and nuclide number densities (atm/b-cm) calculated by the material information processor and used in the subsequent criticality analyses are identical to those shown for intact fuel evaluations, Figure 6.3.4-1. Additional material densities may be obtained from the sample input/output file provided in Section 6.6.10.

Figure 6.3.4-1   Triangular Pitch Lattice Formation of 25 PWR Rods
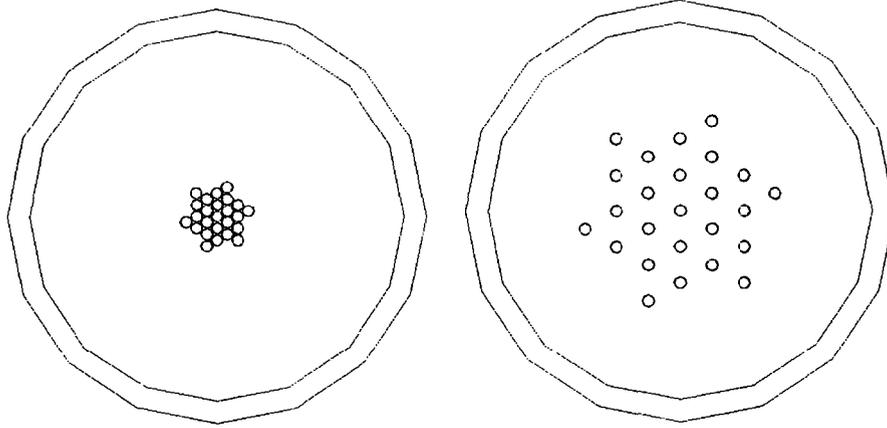
(a) Smallest Pitch   (b) Optimum Pitch
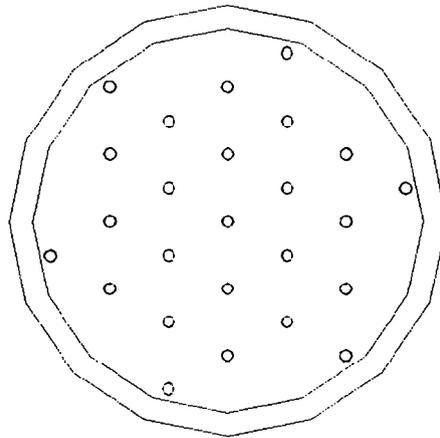
(c) Maximum Pitch

Figure 6.3.4-2   KENO-Va Model of the NAC-LWT Cask with 25 PWR Rods

(Dimensions in centimeters)

☐ WATER

▨ STEEL

☒ LEAD

CUBOID REFLECTING B.C.
ON SIDES, TOP, AND BOTTOM
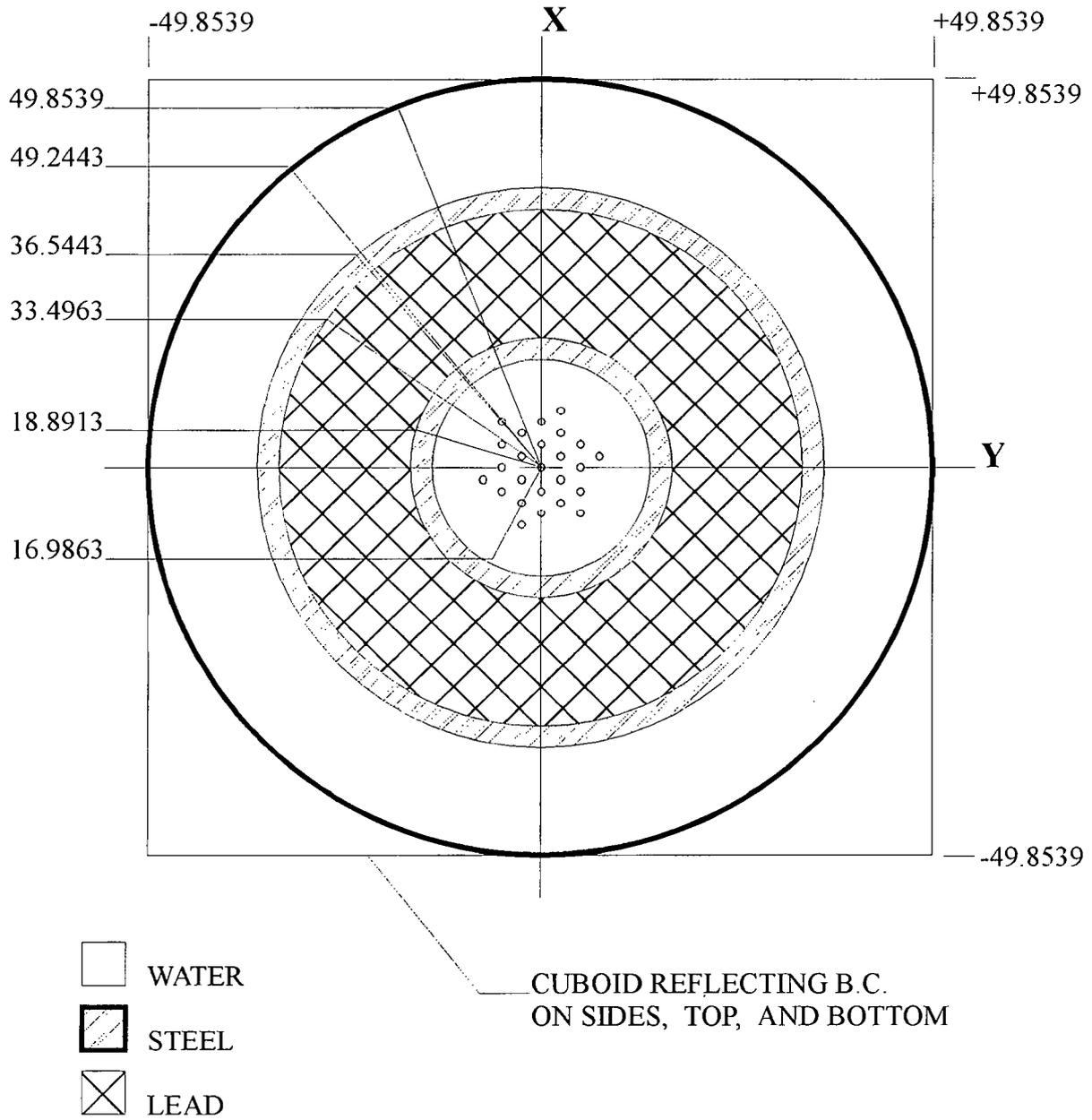
Figure 6.3.4-3   Maximum Reactivity Triangular Pitch Lattice Formation of Damaged Fuel Rods
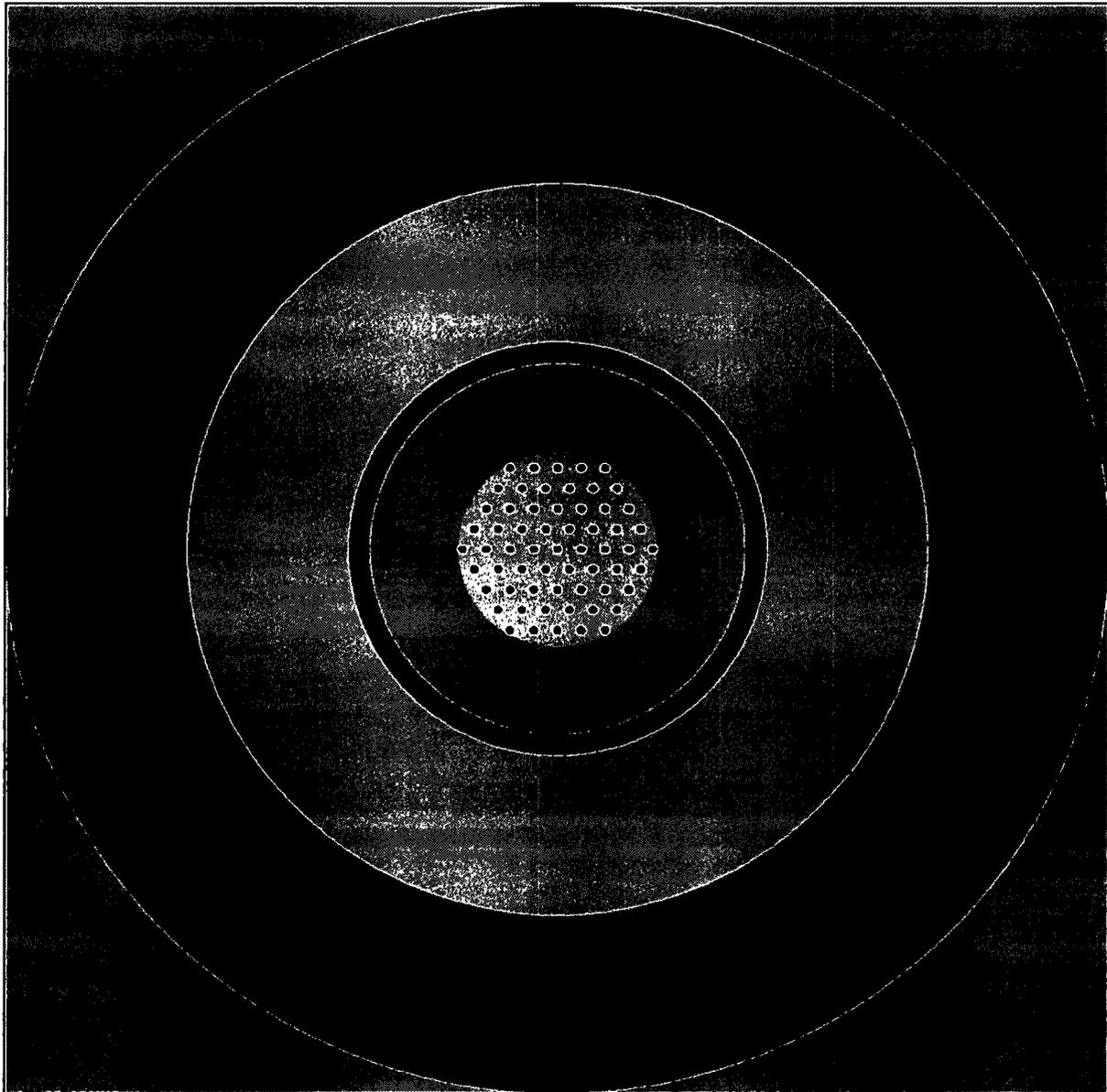
Figure 6.3.4-4   KENO-Va Model of the NAC-LWT Cask with Damaged Fuel Rods –
Radial Detail
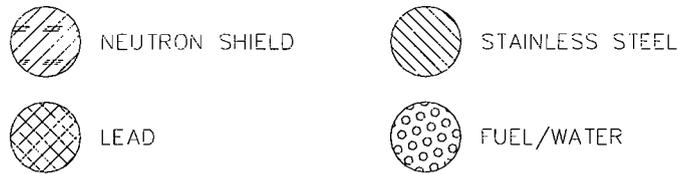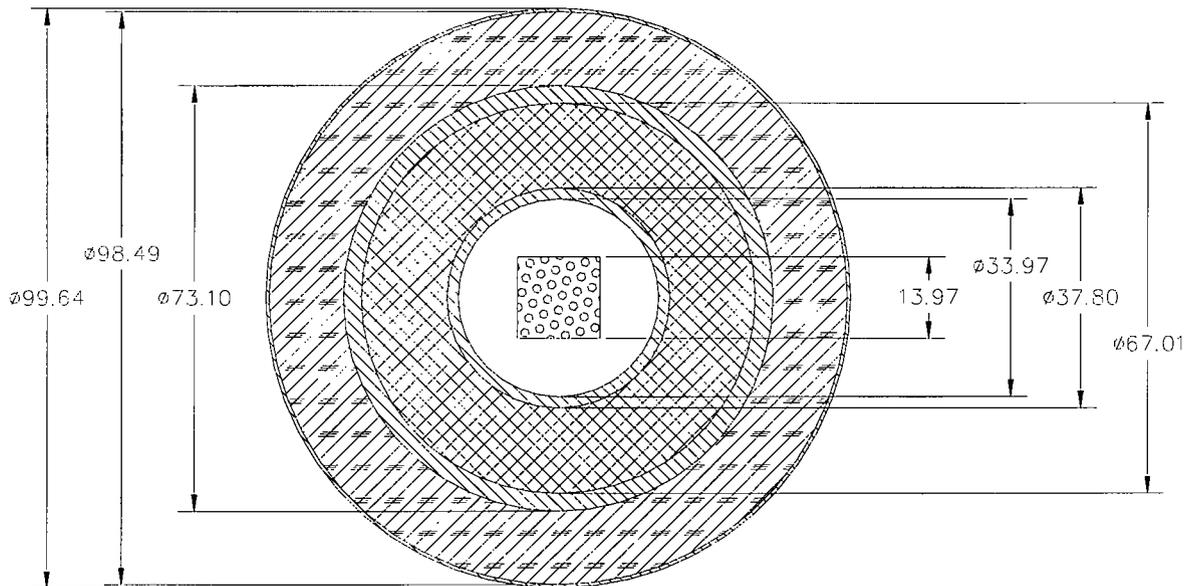
(Dimensions in centimeters)

Figure 6.3.4-5   KENO-Va Model of the NAC-LWT Cask with Damaged Fuel Rods –
Axial Detail

(Dimensions in centimeters)
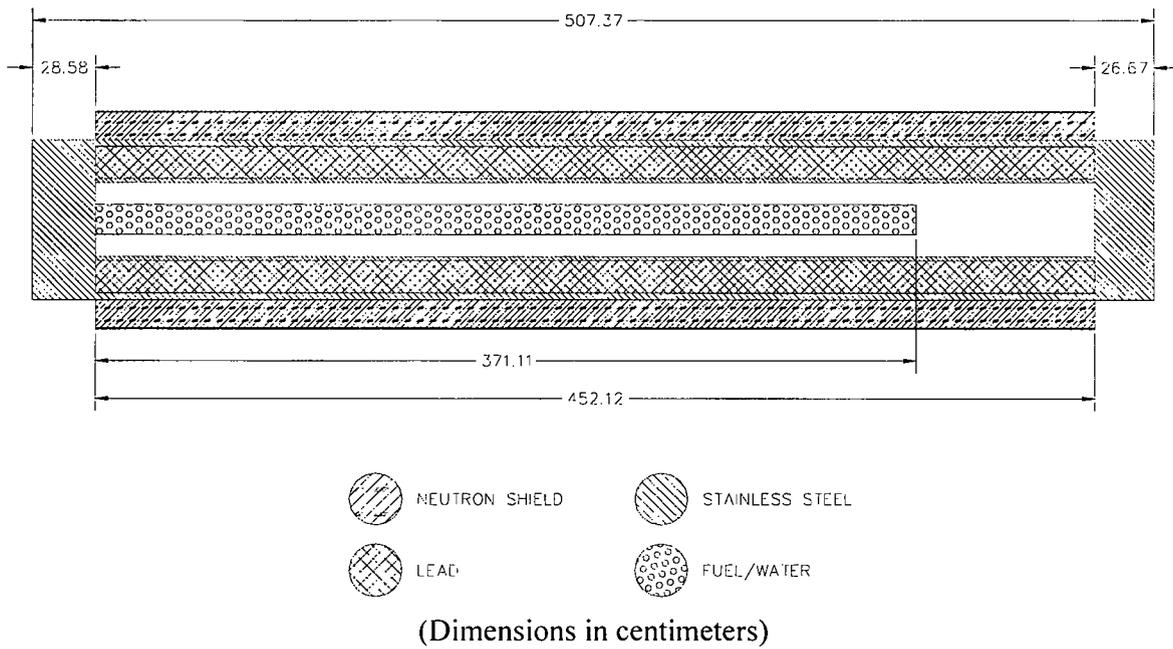
Table 6.3.4-1   Compositions and Number Densities Used in the Criticality Analysis of
PWR and BWR Rods

Material	5.0% Enriched UO2	Zirconium Alloy	H2O	304 Stainless Steel	Pb	Al
Density, gm/cc	10.412	6.56	0.9982	7.920	11.344	2.702
Nuclide	atm/b-cm					
Uranium 235	1.176E-3					
Uranium 238	2.206E-2					
Oxygen	4.647E-2		3.338E-2			
Hydrogen			6.677E-2			
Zirconium Alloy		4.331E-2				
Iron				5.936E-2		
Chromium				1.743E-2		
Nickel				7.721E-3		
Manganese				1.736E-3		
Lead					3.297E-2	
Aluminum						6.031E-2

6.3.5   TRIGA Fuel Elements and Cluster Rods

As previously described, TRIGA fuel elements and fuel cluster rods may be transported in nonpoisoned or poisoned TRIGA basket modules. The following sections detail the analyses performed on these four combinations of design-basis TRIGA fuel types and basket configurations. Nonpoisoned basket designs are analyzed with a maximum of 120 TRIGA fuel elements, or 480 TRIGA fuel cluster rods, while the poisoned basket designs are analyzed with a maximum of 140 TRIGA fuel elements or 560 TRIGA fuel cluster rods.

6.3.5.1   Description of Calculational Models

6.3.5.1.1   TRIGA Fuel Element Methodology

To evaluate the nonpoisoned basket with TRIGA fuel elements, three models are utilized: a fuel/basket unit cell containing four intact TRIGA fuel elements, an axially infinite length cask model and a full cask model. Each of the two NAC-LWT cask models contains up to four TRIGA fuel elements, or screened or sealed cans, in each of the six peripheral TRIGA basket cells. In the case of the axially infinite cask model, a single basket module is surrounded by the cask radial shields and is axially reflected to simulate an infinite length cask. In the case of the full cask model, the NAC-LWT cask is represented with five TRIGA basket modules in the cavity surrounded by the cask radial and axial shields. In this model, the axial shields include an explicit representation of the cask lid and bottom forging. The fuel/basket unit cell model is used to determine the bounding TRIGA fuel element type (Section 6.4.5.1). The cask models are used to determine the maximum k_{eff} of the cask under normal and accident conditions with the bounding fuel element type (Section 6.4.5.2). The infinite length cask model is employed in the criticality evaluation of the intact TRIGA fuel elements in the most reactive basket configuration (Section 6.4.5.3). The full cask model is employed in the criticality evaluation of TRIGA basket modules with failed fuel (top and bottom baskets only) in the NAC-LWT cask under normal and accident conditions (Section 6.4.5.4). A finite cask array is employed in the revised TRIGA fuel element characteristics section (Section 6.4.5.6). The finite cask array model uses the same length cask model developed for the infinite array calculation. However, rather than applying reflective (mirror) boundary conditions to the single cask unit, the cask unit is placed into an 8 (or 4)-cask close-packed configuration.

To evaluate the poisoned basket with TRIGA fuel elements, the non-poisoned axially infinite length cask and full cask models are modified to include the borated stainless steel poison plates. Again, the infinite length cask model is used to evaluate intact TRIGA fuel elements in the most reactive basket configuration (Section 6.4.5.2) and the full cask model is used to evaluate the

basket modules with failed fuel (top and bottom baskets only) in the most reactive basket configuration (Section 6.4.5.3). In the poisoned basket, the central cell, in addition to the six peripheral basket cells, contains intact fuel elements, or (top and bottom baskets only) screened or sealed cans. The bounding TRIGA fuel element type in the non-poisoned basket is verified as the bounding element in the poisoned basket with the axially infinite length cask model.

6.3.5.1.2 TRIGA Fuel Cluster Rod Methodology

To evaluate the nonpoisoned basket with the TRIGA fuel cluster rods, two models are utilized: an axially infinite length cask model and a full cask model. The axially infinite cask model is a single basket module with up to 16 TRIGA fuel cluster rods in a fuel pin handling insert (Figure 6.3.5-1) in the six peripheral basket openings. The single basket module is surrounded by the cask radial shields and is axially reflected to simulate an infinite length cask. The infinite length cask model is employed in the criticality evaluation of the undamaged HEU TRIGA fuel cluster rods at the base material composition in the most reactive basket configuration (Section 6.4.6.1). The full, finite length, cask model used to evaluate the failed (damaged) fuel, contains five TRIGA basket modules in the cavity surrounded by the cask radial and axial shields (Section 6.4.6.2). The three central modules contain intact TRIGA fuel cluster rods in the peripheral openings, and the peripheral openings of the top and bottom modules contain sealed failed fuel cans with up to six rods of TRIGA fuel cluster rod active fuel material. In this model, the axial shields include an explicit representation of the cask lid and bottom forging. The cask models are used to determine the maximum k_{eff} of the cask under normal and accident conditions (Section 6.4.6.3).

To evaluate the poisoned basket with TRIGA fuel cluster rods, the non-poisoned axially infinite length cask and full cask models are modified to include borated stainless steel poison plates. Again, the infinite length cask model is used to evaluate intact TRIGA fuel cluster rods in the most reactive basket configuration (Section 6.4.6.1) and the full cask model is used to evaluate the basket modules with failed fuel (top and bottom baskets only) in the most reactive basket configuration (Section 6.4.6.2). In the poisoned basket, the central cell, in addition to the six peripheral basket cells, contains intact fuel elements, or sealed cans (top and bottom baskets only) with up to six rods of TRIGA fuel cluster rod active fuel material.

The nonpoisoned finite length cask model is also used to evaluate the expanded fuel characteristics for undamaged and damaged HEU fuel cluster rods and the addition of LEU fuel cluster rods (Section 6.4.6.5). For the undamaged fuel configuration, five identical basket modules, with no damaged fuel cans, are located between the cask lid and the bottom forging.

6.3.5.1.3   TRIGA Fuel Element Parametric Study Models

For the parametric evaluation of the most reactive TRIGA fuel element, a unit cell of fuel elements and the basket is modeled for each TRIGA fuel element type (Figure 6.2.5-2). This includes four fuel elements in a 3.44-inch (8.738 cm) square opening surrounded by a 5/16-inch (0.7938 cm) web. The models are evaluated dry and with water at 1 gm/cc in the basket opening.

Reflecting boundary conditions are imposed on the sides, top and bottom simulating an infinite array with no axial leakage. These models were used to determine which of TRIGA fuel element types is most reactive. The most reactive type was then used as the design-basis element in subsequent analyses for normal conditions of transport and hypothetical accident conditions. Combinations of fuel were also analyzed to ensure that fuel enrichment combinations would be bounded by the design-basis loading and enrichment.

6.3.5.1.4   Infinite Axial Length Cask Model

The infinite length models of the NAC-LWT cask with the TRIGA fuel basket are presented in Figure 6.3.5-3 through Figure 6.3.5-5. These models represent TRIGA baskets loaded with up to 24 (nonpoisoned) or 28 (poisoned) TRIGA fuel elements, or 480 (nonpoisoned) or 560 (poisoned) TRIGA fuel cluster rods surrounded by the NAC-LWT radial shields. Since the nonpoisoned TRIGA basket center location is blocked, no fuel elements are present in this location. The models are surrounded by a CUBOID with reflecting boundary conditions imposed on the sides, top and bottom, simulating an infinite array of casks with an infinite axial extent. Water moderator density is allowed to vary in the cavity and outside the cask under normal conditions, and also is allowed to vary inside the neutron shield tank under accident conditions. Cask center-to-center spacing is varied by adjusting the X-Y spacing of the CUBOID surrounding the cask.

6.3.5.1.5   Full (Finite Length) Cask Model

The full cask models are similar to the axially infinite cask models, but rather than axially reflecting single basket modules, five basket module arrays are created (Figure 6.3.5-6). The basket module arrays are enclosed by the modeling of the cask body and the lid. The CUBOID surrounding the cask is surrounded by reflecting boundary conditions on all sides simulating an infinite array of casks. For cask configurations including cans, screened or sealed failed fuel cans are placed into the appropriate openings of the top and bottom basket. The appropriate openings of the three intermediate baskets are filled with uncanned TRIGA fuel elements. Appropriate openings consist of peripheral openings for nonpoisoned baskets and all openings

for poisoned baskets. Moderator variations, including preferential flooding of the screened cans and sealed cans, are evaluated.

6.3.5.1.6   Finite Cask Array Model

The finite cask array model is similar to the infinite array model, but rather than axially and radially reflecting the finite length cask, the KENO-Va HOLE function is used to place a number of casks (either 4 or 8, depending on the configuration evaluated) into a close-packed configuration. The CUBOID surrounding the cask array is reflected by the use of an H_2O reflector card to maximize neutron reflection back into the system.

6.3.5.2   Package Regional Densities

The composition densities (gm/cc) and nuclide number densities (atm/b-cm) calculated by the material information processor and used in the subsequent criticality analyses are shown in Table 6.3.5-1.

Since the SCALE standard composition library does not contain U-ZrH as a standard composition, number densities (atm/barn-cm) were calculated based on dimensional and gram load data from Table 6.2.5-2 (Tomsio). Hydrogen atom densities were calculated based on stoichiometric Zr-H or Zr_5H_8 for the base evaluations. For TRIGA elements in a nonpoisoned basket, variations in ZrH_x composition with a hydrogen-to-zirconium ratio up to the maximum possible (2.0) were evaluated. For TRIGA cluster rods, a stochiometric ratio (H/Zr) of up to 1.7 is evaluated. The homogenized end fitting volume fractions were based on the SCALE default Type 304 stainless steel density and dimensional and gram load data from Table 6.2.5-1. A sample set of TRIGA fuel element number densities used in the criticality analyses is shown in Table 6.3.6-1 and the design basis TRIGA fuel cluster rod number densities are presented in Table 6.3.5-2.

In all criticality models, the fuel elements are explicitly represented. In the case of the TRIGA fuel elements, an explicit 15-inch (38.1 cm) active fuel region of U-ZrH is modeled including 3.42 inches (8.687 cm) of graphite reflector segments above and below the active fuel. TRIGA fuel cluster rods have an active fuel length of 22 inches. All fuel elements are modeled as explicit nested CYLINDERS, but due to their unusual geometry, the TRIGA fuel element end fittings and the spring loaded section of the plenum in the TRIGA fuel cluster rods are modeled as homogenized stainless steel and water. With the exception of the homogenization of fuel debris within the sealed failed fuel cans to represent the worst case damage to the fuel, this is the only homogenization in the geometry.

Figure 6.3.5-1   Fuel Rod Handling Insert for TRIGA Fuel Cluster Rods

(.13)

(.75)

(□ 3.00)

(Nominal Dimensions in Inches)
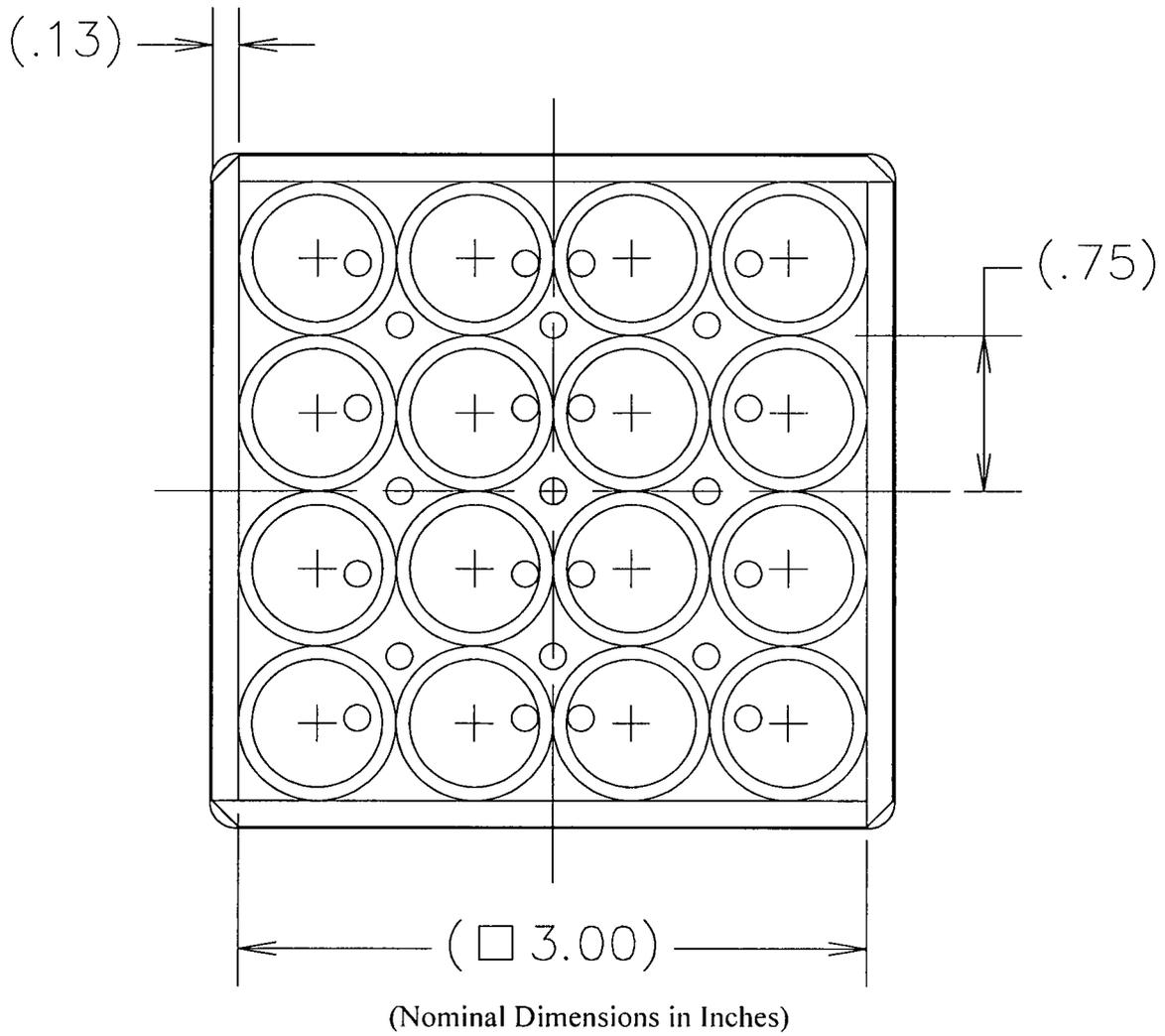
Figure 6.3.5-2　　Fuel/Basket Unit Cell Model for TRIGA Fuel Elements

Four TRIGA Fuel Elements In Opening

1.87706 cm

1.82245 cm

4.7657 cm
4.3688 cm

0.28575 cm

Clad

Zr Rod

UZrH

−4.3688 cm
−4.7657 cm
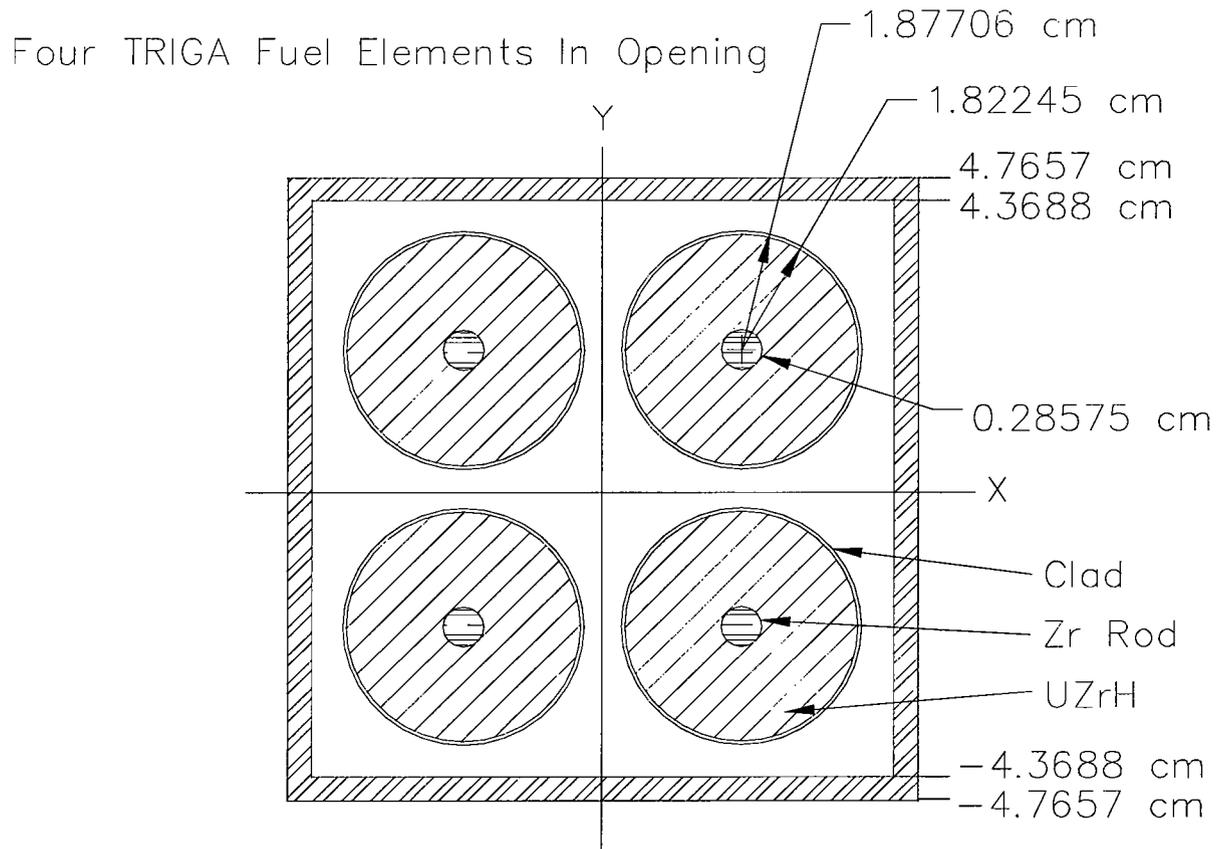
Reflecting Boundary Conditions
on sides top and bottom

Figure 6.3.5-3   NAC-LWT Cask with TRIGA Fuel, Nonpoisoned Basket – Radial View

R49.8221cm   R49.2227cm   R36.5188cm

R33.4645cm
R18.9103cm
R17.1500cm
R17.05cm

Steel

Lead

Liquid Neutron Shield

TRIGA Fuel Elements
Most Reactive
Wet Configuration

TRIGA Fuel Elements
Most Reactive
Dry Configuration

Incoloy 800 Clad Fuel
Nominal Configuration

TRIGA Fuel Cluster Rods
Nominal
Configuration
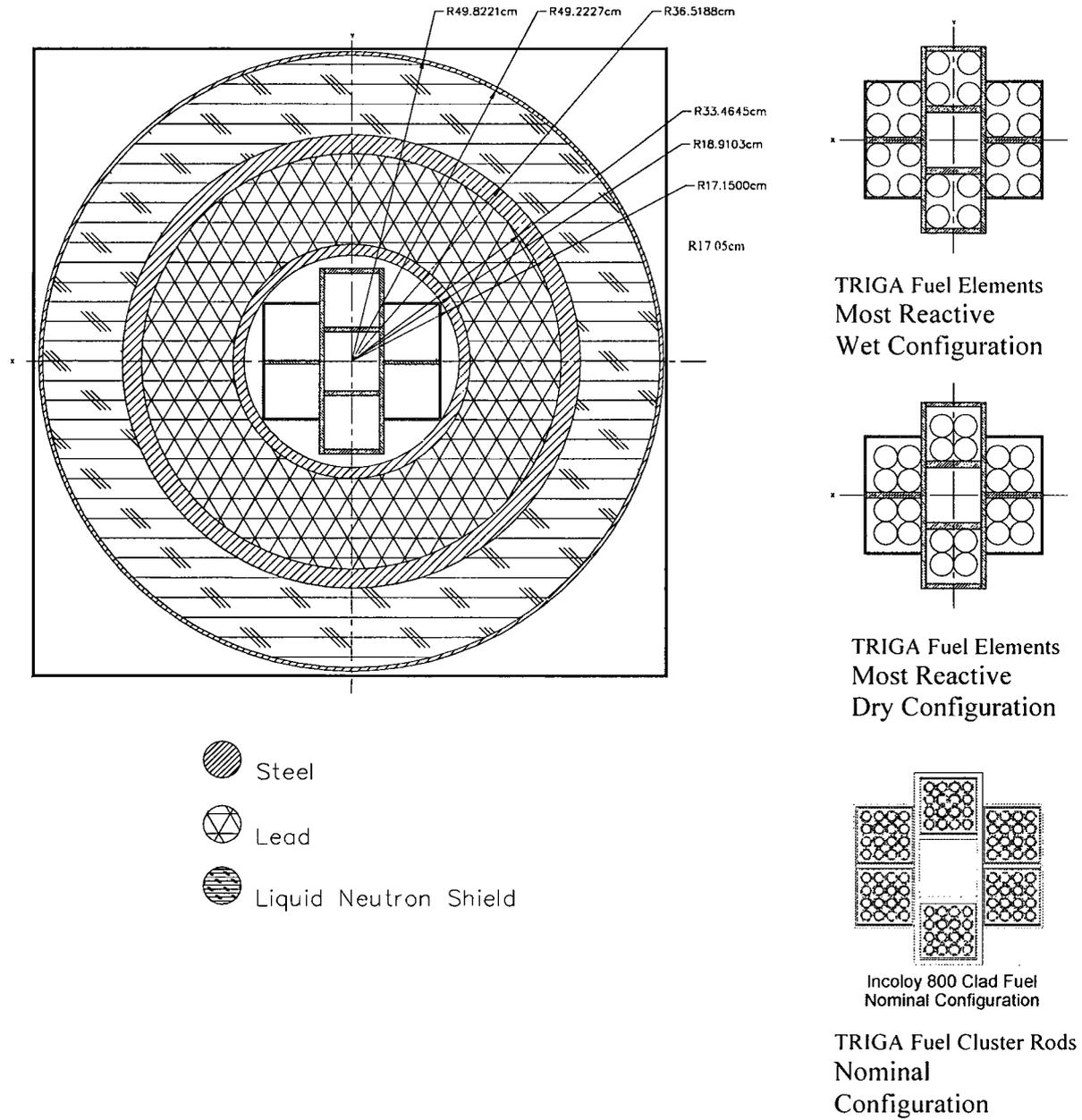
Figure 6.3.5-4   KENO-Va Model of NAC-LWT with Poisoned Basket - Radial View

8.7376 TRIGA Fuel Elements
Most Reactive Dry Configuration

TRIGA Fuel Elements
Most Reactive Wet Configuration

TRIGA Fuel Rods
Nominal Configuration

Steel
Lead
Liquid Neutron Shield
Borated Steel Plate
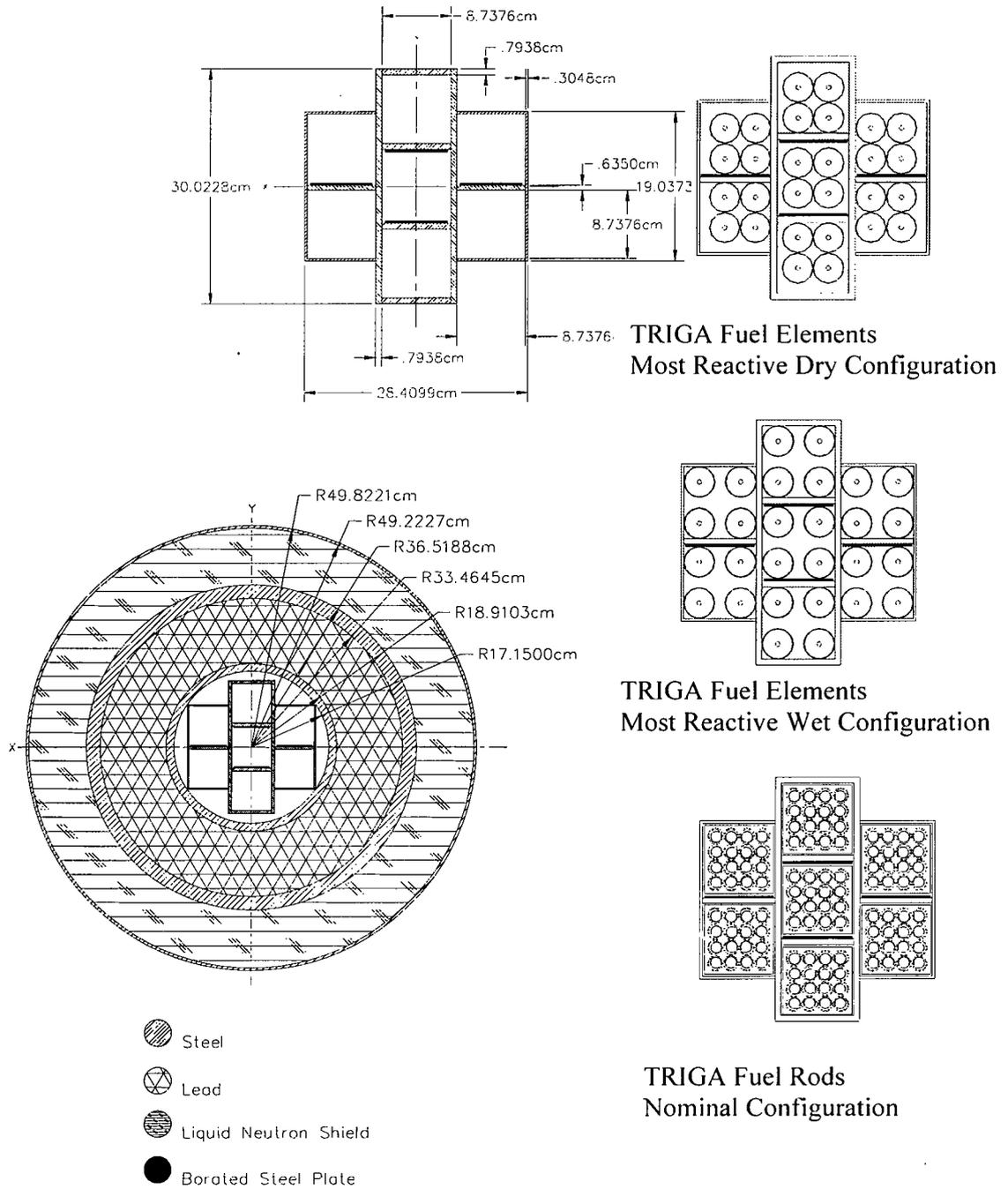
Figure 6.3.5-5   NAC-LWT Cask Model with TRIGA Fuel Elements, Nonpoisoned Basket
– Axial View
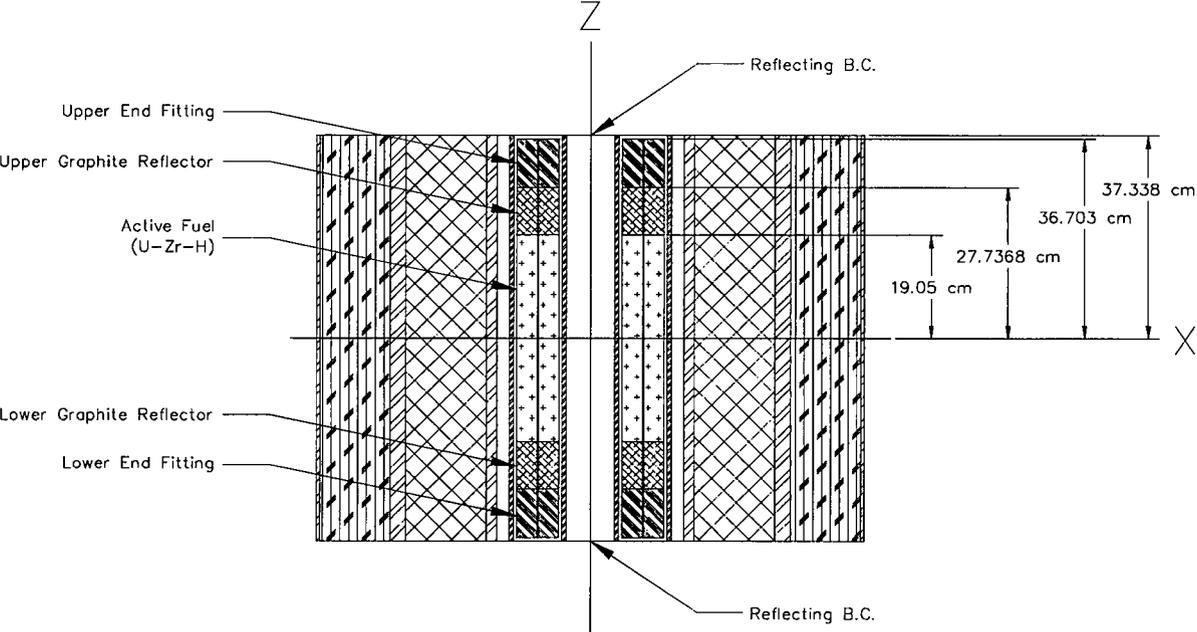
Figure 6.3.5-6   Full-Length NAC-LWT Cask Model with TRIGA Fuel Elements, Nonpoisoned Basket – Axial View
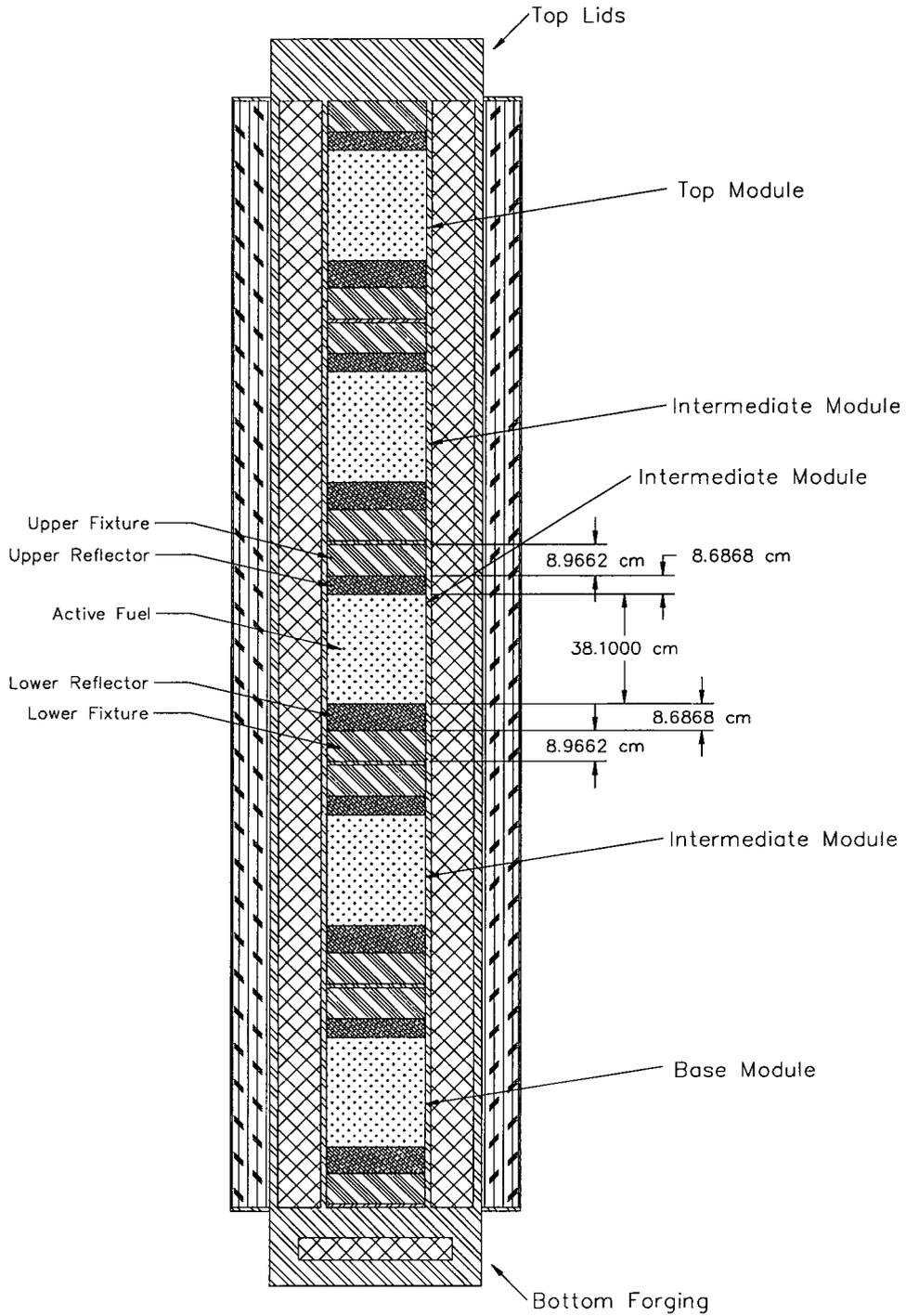
Table 6.3.5-1   Sample Compositions and Number Densities Used in Criticality Analysis
of TRIGA Fuel Elements

Material	FLIP Fuel U-ZrH$_x$	Aluminum	H$_2$O	304 Stainless Steel	Graphite	Lead
Density, gm/cc	--	2.70	0.998	7.920	2.1	11.350
Nuclide				atm/barn-cm		
Uranium 235	9.053E-4	--	--	--	--	--
Uranium 238	3.849E-4	--	--	--	--	--
Zirconium	3.446E-2	--	--	--	--	--
Hydrogen	5.514E-2	--	3.338E-2	--	--	--
Oxygen	--	--	6.675E-2	--	--	--
Carbon	--	--	--	--	1.054E-1	--
Aluminum	--	6.024E-2	--	--	--	--
Iron	--	--	--	5.936E-2	--	--
Chromium	--	--	--	1.743E-2	--	--
Nickel	--	--	--	7.721E-3	--	--
Manganese	--	--	--	1.736E-3	--	--
Lead	--	--	--	--	--	3.297E-2

Table 6.3.5-2   Sample Composition and Number Densities Used in Criticality Analysis of TRIGA Fuel Cluster Rods

Material	U-ZrH$_x$[1]	Aluminum Insert	H$_2$O	304 Stainless Steel	Lead
Density, gm/cc	--	2.70	0.998	7.920	11.350
Nuclide	atm/barn-cm				
Uranium 235	1.46137E-03	--	--	--	--
Uranium 238	1.03065E-04	--	--	--	--
Zirconium	3.40686E-02	--	--	--	--
Hydrogen	5.35638E-02	--	3.338E-2	--	--
Oxygen	--	--	6.675E-2	--	--
Carbon	--	--	--	--	--
Aluminum	--	6.024E-2	--	--	--
Iron	--	--	--	5.936E-2	--
Chromium	--	--	--	1.743E-2	--
Nickel	--	--	--	7.721E-3	--
Manganese	--	--	--	1.736E-3	--
Lead	--	--	--	--	3.297E-2

[1] Sample fuel composition for typical HEU TRIGA cluster rods. Increases in fuel mass, changes in H/Zr ratio, and LEU rods are evaluated in Section 6.4.6.5.

6.3.6   DIDO Fuel Assemblies

6.3.6.1   Description of Calculational Models

Since it is planned to transport many types of DIDO fuel assemblies in the NAC-LWT, a determination of the most limiting, i.e., highest k_{eff}, assembly must be made for criticality purposes. Fuel parameters in Table 6.3.6-1 are employed for the evaluations of HEU, MEU and LEU types and are based on the data presented in Table 6.2.8-1. The tolerances in Table 6.2.8-2 are used in trending reactivity versus the assembly's physical characteristics and produce a bounding fuel assembly characteristic set.

Evaluations are performed with two distinct models. The first stage evaluates reactivity in an infinite array of casks by modeling a single cask with mirrored boundary conditions. The second phase of the evaluations employs a finite array of eight casks. The basket and cask models constructed for the DIDO assembly evaluations are based on the dimensions listed in Table 6.3.6-2.

The KENO-Va model of the NAC-LWT cask with DIDO fuel is centered on a stack of six DIDO baskets. The cask radial shields surround the basket stack. The basket stack surrounded by shields has the lid and bottom weldment added. The module chosen for stacking is the intermediate basket module. While axial extents differ from the bottom and top modules, the basket horizontal cross section is identical in all modules. Axial variations are associated with the stacking of the units, with all units containing the 0.5-inch thick base plate. Figure 6.3.6-1 displays a side view of the intermediate module. A cross-section of the basket with fuel tubes numbered one through seven and the aluminum shell is shown in Figure 6.3.6-2. Two assumptions were made in the DIDO model due to limitation in the KENO-Va input structure and complexity of the model: (1) the heat transfer shunts are modeled as a set of three small cylinders versus a rectangular bar and (2) the aluminum shell is modeled over the full extent of the tube, neglecting the intermediate steel disk. An evaluation is provided in Section 6.4.7 to demonstrate that each of these assumptions is conservative.

Figure 6.3.6-2 also includes a sketch of the two types of fuel configurations evaluated shown in a cross-section, loose and crimped cylinders. The "loose" cylinder configuration spaces the fuel at a constant pitch identical to that of the element during in-core configuration. The second configuration represents the fuel in a "crimped" configuration. For fuel shipment, the assembly can be cut and individual cylinders may be crimped. A radial sketch of the basket cross-section in the cask is shown in Figure 6.3.6-3.

Figure 6.3.6-4 shows this basket module stacked six high inside the NAC-LWT. Reflecting boundary conditions on all sides simulate an infinite array of casks. This model neglects the

impact limiters that would provide additional spacing between casks, and models the cask under accident conditions with the neutron shield voided.

Tubes comprising the basket structure are defined to be stainless steel per licensing drawings. Aluminum tubes are evaluated in the DIDO calculation sets. This evaluation provides significant conservatism in the calculation, as stainless steel contains significant absorber nuclides while aluminum has no significant effect on system reactivity (beyond volume displacement).

The eight-cask array places the casks in a tight triangular pitch configuration. Seven casks are located in a tight cylindrical arrangement similar to that employed in the basket. The eighth cask is placed in a triangular pitch to the lower right corner of the seven cask array.

6.3.6.2   Package Regional Densities

The composition densities (gm/cc) and nuclide number densities (atm/b-cm) calculated by the SCALE material information processor for a range of assemblies evaluated in subsequent criticality analyses are shown in Table 6.3.6-3. Displayed are the HEU, MEU and LEU material densities for the nominal fuel cylinders. Additional material densities may be obtained from the sample input/output files provided in Section 6.6.8.

Figure 6.3.6-1   Intermediate DIDO 42 Basket Module

(Dimensions in inches)
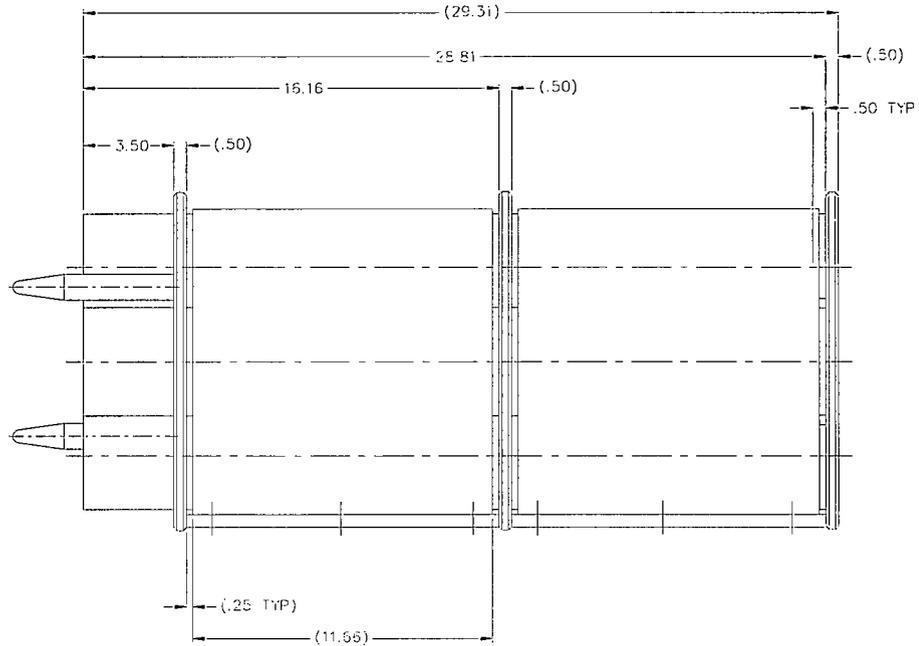
Figure 6.3.6-2   KENO-Va DIDO Fuel in Fuel Tube and Basket Cross-Section
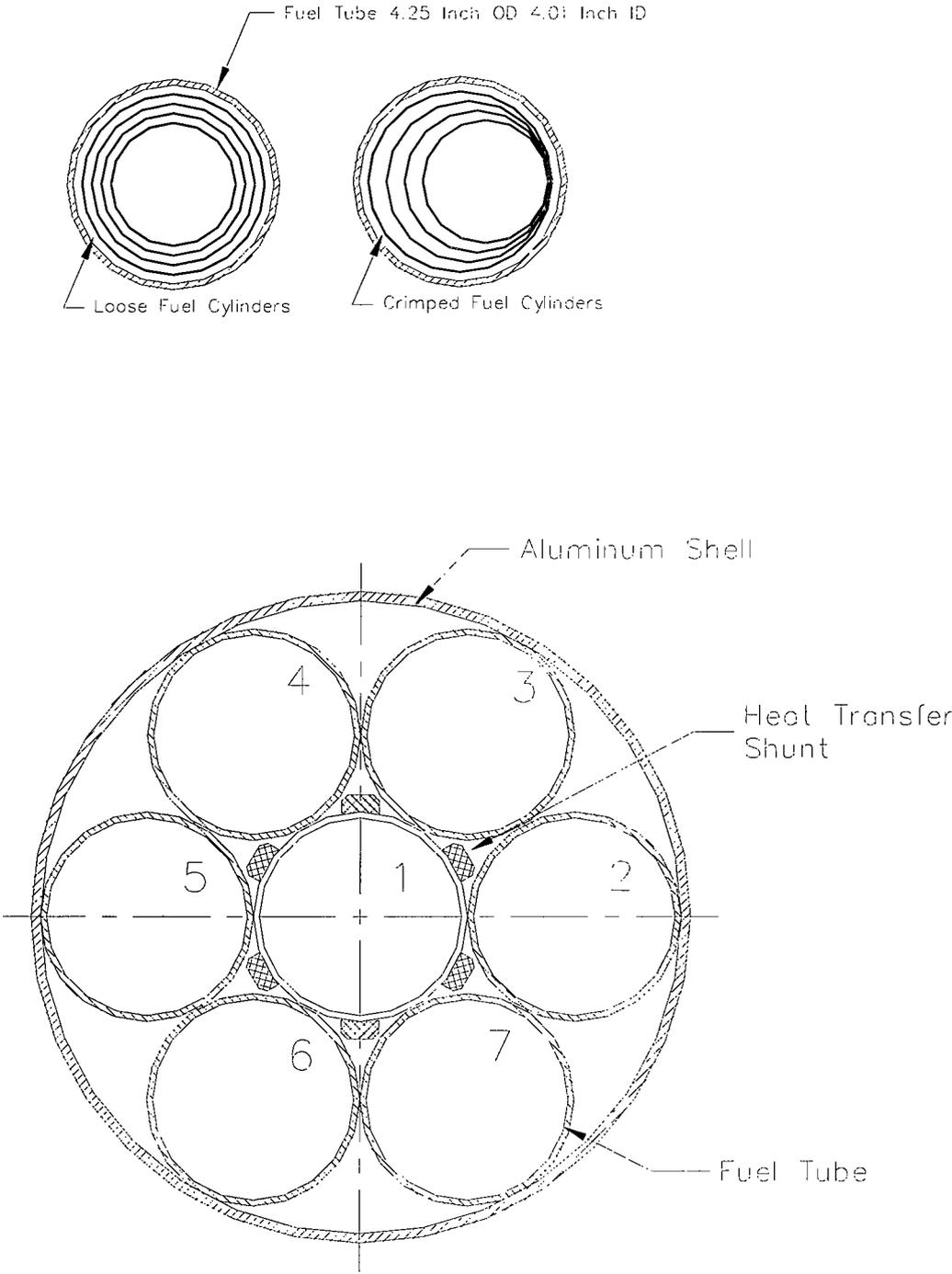
Figure 6.3.6-3   KENO-Va Model of NAC-LWT Cask Cross-Section with DIDO Fuel
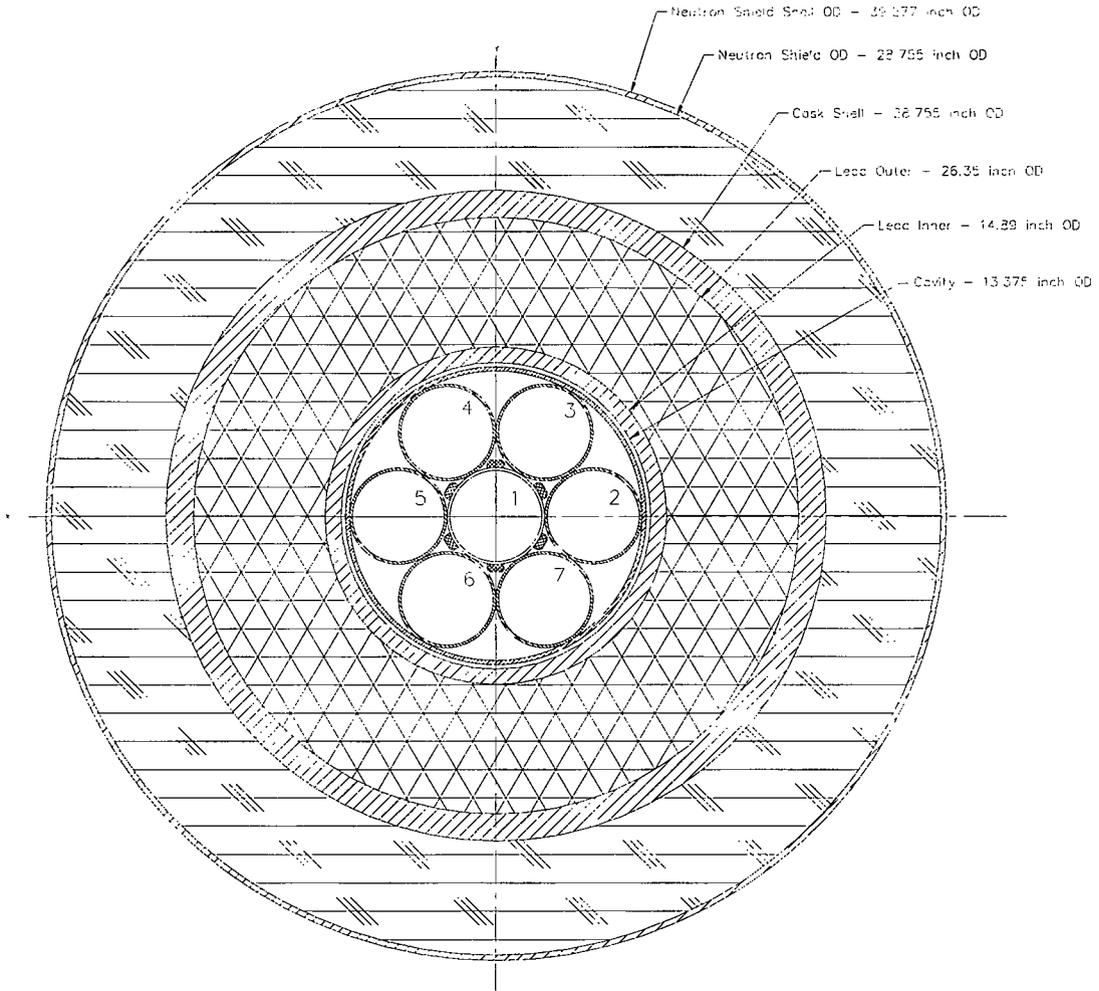
Figure 6.3.6-4   Full Length NAC-LWT Cask Model with 42 DIDO Fuel Assemblies

Upper End Fitting / Plate Material

Active Fuel Region

Lower End Fitting / Plate Material

1.25 cm DIDO
Element End Fitting / Plate Material

60.0 cm DIDO Element
Active Fuel Region

73.125 cm

1.27 cm Basket
Bottom Plate
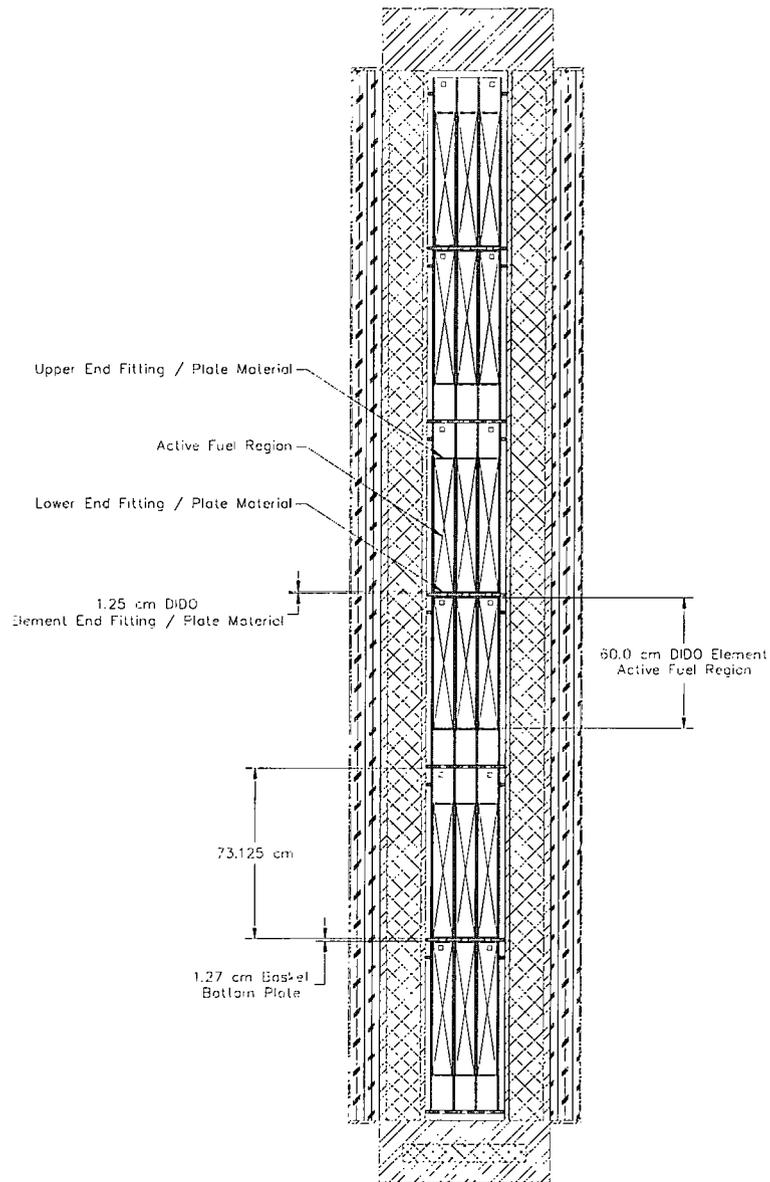
Steel

Lead

Liquid Neutron Shield

Table 6.3.6-1   DIDO Fuel Parameters

Fuel Parameters	Units	Value
Tube 1 Outer Diameter	[cm]	6.38
Tube 2 Outer Diameter	[cm]	7.36
Tube 3 Outer Diameter	[cm]	8.34
Tube 4 Outer Diameter	[cm]	9.32
Clad Thickness	[cm]	0.0425
Tube Thickness	[cm]	0.15
Fuel Meat Thickness	[cm]	0.065
Active Fuel Length	[cm]	60
Total Element Length	[cm]	62.5
Tube Pitch	[cm]	---
Fuel Composition		U-Al
Weight Percent ^{235}U		Note 1
Maximum ^{235}U per Fuel Assembly	[g]	180.0
U wt % in Fuel Composition		Note 1
Mass of Uranium	[g]	Note 1

Note:

1. ^{235}U weight percent, uranium mass and weight percent of uranium in the fuel meat are dependent on the enrichment type evaluated and tolerances employed.

Table 6.3.6-2   DIDO Basket and Cask Parameters

Description	Dimension [in]
Fuel tube outer diameter	4.250
Fuel tube wall thickness	0.120
Fuel tube outer diameter tolerance (maximum)	0.015
Fuel tube outer diameter tolerance (minimum)	0.025
Fuel tube thickness tolerance (maximum)	22%
Fuel tube thickness tolerance (minimum)	0%
Outer ring tube location diameter	8.500
Tube location angle	60.000
Fuel basket outer diameter	13.265
Fuel basket base plate thickness	0.500
Fuel basket base plate thickness tolerance	0.020
Basket bottom plate hole size	1.000
Aluminum shell thickness	0.188
Aluminum shunt width	0.750
Aluminum shunt depth	0.375
Basket cavity height	28.81
Basket cavity height tolerance	0.060
Cask cavity diameter	13.375
Lead shield inner diameter	14.890
Lead shield outer diameter	26.350
Lead shield outer diameter of taper	24.880
Cask outer diameter	28.755
Cask lid thickness	11.250
Bottom forging thickness	10.500
Bottom forging lead insert diameter	20.750
Bottom forging lead insert thickness	3.000
Offset bottom of cask to lead	3.500
Neutron shield thickness	5.000
Neutron shield tank skin	0.236
Number of baskets per cask	6.000

Table 6.3.6-3   Composition Densities Used in Criticality Analysis of DIDO Fuel

Material	HEU U-Al	MEU U-Al	LEU U-Al
Density, gm/cc	U=0.501 Al=2.250	U=1.060,Al=2.085	U=2.415,Al=1.786
Nuclide	Atoms/barn-cm		
Uranium 235	1.222-3	1.222-3	1.222-3
Uranium 238	7.702-5	1.475-3	4.900-3

Material	Al Clad	H2O	304 Stainless Steel	Pb	H2O/ Glycol
Density, gm/cc	2.702	0.998	7.920	11.350	0.9437
Nuclide	Atoms/barn-cm				
Aluminum	6.031E-2				
Oxygen		3.338E-2			2.459E-2
Hydrogen		6.675E-2			5.988E-2
Iron			5.936E-2		
Chromium			1.743E-2		
Nickel			7.721E-3		
Manganese			1.736E-3		
Lead				3.299E-2	
Carbon					1.070E-2

6.3.7   General Atomics Irradiated Fuel Material

6.3.7.1   Description of Calculational Models

Criticality evaluations are performed for three payload combinations: RERTR (TRIGA) fuel only, HTGR fuel only, and both RERTR and HTGR fuel. The results of these analyses show which fuel material is most reactive and establish a basis for choosing a reactivity bias for the combined system. In the models of either RERTR or HTGR fuel, the radial detail of the basket tubes is included. In the combined payload model, the basket tubes are conservatively not modeled, and the RERTR and HTGR enclosures (Fuel Handling Units (FHUs)) intersect tangentially at the centerline of the cask cavity.

The KENO-Va model of the NAC-LWT cask with a combined payload of GA IFM is axially infinite in height, with the active fuel length of the TRIGA elements chosen as the modeled axial extent. Note that two pitch scenarios are evaluated for the 20 TRIGA fuel elements. This first scenario places the elements in a 4×5 rectangular array, as shown in Figure 6.3.7-1, and is denoted as 'Rectangular' in the result tables in Section 6.4.8. The second scenario places 16 elements in a 4×4 array with the remaining four elements inserted in the center of each face on a triangular pitch as shown in Figure 6.3.7-2. For convenience, this scenario is denoted as 'Square' in the result tables in Section 6.4.8. The centerline parameters are calculated as a function of pitch. The HTGR fuel matrix is a homogenized cylinder with outer diameter equal to the inner diameter of the HTGR primary enclosure. The two IFM enclosures intersect tangentially at the centerline of the cask cavity and are surrounded by the cask radial shields. A sketch of the cross-section in the cask is shown in Figure 6.3.7-3. Reflecting boundary conditions on all sides simulate an infinite array of casks. The neutron shield material definition is tied to the exterior moderator definition; a void exterior includes a void neutron shield. Thus, the accident condition of loss of neutron shielding is explicitly modeled when the exterior moderator is set to void.

6.3.7.2   Package Regional Densities

The composition densities (g/cc) and nuclide number densities (atm/b-cm) calculated by the SCALE material information processor are shown in Table 6.3.7-1. Two material descriptions exist for the RERTR/TRIGA fuel: 1) intact fuel with clad; and 2) homogenized fuel without clad.

Figure 6.3.7-1   PICTURE Representation of NAC-LWT Cavity with 'Rectangular'
Array of GA IFM TRIGA Elements
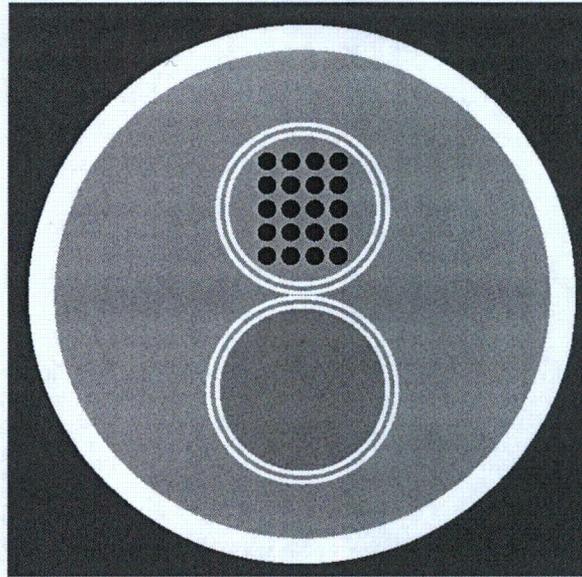
Figure 6.3.7-2   PICTURE Representation of NAC-LWT Cavity with 'Square' Array of
GA IFM TRIGA Elements
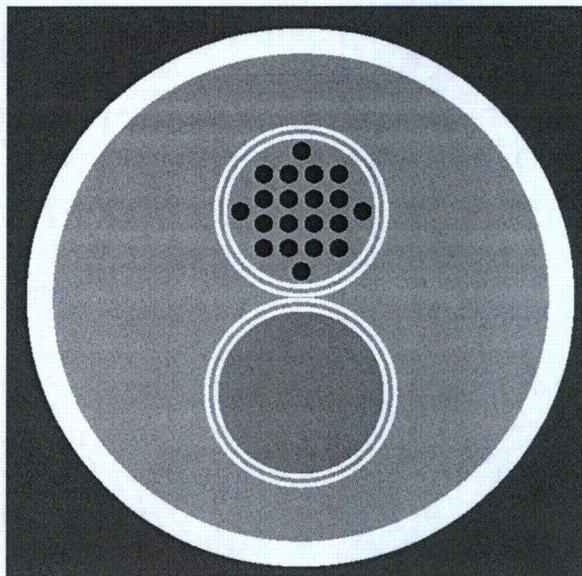
Figure 6.3.7-3   KENO-Va Model of NAC-LWT Cask Cross-Section with GA IFM
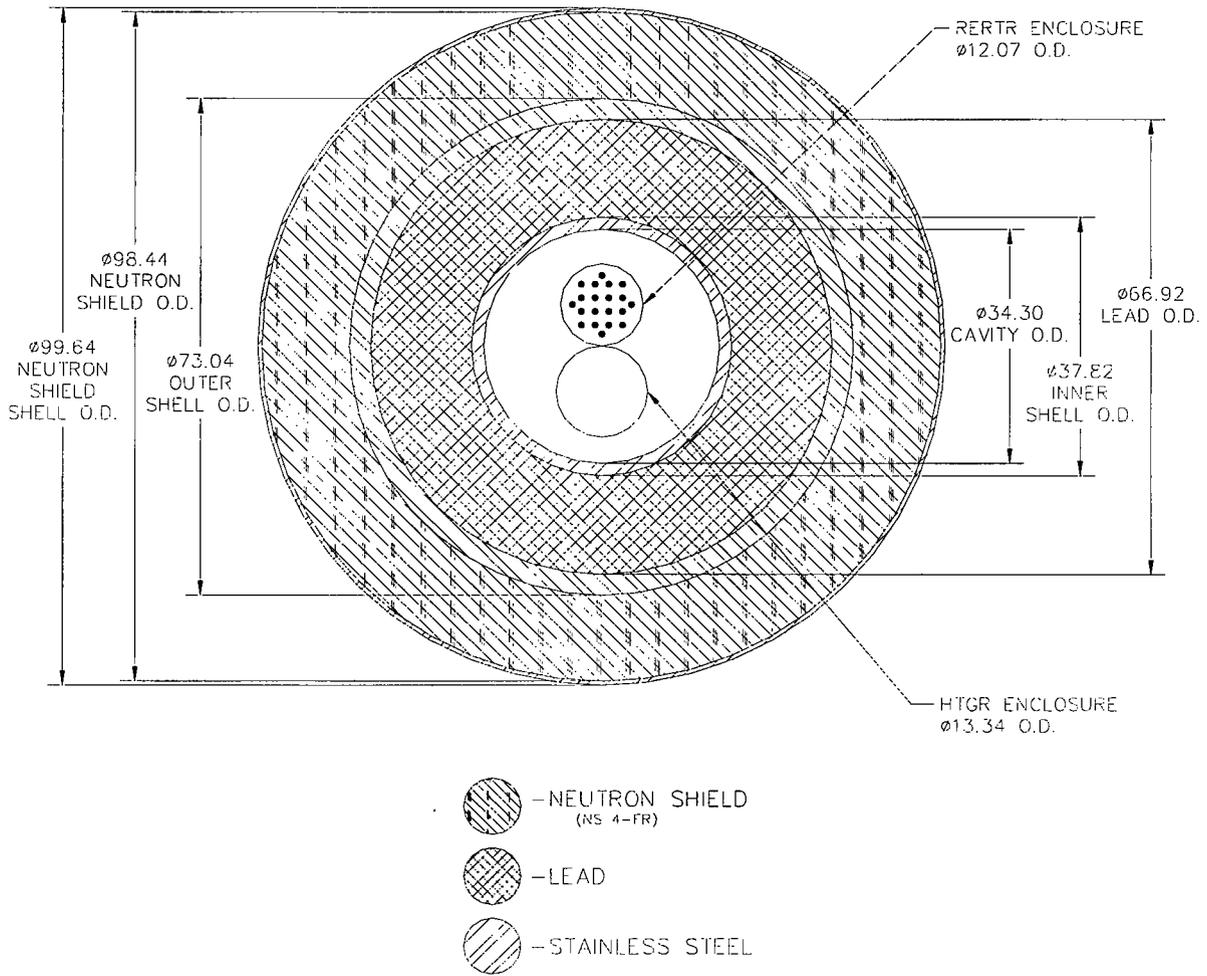
[Dimensions in cm]

Table 6.3.7-1   Composition Densities Used in Criticality Analysis of GA IFM

Material	Intact RERTR Fuel	Intact RERTR Clad	Homog. RERTR Fuel	HTGR Fuel	H2O	304 Stainless Steel	Pb
Density, g/cc	7.409	7.940	1.499	1.116	0.998	7.920	11.344
Nuclide	Atoms/barn-cm						
Hydrogen	4.779E-02		9.717E-03		6.677E-02		
Carbon	5.199E-04		1.084E-04	3.716E-02			
Zirconium	3.052E-02		6.214E-03				
Uranium-235	1.337E-03		2.722E-04	5.117E-05			
Uranium-238	5.382E-03		1.096E-03	3.719E-06			
Chromium		2.298E-02				1.743E-02	
Iron		3.424E-02				5.936E-02	
Nickel		2.850E-02				7.721E-03	
Oxygen				8.810E-05	3.338E-02		
Silicon				3.160E-03			
Thorium				5.315E-04			
Manganese						1.736E-03	
Lead							3.297E-02

6.3.8   PULSTAR Fuel Contents

6.3.8.1   Description of Calculational Models

Four types of basket loadings are considered in the criticality evaluation: (1) intact assemblies loaded directly into the module cell, (2) up to 16 intact elements loaded in the 4×4 fuel rod holder, (3) up to 25 intact or damaged (failed) elements in the PULSTAR failed fuel can, or (4) up to 25 intact or damaged (failed) elements in the PULSTAR screened can. For the evaluation of the canned fuel elements, both discrete and homogenized fuel descriptions are employed.

Fuel elements are modeled using the parameters in Section 6.1.1. Using a conservatively selected enrichment of 6.5 wt % ^{235}U and a loading of 33 grams ^{235}U per element, the calculated UO$_2$ density is 10.38 g/cm^3. The assembly is modeled as a 25-element rectangular rod array with no credit is taken for the assembly upper and lower fittings. The modeled height for intact elements is 26.2 inches, which includes the active fuel height of 24.1 inches and upper and lower end caps. No element (rod) plenum space is modeled.

A bounding can cavity dimension of 3.3-inch width × 30-inch height is chosen to bound the PULSTAR can dimensions. Neither canister wall nor end-plates are included in the model. The 3.3-inch cavity is wider than physically feasible in the minimum 3.38-inch basket opening when adding in the canister wall thicknesses.

PULSTAR fuel evaluations rely on base models developed for the MTR fuel reactivity calculations, as the PULSTAR elements are placed in the 28 MTR basket configuration with spacers. No credit for spacers is taken in the PULSTAR fuel calculations. Base PULSTAR fuel evaluations are performed with minimum basket opening and minimum basket plate thickness, fuel centered within each basket cell, fuel assemblies axially centered in the basket, a flooded cask cavity, and a void cask exterior. Infinite cask arrays are used where possible, with a reduced array specified when necessary to maintain system reactivity below licensing limits.

MTR KENO models are modified to include the PULSTAR fuel assemblies, fuel rod holder and cans. Models are configured to evaluated basket mechanical perturbations and payload radial and axial shifting. Can, cask cavity, neutron shield and cask exterior models are defined as separate materials to allow optimum moderator density and preferential flooding studies.

As indicated in Section 6.1.1, PULSTAR fuel assemblies are rectangular, not square; therefore, assembly alignment (rotation), dubbed 'Xlong' and 'Ylong', is evaluated.

The four types of basket loadings are illustrated in Figure 6.3.8-1 through Figure 6.3.8-4. Dimensioned model sketches with cask materials are shown in Figure 6.3.8-5 and Figure 6.3.8-6. The axial view shows the highest reactivity payload combination of cans and intact fuel assemblies shifted "alternating" into close contact. Note that no spacers are included in the model.

6.3.8.2   Package Regional Densities

The composition densities (g/cc) and nuclide number densities (atm/b-cm) calculated by the SCALE material information processor are shown in Table 6.3.8-1.

Figure 6.3.8-1   PICTURE Representation of NAC-LWT Cavity with PULSTAR
Assemblies
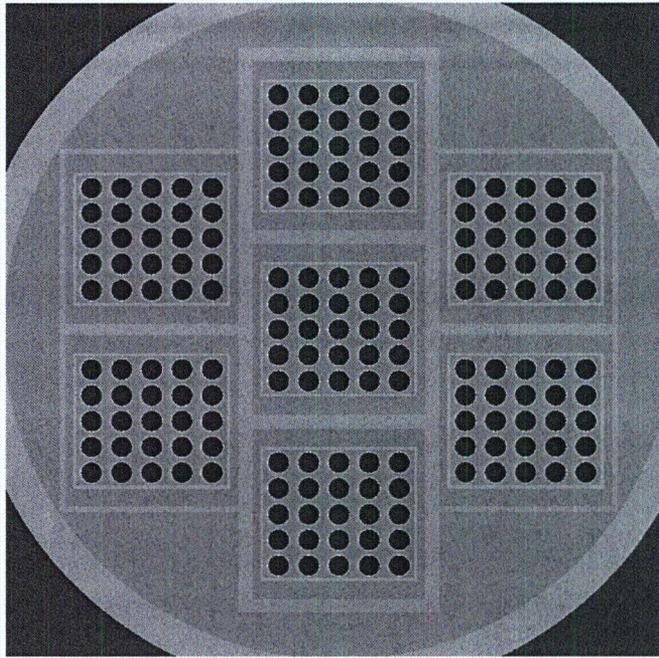
Figure 6.3.8-2   PICTURE Representation of NAC-LWT Cavity with PULSTAR
Elements in 4×4 Rod Insert
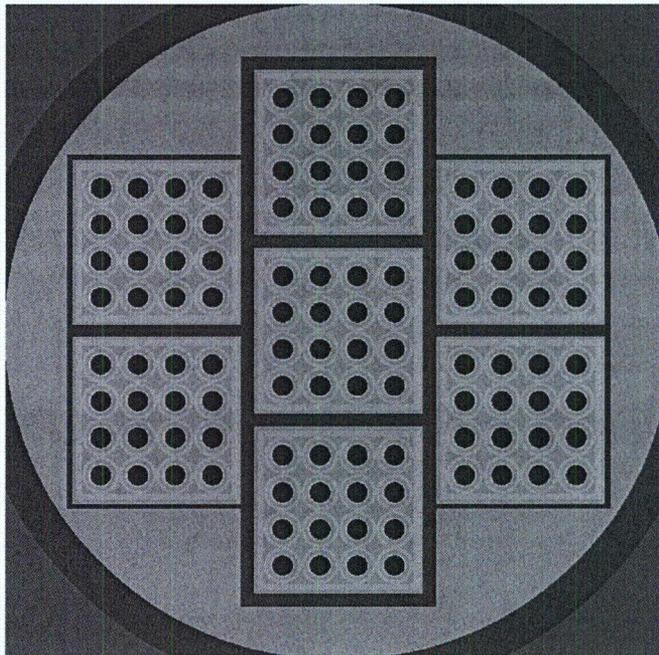
Figure 6.3.8-3   PICTURE Representation of NAC-LWT Cavity with Canned Discrete
PULSTAR Elements
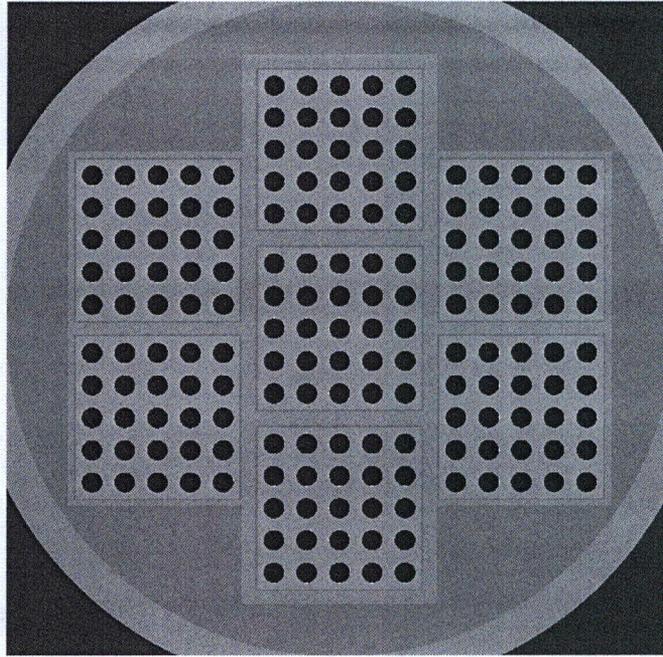
Figure 6.3.8-4   PICTURE Representation of NAC-LWT Cavity with Canned
Homogenized PULSTAR Elements
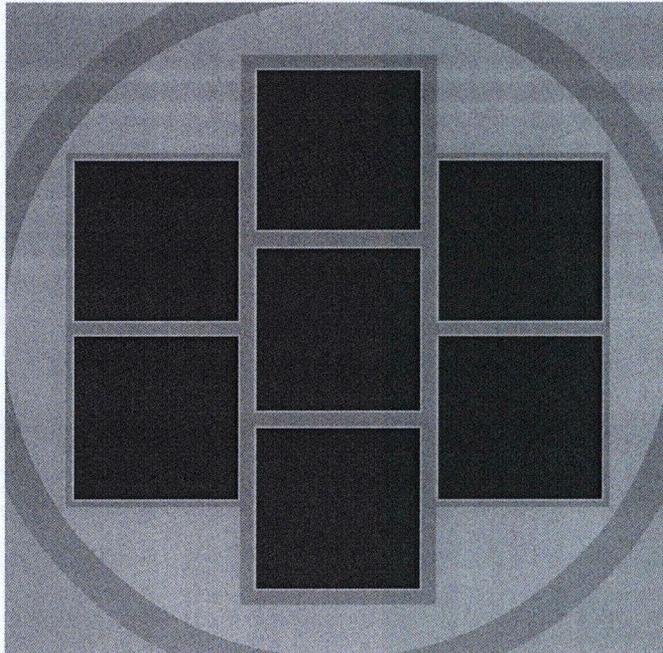
Figure 6.3.8-5   KENO-Va Model of NAC-LWT Cask Cross-Section with 28 MTR
7-Element Basket

Ø98.49 cm
NEUTRON
SHIELD O.D.

Ø99.71 cm
NEUTRON
SHIELD
SHELL O.D

Ø73.09 cm
OUTER
SHELL O.D.

Ø37.78 cm
INNER
SHELL O.D.

Ø34.10 cm
CAVITY O.D.

Ø66.99 cm
LEAD O.D.
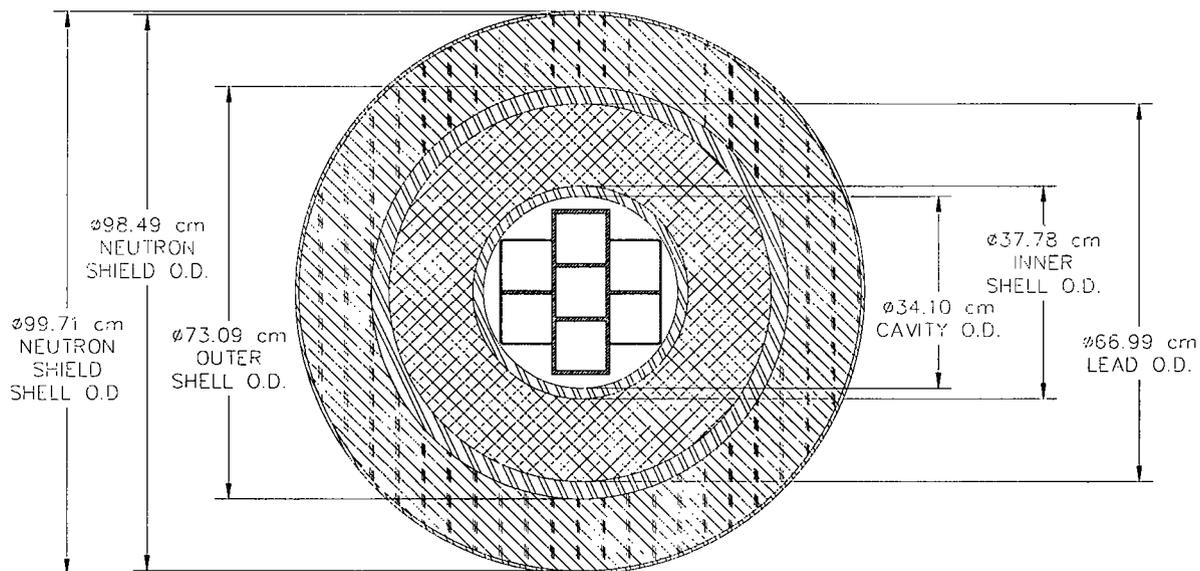
⊘ Neutron Shield

⊘ Lead

⊘ Stainless Steel

Figure 6.3.8-6   Finite Length KENO-Va Model of NAC-LWT Cask with 700 PULSTAR Fuel Elements

76.20 cm
Modeled
Can Height

66.55 cm
PULSTAR
Element
Length

110.49 cm Basket
Content Height

1.27 cm Basket
Bottom Plate

Steel

Lead

Neutron Shield
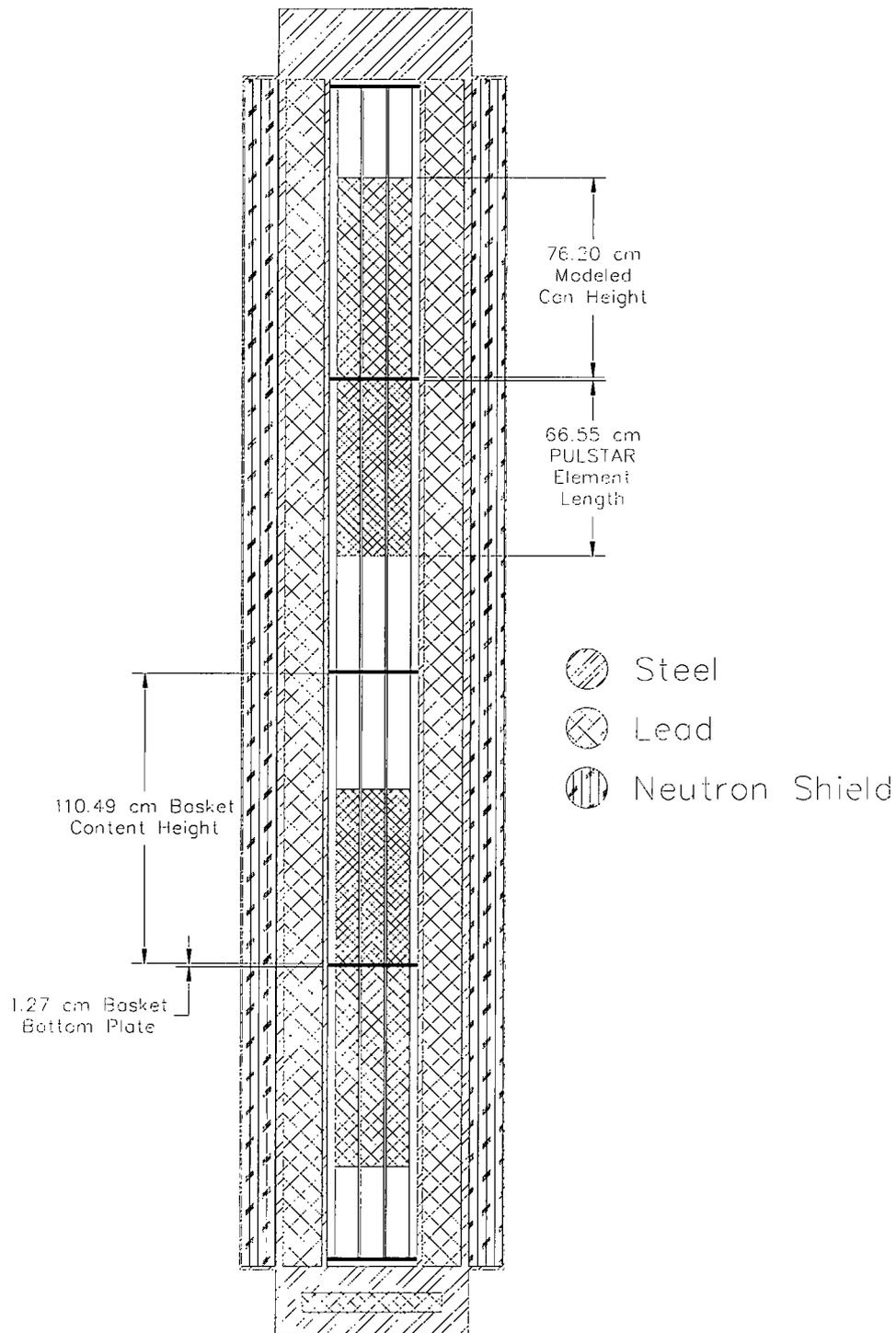
Table 6.3.8-1   Composition Densities Used in Criticality Analysis of PULSTAR Fuel

Material	Intact PULSTAR Fuel	Intact PULSTAR Clad	Homog. PULSTAR Fuel	H2O	304 Stainless Steel	Pb
Density, g/cc	10.38	6.56	3.013.01	0.998	7.920	11.344
Nuclide	Atoms/barn-cm					
Hydrogen				6.677E-02		
Oxygen	4.633E-02			3.338E-02		
Uranium-235	1.524E-03		3.950E-04			
Uranium-238	2.164E-02		5.610E-03			
Zircaloy		4.331E-02	2.096E-03			
Chromium					1.743E-02	
Iron					5.936E-02	
Nickel					7.721E-03	
Manganese					1.736E-03	
Lead						3.297E-02

6.3.9   ANSTO Basket Payload

6.3.9.1   Description of Calculational Models

Fuel parameters in Table 6.2.11-1, spiral fuel assembly, and Table 6.2.12-1, MOATA plate bundle, are employed to build criticality models for the payloads within the NAC-LWT ANSTO baskets. The fuel tolerances in Table 6.2.11-2 and Table 6.2.12-2 are used in trending reactivity versus the assembly's physical characteristics and produce a bounding fuel assembly characteristic set.

Evaluations are performed with an infinite array of casks by modeling a single cask with mirrored boundary conditions. An additional evaluation is performed to demonstrate that a single cask, with containment boundary fully reflected by water, is subcritical with a reactivity below that of the bounding accident configuration array. The ANSTO basket and NAC-LWT cask models are based on the dimensions listed in Table 6.3.9-1 and are identical to the DIDO basket with the exception of slightly larger and thicker fuel tubes and the removal of the aluminum heat transfer components in the basket.

The KENO-Va model of the NAC-LWT cask with the spiral fuel assembly and plate bundle is centered on a stack of six ANSTO baskets. The cask radial shields surround the basket stack. The basket stack, surrounded by shields, has the lid and bottom weldment added. The module chosen for stacking is the intermediate basket module. While axial extents differ from the bottom and top modules, the basket horizontal cross-section is identical in all modules. Axial variations are associated with the stacking of the units, with all units containing the 0.5-inch thick base plate.

Figure 6.3.9-1 displays a side view of the intermediate module. A cross-section of the basket with fuel tubes numbered one through seven is shown in Figure 6.3.9-2. To simplify model construction, the six steel disks surrounding the tubes are not included in the model. They represent a minor amount of parasitic absorber outside the fuel region and, therefore, will have no significant effect on system reactivity.

Figure 6.3.9-2 also includes a sketch of the two types of payload included in the cask. Note that the MOATA plate bundle side plates are modeled without chamfers, allowing additional space for the bundle to move within the tube and allowing a closer approach to adjoining plate bundles than feasible in the as-built assembly configuration. Assembly end-fittings are also not modeled, allowing a significantly closer approach of fuel material in the alternating shifted payload. Structural evaluations of the plate bundle have demonstrated that the as-built configuration of the bundle is maintained through all normal and accident conditions. Structural evaluations of the

spiral fuel assembly demonstrate that the inner and outer shells will maintain their geometry. Since the fuel plates of the spiral assembly are locked into tabs attached to the shells, they will also retain their configuration. To bound a possible reconfiguration of spiral assembly fuel plates within the annular regions, criticality evaluations are performed for variations in fuel locations beyond those feasible by assembly fabrication. Included in the fuel sketches are images of the spiral fuel assembly as-built and the model approximation of three annular fuel rings. A radial sketch of the cask cross-section is shown in Figure 6.3.9-3. The axial stack of baskets is identical to that of the DIDO baskets as shown in Figure 6.3.6-4, with differences limited to payload height. Reflecting boundary conditions on all sides simulate an infinite array of casks. This model neglects the impact limiters that would provide additional spacing between casks, and models the cask under accident conditions with the neutron shield voided.

6.3.9.2   Package Regional Densities

The composition densities (gm/cc) and nuclide number densities (atm/b-cm) calculated by the SCALE material information processor for the nominal characteristic ANSTO payloads used in subsequent criticality analyses are shown in Table 6.3.9-2.

Figure 6.3.9-1   Intermediate ANSTO Basket Module

(Dimensions in inches)
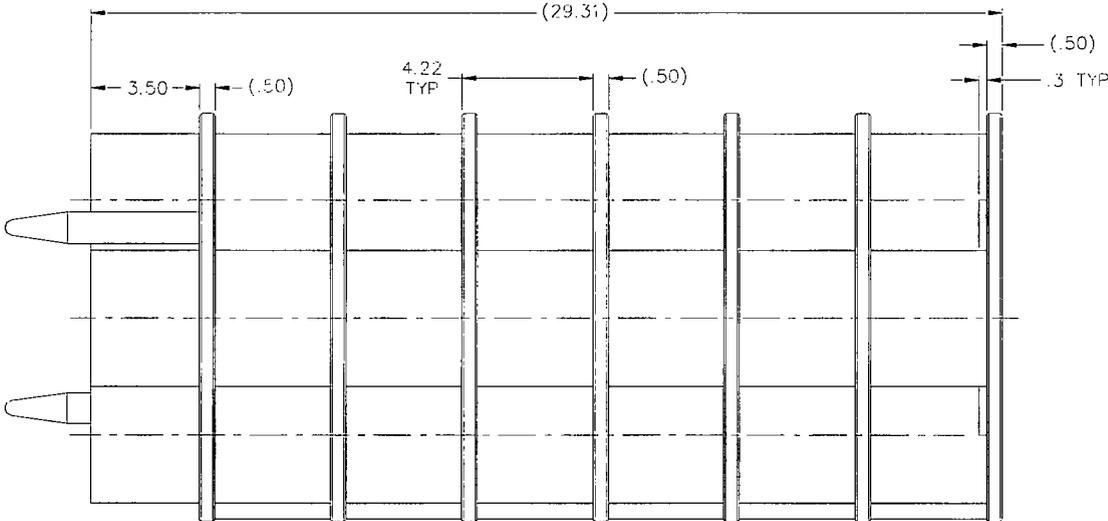
Figure 6.3.9-2   KENO-Va ANSTO Payloads and Basket Cross-Section
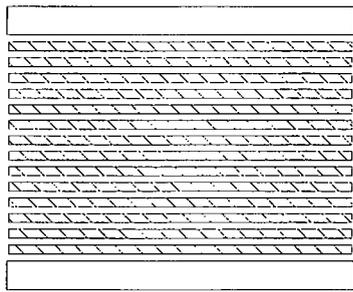
MOATA Plate Bundle Model
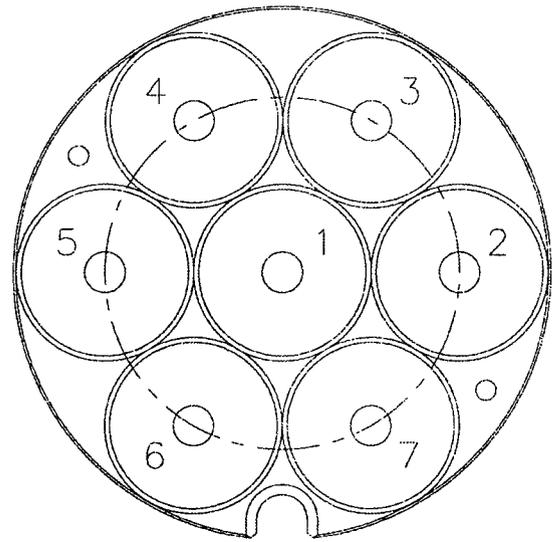
ANSTO Basket
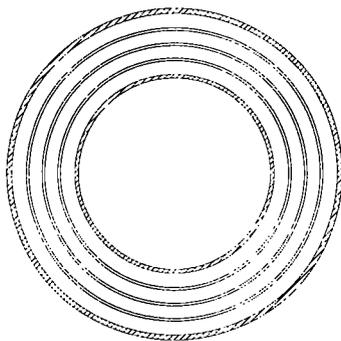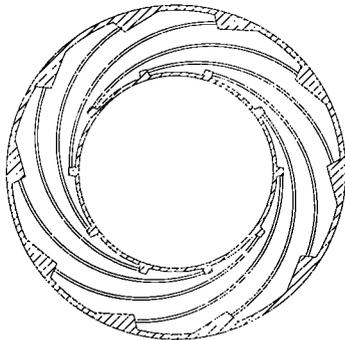
Spiral Fuel Assembly Model

Figure 6.3.9-3   KENO-Va Model of NAC-LWT Cask Cross-Section with ANSTO Basket

Neutron Shield Shell OD – 39.377 inch OD

Neutron Shield OD – 28.755 inch OD

Cask Shell – 28.755 inch OD

Lead Outer – 26.35 inch OD

Lead Inner – 14.89 inch OD

Cavity – 13.375 inch OD

Steel

Lead

Liquid Neutron Shield
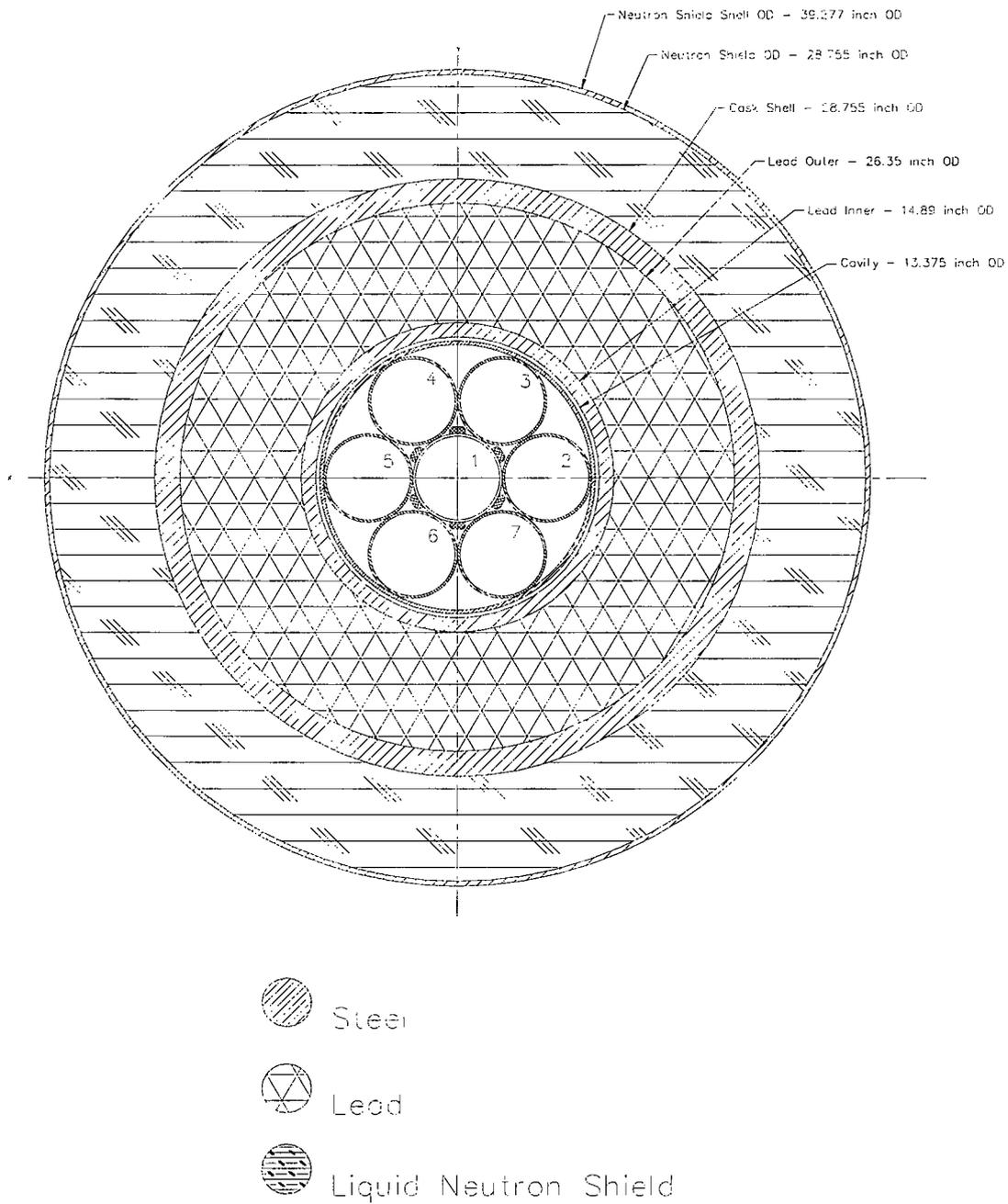
Table 6.3.9-1   ANSTO Basket and Cask Parameters

Description	Dimension [in]
Fuel tube outer diameter	4.375
Fuel tube wall thickness	0.125
Fuel tube outer diameter tolerance (maximum)	0.015
Fuel tube outer diameter tolerance (minimum)	0.025
Fuel tube thickness tolerance (maximum)	22%
Fuel tube thickness tolerance (minimum)	0%
Tube location angle (degrees)	60
Fuel basket outer diameter	13.265
Fuel basket base plate thickness	0.500
Fuel basket base plate thickness tolerance	0.020
Basket bottom plate hole size	1.000
Basket cavity height	28.81
Basket cavity height tolerance	0.060
Cask cavity diameter	13.375
Lead shield inner diameter	14.890
Lead shield outer diameter	26.350
Lead shield outer diameter of taper	24.880
Cask outer diameter	28.755
Cask lid thickness	11.250
Bottom forging thickness	10.500
Bottom forging lead insert diameter	20.750
Bottom forging lead insert thickness	3.000
Offset bottom of cask to lead	3.500
Neutron shield thickness	5.000
Neutron shield tank skin	0.236
Number of baskets per cask	6

Table 6.3.9-2   Composition Densities Used in Criticality Analysis of ANSTO Basket
Payloads

Material	Sprial Assembly U-Al	MOATA Plate Bundles U-Al
Density, gm/cc	U=0.847 Al=1.382	U=0.567,Al=2.517
Nuclide	Atoms/barn-cm	
Uranium 235	1.85E-03	1.34E-03
Uranium 238	3.21E-04	1.15E-04
Al	3.08E-02	5.62E-02

Material	Al Clad	H_2O	304 Stainless Steel	Pb	H_2O/ Glycol
Density, gm/cc	2.702	0.998	7.920	11.350	0.9437
Nuclide	Atoms/barn-cm				
Aluminum	6.031E-2				
Oxygen		3.338E-2			2.459E-2
Hydrogen		6.675E-2			5.988E-2
Iron			5.936E-2		
Chromium			1.743E-2		
Nickel			7.721E-3		
Manganese			1.736E-3		
Lead				3.299E-2	
Carbon					1.070E-2

Note: Fuel material density and composition values are based on nominal fuel
dimensions, mass and enrichment. Values used in the CSAS models vary due
to tolerances applied to the fuel material specification and/or dimension.

6.3.10   ANSTO-DIDO Combined Basket Payload

6.3.10.1   Description of Calculational Models

Mixed ANSTO-DIDO payloads considered in the evaluations include placement of an ANSTO basket top module, containing DIDO and/or ANSTO fuel, on a DIDO basket stack, or including DIDO fuel within the top ANSTO basket module in an ANSTO basket stack. As the results in Section 6.4.7, DIDO, and Section 6.4.10, ANSTO, indicate a higher reactivity for the DIDO basket assembly, the evaluations of the combined payload concentrate on this configuration.

The DIDO and ANSTO fuel models developed in Sections 6.4.7 and 6.4.10 are combined to form a mock-up for a cask model containing both DIDO and ANSTO basket modules. The ANSTO module is modeled to contain DIDO, ANSTO or combination payloads. Fuel parameters are not modified from those described in the individual basket evaluation sections. Model changes are limited to correcting the material composition of the DIDO basket tubes (stainless steel versus aluminum in the Section 6.4.7 evaluations) and the addition of an aluminum damaged fuel can (DFC) to contain intact elements or loose and/or segmented plate material. The DFC can physically only be located in the ANSTO module as its diameter will not allow it to be located in the DIDO basket tube. The inner and outer diameters of the aluminum canister are 98.4 mm and 101.6 mm (see canister sketch in Figure 1.2.3-18) versus a nominal DIDO tube inner diameter of 101.8 mm (including any tube bow or twist, a 0.2-mm gap is insufficient for DFC placement).

Evaluations are performed with an infinite array of casks by modeling a single cask with mirrored boundary conditions. Single cask analyses are not performed as the DIDO and ANSTO calculations in Sections 6.4.7 and 6.4.10 demonstrate that a single cask, with containment boundary fully reflected by water, has a reactivity below that of the bounding accident configuration array. The ANSTO and DIDO basket models are identical with the exception that the ANSTO basket contains slightly larger and thicker fuel tubes and the aluminum heat transfer components are removed from the basket.

The KENO-Va model of the NAC-LWT cask with the combined baskets is composed of a stack of five DIDO basket modules and one top ANSTO basket module. The cask radial shields surround the basket stack. The basket stack, surrounded by shields, has the lid and bottom weldment added. Geometry changes made to the combined model are the inclusion of an aluminum DFC. The only component of the DFC included in the model is the radial aluminum shell. Neglecting the bottom structure allows fissile material in adjoining baskets a closer approach and is, therefore, conservative. The top structure has no effect as the only analysis

component affected is neutron backscatter/reflection that, due to geometry aspects (low radius to height ratio), is not significant to system performance.

The SCALE 4.3 CSAS25 sequence used in this analysis is limited to one material definition within its material information processor geometry cards and is, therefore, limited to calculating a self-shielding correction for only one fuel material. In the combined baskets model, multiple fuel materials may be required. The code input options RES and DAN are, therefore, used to enter the relevant parameters directly. Input values for the resonance correction were calculated with stand-alone CSAS runs for each fuel geometry/material description.

6.3.10.2   Package Regional Densities

The composition densities (gm/cc) and nuclide number densities (atm/b-cm) were calculated by the SCALE material information processor and are identical to those used in Sections 6.4.7 and 6.4.10.

6.4   Criticality Calculations

The criticality calculations for the contents to be transported in the NAC-LWT are described in Sections 6.4.1 through 6.4.10.

6.4.1   PWR Fuel Assemblies

This section presents the criticality analysis for the NAC-LWT cask with the PWR fuel assembly and basket configuration. Criticality analyses of this single assembly arrangement for the most limiting assembly type were performed to satisfy the criticality safety requirements of 10 CFR Parts 71.55 and 71.59 as well as IAEA Transportation Safety Standards (TS-R-1). In these analyses, the bounding PWR fuel assembly was determined for uranium enrichments of 3.7 and 3.5 wt % ^{235}U. Single casks loaded separately with the two design basis PWR fuel assemblies were studied for criticality under both normal and accident conditions. The reactivity effects associated with mechanical and geometric perturbations of the PWR fuel assembly and the basket opening are quantified. The analyses demonstrate that, including all calculational and mechanical uncertainties, the NAC-LWT cask remains subcritical under both normal and accident conditions for all PWR assemblies similar in construction and enrichment to those described herein.

6.4.1.1   Design Basis PWR Fuel Assembly

The k_{eff} values of a single NAC-LWT cask with the PWR fuel assemblies shown in Table 6.2.1-1 and Table 6.2.1-2 are given in Table 6.4.1-1. These results assume a uranium enrichment limit of 3.7 wt % ^{235}U and that full density water is present in the fuel clad gap. As seen in the table, the PWR assembly with the highest reactivity not exceeding 0.95 with uncertainties and bias per Section 6.4.1.6 was found to be the Exxon 15×15ANF WE assembly. Thus, this assembly was selected as the most limiting assembly for a uranium enrichment limit of 3.7 wt % ^{235}U. This assembly will serve as the basis to demonstrate that the CE 14×14, CE 16×16, Exxon 14×14 CE, Exxon 14×14 WE, Westinghouse 14×14, and the Westinghouse 14×14 OFA are sufficiently subcritical under both normal and accident conditions with an enrichment limit of 3.7 wt % ^{235}U.

The PWR fuel assemblies with k_s reactivities exceeding 0.95 were reanalyzed with a uranium enrichment limit of 3.5 wt % ^{235}U. The reactivities of a single NAC-LWT cask with these PWR assemblies and a uranium enrichment of 3.5 wt % ^{235}U are shown in Table 6.4.1-2. From this table it is shown that the reactivity of all re-analyzed assemblies were below the 0.95 limit and that the Westinghouse 17×17 OFA assembly is the most reactive. Consequently, this assembly was selected as the most limiting assembly for a uranium enrichment of 3.5 wt % ^{235}U. This fuel assembly will serve as the basis to demonstrate that the B&W 15×15, B&W 17×17, Exxon

17×17 WE, Westinghouse 15×15, and the Westinghouse 17×17 assemblies are sufficiently subcritical under both normal and accident conditions with an enrichment limit of 3.5 wt % ^{235}U.

6.4.1.2   PWR Fuel Perturbation Studies

The criticality evaluation for the NAC-LWT cask with the design basis PWR assemblies includes studying geometric tolerances and mechanical perturbations. The tolerances and perturbations are independently evaluated for the limiting PWR assemblies at uranium enrichments of 3.5 and 3.7 wt % ^{235}U. The following perturbations and tolerances are analyzed:

I. Mechanical Perturbation
A. Fuel movement in the basket

II. Geometric Tolerances
A. Basket opening size

The geometric tolerance associated with the manufacture of the PWR basket is an opening tolerance of 8.88 ± 0.03 inches. Mechanical perturbations, i.e., fuel movement within the basket, arise from the gap between the assembly and the basket opening.

The effect of these tolerances and perturbations on the reactivity of the most limiting PWR fuel assemblies in the NAC-LWT cask is shown in the results presented in Table 6.4.1-3 and Table 6.4.1-4. Table 6.4.1-3 shows that there is one perturbed configuration with a larger reactivity than the nominal design configuration of the Westinghouse 17×17 OFA fuel assembly. However, the increase in reactivity was not statistically significant, i.e., less than 2σ. Thus, the nominal configuration, i.e. a centered assembly with nominal basket dimensions, of the Westinghouse 17×17 OFA PWR is the most reactive configuration of the most limiting PWR assembly for a uranium enrichment limit of 3.5 wt % ^{235}U. This configuration serves as the design basis and is retained for subsequent moderator density variation studies.

For the Exxon 15×15 ANF WE fuel assembly, the effect of geometrical and mechanical perturbations is presented in Table 6.4.1-4. Analysis of the results reveals that the maximum basket opening causes a statistically significant increase, i.e., >2σ, on reactivity. This configuration serves as the design basis and is retained for subsequent normal and accident condition, moderator density variation studies at the 3.7 wt % enrichment limit.

6.4.1.3   Normal Condition Moderator Density Evaluations

Table 6.4.1-5 presents the cask k_{eff} for the most reactive normal condition configuration as a function of moderator density inside and outside a single cask for enrichment limits of 3.5 and 3.7 wt % ^{235}U. The results show an increase in reactivity with increasing internal moderator density. This indicates that moderator density changes due to increasing temperature have a negative reactivity effect. Low density moderation inside or outside of the cask does not produce abrupt increases in reactivity in comparison to other density values. The calculations show that k_{eff} does not vary significantly when varying external water with constant full density internal moderator. Because external water density does not affect reactivity within statistical limits, the most reactive case is chosen to be internal and external moderator density at 1.0 gm/cc. The k_{eff} in this case for 3.5 and 3.7 wt % ^{235}U are 0.9279 ± 0.0014 and 0.9288 ± 0.0014, respectively. The k_{eff} for the normal condition cask with a dry cavity is very subcritical, i.e., ~ 0.15 and is insensitive to external moderator density variations.

6.4.1.4   Accident Condition Moderator Density Evaluations

Table 6.4.1-6 shows the cask k_{eff} for the most reactive accident condition configuration as a function of moderator density variation in the cavity, neutron shield tank and outside a single cask for enrichment limits of 3.5 and 3.7 wt % ^{235}U. Again, the results show an increase in reactivity with increasing internal moderator density. Low density moderation inside or outside of the cask does not produce abrupt increases in reactivity in comparison to other density values. The calculations show that the k_{eff} for the accident condition with a dry cavity, neutron shield and exterior is very subcritical, i.e., ~ 0.16. The most reactive case occurs with the moderator density at 1.0 gm/cc in the cavity and the neutron shield tank as well as outside. The k_{eff} in this case for 3.5 and 3.7 wt % ^{235}U are 0.9325 ± 0.0013 and 0.9320 ± 0.0013, respectively.

6.4.1.5   Single Package Evaluations

To satisfy 10 CFR 71.55(b)(3), an analysis of the reflection of the containment system (inner shell) by water is performed on a single wet cask. Successive replacement of the cask radial shields with water reflection is also evaluated. The results of this evaluation can be seen in Table 6.4.1-7 and Table 6.4.1-8. The reactivity of the system drops as each radial shield of the cask is replaced by water, k_{eff} = 0.9251 ± 0.013 and k_{eff} = 0.9295 ± 0.0013 for 3.5 and 3.7 wt % ^{235}U, respectively for the full cask surrounded by water to k_{eff} = 0.8372 ± 0.013 and k_{eff} = 0.8363 ± 0.0014 for 3.5 and 3.7 wt % ^{235}U, respectively, for the inner shell surrounded by water.

6.4.1.6   Conclusion

A calculation of k_s under normal and accident conditions can now be made based on the previous results and based on the KENO-Va validation statistics presented in Section 6.5.1 for low enriched uranium fuel. The value k_s is calculated based on the KENO-Va Monte Carlo average plus any biases and uncertainties associated with the methods and the modeling, i.e.:

$$k_s = k_{eff} + 2\sigma_{mc} + \Delta k_{Bias} + \Delta k_{BU}$$

In the validation presented in Section 6.5.1, a bias of 0.0052 (allowance for under prediction of k_{eff}) and a 95/95 method uncertainty of $\pm$ 0.0087 was determined. With this bias and uncertainty, the equation for k_s becomes:

$$k_s = k_{eff} + 2\sigma_{mc} + 0.0052 + 0.0087$$

Thus, $k_s = 0.9446$ and $k_s = 0.9455$ for 3.5 and 3.7 wt % ^{235}U, respectively, under <u>normal conditions</u> for a single NAC-LWT cask with a design basis PWR assembly, and a flooded basket cavity and exterior. Both are below the 0.95 regulatory limit. Under <u>accident conditions</u>, $k_s = 0.9490$ and $k_s = 0.9485$ for 3.5 and 3.7 wt % ^{235}U, respectively, for a single NAC-LWT cask with a design basis PWR assembly with a flooded basket cavity, neutron shield and exterior.

For both normal and accident conditions, the calculated k_{eff} values, after correction for biases and uncertainties, are below the 0.95 limit. The analyses demonstrate that, including all calculational and mechanical uncertainties, a single NAC-LWT cask with PWR fuel assemblies remains subcritical under normal and accident conditions.

Table 6.4.1-1   PWR Fuel Assembly at 3.7% Enrichment Most Reactive Assembly
Results

PWR Fuel	k_{eff} (Dry Gap)	σ (Dry Gap)	k_{eff} (Wet Gap)	σ (Wet Gap)	k_s
W17×17 OFA	N/A	N/A	0.9428	0.0013	0.9593
W15×15	N/A	N/A	0.9407	0.0014	0.9574
B&W 15×15	N/A	N/A	0.9385	0.0014	0.9552
Ex17×17 WE	N/A	N/A	0.9381	0.0013	0.9546
B&W 17×17	N/A	N/A	0.9378	0.0014	0.9545
W17×17	N/A	N/A	0.9375	0.0013	0.9540
Ex15×15 WE	0.9246	0.0013	0.9321	0.0014	0.9488
CE16×16	0.9106	0.0013	0.9117	0.0014	0.9284
CE14×14	0.9059	0.0013	0.9103	0.0014	0.9270
Ex14×14 CE	0.9033	0.0014	0.9087	0.0013	0.9252
W14×14 OFA	0.8959	0.0014	0.9026	0.0014	0.9193
W14×14	0.8919	0.0014	0.9016	0.0013	0.9181
Ex14×14 WE	0.8805	0.0014	0.8944	0.0014	0.9111

Table 6.4.1-2   PWR Fuel Assembly at 3.5% Enrichment Most Reactive Assembly
Results

PWR Fuel	k_{eff} (Dry Gap)	σ (Dry Gap)	k_{eff} (Wet Gap)	σ (Wet Gap)	k_s (Wet Gap)
W17×17 OFA	0.9279	0.0013	0.9326	0.0013	0.9491
B&W 17×17	0.9212	0.0013	0.9314	0.0013	0.9479
Ex17×17 WE	0.9248	0.0012	0.9309	0.0014	0.9476
W15×15	0.9235	0.0012	0.9303	0.0013	0.9468
W17×17	0.9208	0.0013	0.9284	0.0014	0.9451
B&W 15×15	0.9202	0.0013	0.9278	0.0014	0.9445

Table 6.4.1-3   Westinghouse 17×17 OFA Assembly Geometric Tolerances and Mechanical Perturbations Results

Configuration	k_{eff}	σ	$k_{eff} + 2\sigma$
Nominal Configuration	0.9326	0.0013	0.9352
Max. Basket Opening	0.9315	0.0013	0.9341
Min. Basket Opening	0.9342	0.0014	0.9370
Assembly on Side	0.9306	0.0014	0.9334
Assembly in Corner	0.9298	0.0014	0.9326

Table 6.4.1-4   Exxon 15×15 Geometric Tolerances and Mechanical Perturbations Results

Configuration	k_{eff}	σ	$k_{eff} + 2\sigma$
Nominal Configuration	0.9321	0.0014	0.9349
Max. Basket Opening	0.9353	0.0013	0.9379
Min. Basket Opening	0.9316	0.0014	0.9344
Assembly on Side	0.9294	0.0013	0.9320
Assembly in Corner	0.9286	0.0013	0.9312

Table 6.4.1-5   Reactivity with Design Basis PWR Fuel vs. Basket Moderator Density, Normal Conditions

Moderator Density	3.5% Enrichment	3.7% Enrichment
Dry Exterior, Vary Internal Density		
0.0000	0.1496 ± 0.0003	0.1561 ± 0.0003
0.0010	0.1502 ± 0.0003	0.1571 ± 0.0004
0.0100	0.1584 ± 0.0003	0.1656 ± 0.0004
0.0250	0.1733 ± 0.0004	0.1795 ± 0.0004
0.0500	0.1995 ± 0.0005	0.2069 ± 0.0005
0.0750	0.2292 ± 0.0005	0.2347 ± 0.0006
0.1000	0.2588 ± 0.0006	0.2645 ± 0.0006
0.2000	0.3822 ± 0.0009	0.3849 ± 0.0009
0.4000	0.5927 ± 0.0011	0.5926 ± 0.0011
0.6000	0.7417 ± 0.0014	0.7399 ± 0.0013
0.8000	0.8465 ± 0.0013	0.8492 ± 0.0015
0.9000	0.8923 ± 0.0013	0.8896 ± 0.0013
1.0000	0.9279 ± 0.0014	0.9288 ± 0.0014
Wet Interior, Vary External Density		
0.0000	0.9279 ± 0.0014	0.9288 ± 0.0014
0.0010	0.9295 ± 0.0013	0.9284 ± 0.0013
0.0100	0.9251 ± 0.0013	0.9266 ± 0.0013
0.0250	0.9292 ± 0.0013	0.9255 ± 0.0012
0.0500	0.9277 ± 0.0013	0.9297 ± 0.0014
0.0750	0.9284 ± 0.0013	0.9241 ± 0.0014
0.1000	0.9260 ± 0.0013	0.9248 ± 0.0013
0.2000	0.9247 ± 0.0014	0.9289 ± 0.0013
0.4000	0.9254 ± 0.0013	0.9268 ± 0.0013
0.6000	0.9265 ± 0.0013	0.9282 ± 0.0012
0.8000	0.9285 ± 0.0013	0.9271 ± 0.0013
0.9000	0.9266 ± 0.0014	0.9286 ± 0.0013
1.0000	0.9251 ± 0.0013	0.9244 ± 0.0012
Vary Interior and Exterior Density Simultaneously		
0.0000	0.1496 ± 0.0003	0.1561 ± 0.0003
0.0010	0.1508 ± 0.0004	0.1576 ± 0.0004
0.0100	0.1583 ± 0.0004	0.1644 ± 0.0004
0.0250	0.1737 ± 0.0004	0.1784 ± 0.0004
0.0500	0.2004 ± 0.0005	0.2062 ± 0.0005
0.0750	0.2293 ± 0.0006	0.2341 ± 0.0006
0.1000	0.2599 ± 0.0006	0.2637 ± 0.0006
0.2000	0.3834 ± 0.0009	0.3851 ± 0.0009
0.4000	0.5909 ± 0.0011	0.5942 ± 0.0011
0.6000	0.7398 ± 0.0012	0.7416 ± 0.0012
0.8000	0.8486 ± 0.0013	0.8487 ± 0.0014
0.9000	0.8886 ± 0.0014	0.8926 ± 0.0013
1.0000	0.9251 ± 0.0013	0.9244 ± 0.0012

Table 6.4.1-6   Reactivity with Design Basis PWR Fuel vs. Basket Moderator Density, Accident Conditions

Moderator Density	3.5% Enrichment	3.7% Enrichment
Dry Exterior, Vary Internal Density		
0.0000	0.1554 ± 0.0004	0.1637 ± 0.0004
0.0010	0.1561 ± 0.0004	0.1632 ± 0.0003
0.0100	0.1649 ± 0.0004	0.1737 ± 0.0004
0.0250	0.1808 ± 0.0004	0.1883 ± 0.0005
0.0500	0.2096 ± 0.0005	0.2159 ± 0.0005
0.0750	0.2390 ± 0.0006	0.2464 ± 0.0006
0.1000	0.2683 ± 0.0007	0.2767 ± 0.0007
0.2000	0.3928 ± 0.0009	0.3985 ± 0.0009
0.4000	0.5975 ± 0.0012	0.5995 ± 0.0012
0.6000	0.7462 ± 0.0012	0.7478 ± 0.0012
0.8000	0.8510 ± 0.0014	0.8535 ± 0.0014
0.9000	0.8936 ± 0.0012	0.8946 ± 0.0014
1.0000	0.9300 ± 0.0012	0.9296 ± 0.0014
Wet Interior, Vary External Density		
0.0000	0.9300 ± 0.0012	0.9296 ± 0.0014
0.0010	0.9283 ± 0.0014	0.9281 ± 0.0013
0.0100	0.9295 ± 0.0012	0.9303 ± 0.0013
0.0250	0.9304 ± 0.0014	0.9305 ± 0.0014
0.0500	0.9313 ± 0.0014	0.9330 ± 0.0013
0.0750	0.9291 ± 0.0013	0.9334 ± 0.0013
0.1000	0.9308 ± 0.0014	0.9326 ± 0.0013
0.2000	0.9303 ± 0.0013	0.9308 ± 0.0013
0.4000	0.9325 ± 0.0013	0.9319 ± 0.0013
0.6000	0.9310 ± 0.0013	0.9331 ± 0.0014
0.8000	0.9293 ± 0.0014	0.9317 ± 0.0013
0.9000	0.9303 ± 0.0013	0.9322 ± 0.0014
1.0000	0.9325 ± 0.0013	0.9320 ± 0.0013
Vary Interior and Exterior Density Simultaneously		
0.0000	0.1554 ± 0.0004	0.1637 ± 0.0004
0.0010	0.1566 ± 0.0004	0.1642 ± 0.0004
0.0100	0.1659 ± 0.0004	0.1740 ± 0.0004
0.0250	0.1826 ± 0.0004	0.1918 ± 0.0004
0.0500	0.2135 ± 0.0005	0.2220 ± 0.0006
0.0750	0.2450 ± 0.0006	0.2523 ± 0.0006
0.1000	0.2781 ± 0.0007	0.2840 ± 0.0006
0.2000	0.4035 ± 0.0010	0.4059 ± 0.0010
0.4000	0.6045 ± 0.0012	0.6071 ± 0.0012
0.6000	0.7518 ± 0.0012	0.7519 ± 0.0013
0.8000	0.8556 ± 0.0013	0.8572 ± 0.0013
0.9000	0.8988 ± 0.0013	0.8991 ± 0.0014
1.0000	0.9325 ± 0.0013	0.9335 ± 0.0013

Table 6.4.1-7   PWR Single Package 10 CFR 71.55(b)(3) Evaluation k_{eff} Summary for 3.5% Enrichment

Description	$k_{eff} \pm \sigma$	$k_{eff} + 2\sigma$
Single Cask / Inner Shell Reflected with H_2O	0.8372 ± 0.0013	0.8398
Single Cask / Inner Shell and Lead Reflected with H_2O	0.9165 ± 0.0013	0.9191
Single Cask / Inner Shell, Lead & Outer Shell Reflected with H_2O	0.9260 ± 0.0014	0.9288
Single Intact Cask Reflected with H_2O	0.9251 ± 0.0013	0.9277

Table 6.4.1-8   PWR Single Package 10 CFR 71.55(b)(3) Evaluation k_{eff} Summary for 3.7% Enrichment

Description	$k_{eff} \pm \sigma$	$k_{eff} + 2\sigma$
Single Cask / Inner Shell Reflected with H_2O	0.8363 ± 0.0014	0.8391
Single Cask / Inner Shell and Lead Reflected with H_2O	0.9184 ± 0.0014	0.9212
Single Cask / Inner Shell, Lead & Outer Shell Reflected with H_2O	0.9280 ± 0.0013	0.9306
Single Intact Cask Reflected with H_2O	0.9295 ± 0.0013	0.9321

6.4.2   BWR Fuel Assemblies

This section presents the criticality analyses for the NAC-LWT cask with the BWR assembly and basket configuration. Criticality analyses of the two assembly arrangement with the most limiting assembly type are performed to satisfy the criticality safety requirements of 10 CFR Parts 71.55 and 71.59 as well as IAEA Transportation Safety Standards (TS-R-1). In this analysis, the bounding BWR assembly type is determined, and an array of 20 NAC-LWT casks loaded with this design basis BWR assembly is studied for criticality under both normal and accident conditions. Spacing between the casks and moderator density in the cavity, neutron shield tank, and outside is varied to determine the maximum k_{eff}. The reactivity effects of mechanical and geometric perturbations on the assemblies and the basket are quantified. The analyses demonstrate that, including all calculational and mechanical uncertainties, the NAC-LWT remains subcritical under both normal and accident conditions for all BWR assemblies similar in construction to those described herein.

6.4.2.1   Design Basis BWR Fuel Assembly

The k_{eff} values for infinite arrays of BWR assemblies in the basket and cask are shown in Table 6.4.2-1. The arrays contain an infinite number of infinitely long, fully loaded BWR casks on a square pitch with surfaces touching. Conditions include water at 1 gm/cc between the fuel rods and in the basket holes surrounding the assemblies. The neutron shield and cask exterior do not contain water. In addition, the results are reported for wet and dry clad gap configurations. As seen in the table, the Exxon 9×9 assembly with two water rods and an 80 mil channel (Ex 9×9-2/80) is more reactive than the other assembly types. Thus, the Ex 9×9-2/80 assembly is the most limiting, i.e., bounding, BWR assembly.

6.4.2.2   BWR Fuel Perturbation Studies

The criticality evaluation of the NAC-LWT cask with the basket loaded with design basis BWR assemblies includes studying geometric tolerances and mechanical perturbations. The tolerances and perturbations are independently evaluated for the most reactive BWR assembly, i.e., the Ex 9×9-2/80. The following perturbations and tolerances are analyzed:

I. Mechanical Perturbation
A. Fuel movement in the basket

II. Geometric Tolerances
A. Basket opening size
B. Basket divider plate thickness

The geometric tolerances associated with the manufacture of the BWR basket are listed in Table 6.4.2-2. Mechanical perturbations, i.e., fuel movement within the basket, arise from the gap between the fuel and the basket tube. The most reactive configuration analysis that evaluates these effects is performed for an infinite array of casks loaded with the design basis Ex 9×9-2/80 assembly and accident conditions with water at 1 gm/cc modeled between the fuel rods, in the clad gap, and in the basket holes surrounding the assemblies. The neutron shield and cask exterior do not contain water.

The effect of these tolerances and perturbations on the reactivity of BWR assemblies in the BWR basket and NAC-LWT cask is shown in the results presented in Table 6.4.2-3. This table shows that the perturbations do not have a statistically significant, i.e. greater than 2σ, differential in k_{eff} than the nominal case. Thus, the most reactive configuration of BWR assemblies in the basket and cask is the nominal configuration with centered assemblies and nominal basket dimensions. This configuration with the Ex 9×9-2/80 assemblies is utilized in subsequent normal and accident condition moderator density variation analyses.

6.4.2.3   Normal Condition Moderator Density Evaluations

Table 6.4.2-4 presents the cask k_{eff} for the most reactive normal condition configuration as a function of moderator density inside and outside the cask. An array of 20 casks on a triangular pitch is modeled at three cask pitches: touching (99.7 cm), 2-foot surface-to-surface (160.7 cm), and ISO-container spacing (242.84 cm). Moderator density is varied from 1.0 gm/cc to 0.0 gm/cc and for normal conditions. In addition, it is assumed that the neutron shield is filled with water. The results show an increase in reactivity with increasing internal moderator density. This indicates that moderator density changes due to increasing temperature have a negative reactivity effect. Low density moderation inside or outside of the cask does not produce abrupt increases in reactivity in comparison to other density values. The calculations show that cask pitch has no significant impact on the reactivity of the cask array under normal conditions and that k_{eff} does not vary significantly when varying external moderator with constant full density internal moderator. Because external moderator does not affect reactivity within statistical limits, the most reactive case is chosen with both internal and external moderator density at 1.0 gm/cc. The k_{eff} in this case is 0.8447 ± 0.0014. The k_{eff} for the normal condition cask array with a dry cavity is very subcritical, i.e., ~ 0.15 and is insensitive to external moderator density variations.

6.4.2.4   Accident Condition Moderator Density Evaluations

Table 6.4.2-5 shows the cask k_{eff} for the most reactive accident condition configuration as a function of moderator density variation in the cavity, neutron shield tank and outside the cask.

Again, three cask spacings are presented: touching (99.7 cm), 2-foot surface-to-surface (160.7 cm), and the ISO-container spacing (242.84 cm). Moderator density is varied from 1.0 gm/cc to 0.0 gm/cc. For accident conditions it is assumed that the neutron shield tank is punctured and that the moderator density in the tank is the same as the exterior moderator density. Again, the results show an increase in reactivity with increasing internal moderator density. Low density moderation inside or outside of the cask does not produce abrupt increases in reactivity in comparison to other density values. The calculations show that cask pitch does affect reactivity when the neutron shield is empty and that the k_{eff} for the accident condition cask array with a dry cavity, neutron shield and exterior is very subcritical, i.e., ~ 0.24. The most reactive case occurs with casks touching and the moderator density at 1.0 gm/cc in the cavity and at 0.0 gm/cc in the neutron shield tank as well as exterior. The k_{eff} in this case is 0.9232 ± 0.0013. Finally, this configuration has been modified to remove the channel. The resulting k_{eff} is 0.9292 ± 0.0012.

6.4.2.5   Single Package Evaluations

To satisfy 10 CFR 71.55(b)(3), an analysis of the reflection of the containment system (inner shell) by water is performed on a single wet cask. Successive replacement of the cask radial shields with water reflection is also evaluated. The reactivity of the system drops as each radial shield of the cask is replaced by water, from a k_{eff} = 0.8413 ± 0.0014 (k_s = 0.8580) for the full cask surrounded by water, to a k_{eff} = 0.7411 ± 0.0014 (k_s = 0.7578) for the inner shell surrounded by water. The results of this evaluation can be seen in Table 6.4.2-6.

6.4.2.6   Conclusion

A calculation of k_s under normal and accident conditions can now be made based on the previous results and based on the KENO-Va validation statistics presented in Section 6.5.1 for low enriched uranium fuel. The value k_s is calculated based on the KENO-Va Monte Carlo average plus any biases and uncertainties associated with the methods and the modeling, i.e.:

$k_s = k_{eff} + 2\sigma_{mc} + \Delta k_{Bias} + \Delta k_{BU}$

In the validation presented in Section 6.5.1, a bias of 0.0052 (allowance for under prediction of k_{eff}) and a 95/95 method uncertainty of ± 0.0087 was determined. With this bias and uncertainty, the equation for k_s becomes:

$k_s = k_{eff} + 2\sigma_{mc} + 0.0052 + 0.0087$

Thus, k_s = 0.8614 under <u>normal conditions</u> for an array of 20 NAC-LWT casks fully loaded with BWR design basis fuel and a flooded basket cavity and exterior. This is below the 0.95 regulatory limit. Under <u>accident conditions</u>, k_s = 0.9455 for an array of 20 NAC-LWT casks fully loaded with BWR design basis fuel and with a flooded basket cavity and dry neutron shield and exterior.

For both normal and accident conditions, the calculated k_{eff} values, after correction for biases and uncertainties, are below the 0.95 limit. The analyses demonstrate that, including all calculational and mechanical uncertainties, an array of 20 NAC-LWT casks with BWR fuel remains subcritical under normal and accident conditions.

Table 6.4.2-1   BWR Most Reactive Assembly Analysis Results

Assembly Type	Number Rods		Channel Thickness	Dry Gap		Wet Gap	
	Fuel	Water		k_{eff}	σ	k_{eff}	σ
Exxon 9×9	79	2	80 Mil	0.9687	0.0013	0.9766	0.0013
Exxon 9×9	79	2	2mm	0.9711	0.0012	0.9728	0.0013
Exxon 9×9	74	2	2mm	0.9686	0.0013	0.9718	0.0012
GE 8×8	62	2	80 Mil	0.9651	0.0014	0.9711	0.0013
GE 8×8	62	2	100 Mil	0.9643	0.0013	0.9696	0.0013
GE 9×9	74	2	80 Mil	0.9636	0.0013	0.9686	0.0012
GE 7×7	49	0	80 Mil	0.9601	0.0012	0.9682	0.0013
Exxon 8×8 -2	62	2	80 Mil	0.9647	0.0013	0.9672	0.0013
GE 8×8	60	4	2mm	0.9613	0.0013	0.9669	0.0014
GE 9×9	79	2	2mm	0.9609	0.0014	0.9666	0.0012
Exxon 8×8 -1	63	1	80 Mil	0.9585	0.0012	0.9661	0.0013
GE 9×9	79	2	80 Mil	0.9604	0.0014	0.9657	0.0013
Exxon 7×7	49	0	80 Mil	0.9585	0.0013	0.9645	0.0012
GE 8×8	63	1	120 Mil	0.9557	0.0012	0.9641	0.0012
GE 8×8	63	1	100 Mil	0.9597	0.0013	0.9632	0.0012
GE 8×8	63	1	80 Mil	0.9616	0.0013	0.9631	0.0012

Table 6.4.2-2   BWR Basket Tolerances

Component	Dimension / Tolerance
Basket Diameter	13.25 in
Basket Opening	5.75 ± 0.02 in
1/8" Plate Thickness	0.125 / -0.0045 in

Table 6.4.2-3   **BWR Fuel Assembly Geometric Tolerances and Mechanical Perturbations Results**

Configuration	k_{eff}	σ
Nominal Configuration	0.9746	0.0013
Assemblies Moved Out	0.9761	0.0013
Assemblies Moved in Close	0.9654	0.0013
Assemblies on Opposite Sides	0.9711	0.0013
Assemblies on Opposite Corners	0.9737	0.0012
Max. Basket Opening	0.9731	0.0013
Min. Basket Opening	0.9754	0.0013
Min. Basket Plate Thickness	0.9739	0.0013

Table 6.4.2-4   Reactivity with BWR Fuel vs. Basket Moderator Density, Normal Conditions, Array of 20 Casks

Moderator Density	Casks Touching	2 Foot Surf.-to-Surf.	ISO Container 242.84 cm Pitch
Dry Exterior, Vary Internal Density			
0.0000	0.1428 ± 0.0003	0.1425 ± 0.0003	0.1421 ± 0.0003
0.0010	0.1433 ± 0.0004	0.1435 ± 0.0003	0.1432 ± 0.0003
0.0100	0.1508 ± 0.0003	0.1506 ± 0.0004	0.1495 ± 0.0004
0.0250	0.1630 ± 0.0004	0.1632 ± 0.0004	0.1628 ± 0.0004
0.0500	0.1861 ± 0.0005	0.1857 ± 0.0005	0.1854 ± 0.0005
0.0750	0.2096 ± 0.0005	0.2107 ± 0.0005	0.2104 ± 0.0005
0.1000	0.2358 ± 0.0006	0.2359 ± 0.0006	0.2357 ± 0.0006
0.2000	0.3398 ± 0.0008	0.3413 ± 0.0008	0.3408 ± 0.0008
0.4000	0.5272 ± 0.0011	0.5248 ± 0.0011	0.5265 ± 0.0012
0.6000	0.6673 ± 0.0012	0.6673 ± 0.0013	0.6652 ± 0.0013
0.8000	0.7666 ± 0.0013	0.7685 ± 0.0012	0.7684 ± 0.0013
0.9000	0.8107 ± 0.0013	0.8095 ± 0.0013	0.8113 ± 0.0013
1.0000	0.8464 ± 0.0013	0.8412 ± 0.0012	0.8451 ± 0.0014
Wet Interior, Vary External Density			
0.0000	0.8449 ± 0.0013	0.8442 ± 0.0013	0.8441 ± 0.0013
0.0010	0.8441 ± 0.0013	0.8435 ± 0.0014	0.8438 ± 0.0013
0.0100	0.8423 ± 0.0014	0.8437 ± 0.0013	0.8437 ± 0.0013
0.0250	0.8447 ± 0.0014	0.8434 ± 0.0013	0.8429 ± 0.0013
0.0500	0.8438 ± 0.0014	0.8434 ± 0.0013	0.8436 ± 0.0013
0.0750	0.8446 ± 0.0014	0.8445 ± 0.0015	0.8439 ± 0.0014
0.1000	0.8441 ± 0.0014	0.8431 ± 0.0013	0.8429 ± 0.0012
0.2000	0.8437 ± 0.0014	0.8474 ± 0.0013	0.8434 ± 0.0014
0.4000	0.8445 ± 0.0014	0.8435 ± 0.0013	0.8444 ± 0.0014
0.6000	0.8444 ± 0.0013	0.8427 ± 0.0013	0.8437 ± 0.0013
0.8000	0.8457 ± 0.0013	0.8463 ± 0.0013	0.8439 ± 0.0014
0.9000	0.8429 ± 0.0013	0.8439 ± 0.0013	0.8447 ± 0.0012
1.0000	0.8447 ± 0.0014	0.8450 ± 0.0013	0.8447 ± 0.0012
Vary Interior and Exterior Density Simultaneously			
0.0000	0.1428 ± 0.0003	0.1425 ± 0.0003	0.1425 ± 0.0003
0.0010	0.1434 ± 0.0003	0.1431 ± 0.0003	0.1437 ± 0.0003
0.0100	0.1505 ± 0.0004	0.1502 ± 0.0004	0.1501 ± 0.0004
0.0250	0.1625 ± 0.0004	0.1631 ± 0.0004	0.1630 ± 0.0004
0.0500	0.1860 ± 0.0004	0.1856 ± 0.0005	0.1862 ± 0.0004
0.0750	0.2107 ± 0.0005	0.2100 ± 0.0005	0.2109 ± 0.0006
0.1000	0.2351 ± 0.0006	0.2354 ± 0.0006	0.2362 ± 0.0006
0.2000	0.3403 ± 0.0008	0.3402 ± 0.0008	0.3418 ± 0.0009
0.4000	0.5280 ± 0.0011	0.5271 ± 0.0010	0.5264 ± 0.0011
0.6000	0.6658 ± 0.0013	0.6641 ± 0.0013	0.6646 ± 0.0012
0.8000	0.7696 ± 0.0013	0.7681 ± 0.0014	0.7692 ± 0.0013
0.9000	0.8093 ± 0.0013	0.8090 ± 0.0013	0.8087 ± 0.0013
1.0000	0.8446 ± 0.0013	0.8433 ± 0.0014	0.8446 ± 0.0015

Table 6.4.2-5   Reactivity with BWR Fuel vs. Basket Moderator Density, Accident
Conditions, Array of 20 Casks

Moderator Specific Gravity	Casks Touching	2 Foot Surface-to-Surface	ISO 242.84 cm Pitch
Dry Exterior, Vary Internal Density			
0.0000	0.2355 ± 0.0004	0.1849 ± 0.0004	0.1665 ± 0.0004
0.0010	0.2371 ± 0.0004	0.1854 ± 0.0004	0.1681 ± 0.0004
0.0100	0.2479 ± 0.0005	0.1940 ± 0.0004	0.1768 ± 0.0004
0.0250	0.2659 ± 0.0005	0.2105 ± 0.0005	0.1915 ± 0.0005
0.0500	0.2962 ± 0.0006	0.2387 ± 0.0006	0.2166 ± 0.0005
0.0750	0.3271 ± 0.0007	0.2677 ± 0.0006	0.2444 ± 0.0006
0.1000	0.3603 ± 0.0007	0.2970 ± 0.0006	0.2718 ± 0.0007
0.2000	0.4750 ± 0.0009	0.4096 ± 0.0009	0.3814 ± 0.0009
0.4000	0.6534 ± 0.0011	0.5911 ± 0.0011	0.5638 ± 0.0011
0.6000	0.7791 ± 0.0012	0.7212 ± 0.0013	0.6986 ± 0.0012
0.8000	0.8606 ± 0.0013	0.8151 ± 0.0013	0.7950 ± 0.0013
0.9000	0.8970 ± 0.0013	0.8519 ± 0.0014	0.8337 ± 0.0013
1.0000	0.9232 ± 0.0013	0.8822 ± 0.0014	0.8668 ± 0.0013
Wet Interior, Vary External Density			
0.0000	0.9200 ± 0.0012	0.8812 ± 0.0012	0.8678 ± 0.0013
0.0010	0.9220 ± 0.0012	0.8816 ± 0.0014	0.8622 ± 0.0014
0.0100	0.9060 ± 0.0013	0.8690 ± 0.0014	0.8564 ± 0.0014
0.0250	0.8869 ± 0.0013	0.8602 ± 0.0014	0.8491 ± 0.0014
0.0500	0.8719 ± 0.0014	0.8522 ± 0.0014	0.8511 ± 0.0013
0.0750	0.8653 ± 0.0013	0.8498 ± 0.0013	0.8509 ± 0.0012
0.1000	0.8604 ± 0.0014	0.8520 ± 0.0013	0.8506 ± 0.0014
0.2000	0.8513 ± 0.0013	0.8486 ± 0.0014	0.8506 ± 0.0012
0.4000	0.8501 ± 0.0013	0.8507 ± 0.0013	0.8501 ± 0.0013
0.6000	0.8512 ± 0.0013	0.8498 ± 0.0013	0.8512 ± 0.0014
0.8000	0.8494 ± 0.0013	0.8504 ± 0.0014	0.8501 ± 0.0013
0.9000	0.8498 ± 0.0013	0.8486 ± 0.0013	0.8515 ± 0.0013
1.0000	0.8528 ± 0.0014	0.8513 ± 0.0013	0.8500 ± 0.0013
Vary Interior and Exterior Density Simultaneously			
0.0000	0.2364 ± 0.0005	0.1841 ± 0.0004	0.1672 ± 0.0004
0.0010	0.2357 ± 0.0005	0.1855 ± 0.0004	0.1671 ± 0.0004
0.0100	0.2318 ± 0.0005	0.1856 ± 0.0004	0.1709 ± 0.0004
0.0250	0.2279 ± 0.0005	0.1895 ± 0.0004	0.1777 ± 0.0004
0.0500	0.2345 ± 0.0006	0.2051 ± 0.0005	0.1999 ± 0.0005
0.0750	0.2495 ± 0.0006	0.2284 ± 0.0006	0.2254 ± 0.0006
0.1000	0.2688 ± 0.0007	0.2541 ± 0.0007	0.2530 ± 0.0006
0.2000	0.3641 ± 0.0009	0.3563 ± 0.0008	0.3594 ± 0.0008
0.4000	0.5410 ± 0.0011	0.5400 ± 0.0011	0.5417 ± 0.0011
0.6000	0.6790 ± 0.0013	0.6759 ± 0.0013	0.6763 ± 0.0012
0.8000	0.7771 ± 0.0013	0.7756 ± 0.0013	0.7767 ± 0.0013
0.9000	0.8157 ± 0.0014	0.8152 ± 0.0013	0.8199 ± 0.0014
1.0000	0.8519 ± 0.0013	0.8495 ± 0.0013	0.8505 ± 0.0013

Table 6.4.2-6   BWR Single Package 10 CFR 71.55(b)(3) Evaluation k_{eff} Summary

Description	$k_{eff} \pm \sigma$	$k_{eff} + 2\sigma$
Single Cask / Inner Shell Reflected with H_2O	0.7411 ± 0.0014	0.7439
Single Cask / Inner Shell and Lead Reflected with H_2O	0.8331 ± 0.0013	0.8357
Single Cask / Inner Shell, Lead & Outer Shell Reflected with H_2O	0.8417 ± 0.0014	0.8445
Single Intact Cask Reflected with H_2O	0.8413 ± 0.0014	0.8441

6.4.3   MTR Fuel Elements

This section presents the criticality analyses for the NAC-LWT with the MTR fuel element and basket configuration. Criticality analyses of the seven element arrangement with the most limiting assembly type are performed with the SCALE 4.3 CSAS sequence to satisfy the criticality safety requirements of 10 CFR Parts 71.55 and 71.59 as well as IAEA Transportation Safety Standards (TS-R-1). In this analysis, the bounding MTR fuel element type is determined, and an infinite array of NAC-LWT casks loaded with this design basis MTR fuel is studied for criticality under normal and accident conditions. Spacing between the casks and moderator density in the cavity, neutron shield tank and outside is varied to determine the maximum k_{eff}. The reactivity effects of partial basket loading, loss of fuel integrity and mechanical and geometric perturbations of the fuel elements and basket plate material are quantified. The analyses demonstrate that, including all calculational and mechanical uncertainties, the NAC-LWT remains subcritical under normal and accident conditions for all MTR fuel elements that are bounded in enrichment and fissile uranium loading by the design basis assembly.

6.4.3.1   Design Basis MTR Fuel Element

The fuel/basket unit cell k_{eff} values for the HEU and LEU MTR element types are shown in Table 6.4.3-1. The results show that the HEU ORR #2, HEU HFBR and the LEU BSR fuel elements are significantly more reactive than the other element types. In addition, these three element types have the highest fissile loadings, as listed in Table 6.2.3-1 and Table 6.2.3-2. Furthermore, a study of the reactivity of the highest fissile uranium loading HEU (HFBR) and LEU (BSR) elements as a function of the spacing between fuel plates is performed, as shown in Table 6.4.3-2. As shown, the HFBR fuel element is the most reactive when the plates are free to expand to their maximum possible pitch with the basket opening, as is postulated to occur under accident conditions. Also, it is shown that the HFBR element is most reactive with its full load of 18 fuel plates. The greater spacing allowed by fewer fuel plates is shown to be less reactive. Because of this and the minor difference between the other fuel types for intact elements, the HFBR element is chosen as the design basis for further analyses.

6.4.3.2   MTR Fuel Perturbation Studies

The criticality evaluation of the NAC-LWT cask with the baskets fully loaded with design basis HFBR MTR fuel elements includes studying geometric tolerances, mechanical perturbations, moderator (H_2O) density variation and spacing variation between casks. Moderator density is varied from 1.0 gm/cc to 0.0 gm/cc. Cask center-to-center spacing is varied from touching (99.7 cm cask pitch) to ISO-container array spacing (242.84 cm cask pitch). Under normal conditions it is assumed that the neutron shield is filled with water and the fuel element plate

spacing is intact. Under accident conditions it is assumed that the fuel element plate spacing is at its most reactive within each basket opening, the neutron shield tank is punctured, and that the moderator density in the tank is the same as the exterior moderator density.

As shown in Table 6.4.3-2, k_{eff} varies significantly with plate spacing. This is because the intact HFBR fuel element is undermoderated. The largest possible pitch of the HFBR fuel plates within the MTR basket, 0.4572 cm, yields the greatest k_{eff}. Hypothetical accident condition analyses utilize fuel plates with this pitch spacing.

Geometric tolerances and mechanical perturbations are independently evaluated for intact HFBR elements during normal conditions, and optimally spaced HFBR fuel plates during accident conditions. The following perturbations and tolerances are analyzed:

I. Mechanical Perturbation
A. Fuel movement in the basket

II. Geometric Tolerances
A. Basket opening size
B. Basket steel plate thickness

The geometric tolerances associated with the manufacture of the MTR basket are listed in Table 6.4.3-3. Mechanical perturbations, i.e., fuel movement within the basket, arise from the gap between the MTR fuel and the basket tube.

The effect of these tolerances and perturbations on the reactivity of intact elements in the MTR basket and NAC-LWT cask is shown in the results presented in Table 6.4.3-4. This table shows there are three perturbations that have a higher k_{eff} than the nominal case. Two of these cases, "elements moved in close" and "elements moved in closest," are mechanical perturbations. These perturbations correspond to moving the outer elements toward the center element first on one axis and then on two axes, i.e., the top and bottom two elements are first moved down and up, respectively and then moved into the corners nearest to the center of the basket. The complementary configurations are labeled "elements moved out" and "elements moved out farthest," i.e., the top and bottom two elements are first moved up and down, respectively, and then moved into the corners farthest from the center of the basket. Since only one of these mechanical perturbations can occur at a time, the configuration with the greatest reactivity, "elements moved in close" is selected as a significant perturbation. The third case, "basket plate minimum thickness," is a geometric perturbation and is also selected as a significant perturbation. The most reactive configuration of intact elements includes the impact of fuel movement, with the elements moved in close, and the impact of geometric tolerances, by using

the minimum basket plate thickness. This configuration is utilized in the subsequent normal condition moderator density variation analyses.

The results of the mechanical and geometric perturbations for the optimally spaced fuel plates are shown in Table 6.4.3-5. This table shows that there are two perturbations that have a higher k_{eff} than the nominal case. The "minimum basket plate thickness" configuration is a geometric perturbation and the "plates moved in" configuration is a mechanical perturbation. Because the expanded plates cannot move in the vertical direction, the "plates moved in" configuration corresponds to moving the plate bundles on the horizontal axis towards the basket centerline. Conversely, the less reactive "plates moved out" configuration corresponds to moving the plate bundles away from the centerline. The most reactive configuration of optimally spaced fuel plates includes the impact of fuel movement, with the plates moved in, and the impact of geometric tolerances, by using the minimum basket plate thickness. This configuration is utilized in the subsequent hypothetical accident condition moderator density variation analyses. It should be noted that the maximum basket opening perturbation results do not exceed the nominal case by a statistically significant margin and is, therefore, not considered a part of the most reactive configuration.

6.4.3.3   MTR Fuel Moderator Density Criticality Evaluations for Normal Conditions

Table 6.4.3-6 presents the cask k_{eff} for the most reactive normal condition configuration as a function of moderator density inside and outside the cask. An infinite array of casks is modeled at three cask pitches: touching (99.7 cm), 2-foot surface-to-surface (160.7 cm), and ISO-container spacing (242.84 cm). The results show a monotonic increase in reactivity with increasing internal moderator density. This indicates that moderator density changes due to increasing temperature have a negative reactivity effect. Low density moderation inside or outside of the cask does not produce abrupt increases in reactivity in comparison to other density values. The calculations show that cask pitch has no significant impact on the reactivity of the cask array under normal conditions and that k_{eff} does not vary significantly when varying external moderator with constant full density internal moderator. Because external moderator does not affect reactivity within statistical limits, the most reactive case is chosen with both internal and external moderator density at 1.0 gm/cc. The k_{eff} in this case is 0.8107 ± 0.0024. The k_{eff} for the normal condition cask array with a dry cavity is very subcritical, i.e., ~ 0.07 and is insensitive to external moderator density variations.

The effect of partial basket loading on cask k_{eff} under normal conditions is investigated to determine if increased moderation might offset the loss of fuel loading. In this model, the central basket location is empty and filled with water instead of fuel. Also, the outer fuel elements are moved closer to the center. Moderator density is varied from 1.0 gm/cc to 0.01 gm/cc. The

results are shown in the last column of Table 6.4.3-6. These results show the same basic increase in reactivity with increasing moderator density, and a level of k_{eff} consistently below that calculated for the fully loaded basket cases.

6.4.3.4   MTR Fuel Moderator Density Criticality Evaluations for Accident Conditions

Table 6.4.3-7 shows the cask k_{eff} for the most reactive accident condition configuration as a function of moderator density variation in the cavity, neutron shield tank and outside the cask. Again, three cask spacings are presented: touching (99.7 cm), 2-foot surface-to-surface (160.7 cm), and the ISO-container spacing (242.84 cm). Again, the results show a monotonic increase in reactivity with increasing internal moderator density. Low density moderation inside or outside of the cask does not produce abrupt increases in reactivity in comparison to other density values. The calculations show that cask pitch and exterior moderator density variation does significantly affect reactivity when the neutron shield is empty and that the k_{eff} for the accident condition cask array with a dry cavity, neutron shield and exterior is very subcritical, i.e., ~ 0.31. The most reactive case occurs with casks touching and the moderator density at 1.0 gm/cc in the cavity and at 0.0 gm/cc in the neutron shield tank as well as outside. The k_{eff} in this case is 0.9005 ± 0.0021. To address the potential for slightly higher enrichments and fissile uranium loadings, this most reactive case has been analyzed with 94 wt % ^{235}U enrichment and 355 grams ^{235}U per element. The resulting k_{eff} is 0.9021 ± 0.0020.

6.4.3.5   Element Rotation

No controls are placed on the orientation, i.e., plate direction, of MTR elements within a basket opening. Thus, different orientations of MTR elements in the fuel basket are possible. To model this situation, unit cells from the HFBR unit cell analysis are stacked in a 3×3 array. The elements are arranged in several combinations with vacuum boundary conditions. It can be seen in Table 6.4.3-8 that the differences in reactivity of the different orientations are not statistically significant. Therefore, using a single element orientation in the analysis of MTR fuel is sufficient to model all permutations of element orientation.

6.4.3.6   Center Fuel Element Perturbation

The most reactive configurations of intact elements and expanded plates was developed with a nominally positioned, i.e., centered, central element or plate. To verify that these are the most reactive configurations, perturbations of the central component's position have been performed. The results are contained in Table 6.4.3-9. As seen in the table, the reactivity of the perturbations under normal conditions (intact fuel elements) do not vary by a statistically significant margin. Under accident conditions (optimum spaced plates), moving the central

element decreases reactivity. Therefore, it is reasonable to utilize a centered central fuel element for the criticality evaluations.

6.4.3.7   Mixing HEU and LEU MTR Fuel

LEU and HEU fuel elements may be mixed within an MTR basket module. To model this situation, the unit cell models for HFBR and RSG-GAS fuel elements are stacked in a 3×3 array in a KENO-Va model. The RSG-GAS fuel element is selected because, as shown in Table 6.4.3-1.

Table 6.4.3-1 has a relatively high reactivity, but the reactivity is sufficiently lower than the HEU to allow the impact of mixing HEU and LEU elements within the model to be more readily apparent. The fuels are arranged in several combinations within the array with vacuum boundary conditions. It can be seen in Table 6.4.3-10 that the reactivities of the different combinations of the HEU and LEU fuel elements within the model show a trend for lower reactivity with increasing number of LEU fuel elements within the model. Therefore, the mixing of HEU and LEU MTR fuels is bounded by the analysis of HFBR MTR fuel.

6.4.3.8   Uranium Weight Fraction in Fuel Meat

MTR fuel "meat" material is composed of a mixture of the uranium metal, or uranium oxide/silicide, with an aluminum alloying material. The design basis fuel parameters listed in Table 6.2.3-1 and Table 6.2.3-2 include the weight fraction of uranium in the fuel meat. This fraction may vary from the nominal values presented in the tables due to the manufacturing process for the fuel material. Based on the limiting maximum uranium quantities specified for the fuel and the fuel meat volume, the quantity and density of the aluminum in the meat may be calculated. The aluminum densities in the sheet are typically greater than 90% of aluminum's natural density of 2.7 g/cm^3. Since the MTR fuel plates are manufactured from a combination of U-metal, U_3O_8, or U_3Si_2 and aluminum, some variations in the nominal uranium weight fraction reported in Table 6.2.3-1 and Table 6.2.3-2 are expected. A sensitivity study is, therefore, performed on the uranium weight fraction of five types of MTR fuel elements chosen for their bounding configuration (i.e., HEU thin, medium, and thick fuel meat thickness, and LEU thin and thick fuel meat thickness). Because each MTR fuel element type contains effective aluminum densities within 10% of theoretical, the evaluations concentrate on the reactivity effect of reducing the aluminum weight percent while utilizing a fixed maximum uranium mass and enrichment for each fuel element type. This serves to vary the uranium weight fraction in the fuel meat, while maintaining the uranium mass in the fuel element at its fixed maximum value. For a given uranium mass and fuel meat volume, it is expected that reducing the mass of aluminum in the fuel meat volume would serve to increase reactivity by reducing potential neutron absorbers from the system.

The perturbation study of the aluminum weight fraction on reactivity was performed with the infinite lattice cell model used to establish the bounding fuel types as described in Section 6.4.3.1. As shown in Table 6.4.3-12, the reactivity of the system is relatively unaffected by an decrease in the uranium weight percent. For the bounding reactivity MTR fuel element (HFBR), a 50% reduction in aluminum density resulted in an increase in reactivity of less than 0.005 Δk. This compares to a reactivity margin of 0.025 below 0.95 for the highest reactivity MTR fuel element as reported in Section 6.4.3.10. All cases studied resulted in reactivity increases of less than 0.02 Δk, as reported in Table 6.4.3-12. The maximum reactivity increases occurred for the PRR and THOR MTR fuel element designs, which considered aluminum weight fraction reductions of as much as one-third that of the nominal fuel meat. Both the PRR and THOR fuel element designs have reactivities significantly below that of the design basis HFBR fuel element and do not exceed the reactivity of the HFBR element even at the low aluminum densities. Therefore it is concluded that for a fixed uranium mass in the fuel meat, the aluminum weight fraction does not have a significant effect on the bounding reactivity of the MTR fuel elements in the NAC-LWT.

6.4.3.9   Single Package Criticality Evaluation

To satisfy 10 CFR 71.55(b)(3), an analysis of the reflection of the containment system (inner shell) by water is performed on a single wet cask. Successive replacement of the cask radial shields with water reflection is also evaluated (Table 6.4.3-11). The reactivity of the system drops as each radial shield of the cask is replaced by water, from a k_{eff} = 0.8094 ± 0.0021 (k_s = 0.8317) for the full cask surrounded by water, to a k_{eff} = 0.7682 ± 0.0021 (k_s = 0.7905) for the inner shell surrounded by water.

6.4.3.10   MTR Loose Fuel Plate Evaluation

Loose MTR fuel plates may be shipped inside the NAC-LWT using an MTR plate canister. The canister consists of four rectangular aluminum side plates, and top and bottom lids, forming a 2.82 inch by 2.95 inch opening. Two parallel side plates are 0.25 inch (0.635 cm) thick with the remaining two side plates at 0.125-inch (0.3175 cm) thickness. The loose plates are inserted into the canister, which in turn is placed into one of the seven MTR basket openings. The number of fuel plates in each canister is restricted to those of an intact MTR fuel element. By restricting the number of plates to those of an intact fuel element, the criticality evaluation considering optimum pitch of the expanded MTR element, shown in Section 6.4.3.1 and Table 6.4.3-2, is applicable.

While intact, the MTR plate canister restricts the loose fuel plate pitch to a significantly smaller envelope than the basket opening (3.44 inch) employed in the evaluation shown in Table 6.4.3-2.

Since the evaluation results in Table 6.4.3-2 indicate an increase in reactivity up to the maximum fuel plate pitch possible in the basket opening, the reactivity of the MTR plate canister configuration will be significantly lower than that of the uncanistered payload.

Also considered for criticality analysis is a loose plate canister configuration in which the canister plate separates. This configuration is bounded by the accident evaluation of MTR fuel plates where the two MTR element side plates separate from the fuel plates. The accident evaluation of MTR plates is the highest reactivity case for MTR fuel and models the maximum fuel plate pitch obtainable in an MTR basket cell. The additional two canister plates running parallel to the fuel plates restrict the maximum plate pitch possible in the canister opening. The reduced pitch reduces the reactivity of the system.

6.4.3.11   Code Bias and Code Bias Uncertainty Adjustments

A calculation of k_s under normal and accident conditions can now be made based on the previous results and based on the SCALE 4.3 CSAS sequence KENO-Va validation statistics presented in Section 6.5.2 for high enriched uranium fuel. The value k_s is calculated based on the KENO-Va Monte Carlo average plus any biases and uncertainties associated with the methods and the modeling, i.e.:

$$k_s = k_{eff} + \Delta k_{Bias} + \Delta k_{BU} + 2\sigma_{MC} \leq 0.95$$

In the validation presented in Section 6.5.2, a bias of -0.0044 (allowance for overprediction of k_{eff}) and a 95/95 method uncertainty of ± 0.0181 was determined. For added conservatism, the -0.0044 bias correction is neglected. With these biases and uncertainties, the equation for k_s becomes:

$$k_s = k_{eff} + 0.0181 + 2\sigma_{MC}$$

Thus, k_s = 0.8336 under <u>normal conditions</u> for an infinite array of NAC-LWT casks with a full load of HFBR design basis fuel elements, and a flooded basket cavity and exterior. Both are below the 0.95 regulatory limit. Under <u>accident conditions,</u> k_s = 0.9242 for an infinite array of NAC-LWT casks with a full load of 94 wt % / 355 g ^{235}U per element HFBR fuel with plates expanded to their maximum pitch within the basket, and with a flooded basket cavity and dry neutron shield and exterior.

For both normal and accident conditions, the calculated k_{eff} values, after correction for biases and uncertainties, are well below the 0.95 limit. The analyses demonstrate that, including all calculational and mechanical uncertainties, an infinite array of NAC-LWT casks with MTR fuel remains subcritical under normal and accident conditions.

6.4.3.12   Bounding Physical Characteristics for MTR Fuel Elements

The purpose of this section is to document an extended licensing envelope for the NAC-LWT cask. This is accomplished by constructing and evaluating an MTR element with a set of physical characteristics bounding the fuel inventory previously documented, with margin for manufacturing tolerance and expected variations in nominal element characteristics. Since this composite fuel element is expected to significantly increase the maximum reactivity of the NAC-LWT MTR configuration, a finite cask model is constructed. The existing evaluations employed an infinite element length model, which by its nature, contained a significant conservative margin that will be required to maximize the MTR payload fissile material quantities.

To establish bounding fuel element criteria, the analysis trends in Sections 6.4.3.1 through 6.4.3.10 are reviewed. Where necessary, additional analysis is performed to establish reactivity trends on the physical parameters of the elements.

Sections 6.4.3.1 through 6.4.3.4 demonstrate that MTR elements in their intact configuration are undermoderated, and that increased reactivity is achieved by maximizing plate pitch and total fissile material mass. The evaluations also showed that the maximum reactivity basket configuration for the loose fuel plates is obtained by modeling minimum basket plate thickness and fuel plates moved toward the basket center. Fuel element rotation and shifting of the center fuel element in the basket opening have been shown not to impact reactivity of the system significantly. Section 6.4.8 documents the impact of varying the uranium weight fraction at a fixed fissile mass. As the uranium weight fraction increases and the aluminum mass decreases, the system reactivity increases.

To support the addition of MEU fuel elements to the allowable content description, an infinite array of MEU elements was evaluated in the infinite basket cell model. The results of this evaluation, shown in Table 6.4.3-13, show that increasing the ^{235}U enrichment at a fixed fissile mass raises system reactivity. Table 6.4.3-14 demonstrates that the MEU element evaluated (k_{eff} = 0.8312) is lower in reactivity than the HFBR design basis element in the intact configuration (k_{eff} = 0.8471). When evaluating the MEU element in the axially infinite basket model, containing 7 elements inside the radial shields, a maximum reactivity was obtained by maximizing plate pitch (see Table 6.4.3-14). This is consistent with the HEU and LEU evaluations shown in previous sections. The MEU evaluation also demonstrated that moving fuel plates against the basket plates (Configuration B) for a maximum pitch increases reactivity over the configuration with fuel plates separated from the basket plates by a water gap.

Reactivity trends as a function of plate pitch, fuel meat thickness, and fuel plate thickness were obtained from an infinite basket cell model containing McMaster HEU MTR elements. Physical characteristics of the McMaster HEU fuels are provided in Table 6.4.3-15. The McMaster fuel

evaluation results shown in Table 6.4.4-16 and Table 6.4.3-17 document that maximizing plate pitch, decreasing plate thickness, and increasing plate fuel meat thickness produce increases in reactivity. The evaluation also showed increases in reactivity as the result of maximizing the active fuel width.

Based on the above listed trends, the following fuel plate characteristics result in a maximum reactivity configuration.

1. Minimum clad thickness (implies maximum fuel thickness for a given plate thickness)

2. Minimum plate thickness

3. Maximum active fuel width

4. Maximum fuel mass

5. Maximum enrichment (reduces parasitic absorption in ^{238}U)

6. Minimum side plate width/length (increases moderator volume in basket cell)

7. Maximum fissile material density (at a fixed geometry, increasing fissile material mass will increase reactivity)

8. Reducing the number of fuel plates at a fixed fissile material mass per plate decreases reactivity (i.e., the increase in reactivity produced by raising the H/U ratio is offset by the decrease in fissile mass)

No trend to active fuel height is available from previous evaluations. Larger active fuel heights increase reactivity due to improved fuel to moderator ratios, but also lead to separating of the fissile material masses in the finite height basket models. The impact of active fuel height variations is, therefore, evaluated later in this section. To apply the above characteristics to the MTR elements listed in Section 6.2, a set of hybrid bounding element definitions is as shown in Table 6.4.3-18. Limits are established for HEU and LEU elements. MEU element characteristics are enveloped by the HEU fuel characteristics. Various modifications of the listed parameters are addressed in later sections of this evaluation. Modifications to the parameters are made to demonstrate that the listed value is either bounding or provides a maximum licensing envelope value. Little information is available on the tolerances associated with the fuel element parameters; therefore, the larger the envelope, the more likely that any given element will fall within the licensing basis.

Based on the information listed in Table 6.4.3-17 and the analysis trends discussed above, an initial data set with margins in the parameters for tolerances and normal variations in element characteristics is compiled for 94 wt % ^{235}U enriched fuel. The resulting data set is shown in Table 6.4.3-19. The listed data does not represent a bounding configuration for all fuel types, but does represent a starting configuration from which bounding limits for the various fuel types may be determined. The bounding configurations may contain combinations of lower fissile mass per plate, lower enrichment, varying active fuel width or height, a lower number of fuel plates or

reduced enrichment. The fuel plate pitch is determined by spacing the plates to the maximum extent, with the outer fuel plates resting on the basket plates. The resulting basket model serves as the basis for all remaining evaluations.

Results for all MTR criticality evaluations performed in this calculation package are listed in Table 6.4.3-20 and have been divided into matrix cases A through I. Each set (or individual case for certain evaluations) is designed to investigate a potential perturbation of the system or to provide a new group of limiting cask parameters.

Based on the results of analysis documented in Sets A through I, the NAC-LWT MTR cask containing up to 42 elements remains within the subcritical margin ($k_s \leq 0.95$) under the conditions listed in Table 6.4.3-21. Note that the further evaluations documented in Sections 6.4.3.13 and 6.4.3.14 provide additional allowed configurations for MTR fuel elements loaded into the NAC-LWT.

Sets A and B

Set A cases determine the most reactive placement of the fuel plates axially within the basket openings. As shown, the maximum reactivity is obtained by shifting plates toward the adjoining basket (i.e., three groups of two baskets). Set B employs the most reactive shifted scenario and varies the active fuel height. While the fuel plates are undermoderated, increasing the active fuel height serves to separate fissile material in the two baskets. As shown in the result table, the effect of separating the fissile material dominates the undermoderated state of the plates themselves and results in the minimum height model (56 cm) being bounding. Differences in reactivity for both sets of cases (Δk_{eff}) are taken from the 56 cm active fuel height shifted model.

Sets C, D and E

As shown in the Set B evaluation, the maximum bias adjusted reactivity of the NAC-LWT with the MTR containing 20 g ^{235}U per plate is significantly above the 0.95 limit. Set C, therefore, performs a fissile material study to determine the maximum amount of ^{235}U that may be placed in each plate. To remain below a k_s of 0.95, the plates are limited to 18 g ^{235}U each. Evaluating the fuel at a lower enrichment (50 wt % ^{235}U) shows that the HEU (94 wt% ^{235}U) is bounding. To demonstrate that a lower number of plates in the cask is less reactive at the 18g ^{235}U limit, Set D evaluates a reduced number of plates at maximum (optimal) pitch. Reactivity for these cases is significantly lower than that of the 23-plate case. Set E evaluates various perturbations to the input parameters of the model to demonstrate that the given input is bounding. As shown, there is no significant impact of uranium weight percent changes, modeling an aluminum extension to the width of the fuel plate, or shifting of the aluminum side plates within the plane of the basket. Reactivity decreases with a decreasing plate pitch, an extension of the element length by unfueled plate or end fitting, or changes to the plate thickness by either increasing the fuel core

material thickness or the clad thickness. Reactivity increases by decreasing the element side plate thickness, and decreases significantly when inserting two additional aluminum plates approximating the configuration with a loose fuel plate canister inserted into the model. Differences in reactivity (Δk_{eff}) for set C, D, and E are taken from the 56 cm active fuel height shifted model with 18 g ^{235}U.

Set F

Not all MTR fuel plates contain less than 18 g ^{235}U. The HFBR fuel, in particular, contains up to 19.5 g ^{235}U per plate but is limited to 18 fuel plates. An analysis is therefore performed with a bounding 19 plate and 20 g ^{235}U per plate model. The k_s for this system is below 0.95.

Set G

A limited quantity of MTR plates exist with an active fuel width greater than the 6.6 cm evaluated. Therefore, additional analysis is performed at a 7.3 cm active fuel width. Based on the evaluation of an 18 g ^{235}U per plate model, the reactivity of this system is significantly higher than that of the 6.6 cm width case. Therefore, fissile quantity per plate is restricted to 16.5 g ^{235}U.

Set H

Low enriched uranium fuel (LEU) can reach a per plate loading up 21 g ^{235}U. Therefore, evaluations at 7.3 cm and 6.6 cm active fuel width are performed with 23 plates at 22 g of LEU material (maximum 25 wt% ^{235}U). The 7.3 cm active fuel width resulted in a reactivity higher than the allowed limit. The 22 g ^{235}U plates of LEU material are, therefore, restricted to a maximum active fuel width of 6.6 cm.

Set I

NISTR fuel presents an exception to the standard MTR fuel element, since each plate has two fuel sections that are separated by a short section of non fuel-bearing aluminum. These plates may be cut at the aluminum strip, with both sections inserted into a basket opening. This evaluation demonstrates that both an intact and cut element would remain below the licensing limits at 22 grams per plate.

Sets A and B determined that a minimum active fuel should be applied as a constraining parameter. This parameter sets a lower bound on the fissile material axial linear density (g ^{235}U/cm). At a fixed linear fissile material density, while maintaining other fuel bounding parameters, reactivity of the system will be reduced as fissile material is removed from the system. Table 6.4.3-21 footnote 6 credits this system behavior by allowing lower active fuel height when reducing allowed fissile mass per plate/assembly proportionally (i.e., reducing

fissile material content by the ratio of a specific fuel assembly's active fuel height to that of the 56 cm reference minimum height).

6.4.3.13   MTR Fuel Elements with High Fissile Material Loading

This section determines the requirements for loading a high fissile material content MTR fuel element with up to 20 g ^{235}U per plate (460 g ^{235}U per element based on 23 plates). Section 6.4.3.12 has demonstrated that the HEU fuel is more reactive than LEU and MEU fuel. Therefore, only the HEU fuel is evaluated in this section. Additional evaluations are provided with the limiting characteristics of an HEU MTR element containing up to 21g ^{235}U per plate.

The models employed are similar to those of Section 6.4.3.12 with any differences originating in the modified minimum plate thickness and the amount of axial non-active fuel region material (or spacer material) in the basket. Section 6.4.3.12 relied on a minimum plate thickness of 0.115 cm and a minimum 0.7 cm offset of the active fuel region to the end of the fuel element. The offset of 0.7 cm assured an active fuel region separation of 2.67 cm (2 x 0.7 cm plus the 1.27 cm base plate). Section 6.4.3.12 analyses have shown that increasing the axial separation distance between the fissile material or increasing plate thickness will decrease system reactivity. Both of these effects are taken credit for in the evaluation of the high fissile material loaded MTR element. The minimum plate thickness and element axial end region hardware length are adjusted until k_s is below 0.95.

Evaluations for various amounts of axial hardware material reveal that with only this change, a minimum 4 cm offset, 8 cm total hardware (spacer material) must be provided for the system reactivity to remain below 0.95 (Table 6.4.3-23). Similarly, Table 6.4.3-23 shows that increasing the fuel plate thickness to 0.123 cm (1.23 mm) is insufficient by itself to reduce reactivity below 0.95. A combination of 2 cm of hardware at the top and bottom of the element, for a total of 4 cm fuel element hardware, in combination with the 0.123 cm minimum plate thickness produces the required result. While the model employed a symmetric 2 cm fuel plate extension on each end of the active fuel region, any combination of top or bottom hardware or basket spacer material resulting in a 4 cm total is sufficient to assure criticality safety. Based on this evaluation, it is permissible to load a 460 g ^{235}U element, provided that the fuel plates are at minimum 0.123 cm in thickness and that cropping of the fuel element or basket spacer material assures 4 cm axial element material separating the active fuel region. Note that 4 cm of fuel element or spacer material plus the 1.27 cm basket base plate result in a total 5.27 cm of axial separation for the limiting configuration. An enhanced fuel characteristic set is generated and shown in Table 6.4.3-22 to reflect the requirements for loading of the increased fissile material element.

At 21g ^{235}U per plate, additional loading constraint must be applied. The evaluations of the 21g ^{235}U per plate HEU elements are based on the 0.7 cm minimum offset of the active fuel region and decrease the number of plates per element and/or increase the plate minimum thickness. The results of this evaluation are added to Table 6.4.3-23 with a bounding set of fuel characteristics added to Table 6.4.3-22.

6.4.3.14   LEU MTR Fuel Elements with Increased Active Fuel Width and/or Increased Fissile Material Mass

Increased Active Fuel Width

This section determines the requirements for loading LEU fuel elements with an active fuel width larger than 6.6 cm. Section 6.4.3.12 has demonstrated an active fuel width of 7.3 cm yields a k_s of greater than 0.95. This section extends the licensing envelope to a maximum active fuel width of 7.0, 7.1 or 7.15 cm for LEU fuel.

The models employed are similar to those of Section 6.4.3.12 with differences originating in the modifications made in active fuel width, plate thickness, ^{235}U loading per plate, active fuel height, and number of fuel plates.

The 7.0 cm active fuel width evaluation shows that plate thickness, ^{235}U loading per plate, and active fuel height adjustments were sufficient to reduce system reactivity below 0.95. Evaluations of the 7.1 cm active fuel width envelope relied on changes in the number of fuel plates and plate thickness. Extending the active fuel width to 7.15 cm required an increased plate minimum thickness (0.119 cm) in conjunction with a decreased number of fuel plates, increased minimum active fuel height, or decreased fissile material load per plate. Evaluation results are shown in Table 6.4.3-24. A summary of the allowable LEU fuel characteristics is shown in Table 6.4.3-25.

An additional 7.0 cm active width plate configuration is evaluated with a maximum a 23.5 g ^{235}U per plate. To reduce system reactivity to levels bounded by the HEU design basis element (the "generic" element defined in Table 6.4.3-21) the plate thickness in this case is increased to a minimum 0.13 cm. Table 6.4.3-30 contains the results of the element characteristic analyses demonstrating that at a minimum thickness of 0.13 inch up to 23 plates of 23.5 g ^{235}U may be loaded with a maximum active fuel width of 7.0 cm, minimum active fuel height of 56 cm, and clad thickness of 0.02 cm. A maximum number of plates is defined as the limiting quantity per Section 6.4.3-12. To verify that this analysis result holds true for the thicker minimum plate thickness of 0.13 cm, a study on the number of plates in the element was performed. Table 6.4.3-30 contains the data demonstrating that no reactivity increase occurs as plate number is decreased at the minimum 0.13 cm plate thickness specified for this evaluation.

Increased Fissile Material Mass (32 g ^{235}U per plate)

LEU fuel elements may contain a ^{235}U content of up to 32 grams per plate. Based on the analysis trends observed in the previous sections, a full cask load of elements containing fissile material significantly above 22 grams per plate will exceed safety limits. Additional analyses are, therefore, performed limiting the contents of the basket module with 32 gram ^{235}U plates to four elements per basket. The center row of elements (locations 1, 2 and 3 in Figure 6.3.3-5) are not loaded. The LEU plate characteristics applied are a maximum 7.3 cm active fuel width, a minimum 56 cm fuel height, and a minimum 0.115 cm plate thickness. Twenty-three plate elements are modeled.

Table 6.4.3-27 contains the results of the criticality evaluations with the revised model. Each of the bounding MTR configurations (summarized in Table 6.4.3-26) is evaluated at full load and with a partial load in the top and bottom baskets. A single fuel type is included in this analysis set. As shown in Table 6.4.3-26, the system reactivity of the 32 gram ^{235}U per plate element (Case 25%-J) is above safety limits for both full and partially loaded top and bottom baskets (k_s must be less than 0.95). Partially loading the top and bottom baskets reduces system reactivity by approximately 0.01 Δk across all fuel types. Loading the high fissile mass (high reactivity) 32 g ^{235}U per plate LEU elements in a partially loaded basket, and locating the partially loaded baskets at the top and bottom of the basket stack have no significant effect on system reactivities — i.e., system reactivity is controlled by the adjacent (cask center) baskets containing higher reactivity, fully loaded baskets.

An evaluation of six baskets with four elements per basket of the 32 gram ^{235}U per plate LEU fuel element results in a k_{eff} of approximately 0.7. This clearly demonstrates that removing three elements from the basket reduces the basket reactivity significantly, and that replacing any fully loaded basket by the partially loaded high fissile material content element basket is bounded by the evaluations of a fully loaded (42 element) cask configuration.

Loading of the high fissile material elements is, therefore, allowed provided that the elements meet the characteristics of Table 6.4.3-28, including the limitation that any basket containing LEU MTR plates above 22 gram ^{235}U must be limited to four elements (or an equivalent number of fuel plates in a plate canister) with no fuel material in basket openings 1, 2 and 3 per Figure 6.3.3-5.

The specified (partially loaded) basket configuration relies on the moderator in the center basket row to neutronically separate the fissile material in the outer sections. As moderator density in the cask decreases, neutronic interaction among the high fissile mass LEU elements in the outer basket sections will increase. Because previous evaluations have demonstrated that the MTR element reactivity rapidly decreases as moderator density is decreased, it is, therefore, not expected that reduced moderator density will result in a system reactivity increase. To provide

quantitative support to this conclusion, moderator density studies are performed for the system with partially loaded baskets located at the top and bottom of the stack, for a system with partially loaded baskets in the cask center baskets, and for a system containing six partially loaded baskets. The partially loaded baskets contain the high fissile mass LEU elements, while the fully loaded baskets contain the maximum reactivity HEU elements ("94%-D").

As demonstrated in Figure 6.4.3-1 and Table 6.4.3-29, maximum reactivity is achieved by a fully moderated cask interior for all conditions.

Figure 6.4.3-1 also contains the results of a full set of moderator density evaluations for a system containing cell blocks that will physically prevent elements from being loaded into baskets containing high fissile mass LEU elements. The block body is composed of an aluminum tube and an aluminum top plate. As the length of the block depends on the type of MTR basket employed, and the tube represents the majority of the block mass (the top plate occupies less than three cubic inches), only the tube portion of the block is included in the model. As shown in the moderator density plot, Figure 6.4.3-1, and the result summary in Table 6.4.3-29, there is no effect from the insertion of the cell block on the models containing both full and partially loaded baskets, and only a minor effect on the lower reactivity models containing all partially loaded baskets.

6.4.3.15   MTR Payload Criticality Safety Index

Evaluations included in Sections 6.4.3.1 through 6.4.3.14 demonstrate that the bias and uncertainty adjusted reactivity (k_s) for an infinite array of NAC-LWT casks containing MTR fuel elements remains below 0.95. Therefore, the Criticality Safety Index (CSI) for all MTR payloads is 0.

Figure 6.4.3-1   Cask Interior Moderator Density and Blocked Cell Study Results
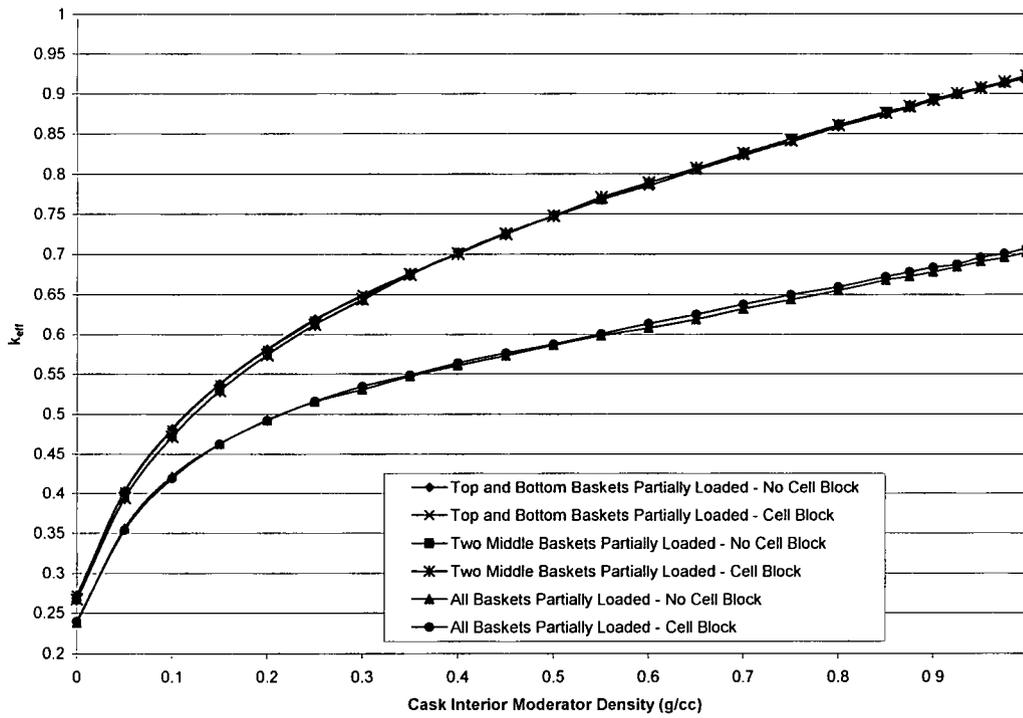
Table 6.4.3-1   Fuel/Basket Unit Cell k$_{eff}$ versus MTR Fuel Element Type

MTR Type	Plate Pitch (cm)	^{235}U Loading (grams)	k$_{eff}$ ± σ
HEU ORR	0.422	285	1.2475 ± 0.0025
LEU BSR	0.422	340	1.2486 ± 0.0022
HEU HFBR	0.371[1]	351	1.2396 ± 0.0022
HEU NISTR	0.422[2]	362	1.1808 ± 0.0027
LEU RSG-GAS	0.369	271	1.1502 ± 0.0033
HEU PRR	0.432	247	1.1594 ± 0.0027
LEU THOR	0.761	210	1.0600 ± 0.0032
LEU ZPRL	0.776	210	1.0596 ± 0.0030
LEU IEA-R1	0.431	180	1.0219 ± 0.0039
HEU THOR	0.761	140	0.9479 ± 0.0039
GRR	0.442	187.2	1.0982 ± 0.0037

1. Variable outer plate spacing.

2. Two half-sections stacked together in the basket cell. Section cuts are a minimum of 1 inch from active fuel on each end.

Table 6.4.3-2   Cask k$_{eff}$ versus Fuel Plate Spacing

Fuel Type	# of Fuel Plates	Pitch (cm)	k$_{eff}$	σ	k$_{eff}$ + 2σ
HFBR	13	0.6330*	0.7901	0.0034	0.7969
	14	0.5878*	0.8120	0.0036	0.8192
	15	0.5486*	0.8161	0.0040	0.8241
	16	0.5142*	0.8341	0.0034	0.8409
	17	0.4840*	0.8398	0.0030	0.8458
	18	0.4572*	0.8471	0.0033	0.8537
	18	0.3708	0.7918	0.0043	0.8004
	18	0.2921	0.7131	0.0040	0.7211
	18	0.2250	0.6462	0.0039	0.6540
	18	0.1270	0.5166	0.0035	0.5236
BSR	19	0.4782	0.8375	0.0027	0.8429
	19	0.3878	0.7967	0.0029	0.8027

*   Maximum possible spacing of fuel and end plates of HFBR fuel element within basket opening.

Table 6.4.3-3   MTR Basket Geometric Tolerances

Component	Dimension / Tolerance
Basket Opening	3.44 inch + 0.04 / - 0.06 inch
5/16 inch Plate Thickness	0.3125 nom. / 0.28 inch min.
1/4 inch Plate Thickness	0.25 nom. / 0.24 inch min.
11 Gauge Sheet	0.12 inch min.

Table 6.4.3-4   MTR Basket/Intact Fuel Element Geometric Tolerances and Mechanical
Perturbations Results

Configuration	k_{eff}	σ	k_{eff} + 2σ
Elements Moved in Close	0.8023	0.0021	0.8065
Min. Basket Plate Thickness	0.8014	0.0032	0.8078
Elements Moved in Closest	0.7969	0.0021	0.8011
Nominal Configuration	0.7943	0.0031	0.8005
Elements Resting on Basket	0.7928	0.0020	0.7968
Max. Basket Opening	0.7898	0.0035	0.7960
Min. Basket Opening	0.7931	0.0032	0.7995
Elements Moved Out	0.7759	0.0019	0.7797
Elements Moved Out Furthest	0.7667	0.0020	0.7707

Table 6.4.3-5   MTR Basket/Optimally Spaced Fuel Plates Geometric Tolerances and
Mechanical Perturbations Results

Configuration	k_{eff}	σ	k_{eff} + 2σ
Min. Basket Plate Thickness	0.8585	0.0035	0.8655
Plates Moved In	0.8577	0.0020	0.8617
Nominal Configuration	0.8471	0.0033	0.8537
Max. Basket Opening	0.8485	0.0037	0.8559
Min. Basket Opening	0.8406	0.0031	0.8468
Plates Moved Out	0.8290	0.0019	0.8328

Table 6.4.3-6   Reactivity with MTR Fuel vs. Basket Moderator Density, Normal
                   Conditions, Dry Exterior, Infinite Array of Casks

Moderator Density	Casks Touching	2 Foot Surf.-to-Surf.	ISO Container 242.84 cm Pitch	Touching, Center Position Empty
Dry Exterior, Vary Internal Density				
0.0000	0.0705 ± 0.0004	0.0700 ± 0.0004	0.0716 ± 0.0004	N/A
0.0010	0.0728 ± 0.0004	0.0725 ± 0.0004	0.0722 ± 0.0004	N/A
0.0100	0.0912 ± 0.0006	0.0910 ± 0.0005	0.0912 ± 0.0005	0.0793 ± 0.0010
0.0250	0.1227 ± 0.0007	0.1231 ± 0.0007	0.1246 ± 0.0008	N/A
0.0500	0.1789 ± 0.0009	0.1795 ± 0.0009	0.1779 ± 0.0009	0.1612 ± 0.0018
0.0750	0.2285 ± 0.0011	0.2294 ± 0.0011	0.2292 ± 0.0011	N/A
0.1000	0.2741 ± 0.0012	0.2772 ± 0.0013	0.2771 ± 0.0012	0.2513 ± 0.0025
0.2000	0.4207 ± 0.0016	0.4211 ± 0.0016	0.4178 ± 0.0017	0.3886 ± 0.0032
0.4000	0.5868 ± 0.0019	0.5861 ± 0.0018	0.5864 ± 0.0019	0.5170 ± 0.0037
0.6000	0.6831 ± 0.0021	0.6792 ± 0.0020	0.6817 ± 0.0019	0.5829 ± 0.0037
0.8000	0.7511 ± 0.0020	0.7515 ± 0.0020	0.7539 ± 0.0020	0.6289 ± 0.0041
0.9000	0.7830 ± 0.0019	0.7773 ± 0.0021	0.7827 ± 0.0020	N/A
1.0000	0.8072 ± 0.0019	0.8105 ± 0.0020	0.8102 ± 0.0019	0.6639 ± 0.0041
Wet Interior, Vary External Density				
0.0000	0.8139 ± 0.0021	0.8067 ± 0.0020	0.8080 ± 0.0022	N/A
0.0010	0.8116 ± 0.0020	0.8128 ± 0.0020	0.8136 ± 0.0023	N/A
0.0100	0.8108 ± 0.0021	0.8061 ± 0.0019	0.8085 ± 0.0022	N/A
0.0250	0.8078 ± 0.0019	0.8107 ± 0.0021	0.8074 ± 0.0021	N/A
0.0500	0.8066 ± 0.0022	0.8082 ± 0.0020	0.8072 ± 0.0020	N/A
0.0750	0.8113 ± 0.0020	0.8054 ± 0.0022	0.8082 ± 0.0022	N/A
0.1000	0.8097 ± 0.0020	0.8075 ± 0.0019	0.8081 ± 0.0019	N/A
0.2000	0.8133 ± 0.0020	0.8075 ± 0.0023	0.8087 ± 0.0020	N/A
0.4000	0.8096 ± 0.0018	0.8113 ± 0.0020	0.8087 ± 0.0018	N/A
0.6000	0.8110 ± 0.0018	0.8098 ± 0.0020	0.8103 ± 0.0020	N/A
0.8000	0.8072 ± 0.0023	0.8108 ± 0.0019	0.8096 ± 0.0018	N/A
0.9000	0.8133 ± 0.0021	0.8080 ± 0.0021	0.8069 ± 0.0020	N/A
1.0000	0.8107 ± 0.0024	0.8096 ± 0.0022	0.8103 ± 0.0021	N/A
Vary Interior and Exterior Density Simultaneously				
0.0000	0.0705 ± 0.0004	0.0700 ± 0.0004	0.0716 ± 0.0004	N/A
0.0010	0.0736 ± 0.0004	0.0724 ± 0.0005	0.0733 ± 0.0004	N/A
0.0100	0.0906 ± 0.0005	0.0909 ± 0.0005	0.0895 ± 0.0005	N/A
0.0250	0.1239 ± 0.0007	0.1244 ± 0.0007	0.1245 ± 0.0007	N/A
0.0500	0.1774 ± 0.0008	0.1774 ± 0.0009	0.1778 ± 0.0009	N/A
0.0750	0.2291 ± 0.0011	0.2272 ± 0.0010	0.2307 ± 0.0010	N/A
0.1000	0.2750 ± 0.0011	0.2741 ± 0.0012	0.2753 ± 0.0013	N/A
0.2000	0.4204 ± 0.0016	0.4215 ± 0.0016	0.4187 ± 0.0015	N/A
0.4000	0.5809 ± 0.0018	0.5829 ± 0.0018	0.5825 ± 0.0019	N/A
0.6000	0.6833 ± 0.0020	0.6811 ± 0.0021	0.6802 ± 0.0020	N/A
0.8000	0.7547 ± 0.0020	0.7521 ± 0.0019	0.7495 ± 0.0022	N/A
0.9000	0.7821 ± 0.0021	0.7822 ± 0.0018	0.7828 ± 0.0021	N/A
1.0000	0.8107 ± 0.0024	0.8096 ± 0.0022	0.8103 ± 0.0021	N/A

Table 6.4.3-7   Reactivity with MTR Fuel vs. Basket Moderator Density, Accident
                 Conditions, Dry Exterior, Infinite Array of Casks

Moderator Specific Gravity	Casks Touching	2 Foot Surface-to-Surface	ISO 242.84 cm Pitch
Dry Exterior, Vary Internal Density			
0.0000	0.3126 ± 0.0009	0.1031 ± 0.0005	0.1000 ± 0.0005
0.0010	0.3169 ± 0.0009	0.1071 ± 0.0005	0.1024 ± 0.0005
0.0100	0.3493 ± 0.0010	0.1316 ± 0.0006	0.1266 ± 0.0006
0.0250	0.3980 ± 0.0010	0.1720 ± 0.0008	0.1686 ± 0.0007
0.0500	0.4629 ± 0.0011	0.2343 ± 0.0010	0.2336 ± 0.0010
0.0750	0.5152 ± 0.0013	0.2910 ± 0.0010	0.2845 ± 0.0012
0.1000	0.5592 ± 0.0015	0.3425 ± 0.0012	0.3335 ± 0.0013
0.2000	0.6643 ± 0.0018	0.4836 ± 0.0014	0.4830 ± 0.0016
0.4000	0.7625 ± 0.0019	0.6440 ± 0.0018	0.6424 ± 0.0019
0.6000	0.8138 ± 0.0021	0.7390 ± 0.0019	0.7367 ± 0.0020
0.8000	0.8598 ± 0.0021	0.8138 ± 0.0021	0.8061 ± 0.0021
0.9000	0.8777 ± 0.0022	0.8428 ± 0.0021	0.8411 ± 0.0019
1.0000	0.9005 ± 0.0021	0.8717 ± 0.0021	0.8690 ± 0.0019
Wet Interior, Vary External Density			
0.0000	0.9005 ± 0.0021	0.8694 ± 0.0021	0.8739 ± 0.0020
0.0010	0.8975 ± 0.0020	0.8686 ± 0.0023	0.8680 ± 0.0022
0.0100	0.8851 ± 0.0022	0.8673 ± 0.0020	0.8683 ± 0.0021
0.0250	0.8737 ± 0.0022	0.8648 ± 0.0022	0.8671 ± 0.0020
0.0500	0.8709 ± 0.0020	0.8656 ± 0.0021	0.8648 ± 0.0022
0.0750	0.8681 ± 0.0020	0.8648 ± 0.0020	0.8658 ± 0.0020
0.1000	0.8645 ± 0.0019	0.8614 ± 0.0020	0.8618 ± 0.0020
0.2000	0.8625 ± 0.0020	0.8632 ± 0.0021	0.8616 ± 0.0021
0.4000	0.8625 ± 0.0020	0.8601 ± 0.0022	0.8594 ± 0.0019
0.6000	0.8592 ± 0.0021	0.8589 ± 0.0020	0.8591 ± 0.0021
0.8000	0.8600 ± 0.0020	0.8611 ± 0.0020	0.8589 ± 0.0021
0.9000	0.8629 ± 0.0020	0.8599 ± 0.0022	0.8584 ± 0.0021
1.0000	0.8606 ± 0.0023	0.8591 ± 0.0022	0.8602 ± 0.0020
Vary Interior and Exterior Density Simultaneously			
0.0000	0.3126 ± 0.0009	0.1031 ± 0.0005	0.1000 ± 0.0005
0.0010	0.2985 ± 0.0008	0.1054 ± 0.0005	0.1025 ± 0.0005
0.0100	0.2306 ± 0.0008	0.1270 ± 0.0006	0.1245 ± 0.0007
0.0250	0.2097 ± 0.0009	0.1579 ± 0.0008	0.1594 ± 0.0008
0.0500	0.2286 ± 0.0010	0.2072 ± 0.0010	0.2092 ± 0.0009
0.0750	0.2640 ± 0.0011	0.2534 ± 0.0011	0.2533 ± 0.0012
0.1000	0.2996 ± 0.0011	0.2963 ± 0.0012	0.2972 ± 0.0012
0.2000	0.4348 ± 0.0015	0.4337 ± 0.0015	0.4332 ± 0.0017
0.4000	0.6048 ± 0.0017	0.6066 ± 0.0020	0.6037 ± 0.0018
0.6000	0.7126 ± 0.0021	0.7144 ± 0.0020	0.7134 ± 0.0019
0.8000	0.7960 ± 0.0019	0.7892 ± 0.0022	0.7984 ± 0.0022
0.9000	0.8295 ± 0.0020	0.8303 ± 0.0021	0.8289 ± 0.0021
1.0000	0.8606 ± 0.0023	0.8591 ± 0.0022	0.8602 ± 0.0020

Table 6.4.3-8   MTR Fuel Element Rotation Perturbation Study

Case	k_{eff}	σ	$k_{eff} + 2\sigma$
All Horizontal Plates	0.6011	0.0027	0.6065
Corners-Only Horizontal	0.6033	0.0025	0.6083
Corners-Only Vertical	0.6045	0.0027	0.6099
All Vertical Plates	0.6053	0.0027	0.6107

Table 6.4.3-9   MTR Basket/Center Fuel Element Perturbation Study

Fuel Type	Center Element Configuration	k_{eff}	σ	$k_{eff} + 2\sigma$
Intact Elements	Centered	0.8107	0.0020	0.8147
Intact Elements	Corner	0.8066	0.0021	0.8108
Intact Elements	Right	0.8122	0.0021	0.8164
Intact Elements	Up	0.8133	0.0021	0.8175
Expanded Plates	Centered	0.8606	0.0023	0.8652
Expanded Plates	Right	0.8547	0.0019	0.8585

Table 6.4.3-10   Mixed HEU/LEU MTR Fuel Perturbation Study

Case	k_{eff}	σ	$k_{eff} + 2\sigma$
9 HEU	0.6011	0.0027	0.6065
8 HEU 1 LEU centered	0.6033	0.0030	0.6093
6 HEU 3 LEU center row	0.5976	0.0030	0.6036
4 HEU 5 LEU + pattern	0.5894	0.0026	0.5946
8 LEU 1 HEU centered	0.5789	0.0027	0.5843
9 LEU	0.5685	0.0025	0.5735

Table 6.4.3-11   MTR Single Package 10 CFR 71.55(b)(3) Evaluation k_{eff} Summary

Description	$k_{eff} \pm \sigma$	$k_{eff} + 2\sigma$
Single Cask / Inner Shell Reflected with H_2O	0.7682 ± 0.0021	0.7724
Single Cask / Inner Shell and Lead Reflected with H_2O	0.8043 ± 0.0021	0.8085
Single Cask / Inner Shell, Lead & Outer Shell Reflected with H_2O	0.8047 ± 0.0022	0.8091
Single Intact Cask Reflected with H_2O	0.8094 ± 0.0021	0.8136

Table 6.4.3-12   MTR Fuel Uranium Weight Percentage Perturbations

Fuel Type	U wt%[1]	Effective Al Density (g/cm3)	% of Theoretical Al Density	k_{eff}	Δk_{eff}
HEU HFBR	30%[2]	2.58	96%	1.2396 ± 0.0022	n/a
	45%	1.25	46%	1.2426 ± 0.0027	0.0030
HEU PRR	12.5%[2]	2.65	98%	1.1594 ± 0.0027	n/a
	18.75%	1.64	61%	1.1679 ± 0.0025	0.0085
	33%	0.77	28%	1.1763 ± 0.0024	0.0169
HEU THOR	8.0%[2]	2.67	99%	0.9479 ± 0.0039	n/a
	12%	1.75	65%	0.9530 ± 0.0035	0.0051
	20%	0.95	35%	0.9647 ± 0.0035	0.0168
LEU THOR	40%[2]	2.46	91%	1.0600 ± 0.0032	n/a
	50%	1.64	61%	1.0628 ± 0.0035	0.0028
	60%	1.09	41%	1.0718 ± 0.0036	0.0118
LEU IEA	40%[2]	2.47	91%	1.0219 ± 0.0039	n/a
	50%	1.64	61%	1.0266 ± 0.0036	0.0047
	60%	1.09	40%	1.0272 ± 0.0042	0.0053

Notes:

[1] Uranium in Fuel Composition (wt %)

[2] Nominal value

n/a – not applicable

Table 6.4.3-13   MEU MTR Unit Cell k_{eff} Comparison (Enrichment Variation)

Description	k_{eff}	σ
13.91 g ^{235}U - 44.44 wt% ^{235}U – Al Clad	1.2476	0.0008
13.91 g ^{235}U - 44.44 wt% ^{235}U – AlMg Clad	1.2475	0.0008
14.5 g ^{235}U – 35 wt% ^{235}U – Al Clad	1.2501	0.0008
14.5 g ^{235}U – 50 wt% ^{235}U – Al Clad	1.2642	0.0008
14.5 g ^{235}U – 80 wt% ^{235}U – Al Clad	1.2844	0.0008

Table 6.4.3-14   MEU MTR Basket k_{eff} Comparison (Plate Location)

Number of Plates	Configuration(1)	k_{eff}	σ
23	A	0.8242	0.0011
22	A	0.8230	0.0010
21	A	0.8176	0.0010
23	B	0.8312	0.0010
22	B	0.8265	0.0010
21	B	0.8206	0.0010

Note:

1. Configuration A places the outer fuel plates separated from the basket plates by a space equal to one-half the spacing between the interior plates. Configuration B places the plates directly against the basket plates.

Table 6.4.3-15   Physical Characteristics of McMaster MTR Fuels

Fuel Parameters	10 Plate	18 Plate
Element Width (cm)	7.61	7.61
Element Depth (cm)	8.03	8.23
Side Plate Thickness (cm)	0.48 (0.19 inch)	0.48
No. of Plates	10	18
Plate Thickness (cm)	0.153 ± 0.005	0.127 ± 0.005
Active Fuel Length (cm)	61.0	59.1 to 60.0
Active Fuel Width (cm)	7.3	5.92 to 6.54
Active Fuel Thickness (cm)	0.051	0.0508
Clad Thickness (cm)	0.05 ± 0.008	0.038 ± 0.008
Plate Pitch	0.319 ± 0.004 inch	0.442 ± 0.004 cm
Fuel Composition	U-Al	U-Al
Wt % ^{235}U (nominal)	93.1 ± 0.1	93.1 ± 0.1
^{235}U per Fuel Element (g)	161.4 ± 0.1	212.1 ± 6
^{235}U per Plate (g)	16.0 ± 0.48	12.25 ± 0.37
Alloy per Plate (Al) (g)	58.9	50.4

Table 6.4.3-16   Reactivity of Various Parameter Variations for 10-Plate McMaster
Element

k_{eff}	σ	k_{eff}+2σ	Δk_{eff}	$\Delta k_{eff}/\sigma$	Description
1.11679	0.00083	1.11845	-	-	nominal fuel (0.153 cm plate, 0.051 cm meat, 0.8103 cm pitch)
1.11451	0.00077	1.11605	-0.00240	-3.1	decreased pitch -0.010 cm
1.11975	0.00078	1.12131	0.00286	3.7	increased pitch +0.010 cm
1.12042	0.00079	1.12200	0.00069	0.9	max pitch and decreased plate thickness -0.008
1.12020	0.00080	1.12180	0.00049	0.6	max pitch and increased plate thickness +0.008
1.11680	0.00080	1.11840	-0.00291	-3.6	max pitch/min plate thickness and decreased fuel meat thick. (0.029 cm)
1.12154	0.00080	1.12314	0.00183	2.3	max pitch/min plate thickness and increased fuel meat thick. (0.061 cm)
1.12346	0.00081	1.12508	0.00377	4.7	max pitch/min plate thickness and increased fuel meat thick. (0.077 cm)
1.13520	0.00080	1.13680	0.01549	19.4	max pitch/min plate thickness and increased fuel meat thick. (0.145 cm)

Table 6.4.3-17   Reactivity of Various Parameter Variations for 18-Plate McMaster
Element

k_{eff}	σ	k_{eff}+2σ	Δk_{eff}	$\Delta k_{eff}/\sigma$	Description
1.17730	0.00111	1.17952	-	-	nominal fuel (0.127 cm plate, 0.051 cm meat, 0.8103 cm pitch)
1.17068	0.00117	1.17302	-0.00650	-5.6	decreased pitch -0.010 cm
1.17810	0.00112	1.18034	0.00082	0.7	increased pitch +0.010 cm
1.17956	0.00119	1.18194	0.00160	1.3	max pitch and decreased plate thickness -0.008
1.17753	0.00117	1.17987	-0.00047	-0.4	max pitch and increased plate thickness +0.008
1.17646	0.00114	1.17874	-0.00160	-1.4	max pitch/min plate thickness and decreased fuel meat thick. (0.029 cm)
1.18002	0.00117	1.18236	0.00202	1.7	max pitch/min plate thickness and increased fuel meat thick. (0.061 cm)
1.19393	0.00116	1.19625	0.01591	13.7	max pitch/min plate thickness and increased fuel meat thick. (0.119 cm)
1.15124	0.00122	1.15368	-0.02584	-21.2	nominal case at minimum active fuel width (5.92 cm)

Table 6.4.3-18   MTR Limiting Fuel Configurations

Parameter	HEU/MEU	LEU
Min. side plate thickness (cm)	0.45	0.475
Min. side plate length (cm)	7.6	7.62
Min. plate thickness (cm)	0.122	0.127
Min. clad thickness (cm)	0.024	0.033
Maximum number of fuel plates	23	21
235U content per plate (g)	19.5	21
Enrichment (wt % 235U)	94	20
Max. Active Width (cm)	6.54(1)	6.0
Max. Active Fuel Height (cm)	62.5	60.0
Max. Uranium Wt %	50(2)	74

Notes:

1. A 7.3 cm active fuel width is modeled for reduced fissile material mass (^{235}U) and/or a reduced number of fuel plates.
2. Based on MEU fuel.

Table 6.4.3-19   Initial Fuel Configurations for MTR Bounding Evaluations

Variable	Value
Min. side plate thickness (cm)	0.40
Min. side plate length (cm)	7.5
Min. plate thickness (cm)	0.115
Min. clad thickness (cm)	0.020
Maximum number of fuel plates	23
235U content per plate (g)	21
Enrichment (wt % 235U)	94
Max. Active Width (cm)	6.6
Max. Active Fuel Height (cm)	65
Max. Uranium Wt %	50
Element/Plate Material Above/Below Active Fuel (cm)	0.7

Table 6.4.3-20   Reactivity Impact of Parameter Variations in the Finite Cask Model

Set	Number of Plates	^{235}U per Plate (g)	U wt %	^{235}U wt %	Fuel Width (cm)	Fuel Height (cm)	Additional Description of File Parameters	k_{eff}	σ	$k_{eff}+2\sigma$	k_s	Δk	$\Delta k_{eff}/\sigma$
A	23	20	50%	94%	6.6	65.0	Plates at bottom	0.91822	0.00093	0.92008	0.93818	-0.01358	-14.6
	23	20	50%	94%	6.6	65.0	Axial shift to cask center	0.92549	0.00094	0.92737	0.94547	-0.00631	-6.7
	23	20	50%	94%	6.6	65.0	Axial shift alternating	0.93180	0.00091	0.93362	0.95172	--	--
B	23	20	50%	94%	6.6	56.0	Alternating shift (a.s.)	0.94724	0.00091	0.94906	0.96716	0.01544	17.0
	23	20	50%	94%	6.6	60.0	Alternating shift	0.94157	0.00092	0.94341	0.96151	0.00977	10.6
	23	20	50%	94%	6.6	71.752	Alternating shift	0.93015	0.00092	0.93199	0.95009	-0.00165	-1.8
C	23	30	50%	94%	6.6	56.0	Alternating shift	1.01772	0.00097	1.01966	1.03776	0.09128	94.1
	23	19	50%	94%	6.6	56.0	Alternating shift	0.93739	0.00091	0.93921	0.95731	0.01095	12.0
	23	18	50%	94%	6.6	56.0	Alternating shift	0.92644	0.00093	0.92830	0.94640	--	--
	23	17	50%	94%	6.6	56.0	Alternating shift	0.91468	0.00099	0.91666	0.93476	-0.01176	-11.9
	23	18	50%	50%	6.6	56.0	a.s.; MEU Core	0.90732	0.00092	0.90916	0.92726	-0.01912	-20.8
D	21	18	50%	94%	6.6	56.0	Alternating shift	0.91806	0.00092	0.91990	0.93800	-0.00838	-9.1
	19	18	50%	94%	6.6	56.0	Alternating shift	0.90657	0.00097	0.90851	0.92661	-0.01987	-20.5
E	23	18	75%	94%	6.6	56.0	Alternating shift	0.92567	0.00091	0.92749	0.94559	-0.00077	-0.8
	23	18	30%	94%	6.6	56.0	Alternating shift	0.92753	0.00097	0.92947	0.94757	0.00109	1.1
	23	18	50%	94%	6.6	56.0	a.s.; pitch -0.02 cm	0.91104	0.00096	0.91296	0.93106	-0.01540	-16.0
	23	18	50%	94%	6.6	56.0	a.s.; pitch -0.04 cm	0.89691	0.00095	0.89881	0.91691	-0.02953	-31.1
	23	18	50%	94%	6.6	56.0	a.s.; side plate lateral shift	0.92711	0.00094	0.92899	0.94709	0.00067	0.7
	23	18	50%	94%	6.6	56.0	a.s.; side plates 0.5 cm	0.92357	0.00093	0.92543	0.94353	-0.00287	-3.1
	23	18	50%	94%	6.6	56.0	a.s.; side plates 0.3 cm	0.92975	0.00093	0.93161	0.94971	0.00331	3.6
	23	18	50%	94%	6.6	56.0	a.s.; canister plates added	0.89768	0.00193	0.90154	0.91964	-0.02876	-14.9
	23	18	50%	94%	6.6	56.0	a.s.; clad width +1cm	0.92573	0.00097	0.92767	0.94577	-0.00071	-0.7
	23	18	50%	94%	6.6	56.0	a.s.; clad length +4cm	0.91304	0.00094	0.91492	0.93302	-0.01340	-14.3
	23	18	50%	94%	6.6	56.0	a.s.; plate 0.125, clad 0.025	0.91525	0.00094	0.91713	0.93523	-0.01119	-11.9
	23	18	50%	94%	6.6	56.0	a.s.; plate 0.115, clad 0.020	0.91405	0.00094	0.91593	0.93403	-0.01239	-13.2
F	19	20	50%	94%	6.6	56.0	Alternating shift	0.92822	0.00096	0.93014	0.94824	--	--
G	23	18	50%	94%	7.3	56.0	Alternating shift	0.94448	0.00090	0.94628	0.96438	--	--
	23	17	50%	94%	7.3	56.0	Alternating shift	0.93237	0.00092	0.93421	0.95231	--	--
	23	16.5	50%	94%	7.3	56.0	Alternating shift	0.92550	0.00094	0.92738	0.94548	--	--
H	23	22	75%	25%	7.3	56.0	Alternating shift; LEU Core	0.94090	0.00091	0.94272	0.96082	--	--
	23	22	75%	25%	6.6	56.0	Alternating shift; LEU Core	0.91993	0.00092	0.92177	0.93987	--	--
I	34	11	50%	94%	6.6	26.0	Alternating shift	0.87068	0.00094	0.87256	0.89066	--	--
	34	11	50%	94%	6.6	30.0	Alternating shift	0.87146	0.00095	0.87336	0.89146	--	--
	17	22	50%	94%	6.6	26.0	Fuel split by 2 cm spacer	0.92616	0.00091	0.92798	0.94608	--	--

NAC International

6.4.3-26

Table 6.4.3-21   Baseline MTR Bounding Configurations

Parameter[1]	Generic	NISTR[2]
Plate thickness	≥ 0.115 cm	≥ 0.115 cm
Clad thickness	≥ 0.02 cm	≥ 0.02 cm
Number of fuel plates	≤ 23[3]	≤ 17
^{235}U content per plate	≤ 18 g[3,4,5]	≤ 22 g
Enrichment wt % ^{235}U	≤ 94[4]	≤ 94
Active width	≤ 6.6 cm[5]	≤ 6.6 cm
Active fuel height	≥ 56 cm[6]	≥ 54 cm
Maximum reactivity (k_s)	0.9482	0.9461

Notes:

[1]   Loose fuel plates meeting the requirements in this table must be loaded into a MTR plate canister.

[2]   Fuel plates may be cut in half with each half limited to 11g ^{235}U and an active fuel length between 27 and 30 cm.

[3]   At a 19 fuel plate maximum, the plates are limited to 20g ^{235}U per plate.

[4]   LEU fuel plate with up to 22g ^{235}U may be loaded at a maximum enrichment of 25 wt % ^{235}U.

[5]   At a maximum active fuel width of 7.3 cm, the plates are limited to 16.5g ^{235}U.

[6]   Active fuel height below 56 cm is allowed provided the axial (height) fissile material linear density is maintained. This is achieved by a proportionate reduction in the maximum allowed fissile material mass per plate by the ratio of the fuel plate fissile material height to the 56 cm reference height. As an example, at a minimum 42 cm active fuel height, the generic 18 g ^{235}U maximum plate (56 cm minimum active fuel height) would be reduced to an allowable maximum of 13.5 g ^{235}U (18g ^{235}U * 42/56) per plate. Reduced fuel heights may similarly be applied to the fuel configurations described in Notes 2, 3 and 4.

Table 6.4.3-22   High Fissile Mass MTR Fuel – Bounding Parameter Analysis

Parameter	Variation From Baseline (Generic) MTR		
	Increased Plate Thickness and Fissile Mass [1]	Increased Plate Thickness and Fissile Mass and Decreased Number of Plates	Increased Fissile Mass and Decreased Number of Plates
Plate thickness [cm]	≥ 0.123	≥ 0.200	≥ 0.115
Clad thickness [cm]	≥ 0.02	≥ 0.02	≥ 0.02
Number of fuel plates	≤ 23	≤ 19	≤ 17
^{235}U content per plate [g]	≤ 20	≤ 21	≤ 21
Enrichment [wt % ^{235}U]	≤ 94	≤ 94	≤ 94
Active Width [cm]	≤ 6.6	≤ 6.6	≤ 6.6
Active Fuel Height [cm]	≥ 56	≥ 56	≥ 56
Maximum reactivity (k_s)	0.9488	0.8753	0.9451

[1]   Requires a minimum 4 cm of fuel element hardware (or spacer material) separating the fuel segments axially.

Table 6.4.3-23   MTR High Fissile Content Loading Evaluation (460 g ^{235}U)

Number of Plates	^{235}U per Plate (g)	Fuel Width (cm)	Fuel Height (cm)	Plate Thickness (cm)	Offset (cm)	k_{eff}	σ	$k_{eff}+2\sigma$	k_s	Δk
23	20.0	6.6	56.0	0.115	0.7	0.94724	0.00091	0.94906	0.96716	--
23	20.0	6.6	56.0	0.115	1.7	0.94161	0.00093	0.94347	0.96157	-0.00563
23	20.0	6.6	56.0	0.115	2.0	0.93810	0.00094	0.93998	0.95808	-0.00914
23	20.0	6.6	56.0	0.115	3.0	0.93339	0.00112	0.93563	0.95373	-0.01385
23	20.0	6.6	56.0	0.115	4.0	0.92770	0.00107	0.92984	0.94794	-0.01954
23	20.0	6.6	56.0	0.123	0.7	0.93729	0.00095	0.93919	0.95729	-0.00995
23	20.0	6.6	56.0	0.123	1.7	0.93036	0.00093	0.93222	0.95032	-0.01688
23	20.0	6.6	56.0	0.123	2.0	0.92883	0.00093	0.93069	0.94879	-0.01841
19	21.0	6.6	56.0	0.200	0.7	0.85540	0.0093	0.85726	0.87526	--
17	21.0	6.6	56.0	0.115	0.7	0.92509	0.0095	0.92699	0.94509	--

Table 6.4.3-24   LEU MTR Active Fuel Width Increase Evaluation

Number of Plates	^{235}U per Plate (g)	U wt%	^{235}U wt%	Fuel Width (cm)	Fuel Height (cm)	Plate Thickness (cm)	k_{eff}	σ	$k_{eff}+2\sigma$	k_s
23	22.0	75%	25%	6.6	56.0	0.115	0.91993	0.00092	0.92177	0.93987
23	22.0	75%	25%	7.0	56.0	0.115	0.93387	0.00093	0.93573	0.95383
23	22.0	75%	25%	7.0	56.0	0.119	0.92717	0.00090	0.92897	0.94707
23	21.5	75%	25%	7.0	56.0	0.115	0.92915	0.00087	0.93089	0.94899
23	22.0	75%	25%	7.0	63.0	0.115	0.92154	0.00087	0.92328	0.94138
17	22.0	75%	25%	7.1	56.0	0.115	0.90885	0.00093	0.91071	0.92881
23	22.0	75%	25%	7.1	56.0	0.200	0.81898	0.00089	0.82076	0.83886
23	22.0	75%	25%	7.15	56.0	0.119	0.93169	0.00086	0.93341	0.95151
22	22.0	75%	25%	7.15	56.0	0.119	0.92981	0.00092	0.93165	0.94975
23	21.5	75%	25%	7.15	56.0	0.119	0.92662	0.00090	0.92842	0.94652
23	22.0	75%	25%	7.15	61.0	0.119	0.92512	0.00091	0.92694	0.94504

Table 6.4.3-25   Summary of LEU MTR Bounding Configurations

Parameter	LEU Baseline	7.0 cm Active Width			7.1 cm Active Width		7.15 cm Active Width		
		Plate Thickness	^{235}U Content	Active Length	Plate Thickness	Number of Plates	Number of Plates	^{235}U Content	Active Length
Plate thickness [cm]	≥ 0.115	≥ 0.119	≥ 0.115	≥ 0.115	≥ 0.200	≥ 0.115	≥ 0.119	≥ 0.119	≥ 0.119
Clad thickness [cm]	≥ 0.02	≥ 0.02	≥ 0.02	≥ 0.02	≥ 0.02	≥ 0.02	≥ 0.02	≥ 0.02	≥ 0.02
Number of fuel plates	≤ 23	≤ 23	≤ 23	≤ 23	≤ 23	≤ 17	≤ 22	≤ 23	≤ 23
^{235}U content per plate [g]	≤ 22	≤ 22	≤ 21.5	≤ 22	≤ 22	≤ 22	≤ 22	≤ 21.5	≤ 22
Enrichment [wt % ^{235}U]	≤ 25	≤ 25	≤ 25	≤ 25	≤ 25	≤ 25	≤ 25	≤ 25	≤ 25
Active Width [cm]	≤ 6.6	≤ 7.0	≤ 7.0	≤ 7.0	≤ 7.1	≤ 7.1	≤ 7.15	≤ 7.15	≤ 7.15
Active Fuel Height [cm]	≥ 56	≥ 56	≥ 56	≥ 63	≥ 56	≥ 56	≥ 56	≥ 56	≥ 61
Maximum reactivity (k_s)	0.93987	0.94707	0.94899	0.94138	0.83886	0.92881	0.94975	0.94652	0.94504

Table 6.4.3-26   Summary of Previous Bounding Configurations for Use in High Mass
LEU Calculations

Fuel ID	Plate Thickness [cm]	Clad Thickness [cm]	Number of Fuel Plates	^{235}U per Plate [g]	Enrichment [wt % ^{235}U]	Active Width [cm]	Active Height [cm]	Fuel Offset [cm]
25%-A	0.115	0.02	23	22	25	6.6	56	0.7
25%-B	0.119	0.02	23	22	25	7	56	0.7
25%-C	0.115	0.02	23	21.5	25	7	56	0.7
25%-D	0.115	0.02	23	22	25	7	63	0.7
25%-E	0.2	0.02	23	22	25	7.1	56	0.7
25%-F	0.115	0.02	17	22	25	7.1	56	0.7
25%-G	0.119	0.02	22	22	25	7.15	56	0.7
25%-H	0.119	0.02	23	21.5	25	7.15	56	0.7
25%-I	0.119	0.02	23	22	25	7.15	61	0.7
25%-J[1]	0.115	0.02	23	32	25	7.3	56	0.7
25%-K[1]	0.130	0.02	23	23.5	25	7.0	56	0.7
94%-A	0.115	0.02	23	18	94	6.6	56	0.7
94%-B	0.115	0.02	19	20	94	6.6	56	0.7
94%-C	0.115	0.02	23	16.5	94	7.3	56	0.7
94%-D	0.123	0.02	23	20	94	6.6	56	2.0
94%-E	0.2	0.02	19	21	94	6.6	56	0.7
94%-F	0.115	0.02	17	21	94	6.6	56	0.7

Note: All configurations previously evaluated as bounding are included with the
exception of NISTR fuel plates. The split plate design adds an additional
model complexity not required in the evaluations. The LEU high fissile mass
analysis scope is designed to demonstrate that the addition of a partially loaded
basket to the previous payloads is bounded by the maximum reactivities
already documented. Conclusions drawn from the remaining payloads are
applicable to the NISTR fuel.

---

[1] Content added in Section 6.4.3.14

Table 6.4.3-27   High Fissile Mass LEU (32 g ^{235}U per Plate) Analysis Results

| Fuel ID[1] | Same Fuel All Baskets | | | | 32g ^{235}U PBL[2] - 7.3 cm Width | | |
| | Full Load | | Partial Top/Bottom | | | Full Load | Partial Load |
	k_{eff}	Dancoff Factor	k_{eff}	Δk	k_{eff}	Δk	Δk
25%-A	0.92134	0.50241715	0.91073	-0.011	0.91254	-0.009	0.002
25%-B	0.92813	0.50706971	0.91656	-0.012	0.91521	-0.013	-0.001
25%-C	0.92913	0.50241715	0.91915	-0.010	0.91769	-0.011	-0.001
25%-D	0.92391	0.50241715	0.91091	-0.013	0.91053	-0.013	0.000
25%-E	0.81720	0.61588436	0.80189	-0.015	0.80451	-0.013	0.003
25%-F	0.91075	0.36430386	0.89951	-0.011	0.89608	-0.015	-0.003
25%-G	0.92995	0.48636374	0.91938	-0.011	0.91798	-0.012	-0.001
25%-H	0.92940	0.50706971	0.91356	-0.016	0.91640	-0.013	0.003
25%-I	0.92533	0.50706971	0.90939	-0.016	0.91298	-0.012	0.004
25%-J[3]	0.99842	0.50241715	0.98432	-0.014	--	--	--
94%-A	0.92885	0.50241715	0.91645	-0.012	0.91873	-0.010	0.002
94%-B	0.92823	0.41448367	0.91949	-0.009	0.91825	-0.010	-0.001
94%-C	0.92533	0.50241715	0.91439	-0.011	0.91572	-0.010	0.001
94%-D	0.93162	0.51188898	0.91978	-0.012	0.92071	-0.011	0.001
94%-E	0.85605	0.50536168	0.84241	-0.014	0.84414	-0.012	0.002
94%-F	0.92381	0.36430386	0.91394	-0.010	0.91466	-0.009	0.001

Note: LEU payload defined as 25%-K case in Table 6.4.3-27 is not evaluated for interface with the 32g ^{235}U top/bottom basket loading. As demonstrated in Table 6.4.3-30 the 25%-K case element reactivity is lower than other elements in this table. The table demonstrates that addition of a partial loaded basket reduces system reactivity for the full range of MTR fuel types making the evaluation of mixed load with the 25%-K case unnecessary.

---

[1] Fuel ID is the identifier for the fuel material contained in all baskets for the cases containing one fuel type, and for the fuel material in the middle baskets for cases containing two fuel types.

[2] Partial basket loading (PBL) in the top and bottom baskets. Partially loaded baskets contain four 32 g ^{235}U per plate LEU elements per basket loaded in locations 4, 5, 6 and 7 per Figure 6.3.3-5.

[3] LEU fuel material of 32 g ^{235}U per plate, up to 23 plates.

Table 6.4.3-28   LEU High Fissile Mass Bounding Configuration

Parameter	Value
Number of Elements per Basket	4
Plate thickness [cm]	≥ 0.115
Clad thickness [cm]	≥ 0.02
Number of fuel plates	≤ 23
^{235}U content per plate [g]	≤ 32
Enrichment [wt % ^{235}U]	≤ 25
Active Width [cm]	≤ 7.3
Active Fuel Height [cm]	≥ 56

Table 6.4.3-29   Cask Interior Moderator Density and Blocked Cell Study Results

Water Density	k$_{eff}$ - No Block in Cells			k$_{eff}$ - Cells Blocked		
(g/cc)	Top/Bottom	Middle	All	Top/Bottom	Middle	All
0.0001	0.27234	0.26713	0.23817	0.27245	0.26739	0.23954
0.05	0.40294	0.39430	0.35646	0.40162	0.39373	0.35399
0.1	0.48197	0.47202	0.42209	0.48063	0.47190	0.41877
0.15	0.53747	0.52908	0.46242	0.53688	0.52916	0.46267
0.2	0.58102	0.57382	0.49272	0.57990	0.57397	0.49199
0.25	0.61913	0.61263	0.51513	0.61741	0.61234	0.51569
0.3	0.64772	0.64313	0.53051	0.64984	0.64416	0.53452
0.35	0.67598	0.67399	0.54706	0.67618	0.67494	0.54860
0.4	0.70176	0.70168	0.56069	0.70205	0.70071	0.56383
0.45	0.72644	0.72472	0.57294	0.72649	0.72528	0.57630
0.5	0.74703	0.74779	0.58607	0.74782	0.74773	0.58752
0.55	0.76761	0.76773	0.59845	0.76797	0.77091	0.60062
0.6	0.78894	0.78853	0.60810	0.78536	0.78906	0.61363
0.65	0.80652	0.80700	0.61890	0.80456	0.80727	0.62501
0.7	0.82463	0.82581	0.63197	0.82236	0.82511	0.63753
0.75	0.83955	0.84342	0.64340	0.84073	0.84144	0.64965
0.8	0.85813	0.86053	0.65486	0.86006	0.86031	0.65927
0.85	0.87370	0.87748	0.66785	0.87507	0.87554	0.67184
0.875	0.88346	0.88416	0.67243	0.88172	0.88412	0.67783
0.9	0.89071	0.89426	0.67804	0.89148	0.89217	0.68348
0.925	0.89848	0.89942	0.68416	0.89951	0.90069	0.68737
0.95	0.90695	0.90763	0.69048	0.90568	0.90782	0.69599
0.975	0.91266	0.91418	0.69592	0.91351	0.91492	0.70057
0.9982	0.92071	0.92323	0.70202	0.91870	0.92264	0.70720

Table 6.4.3-30   LEU MTR Element Specification Studies (23.5g ^{235}U per Plate)

Enrichment [wt % ^{235}U]	Plate thickness [cm]	Clad thickness [cm]	Number of fuel plates	^{235}U per plate [g]	Active Width [cm]	k_{eff}	Delta to Base [Δk]
94	0.115	0.02	23	18	6.6	0.92885	N/A
25	0.13	0.02	23	23.5	7.0	0.92525	-0.0036
25	0.13	0.02	22	23.5	7.0	0.9237	-0.00515
25	0.13	0.02	21	23.5	7.0	0.92355	-0.0053
25	0.13	0.02	20	23.5	7.0	0.91981	-0.00904
25	0.13	0.02	19	23.5	7.0	0.91896	-0.00989

6.4.4   PWR and BWR Rods in a Rod Holder or Fuel Assembly Lattice

The NAC-LWT cask may transport up to 25 intact PWR or BWR fuel rods that are in a fuel rod holder or fuel assembly lattice. Up to 14 of 25 PWR or BWR fuel rods in a fuel rod holder may be classified as damaged.

6.4.4.1   Intact PWR and BWR Rods in a Rod Holder or Fuel Assembly Lattice

This section presents the criticality analysis for the NAC-LWT with up to 25 PWR or 25 BWR fuel rods of up to 5.0 wt % ^{235}U initial enrichment. No credit is taken for geometry control that is provided by the rod holder and no rod positions are specified for the rods in the lattice. Since various fuel rod arrangements may be shipped, the criticality of the PWR and BWR rods in the NAC-LWT cask cavity is studied to determine the optimum pitch and, therefore, the maximum k_{eff} for the cask. Both PWR and BWR studies evaluate rods unrestrained in the cavity. No credit is taken for any basket structure.

Cask k_{eff} versus rod fuel rod pitch is shown in Table 6.4.4-1 for the PWR analysis and Table 6.4.4-5 for the BWR study. The rod pitch, which corresponds to center-to-center spacing in a triangular and most reactive lattice formation, is varied from 1.128 cm to 5.997 cm. The limits 1.1278 cm and 5.997 cm correspond to the most compact and the most dispersed PWR rod formations in a triangular pitch, respectively. Due to the larger rod diameter, the BWR range is from 1.640 cm to 5.228 cm. These evaluations are based on an infinite array of casks with water at 1 gm/cc between the fuel rods and in the basket cavity. The neutron shield and cask exterior do not contain water and the results are reported for wet and dry clad gap configurations.

Table 6.4.4-1 and Table 6.4.4-5 show that a broad peak in k_{eff} occurs in the rod pitch range from 2.5 to 3.5 cm for the PWR rods and 3.0 to 4.0 for the BWR rods, and that there is no statistically significant difference between wet gap and dry gap reactivities. Therefore, the most reactive configuration is chosen for the PWR rod system with a wet gap and a pitch of 2.922 cm and $k_{eff} = 0.6082 \pm 0.0035$. The BWR rod most reactive configuration occurs at a pitch of 3.691 cm and a dry gap $k_{eff} = 0.7045 \pm 0.0033$. These pitches will be used in the subsequent moderator studies.

25 PWR or BWR Rods Moderator Density Criticality Evaluations for Normal Conditions

With the fuel rods at optimum pitch (2.922 cm, PWR, or 3.691 cm, BWR), Table 6.4.4-2 and Table 6.4.4-6 present the cask k_{eff} as a function of moderator density inside and outside the cask.

An infinite array of casks on a square pitch is modeled at three cask pitches: touching (99.7 cm), 2-foot surface-to-surface (160.7 cm), and ISO-container spacing (242.84 cm). The water moderator density is varied from 1.0 gm/cc to 0.0 gm/cc, and for normal conditions it is assumed

that the clad gap is dry and the neutron shield is filled with water. The results show an increase in reactivity with increasing internal moderator density. This indicates that moderator density changes due to increasing temperature have a negative reactivity effect. Low density moderation inside or outside of the cask does not produce abrupt increases in reactivity in comparison to other density values. There is no optimum at low density as expected from an undermoderated system. The calculations show that cask pitch has no significant impact on the reactivity of the cask array under normal conditions and that k_{eff} does not vary significantly when varying external moderator with constant full density internal moderator. For the PWR cases, the external moderator does not affect reactivity within statistical limits, and the most reactive case is chosen with both internal and external moderator density at 1.0 gm/cc. The k_{eff} in this case is 0.6070 ± 0.0033. Similarly, the most reactive BWR case is for a fully moderated interior, but a dry exterior, resulting in a k_{eff} of 0.7045 ± 0.0038. The external moderator does not affect reactivity since the fully moderated exterior case produces a slightly lower k_{eff} that is within statistics. For both the PWR and BWR analysis, the k_{eff} for the normal condition cask array with a dry cavity is very subcritical, i.e. ~ <0.1 and is insensitive to external moderator density variations.

Thus, up to 25 PWR or BWR rods with 5.0 wt % ^{235}U initial enrichment are acceptable in the NAC-LWT cask. An infinite array of casks with optimum interspersed moderation has been analyzed and the NAC-LWT cask with up to 25 PWR or BWR fuel rod of up to 5.0 wt % ^{235}U remains subcritical in all of the normal transport and accident conditions.

25 PWR or BWR Rods Moderator Density Criticality Evaluations for Accident Conditions

With the fuel rods at optimum pitch, Table 6.4.4-3 (PWR) and Table 6.4.4-7 (BWR) show the cask k_{eff} for the most reactive accident condition configuration as a function of moderator density variation in the cavity, neutron shield tank and outside the cask. Again, three cask spacings are presented: touching (99.7 cm), 2-foot surface-to-surface (160.7 cm), and the ISO-container spacing (242.84 cm). Moderator density is varied from 1.0 gm/cc to 0.0 gm/cc. For accident conditions it is assumed that the clad gap contains full density water and that the neutron shield tank is punctured and the moderator density in the tank is the same as the exterior moderator density. Again, the results show an increase in reactivity with increasing internal moderator density. Low density moderation inside or outside of the cask does not produce abrupt increases in reactivity in comparison to other density values. For both the PWR and BWR analyses, the calculations show that cask pitch does affect reactivity and that the k_{eff} for the accident condition cask array with a dry cavity, neutron shield and exterior is very subcritical, i.e. is less than 0.20. Reactivity is dominated by full density internal moderator. All other variations do not affect reactivity significantly. Therefore, the most reactive PWR case is chosen with casks touching and the moderator density at 1.0 gm/cc in the cavity and at 0.0 gm/cc in the neutron shield tank

as well as exterior. The k_{eff} in this case is 0.6077 ± 0.0030. Likewise, the most reactive BWR case is chosen with casks that are 242.82 cm apart (ISO case) and the moderator density at 1.0 gm/cc in the cavity and at 0.0 gm/cc in the neutron shield tank as well as exterior. The k_{eff} in this case is 0.7135 ± 0.0033.

Single Package Criticality Evaluation

To satisfy 10 CFR 71.55(b)(3), an analysis of the reflection of the containment system (inner shell) by water is performed on a single wet cask. Successive replacement of the cask radial shields with water reflection is also evaluated. The reactivity of the PWR system does not vary with statistical significance as each radial shield of the cask is replaced by water, from a k_{eff} = 0.6008 ± 0.0034 ($k_s = 0.6215$) for the full cask surrounded by water, to a $k_{eff} = 0.6001 \pm 0.0030$ ($k_s = 0.6200$) for the inner shell surrounded by water. BWR results are k_{eff}s of 0.6932 and 0.6943 for a full cask reflected and the inner shell water reflected, respectively. The results from this evaluation can be seen in Table 6.4.4-4 (PWR) and Table 6.4.4-8 (BWR).

Conclusion

A calculation of k_s under normal and accident conditions can now be made based on the previous results and based on the KENO-Va validation statistics presented in Section 6.5.1 for low enriched uranium fuel. The value k_s is calculated based on the KENO-Va Monte Carlo average plus any biases and uncertainties associated with the methods and the modeling, i.e.:

$$k_s = k_{eff} + 2\sigma_{mc} + \Delta k_{Bias} + \Delta k_{BU}$$

In the validation presented in Section 6.5.1, a bias of 0.0052 (allowance for under prediction of k_{eff}) and a 95/95 method uncertainty of ± 0.0087 was determined. With this bias and uncertainty, the equation for k_s becomes:

$$k_s = k_{eff} + 2\sigma_{mc} + 0.0052 + 0.0087$$

Thus, $k_s = 0.6275$ under normal conditions for an infinite array of NAC-LWT casks loaded with 25 PWR design basis fuel rods and a flooded basket cavity and exterior. This is below the 0.95 regulatory limit. Under accident conditions, $k_s = 0.6276$ for an infinite array of NAC-LWT casks loaded with 25 PWR design basis fuel rods and with a flooded basket cavity and dry neutron shield and exterior.

Under normal conditions, $k_s = 0.7251$ for an infinite array of NAC-LWT casks loaded with 25 BWR design basis fuel rods and a flooded basket cavity and a dry exterior. This is below the 0.95 regulatory limit. Under accident conditions, $k_s = 0.7340$ for an infinite array of NAC-LWT casks loaded with 25 BWR design basis fuel rods and with a flooded basket cavity and dry neutron shield and exterior.

For both normal and accident conditions, the calculated k_{eff} values, after correction for biases and uncertainties, are below the 0.95 limit. The analyses demonstrate that, including all calculational and mechanical uncertainties, an infinite array of NAC-LWT casks with 25 PWR or BWR fuel rods remains subcritical under normal and accident conditions.

For both normal and accident conditions, the calculated k_{eff} values, after correction for biases and uncertainties, are below the 0.95 limit. The analyses demonstrate that, including all calculational and mechanical uncertainties, an infinite array of NAC-LWT casks with 25 PWR fuel remains subcritical under normal and accident conditions.

6.4.4.2   Damaged PWR and BWR Rods in a Rod Holder

This section presents the criticality analysis for the NAC-LWT with 25 PWR or BWR fuel rods of up to 5.0 wt % ^{235}U initial enrichment classified as damaged. Although the contents is limited to 14 damaged fuel rods in a 25-rod shipment, the analysis conservatively considers all 25 rods as failing during transport. No credit is taken for any parasitic absorption in the basket, fuel can or rod holder structure. Credit is taken for the rod holder weldment to contain the fissile material during water-fuel mixture studies. Criticality analyses are performed to satisfy the criticality safety requirements of 10 CFR Parts 71.55 and 71.59, as well as IAEA Transportation Safety Standards (TS-R-1). A single cask evaluation is also performed to comply with 10CFR71.55(b)(3). The analyses demonstrate that, including all calculational and mechanical uncertainties, the NAC-LWT is subcritical during normal and accident conditions with up to 25 damaged PWR or BWR rods.

Damaged Fuel Rod Evaluation – Heterogeneous (Rod) Configurations

Damaged fuel rods are evaluated in heterogeneous configurations by analyzing unclad fuel rods in a triangular pitch. Removing the cladding conservatively removes any potential parasitic absorbers while increasing the available volume for water moderator. Three rod arrays are considered: 25 rods, 37 rods, and 61 rods. The latter two arrays are complete hexagonal arrays. The limiting pitch is determined for each PWR and BWR array. The fuel region cross-sectional area is conserved in each of the configurations. The fuel rod radii for the various arrays are summarized in Table 6.4.4-19.

Water Exterior Evaluations

As shown in Table 6.4.4-9 through Table 6.4.4-14 and Figure 6.4.4-1 and Figure 6.4.4-2, the system reactivity increases as the number of rods is increased. As the number of rods increases, so does the cross-sectional area occupied by the rod array. Since the canister provides a limited cross-sectional area for the rod array, evaluations for arrays larger than 61 rods are not required.

Based on the can outer width of 5.5 inches (13.97 cm), the can cross-sectional area is 195.16 cm^2. Using the rod radius, rod pitch, and number of rods, the area of an enclosing hexagon is calculated for each of the three PWR and BWR arrays, shown in Table 6.4.4-19. This area is compared to the can area. For both BWR and PWR fuel, the 37-rod array results in an enclosing area that is larger than the can. A further increase in the cross-sectional lattice area, required for maximum reactivity, is seen in the 61-rod array. Therefore, the use of a 61-rod array is bounding for the NAC-LWT with no larger arrays requiring analysis.

Void Exterior/Preferential Flooding Evaluations

To increase the coupling of adjacent casks in the infinite array, system reactivity is evaluated for two additional scenarios: void exterior with fully flooded cask cavity and void exterior with preferentially flooded cask cavity. Preferential flooding removes the cask interior moderator outside the fuel rod lattice providing for increased neutronic interaction between casks in the infinite array. The 61-rod hexagonal array is employed.

As shown in Table 6.4.4-15 and Table 6.4.4-16, the void exterior, completely flooded cask cavity, scenario produced slightly higher reactivities than the scenario containing a water cask exterior. This is the result of increased neutronic interaction between casks and indicates the need for preferential flooding evaluations.

The preferential flooding model encloses the 61-rod array in a fully flooded cylinder with the remaining cask cavity filled with the exterior moderator material. This allows the array to remain flooded while voiding from the remaining cask cavity space, the neutron shield and cask exterior. A range of rod pitches is evaluated for both BWR and PWR fuel to determine the maximum reactivity pitch in this configuration. Given the increased neutronic interaction between casks, the most reactive rod pitch of the previously evaluated isolated cask changes. A check is also made to determine whether the modeled array remains conservative with respect to the envelope of the rod holder.

As shown in Table 6.4.4-17 and Table 6.4.4-18, system reactivity is much higher given the preferential flooding scenario. As shown in Table 6.4.4-20, the 61-rod array remains conservative for BWR fuel under the preferential flooding scenario. A 61-rod array of PWR fuel at its most reactive pitch produces a cross sectional area slightly smaller than that produced by the rod holder exterior (186.9 cm^2 versus 195.2 cm^2 calculated for the canister). However, the area calculation takes no credit for the rod holder wall material and fuel rod tube insert, which reduce the available cross-sectional area significantly. A larger array of PWR fuel rods (with reduced diameter) is, therefore, not investigated.

Single Cask Evaluation

10 CFR 71.55(b)(3) requires an evaluation of the NAC-LWT with the containment system fully reflected by water. The containment for the NAC-LWT is the cask inner shell. While no operating condition results in a removal of the cask outer shell and lead gamma shield, the most reactive preferential flooding case for BWR fuel is reevaluated by removing the lead and outer shells (including neutron shield), and reflecting the system by water at full density on the X and Y faces (the Z boundary condition remains mirrored). The results of this analysis, a k_s = 0.60117, demonstrates that the system reactivity of the single cask, with containment fully reflected, is significantly below regulatory limits.

Homogenized Fuel/Water Evaluation

A homogenized mixture of UO_2 and water is analyzed in a finite axial model with an infinite array of casks. The width chosen for the fuel homogenization, 13.97 cm, is conservative in that the fuel material must be enclosed by the inner dimension of the rod holder.

Given the maximum fuel volume for 25 BWR fuel rods, 11588 cm^3, and a UO_2 volume fraction, the height of the homogenized mixture of UO_2 and water is calculated. For a UO_2 volume fraction of 0.16, the cross-sectional area of UO_2 is 31.23 cm^2 (195.16 cm^2 × 0.16) and the resultant axial extent is 371.11 cm. The fuel mixture is modeled at the top of the cask cavity.

The limiting UO_2 volume fraction is calculated using a void cask cavity (i.e., preferential flooding), cask exterior and neutron shield to maximize neutron interaction in the cask array. As shown in Table 6.4.4-21 and Figure 6.4.4-3, the maximum reactivity is calculated with a UO_2 volume fraction of 16 percent.

Four sets of moderator density studies are performed, as shown in Table 6.4.4-22 through Table 6.4.4-25. The studies all serve to demonstrate the maximum reactivity configuration of the voided cask cavity and cask exterior. All cases with a voided cask exterior also have a voided neutron shield; thus, the accident condition of loss of neutron shield is explicitly considered.

Single Cask Evaluation

10 CFR 71.55(b)(3) requires an evaluation of the NAC-LWT with the containment system fully reflected by water. The containment for the NAC-LWT is the cask inner shell. While no operating condition results in a removal of the cask outer shell and lead gamma shield, each of the partial flooding cases is reevaluated by removing the lead and outer shells (including neutron shield), and reflecting the system by full density water on the X and Y faces. The results of this analysis are shown in Table 6.4.4-26 and demonstrate that the system reactivity decreases with the removal of the lead, outer shell and neutron shield reflectors.

Code Bias and Code Bias Uncertainty Adjustments

A calculation of k_s under normal and accident conditions can now be made based on the results for the heterogeneous rod and the homogenized fuel/water evaluatons. Since the fuel rod (heterogeneous) configuration resulted in a significantly higher k_{eff} than the homogeneous configuration the KENO-Va validation statistics presented in Section 6.5.1 for low enriched uranium fuel are applied. The value k_s is calculated based on the KENO-Va Monte Carlo average plus any biases and uncertainties associated with the methods and the modeling, i.e.:

$$k_s = k_{eff} + 2\sigma_{mc} + \Delta k_{Bias} + \Delta k_{BU}$$

In the validation presented in Section 6.5.1, a bias of 0.0052 (allowance for under prediction of k_{eff}) and a 95/95 method uncertainty of $\pm$ 0.0087 were determined. With this bias and uncertainty, the equation for k_s becomes:

$$k_s = k_{eff} + 2\sigma_{mc} + 0.0052 + 0.0087$$

Each of the resulting tables for arrays of damaged fuel rods, Table 6.4.4-19 through Table 6.4.4-26, includes the calculated k_s. Mixtures with significantly lower k_{eff} results are not limiting.

Under accident conditions (i.e., dry neutron shield) and preferential flooding, $k_s = 0.89950$ for an infinite array of NAC-LWT casks loaded with 25 BWR design basis damaged fuel rods. The calculated k_s for PWR fuel rods is 0.77156.

The calculated k_{eff} values, after correction for biases and uncertainties, are below the 0.95 limit. The analyses demonstrate that, including all calculational and mechanical uncertainties, an infinite array of NAC-LWT casks with 25 PWR or BWR damaged fuel rods remains subcritical under normal and accident conditions.

Figure 6.4.4-1   Maximum Reactivity Pitch Determination for Damaged BWR Rod
Arrays – Water Exterior
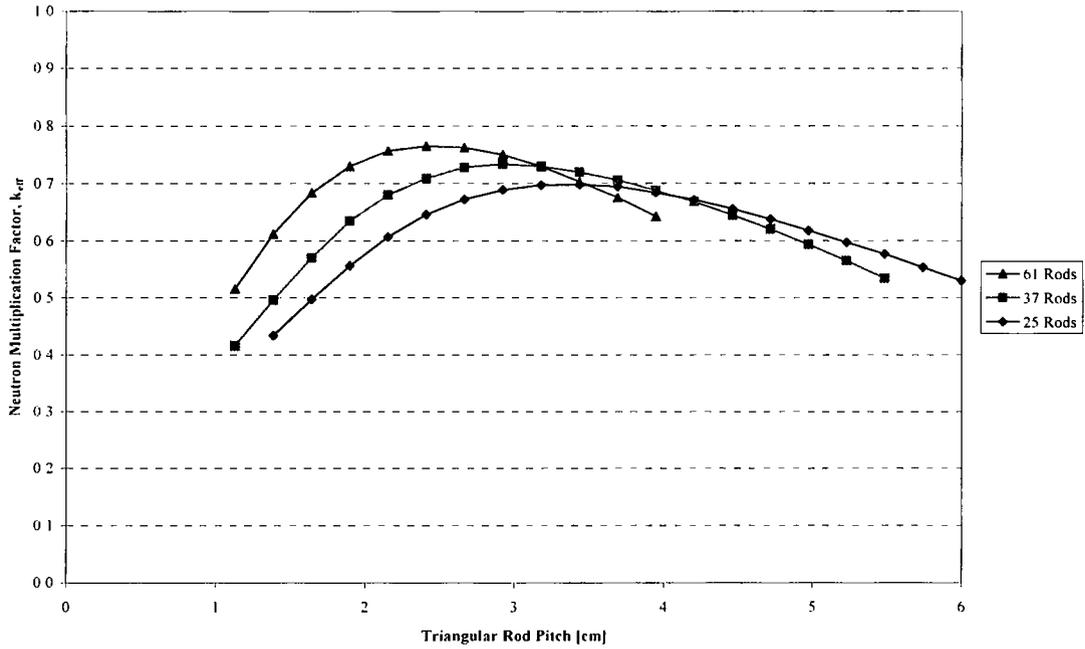
Figure 6.4.4-2   Maximum Reactivity Pitch Determination for Damaged PWR Rod
Arrays – Water Exterior
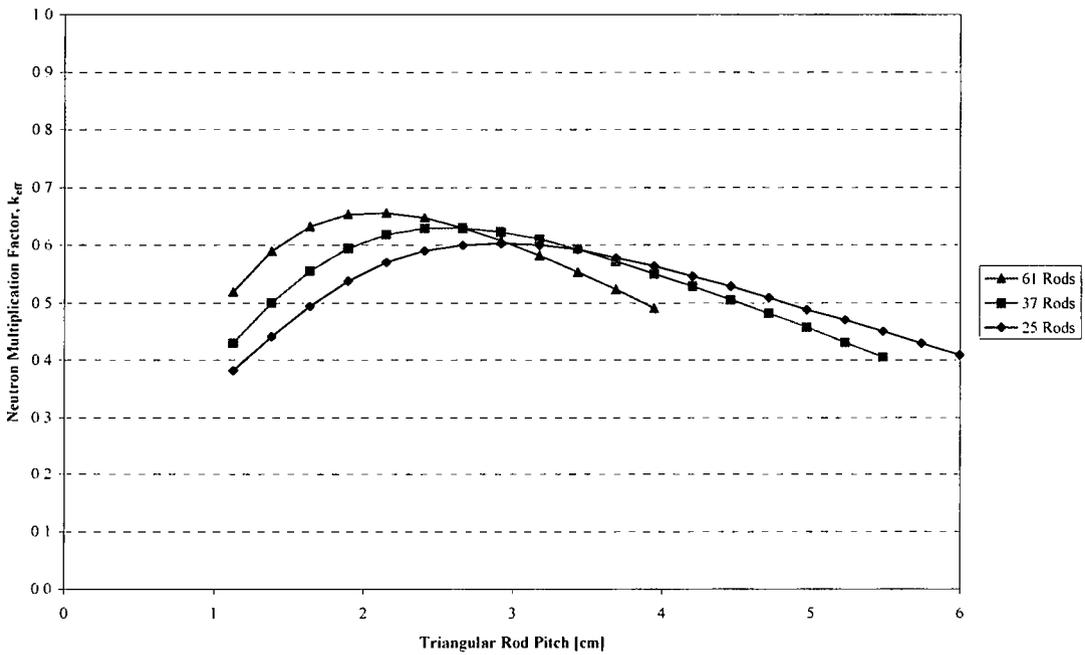
Figure 6.4.4-3   Maximum Reactivity Determination for Homogenized UO_2/Water Mixture
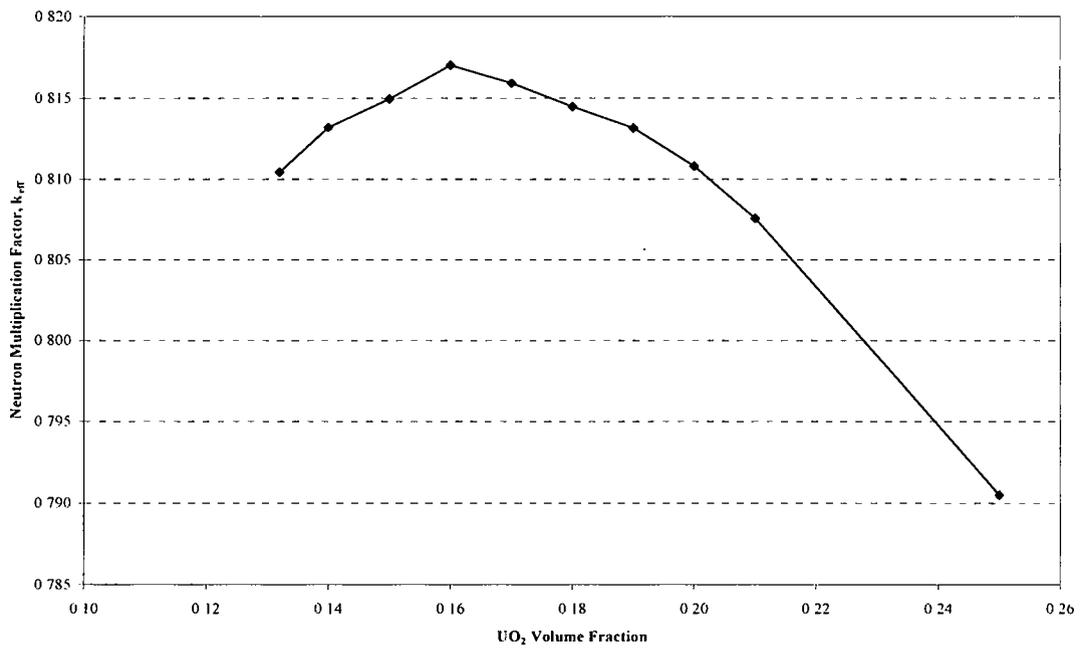
Table 6.4.4-1   NAC-LWT Cask with 25 PWR Rods, k_{eff} versus Fuel Rod Pitch, 5.0 wt %
^{235}U Initial Enrichment

Fuel Rod Pitch (cm)	Cask $k_{eff} \pm \sigma$ Wet Gap	Cask $k_{eff} \pm \sigma$ Dry Gap
1.12769	0.3581 ± 0.0027	0.3577 ± 0.0029
1.38399	0.4150 ± 0.0030	0.4167 ± 0.0033
1.64029	0.4757 ± 0.0032	0.4705 ± 0.0034
1.89659	0.5250 ± 0.0039	0.5268 ± 0.0032
2.15289	0.5578 ± 0.0035	0.5588 ± 0.0035
2.40919	0.5841 ± 0.0034	0.5801 ± 0.0035
2.66539	0.6018 ± 0.0033	0.6030 ± 0.0034
2.92169	0.6082 ± 0.0035	0.6037 ± 0.0035
3.17799	0.6037 ± 0.0034	0.6102 ± 0.0035
3.43429	0.5988 ± 0.0033	0.6002 ± 0.0033
3.69059	0.5838 ± 0.0034	0.5847 ± 0.0035
3.94689	0.5743 ± 0.0036	0.5725 ± 0.0033
4.20319	0.5610 ± 0.0032	0.5582 ± 0.0027
4.45949	0.5415 ± 0.0028	0.5464 ± 0.0036
4.71579	0.5217 ± 0.0027	0.5286 ± 0.0026
4.97209	0.5113 ± 0.0028	0.5109 ± 0.0028
5.22839	0.4858 ± 0.0026	0.4885 ± 0.0032
5.48459	0.4756 ± 0.0026	0.4763 ± 0.0030
5.74089	0.4562 ± 0.0029	0.4564 ± 0.0029
5.99719	0.4402 ± 0.0029	0.4385 ± 0.0028

Table 6.4.4-2   Reactivity with 25 PWR Rods vs. Basket Moderator Density, Normal
Conditions, Infinite Array of Casks

Moderator Density	Casks Touching	2 Foot Surf.-to-Surf.	ISO Container 242.84 cm Pitch
Dry Exterior, Vary Internal Density			
0.0000	0.0413 ± 0.0004	0.0410 ± 0.0004	0.0410 ± 0.0005
0.0010	0.0414 ± 0.0005	0.0419 ± 0.0004	0.0421 ± 0.0004
0.0100	0.0483 ± 0.0005	0.0477 ± 0.0006	0.0488 ± 0.0005
0.0250	0.0652 ± 0.0008	0.0664 ± 0.0008	0.0645 ± 0.0008
0.0500	0.1026 ± 0.0014	0.1036 ± 0.0012	0.1051 ± 0.0012
0.0750	0.1429 ± 0.0017	0.1424 ± 0.0016	0.1453 ± 0.0015
0.1000	0.1845 ± 0.0021	0.1828 ± 0.0019	0.1860 ± 0.0022
0.2000	0.3075 ± 0.0029	0.3053 ± 0.0027	0.3070 ± 0.0026
0.4000	0.4296 ± 0.0033	0.4237 ± 0.0034	0.4265 ± 0.0036
0.6000	0.4959 ± 0.0036	0.4988 ± 0.0037	0.4931 ± 0.0030
0.8000	0.5615 ± 0.0035	0.5562 ± 0.0038	0.5560 ± 0.0034
0.9000	0.5823 ± 0.0035	0.5868 ± 0.0033	0.5866 ± 0.0036
1.0000	0.6056 ± 0.0036	0.6002 ± 0.0035	0.6030 ± 0.0030
Wet Interior, Vary External Density			
0.0000	0.5993 ± 0.0031	0.6027 ± 0.0036	0.6035 ± 0.0036
0.0010	0.5976 ± 0.0036	0.6021 ± 0.0034	0.6028 ± 0.0035
0.0100	0.6079 ± 0.0036	0.6052 ± 0.0037	0.6005 ± 0.0035
0.0250	0.6050 ± 0.0036	0.6034 ± 0.0033	0.6027 ± 0.0036
0.0500	0.6003 ± 0.0030	0.6005 ± 0.0034	0.6100 ± 0.0036
0.0750	0.6072 ± 0.0036	0.6009 ± 0.0033	0.5996 ± 0.0035
0.1000	0.6042 ± 0.0036	0.6038 ± 0.0036	0.5995 ± 0.0030
0.2000	0.6032 ± 0.0035	0.6034 ± 0.0035	0.6016 ± 0.0036
0.4000	0.6050 ± 0.0031	0.6032 ± 0.0031	0.5987 ± 0.0034
0.6000	0.6025 ± 0.0032	0.6071 ± 0.0037	0.6003 ± 0.0031
0.8000	0.5975 ± 0.0030	0.6045 ± 0.0034	0.6040 ± 0.0030
0.9000	0.5993 ± 0.0034	0.6033 ± 0.0039	0.6082 ± 0.0037
1.0000	0.6037 ± 0.0037	0.5970 ± 0.0033	0.6036 ± 0.0033
Vary Interior and Exterior Density Simultaneously			
0.0000	0.0407 ± 0.0005	0.0405 ± 0.0004	0.0409 ± 0.0004
0.0010	0.0418 ± 0.0004	0.0411 ± 0.0004	0.0418 ± 0.0005
0.0100	0.0480 ± 0.0005	0.0481 ± 0.0005	0.0488 ± 0.0005
0.0250	0.0669 ± 0.0008	0.0656 ± 0.0008	0.0649 ± 0.0007
0.0500	0.1051 ± 0.0012	0.1002 ± 0.0013	0.1034 ± 0.0012
0.0750	0.1415 ± 0.0016	0.1430 ± 0.0016	0.1464 ± 0.0018
0.1000	0.1850 ± 0.0020	0.1865 ± 0.0022	0.1826 ± 0.0019
0.2000	0.3014 ± 0.0025	0.3043 ± 0.0028	0.3011 ± 0.0027
0.4000	0.4245 ± 0.0030	0.4246 ± 0.0033	0.4193 ± 0.0032
0.6000	0.5022 ± 0.0037	0.4916 ± 0.0036	0.4998 ± 0.0031
0.8000	0.5567 ± 0.0034	0.5551 ± 0.0029	0.5550 ± 0.0034
0.9000	0.5865 ± 0.0035	0.5810 ± 0.0031	0.5725 ± 0.0033
1.0000	0.6070 ± 0.0033	0.6012 ± 0.0032	0.6012 ± 0.0034

Table 6.4.4-3   Reactivity with 25 PWR Rods vs. Basket Moderator Density, Accident Conditions, Infinite Array of Casks

Moderator Specific Gravity	Casks Touching	2 Foot Surface-to-Surface	ISO 242.84 cm Pitch
Dry Exterior, Vary Internal Density			
0.0000	0.1127 ± 0.0008	0.1135 ± 0.0008	0.1125 ± 0.0006
0.0010	0.1158 ± 0.0007	0.1161 ± 0.0007	0.1149 ± 0.0007
0.0100	0.1365 ± 0.0009	0.1377 ± 0.0009	0.1355 ± 0.0009
0.0250	0.1782 ± 0.0013	0.1778 ± 0.0012	0.1761 ± 0.0013
0.0500	0.2438 ± 0.0019	0.2392 ± 0.0018	0.2401 ± 0.0019
0.0750	0.2971 ± 0.0021	0.2974 ± 0.0021	0.2982 ± 0.0022
0.1000	0.3442 ± 0.0028	0.3404 ± 0.0027	0.3392 ± 0.0025
0.2000	0.4417 ± 0.0034	0.4417 ± 0.0030	0.4381 ± 0.0035
0.4000	0.4958 ± 0.0031	0.4941 ± 0.0032	0.4852 ± 0.0036
0.6000	0.5290 ± 0.0033	0.5228 ± 0.0034	0.5297 ± 0.0037
0.8000	0.5701 ± 0.0036	0.5689 ± 0.0034	0.5667 ± 0.0031
0.9000	0.5952 ± 0.0034	0.5842 ± 0.0030	0.5853 ± 0.0034
1.0000	0.6045 ± 0.0033	0.6040 ± 0.0032	0.6101 ± 0.0032
Wet Interior, Vary External Density			
0.0000	0.6008 ± 0.0033	0.6057 ± 0.0032	0.6047 ± 0.0034
0.0010	0.6053 ± 0.0033	0.6023 ± 0.0031	0.6046 ± 0.0036
0.0100	0.6010 ± 0.0033	0.6031 ± 0.0030	0.6036 ± 0.0032
0.0250	0.6058 ± 0.0035	0.6056 ± 0.0034	0.6002 ± 0.0029
0.0500	0.6052 ± 0.0035	0.5996 ± 0.0036	0.6028 ± 0.0037
0.0750	0.5991 ± 0.0035	0.6043 ± 0.0032	0.6017 ± 0.0034
0.1000	0.6022 ± 0.0037	0.6007 ± 0.0033	0.6081 ± 0.0036
0.2000	0.5975 ± 0.0033	0.6064 ± 0.0034	0.6016 ± 0.0032
0.4000	0.6063 ± 0.0038	0.6020 ± 0.0032	0.6090 ± 0.0035
0.6000	0.6063 ± 0.0032	0.6024 ± 0.0032	0.6014 ± 0.0035
0.8000	0.6044 ± 0.0035	0.6016 ± 0.0035	0.6018 ± 0.0034
0.9000	0.6010 ± 0.0033	0.6069 ± 0.0029	0.6041 ± 0.0035
1.0000	0.5986 ± 0.0031	0.6024 ± 0.0038	0.6060 ± 0.0034
Vary Interior and Exterior Density Simultaneously			
0.0000	0.1136 ± 0.0006	0.1110 ± 0.0006	0.1134 ± 0.0007
0.0010	0.1100 ± 0.0006	0.0985 ± 0.0007	0.0825 ± 0.0006
0.0100	0.0989 ± 0.0008	0.0696 ± 0.0007	0.0556 ± 0.0007
0.0250	0.1031 ± 0.0010	0.0769 ± 0.0010	0.0670 ± 0.0008
0.0500	0.1312 ± 0.0013	0.1090 ± 0.0013	0.1037 ± 0.0014
0.0750	0.1628 ± 0.0019	0.1483 ± 0.0018	0.1453 ± 0.0016
0.1000	0.1977 ± 0.0021	0.1854 ± 0.0020	0.1853 ± 0.0020
0.2000	0.3101 ± 0.0029	0.3018 ± 0.0025	0.3069 ± 0.0028
0.4000	0.4269 ± 0.0029	0.4287 ± 0.0032	0.4225 ± 0.0035
0.6000	0.4965 ± 0.0033	0.4952 ± 0.0035	0.4983 ± 0.0038
0.8000	0.5606 ± 0.0032	0.5614 ± 0.0035	0.5572 ± 0.0035
0.9000	0.5803 ± 0.0032	0.5782 ± 0.0037	0.5837 ± 0.0036
1.0000	0.6077 ± 0.0030	0.6011 ± 0.0037	0.5974 ± 0.0036

Table 6.4.4-4   PWR Rods, Single Package 10 CFR 71.55(b)(3) Evaluation k_{eff} Summary

Description	$k_{eff} \pm \sigma$	$k_{eff} + 2\sigma$
Single Cask / Inner Shell Reflected with H_2O	0.6001 ± 0.0030	0.6061
Single Cask / Inner Shell and Lead Reflected with H_2O	0.6079 ± 0.0036	0.6151
Single Cask / Inner Shell, Lead & Outer Shell Reflected with H_2O	0.6020 ± 0.0031	0.6082
Single Intact Cask Reflected with H_2O	0.6008 ± 0.0034	0.6076

Table 6.4.4-5   NAC-LWT Cask with 25 BWR rods, k_{eff} versus Fuel Rod Pitch, 5.0 wt % ^{235}U Initial Enrichment

Fuel Rod Pitch (cm)	Cask $k_{eff} \pm \sigma$ Wet Gap			Cask $k_{eff} \pm \sigma$ Dry Gap		
1.64029	0.45706	±	0.00286	0.45873	±	0.00342
1.89659	0.52452	±	0.00385	0.52673	±	0.00355
2.15289	0.58707	±	0.00413	0.57828	±	0.00381
2.40919	0.62675	±	0.00393	0.62288	±	0.00333
2.66539	0.66556	±	0.00348	0.66648	±	0.00382
2.92169	0.68714	±	0.00383	0.68098	±	0.00317
3.17799	0.69181	±	0.00380	0.70311	±	0.00372
3.43429	0.69862	±	0.00368	0.70173	±	0.00300
3.69059	0.70297	±	0.00367	0.70447	±	0.00333
3.94689	0.69617	±	0.00347	0.69925	±	0.00329
4.20319	0.68521	±	0.00315	0.68556	±	0.00301
4.45949	0.67665	±	0.00369	0.6743	±	0.00337
4.71579	0.65473	±	0.00331	0.66008	±	0.00322
4.97209	0.64283	±	0.00344	0.64691	±	0.00330
5.22839	0.62652	±	0.00300	0.62668	±	0.00293

Table 6.4.4-6 Reactivity with 25 BWR Rods vs. Basket Moderator Density, Normal Conditions, Infinite Array of Casks

Moderator Specific Gravity	Casks Touching			2 Foot Surface-to-Surface			ISO 242.82 cm		
Dry Exterior, Vary Internal Density									
0.0000	0.05656	+ OR -	0.00055	0.05605	+ OR -	0.00059	0.05682	+ OR -	0.00057
0.0010	0.05819	+ OR -	0.00054	0.05788	+ OR -	0.00052	0.05871	+ OR -	0.00055
0.0100	0.06800	+ OR -	0.00062	0.06777	+ OR -	0.00073	0.06698	+ OR -	0.00065
0.0250	0.09072	+ OR -	0.00091	0.09067	+ OR -	0.00099	0.09127	+ OR -	0.00093
0.0500	0.13923	+ OR -	0.00146	0.13684	+ OR -	0.00140	0.13990	+ OR -	0.00125
0.0750	0.18606	+ OR -	0.00191	0.18738	+ OR -	0.00173	0.18799	+ OR -	0.00184
0.1000	0.23476	+ OR -	0.00216	0.23439	+ OR -	0.00210	0.23364	+ OR -	0.00212
0.2000	0.38517	+ OR -	0.00344	0.37607	+ OR -	0.00269	0.37838	+ OR -	0.00317
0.4000	0.53477	+ OR -	0.00344	0.53398	+ OR -	0.00357	0.53238	+ OR -	0.00399
0.6000	0.61570	+ OR -	0.00363	0.61111	+ OR -	0.00332	0.61508	+ OR -	0.00342
0.8000	0.66499	+ OR -	0.00388	0.66829	+ OR -	0.00360	0.66555	+ OR -	0.00367
0.9000	0.67966	+ OR -	0.00366	0.68529	+ OR -	0.00334	0.68097	+ OR -	0.00328
1.0000	0.69240	+ OR -	0.00386	0.70201	+ OR -	0.00364	0.69756	+ OR -	0.00346
Moderator Specific Gravity	**Casks Touching**			**2 Foot Surface-to-Surface**			**ISO 242.82 cm**		
Wet Interior, Vary External Density									
0.0000	0.69610	+ OR -	0.00339	0.69135	+ OR -	0.00338	0.69935	+ OR -	0.00329
0.0010	0.70161	+ OR -	0.00391	0.70301	+ OR -	0.00358	0.69066	+ OR -	0.00388
0.0100	0.69020	+ OR -	0.00397	0.69402	+ OR -	0.00352	0.70044	+ OR -	0.00329
0.0250	0.69884	+ OR -	0.00379	0.69871	+ OR -	0.00389	0.70458	+ OR -	0.00381
0.0500	0.69110	+ OR -	0.00349	0.69663	+ OR -	0.00384	0.69940	+ OR -	0.00326
0.0750	0.69634	+ OR -	0.00374	0.70282	+ OR -	0.00323	0.69400	+ OR -	0.00373
0.1000	0.69592	+ OR -	0.00367	0.69793	+ OR -	0.00317	0.69605	+ OR -	0.00352
0.2000	0.69566	+ OR -	0.00323	0.69491	+ OR -	0.00368	0.69803	+ OR -	0.00339
0.4000	0.69463	+ OR -	0.00382	0.69520	+ OR -	0.00331	0.70063	+ OR -	0.00348
0.6000	0.69541	+ OR -	0.00364	0.69413	+ OR -	0.00337	0.69327	+ OR -	0.00354
0.8000	0.69669	+ OR -	0.00329	0.69355	+ OR -	0.00380	0.69196	+ OR -	0.00365
0.9000	0.69587	+ OR -	0.00348	0.70373	+ OR -	0.00343	0.70134	+ OR -	0.00335
1.0000	0.70298	+ OR -	0.00377	0.70245	+ OR -	0.00365	0.69863	+ OR -	0.00333
Moderator Specific Gravity	**Casks Touching**			**2 Foot Surface-to-Surface**			**ISO 242.82 cm**		
Vary Interior and Exterior Density Simultaneously									
0.0000	0.05730	+ OR -	0.00053	0.05650	+ OR -	0.00052	0.05718	+ OR -	0.00049
0.0010	0.05797	+ OR -	0.00060	0.05815	+ OR -	0.00056	0.05839	+ OR -	0.00059
0.0100	0.06703	+ OR -	0.00062	0.06801	+ OR -	0.00070	0.06772	+ OR -	0.00074
0.0250	0.09224	+ OR -	0.00088	0.09213	+ OR -	0.00091	0.09063	+ OR -	0.00087
0.0500	0.14064	+ OR -	0.00150	0.13757	+ OR -	0.00153	0.13709	+ OR -	0.00145
0.0750	0.18790	+ OR -	0.00202	0.18714	+ OR -	0.00212	0.18650	+ OR -	0.00176
0.1000	0.23532	+ OR -	0.00225	0.23607	+ OR -	0.00229	0.23225	+ OR -	0.00256
0.2000	0.38056	+ OR -	0.00314	0.38750	+ OR -	0.00297	0.37600	+ OR -	0.00334
0.4000	0.53150	+ OR -	0.00323	0.53738	+ OR -	0.00338	0.53434	+ OR -	0.00372
0.6000	0.61988	+ OR -	0.00371	0.61154	+ OR -	0.00338	0.61457	+ OR -	0.00380
0.8000	0.66446	+ OR -	0.00377	0.66538	+ OR -	0.00334	0.66393	+ OR -	0.00362
0.9000	0.68590	+ OR -	0.00405	0.68149	+ OR -	0.00338	0.68109	+ OR -	0.00357
1.0000	0.70435	+ OR -	0.00312	0.69210	+ OR -	0.00383	0.69897	+ OR -	0.00348

Table 6.4.4-7   Reactivity with 25 BWR Rods vs. Basket Moderator Density, Accident Conditions, Infinite Array of Casks

Moderator Specific Gravity	Casks Touching			2 Foot Surface-to-Surface			ISO 242.82 cm		
Dry Exterior, Vary Internal Density									
0.0000	0.16678	+ OR -	0.00082	0.16532	+ OR -	0.00081	0.16417	+ OR -	0.00076
0.0010	0.16927	+ OR -	0.00092	0.16818	+ OR -	0.00076	0.16919	+ OR -	0.00083
0.0100	0.19533	+ OR -	0.00098	0.19554	+ OR -	0.00111	0.19714	+ OR -	0.00108
0.0250	0.24529	+ OR -	0.00150	0.24317	+ OR -	0.00136	0.24647	+ OR -	0.00156
0.0500	0.32172	+ OR -	0.00192	0.32000	+ OR -	0.00171	0.32349	+ OR -	0.00190
0.0750	0.38479	+ OR -	0.00267	0.38527	+ OR -	0.00234	0.38571	+ OR -	0.00253
0.1000	0.44132	+ OR -	0.00298	0.43394	+ OR -	0.00301	0.43722	+ OR -	0.00262
0.2000	0.56027	+ OR -	0.00330	0.56105	+ OR -	0.00321	0.55792	+ OR -	0.00334
0.4000	0.62723	+ OR -	0.00380	0.63534	+ OR -	0.00388	0.62068	+ OR -	0.00368
0.6000	0.65834	+ OR -	0.00371	0.65642	+ OR -	0.00342	0.65566	+ OR -	0.00399
0.8000	0.68180	+ OR -	0.00370	0.67879	+ OR -	0.00333	0.68134	+ OR -	0.00369
0.9000	0.69219	+ OR -	0.00333	0.69177	+ OR -	0.00348	0.69876	+ OR -	0.00338
1.0000	0.70574	+ OR -	0.00346	0.70062	+ OR -	0.00308	0.70613	+ OR -	0.00336
Moderator Specific Gravity	**Casks Touching**			**2 Foot Surface-to-Surface**			**ISO 242.82 cm**		
Wet Interior, Vary External Density									
0.0000	0.70485	+ OR -	0.00350	0.70537	+ OR -	0.00380	0.71353	+ OR -	0.00333
0.0010	0.70559	+ OR -	0.00330	0.70379	+ OR -	0.00376	0.70277	+ OR -	0.00317
0.0100	0.69932	+ OR -	0.00319	0.69971	+ OR -	0.00303	0.69208	+ OR -	0.00359
0.0250	0.69882	+ OR -	0.00378	0.69308	+ OR -	0.00346	0.69471	+ OR -	0.00343
0.0500	0.69939	+ OR -	0.00409	0.68428	+ OR -	0.00368	0.69751	+ OR -	0.00374
0.0750	0.69777	+ OR -	0.00369	0.69635	+ OR -	0.00352	0.69247	+ OR -	0.00358
0.1000	0.70068	+ OR -	0.00317	0.69051	+ OR -	0.00326	0.70317	+ OR -	0.00354
0.2000	0.69652	+ OR -	0.00304	0.69519	+ OR -	0.00337	0.69979	+ OR -	0.00329
0.4000	0.69578	+ OR -	0.00351	0.70041	+ OR -	0.00331	0.69308	+ OR -	0.00310
0.6000	0.69367	+ OR -	0.00362	0.69188	+ OR -	0.00404	0.69766	+ OR -	0.00327
0.8000	0.70330	+ OR -	0.00363	0.69912	+ OR -	0.00373	0.70236	+ OR -	0.00344
0.9000	0.69400	+ OR -	0.00340	0.69387	+ OR -	0.00385	0.69551	+ OR -	0.00386
1.0000	0.69902	+ OR -	0.00350	0.69844	+ OR -	0.00344	0.70029	+ OR -	0.00335
Moderator Specific Gravity	**Casks Touching**			**2 Foot Surface-to-Surface**			**ISO 242.82 cm**		
Vary Interior and Exterior Density Simultaneously									
0.0000	0.16499	+ OR -	0.00076	0.16534	+ OR -	0.00084	0.16534	+ OR -	0.00084
0.0010	0.15978	+ OR -	0.00082	0.11798	+ OR -	0.00081	0.11798	+ OR -	0.00081
0.0100	0.14066	+ OR -	0.00100	0.07981	+ OR -	0.00085	0.07981	+ OR -	0.00085
0.0250	0.14370	+ OR -	0.00128	0.09501	+ OR -	0.00100	0.09501	+ OR -	0.00100
0.0500	0.17380	+ OR -	0.00174	0.13825	+ OR -	0.00129	0.13825	+ OR -	0.00129
0.0750	0.21261	+ OR -	0.00179	0.19305	+ OR -	0.00197	0.19305	+ OR -	0.00197
0.1000	0.25648	+ OR -	0.00229	0.23437	+ OR -	0.00233	0.23437	+ OR -	0.00233
0.2000	0.38917	+ OR -	0.00323	0.37995	+ OR -	0.00299	0.37995	+ OR -	0.00299
0.4000	0.53569	+ OR -	0.00371	0.52997	+ OR -	0.00334	0.52997	+ OR -	0.00334
0.6000	0.61450	+ OR -	0.00367	0.61391	+ OR -	0.00352	0.61391	+ OR -	0.00352
0.8000	0.66387	+ OR -	0.00329	0.66631	+ OR -	0.00384	0.66631	+ OR -	0.00384
0.9000	0.68209	+ OR -	0.00360	0.68136	+ OR -	0.00384	0.68136	+ OR -	0.00384
1.0000	0.69742	+ OR -	0.00378	0.68992	+ OR -	0.00387	0.68992	+ OR -	0.00387

Table 6.4.4-8   BWR Rods, Single Package 10 CFR 71.55(b)(3) Evaluation k_{eff} Summary

Description	$k_{eff} \pm \sigma$			$k_{eff} + 2\sigma$
Single Cask/ Inner Shell H₂O Reflected	0.69428	±	0.00368	0.70164
Single Cask/ Inner Shell & Lead H₂O Reflected	0.69355	±	0.00397	0.70149
Single Cask/ Inner Shell, Lead, & Outer Shell H₂O Reflected	0.69532	±	0.00373	0.70278
Single Cask H₂O Reflected	0.69322	±	0.00381	0.70084

Table 6.4.4-9   Maximum Reactivity Pitch Determination for 25 BWR Rods – Water Exterior

Cask Cavity (g/cc)	Exterior (g/cc)	Pitch (cm)	k_{eff}	σ	k_s	$k_{eff}+2\sigma$	Δk	$\Delta k/\sigma$
1	1	1.3840	0.43688	0.00070	0.45218	0.43828	-0.26228	-374.7
1	1	1.6403	0.49775	0.00076	0.51317	0.49927	-0.20129	-264.9
1	1	1.8966	0.55826	0.00078	0.57372	0.55982	-0.14074	-180.4
1	1	2.1529	0.60670	0.00083	0.62226	0.60836	-0.09220	-111.1
1	1	2.4092	0.64459	0.00080	0.66009	0.64619	-0.05437	-68.0
1	1	2.6654	0.67337	0.00081	0.68889	0.67499	-0.02557	-31.6
1	1	2.9217	0.68893	0.00084	0.70451	0.69061	-0.00995	-11.8
1	1	3.1780	0.69768	0.00080	0.71318	0.69928	-0.00128	-1.6
1	1	3.4343	0.69896	0.00080	0.71446	0.70056	--	--
1	1	3.6906	0.69337	0.00077	0.70881	0.69491	-0.00565	-7.3
1	1	3.9469	0.68509	0.00075	0.70049	0.68659	-0.01397	-18.6
1	1	4.2032	0.66997	0.00075	0.68537	0.67147	-0.02909	-38.8
1	1	4.4595	0.65593	0.00074	0.67131	0.65741	-0.04315	-58.3
1	1	4.7158	0.63801	0.00076	0.65343	0.63953	-0.06103	-80.3
1	1	4.9721	0.61716	0.00072	0.63250	0.61860	-0.08196	-113.8
1	1	5.2284	0.59692	0.00070	0.61222	0.59832	-0.10224	-146.1
1	1	5.4846	0.57611	0.00073	0.59147	0.57757	-0.12299	-168.5
1	1	5.7409	0.55318	0.00068	0.56844	0.55454	-0.14602	-214.7
1	1	5.9972	0.53013	0.00070	0.54543	0.53153	-0.16903	-241.5

Table 6.4.4-10   Maximum Reactivity Pitch Determination for 25 PWR Rods – Water Exterior

Cask Cavity (g/cc)	Exterior (g/cc)	Pitch (cm)	k_{eff}	σ	k_s	$k_{eff}+2\sigma$	Δk	$\Delta k/\sigma$
1	1	1.1277	0.38430	0.00070	0.39960	0.38570	-0.21964	-313.8
1	1	1.3840	0.44279	0.00072	0.45813	0.44423	-0.16111	-223.8
1	1	1.6403	0.49656	0.00077	0.51200	0.49810	-0.10724	-139.3
1	1	1.8966	0.53980	0.00073	0.55516	0.54126	-0.06408	-87.8
1	1	2.1529	0.56950	0.00075	0.58490	0.57100	-0.03434	-45.8
1	1	2.4092	0.59041	0.00078	0.60587	0.59197	-0.01337	-17.1
1	1	2.6654	0.60073	0.00077	0.61617	0.60227	-0.00307	-4.0
1	1	2.9217	0.60380	0.00077	0.61924	0.60534	--	--
1	1	3.1780	0.59904	0.00074	0.61442	0.60052	-0.00482	-6.5
1	1	3.4343	0.59206	0.00078	0.60752	0.59362	-0.01172	-15.0
1	1	3.6906	0.57836	0.00069	0.59364	0.57974	-0.02560	-37.1
1	1	3.9469	0.56256	0.00068	0.57782	0.56392	-0.04142	-60.9
1	1	4.2032	0.54640	0.00070	0.56170	0.54780	-0.05754	-82.2
1	1	4.4595	0.52823	0.00069	0.54351	0.52961	-0.07573	-109.8
1	1	4.7158	0.51025	0.00067	0.52549	0.51159	-0.09375	-139.9
1	1	4.9721	0.49011	0.00068	0.50537	0.49147	-0.11387	-167.5
1	1	5.2284	0.47064	0.00066	0.48586	0.47196	-0.13338	-202.1
1	1	5.4846	0.45036	0.00063	0.46552	0.45162	-0.15372	-244.0
1	1	5.7409	0.42865	0.00062	0.44379	0.42989	-0.17545	-283.0
1	1	5.9972	0.40918	0.00059	0.42426	0.41036	-0.19498	-330.5

Table 6.4.4-11   Maximum Reactivity Pitch Determination for 37 BWR Rods – Water Exterior

Cask Cavity (g/cc)	Exterior (g/cc)	Pitch (cm)	k_{eff}	σ	k_s	$k_{eff}+2\sigma$	Δk	$\Delta k/\sigma$
1	1	1.1277	0.41793	0.00067	0.43317	0.41927	-0.31608	-471.8
1	1	1.3840	0.49679	0.00073	0.51215	0.49825	-0.23710	-324.8
1	1	1.6403	0.57355	0.00077	0.58899	0.57509	-0.16026	-208.1
1	1	1.8966	0.63372	0.00081	0.64924	0.63534	-0.10001	-123.5
1	1	2.1529	0.67993	0.00087	0.69557	0.68167	-0.05368	-61.7
1	1	2.4092	0.71022	0.00085	0.72582	0.71192	-0.02343	-27.6
1	1	2.6654	0.72818	0.00082	0.74372	0.72982	-0.00553	-6.7
1	1	2.9217	0.73371	0.00082	0.74925	0.73535	--	--
1	1	3.1780	0.73076	0.00082	0.74630	0.73240	-0.00295	-3.6
1	1	3.4343	0.72100	0.00078	0.73646	0.72256	-0.01279	-16.4
1	1	3.6906	0.70690	0.00076	0.72232	0.70842	-0.02693	-35.4
1	1	3.9469	0.68847	0.00081	0.70399	0.69009	-0.04526	-55.9
1	1	4.2032	0.66618	0.00075	0.68158	0.66768	-0.06767	-90.2
1	1	4.4595	0.64430	0.00073	0.65966	0.64576	-0.08959	-122.7
1	1	4.7158	0.61821	0.00071	0.63353	0.61963	-0.11572	-163.0
1	1	4.9721	0.59337	0.00073	0.60873	0.59483	-0.14052	-192.5
1	1	5.2284	0.56602	0.00068	0.58128	0.56738	-0.16797	-247.0
1	1	5.4846	0.53531	0.00068	0.55057	0.53667	-0.19868	-292.2

Table 6.4.4-12   Maximum Reactivity Pitch Determination for 37 PWR Rods – Water
Exterior

Cask Cavity (g/cc)	Exterior (g/cc)	Pitch (cm)	k_{eff}	σ	k_s	$k_{eff}+2\sigma$	Δk	$\Delta k/\sigma$
1	1	1.1277	0.43247	0.00068	0.44773	0.43383	-0.19855	-292.0
1	1	1.3840	0.50187	0.00077	0.51731	0.50341	-0.12897	-167.5
1	1	1.6403	0.55749	0.00078	0.57295	0.55905	-0.07333	-94.0
1	1	1.8966	0.59561	0.00081	0.61113	0.59723	-0.03515	-43.4
1	1	2.1529	0.61842	0.00078	0.63388	0.61998	-0.01240	-15.9
1	1	2.4092	0.62864	0.00079	0.64412	0.63022	-0.00216	-2.7
1	1	2.6654	0.63084	0.00077	0.64628	0.63238	--	--
1	1	2.9217	0.62153	0.00072	0.63687	0.62297	-0.00941	-13.1
1	1	3.1780	0.60939	0.00072	0.62473	0.61083	-0.02155	-29.9
1	1	3.4343	0.59297	0.00070	0.60827	0.59437	-0.03801	-54.3
1	1	3.6906	0.57112	0.00067	0.58636	0.57246	-0.05992	-89.4
1	1	3.9469	0.54994	0.00067	0.56518	0.55128	-0.08110	-121.0
1	1	4.2032	0.52793	0.00069	0.54321	0.52931	-0.10307	-149.4
1	1	4.4595	0.50588	0.00065	0.52108	0.50718	-0.12520	-192.6
1	1	4.7158	0.48106	0.00066	0.49628	0.48238	-0.15000	-227.3
1	1	4.9721	0.45664	0.00063	0.47180	0.45790	-0.17448	-277.0
1	1	5.2284	0.43149	0.00061	0.44661	0.43271	-0.19967	-327.3
1	1	5.4846	0.40582	0.00062	0.42096	0.40706	-0.22532	-363.4

Table 6.4.4-13   Maximum Reactivity Pitch Determination for 61 BWR Rods – Water
Exterior

Cask Cavity (g/cc)	Exterior (g/cc)	Pitch (cm)	k_{eff}	σ	k_s	$k_{eff}+2\sigma$	Δk	$\Delta k/\sigma$
1	1	1.1277	0.52008	0.00072	0.53542	0.52152	-0.24512	-340.4
1	1	1.3840	0.61379	0.00081	0.62931	0.61541	-0.15123	-186.7
1	1	1.6403	0.68471	0.00083	0.70027	0.68637	-0.08027	-96.7
1	1	1.8966	0.73218	0.00083	0.74774	0.73384	-0.03280	-39.5
1	1	2.1529	0.75701	0.00082	0.77255	0.75865	-0.00799	-9.7
1	1	2.4092	0.76498	0.00083	0.78054	0.76664	--	--
1	1	2.6654	0.76171	0.00078	0.77717	0.76327	-0.00337	-4.3
1	1	2.9217	0.74933	0.00075	0.76473	0.75083	-0.01581	-21.1
1	1	3.1780	0.72877	0.00074	0.74415	0.73025	-0.03639	-49.2
1	1	3.4343	0.70376	0.00073	0.71912	0.70522	-0.06142	-84.1
1	1	3.6906	0.67540	0.00072	0.69074	0.67684	-0.08980	-124.7
1	1	3.9469	0.64190	0.00069	0.65718	0.64328	-0.12336	-178.8

Table 6.4.4-14   Maximum Reactivity Pitch Determination for 61 PWR Rods – Water
Exterior

Cask Cavity (g/cc)	Exterior (g/cc)	Pitch (cm)	k_{eff}	σ	k_s	$k_{eff}+2\sigma$	Δk	$\Delta k/\sigma$
1	1	1.1277	0.52230	0.00075	0.53770	0.52380	-0.13379	-178.4
1	1	1.3840	0.58974	0.00078	0.60520	0.59130	-0.06629	-85.0
1	1	1.6403	0.63319	0.00083	0.64875	0.63485	-0.02274	-27.4
1	1	1.8966	0.65233	0.00077	0.66777	0.65387	-0.00372	-4.8
1	1	2.1529	0.65607	0.00076	0.67149	0.65759	--	--
1	1	2.4092	0.64753	0.00076	0.66295	0.64905	-0.00854	-11.2
1	1	2.6654	0.63012	0.00072	0.64546	0.63156	-0.02603	-36.2
1	1	2.9217	0.60859	0.00073	0.62395	0.61005	-0.04754	-65.1
1	1	3.1780	0.58257	0.00070	0.59787	0.58397	-0.07362	-105.2
1	1	3.4343	0.55274	0.00066	0.56796	0.55406	-0.10353	-156.9
1	1	3.6906	0.52407	0.00066	0.53929	0.52539	-0.13220	-200.3
1	1	3.9469	0.49246	0.00062	0.50760	0.49370	-0.16389	-264.3

Table 6.4.4-15   Maximum Reactivity Pitch Determination for 61 BWR Rods – Void
Exterior

Cask Cavity (g/cc)	Exterior (g/cc)	Pitch (cm)	k_{eff}	σ	k_s	$k_{eff}+2\sigma$	Δk	$\Delta k/\sigma$
1	0	1.1277	0.52156	0.00075	0.53696	0.52306	-0.25209	-336.1
1	0	1.3840	0.61695	0.00083	0.63251	0.61861	-0.15654	-188.6
1	0	1.6403	0.68835	0.00083	0.70391	0.69001	-0.08514	-102.6
1	0	1.8966	0.73509	0.00085	0.75069	0.73679	-0.03836	-45.1
1	0	2.1529	0.76248	0.00083	0.77804	0.76414	-0.01101	-13.3
1	0	2.4092	0.77355	0.00080	0.78905	0.77515	--	--
1	0	2.6654	0.77146	0.00079	0.78694	0.77304	-0.00211	-2.7
1	0	2.9217	0.76267	0.00075	0.77807	0.76417	-0.01098	-14.6
1	0	3.1780	0.74480	0.00072	0.76014	0.74624	-0.02891	-40.2
1	0	3.4343	0.72517	0.00073	0.74053	0.72663	-0.04852	-66.5
1	0	3.6906	0.70227	0.00069	0.71755	0.70365	-0.07150	-103.6
1	0	3.9469	0.67451	0.00071	0.68983	0.67593	-0.09922	-139.7

Table 6.4.4-16   Maximum Reactivity Pitch Determination for 61 PWR Rods – Void
Exterior

Cask Cavity (g/cc)	Exterior (g/cc)	Pitch (cm)	k_{eff}	σ	k_s	$k_{eff}+2\sigma$	Δk	$\Delta k/\sigma$
1	0	1.1277	0.52341	0.00079	0.53889	0.52499	-0.13907	-176.0
1	0	1.3840	0.59319	0.00077	0.60863	0.59473	-0.06933	-90.0
1	0	1.6403	0.63388	0.00079	0.64936	0.63546	-0.02860	-36.2
1	0	1.8966	0.65655	0.00078	0.67201	0.65811	-0.00595	-7.6
1	0	2.1529	0.66256	0.00075	0.67796	0.66406	--	--
1	0	2.4092	0.65394	0.00072	0.66928	0.65538	-0.00868	-12.1
1	0	2.6654	0.63865	0.00070	0.65395	0.64005	-0.02401	-34.3
1	0	2.9217	0.61660	0.00069	0.63188	0.61798	-0.04608	-66.8
1	0	3.1780	0.59274	0.00066	0.60796	0.59406	-0.07000	-106.1
1	0	3.4343	0.56934	0.00065	0.58454	0.57064	-0.09342	-143.7
1	0	3.6906	0.54287	0.00064	0.55805	0.54415	-0.11991	-187.4
1	0	3.9469	0.51595	0.00063	0.53111	0.51721	-0.14685	-233.1

Table 6.4.4-17   Maximum Reactivity Pitch Determination for 61 BWR Rods – Void
Exterior and Preferential Flooding of Cask Cavity

Cask Cavity (g/cc)	Exterior (g/cc)	Pitch (cm)	k_{eff}	σ	k_s	$k_{eff}+2\sigma$	Δk	$\Delta k/\sigma$
0	0	1.1277	0.53776	0.00070	0.55306	0.53916	-0.34644	-494.9
0	0	1.3840	0.70636	0.00077	0.72180	0.70790	-0.17770	-230.8
0	0	1.6403	0.81018	0.00082	0.82572	0.81182	-0.07378	-90.0
0	0	1.8966	0.86442	0.00079	0.87990	0.86600	-0.01960	-24.8
0	0	2.1529	0.88400	0.00080	0.89950	0.88560	--	--
0	0	2.4092	0.87897	0.00077	0.89441	0.88051	-0.00509	-6.6
0	0	2.6654	0.86184	0.00079	0.87732	0.86342	-0.02218	-28.1
0	0	2.9217	0.83244	0.00073	0.84780	0.83390	-0.05170	-70.8
0	0	3.1780	0.79468	0.00071	0.81000	0.79610	-0.08950	-126.1
0	0	3.4343	0.75931	0.00070	0.77461	0.76071	-0.12489	-178.4
0	0	3.6906	0.71973	0.00073	0.73509	0.72119	-0.16441	-225.2

Table 6.4.4-18   Maximum Reactivity Pitch Determination for 61 PWR Rods – Void
Exterior and Preferential Flooding of Cask Cavity

Cask Cavity (g/cc)	Exterior (g/cc)	Pitch (cm)	k_{eff}	σ	k_s	$k_{eff}+2\sigma$	Δk	$\Delta k/\sigma$
0	0	1.1277	0.55291	0.00071	0.56823	0.55433	-0.20333	-286.4
0	0	1.3840	0.67194	0.00076	0.68736	0.67346	-0.08420	-110.8
0	0	1.6403	0.73270	0.00078	0.74816	0.73426	-0.02340	-30.0
0	0	1.8966	0.75614	0.00076	0.77156	0.75766	--	--
0	0	2.1529	0.75121	0.00076	0.76663	0.75273	-0.00493	-6.5
0	0	2.4092	0.73087	0.00076	0.74629	0.73239	-0.02527	-33.3
0	0	2.6654	0.70242	0.00072	0.71776	0.70386	-0.05380	-74.7
0	0	2.9217	0.66618	0.00068	0.68144	0.66754	-0.09012	-132.5
0	0	3.1780	0.62965	0.00067	0.64489	0.63099	-0.12667	-189.1
0	0	3.4343	0.59036	0.00065	0.60556	0.59166	-0.16600	-255.4
0	0	3.6906	0.55310	0.00063	0.56826	0.55436	-0.20330	-322.7

Table 6.4.4-19   Damaged Rod Array Area Calculation – Flooded Cask Cavity

Moderation	Number of Rods	Fuel Type	Pitch [cm]	Rod Radius [cm]	# Rods Max	Diameter [cm]	$Area_{Hex}$ [cm^2]
Water Cavity	25	BWR	3.434	0.622	5	14.98	168.3
Water Exterior		PWR	2.922	0.478	5	12.64	119.9
Water Cavity	37	BWR	2.922	0.512	7	18.55	258.2
Water Exterior		PWR	2.665	0.393	7	16.78	211.1
Water Cavity	61	BWR	2.409	0.398	9	20.07	302.1
Water Exterior		PWR	2.153	0.306	9	17.84	238.6

Table 6.4.4-20   Damaged Rod Array Area Calculation – Preferential Flooding

Moderation	Number of Rods	Fuel Type	Pitch [cm]	Rod Radius [cm]	# Rods Max	Diameter [cm]	Area$_{Hex}$ [cm^2]
Partially Flooded Cavity	61	BWR	2.153	0.398	9	18.02	243.5
Void Exterior		PWR	1.897	0.306	9	15.78	186.9

Table 6.4.4-21   Maximum Reactivity Determination for Homogenized UO$_2$/Water Mixture

Cask Cavity (g/cc)	Exterior (g/cc)	UO$_2$ Vol Frac	k$_{eff}$	σ	k$_{eff}$+2σ	Δk	Δk/σ
0	0	0.132	0.81043	0.00075	0.81193	-0.00665	-8.9
0	0	0.14	0.81319	0.00075	0.81469	-0.00389	-5.2
0	0	0.15	0.81495	0.00071	0.81637	-0.00221	-3.1
0	0	0.16	0.81702	0.00078	0.81858	--	--
0	0	0.17	0.81592	0.00076	0.81744	-0.00114	-1.5
0	0	0.18	0.81448	0.00078	0.81604	-0.00254	-3.3
0	0	0.19	0.81315	0.00079	0.81473	-0.00385	-4.9
0	0	0.20	0.81080	0.00080	0.81240	-0.00618	-7.7

Table 6.4.4-22   Homogenized UO$_2$/Water Cask Cavity Moderator Density Study Results - Void Exterior

Cask Cavity (g/cc)	Exterior (g/cc)	UO$_2$ Vol Frac	k$_{eff}$	σ	k$_{eff}$+2σ	Δk	Δk/σ
0.0	0	0.16	0.81702	0.00078	0.81858	--	--
0.1	0	0.16	0.80234	0.00078	0.80390	-0.01468	-18.8
0.2	0	0.16	0.79078	0.00083	0.79244	-0.02614	-31.5
0.3	0	0.16	0.77986	0.00082	0.78150	-0.03708	-45.2
0.4	0	0.16	0.77082	0.00084	0.77250	-0.04608	-54.9
0.5	0	0.16	0.76440	0.00086	0.76612	-0.05246	-61.0
0.6	0	0.16	0.75856	0.00081	0.76018	-0.05840	-72.1
0.7	0	0.16	0.75823	0.00079	0.75981	-0.05877	-74.4
0.8	0	0.16	0.75812	0.00079	0.75970	-0.05888	-74.5
0.9	0	0.16	0.75836	0.00080	0.75996	-0.05862	-73.3
1.0	0	0.16	0.76077	0.00085	0.76247	-0.05611	-66.0

Table 6.4.4-23   Homogenized UO₂/Water Cask Cavity Moderator Density Study
Results - Water Exterior

Cask Cavity (g/cc)	Exterior (g/cc)	UO₂ Vol Frac	k_eff	σ	k_eff+2σ	Δk	Δk/σ
0.0	1	0.16	0.65512	0.00078	0.65668	-0.10233	-131.2
0.1	1	0.16	0.68935	0.00083	0.69101	-0.06800	-81.9
0.2	1	0.16	0.70977	0.00084	0.71145	-0.04756	-56.6
0.3	1	0.16	0.72173	0.00084	0.72341	-0.03560	-42.4
0.4	1	0.16	0.72868	0.00079	0.73026	-0.02875	-36.4
0.5	1	0.16	0.73455	0.00083	0.73621	-0.02280	-27.5
0.6	1	0.16	0.73958	0.00081	0.74120	-0.01781	-22.0
0.7	1	0.16	0.74478	0.00082	0.74642	-0.01259	-15.4
0.8	1	0.16	0.74887	0.00084	0.75055	-0.00846	-10.1
0.9	1	0.16	0.75191	0.00082	0.75355	-0.00546	-6.7
1.0	1	0.16	0.75743	0.00079	0.75901	--	--

Table 6.4.4-24   Homogenized UO₂/Water Exterior Moderator Density Study Results –
Void Cask Cavity

Cask Cavity (g/cc)	Exterior (g/cc)	UO₂ Vol Frac	k_eff	σ	k_eff+2σ	Δk	Δk/σ
0	0.0	0.16	0.81702	0.00078	0.81858	--	--
0	0.1	0.16	0.66923	0.00081	0.67085	-0.14773	-182.4
0	0.2	0.16	0.65897	0.00080	0.66057	-0.15801	-197.5
0	0.3	0.16	0.65619	0.00078	0.65775	-0.16083	-206.2
0	0.4	0.16	0.65607	0.00078	0.65763	-0.16095	-206.3
0	0.5	0.16	0.65449	0.00079	0.65607	-0.16251	-205.7
0	0.6	0.16	0.65513	0.00081	0.65675	-0.16183	-199.8
0	0.7	0.16	0.65479	0.00077	0.65633	-0.16225	-210.7
0	0.8	0.16	0.65445	0.00077	0.65599	-0.16259	-211.2
0	0.9	0.16	0.65591	0.00081	0.65753	-0.16105	-198.8
0	1.0	0.16	0.65512	0.00078	0.65668	-0.16190	-207.6

Table 6.4.4-25   Homogenized UO₂/Water Exterior Moderator Density Study Results –
Water Cask Cavity

Cask Cavity (g/cc)	Exterior (g/cc)	UO₂ Vol Frac	k_{eff}	σ	k_{eff}+2σ	Δk	Δk/σ
1	0.0	0.16	0.76077	0.00085	0.76247	--	--
1	0.1	0.16	0.75700	0.00085	0.75870	-0.00377	-4.4
1	0.2	0.16	0.75719	0.00080	0.75879	-0.00368	-4.6
1	0.3	0.16	0.75696	0.00081	0.75858	-0.00389	-4.8
1	0.4	0.16	0.75430	0.00083	0.75596	-0.00651	-7.8
1	0.5	0.16	0.75574	0.00081	0.75736	-0.00511	-6.3
1	0.6	0.16	0.75516	0.00080	0.75676	-0.00571	-7.1
1	0.7	0.16	0.75480	0.00085	0.75650	-0.00597	-7.0
1	0.8	0.16	0.75601	0.00084	0.75769	-0.00478	-5.7
1	0.9	0.16	0.75542	0.00081	0.75704	-0.00543	-6.7
1	1.0	0.16	0.75743	0.00079	0.75901	-0.00346	-4.4

Table 6.4.4-26   Single Cask Containment Reflected Results Comparison for
Homogenized UO₂/Water Model

Cask Configuration	Cask Cavity (g/cc)	Exterior (g/cc)	UO₂ Vol Frac	k_{eff}	σ	k_{eff}+2σ	Δk	Δk/σ
Array	0	0	0.16	0.81702	0.00078	0.81858	--	--
Single	0	0	0.16	0.50369	0.00076	0.50521	-0.31337	-412.3
Array	1	0	0.16	0.76077	0.00085	0.76247	--	--
Single	1	0	0.16	0.74882	0.00085	0.75052	-0.01195	-14.1
Array	1	1	0.16	0.75743	0.00079	0.75901	--	--
Single	1	1	0.16	0.75043	0.00080	0.75203	-0.00698	-8.7
Array	0	1	0.16	0.65512	0.00078	0.65668	--	--
Single	0	1	0.16	0.54351	0.00078	0.54507	-0.11161	-143.1

6.4.5   TRIGA Fuel Elements

This section presents the criticality evaluation for TRIGA fuel elements in the NAC-LWT with nonpoisoned and poisoned basket modules for intact and failed fuel. In the non-poisoned configuration, up to 120 intact TRIGA fuel elements can be transported in the NAC-LWT cask. In the poisoned configuration, up to 140 intact TRIGA elements can be transported in the NAC-LWT cask. Up to four TRIGA fuel elements can be contained in screened canisters. Up to two failed TRIGA fuel elements can be contained in sealed canisters. The analyses are performed to satisfy the requirements of 10 CFR Parts 71.55 and 71.59 as well as IAEA Transportation Safety Standards (TS-R-1).

The most reactive TRIGA fuel element type in the NAC-LWT TRIGA basket is evaluated in Section 6.4.5.1. The most reactive basket and intact fuel configurations, including both geometric perturbations and manufacturing tolerances, under wet and dry conditions are evaluated in Section 6.4.5.2. The most reactive cask configuration with three baskets of intact design-basis TRIGA fuel and two baskets of fuel, either in screened cans or in sealed cans, is evaluated under normal and accident conditions in Section 6.4.5.3. Preferential flooding of the screened and sealed failed fuel cans is also evaluated. The maximum k_{eff} of the NAC-LWT cask loaded with design-basis TRIGA fuel is evaluated under normal and accident conditions in Section 6.4.5.4. A single package evaluation, in accordance with 10 CFR 71.55(b)(3), is performed in Section 6.4.5.5. An expanded set of TRIGA fuel characteristics is evaluated in Section 6.4.5.6. The analyses demonstrate that, including all calculational and mechanical uncertainties, the NAC-LWT cask remains subcritical ($k_s < 0.95$) under normal and accident conditions.

Any combination of TRIGA fuel element types can be placed in the NAC-LWT TRIGA baskets. TRIGA fuel cluster rods are analyzed as separate loadings in Section 6.4.6 and will not be shipped with TRIGA fuel elements. Transportation of a limited quantity of cluster rods within a TRIGA fuel element shipment is analyzed in Section 6.4.5.6.5.

6.4.5.1   Most Reactive TRIGA Fuel Element

Of the four main types of TRIGA fuel elements (Table 6.2.5-1), three (aluminum clad, stainless steel clad, and FFCR) are explicitly analyzed to determine which element is bounding in terms of criticality. The ACPR fuel element and fuel follower control rod types are eliminated from consideration due to their low [235]U loading. For steel clad fuel, the standard, and FLIP LEU-I compositions (Table 6.2.5-2) are also eliminated from further consideration due to their low [235]U loading. These element types are bounded by this analysis. The two types of Al clad fuel elements, each with 20 wt % [235]U loading are analyzed, and the two types of stainless steel clad elements (standard streamlined and standard plain) both enriched to either 20 wt % or 70 wt % in

^{235}U are analyzed. The FFCR element is analyzed with FLIP LEU-I composition enriched to 20 wt % ^{235}U. Higher enrichment elements, evaluated to 95 wt % ^{235}U, and minor increases in the 20 wt % ^{235}U and 70 wt% ^{235}U fuel elements fissile mass and enrichment are evaluated in Section 6.4.5.6.4.

6.4.5.1.1   Nonpoisoned Basket Most Reactive TRIGA Fuel Element Evaluation

The parametric evaluation of the TRIGA fuel element types for the nonpoisoned basket is performed with the fuel/basket unit cell infinite array model. The reactivities of the seven candidate fuel types are presented in Table 6.4.5-1. The results show that the stainless steel clad, standard plain, TRIGA fuel element with FLIP composition at 70 wt % ^{235}U is the most reactive of all TRIGA fuel element types. Table 6.4.5-1 also includes the results for several combinations of steel FLIP LEU (20 wt % ^{235}U) and FLIP HEU (70 wt % ^{235}U) which are bounded by the results for four 70 wt % ^{235}U elements per basket cell.

6.4.5.1.2   Poisoned Basket Most Reactive TRIGA Fuel Element Evaluation

The parametric evaluation of TRIGA fuel element types for the poisoned basket is performed with an infinite cask array model. The reactivity of the candidate fuel types is presented in Table 6.4.5-2. Again, the results show that the stainless steel clad, standard plain, TRIGA fuel element with FLIP composition at 70 wt % ^{235}U is the most reactive of all TRIGA fuel element types, and combinations of steel FLIP LEU (20 wt % ^{235}U) and FLIP HEU (70 wt % ^{235}U) are bounded by the results for four 70 wt % ^{235}U elements per basket cell. Because of the low relative reactivity of the 14-inch aluminum clad and FFCR (Table 6.4.5-1) elements, it is not necessary to re-analyze these elements.

6.4.5.1.3   Summary of Most Reactive TRIGA Fuel Element Evaluation

The stainless steel clad, standard plain, TRIGA fuel element with FLIP composition at 70 wt% ^{235}U is the most reactive of all TRIGA fuel element types in the poisoned and non-poisoned baskets. Four of these elements in basket openings bound the other element types and any combination with other such elements. This TRIGA fuel element type and the TRIGA fuel cluster rods will be utilized in subsequent evaluations of the NAC-LWT cask with poisoned and nonpoisoned baskets.

6.4.5.2   Most Reactive Fuel Element and Basket Configurations

The primary basket tolerances affecting system reactivity are geometric tolerances, including the positioning of the fuel elements in the cell opening, the size of the cell opening; and manufacturing tolerances, including the thickness of the steel plate dividing the basket openings. The effect of these tolerances is evaluated sequentially in this section.

6.4.5.2.1   Geometric Perturbations

The TRIGA fuel elements are held in place by basket modules. Each cell opening in the basket module can contain up to four TRIGA fuel elements. The TRIGA fuel elements are not constrained in the opening and, therefore, may shift to any location in the opening. Wet and dry conditions of the TRIGA fuel are evaluated to determine the most reactive fuel element and basket configuration.

Table 6.4.5-3 and Table 6.4.5-4 show the nonpoisoned and poisoned axially infinite basket cask k_{eff} with design-basis TRIGA fuel elements. The effects evaluated in the tables include fuel element movement and partial loading in wet and dry basket openings.

For each basket configuration, the most reactive wet configuration contains four design-basis TRIGA fuel elements moved outward to the corners of each cell opening, with k_{eff} = 0.83468 ± 0.00101 and 0.87874 ± 0.00123 for nonpoisoned and poisoned basket configurations, respectively. Although the reactivity of the nonpoisoned basket configurations with three fuel elements in a cell are similar to that with four rods, the four rod configuration is selected as the most reactive because it contains the greatest amount of ^{235}U. The wet configuration maximizes the moderation between TRIGA fuel elements within the wet cavity and is referred to as the wet configuration for TRIGA fuel elements.

The most reactive dry configuration, with no water in the neutron shield, contains four design-basis TRIGA fuel elements touching in each opening and moved inward to the basket center with k_{eff} = 0.93434 ± 0.00115 and 0.88969 ± 0.00122 for nonpoisoned and poisoned basket configurations, respectively. This dry configuration minimizes the neutron leakage of TRIGA fuel elements within the dry basket and is referred to as the dry configuration for TRIGA fuel elements. The partial loading evaluations show a general decrease in reactivity with a decreasing number of fuel elements.

6.4.5.2.2   Manufacturing Tolerance Perturbations

In addition to geometric tolerances, the wet and dry configurations were evaluated to determine the effect of manufacturing tolerances. The dimensional ranges of the plate materials used to construct the basket openings are 0.28 inch minimum/0.3125 inch maximum for the center plate, 0.24 inch minimum/0.295 inch maximum for the outside divider plate, and 0.12 inch minimum/0.13 inch maximum for the outside plate. The cell opening is checked during fabrication to ensure a minimum cell opening of 3.38 inches square, and a maximum cell opening size of 3.48 inches square. The most reactive configurations based on geometric tolerances are utilized in this analysis.

Table 6.4.5-5 and Table 6.4.5-6 show the nonpoisoned and poisoned basket, cask k_{eff} with design-basis TRIGA fuel elements. The effects evaluated in the tables include perturbations on

basket plate thickness and basket opening size. For the nonpoisoned basket, within statistical limits, the most reactive wet and dry configurations contain baskets with the minimum stainless steel thickness divider plates. The reactivity of these wet and dry configurations are k_{eff} = 0.86861 ± 0.00094 and k_{eff} = 0.90501 ± 0.00109, respectively. Furthermore, the most reactive dry configuration for manufacturing tolerances contains the minimum basket opening, k_{eff} = 0.90817 ± 0.00105. For the poisoned basket configuration, the perturbations do not significantly increase reactivity.

6.4.5.3   Sealed and Screened Cans Criticality Evaluation

Criticality calculations were performed in screened and sealed failed fuel cans in the top and base basket modules of the cask. Three cases are examined for each basket combination, an all dry system, a full wet system, and a preferentially wet system with water only in the screened or sealed failed fuel can. Fuel in sealed cans is modeled both homogeneously, heterogeneously, and with partial loadings. The three central modules contain intact fuel in the most reactive wet or dry configurations, as appropriate, as determined in Section 6.4.5.2. The reactivities of the failed fuel combinations are compared to the reactivities of respective intact fuel configurations, and moderator density studies are performed on the most reactive configurations in Section 6.4.5.4.

6.4.5.3.1   Screened Failed Fuel Can Evaluations

Table 6.4.5-7 shows the results of the preferential flooding and partial loading studies of the screened failed fuel can configurations with design-basis TRIGA fuel elements in non-poisoned and poisoned baskets. As seen in the table, the most reactive configurations for the NAC-LWT cask containing screened cans with TRIGA fuel elements is an infinite array of casks with dry cavities, loaded with preferentially flooded screened cans, with each can containing four fuel elements in the corners of the cans. The most reactive poisoned configuration also contains the maximum can opening size.

The reactivity, k_{eff}, for the nonpoisoned and poisoned configurations is 0.90926 ± 0.00126 and 0.90224 ± 0.00128, respectively. The reactivity of the screened cans in the nonpoisoned basket configuration is bounded by the sealed can evaluations presented in Section 6.4.5.3.2.

6.4.5.3.2   Sealed Failed Fuel Can Evaluations

Table 6.4.5-8 shows the results of the preferential flooding and partial loading studies of the sealed failed fuel can configurations with TRIGA fuel elements in non-poisoned and poisoned baskets. Included in the sealed can evaluations are homogenous fuel/moderator mixture cases, representing fuel debris, with the mixture either being solid (no water), filling one half of the can

or filling the whole can. Cases are evaluated for the solid in the mixture both with and without graphite.

As seen in the table, the most reactive configuration for the NAC-LWT cask with the non-poisoned basket containing sealed cans is for an infinite array of casks with dry cavities loaded with preferentially flooded, maximum diameter, sealed cans, each can containing a homogeneous mixture of water and the fissile material equivalent to two TRIGA fuel elements. The most reactive nonpoisoned configuration is k_{eff} = 0.91355 ± 0.00119. The "Wet Cask / Wet Can, Elements Out" case for the non-poisoned basket was not analyzed because the reactivity of the element configurations is significantly lower than the homogenized mixture configurations.

The most reactive poisoned basket configuration is selected as the case containing flooded cask and cans with elements touching the can wall. The reactivity, k_{eff}, for this configuration is 0.88574 ± 0.00130. Since the screened can reactivity presented in Section 6.4.5.3.1 is higher, this configuration is bounded.

6.4.5.4 Moderator Density Criticality Evaluations for Intact TRIGA Fuel Elements

The evaluations for normal and accident conditions include moderator density variations in the cask cavity and external environment to the cask. One evaluation is performed for each basket (non-poisoned / poisoned) combination.

Table 6.4.5-9 and Table 6.4.5-10 show the most reactive configurations for these combinations as determined in Section 6.4.5.3. The tables contain results for infinite axial length models for the intact fuel and finite axial length models with cask end caps for failed fuel. Comparing the reactivity of the more conservative infinite models with finite models is acceptable, provided the result with the highest k_{eff} is always selected. Alternately, converting conservative infinite axial length models to finite axial length models is equally acceptable.

As seen in Table 6.4.5-9, k_{eff} = 0.93434 ± 0.00115 for the most reactive dry configuration with intact, TRIGA fuel elements in the non-poisoned basket. When reevaluated as a finite axial length cask model with end caps, the resulting k_{eff} = 0.89731 ± 0.00117. As a result, the most reactive configuration of TRIGA fuel elements in the nonpoisoned basket becomes the configuration with two baskets with sealed cans preferentially flooded with a dry cask, k_{eff} =

0.91355 ± 0.00119. This configuration is chosen for further moderator density variation evaluations. As seen in Table 6.4.5-10, the most reactive configuration of TRIGA fuel elements in the poisoned basket contains two screened cans preferentially flooded with a dry cask. This configuration is chosen for moderator density variations. Results of the moderator density

variation cases for normal and accident conditions for the two basket configurations are presented in Table 6.4.5-11 through Table 6.4.5-14.

As seen in Table 6.4.5-12, the most reactive configuration for the TRIGA fuel elements in the nonpoisoned basket contains two baskets with sealed cans, preferentially flooded, under accident conditions with no water in the cask interior, neutron shield, or exterior, $k_{eff} = 0.9136 \pm 0.0012$. Per Section 6.1.1, this corresponds to $k_s = 0.9328$.

As seen in Table 6.4.5-14, the most reactive configuration for the TRIGA fuel elements in the poisoned basket, contains two baskets with sealed cans, preferentially flooded, under accident conditions with no water in the cask interior, neutron shield, or exterior, $k_{eff} = 0.9022 \pm 0.0015$. Per Section 6.1.1, this corresponds to $k_s = 0.9220$.

6.4.5.5 Single Package Criticality Evaluation

To satisfy 10 CFR 71.55(b)(3), an analysis of the reflection of the containment system (inner shell) by water is performed on a single wet cask. Successive replacement of the cask radial shields with water reflection is also evaluated for each basket (nonpoisoned/poisoned) combination. As seen in Table 6.4.5-15 and Table 6.4.5-16, the reactivity of the system drops as each radial shield of the cask is replaced by water from the full cask surrounded by water, to the inner shell surrounded by water.

6.4.5.6 Revised TRIGA Fuel Element Characteristics for Nonpoisoned Baskets

The purpose of this section is to demonstrate reactivity results for a revised set of TRIGA fuel element characteristics.

The analysis is broken into five sections. The first section establishes a minimum number of fuel characteristics meeting criticality safety limits for intact fuel (cask shipments with no cans). The second section evaluates severely damaged TRIGA fuel, including debris, in sealed and screened cans. The third section contains the evaluations for a screened can containing TRIGA elements with potential clad damage, but meeting structural requirements for transport. The fourth section evaluates increases in the range of enrichment and fissile material mass of TRIGA fuel elements in intact, screened, and sealed canister configurations. The fifth section contains the evaluation of a mixed shipment of TRIGA fuel elements and TRIGA cluster rods. Unless otherwise indicated, all models represent the accident condition cask (i.e., no neutron shield) in a finite cask array of eight casks. The array of eight casks is placed in a close-pack triangular pitch configuration as shown in Figure 6.4.5-9. As demonstrated in the analysis results sections, neutronic coupling between casks in an array, with void between casks, maximizes reactivity. Placing the casks in a tight pitch array, therefore, represents the most reactive configuration. The

CSI based on the eight-cask accident array is 12.5 (N=4, CSI=50/N). Under normal conditions, with the neutron shield in place, the system is evaluated for an infinite array of casks (reflective boundary condition on a cuboid surrounding the cask) producing a CSI of 0.

While the analyses evaluate both screened and sealed cans, shipment is only permitted in the sealed canister configuration.

6.4.5.6.1   Intact Fuel Elements (No Can)

Basic TRIGA fuel element characteristics affecting system reactivity are itemized in the following paragraphs, with a qualitative description as to their effect on system reactivity.

Following the qualitative description are the result discussions of the KENO-Va calculations for the individual parameters.

Enrichment

TRIGA fuel elements are constructed at two basic enrichment levels (20 wt % and 70 wt % ^{235}U).

Fissile Material Mass

Maximum fissile material mass for each enrichment/fuel clad material combination is assigned to the models. Maximum fissile material mass will result in maximum system reactivity.

Zirconium Mass and Hydrogen-to-Zirconium (H/Zr) Ratio

The combination of zirconium mass and the H/Zr ratio determines the quantity of moderator (hydrogen) within the fuel matrix. Previous evaluations indicate that increasing the moderator quantity has the potential to increase system reactivity (i.e., the fuel element itself is under-moderated). Therefore, maximum system reactivity is obtained from a H/Zr ratio of 2.0 (maximum for zirconium hydride) and a maximum fuel zirconium content (limited by the fuel region volume).

Rod Diameter

Modifying rod diameter at a fixed fuel geometry and mass has a small negative effect for stainless steel clad elements, as it increases clad volume (stainless steel is a parasitic absorber). There is no significant effect on aluminum clad fuel. A secondary effect of a rod diameter increase is the separation of the fuel in the dry cavity cask case and reduction in water between elements in the wet cavity cask case. Both result in minor negative reactivity trends.

When allowing the fuel to expand to the clad inner surface, a maximum rod OD allows for additional moderator (in the form of ZrH), which more than offsets the minor reactivity effects discussed previously and, therefore, represents a bounding configuration.

Clad Thickness

Reducing clad thickness removes parasitic absorber for the stainless steel clad fuel element. At a
fixed outer diameter, reduced clad thickness provides additional rod interior volume. For a fixed
fuel mass, the reactivity effect of a reduced clad thickness is, therefore, limited to the parasitic
absorber removal while, at a maximum fuel mass, the reduced thickness clad provides volume
for additional ZrH.

Fuel Outer and Inner Diameter

Inner and outer fuel diameters have no effect on system reactivity at a fixed fuel mass.
Maximum outer diameter (i.e., contact with the clad) and minimum inner diameter (i.e., contact
with the center zirconium rod where applicable) provide for additional ZrH volume and,
therefore, represent a bounding configuration.

Central Zirconium Rod Diameter

A change in the diameter of the central zirconium rod at a fixed fuel geometry has no significant
system reactivity effect, as it involves neutronically transparent material. A minimum zirconium
rod is bounding for the modified fuel dimensions (maximum ZrH).

Active Fuel Length

The reactivity variations associated with the active fuel length have distinctly different trends
when considering a system at a fixed (nominal) ZrH quantity and for a system maximizing the
ZrH quantity. At a fixed ZrH quantity, the minimum active fuel height compacts the fissile
material region (potentially above theoretical density) and, therefore, increases system reactivity.
At the maximum ZrH quantity, the effect of a compacted (reduced leakage) fuel region is offset
by the reduced moderator ratio in the fuel region, resulting in a slight decrease in reactivity for a
dry cask cavity and no statistically resolvable effect for a wet cask cavity (bounding for the finite
array of casks modeled). Therefore, active fuel length variations have no significant effects on
the highest system reactivity cases containing maximum ZrH.

Zirconium Content and H/Zr Ratio

The effect of zirconium mass changes at a fixed H/Zr ratio of 1.6 is illustrated in Figure 6.4.5-1
for a finite cask array of eight casks. Similar reactivity changes as a function of H/Zr ratio are
shown in Figure 6.4.5-2. Both figures clearly demonstrate that maximum zirconium quantity and
H/Zr ratio are bounding for the system. Analysis trends hold true for both wet and dry cask
cavity cases. Note that the 20% enriched material curve indicates a higher reactivity than the
70% enriched curve for the H/Zr ratio study (dry cask cavity). This is the result of specifying an
artificially high zirconium content of the fuel material. The composition for the 20 wt % rod
with 2,300 grams of zirconium in the fuel results in a ZrH_x density of approximately 6.9 g/cm^3,

well above the actual density of 5.61 g/cm3. The 2,300 grams base value is obtained from a fuel element with only 41 grams of ^{235}U versus 167 grams in the design basis element. Figure 6.4.5-3 demonstrates that a maximum fissile material content is bounding for fuel containing the maximum ZrH content feasible at a maximum H/Zr ratio of 2.0.

At the maximum ZrH quantity possible in the fuel rod, the 70 wt % case is bounding as demonstrated in Table 6.4.5-20 and discussed later in this section.

Maximum Reactivity Fuel Element Configuration

Fuel assembly characteristics are evaluated by allowing:

- Rod diameter to reach a maximum of 1.5 inches

- Clad to be reduced to 0.0001 cm (essentially a no clad case, allowing the basic KENO cells to be retained within the input file structure)

- Fuel outer diameter to be maximized into contact with the clad inner surface and be minimized by 0.1 inch (arbitrary value chosen for study purposes)

- Fuel inner diameter to be minimized into contact with the zirconium center rod (no maximum was evaluated as analysis trends all indicate a reduced fuel volume to be bounding)

- Zirconium inner rod to be reduced (minimum) to a 0.0001 cm radius (essentially a "no inner rod" case with the KENO cell for the rod retained) or increased (maximum) to contact the fuel inner diameter

- Active fuel length to be varied by 0.5 inch

As shown in Table 6.4.5-17, maximum system reactivity is achieved for a fuel element with the following characteristics:

- Maximum zirconium content

  Calculated based on the physical dimensions of the fuel region and zirconium hydride at full density (occupying all nonuranium volume)

- Maximum H/Zr atom ratio (2.0)

  Based on the H/Zr ratio study in the previous section having determined a maximum H/Zr ratio to be bounding for wet and dry cask configurations, all fuel element physical characteristic studies applied the maximum ratio of 2.0.

- Maximum rod outer diameter of 1.5 inches

  Fixed fuel mass cases show a slight decrease in reactivity due to the additional clad volume (stainless steel) associated with a larger fuel rod at a constant clad thickness. When considering increased fuel diameter and the associated increase in volume for zirconium hydride, a maximum rod diameter is bounding.

- Minimum clad thickness

Provides a significant increase in reactivity as the result of reduced parasitic absorber and increased volume for the fuel. Note that bias adjusted reactivities for a 0.0001 cm clad case exceed a 0.95 limit. Further evaluations documented in Table 6.4.5-18 indicate a model containing a 0.01 inch clad is sufficient to demonstrate reactivity below the 0.95 limit. This model change is adopted for the screened and sealed can evaluations.

- Maximum fuel outer diameter, minimum inner diameter and a minimum (removed) central rod

  All three properties increase the potential fuel volume and, therefore, provide additional ZrH volume.

- No significant reactivity effect of fuel length for the bounding (wet) fuel configurations

  The maximum active fuel length is specified to be a bounding configuration as it provides the largest amount of integral fuel moderator (ZrH$_x$) to the system.

Optimum Moderation, Fuel Element Location and Basket Manufacturing Tolerances

Reference criticality calculations for TRIGA fuel in either an infinite basket cell or infinite cask array configuration indicate that maximum system reactivity is obtained from a dry cask cavity with fuel elements shifted toward the basket center in a minimum opening size basket. Finite cask array calculations on the fuel parameters evaluated herein indicate that this configuration is not bounding for a finite cask array. Water in the model not only thermalizes neutrons to support reactions with the fissile material, but also absorbs neutrons. Since the TRIGA elements contain moderator in the fuel matrix, independent of the water in the element-to-basket gaps, an infinite array of casks provides significant neutronic interactions on a dry cask basis. In the finite array models, the additional neutrons supplied by other casks are significantly reduced, resulting in a system with a water cavity being bounding.

A sample evaluation of reactivity trends as a function of model configuration is shown in Table 6.4.5-19. The data demonstrate a sharp drop-off in reactivity as the number of fuel units is reduced (infinite basket unit cell to finite cask model, to finite cask array, and finally to a single cask model) for a dry cask, while reactivity for a wet cask remains relatively constant across array sizes. Initial reactivity studies for the 70 wt % enriched steel clad fuel at various moderator quantities (accomplished by varying fuel zirconium quantity at a fixed H/Zr ratio) confirm that system reactivity increases with increased moderator density, but levels off at densities above 0.5 g/cm3 (see Figure 6.4.5-4). At this level, increased moderation between elements in a basket opening is offset by reduced interaction between the basket opening, baskets in the cask, and casks in the array. Detailed moderator density studies for the system considering various fuel element moderator quantities (adjusted by H/Zr ratio), TRIGA element configuration (nominal

and most reactive element), rod locations (shifted in – optimal for dry system; shifted to basket corners – optimal for wet system), and basket opening size (minimum and maximum) are illustrated in Figure 6.4.5-5. These studies demonstrate that maximum reactivity is the result of:

- Fully moderated cask cavity (water density 1 g/cm^3)

- Most reactive element configuration defined in the previous section

- Shifted out (to basket corners) fuel elements

No significant changes in reactivity occurred as the result of basket opening size changes for a fully flooded (maximum reactivity) basket configuration.

<u>Maximum Intact Fuel Reactivity and Criticality Safety Index</u>

Based on a 1.5-inch maximum rod diameter, a minimum clad thickness of 0.01 inch, a conservatively removed central zirconium rod, and a maximum ZrH content system, reactivities are calculated for each of the primary TRIGA fuel types. Results for the analyses are listed in Table 6.4.5-20. Maximum bias adjusted reactivity (k_s) for the revised TRIGA fuel description is 0.94842 (k_{eff} = 0.93024 ± 0.00069) under accident conditions with a cask array limited to eight casks (CSI = 12.5). Table 6.4.5-4 also illustrates the large reactivity increase associated with the move from a nominal fuel element to the bounding configuration specified here.

The normal condition (intact neutron shield) maximum reactivity for the system is shown in Table 6.4.5-21 for an infinite cask array. Therefore, the CSI for intact fuel shipments is 12.5.

6.4.5.6.2   Screened and Sealed Can Criticality Evaluations for Severely Damaged Fuel (Up to Two Elements per Can)

The NAC-LWT system may be loaded with screened or sealed cans in the top and bottom basket modules. The sealed can was previously evaluated for a damaged content of up to two equivalent intact rods. Based on an accident cask condition (i.e., no neutron shield), reactivity evaluations for a finite array of eight casks are repeated in this section for the revised TRIGA fuel element definition. In addition, the screened can is similarly evaluated to contain up to two equivalent intact rods.

Screened and sealed can reactivity evaluations are performed at various cask cavity and can moderator combinations for a solid fuel material and for a fuel mixture filling the can cavity. The results plotted in Figure 6.4.5-6 demonstrate that the reactivity of the system is controlled by the uncanned baskets with no significant feedback from the can locations regardless of can fuel height or moderator fraction. Note that the can contents are limited to the equivalent of two fuel elements, while uncanned basket locations contain up to four rods. Similar results are obtained from a study of debris height at various can moderator densities as shown in Figure 6.4.5-7. The study demonstrates no statistically significant effect of debris height on system reactivity.

Maximum system reactivity was calculated at a k_{eff} of 0.93159 ± 0.00066 for a k_s of 0.94971 after adjusting for a calculation bias uncertainty of 0.0168 (code bias is an approximately 0.02 □k over-prediction and is, therefore, set to 0 for the bias adjusted reactivity). This reactivity is not statistically different from that of the intact fuel. As an eight-cask array was modeled under accident conditions, the system CSI is 12.5.

Maximum normal condition reactivity for an infinite array of casks containing cans with up to two TRIGA elements worth of fuel material is 0.92351 ± 0.00071 (wet cask and can).

The overall system CSI for casks containing cans with up to four fuel elements per can, including fuel debris, is 12.5.

6.4.5.6.3   Screened Can Criticality Evaluations (Four Elements per Can – Elements Retaining Structural Integrity)

The NAC-LWT system may be loaded with screened cans in the top and bottom basket modules. The screened can was previously evaluated for a content of up to four intact TRIGA elements. Based on an accident cask condition (i.e., no neutron shield), reactivity evaluations for a finite array of casks are repeated in this section for the revised TRIGA fuel element definition.

Reactivity evaluations are performed at various cask cavity and can moderator combinations for four elements per can in an eight-cask array. The results plotted in Figure 6.4.5-8 demonstrate that the maximum reactivity is achieved by a dry cask cavity with a full density, preferentially flooded can. Bias adjusted reactivity for this system is slightly above 0.95. Evaluations are, therefore, repeated for a four-cask array (CSI = 25) with the corresponding results added to the Figure 6.4.5-8 plot. Maximum system reactivity for the four-cask array is k_{eff} of 0.92798 ± 0.00070 for a k_s of 0.94618. Moderator condition for the maximum reactivity case is a wet (1 g/cm³) cask and wet can at 0.4 g/cm³ moderator density (note that there is no statistically significant change in system reactivity as a function of can cavity moderator density).

Maximum normal condition reactivity for an infinite array of casks containing the screened cans with four TRIGA elements is 0.92484 ± 0.00068 (wet cask/wet can).

The overall system CSI for casks containing cans with up to four fuel elements per can, including fuel debris, is 25.

6.4.5.6.4   Higher Fissile Material Mass and Enrichment Study

The NAC-LWT cask is evaluated to contain increased fissile material mass and enrichment elements. Revised parameters are designed to bound TRIGA fuel elements up to 25 wt % enriched with 275g ^{235}U fissile mass, up to 71 wt % enriched with up to 138g ^{235}U, and up to 95 wt % enriched with up to 175g ^{235}U. The evaluation justifying the slight increase in fissile

content for 20 wt % and 70 wt % elements and the signficantly higher 95 wt % elements is divided into intact and damaged fuel sections.

Intact Fuel Elements (No Canister)

Analysis in this section evaluates increases in fissile material mass and enrichment and provides loading restrictions where necessary for the increased payload definition.

Increased Fuel Enrichment (20 wt % ^{235}U and 70 wt % ^{235}U Base Cases)

The first analysis phase was an increase in the ^{235}U enrichment. The LEU was increased from 20 to 25 wt % ^{235}U, while the HEU had a smaller increase from 70 to 71 wt %. The cases model an NAC-LWT cask with a full payload of maximum reactivity fuel (maximum clad diameter, minimum clad thickness, and maximum H/Zr ratio). This fuel type has been documented in the previous TRIGA analysis section to be bounding. Table 6.4.5-22 displays the results of the increased enrichment analysis for the 20 wt % and 70 wt % fuels. The 20 wt % enriched fuel showed a small increase in reactivity, but is still significantly below the 70 wt % fuel in reactivity. The small increase in enrichment in the 70 wt % fuel yielded a similarly small change in reactivity. The change in reactivity is a fraction of the uncertainty associated with the reactivity and is statistically insignificant. The increased enrichment fuel payload remained well under the reactivity limit of 0.95.

Increased Mass of ^{235}U (25 wt % ^{235}U and 71 wt % ^{235}U Base Cases)

The next phase of the analysis increased the mass of ^{235}U in addition to the increased enrichment. The 71 wt % maximum ^{235}U mass was increased from 137 to 138 grams, while the LEU (25 wt %) maximum was increased from 169 to 275 grams. Results for this analysis, with four elements per basket opening, are documented in Table 6.4.5-23. The increase in fissile material in the HEU fuel was small and, again, produced an insignificant change in reactivity when compared to the previous HEU run. All HEU reactivities remained under the 0.95 limit.

Because the full payload of 25%, 275g ^{235}U enriched LEU exceeds the reactivity limit, the fuel must have loading restrictions implemented to meet the limits. The 275g ^{235}U LEU is restricted to the bottom and top baskets of the previously most reactive payload, the 71%, 138 g loading. To implement the restrictions, the material cards of the 25%, 275g LEU were copied and added to the input file of the 138g HEU and a MORE DATA card was added to allow for the Dancoff correction of the second fuel. The result of the LEU restriction to the bottom and top baskets of the HEU payload also exceeded the reactivity limit, so the LEU basket was further restricted, allowing only three rods per basket opening instead of four. Table 6.4.5-24 displays the results of the TRIGA payloads containing the 25%, 275g LEU fuel, as well as comparing them to the full payload of 71%, 138g fuel. A tube basket spacer will be used to limit the loading within the basket opening, while retaining the ability to flood and drain the basket freely.

95% HEU Fuel Loading

A full payload of 95% weight enriched and 175g ^{235}U HEU fuel was evaluated. As with the 25%, 275g LEU fuel, the full payload of 95% HEU fuel resulted in a reactivity over 0.95. The same loading restrictions were tested with the 95% HEU fuel, including restricting the fuel to the bottom and top baskets and only allowing three rods per basket opening. The loading evaluation, documented in Table 6.4.5-25, found that to remain under the 0.95 reactivity limit, the 95% HEU fuel must be restricted to the top and bottom baskets with only three rods per opening. The 71%, 138g HEU fuel was loaded in the middle three baskets of the payloads, while the 95% HEU fuel was restricted to the top and bottom baskets. Figure 6.4.5-12 lists the input for the 95% HEU three-element restricted configuration.

PICTURE, a module within the SCALE package, is used to generate representations of the system geometry. Figure 6.4.5-10 contains the image of a fully loaded basket containing four TRIGA elements or mixed loading of TRIGA elements and TRIGA cluster rods. This evaluation represents the center baskets of the transport configuration containing the 95 wt % enriched fuel in the top and bottom baskets. Figure 6.4.5-11 displays the cross-section of the top and bottom baskets with payload limited to three elements. A dummy TRIGA tube will be inserted into the basket to prohibit loading of a fourth element into the basket cell. The dummy tube is not included in the model.

Damaged Fuel

The NAC-LWT cask is licensed to transport both intact and damaged TRIGA fuel elements. Damaged fuel is restricted to the top and bottom basket modules. The most reactive 25%, 275g ^{235}U LEU, 71%, 138g ^{235}U HEU fuel and 95%, 175g ^{235}U HEU TRIGA fuel were modeled as damaged fuel and restricted to the top and bottom baskets of a payload. The remaining baskets were loaded with the previously most reactive full payload, which was the 71%, 138g HEU fuel.

The damaged fuel model was used as the base model, and the 71%, 138g HEU material cards were inserted into the input file. The damaged fuel was modeled as both intact and rubble fuel. The rubble fuel is sealed in a damaged fuel canister and limited to two rods worth of fuel, while the intact fuel was placed into basket openings in a screened canister and can contain full four rods per canister.

Results of the damaged, rubble fuel analyses shown in Table 6.4.5-26 demonstrate that the restriction to two fuel rods in the sealed canister reduces basket reactivity in the damaged fuel locations to that below the intact fuel center baskets (i.e., system reactivity is controlled by the center intact fuel baskets, and no significant system reactivity change results from the placement of the sealed damaged fuel canisters). Figure 6.4.5-13 lists the input for the 95% HEU damaged fuel configuration.

Screened canisters are expected to reduce reactivity for the full, four element per basket opening payload as a result of the additional stainless steel material in the canister body, axial fuel offset produced by the canister bottom and lid structure, and reduced element pitch available in the canister. The most reactive configuration study in previous evaluations documented the reduced reactivity for smaller fuel element pitch. This effect is verified for the higher load fuel elements in Table 6.4.5-27. Results in Table 6.4.5-27 also include the additional effect of adding the canister materials and the axial offset produced by the canister. The combination of these effects results in a lower screened canister basket reactivity than that of the central baskets with a resulting statistically insignificant change in system reactivity. Screened canister evaluations are performed for all increased payload definitions with the results documented in Table 6.4.5-28. None of the cases showed a statistically significant change in reactivity and no case exceeds the 0.95 allowable k_s.

6.4.5.6.5   Mixed TRIGA Fuel Element and Cluster Rod Study

The NAC-LWT cask may contain a mix payload of TRIGA fuel including cluster rods. The most reactive payload (71%, 138g HEU) was modeled with one of the basket openings loaded with TRIGA cluster fuel. The cluster rods were modeled both as intact in a 4 × 4 holder, and as damaged fuel rods as rubble in a sealed canister. The intact rods had a full loading of 16 rods per basket opening, while the damaged fuel was restricted to the equivalent of six rods in the sealed canister. The resulting reactivity is displayed in Table 6.4.5-29. Replacing the 71 wt % HEU rods with cluster rods in one basket opening shows no stastical change in reactivity, as the system reactivity is driven by the fully loaded fuel element baskets.

6.4.5.6.6   Revised Fuel Parameter Reactivity Summary

The reactivity evaluation of the NAC-LWT cask containing up to 120 TRIGA elements demonstrates that subcritical margin ($k_s \leq 0.95$) can be maintained under the following condition:

		Any Mix Loading			Top/Bottom Basket Only	
Fuel Type	LEU	LEU	HEU	Cluster	LEU	HEU
Clad Type	SS	Al	SS	Incoloy	SS	SS
^{235}U Enrichment (wt %)	25%	25%	71%	95%	25%	95%
^{235}U Content (grams)	≤ 169	≤ 41	≤ 138	≤ 46.5	≤ 275	≤ 175
Max.# of Elements/Rods per Opening — Intact	4			16	3	3
Max.# of Elements/Rods per Opening — Sealed	2			6	2	2
Rod Diameter	≤ 1.5 inch			≤ 0.53	≤ 1.5 inch	
H/ZR Ratio	2.0			1.7	2.0	
Fuel Material	$U\text{-}ZrH_x$					
Clad Thickness	≥ 0.01 inch					
Maximum Reactivity (k_s)	0.949					

Due to limitations on the array size for accident conditions, the criticality safety index (CSI) for the package is 12.5 for loading of intact fuel and sealed cans containing up to two fuel elements (in any condition, including severely damaged fuel and debris). The basket top module may contain TRIGA cluster rods in either intact or canned form.

6.4.5.7   Conclusion

Thus, including all calculational and mechanical uncertainties, an infinite array of NAC-LWT casks remains subcritical, and is below the 0.95 limit, corrected for bias and uncertainty, under normal and accident conditions with:

Nonpoisoned Baskets:

1. 120 TRIGA fuel elements,
2. Sealed cans (top and bottom baskets only) with two damaged TRIGA fuel elements or fuel debris equivalent to two elements.
3. TRIGA cluster rods in the rod holder desribed in Section 6.4.6 inserted into the top basket module of a TRIGA fuel element shipment.

Poisoned Baskets:

4. 140 TRIGA fuel elements,
5. Sealed cans (top and bottom baskets only) with two damaged TRIGA fuel elements or fuel debris equivalent to two elements.

Figure 6.4.5-1   Finite Cask Array Reactivity versus Fuel Zirconium Mass
(Dry Cask Cavity)
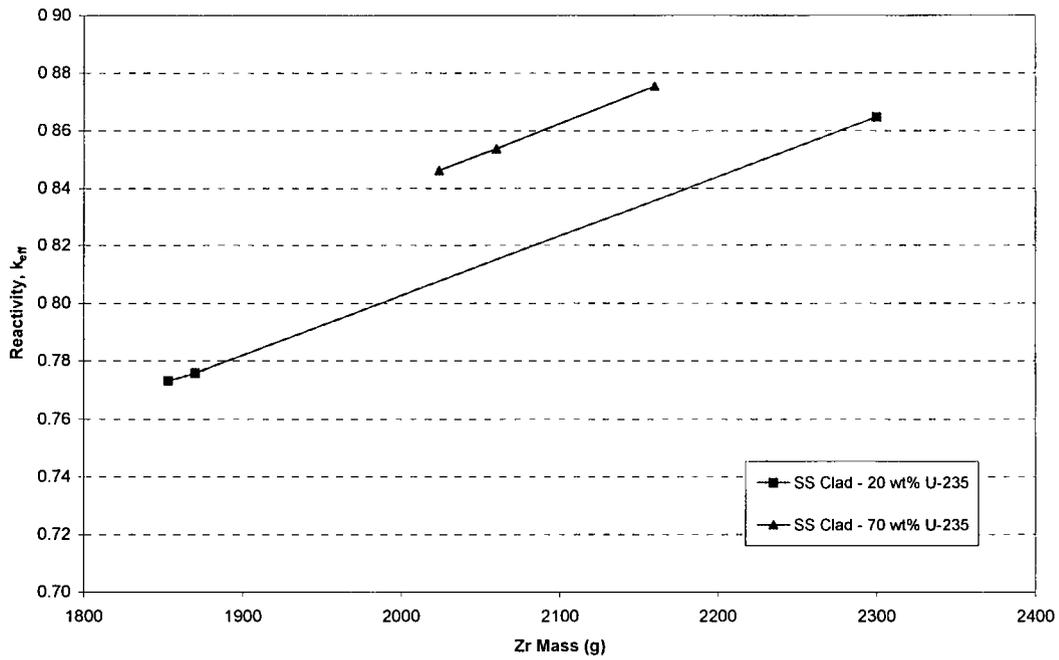
Figure 6.4.5-2   Finite Cask Array Reactivity versus H/Zr Ratio (Dry Cask Cavity)
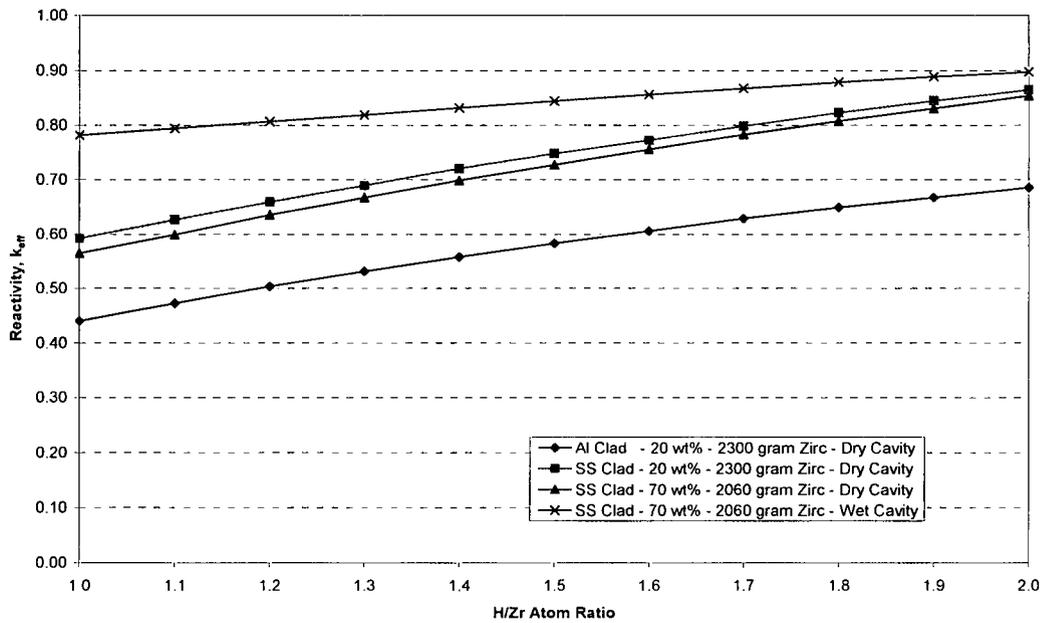
Figure 6.4.5-3   Finite Cask Array Reactivity versus Fuel Mass (Study of ZrH Displacement of Fissile Material for a Fixed Fuel Geometry)
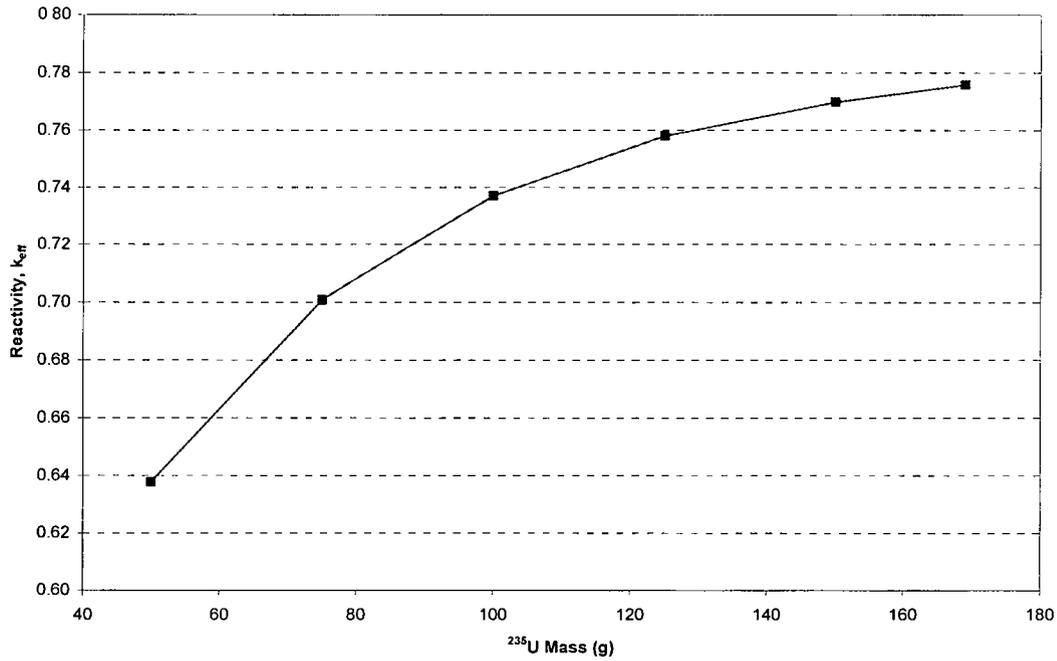
Figure 6.4.5-4   Intact Fuel Optimum Moderator Study – 70 wt % ^{235}U Various Zirconium Masses
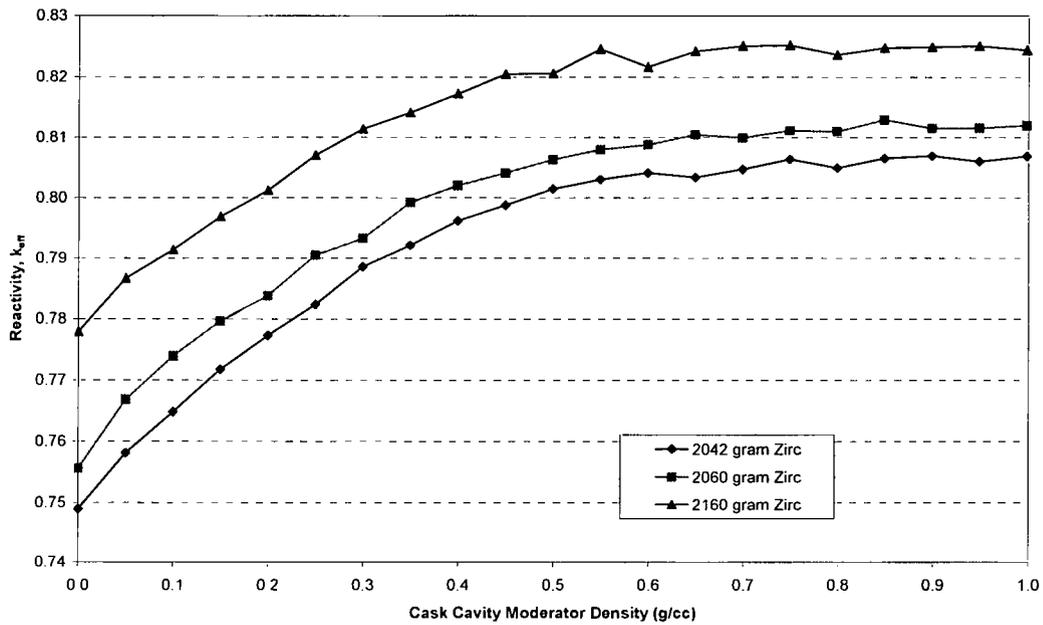
Figure 6.4.5-5   Detailed Intact Fuel Optimum Moderator Study – H/Zr Ratio, Fuel
Element Characteristics and Location Varied
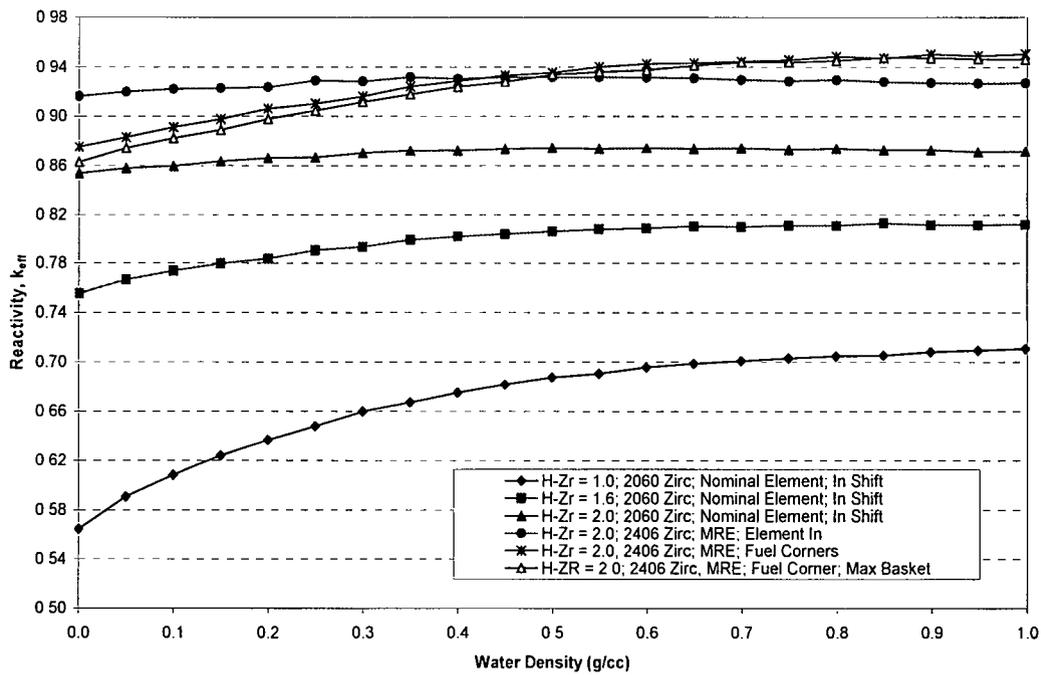
Figure 6.4.5-6   Screened and Sealed Can Optimum Moderator Study – Maximum
Reactivity Fuel Configuration – 70 wt% ^{235}U Steel Clad
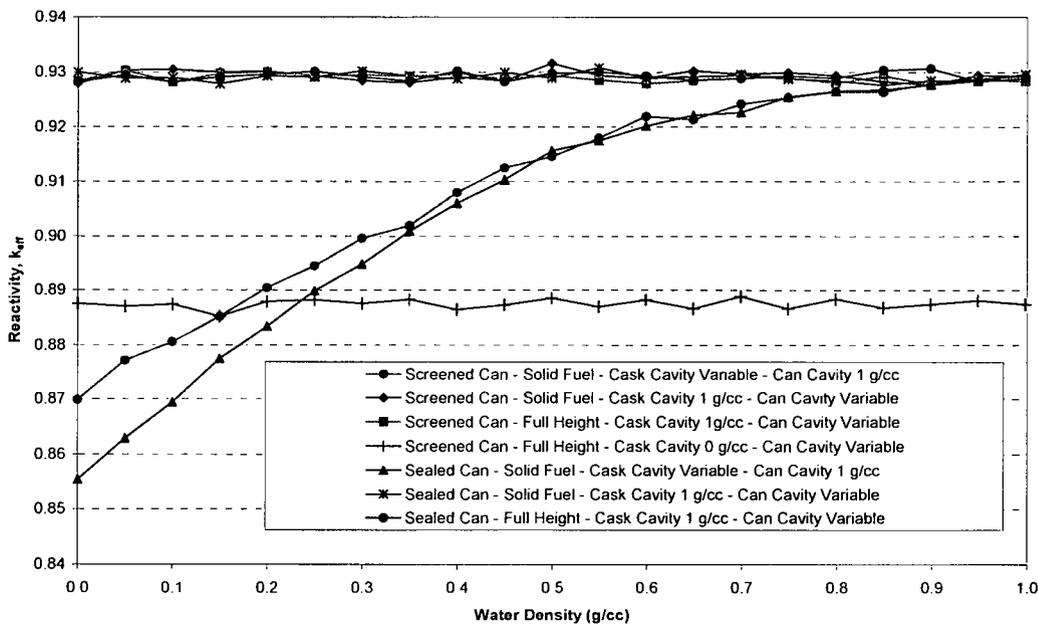
Figure 6.4.5-7   Screened and Sealed Can Debris Height Study – Maximum Reactivity
Fuel Configuration – 70 wt% ^{235}U Steel Clad
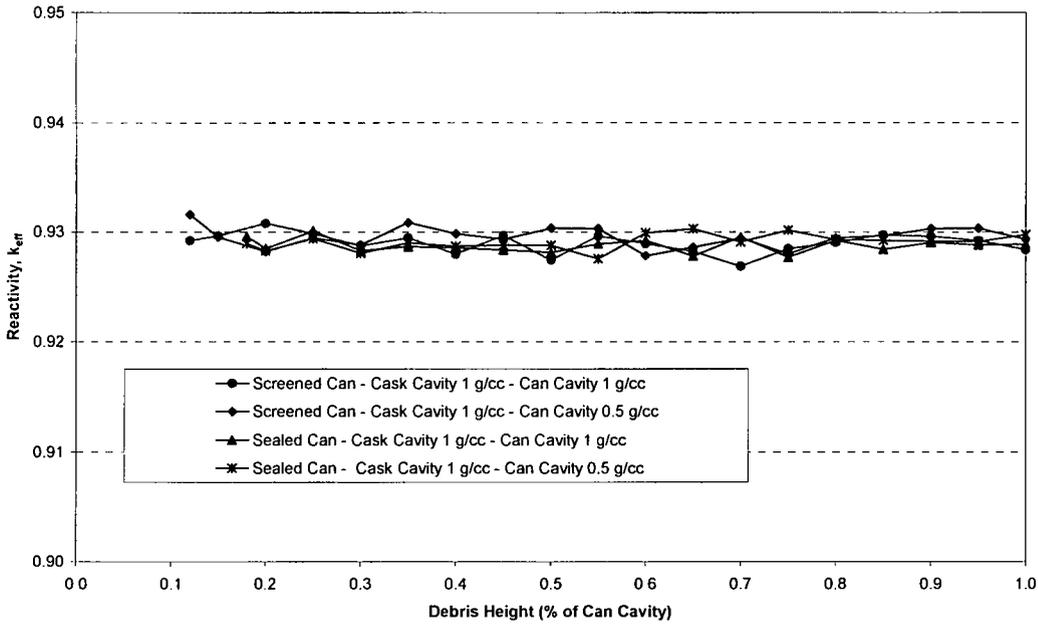
Figure 6.4.5-8   Screened Can – 4 Elements per Can – Maximum Reactivity Fuel
Configuration – 70 wt% ^{235}U Steel Clad
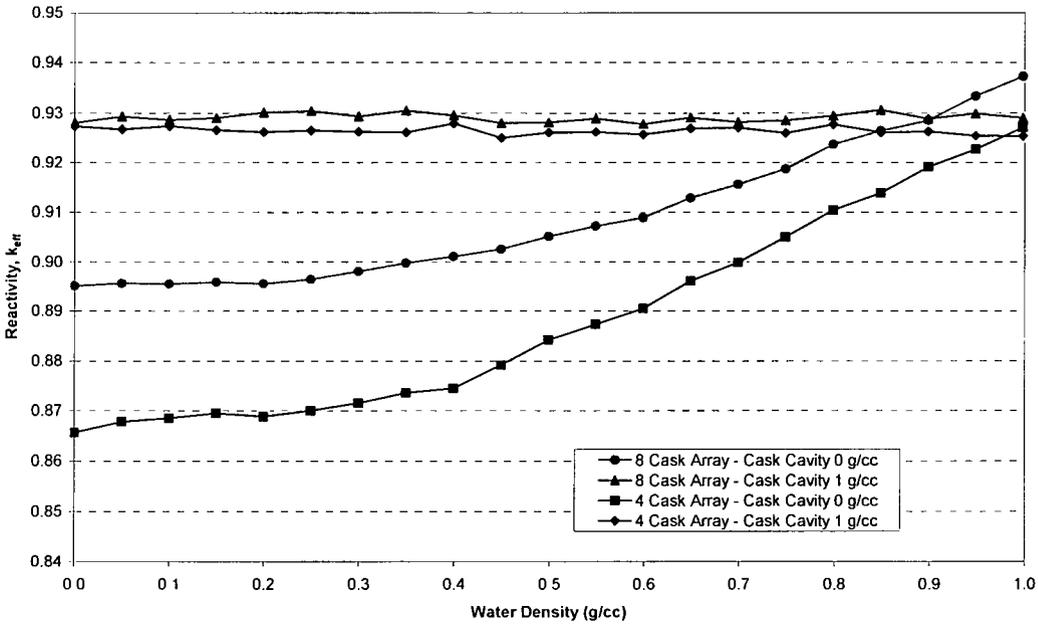
Figure 6.4.5-9   PICTURE Representation of NAC-LWT Eight Cask Array for Accident
Condition TRIGA Unpoisoned Basket Analysis
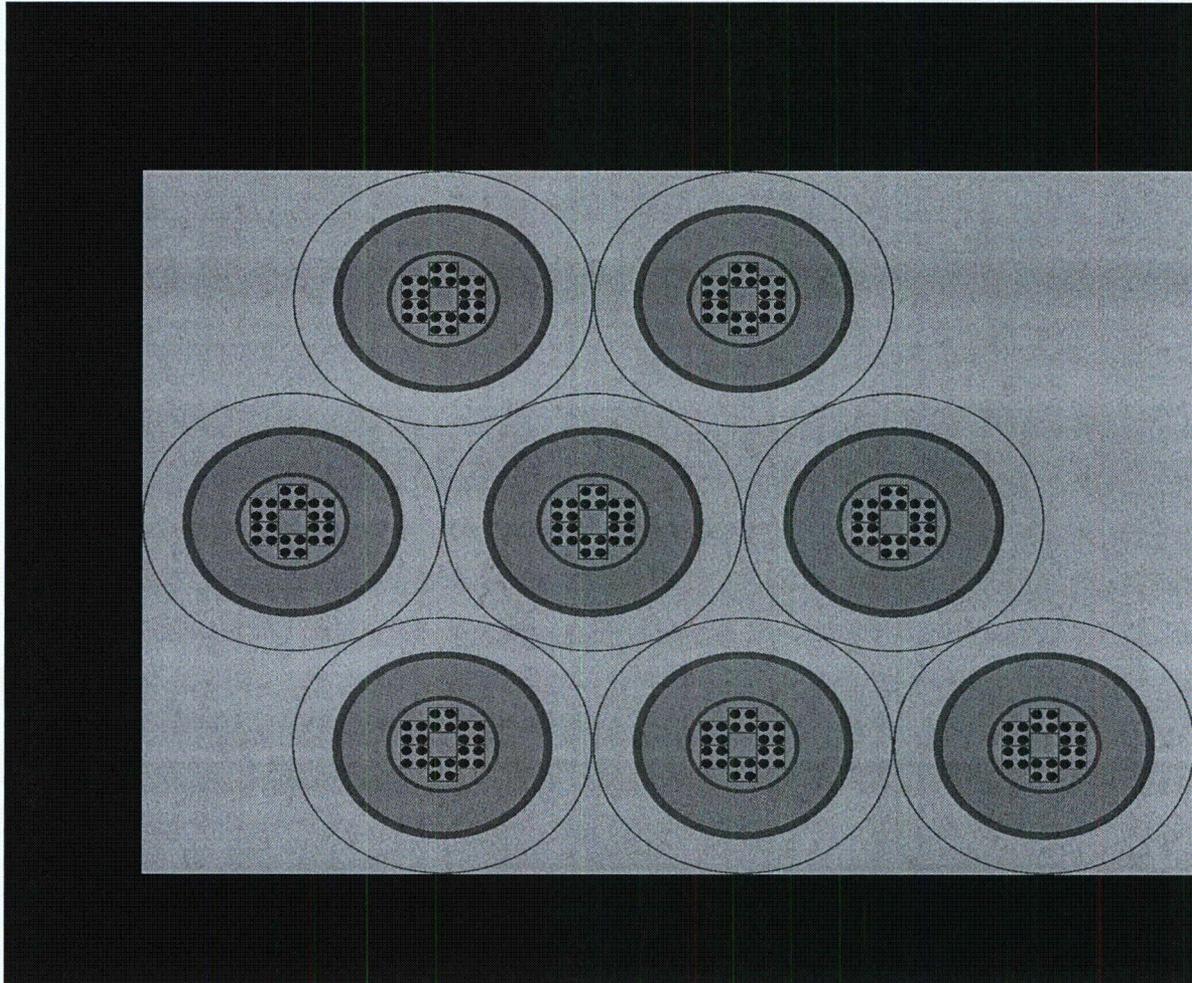
Figure 6.4.5-10   PICTURE Representation of NAC-LWT TRIGA Payload – Fully Loaded Basket Analysis and Mixed TRIGA Loading[4]
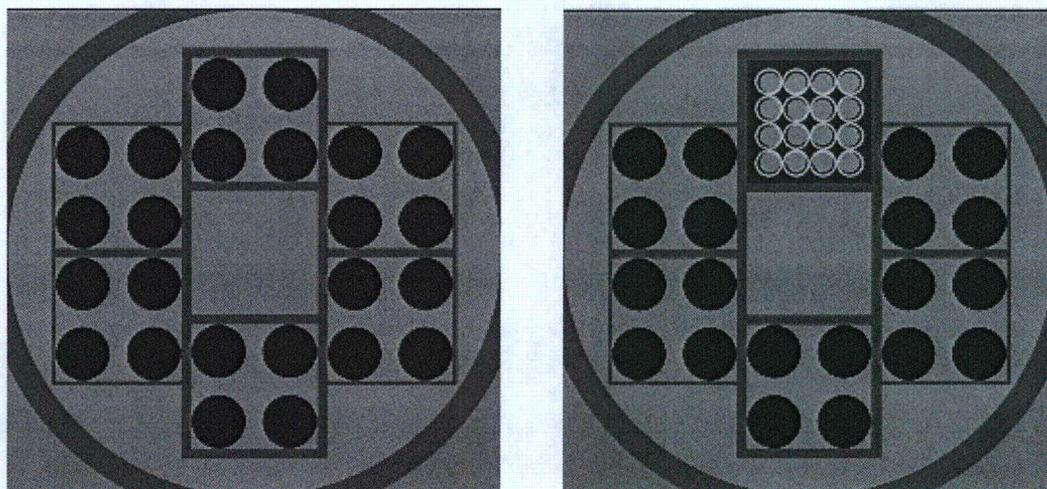
Figure 6.4.5-11   PICTURE Representation of NAC-LWT TRIGA Payload – Reduced Number of Elements in High Fissile Material Element Basket – Top and Bottom Baskets
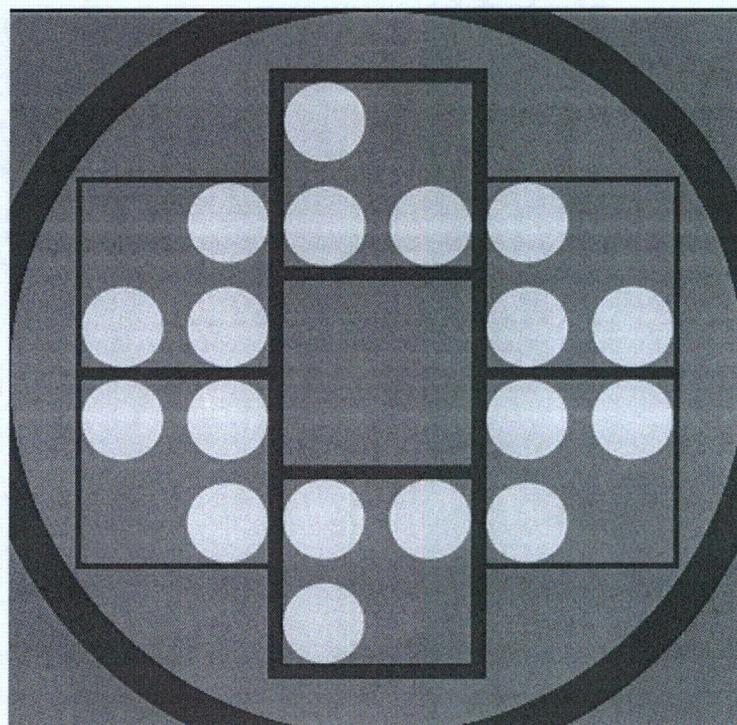
[4] Fully loaded baskets represent the center baskets for the high fissile material load analysis (>138g ^{235}U for HEU and >169g ^{235}U for LEU) and any basket for lower fissile mass and/or mixed TRIGA element/TRIGA cluster rod contents.

Figure 6.4.5-12   Sample Input File for High Mass HEU TRIGA Analysis – 3 Intact
Elements of 175 g ^{235}U at 95 wt % ^{235}U per Basket Opening in Top and Bottom
Basket –Accident Array Calculation with 8 Casks

```
=CSAS25
TRIGA - WET INTERIOR, DRY EXTERIOR - FINITE CASK ARRAY
'2 Fuel run with 2nd fuel in bottom and top baskets
'Fuel 1: 71_2342Zr_U5_138g - middle 3 baskets
'Fuel 2: 95_2345Zr_U5_175g - top and bottom baskets
27GROUPNDF4 LATTICECELL
'FUEL 1
U-235     1 0.0 8.09244E-04 293.0 END
U-238     1 0.0 3.24241E-04 293.0 END
ZR        1 0.0 3.53871E-02 293.0 END
H         1 0.0 7.07742E-02 293.0 END
'CLAD
SS304     2 1.0 293.0 END
'CASK INTERNAL MODERATOR
H2O       3 1.0 293.0 END
'ZIRCONIUM ROD
ZR        4 1.0 293.0 END
'GRAPHITE REFLECTOR
C         5 1.0 293.0 END
'BASKET AND CASK STEEL
SS304     6 1.0 293.0 END
'LEAD SHIELD
PB        7 1.0 293.0 END
'NEUTRON SHIELD
H2O       8 1.0 293.0 END
'CASK EXTERNAL MATERIAL
H2O       9 1E-20 293.0 END
'END FITTING FOR FUEL ELEMENT
SS304     10 0.337137 293.0 END
H2O       10 0.662863 293.0 END
'FUEL 2
U-235     11 0.0 1.02622E-03 293.0 END
U-238     11 0.0 5.21101E-05 293.0 END
ZR        11 0.0 3.54310E-02 293.0 END
H         11 0.0 7.08620E-02 293.0 END
END COMP
SQUAREPITCH 3.8101 3.7592 1 3 3.81 2 3.7592 0 END
MORE DATA
RES=11  CYLINDER 1.87960  DAN(11)=8.52196E-01   END
TRIGA - WET INTERIOR, DRY EXTERIOR - MOST REACTIVE CONFIGURATION
READ PARAM TME=170.0 GEN=803 NPG=2000 RUN=YES PLT=NO
TBA=2.0 END PARAM
READ GEOM
UNIT 41
COM='TRIGA FUEL ELEMENT'
CYLINDER 4 1 0.00010 2P19.6850
'
CYLINDER 1 1 1.87960 2P19.6850
CYLINDER 5 1 1.87960 2P28.3718
'
CYLINDER 2 1 1.90500 2P28.3718
CYLINDER 10 1 1.90500 2P36.7030
UNIT 45
COM='3.38 in Width / 0.28 in Thickness DIVIDER CENTER STACK'
CUBOID   6 1 2P4.29260 0.71120 0.00000 2P36.7030
```

Figure 6.4.5-12   Sample Input File for High Mass HEU TRIGA Analysis – 3 Intact
Elements of 175 g ²³⁵U at 95 wt % ²³⁵U per Basket Opening in Top and Bottom
Basket –Accident Array Calculation with 8 Casks (continued)

```
UNIT 46
COM='3.38 in Width / 0.24 in Thickness DIVIDER OUTSIDE STACK'
CUBOID   6 1 2P4.29260 0.60960 0.00000 2P36.7030
UNIT 50
COM='TRIGA ELEMENTS - Top of 3.38 in x 3.38 in OPENING'
CUBOID   3 1 2P4.29260 2P4.29260 2P36.7030
HOLE     41 +2.3875 +2.3875 0.0000
HOLE     41 -2.3875 +2.3875 0.0000
HOLE     41 -2.3875 -2.3875 0.0000
HOLE     41 +2.3875 -2.3875 0.0000
UNIT 51
COM='TRIGA ELEMENTS - Bottom of 3.38 in x 3.38 in OPENING'
CUBOID   3 1 2P4.29260 2P4.29260 2P36.7030
HOLE     41 +2.3875 +2.3875 0.0000
HOLE     41 -2.3875 +2.3875 0.0000
HOLE     41 -2.3875 -2.3875 0.0000
HOLE     41 +2.3875 -2.3875 0.0000
UNIT 52
COM='TRIGA ELEMENTS - Bottom Right of 3.38 in x 3.38 in OPENING'
CUBOID   3 1 2P4.29260 2P4.29260 2P36.7030
HOLE     41 +2.3875 +2.3875 0.0000
HOLE     41 -2.3875 +2.3875 0.0000
HOLE     41 -2.3875 -2.3875 0.0000
HOLE     41 +2.3875 -2.3875 0.0000
UNIT 53
COM='TRIGA ELEMENTS - Top Right of 3.38 in x 3.38 in OPENING'
CUBOID   3 1 2P4.29260 2P4.29260 2P36.7030
HOLE     41 +2.3875 +2.3875 0.0000
HOLE     41 -2.3875 +2.3875 0.0000
HOLE     41 -2.3875 -2.3875 0.0000
HOLE     41 +2.3875 -2.3875 0.0000
UNIT 54
COM='TRIGA ELEMENTS - Bottom Left of 3.38 in x 3.38 in OPENING'
CUBOID   3 1 2P4.29260 2P4.29260 2P36.7030
HOLE     41 +2.3875 +2.3875 0.0000
HOLE     41 -2.3875 +2.3875 0.0000
HOLE     41 -2.3875 -2.3875 0.0000
HOLE     41 +2.3875 -2.3875 0.0000
UNIT 55
COM='TRIGA ELEMENTS - Top Left of 3.38 in x 3.38 in OPENING'
CUBOID   3 1 2P4.29260 2P4.29260 2P36.7030
HOLE     41 +2.3875 +2.3875 0.0000
HOLE     41 -2.3875 +2.3875 0.0000
HOLE     41 -2.3875 -2.3875 0.0000
HOLE     41 +2.3875 -2.3875 0.0000
UNIT 56
COM='TRIGA BASKET 3.38 in x 3.38 in CENTER OPENING'
CUBOID   3 1 2P4.29260 2P4.29260 2P36.7030
UNIT 60
COM='CENTER COLUMN OF THREE OPENINGS w/ 0.28 in plate'
ARRAY 11 -4.2926 -13.5890 -36.7030
REPLICATE 6 1 4R0.7112 2R0.0 1
UNIT 61
COM='LEFT OUTSIDE COLUMN OF TWO OPENINGS w/ 0.12 in plate'
ARRAY 12 -4.2926 -8.8900 -36.7030
```

Figure 6.4.5-12   Sample Input File for High Mass HEU TRIGA Analysis – 3 Intact
Elements of 175 g ^{235}U at 95 wt % ^{235}U per Basket Opening in Top and Bottom
Basket –Accident Array Calculation with 8 Casks (continued)

```
REPLICATE 6 1 0.0 0.3048 2R0.3048 2R0.0 1
UNIT 62
COM='RIGHT OUTSIDE COLUMN OF TWO OPENINGS w/ 0.12 in plate'
ARRAY 13 -4.2926 -8.8900 -36.7030
REPLICATE 6 1 0.3048 0.0 2R0.3048 2R0.0 1
UNIT 70
COM='NAC-LWT TRIGA BASKET WITH RADIAL CASK SHIELD'
CYLINDER 3 1 17.15000 2P36.7030
HOLE      60 0.0000 0.0000 0.0000
HOLE      61 -9.2965 0.0000 0.0000
HOLE      62 +9.2965 0.0000 0.0000
CYLINDER 6 1 18.91030 2P37.3379
CYLINDER 7 1 33.46450 2P37.3379
CYLINDER 6 1 36.51880 2P37.3379
CYLINDER 9 1 49.22270 2P37.3379
CYLINDER 6 1 49.82210 2P37.3379
'---------------2nd Fuel Units-----------------------------
UNIT 141
COM='TRIGA FUEL ELEMENT'
CYLINDER 4 1 0.00010 2P19.6850
'
CYLINDER 11 1 1.87960 2P19.6850
CYLINDER 5 1 1.87960 2P28.3718
'
CYLINDER 2 1 1.90500 2P28.3718
CYLINDER 10 1 1.90500 2P36.7030

UNIT 150
COM='TRIGA ELEMENTS - Top of 3.38 in x 3.38 in OPENING (Fuel 2)'
CUBOID    3 1 2P4.29260 2P4.29260 2P36.7030
'HOLE      141 +2.3875 +2.3875 0.0000
HOLE      141 -2.3875 +2.3875 0.0000
HOLE      141 -2.3875 -2.3875 0.0000
HOLE      141 +2.3875 -2.3875 0.0000
UNIT 151
COM='TRIGA ELEMENTS - Bottom of 3.38 in x 3.38 in OPENING (Fuel 2)'
CUBOID    3 1 2P4.29260 2P4.29260 2P36.7030
HOLE      141 +2.3875 +2.3875 0.0000
HOLE      141 -2.3875 +2.3875 0.0000
HOLE      141 -2.3875 -2.3875 0.0000
'HOLE      141 +2.3875 -2.3875 0.0000
UNIT 152
COM='TRIGA ELEMENTS - Bottom Right of 3.38 in x 3.38 in OPENING (Fuel 2)'
CUBOID    3 1 2P4.29260 2P4.29260 2P36.7030
HOLE      141 +2.3875 +2.3875 0.0000
HOLE      141 -2.3875 +2.3875 0.0000
HOLE      141 -2.3875 -2.3875 0.0000
'HOLE      141 +2.3875 -2.3875 0.0000
UNIT 153
COM='TRIGA ELEMENTS - Top Right of 3.38 in x 3.38 in OPENING (Fuel 2)'
CUBOID    3 1 2P4.29260 2P4.29260 2P36.7030
'HOLE      141 +2.3875 +2.3875 0.0000
HOLE      141 -2.3875 +2.3875 0.0000
HOLE      141 -2.3875 -2.3875 0.0000
HOLE      141 +2.3875 -2.3875 0.0000
```

Figure 6.4.5-12   Sample Input File for High Mass HEU TRIGA Analysis – 3 Intact
Elements of 175 g ^{235}U at 95 wt % ^{235}U per Basket Opening in Top and Bottom
Basket –Accident Array Calculation with 8 Casks (continued)

```
UNIT 154
COM='TRIGA ELEMENTS - Bottom Left of 3.38 in x 3.38 in OPENING (Fuel 2)'
CUBOID   3 1 2P4.29260 2P4.29260 2P36.7030
HOLE      141 +2.3875 +2.3875 0.0000
HOLE      141 -2.3875 +2.3875 0.0000
'HOLE     141 -2.3875 -2.3875 0.0000
HOLE      141 +2.3875 -2.3875 0.0000
UNIT 155
COM='TRIGA ELEMENTS - Top Left of 3.38 in x 3.38 in OPENING (Fuel 2)'
CUBOID   3 1 2P4.29260 2P4.29260 2P36.7030
HOLE      141 +2.3875 +2.3875 0.0000
'HOLE     141 -2.3875 +2.3875 0.0000
HOLE      141 -2.3875 -2.3875 0.0000
HOLE      141 +2.3875 -2.3875 0.0000
UNIT 160
COM='CENTER COLUMN OF THREE OPENINGS w/ 0.28 in plate'
ARRAY 111 -4.2926 -13.5890 -36.7030
REPLICATE 6 1 4R0.7112 2R0.0 1
UNIT 161
COM='LEFT OUTSIDE COLUMN OF TWO OPENINGS w/ 0.12 in plate'
ARRAY 112 -4.2926 -8.8900 -36.7030
REPLICATE 6 1 0.0 0.3048 2R0.3048 2R0.0 1
UNIT 162
COM='RIGHT OUTSIDE COLUMN OF TWO OPENINGS w/ 0.12 in plate'
ARRAY 113 -4.2926 -8.8900 -36.7030
REPLICATE 6 1 0.3048 0.0 2R0.3048 2R0.0 1
UNIT 170
COM='NAC-LWT TRIGA BASKET WITH RADIAL CASK SHIELD'
CYLINDER 3 1 17.15000 2P36.7030
HOLE      160 0.0000 0.0000 0.0000
HOLE      161 -9.2965 0.0000 0.0000
HOLE      162 +9.2965 0.0000 0.0000
CYLINDER 6 1 18.91030 2P37.3379
CYLINDER 7 1 33.46450 2P37.3379
CYLINDER 6 1 36.51880 2P37.3379
CYLINDER 9 1 49.22270 2P37.3379
CYLINDER 6 1 49.82210 2P37.3379
'----------End 2nd Fuel Units----------------------------
UNIT 80
COM='NAC-LWT WITH 5 TRIGA BASKETS - NO LID OR BOTTOM WELDMENT'
CYLINDER 3 1 49.82210 373.3800 0.0000
HOLE      170 0.0000 0.0000 +37.3380
HOLE      70 0.0000 0.0000 +112.0140
HOLE      70 0.0000 0.0000 +186.6900
HOLE      70 0.0000 0.0000 +261.3660
HOLE      170 0.0000 0.0000 +336.0420
UNIT 90
COM='SIMPLIFIED LID STRUCTURE NAC-LWT'
CYLINDER 6 1 36.5188 2P14.1351
CYLINDER 9 1 49.8221 2P14.1351
UNIT 91
COM='SIMPLIFIED CASK BOTTOM STRUCTURE NAC-LWT'
CYLINDER 7 1 26.3525 2P3.81
CYLINDER 6 1 36.6188 +13.97 -12.7
CYLINDER 9 1 49.8221 +13.97 -12.7
UNIT 92
COM='SINGLE CASK'
```

Figure 6.4.5-12   Sample Input File for High Mass HEU TRIGA Analysis – 3 Intact Elements of 175 g ^{235}U at 95 wt % ^{235}U per Basket Opening in Top and Bottom Basket –Accident Array Calculation with 8 Casks (continued)

```
CYLINDER 9 1 49.82210 428.3204 0.0000
HOLE      91 0.0000 0.0000 +12.7000
HOLE      80 0.0000 0.0000 +26.6700
HOLE      90 0.0000 0.0000 +414.1852
GLOBAL UNIT 93
COM='FINITE CASK ARRAY - 8 CASKS'
CUBOID    9 1 199.28960 -149.46660 2P136.11700 428.3204 0.0000
HOLE      92 0.0000 0.0000 0.0000
HOLE      92 +99.6444 0.0000 0.0000
HOLE      92 +49.8222 +86.2946 0.0000
HOLE      92 -49.8222 +86.2946 0.0000
HOLE      92 -99.6444 0.0000 0.0000
HOLE      92 -49.8222 -86.2946 0.0000
HOLE      92 +49.8222 -86.2946 0.0000
HOLE      92 +149.4666 -86.2946 0.0000
END GEOM
READ ARRAY
ARA=11 NUX=1 NUY=5 NUZ=1 FILL 50 45 56 45 51 END FILL
ARA=12 NUX=1 NUY=3 NUZ=1 FILL 53 46 52 END FILL
ARA=13 NUX=1 NUY=3 NUZ=1 FILL 55 46 54 END FILL
ARA=111 NUX=1 NUY=5 NUZ=1 FILL 151 45 56 45 150 END FILL
ARA=112 NUX=1 NUY=3 NUZ=1 FILL 154 46 155 END FILL
ARA=113 NUX=1 NUY=3 NUZ=1 FILL 152 46 153 END FILL
END ARRAY
READ BOUNDS ALL=H2O END BOUNDS
READ PLOT
TTL='X-Y PLOT OF BASKET'
SCR=YES PIC=MAT LPI=10
UAX=1.0 VDN=-1.0 NAX=1600
XUL=-17.2 YUL=17.2 ZUL=215
XLR=17.2 YLR=-17.2 ZLR=215 END
TTL='X-Y PLOT OF PERIPHERAL OPENING'
SCR=YES PIC=MAT LPI=10
UAX=1.0 VDN=-1.0 NAX=1600
XUL=-7.0 YUL=16.0 ZUL=215
XLR=7.0  YLR=4.0 ZLR=215 END
TTL='Y-Z PLOT OF BASKET (CENTER OF FUEL ELEMENTS,CANISTER ELEVATION)'
SCR=YES PIC=MAT LPI=10
VAX=1.0 WDN=-1.0 NAX=1600
XUL=2.12 YUL=-14.0 ZUL=330
XLR=2.12 YLR=-4.5 ZLR=235 END
TTL='Y-Z PLOT OF BASKET (CASK)'
SCR=YES PIC=MAT LPI=10
VAX=1.0 WDN=-1.0 NAX=1600
XUL=2.12 YUL=-51 ZUL=465
XLR=2.12 YLR=+51 ZLR=0 END
TTL='X-Y PLOT OF ARRAY'
SCR=YES PIC=MAT LPI=10
UAX=1.0 VDN=-1.0 NAX=1600
XUL=-200 YUL=200 ZUL=215
XLR=200  YLR=-200 ZLR=215
END PLOT
END DATA
END
```

Figure 6.4.5-13   Sample Input File for High Mass HEU TRIGA Analysis – 2 Damaged
Elements of 175 g ^{235}U at 95 wt % ^{235}U per Basket Opening in Top and Bottom
Basket – Accident Array Calculation with 8 Casks

```
=CSAS25
TRIGA - PREF. FLOOD DEBRIS CANISTER - SEALED CAN - 2 RODS
27GROUPNDF4  INFHOMMEDIUM
'Sealed Fuel: 95_2345Zr_U5_175g
'Middle Baskets Fuel: 71_2342Zr_U5_138g'FUEL
U-235      1 0.0 1.80754E-04 293.0 END
U-238      1 0.0 9.17849E-06 293.0 END
ZR         1 0.0 6.24069E-03 293.0 END
H          1 0.0 1.24814E-02 293.0 END
H2O        1 0.823864 293.0 END
'
'
'CANISTER INTERNAL MODERATOR
H2O        3 1.0 293.0 END
'ZIRCONIUM ROD
ZR         4 1.0 293.0 END
'GRAPHITE REFLECTOR
C          5 1.0 293.0 END
'BASKET AND CASK STEEL
SS304      6 1.0 293.0 END
'LEAD SHIELD
PB         7 1.0 293.0 END
'NEUTRON SHIELD
H2O        8 1.0 293.0 END
'CASK EXTERNAL MATERIAL
H2O        9 1E-20 293.0 END
'
'
'
'INTACT FUEL MATERIAL COMPOSITION
U-235     11 0.0 8.09244E-04 293.0 END
U-238     11 0.0 3.24241E-04 293.0 END
ZR        11 0.0 3.53871E-02 293.0 END
H         11 0.0 7.07742E-02 293.0 END
'INTACT FUEL CLAD
SS304     12 1.0 293.0 END
'CASK INTERIOR MODERATOR MATERIAL
H2O       13 1.0 293.0 END
'INTACT FUEL END-FITTING
SS304     14 0.337137 293.0 END
H2O       14 0.662863 293.0 END
END COMP
MORE DATA
RES=11  CYLINDER 1.8796 DAN(11)=8.52196E-01
END MORE
TRIGA - PREF. FLOOD CANISTER  - 2 ROD FILLING CANISTER + TOLERANCE
READ PARAM TME=170.0 GEN=803 NPG=2000 RUN=YES PLT=NO
TBA=2.0 END PARAM
READ GEOM
UNIT 1
COM='TRIGA FUEL (SEALED)'
CYLINDER 1 1 3.98770 99.3130 0.0010
UNIT 5
COM='3.38 in Width / 0.28 in Thickness DIVIDER CENTER STACK (SEALED)'
CUBOID    6 1 2P4.29260 0.71120 0.00000 112.6490 -8.2550
UNIT 6
```

Figure 6.4.5-13   Sample Input File for High Mass HEU TRIGA Analysis – 2 Damaged
Elements of 175 g ^{235}U at 95 wt % ^{235}U per Basket Opening in Top and Bottom
Basket – Accident Array Calculation with 8 Casks (continued)

```
COM='3.38 in Width / 0.24 in Thickness DIVIDER OUTSIDE STACK (SEALED)'
CUBOID   6 1 2P4.29260 0.60960 0.00000 112.6490 -8.2550
UNIT 7
COM=' SEALED CANISTER'
CYLINDER 3 1 3.98780 99.3140 0.0000
HOLE     1 0.0000 0.0000 0.0000
CYLINDER 6 1 4.15290 101.8540 -1.2700
CYLINDER 13 1 4.15290 112.6490 -8.2550
UNIT 10
COM='TRIGA ELEMENTS - Top of 3.38 in x 3.38 in OPENING (SEALED)'
CUBOID   13 1 2P4.29260 2P4.29260 112.6490 -8.2550
HOLE     7 0.0000 +0.1396 0.0000
UNIT 11
COM='TRIGA ELEMENTS - Bottom of 3.38 in x 3.38 in OPENING (SEALED)'
CUBOID   13 1 2P4.29260 2P4.29260 112.6490 -8.2550
HOLE     7 0.0000 -0.1396 0.0000
UNIT 12
COM='TRIGA ELEMENTS - Bottom Right of 3.38 in x 3.38 in OPENING (SEALED)'
CUBOID   13 1 2P4.29260 2P4.29260 112.6490 -8.2550
HOLE     7 +0.1396 -0.1396 0.0000
UNIT 13
COM='TRIGA ELEMENTS - Top Right of 3.38 in x 3.38 in OPENING (SEALED)'
CUBOID   13 1 2P4.29260 2P4.29260 112.6490 -8.2550
HOLE     7 +0.1396 +0.1396 0.0000
UNIT 14
COM='TRIGA ELEMENTS - Bottom Left of 3.38 in x 3.38 in OPENING (SEALED)'
CUBOID   13 1 2P4.29260 2P4.29260 112.6490 -8.2550
HOLE     7 -0.1396 -0.1396 0.0000
UNIT 15
COM='TRIGA ELEMENTS - Top Left of 3.38 in x 3.38 in OPENING (SEALED)'
CUBOID   13 1 2P4.29260 2P4.29260 112.6490 -8.2550
HOLE     7 -0.1396 +0.1396 0.0000
UNIT 16
COM='TRIGA BASKET 3.38 in x 3.38 in CENTER OPENING (SEALED)'
CUBOID   13 1 2P4.29260 2P4.29260 112.6490 -8.2550
UNIT 20
COM='CENTER COLUMN OF THREE OPENINGS w/ 0.28 in plate (SEALED)'
ARRAY 1 -4.2926 -13.5890 -8.2550
REPLICATE 6 1 4R0.7112 2R0.0 1
UNIT 21
COM='LEFT OUTSIDE COLUMN OF TWO OPENINGS w/ 0.12 in plate (SEALED)'
ARRAY 2 -4.2926 -8.8900 -8.2550
REPLICATE 6 1 0.0 0.3048 2R0.3048 2R0.0 1
UNIT 22
COM='RIGHT OUTSIDE COLUMN OF TWO OPENINGS w/ 0.12 in plate (SEALED)'
ARRAY 3 -4.2926 -8.8900 -8.2550
REPLICATE 6 1 0.3048 0.0 2R0.3048 2R0.0 1
UNIT 30
COM='NAC-LWT TRIGA BASKET (SEALED)'
CYLINDER 13 1 17.15000 112.6491 -8.2551
HOLE     20 0.0000 0.0000 0.0000
HOLE     21 -9.2965 0.0000 0.0000
HOLE     22 +9.2965 0.0000 0.0000
CYLINDER 6 1 18.91030 113.2838 -8.8898
CYLINDER 7 1 33.46450 113.2838 -8.8898
CYLINDER 6 1 36.51880 113.2838 -8.8898
```

Figure 6.4.5-13   Sample Input File for High Mass HEU TRIGA Analysis – 2 Damaged
Elements of 175 g ^{235}U at 95 wt % ^{235}U per Basket Opening in Top and Bottom
Basket – Accident Array Calculation with 8 Casks (continued)

```
CYLINDER 9 1 49.22270 113.2838 -8.8898
CYLINDER 6 1 49.82210 113.2838 -8.8898
UNIT 41
COM='TRIGA FUEL ELEMENT'
CYLINDER 4 1 0.00010 2P19.6850

CYLINDER 11 1 1.87960 2P19.6850
CYLINDER 5 1 1.87960 2P28.3718

CYLINDER 12 1 1.90500 2P28.3718
CYLINDER 14 1 1.90500 2P36.7030
UNIT 45
COM='3.38 in Width / 0.28 in Thickness DIVIDER CENTER STACK'
CUBOID   6 1 2P4.29260 0.71120 0.00000 2P36.7030
UNIT 46
COM='3.38 in Width / 0.24 in Thickness DIVIDER OUTSIDE STACK'
CUBOID   6 1 2P4.29260 0.60960 0.00000 2P36.7030
UNIT 50
COM='TRIGA ELEMENTS - Top of 3.38 in x 3.38 in OPENING'
CUBOID   13 1 2P4.29260 2P4.29260 2P36.7030
HOLE     41 +2.3875 +2.3875 0.0000
HOLE     41 -2.3875 +2.3875 0.0000
HOLE     41 -2.3875 -2.3875 0.0000
HOLE     41 +2.3875 -2.3875 0.0000
UNIT 51
COM='TRIGA ELEMENTS - Bottom of 3.38 in x 3.38 in OPENING'
CUBOID   13 1 2P4.29260 2P4.29260 2P36.7030
HOLE     41 +2.3875 +2.3875 0.0000
HOLE     41 -2.3875 +2.3875 0.0000
HOLE     41 -2.3875 -2.3875 0.0000
HOLE     41 +2.3875 -2.3875 0.0000
UNIT 52
COM='TRIGA ELEMENTS - Bottom Right of 3.38 in x 3.38 in OPENING'
CUBOID   13 1 2P4.29260 2P4.29260 2P36.7030
HOLE     41 +2.3875 +2.3875 0.0000
HOLE     41 -2.3875 +2.3875 0.0000
HOLE     41 -2.3875 -2.3875 0.0000
HOLE     41 +2.3875 -2.3875 0.0000
UNIT 53
COM='TRIGA ELEMENTS - Top Right of 3.38 in x 3.38 in OPENING'
CUBOID   13 1 2P4.29260 2P4.29260 2P36.7030
HOLE     41 +2.3875 +2.3875 0.0000
HOLE     41 -2.3875 +2.3875 0.0000
HOLE     41 -2.3875 -2.3875 0.0000
HOLE     41 +2.3875 -2.3875 0.0000
UNIT 54
COM='TRIGA ELEMENTS - Bottom Left of 3.38 in x 3.38 in OPENING'
CUBOID   13 1 2P4.29260 2P4.29260 2P36.7030
HOLE     41 +2.3875 +2.3875 0.0000
HOLE     41 -2.3875 +2.3875 0.0000
HOLE     41 -2.3875 -2.3875 0.0000
HOLE     41 +2.3875 -2.3875 0.0000
UNIT 55
COM='TRIGA ELEMENTS - Top Left of 3.38 in x 3.38 in OPENING'
CUBOID   13 1 2P4.29260 2P4.29260 2P36.7030
HOLE     41 +2.3875 +2.3875 0.0000
```

Figure 6.4.5-13   Sample Input File for High Mass HEU TRIGA Analysis – 2 Damaged
Elements of 175 g ^{235}U at 95 wt % ^{235}U per Basket Opening in Top and Bottom
Basket – Accident Array Calculation with 8 Casks (continued)

```
HOLE      41 -2.3875 +2.3875 0.0000
HOLE      41 -2.3875 -2.3875 0.0000
HOLE      41 +2.3875 -2.3875 0.0000
UNIT 56
COM='TRIGA BASKET 3.38 in x 3.38 in CENTER OPENING'
CUBOID   13 1 2P4.29260 2P4.29260 2P36.7030
UNIT 60
COM='CENTER COLUMN OF THREE OPENINGS w/ 0.28 in plate'
ARRAY 11 -4.2926 -13.5890 -36.7030
REPLICATE 6 1 4R0.7112 2R0.0 1
UNIT 61
COM='LEFT OUTSIDE COLUMN OF TWO OPENINGS w/ 0.12 in plate'
ARRAY 12 -4.2926 -8.8900 -36.7030
REPLICATE 6 1 0.0 0.3048 2R0.3048 2R0.0 1
UNIT 62
COM='RIGHT OUTSIDE COLUMN OF TWO OPENINGS w/ 0.12 in plate'
ARRAY 13 -4.2926 -8.8900 -36.7030
REPLICATE 6 1 0.3048 0.0 2R0.3048 2R0.0 1
UNIT 70
COM='NAC-LWT TRIGA BASKET WITH RADIAL CASK SHIELD'
CYLINDER 13 1 17.15000 2P36.7030
HOLE      60 0.0000 0.0000 0.0000
HOLE      61 -9.2965 0.0000 0.0000
HOLE      62 +9.2965 0.0000 0.0000
CYLINDER 6 1 18.91030 2P37.3379
CYLINDER 7 1 33.46450 2P37.3379
CYLINDER 6 1 36.51880 2P37.3379
CYLINDER 9 1 49.22270 2P37.3379
CYLINDER 6 1 49.82210 2P37.3379
UNIT 81
COM='NAC-LWT WITH 5 TRIGA BASKETS - NO LID OR BOTTOM WELDMENT'
CYLINDER 13 1 49.82210 468.3760 0.0000
HOLE      30 0.0000 0.0000 +8.8900
HOLE      70 0.0000 0.0000 +159.5120
HOLE      70 0.0000 0.0000 +234.1880
HOLE      70 0.0000 0.0000 +308.8640
HOLE      30 0.0000 0.0000 +355.0920
UNIT 90
COM='SIMPLIFIED LID STRUCTURE NAC-LWT'
CYLINDER 6 1 36.5188 2P14.1351
CYLINDER 9 1 49.8221 2P14.1351
UNIT 91
COM='SIMPLIFIED CASK BOTTOM STRUCTURE NAC-LWT'
CYLINDER 7 1 26.3525 2P3.81
CYLINDER 6 1 36.6188 +13.97 -12.7
CYLINDER 9 1 49.8221 +13.97 -12.7
UNIT 92
COM='SINGLE CASK'
CYLINDER 9 1 49.82210 523.3164 0.0000
HOLE      91 0.0000 0.0000 +12.7000
HOLE      81 0.0000 0.0000 +26.6700
HOLE      90 0.0000 0.0000 +509.1812
GLOBAL UNIT 93
COM='FINITE CASK ARRAY - 8 CASKS'
CUBOID   9 1 199.28960 -149.46660 2P136.11700 523.3164 0.0000
HOLE      92 0.0000 0.0000 0.0000
HOLE      92 +99.6444 0.0000 0.0000
HOLE      92 +49.8222 +86.2946 0.0000
```

Figure 6.4.5-13   Sample Input File for High Mass HEU TRIGA Analysis – 2 Damaged
Elements of 175 g ^{235}U at 95 wt % ^{235}U per Basket Opening in Top and Bottom
Basket – Accident Array Calculation with 8 Casks (continued)

```
HOLE      92 -49.8222 +86.2946 0.0000
HOLE      92 -99.6444 0.0000 0.0000
HOLE      92 -49.8222 -86.2946 0.0000
HOLE      92 +49.8222 -86.2946 0.0000
HOLE      92 +149.4666 -86.2946 0.0000
END GEOM
READ ARRAY
ARA=1 NUX=1 NUY=5 NUZ=1 FILL 10 5 16 5 11 END FILL
ARA=2 NUX=1 NUY=3 NUZ=1 FILL 13 6 12 END FILL
ARA=3 NUX=1 NUY=3 NUZ=1 FILL 15 6 14 END FILL
ARA=11 NUX=1 NUY=5 NUZ=1 FILL 50 45 56 45 51 END FILL
ARA=12 NUX=1 NUY=3 NUZ=1 FILL 53 46 52 END FILL
ARA=13 NUX=1 NUY=3 NUZ=1 FILL 55 46 54 END FILL
END ARRAY
READ BOUNDS ALL=H2O END BOUNDS
READ PLOT
TTL='X-Y PLOT OF CASK (CANISTER ELEVATION)'
SCR=YES PIC=MAT LPI=10
UAX=1.0 VDN=-1.0 NAX=1600
XUL=-50.0 YUL=50.0 ZUL=50
XLR=50.0 YLR=-50.0 ZLR=50 END
TTL='X-Y PLOT OF BASKET (CANISTER ELEVATION)'
SCR=YES PIC=MAT LPI=10
UAX=1.0 VDN=-1.0 NAX=1600
XUL=-17.2 YUL=17.2 ZUL=50
XLR=17.2 YLR=-17.2 ZLR=50 END
TTL='X-Y PLOT OF BASKET (CAVITY MID PLANE)'
SCR=YES PIC=MAT LPI=10
UAX=1.0 VDN=-1.0 NAX=1600
XUL=-17.2 YUL=17.2 ZUL=210.0
XLR=17.2 YLR=-17.2 ZLR=210.0 END
TTL='X-Y PLOT OF CENTER OPENING (CANISTER ELEVATION)'
SCR=YES PIC=MAT LPI=10
UAX=1.0 VDN=-1.0 NAX=1600
XUL=-7.0 YUL=7.0 ZUL=50
XLR=7.0 YLR=-7.0 ZLR=50 END
TTL='X-Y PLOT OF PERIPHERAL OPENING (CANISTER ELEVATION)'
SCR=YES PIC=MAT LPI=10
UAX=1.0 VDN=-1.0 NAX=1600
XUL=-7.0 YUL=16.0 ZUL=50
XLR=7.0  YLR=4.0 ZLR=50 END
TTL='Y-Z PLOT OF BASKET (CENTER OF FUEL ELEMENTS,CANISTER ELEVATION)'
SCR=YES PIC=MAT LPI=10
VAX=1.0 WDN=-1.0 NAX=1600
XUL=2.12 YUL=-14.0 ZUL=100.69
XLR=2.12 YLR=-4.5 ZLR=20 END
TTL='Y-Z PLOT OF BASKET (CASK)'
SCR=YES PIC=MAT LPI=10
VAX=1.0 WDN=-1.0 NAX=1600
XUL=2.12 YUL=-51 ZUL=500
XLR=2.12 YLR=+51 ZLR=0 END
TTL='X-Y PLOT OF ARRAY'
SCR=YES PIC=MAT LPI=10
UAX=1.0 VDN=-1.0 NAX=1600
```

Figure 6.4.5-13   Sample Input File for High Mass HEU TRIGA Analysis – 2 Damaged Elements of 175 g ^{235}U at 95 wt % ^{235}U per Basket Opening in Top and Bottom Basket – Accident Array Calculation with 8 Casks (continued)

```
XUL=-200 YUL=200 ZUL=215
XLR=200  YLR=-200 ZLR=215
END PLOT
END DATA
END
```

Table 6.4.5-1   Parametric Study – Fuel / Basket k-infinity versus TRIGA Fuel Element
Type, Nonpoisoned Basket

(Infinite Array of Nonpoisoned TRIGA Basket Cells with Four (4) Elements)

Fuel Element Type	Initial U Content wt%	Total U grams	^{235}U wt%	Wet Case Results K(infinity) ± σ	Dry Case Results k(infinity) ± σ
Original Al Clad 14 inch Active Fuel	8-8.5	205	20.0	1.01740 ± 0.00081	1.04129 ± 0.00066
Original Al Clad 15 inch Active Fuel	8-8.5	205	20.0	1.00636 ± 0.00081	1.02634 ± 0.00065
Stand. Streamlined Steel Clad 15 inch Active Fuel (FLIP)	8.5	196	70.0	1.33900 ± 0.00094	1.43012 ± 0.00078
Stand. Plain Steel Clad 15 Active Fuel (FLIP)	8.5	196	70.0	1.33969 ± 0.00097	1.43009 ± 0.00077
Stand. Streamlined Steel Clad FLIP-LEU-II	30.6	845	20.0	1.28517 ± 0.00087	1.31180 ± 0.00073
Stand. Plain Steel Clad FLIP-LEU-II	30.6	845	20.0	1.28512 ± 0.00088	1.31198 ± 0.00072
FFCR Element FLIP-LEU-I	20.0	484	20.0	1.16407 ± 0.00086	1.23186 ± 0.00071
1-70 wt% ^{235}U + 3-20 wt% ^{235}U	--	--	--	1.30429 ± 0.00091	1.34060 ± 0.00071
3-70 wt% ^{235}U + 1-20 wt% ^{235}U	--	--	--	1.32896 ± 0.00092	1.40083 ± 0.00077
2-70 wt% ^{235}U + 2-20 wt% ^{235}U	--	--	--	1.31601 ± 0.00094	1.37156 ± 0.00076

LEU   Low Enriched Uranium
FLIP   Fuel Life Improvement Program
FFCR   Fuel Follower Control Rod
* Resonance treatment for two different fuel types is included.

Table 6.4.5-2   Parametric Study – Cask k_{eff} versus TRIGA Fuel Element Type,
Poisoned Basket

Fuel Element Type	Initial U Content wt%	Total U grams	235U wt%	Wet Case Results $k_{eff} \pm \sigma$	Dry Case Results $K_{eff} \pm \sigma$
Original Al Clad 15 inch Active Fuel	8-8.5	205	20.0	0.58906 ± 0.00097	0.47118 ± 0.00076
Stand. Streamlined Steel Clad 15 inch Active Fuel (FLIP)	8.5	196	70.0	0.86504 ± 0.00134	0.85705 ± 0.00112
Stand. Plain Steel Clad 15 Active Fuel (FLIP)	8.5	196	70.0	0.86647 ± 0.00137	0.86610 ± 0.00115
Stand. Streamlined Steel Clad FLIP-LEU-II	30.6	845	20.0	0.83413 ± 0.00130	0.80073 ± 0.00103
Stand. Plain Steel Clad FLIP-LEU-II	30.6	845	20.0	0.83604 ± 0.00127	0.80492 ± 0.00099
1-70 wt% 235U + 3-20 wt% 235U	--	--	--	0.84391 ± 0.00133	0.81589 ± 0.00101
3-70 wt% 235U + 1-20 wt% 235U	--	--	--	0.85826 ± 0.00131	0.84917 ± 0.00108
2-70 wt% 235U + 2-20 wt% 235U	--	--	--	0.85162 ± 0.00129	0.83177 ± 0.00103

Table 6.4.5-3   Axially Infinite Cask k_{eff} with TRIGA Fuel Elements – Fuel Element Placement Perturbations, Nonpoisoned Basket

Basket Configuration	Wet Case Results $k_{eff} \pm \sigma$	Dry Case Results $k_{eff} \pm \sigma$
Elements Touching, Moved In	-	0.93434 ± 0.00115
Elements Touching, Centered	0.77382 ± 0.00109	0.92672 ± 0.00185
Elements Out	0.83468 ± 0.00101	0.90817 ± 0.00105
Elements Centered, Quadrants	0.81340 ± 0.00107	-
Three - 70 wt% ^{235}U Elements (Equilateral)	0.83646 ± 0.00112	-
Three - 70 wt% ^{235}U Elements (in corner)	0.83579 ± 0.00101	0.80629 ± 0.00110
Three - 70 wt% ^{235}U Elements (Isosceles)	0.83468 ± 0.00101	-
Two - 70 wt% ^{235}U Elements (Center)	0.67480 ± 0.00097	0.63503 ± 0.00108
One - 70 wt% ^{235}U Elements (Center)	0.44428 ± 0.00091	-

Table 6.4.5-4   Axially Infinite Cask k_{eff} with TRIGA Fuel Elements – Fuel Element Placement Perturbations, Poisoned Basket

Basket Configuration	Wet Case Results $k_{eff} \pm \sigma$	Dry Case Results $k_{eff} \pm \sigma$
Elements Touching, Moved In	-	0.88969 ± 0.00122
Elements Touching, Centered	0.82705 ± 0.00136	0.87833 ± 0.00122
Elements Touching, Moved Out	-	0.87871 ± 0.00112
Elements Centered, Quadrants	0.86647 ± 0.00134	0.86610 ± 0.00115
Elements Out	0.87874 ± 0.00123	0.85348 ± 0.00114
27 Elements, Touching	0.85014 ± 0.00131	0.66829 ± 0.00114
27 Elements, Corners	0.84686 ± 0.00124	-
26 Elements, Touching	0.82959 ± 0.00124	0.64354 ± 0.00117
26 Elements, Corners	0.81959 ± 0.00126	-
21 Elements, Touching	0.70693 ± 0.00127	0.55021 ± 0.00110
21 Elements, Corners	0.73134 ± 0.00133	-
14 Elements, Touching	0.58154 ± 0.00136	0.39354 ± 0.00097
14 Elements, Corners	0.55112 ± 0.00117	-

Table 6.4.5-5   Axially Infinite Cask k_{eff} with TRIGA Fuel Elements – Basket
Manufacturing Tolerance Perturbations, Nonpoisoned Basket

Basket Configuration	Wet Case Results w/ Dry Neutron Shield $k_{eff} \pm \sigma$	Dry Case Results $k_{eff} \pm \sigma$
Base Case[1]	0.86190 ± 0.00089[3]	0.90053 ± 0.00115[4]
Thin SS Plates	0.86861 ± 0.00094	0.90501 ± 0.00109
Maximum Basket Opening[2]	0.86864 ± 0.00097	0.90023 ± 0.00107
Minimum Basket Opening[2]	0.86489 ± 0.00091	0.90817 ± 0.00105

Notes:

1. Both wet and dry base case configurations include elements out to corners of basket openings.
2. Incorporates minimum thickness stainless steel, basket divider plates.
3. Comparable to the "elements out," k_{eff} = 0.83468 ± 0.00101, configuration of Table 6.4.5-3 except the neutron shield is dry.
4. Incorporates the "elements out" configuration.

Table 6.4.5-6   Axially Infinite Cask k_{eff} with TRIGA Fuel Elements – Basket
Manufacturing Tolerance Perturbations, Poisoned Basket

Basket Configuration	Wet Case Results $k_{eff} \pm \sigma$	Dry Case Results $k_{eff} \pm \sigma$
Base Case[1]	0.87874 ± 0.00123	0.88969 ± 0.00122
Minimum Opening[2]	0.87832 ± 0.00127	0.89054 ± 0.00107
Increased Central Opening[2]	0.87981 ± 0.00133	0.88722 ± 0.00118
Increased Exterior Openings[2]	0.87875 ± 0.00134	0.88998 ± 0.00120
Increased Central Opening, Decreased Exterior Openings[2]	0.87475 ± 0.00134	0.88724 ± 0.00116

Notes:

1. Most reactive configurations from Table 6.4.5-4.
2. Incorporates minimum thickness stainless steel, basket divider plates.

Table 6.4.5-7   Screened Can Preferential Flooding and Partial Loading Reactivity
Evaluations for TRIGA Fuel Elements, Nonpoisoned and Poisoned Baskets

Description	$k_{eff} \pm \sigma$ Nonpoisoned Basket	$k_{eff} \pm \sigma$ Poisoned Basket
Wet Cask / Wet Can	0.84040 ± 0.00132	0.88010 ± 0.00139
Dry Cask / Dry Can	0.89383 ± 0.00120	0.86228 ± 0.00128
Dry Cask / Wet Can – Elements To Center of Cask	0.89778 ± 0.00124	0.88272 ± 0.00124
Dry Cask / Wet Can – Elements To Center of Can	0.89435 ± 0.00124	0.87727 ± 0.00124
Dry Cask / Wet Can – Elements Quadrant Centered	0.89821 ± 0.00129	0.88737 ± 0.00123
Dry Cask / Wet Can – Elements in Corners	0.90926 ± 0.00126	0.89957 ± 0.00118
Dry Cask / Wet Can – Elements in Corners, Max. Can	0.90673 ± 0.00123	0.90224 ± 0.00128
18 Elements per Basket Module	0.84896 ± 0.00121	0.82527 ± 0.00114
12 Elements per Basket Module	0.82532 ± 0.00125	0.80281 ± 0.00119

Table 6.4.5-8   Sealed Can Preferential Flooding and Partial Loading Reactivity
Evaluations for TRIGA Fuel Elements, Nonpoisoned and Poisoned Baskets

Description	$k_{eff} \pm \sigma$ Nonpoisoned Basket	$k_{eff} \pm \sigma$ Poisoned Basket
Wet Cask / Wet Can, Elements Out	-	0.88574 ± 0.00130
Wet Cask / Wet Can	0.84331 ± 0.00129	0.88036 ± 0.00125
Dry Cask / Dry Can	0.85693 ± 0.00121	0.83021 ± 0.00118
Dry Cask / Wet Can	0.84376 ± 0.00129	0.78084 ± 0.00114
2 Rods per Can - 3 Five Inch Fuel Pellets	0.84346 ± 0.00128	0.88212 ± 0.00133
Mixture Solid (No Moderator)- 2 Rods Per Can	0.87512 ± 0.00122	0.88371 ± 0.00125
Mixture Half Can Height - 2 Rods Per Can	0.90691 ± 0.00212	0.88564 ± 0.00146
Mixture Full Can Height - 2 Rods Per Can	0.91088 ± 0.00106	0.88411 ± 0.00129
Mixture - Solid (No Moderator) - 1 Rod Per Can	0.85868 ± 0.00132	0.88472 ± 0.00131
Mixture - Half Can Height - 1 Rod Per Can	0.87411 ± 0.00117	0.88204 ± 0.00130
Mixture - Full Can Height - 1 Rod Per Can	0.85913 ± 0.00117	0.88477 ± 0.00142
2 Rods Per Can + Graphite – Solid	0.87208 ± 0.00117	0.88616 ± 0.00138
2 Rods Per Can + Graphite – Full Can Height	0.89867 ± 0.00118	0.88431 ± 0.00129
Increased Can Diameter (+0.02 inch)[1]	0.91355 ± 0.00119	0.88436 ± 0.00138

Note:

1. The increased can diameter cases were analyzed using the most reactive cases for each basket configuration (nonpoisoned / poisoned). The "Wet Cask / Wet Can, Elements Out" case was selected for the poisoned basket configuration due to the lack of statistically significant differences in the above reported results.

Table 6.4.5-9   Summary of Most Reactive Configurations, TRIGA Fuel Elements,
Nonpoisoned Basket

	Wet	Dry	Preferential
Intact Fuel	0.86861 ± 0.00094	0.93434 ± 0.00115 [1]	-
Screened Fuel Cans	0.84040 ± 0.00132	0.89383 ± 0.00120	0.90926 ± 0.00126
Sealed Fuel Cans	0.84331 ± 0.00129	0.85693 ± 0.00121	0.91355 ± 0.00199

Note:

1. As reported in Section 6.4.5.4, this case is reevaluated with a finite axial length model, making
    the preferentially flooded, sealed can case the most reactive.

Table 6.4.5-10   Summary of Most Reactive Configurations, TRIGA Fuel Elements,
Poisoned Basket

	Wet	Dry	Preferential
Intact Fuel	0.87874 ± 0.00123	0.88969 ± 0.00122	-
Screened Fuel Cans	0.88010 ± 0.00139	0.86228 ± 0.00128	0.90224 ± 0.00128
Sealed Fuel Cans	0.88574 ± 0.00130	0.83021 ± 0.00118	0.88564 ± 0.00146

Table 6.4.5-11   Reactivity Results for TRIGA Fuel Elements, Sealed Cans, Normal
Conditions, Nonpoisoned Basket

Moderator SG	Casks Touching ($k_{eff} \pm \sigma$)	8 Foot Center-To-Center ($k_{eff} \pm \sigma$)
Dry Exterior, Vary Internal Density		
0.00000	0.7239 ± 0.0012	0.7203 ± 0.0012
0.00100	0.7205 ± 0.0012	0.7212 ± 0.0012
0.00178	0.7231 ± 0.0013	0.7201 ± 0.0012
0.00316	0.7216 ± 0.0012	0.7202 ± 0.0012
0.00562	0.7227 ± 0.0012	0.7181 ± 0.0012
0.01000	0.7234 ± 0.0012	0.7224 ± 0.0012
0.01780	0.7205 ± 0.0012	0.7223 ± 0.0013
0.03160	0.7249 ± 0.0012	0.7242 ± 0.0012
0.05620	0.7263 ± 0.0012	0.7285 ± 0.0012
0.10000	0.7295 ± 0.0012	0.7303 ± 0.0012
0.17800	0.7446 ± 0.0012	0.7415 ± 0.0012
0.31600	0.7674 ± 0.0012	0.7647 ± 0.0013
0.56200	0.7887 ± 0.0013	0.7884 ± 0.0013
0.70000	0.7977 ± 0.0014	0.7961 ± 0.0014
0.80000	0.8009 ± 0.0013	0.7974 ± 0.0013
0.90000	0.8000 ± 0.0013	0.8008 ± 0.0012
1.00000	0.8020 ± 0.0013	0.8022 ± 0.0014
Optimally Moderated Cask Interior (SG = 1.0), Vary External Density		
0.00000	0.8020 ± 0.0013	0.8022 ± 0.0013
0.00100	0.8013 ± 0.0014	0.8010 ± 0.0013
0.00178	0.7993 ± 0.0014	0.8003 ± 0.0013
0.00316	0.8017 ± 0.0014	0.8024 ± 0.0013
0.00562	0.8041 ± 0.0014	0.8002 ± 0.0013
0.01000	0.8018 ± 0.0013	0.8032 ± 0.0013
0.01780	0.8025 ± 0.0013	0.8018 ± 0.0013
0.03160	0.8001 ± 0.0013	0.8023 ± 0.0013
0.05620	0.8004 ± 0.0014	0.7993 ± 0.0013
0.10000	0.8008 ± 0.0012	0.8000 ± 0.0013
0.17800	0.8018 ± 0.0014	0.8019 ± 0.0013
0.31600	0.8034 ± 0.0014	0.8019 ± 0.0013
0.56200	0.7996 ± 0.0013	0.8025 ± 0.0013
0.70000	0.8018 ± 0.0014	0.8026 ± 0.0014
0.80000	0.8013 ± 0.0013	0.8009 ± 0.0013
0.90000	0.7998 ± 0.0013	0.8009 ± 0.0012
1.00000	0.8019 ± 0.0015	0.8003 ± 0.0013
Vary Internal and External Density Simultaneously		
0.00000	0.7239 ± 0.0012	0.7203 ± 0.0013
0.00100	0.7212 ± 0.0012	0.7192 ± 0.0012
0.00178	0.7210 ± 0.0011	0.7236 ± 0.0012
0.00316	0.7202 ± 0.0012	0.7217 ± 0.0012
0.00562	0.7225 ± 0.0012	0.7218 ± 0.0012
0.01000	0.7229 ± 0.0012	0.7236 ± 0.0012
0.01780	0.7230 ± 0.0012	0.7239 ± 0.0012
0.03160	0.7253 ± 0.0013	0.7236 ± 0.0012
0.05620	0.7273 ± 0.0012	0.7261 ± 0.0013
0.10000	0.7311 ± 0.0012	0.7296 ± 0.0013
0.17800	0.7439 ± 0.0013	0.7429 ± 0.0012
0.31600	0.7634 ± 0.0013	0.7650 ± 0.0013
0.56200	0.7882 ± 0.0014	0.7898 ± 0.0013
0.70000	0.7950 ± 0.0014	0.7941 ± 0.0012
0.80000	0.7950 ± 0.0013	0.7973 ± 0.0013
0.90000	0.7984 ± 0.0012	0.8002 ± 0.0012
1.00000	0.8000 ± 0.0013	0.8029 ± 0.0014

Table 6.4.5-12   Reactivity Results for TRIGA Fuel Elements, Sealed Cans, Accident Conditions, Nonpoisoned Basket

Moderator SG	Casks Touching (k$_{eff}$ ± σ)	8 Foot Center-To-Center (k$_{eff}$ ± σ)
Dry Exterior and Neutron Shield, Vary Internal Moderator		
0.00000	0.9136 ± 0.0012	0.9057 ± 0.0011
0.00100	0.9119 ± 0.0012	0.9054 ± 0.0011
0.00178	0.9101 ± 0.0012	0.9041 ± 0.0011
0.00316	0.9110 ± 0.0011	0.9040 ± 0.0011
0.00562	0.9095 ± 0.0012	0.9046 ± 0.0011
0.01000	0.9059 ± 0.0012	0.8999 ± 0.0012
0.01780	0.9021 ± 0.0012	0.8979 ± 0.0012
0.03160	0.8965 ± 0.0012	0.8908 ± 0.0011
0.05620	0.8842 ± 0.0013	0.8793 ± 0.0012
0.10000	0.8660 ± 0.0012	0.8622 ± 0.0012
0.17800	0.8432 ± 0.0012	0.8419 ± 0.0012
0.31600	0.8275 ± 0.0013	0.8222 ± 0.0012
0.56200	0.8185 ± 0.0013	0.8153 ± 0.0014
0.70000	0.8144 ± 0.0013	0.8124 ± 0.0013
0.80000	0.8140 ± 0.0013	0.8091 ± 0.0013
0.90000	0.8154 ± 0.0012	0.8082 ± 0.0013
1.00000	0.8117 ± 0.0013	0.8081 ± 0.0013
Optimally Moderated Internal (SG = 0.0), Vary Neutron Shield and Exterior		
0.00000	0.9136 ± 0.0012	0.9057 ± 0.0011
0.00100	0.8950 ± 0.0011	0.8208 ± 0.0012
0.00178	0.8887 ± 0.0011	0.7931 ± 0.0012
0.00316	0.8732 ± 0.0012	0.7651 ± 0.0012
0.00562	0.8505 ± 0.0012	0.7454 ± 0.0011
0.01000	0.8210 ± 0.0011	0.7311 ± 0.0012
0.01780	0.7957 ± 0.0012	0.7233 ± 0.0012
0.03160	0.7655 ± 0.0012	0.7192 ± 0.0011
0.05620	0.7432 ± 0.0012	0.7195 ± 0.0013
0.10000	0.7325 ± 0.0013	0.7177 ± 0.0012
0.17800	0.7252 ± 0.0011	0.7206 ± 0.0012
0.31600	0.7216 ± 0.0012	0.7213 ± 0.0012
0.56200	0.7211 ± 0.0012	0.7211 ± 0.0012
0.70000	0.7199 ± 0.0012	0.7190 ± 0.0012
0.80000	0.7213 ± 0.0012	0.7184 ± 0.0012
0.90000	0.7183 ± 0.0013	0.7196 ± 0.0012
1.00000	0.7189 ± 0.0011	0.7194 ± 0.0013
Vary Interior, Exterior and Neutron Shield Simultaneously		
0.00000	0.9136 ± 0.0012	0.9057 ± 0.0011
0.00100	0.8964 ± 0.0012	0.8189 ± 0.0012
0.00178	0.8879 ± 0.0011	0.7913 ± 0.0013
0.00316	0.8726 ± 0.0012	0.7673 ± 0.0013
0.00562	0.8496 ± 0.0011	0.7459 ± 0.0012
0.01000	0.8223 ± 0.0012	0.7345 ± 0.0012
0.01780	0.7903 ± 0.0012	0.7237 ± 0.0012
0.03160	0.7685 ± 0.0012	0.7223 ± 0.0011
0.05620	0.7504 ± 0.0012	0.7242 ± 0.0012
0.10000	0.7415 ± 0.0013	0.7296 ± 0.0012
0.17800	0.7445 ± 0.0013	0.7404 ± 0.0013
0.31600	0.7674 ± 0.0013	0.7658 ± 0.0013
0.56200	0.7904 ± 0.0013	0.7898 ± 0.0013
0.70000	0.7972 ± 0.0014	0.7936 ± 0.0014
0.80000	0.7969 ± 0.0013	0.7956 ± 0.0014
0.90000	0.8003 ± 0.0013	0.8007 ± 0.0013
1.00000	0.8000 ± 0.0013	0.8013 ± 0.0013

Table 6.4.5-13   Reactivity Results for TRIGA Fuel Elements, Screened Cans, Normal Conditions, Poisoned Basket

Moderator SG	Casks Touching (keff ± σ)	8 Foot Center-To-Center (keff ± σ)
Dry Exterior, Vary Internal Density		
0.00000	0.8376 ± 0.0018	0.8381 ± 0.0017
0.00100	0.8408 + 0.0017	0.8418 + 0.0016
0.00178	0.8408 + 0.0018	0.8412 + 0.0018
0.00316	0.8390 + 0.0017	0.8432 + 0.0016
0.00562	0.8371 + 0.0017	0.8399 + 0.0017
0.01000	0.8420 + 0.0017	0.8397 + 0.0018
0.01780	0.8383 + 0.0017	0.8419 + 0.0017
0.03160	0.8413 + 0.0017	0.8427 + 0.0017
0.05620	0.8466 + 0.0017	0.8448 + 0.0017
0.10000	0.8433 ± 0.0016	0.8479 ± 0.0017
0.17800	0.8510 + 0.0017	0.8502 + 0.0017
0.31600	0.8497 + 0.0016	0.8505 + 0.0016
0.56200	0.8453 + 0.0017	0.8484 + 0.0017
0.70000	0.8444 + 0.0016	0.8464 + 0.0017
0.80000	0.8321 + 0.0017	0.8432 + 0.0017
0.90000	0.8458 + 0.0017	0.8437 + 0.0017
1.00000	0.8527 + 0.0017	0.8540 + 0.0017
Optimally Moderated Cask Interior (SG = 1.0), Vary External Density		
0.00000	0.8527 ± 0.0017	0.8540 ± 0.0017
0.00100	0.8482 + 0.0018	0.8513 + 0.0016
0.00178	0.8532 + 0.0017	0.8513 + 0.0016
0.00316	0.8516 + 0.0017	0.8531 + 0.0017
0.00562	0.8546 + 0.0017	0.8539 + 0.0017
0.01000	0.8521 + 0.0018	0.8517 + 0.0019
0.01780	0.8528 + 0.0018	0.8515 + 0.0018
0.03160	0.8543 + 0.0017	0.8526 + 0.0017
0.05620	0.8506 + 0.0018	0.8503 + 0.0017
0.10000	0.8523 + 0.0018	0.8542 + 0.0016
0.17800	0.8507 + 0.0018	0.8478 + 0.0016
0.31600	0.8539 + 0.0017	0.8518 + 0.0016
0.56200	0.8545 + 0.0017	0.8525 + 0.0017
0.70000	0.8512 + 0.0017	0.8534 + 0.0017
0.80000	0.8548 + 0.0017	0.8529 + 0.0017
0.90000	0.8523 + 0.0016	0.8522 + 0.0017
1.00000	0.8540 + 0.0018	0.8523 + 0.0017
Vary Internal and External Density Simultaneously		
0.00000	0.8376 ± 0.0018	0.8381 ± 0.0017
0.00100	0.8396 + 0.0017	0.8382 + 0.0017
0.00178	0.8404 + 0.0016	0.8404 + 0.0017
0.00316	0.8430 + 0.0016	0.8413 + 0.0017
0.00562	0.8448 + 0.0017	0.8391 + 0.0016
0.01000	0.8400 + 0.0017	0.8398 + 0.0017
0.01780	0.8419 + 0.0017	0.8424 + 0.0018
0.03160	0.8394 + 0.0017	0.8439 + 0.0017
0.05620	0.8437 + 0.0017	0.8385 + 0.0017
0.10000	0.8477 + 0.0017	0.8477 + 0.0017
0.17800	0.8502 + 0.0017	0.8469 + 0.0017
0.31600	0.8463 + 0.0017	0.8494 + 0.0018
0.56200	0.8484 + 0.0017	0.8513 + 0.0017
0.70000	0.8471 + 0.0017	0.8459 + 0.0018
0.80000	0.8440 + 0.0017	0.8462 + 0.0016
0.90000	0.8429 + 0.0017	0.8451 + 0.0017
1.00000	0.8540 ± 0.0018	0.8523 ± 0.0017

Table 6.4.5-14   Reactivity Results for TRIGA Fuel Elements, Screened Cans, Accident
Conditions, Poisoned Basket

Moderator SG	Casks Touching ($k_{eff} \pm \sigma$)	8 Foot Center-To-Center ($k_{eff} \pm \sigma$)
Dry Exterior and Neutron Shield, Vary Internal Moderator		
0.00000	0.9022 ± 0.0015	0.9015 ± 0.0016
0.00100	0.9019 ± 0.0016	0.9022 ± 0.0016
0.00178	0.8998 ± 0.0016	0.9003 ± 0.0016
0.00316	0.8992 ± 0.0016	0.9009 ± 0.0016
0.00562	0.8995 ± 0.0017	0.9015 ± 0.0017
0.01000	0.8998 ± 0.0017	0.8956 ± 0.0017
0.01780	0.8979 ± 0.0017	0.9003 ± 0.0017
0.03160	0.8966 ± 0.0018	0.8946 ± 0.0016
0.05620	0.8949 ± 0.0015	0.8889 ± 0.0015
0.10000	0.8893 ± 0.0018	0.8844 ± 0.0017
0.17800	0.8843 ± 0.0018	0.8822 ± 0.0016
0.31600	0.8772 ± 0.0017	0.8765 ± 0.0016
0.56200	0.8635 ± 0.0018	0.8640 ± 0.0017
0.70000	0.8586 ± 0.0017	0.8657 ± 0.0017
0.80000	0.8620 ± 0.0016	0.8594 ± 0.0016
0.90000	0.8622 ± 0.0016	0.8600 ± 0.0017
1.00000	0.8662 ± 0.0017	0.8629 ± 0.0018
Optimally Moderated Internal (SG = 0.0), Vary Neutron Shield and Exterior		
0.00000	0.9022 ± 0.0015	0.9015 ± 0.0016
0.00100	0.8970 ± 0.0016	0.8644 ± 0.0017
0.00178	0.8910 ± 0.0016	0.8596 ± 0.0018
0.00316	0.8862 ± 0.0015	0.8542 ± 0.0016
0.00562	0.8789 ± 0.0016	0.8457 ± 0.0016
0.01000	0.8687 ± 0.0015	0.8438 ± 0.0017
0.01780	0.8618 ± 0.0017	0.8409 ± 0.0018
0.03160	0.8539 ± 0.0016	0.8386 ± 0.0017
0.05620	0.8482 ± 0.0017	0.8403 ± 0.0018
0.10000	0.8427 ± 0.0015	0.8381 ± 0.0017
0.17800	0.8433 ± 0.0017	0.8418 ± 0.0016
0.31600	0.8424 ± 0.0018	0.8405 ± 0.0018
0.56200	0.8422 ± 0.0017	0.8391 ± 0.0017
0.70000	0.8438 ± 0.0017	0.8399 ± 0.0016
0.80000	0.8429 ± 0.0018	0.8407 ± 0.0017
0.90000	0.8423 ± 0.0017	0.8445 ± 0.0016
1.00000	0.8398 ± 0.0016	0.8383 ± 0.0017
Vary Interior, Exterior and Neutron Shield Simultaneously		
0.00000	0.9022 ± 0.0015	0.9015 ± 0.0016
0.00100	0.8948 ± 0.0016	0.8662 ± 0.0016
0.00178	0.8932 ± 0.0017	0.8577 ± 0.0016
0.00316	0.8881 ± 0.0016	0.8524 ± 0.0017
0.00562	0.8762 ± 0.0016	0.8429 ± 0.0017
0.01000	0.8722 ± 0.0017	0.8431 ± 0.0017
0.01780	0.8628 ± 0.0016	0.8412 ± 0.0017
0.03160	0.8586 ± 0.0016	0.8450 ± 0.0017
0.05620	0.8533 ± 0.0017	0.8448 ± 0.0018
0.10000	0.8496 ± 0.0017	0.8458 ± 0.0017
0.17800	0.8494 ± 0.0017	0.8489 ± 0.0017
0.31600	0.8500 ± 0.0017	0.8459 ± 0.0017
0.56200	0.8489 ± 0.0018	0.8488 ± 0.0018
0.70000	0.8443 ± 0.0017	0.8463 ± 0.0017
0.80000	0.8459 ± 0.0017	0.8407 ± 0.0018
0.90000	0.8421 ± 0.0017	0.8483 ± 0.0017
1.00000	0.8540 ± 0.0018	0.8504 ± 0.0019

Table 6.4.5-15   Single Package 10 CFR 71.55(b)(3) Evaluation k_{eff} Summary, TRIGA
Fuel Element, Nonpoisoned Basket

Description	$k_{eff} \pm \sigma$	k_s
Single Cask / Inner Shell Reflected with H_2O	0.80664 ± 0.00136	0.82616
Single Cask / Inner Shell and Lead Reflected with H_2O	0.84194 ± 0.00130	0.86134
Single Cask / Inner Shell, Lead & Outer Shell Reflected with H_2O	0.84398 ± 0.00128	0.86334
Single Intact Cask Reflected with H_2O	0.84446 ± 0.00126	0.86392

Table 6.4.5-16   Single Package 10 CFR 71.55(b)(3) Evaluation k_{eff} Summary, TRIGA
Fuel Element, Poisoned Basket

Description	$k_{eff} \pm \sigma$	k_s
Single Cask / Inner Shell Reflected with H_2O	0.85480 ± 0.00135	0.87430
Single Cask / Inner Shell and Lead Reflected with H_2O	0.87788 ± 0.00136	0.89740
Single Cask / Inner Shell, Lead & Outer Shell Reflected with H_2O	0.88369 ± 0.00133	0.90315
Single Intact Cask Reflected with H_2O	0.88117 ± 0.00131	0.90059

Table 6.4.5-17   Fuel Element Physical Characteristics Evaluation

Parameter							Cask Cavity Moderator Condition/Fuel Location							
							Dry - In Shift		0.5 g/cc - In Shift		1 g/cc - In Shift		1 g/cc – Shifted Out	
Fuel Rod OD	Clad Thickness	Fuel OD	Fuel ID	Active Fuel Length	Zirc Interior Rod OD	Zirc Mass (gram)	k_{eff}	$\Delta k/\sigma$	k_{eff}	$\Delta k/\sigma$	k_{eff}	$\Delta k/\sigma$	k_{eff}	$\Delta k/\sigma$
Nominal	Nominal	Nominal	Nominal	Nominal	Nominal	2059	0.85521	-	0.87591	-	0.87217	-	0.89939	-
Max	Nominal	Nominal	Nominal	Nominal	Nominal	2059	0.85102	-2.8	0.87063	-5.6	0.86795	-4.4	0.89480	-4.8
Nominal	Min	Nominal	Nominal	Nominal	Nominal	2059	0.85966	6.2	0.88920	14.0	0.89067	19.4	0.92184	23.3
Nominal	Nominal	Min	Nominal	Nominal	Nominal	1765	0.78425	-72.2	0.82168	-58.1	0.82388	-51.7	0.85987	-42.6
Nominal	Nominal	Max	Nominal	Nominal	Nominal	2068	0.85611	2.6	0.87530	-0.6	0.87327	1.2	0.90107	1.8
Nominal	Nominal	Nominal	Min	Nominal	Nominal	2071	0.85409	0.4	0.87776	2.0	0.87334	1.2	0.90196	2.7
Nominal	Nominal	Nominal	Nominal	Min	Nominal	1988	0.84974	-4.2	0.87304	-3.0	0.87192	-0.3	0.89885	-0.6
Nominal	Nominal	Nominal	Nominal	Max	Nominal	2129	0.85762	4.2	0.87705	1.2	0.87078	-1.5	0.89995	0.6
Nominal	Nominal	Nominal	Nominal	Nominal	Min	2059	0.85370	0.0	0.87322	-2.8	0.87095	-1.3	0.89785	-1.6
Nominal	Nominal	Nominal	Nominal	Nominal	Max	2059	0.85360	-0.1	0.87502	-0.9	0.87125	-1.0	0.89966	0.3
Nominal	Min	Max	Nominal	Nominal	Nominal	2191	0.88846	36.9	0.91259	37.9	0.91057	39.6	0.93977	42.6
Max	Min	Max	Nominal	Nominal	Nominal	2261	0.89797	46.7	0.92086	47.8	0.91631	44.9	0.94365	46.4
Max	Min	Max	Nominal	Nominal	Min	2261	0.89729	45.3	0.92035	46.6	0.91583	46.1	0.94260	44.9
Max	Min	Max	Min	Nominal	Min	2327	0.91165	60.7	0.92950	55.7	0.92648	56.0	0.94983	51.3
Max	Min	Max	Min	Max	Min	2406	0.91646	66.2	0.93183	57.7	0.92716	56.3	0.95048	52.7
Max	Min	Max	Min	Min	Min	2248	0.90919	58.1	0.92962	57.1	0.92491	54.8	0.95030	52.2

Table 6.4.5-18   Element Variation to Reduce k_s Below 0.95

Variation	k_{eff}	σ	k_s	Δk
Base	0.95048	0.00069	0.9687	
Single Cask	0.94221	0.00068	0.9604	-0.00827
Min Clad 0.01 inch	0.93007	0.00068	0.9482	-0.02041
Center rod 0.1 inch	0.94559	0.00066	0.9637	-0.00489
Center Rod 0.1 inch and Clad 0.01 inch	0.92465	0.00069	0.9428	-0.02583

Table 6.4.5-19   General Model Configuration – Dry to Wet System Reactivity Changes, 70 wt% ^{235}U Stainless Steel Clad Fuel - Nominal Fuel Parameters

Model Type	Fuel Material	Dry Interior		Wet Interior		Dry to Wet	Dry to Wet
		k_{eff}	σ	k_{eff}	σ	Δk	$\Delta k / \sigma$
Unit Cell	2060 g Zirc 1.6 H/Zr	1.43854	0.00074	1.34434	0.00088	-0.0942	-82
Unit Cell	2060 g Zirc 2.0 H/Zr	1.47297	0.00072	1.37063	0.00095	-0.1023	-86
Infinite Cask Array	2060 g Zirc 1.6 H/Zr	0.91389	0.00058	0.82201	0.00069	-0.0919	-102
Infinite Cask Array	2060 g Zirc 2.0 H/Zr	0.99893	0.00060	0.87887	0.00069	-0.1201	-131
Finite Cask Array	2060 g Zirc 2.0 H/Zr	0.85371	0.00068	0.87160	0.00067	0.0179	19
Single Cask	2060 g Zirc 1.6 H/Zr	0.69491	0.00059	0.80561	0.00066	0.1107	125

Table 6.4.5-20   Primary Fuel Type Reactivity Comparison[1] – Accident Conditions Eight-Cask Array (No Cans)

Fuel Type	Cask Cavity Moderator	Fuel Characteristics	Rod Location	k_{eff}	σ	k_s	Δk/σ
Al Clad	Dry	Nominal	Shifted In	0.61831	0.00053	0.63617	-
14 inch	Wet	Nominal	Shifted In	0.67516	0.00056	0.69308	73.7
	Wet	Most Reactive	Shifted In	0.68914	0.00056	0.70706	91.9
	Wet	Most Reactive	Shifted Out	0.68690	0.00054	0.70478	90.7
Al Clad -	Dry	Nominal	Shifted In	0.60606	0.00051	0.62388	-
15 inch	Wet	Nominal	Shifted In	0.66104	0.00058	0.67900	71.2
	Wet	Most Reactive	Shifted In	0.68272	0.00055	0.70062	102.2
	Wet	Most Reactive	Shifted Out	0.67985	0.00052	0.69769	101.3
SS Clad -	Dry	Nominal	Shifted In	0.77575	0.00058	0.79371	-
20% Enriched	Wet	Nominal	Shifted In	0.82684	0.00064	0.84492	59.2
	Wet	Most Reactive	Shifted In	0.86114	0.00061	0.87916	101.4
	Wet	Most Reactive	Shifted Out	0.89909	0.00064	0.91717	142.8
SS Clad	Dry	Nominal	Shifted In	0.85521	0.00068	0.87337	-
70% Enriched	Wet	Nominal	Shifted In	0.87217	0.00067	0.89031	17.8
	Wet	Most Reactive	Shifted In	0.90587	0.00069	0.92405	52.3
	Wet	Most Reactive	Shifted Out	0.93024	0.00069	0.94842	77.4

Table 6.4.5-21   Normal Condition Maximum System Reativities (No Cans)[2]

Array Size	Neutron Shield	Cask Cavity	Fuel Config	k_{eff}	σ	k_s
Infinite	Yes	Dry	MRE	0.84554	0.00066	0.86366
Infinite	Yes	Wet	MRE	0.92398	0.00068	0.94214

---

[1] Fueled follower rods are not evaluated separately as their physical characteristics and fuel compositions are bounded by a stainless steel clad 20% enriched element.

[2] Most reactive element configuration as documented under accident conditions.

Table 6.4.5-22   Increased Enrichment for 20 wt % and 70 wt % TRIGA Fuel Elements

wt %	g ^{235}U	k_{eff}	σ	k_s	$\Delta k_s/\sigma$
20	169	0.89973	0.00064	0.91781	--
25	169	0.91236	0.00065	0.93046	13.9
70	137	0.93063	0.00067	0.94877	--
71	137	0.93066	0.00068	0.94882	0.1

Table 6.4.5-23   Increased ^{235}U Mass TRIGA Fuel Elements

wt %	g ^{235}U	k_{eff}	σ	k_s	$\Delta k_s/\sigma$
25	169	0.91236	0.00065	0.93046	--
25	275	0.95139	0.00068	0.96955	41.6
71	137	0.93066	0.00068	0.94882	--
71	138	0.93159	0.00066	0.94971	0.9

Table 6.4.5-24   Limited Quantity Study for LEU Fissile Mass Increase

Baskets									
Bottom/Top			Three Middle						
# Rods	wt %	g ^{235}U	# Rods	wt %	g ^{235}U	k_{eff}	σ	k_s	$\Delta k_s/\sigma$
4	71	138	4	71	138	0.93159	0.00066	0.94971	--
4	25	275	4	25	275	0.95139	0.00068	0.96955	20.9
4	25	275	4	71	138	0.94928	0.00067	0.96742	18.8
3	25	275	4	71	138	0.92997	0.00067	0.94811	-1.7

Table 6.4.5-25   95 wt% TRIGA Fuel Elements

Baskets									
Bottom/Top			Three Middle						
# Rods	wt %	g ^{235}U	# Rods	wt %	g ^{235}U	k_{eff}	σ	k_s	$\Delta k_s/\sigma$
4	71	138	4	71	138	0.93159	0.00066	0.94971	--
4	95	175	4	95	175	0.97990	0.00069	0.99808	50.7
4	95	175	4	71	138	0.97662	0.00066	0.99474	48.2
3	95	175	4	71	138	0.93030	0.00064	0.94838	-1.4

Table 6.4.5-26   TRIGA Damaged Fuel Canister – Sealed Canister in Top and Bottom Basket Module

Baskets									
Bottom / Top			Three Middle						
# Rods	wt %	g ^{235}U	# Rods	wt %	g ^{235}U	k_{eff}	σ	k_s	$\Delta k_s/\sigma$
4	71	138	4	71	138	0.93159	0.00066	0.94971	--
2	71	138	4	71	138	0.93032	0.00068	0.94848	-1.3
2	25	275	4	71	138	0.93109	0.00070	0.94929	-0.4
2	95	175	4	71	138	0.93071	0.00068	0.94887	-0.9

Table 6.4.5-27   TRIGA Fuel Element Pitch/Screened Canister Evaluation

Baskets									
	Bottom / Top			Three Middle					
DFC	Pitch	wt %	g ^{235}U	Pitch	wt %	g ^{235}U	k_{eff}	σ	k_s	$\Delta k_s/\sigma$
No	4.7750	95	175	4.775	71	138	0.97662	0.00066	0.99474	--
No	4.1924	95	175	4.775	71	138	0.95679	0.00068	0.97495	-20.9
Yes	4.1924	95	175	4.775	71	138	0.92977	0.00068	0.94793	-49.4

Table 6.4.5-28   TRIGA Structural Intact Fuel Canister -- Screened Canister in Top and Bottom Basket Module

Baskets									
Bottom / Top			Three Middle						
# Rods	wt %	g ^{235}U	# Rods	wt %	g ^{235}U	k_{eff}	σ	k_s	$\Delta k_s/\sigma$
4	71	138	4	71	138	0.93159	0.00066	0.94971	--
4	71	138	4	71	138	0.92971	0.00069	0.94789	-1.9
4	25	275	4	71	138	0.93055	0.00065	0.94865	-1.1
4	95	175	4	71	138	0.92977	0.00068	0.94793	-1.9

Table 6.4.5-29   TRIGA Cluster Rod Study in TRIGA Fuel Element Shipment

| Baskets | | | | | | | | | |
| 1 Opening | | | Remaining Payload | | | | | | |
# Rods	wt %	g ^{235}U	# Rods	wt %	g ^{235}U	k_{eff}	σ	k_s	$\Delta k_s/\sigma$
4	71	138	4	71	138	0.93159	0.00066	0.94971	--
6	95	46.5	4	71	138	0.93085	0.00064	0.94893	-0.8
16	95	46.5	4	71	138	0.93141	0.00065	0.94951	-0.2

6.4.6   TRIGA Fuel Cluster Rods

This section presents the criticality evaluation for the NAC-LWT with nonpoisoned and poisoned basket modules for intact and failed TRIGA fuel cluster rods. In the nonpoisoned configuration, up to 480 intact TRIGA fuel cluster rods can be transported in the NAC-LWT cask. In the poisoned configuration, up to 560 intact TRIGA fuel cluster rods can be transported in the NAC-LWT cask. Up to six TRIGA fuel cluster rods can be contained in sealed canisters. The analyses are performed to satisfy the requirements of 10 CFR Parts 71.55 and 71.59, as well as IAEA Transportation Safety Standards (TS-R-1).

The design basis TRIGA fuel cluster rod is evaluated for the most reactive basket and intact fuel configurations, including both geometric perturbations and manufacturing tolerances, under wet and dry conditions in Section 6.4.6.1. The most reactive cask configuration with three baskets of intact design-basis TRIGA fuel and two baskets of fuel in sealed cans, is evaluated under normal and accident conditions in Section 6.4.6.2. Preferential flooding of the sealed failed fuel cans is also evaluated. The maximum k_{eff} of the NAC-LWT cask loaded with design-basis TRIGA fuel cluster rods is evaluated under normal and accident conditions in Section 6.4.6.3. A single package evaluation, in accordance with 10 CFR 71.55(b)(3), is performed in Section 0. The analyses demonstrate that, including all calculational and mechanical uncertainties, the NAC-LWT cask remains subcritical ($k_s < 0.95$) under normal and accident conditions.

The poisoned and nonpoisoned basket may contain both HEU and LEU cluster rods. The evaluations of LEU cluster rods are based on the analysis trends observed for the HEU rods. As the nonpoisoned basket is significantly more reactive than the poisoned basket configuration, expanded scope HEU and LEU evaluations are based on the nonpoisoned basket model. LEU evaluations, in conjunction with expanded HEU characteristics, are included in Section 6.4.6.5.

6.4.6.1   Most Reactive Fuel and Basket Configurations

The primary basket tolerances affecting system reactivity are geometric tolerances, including the positioning of the fuel cluster rods and aluminum tube insert in the cell opening, the size of the cell opening; and manufacturing tolerances, including the thickness of the steel plate dividing the basket openings. The effect of these tolerances is evaluated sequentially in this section.

6.4.6.1.1   Geometric Perturbations

The TRIGA fuel cluster rods are held in place by basket modules and a fuel rod insert (Figure 6.2.6-1) with a welded, 4 × 4 array of 0.75-inch OD aluminum tubes. The TRIGA fuel cluster rods, one per insert tube, may shift to any location in a tube. Wet and dry conditions of the

TRIGA fuel cluster rods are evaluated to determine the most reactive fuel and basket configuration.

Table 6.4.6-1 and Table 6.4.6-2 show the cask k_{eff} for the nonpoisoned and poisoned baskets with TRIGA fuel cluster rods. The effects evaluated in the tables include fuel movement within the fuel rod inserts and partial loadings under wet and dry moderation conditions.

The most reactive wet configuration contains 16 TRIGA fuel cluster rods moved outward from the center of each 4 × 4 insert array and the inserts moved to the center of the basket with k_{eff} = 0.7571 ± 0.0025 and 0.7995 ± 0.0026, for the nonpoisoned and poisoned basket configurations, respectively. This wet configuration maximizes the moderation between TRIGA fuel cluster rods within wet inserts and maximizes the interaction between inserts. It is referred to as the wet configuration for TRIGA fuel cluster rods.

The dry configuration selected as most reactive, including no water in the neutron shield, contains 16 TRIGA fuel cluster rods moved inward to the center of each 4 × 4 insert array and the inserts moved to the center of the basket with k_{eff} = 0.8047 ± 0.0020 and 0.7489 ± 0.0019 for the non-poisoned and poisoned basket configurations, respectively. This dry configuration minimizes the neutron leakage of TRIGA fuel cluster rods within the dry basket and is referred to as the dry configuration.

Finally, the effect of partial fuel element loading was examined. Table 6.4.6-1 and Table 6.4.6-2 show that partial loading of the elements in the basket generally serves to decrease the reactivity for both the wet and dry poisoned and non-poisoned baskets. Although the case with one rod removed from the wet, nonpoisoned basket has a higher k_{eff} than the most reactive full load configuration, the difference in k_{eff} values is significantly less than 2σ. This makes the result statistically insignificant, and the full loading cases can be selected for further evaluation as stated above.

6.4.6.1.2   Manufacturing Tolerance Perturbations

The manufacturing tolerance analyses were performed by sequentially analyzing perturbations to the most reactive configurations from Section 6.4.6.1.1 and retaining appropriate perturbations. First, the effect of reducing the basket plate thickness was examined. Table 6.4.6-3 and Table 6.4.6-4 show that, for the non-poisoned and poisoned baskets, reducing the thickness of the basket plates increases the reactivity of the system. Thus, this configuration is utilized for the subsequent analyses.

Next, the dimensional tolerances of the aluminum tube inserts were evaluated. Three different cases were examined. The first case examined an increase in the aluminum tube diameter, while retaining the nominal thickness, the second case examined a decrease in the aluminum tube

diameter while retaining the nominal wall thickness, and the third case examined the effect of reducing the aluminum tube thickness. The results presented in Table 6.4.6-3 and Table 6.4.6-4 show that, for the non-poisoned and poisoned basket configurations, the highest k_{eff} values are obtained for the aluminum tubes at maximum diameter, and for the dry case with the aluminum tubes at minimum thickness. While these cases produced the highest values of k_{eff}, it should be noted that the differences between these results and the previous case is insignificant because they are within 2σ of one another.

After incorporating the previously described modifications, the effect of minimizing the basket insert opening was examined. As shown in Table 6.4.6-3 and Table 6.4.6-4, this perturbation results in equal or higher k_{eff} values for 3 of the 4 cases, with the dry, non-poisoned case resulting in a slight decrease in k_{eff}. As previously described, these differences are considered insignificant because they differ by less than 2σ. Nevertheless, because this perturbation is expected to increase the interaction between the individual baskets, it is retained in the most reactive configuration for further analysis.

Therefore, the most reactive case for intact fuel in the poisoned basket is selected as a wet configuration consisting of the following features: fuel elements moved away from the center of the aluminum center, aluminum insert moved towards the basket center, minimum divider plate thickness, minimum basket opening, and maximum aluminum tube insert diameter. The resulting reactivity for this system is, $k_{eff} = 0.8025 \pm 0.0025$. Likewise, the most reactive case for intact fuel in the non-poisoned basket is selected as a dry configuration consisting of the following features: fuel elements moved toward the center of the aluminum insert, aluminum insert moved towards the basket center, minimum divider plate thickness, and minimum basket opening. The resulting reactivity for this system is, $k_{eff} = 0.8129 \pm 0.0021$.

6.4.6.2   Sealed Cans Criticality Evaluation

Criticality calculations were performed for sealed failed fuel cans in the top and base basket modules of the cask. Three cases are examined for each basket combination, an all dry system, a full wet system, and a preferentially wet system with water only in the sealed failed fuel can. Fuel in sealed cans is modeled homogeneously, heterogeneously, and with partial loadings. The three central modules contain intact fuel in the most reactive wet or dry configurations, as appropriate, as determined in Section 6.4.5.2. The reactivities of the failed fuel combinations are compared to the reactivities of respective intact fuel configurations, and moderator density studies are performed on the most reactive configurations in Section 6.4.6.3.

Table 6.4.6-5 and Table 6.4.6-6 show the results of the preferential flooding and partial loading studies of the sealed failed fuel can configurations with TRIGA fuel cluster rods in nonpoisoned and poisoned baskets. Each sealed can contains up to six equivalent TRIGA fuel cluster rods.

The most reactive cases for the non-poisoned and poisoned baskets contain maximum outer diameter, preferential wet sealed fuel cans filled with a homogeneous mixture of fuel material and water. The most reactive nonpoisoned and poisoned cases are k_{eff} = 0.8669 ± 0.0022 and k_{eff} = 0.8384 ± 0.0021, respectively.

6.4.6.3   Moderator Density Criticality Evaluations for TRIGA Fuel Cluster Rods

The evaluations for normal and accident conditions include moderator density variations in the cask cavity and external environment to the cask. One evaluation is performed for each basket (non-poisoned / poisoned) combination. Table 6.4.6-7 and Table 6.4.6-8 show the most reactive configurations for these combinations as determined in Section 6.4.6.2. The tables contain results for infinite axial length models for the intact fuel and finite models with cask end caps for failed fuel. Comparing the reactivity of the more conservative infinite models with finite models is acceptable, provided the result with the highest k_{eff} is always selected. Alternately, converting infinite models to finite models is equally acceptable.

As seen in Table 6.4.6-7 and Table 6.4.6-8, the most reactive nonpoisoned and poisoned basket configurations with TRIGA fuel cluster rods contain two baskets with sealed cans preferentially flooded with a dry cask, k_{eff} = 0.8669 ± 0.0022 and k_{eff} = 0.8384 ± 0.0021, respectively. These configurations are chosen for moderator density variations.

Results of the moderator density variation cases for normal and accident conditions for the nonpoisoned and poisoned basket configurations are presented in Table 6.4.6-9 through Table 6.4.6-12.

As seen in Table 6.4.6-10, the most reactive configuration for the TRIGA fuel cluster rods in the non-poisoned basket, analyzed conservatively without end caps, contains 5 baskets with intact fuel under accident conditions with no water in the cask interior, neutron shield, or exterior, k_{eff} = 0.8756 ± 0.0023. Per Section 6.1.1, this corresponds to k_s = 0.8970.

As seen in Table 6.4.6-12, the most reactive configuration for the TRIGA fuel cluster rods in the poisoned basket, contains two baskets with maximum diameter sealed cans, preferentially flooded, under accident conditions with no water in the cask interior, neutron shield, or exterior, k_{eff} = 0.8399 ± 0.0021. Per Section 6.1.1, this corresponds to k_s = 0.8609.

6.4.6.4   Single Package Criticality Evaluation

To satisfy 10 CFR 71.55(b)(3), an analysis of the reflection of the containment system (inner shell) by water is performed on a single wet cask. Successive replacement of the cask radial shields with water reflection is also evaluated for each basket (poisoned/nonpoisoned)

configuration. As seen in Table 6.4.6-13 and Table 6.4.6-14, the reactivity of the system drops as each radial shield of the cask is replaced by water, from the full cask surrounded by water, to the inner shell surrounded by water.

6.4.6.5   Increased Content Scope for TRIGA Cluster Rods

The TRIGA cluster rod content is modified by first expanding on the HEU fuel characteristics, i.e., fuel volume and clad thickness, followed by evaluations increasing the allowed fuel composition range, i.e. changes in H/Zr ratio, ^{235}U enrichment, wt % U in the fuel matrix, and ^{235}U mass.

6.4.6.5.1   Increased Fuel Volume and Reduced Clad Thickness Evaluations for HEU Fuel

The HEU TRIGA fuel cluster rod contents evaluated previously in this section, and as presented in Table 6.2.6-1 and Table 6.2.6-2, are based on nominal, dimensional and compositional values. To ensure that criticality safety is maintained for parameter values slightly different from those listed in the tables, a set of calculations are performed with increased active fuel length, increased fuel pellet diameter, decreased cladding thickness, and corresponding increases in the uranium and zirconium masses due to the increased volume.

Calculations are performed for two cases based on the most reactive configuration presented in Section 6.4.6.3, which is for the nonpoisoned basket configuration. In each case, the active fuel length is increased to 22.5 inches, the cladding thickness is decreased to 0.015 inch, and the pellet diameter is set at 0.52 inch for the first case, then 0.53 inch for the second case. The results are presented in Table 6.4.6-15. As seen in the results, the increase in the fuel volume for the maximum pellet diameter (0.53 inch) results in an increase in k_s of 1.2 percent. The resulting value is well below the 0.95 limit. Note that for the dry system, reducing clad thickness allows the fuel rods to shift closer to the center of each cluster rod insert. For the wet system, a reduced clad thicknessincreases the moderator volume.

6.4.6.5.2   Variations in Fuel Material Compostions Including the Addition of LEU Fuel Material

Criticality evaluations for the fuel material composition changes are divided into three sets of analysis. The first analysis stage uses the HEU and LEU intact and damaged fuel models to

determine the effect of the H/Zr ratio on system reactivity. Next, cask cavity moderator density studies confirm that the most reactive system configuration at the requested fissile material mass, enrichment, and H/Zr ratio remains the preferentially flooded cask with dry cask cavity. These evaluations all rely on an accident cask configuration with no neutron shield, coupling the casks in the infinite array modeled. The final set of evaluations runs normal condition models to

demonstrate that the accident condition bounds and the criticality safety index (CSI) is 0 for all conditions. The set also includes the necessary analysis to demonstrate that the results from a single cask, containment reflected, is bounded. TRIGA fuel rod geometry for the HEU and LEU evaluations is based on the previously determined geometry summarized in Table 6.4.6-20. The maximum fuel mass (grams ^{235}U), maximum enrichment (wt % ^{235}U), and minimum weight percent uranium employed in the analysis are also contained in Table 6.4.6-20. In conjunction with the hydrogen to zirconium ratio, the minimum uranium weight percent in the fuel matrix determines the maximum quantity of moderator (hydrogen) within the fuel matrix.

Hydrogen to Zirconium Ratio Studies

For the accident condition cask array model, including loss of neutron shield with a dry cask exterior, the system reactivities are evaluated for H/Zr ratios from 1.5 to 1.7. The system is evaluated for intact fuel and damaged fuel with a flooded and a dry cask cavity. For the dry cavity, the fuel is placed in the maximum reactivity dry cavity geometry configuration, while for the flooded cavity, the wet cavity most reactive geometry configuration is used. Note that for the dry cask cavity damaged fuel case, a preferentially flooded (full density water) canister is modeled. As seen in Figure 6.4.6-1 and Figure 6.4.6-2, the maximum reactivity is associated with a maximum H/Zr ratio (1.7) for LEU and HEU fuel under both dry and wet conditions. The magnitude of the increase varies by configuration and ranges from Δk=0.011 to 0.045. Increases in reactivity are higher for the HEU material than for the LEU configuration. Therefore, a maximum H/Zr ratio of 1.7 is used for the optimum moderator density evaluation.

Maximum Reactivity Moderator / Optimum Moderator Condition Study

HEU and LEU configurations are evaluated at various cask cavity moderator density conditions. All models employ fuel at the maximum H/Zr ratio of 1.7. The maximum reactivity condition cask, i.e., preferentially flooded damaged fuel can (damaged fuel model only), cask accident model, and exterior moderator (dry), is used in these evaluations. HEU and LEU optimum moderator density plots for the dry cavity most reactive basket configuration ("Dry Cavity MRC") and the wet cavity most reactive basket configuration ("Wet Cavity MRC") are included in Figure 6.4.6-3 and Figure 6.4.6-4. Maximum system reactivity is obtained from the damaged fuel can model with a dry cask cavity. Figure 6.4.6-5 confirms that the fully flooded damaged fuel can represents the bounding scenario.

The maximum system reactivities for the accident models are summarized in Table 6.4.6-16.

Single Cask Containment (Fully Reflected) and Normal Condition Array Evaluations

A normal condition infinite cask array is evaluated to demonstrate compliance with 10 CFR 71.55 and 71.59. Normal condition cask array results are summarized in Table 6.4.6-17.

Reactivity of the normal condition array is lower, as the radial neutron shield reduces neutronic interaction between casks.

A single cask evaluation is performed to comply with 10 CFR 71.55(b)(3). The containment for the NAC-LWT is the cask inner shell. While no operating condition results in removal of the cask outer shell and lead gamma shield, the most reactive preferential flooded and fully flooded cases are reevaluated by removing the lead and outer shells (including neutron shield), and reflecting the system by 20 cm water at full density on the X, Y and Z faces. Single cask, with containment fully water reflected reactivities are summarized in Table 6.4.6-18.

Maximum Reactivities and Comparison to Limits

Based on the TRIGA bias k_s, the bias and uncertainty adjusted Monte Carlo-generated system reactivity is summarized in Table 6.4.6-19 for each of the three primary analysis groups.

The maximum adjusted neutron multiplication factor, (k_s), is 0.9303. The maximum reactivity is based on the following model characteristics:

- HEU rods
- 0.53-inch pellet diameter, 0.015-inch clad thickness and 22.5 inches active fuel length
- Maximum 95 wt % ^{235}U enriched material with a minimum 9.5 wt % U in the fuel meat (bounds LEU fuel material maximum 20 wt % ^{235}U enriched material with a minimum 43 wt % U in the fuel meat)
- Damaged fuel cans containing an equivalent 6 intact fuel rods per can
- Preferentially flooded can
- Void cask cavity and exterior
- Loss of neutron shield

The maximum reactivity is calculated under hypothetical accident conditions. As an infinite cask array remains subcritical under normal and accident conditions, the criticality safety index (CSI) is 0.

6.4.6.6   Conclusion

Thus, including all calculational and mechanical uncertainties, an infinite array of NAC-LWT casks remains subcritical, and is below the 0.95 limit, corrected for bias and uncertainty, under normal and accident conditions with fuel rod parameters as defined in Table 6.4.6-20 and the following defined quantity limits:

Nonpoisoned Baskets:
1. 480 TRIGA fuel cluster rods.

2. Sealed damaged fuel cans (DFCs), top and bottom baskets only, with up to six damaged TRIGA fuel cluster rods or fuel debris and remainder of baskets filled with undamaged fuel.

<u>Poisoned Baskets:</u>

1. 560 TRIGA fuel cluster rods.

2. Sealed DFCs, top and bottom baskets only, with up to six damaged TRIGA fuel cluster rods or fuel debris and remainder of baskets filled with undamaged fuel.

Figure 6.4.6-1   HEU Cluster Rod Reactivity versus H/Zr Ratio – Accident Condition
Cask Array
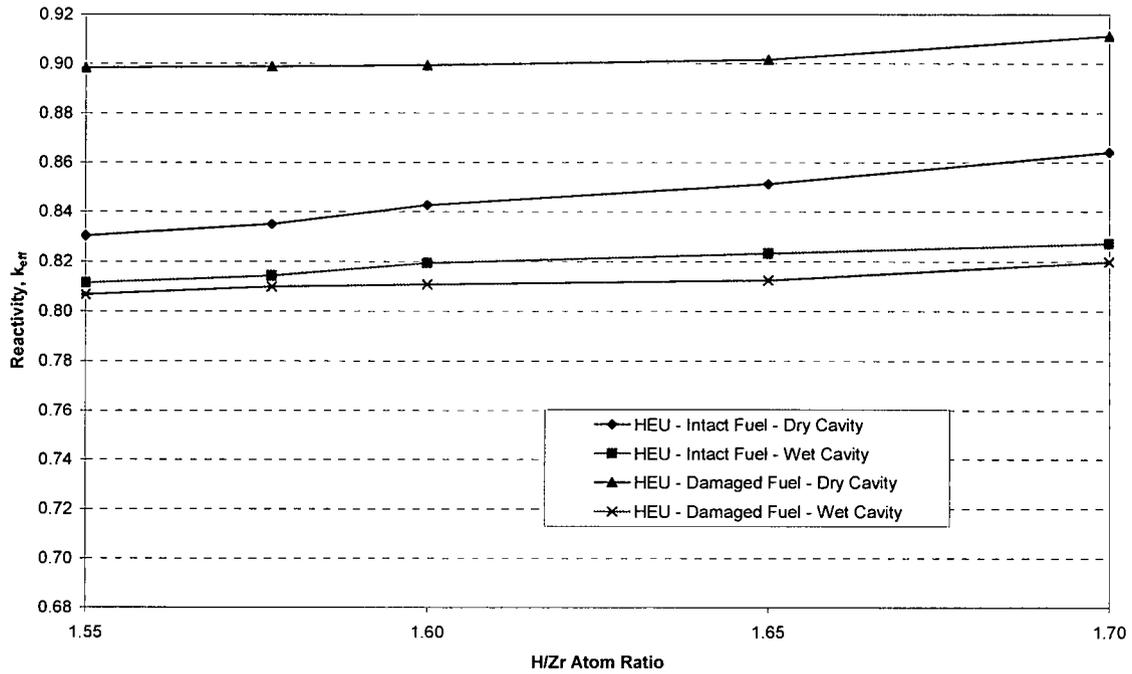
Figure 6.4.6-2   LEU Cluster Rod Reactivity versus H/Zr Ratio – Accident Condition
Cask Array
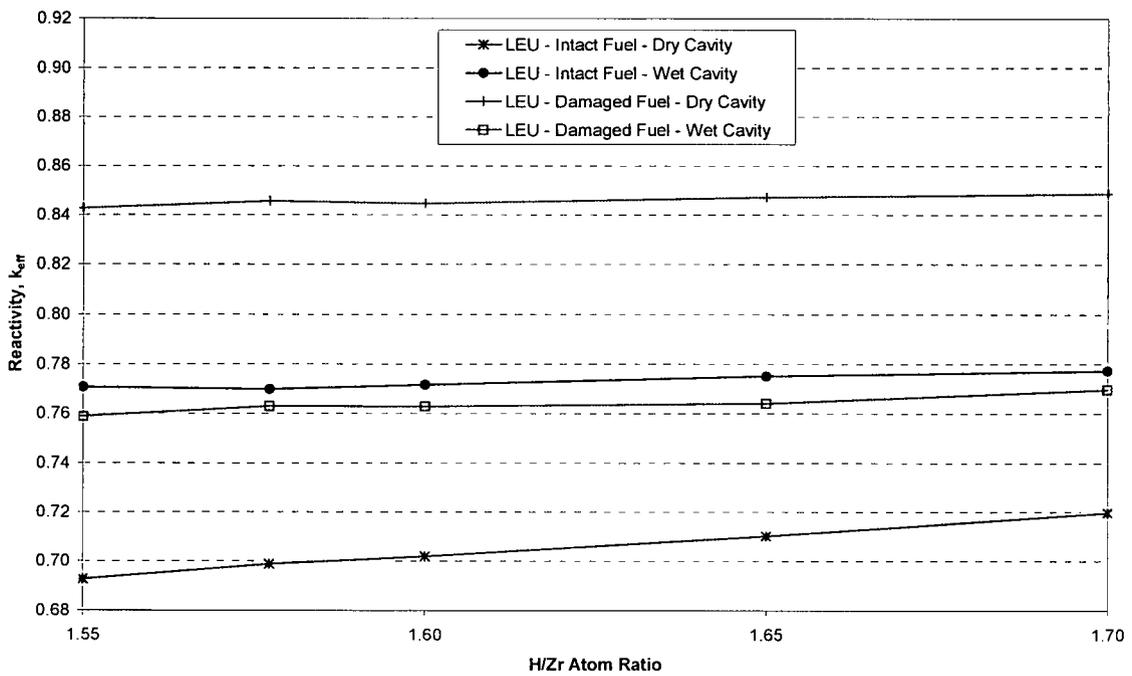
Figure 6.4.6-3   HEU TRIGA Cluster Rod System Reactivity versus Cask Cavity
Moderator
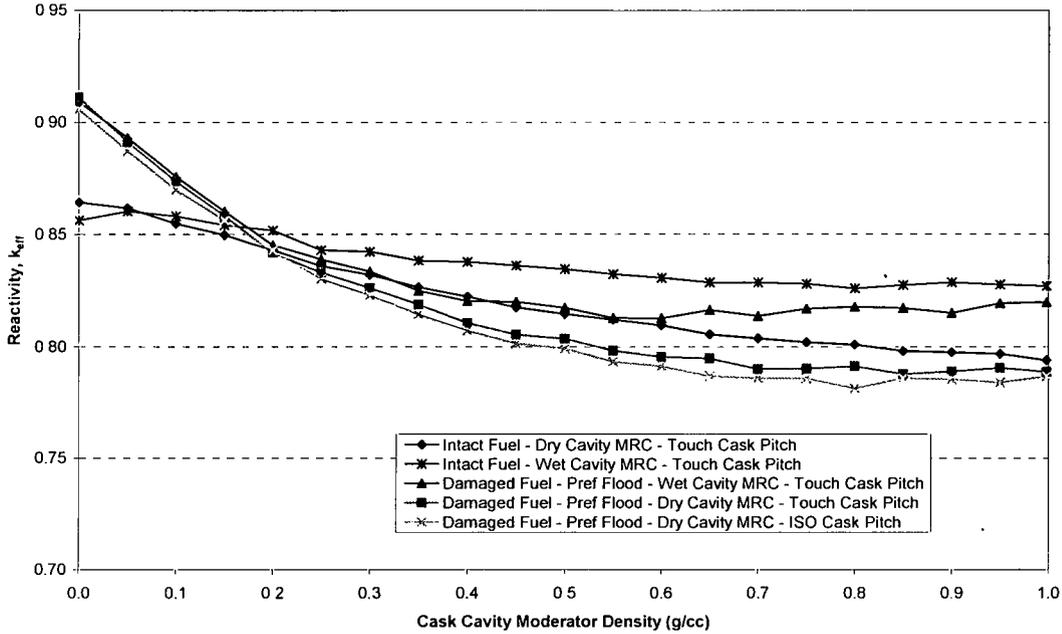
Figure 6.4.6-4   LEU TRIGA Cluster Rod System Reactivity versus Cask Cavity
Moderator
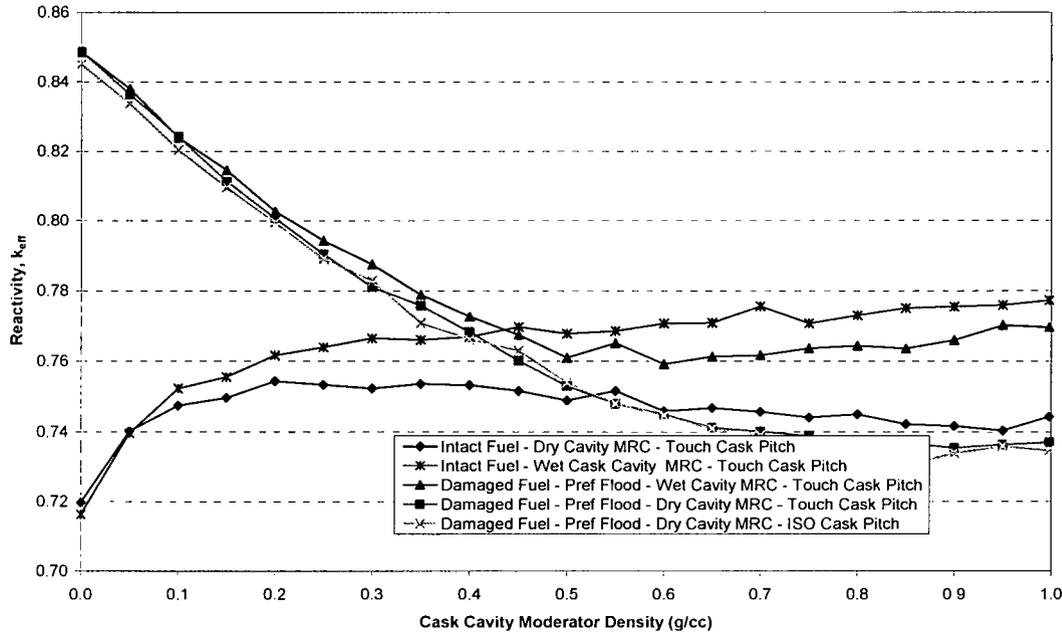
Figure 6.4.6-5   TRIGA Cluster Rod Reactivity versus Damaged Fuel Can Moderator
(Pref Flood – Dry Cask Cavity)
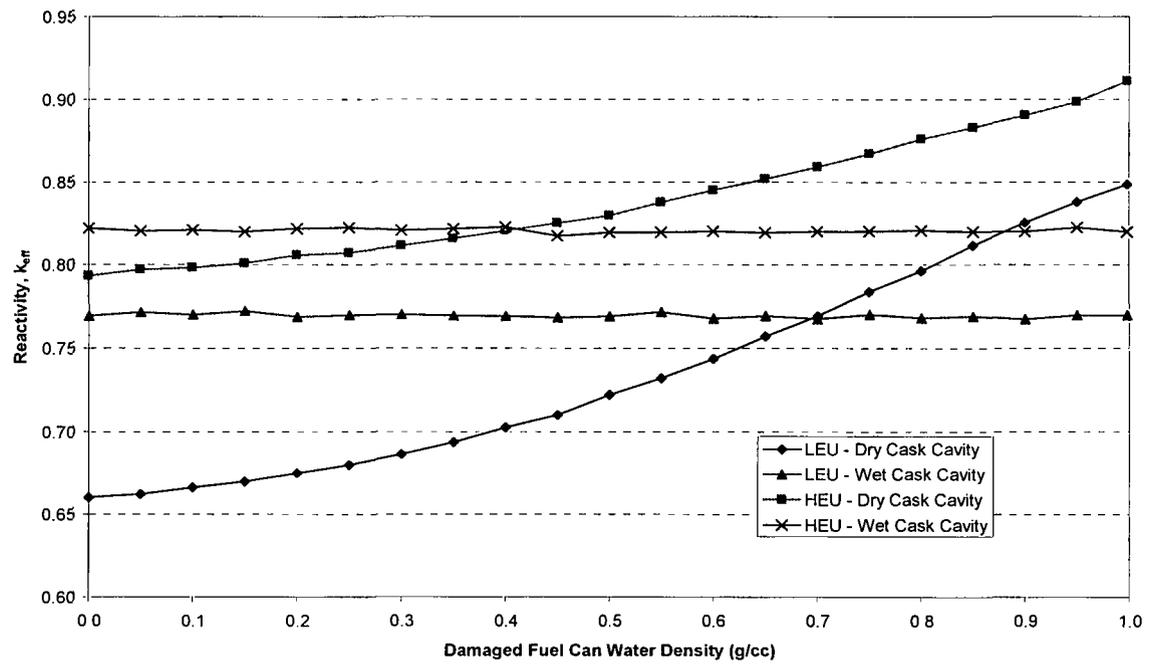
Table 6.4.6-1   Cask k_eff with TRIGA Fuel Cluster Rods – Fuel Rod Placement Perturbations, Nonpoisoned Basket

Basket Configuration	Wet Case Results $k_{eff} \pm \sigma$	Dry Case Results $k_{eff} \pm \sigma$
Nominal Centered Fuel and Al Insert	0.7340 ± 0.0026	0.8001 ± 0.0019
Elements Moved To Al Insert Center	0.7110 ± 0.0027	0.8076 ± 0.0019
Elements Moved Away From Al Insert Center	0.7458 ± 0.0026	0.8005 ± 0.0020
Al Insert Moved To Basket Center[1]	0.7571 ± 0.0025	0.8047 ± 0.0020
Al Insert Moved Away From Basket Center[1]	0.7391 ± 0.0025	0.8027 ± 0.0020
1 Rod Removed From Each Al Insert	0.7576 ± 0.0026	0.7782 ± 0.0020
2 Rods Removed From Each Al Insert	0.7558 ±0.0024	0.7503 ± 0.0020
3 Rods Removed From Each Al Insert	0.7414 ± 0.0022	-

Note:

[1]   The most reactive fuel positioning is retained.

Table 6.4.6-2   Cask k_eff with TRIGA Fuel Cluster Rods – Fuel Rod Placement Perturbations, Poisoned Basket

Basket Configuration	Wet Case Results $k_{eff} \pm \sigma$	Dry Case Results $k_{eff} \pm \sigma$
Nominal Centered Fuel and Al Insert	0.7809 ± 0.0026	0.7435 ± 0.0020
Elements Moved To Al Insert Center	0.7654 ± 0.0025	0.7501 ± 0.0019
Elements Moved Away From Al Insert Center	0.7922 ± 0.0027	0.7468 ± 0.0020
Al Insert Moved To Basket Center[1]	0.7995 ± 0.0026	0.7489 ± 0.0019
Al Insert Moved Away From Basket Center[1]	0.7914 ± 0.0027	0.7476 ± 0.0022
1 Rod Removed From Each Al Insert	0.7956 ± 0.0027	0.7163 ± 0.0019
2 Rods Removed From Each Al Insert	0.7882 ± 0.0026	0.6831 ± 0.0019
3 Rods Removed From Each Al Insert	0.7764 ± 0.0026	-

Note:

[1]   The most reactive fuel in tube motion is retained.

Table 6.4.6-3   Axially Infinite Cask k_{eff} with TRIGA Fuel Cluster Rods – Basket and Insert Manufacturing Tolerance Perturbations, Nonpoisoned Basket

Basket Configuration	Wet Case Results $k_{eff} \pm \sigma$	Dry Case Results $k_{eff} \pm \sigma$
Base Case[1]	0.7571 ± 0.0025	0.8047 ± 0.0020
Thin SS Basket Plates	0.7652 ± 0.0025	0.8140 ± 0.0020
Maximum Al Insert Tube Diameter[2]	0.7653 ± 0.0027	0.8146 ± 0.0022
Minimum Al Insert Tube Diameter[2]	0.7487 ± 0.0025	0.8084 ± 0.0019
Minimum Al Insert Tube Thickness[2]	0.7625 ± 0.0026	0.8157 ± 0.0021
Minimum Basket Opening[2]	0.7682 ± 0.0026 [3]	0.8129 ± 0.0021

Notes:

[1]   Most reactive configurations as determined in Section 6.4.6.1.1.

[2]   Incorporates minimum thickness stainless steel, basket divider plates.

[3]   Maximum aluminum tube diameter.

Table 6.4.6-4   Axially Infinite Cask k_{eff} with TRIGA Fuel Cluster Rods – Basket and Insert Manufacturing Tolerance Perturbations, Poisoned Basket

Basket Configuration	Wet Case Results $k_{eff} \pm \sigma$	Dry Case Results $k_{eff} \pm \sigma$
Base Case[1]	0.7995 ± 0.0026	0.7489 ± 0.0019
Thin SS Basket Plates	0.8019 ± 0.0024	0.7513 ± 0.0020
Maximum Al Insert Tube Diameter[2]	0.8055 ± 0.0027	0.7512 ± 0.0019
Minimum Al Insert Tube Diameter[2]	0.7969 ± 0.0026	0.7507 ± 0.0018
Minimum Al Insert Tube Thickness[2]	0.7995 ± 0.0023	0.7518 ± 0.0019
Minimum Basket Opening[2]	0.8025 ± 0.0025 [3]	0.7518 ± 0.0018 [4]

Notes:

[1]   Most reactive configurations as determined in Section 6.4.6.1.1.

[2]   Incorporates minimum thickness stainless steel, basket divider plates.

[3]   Maximum aluminum tube diameter.

[4]   Minimum aluminum tube thickness.

Table 6.4.6-5   Sealed Can Preferential Flooding and Partial Loading Reactivity
Evaluations for TRIGA Fuel Rod Clusters, Nonpoisoned Basket

Description	$k_{eff} \pm \sigma$ Dry Cask/Dry Can	$k_{eff} \pm \sigma$ Wet Cask/Wet Can	$k_{eff} \pm \sigma$ Dry Cask/Wet Can
1 Solid Fuel Lump	0.7184 ± 0.0025	0.7654 ± 0.0024	0.6954 ± 0.0022
2 Solid Fuel Lumps	0.7053 ± 0.0021	0.7546 ± 0.0025	0.6721 ± 0.0020
3 Solid Fuel Lumps	0.6946 ± 0.0022	0.7597 ± 0.0025	0.6704 ± 0.0022
4 Solid Fuel Lumps	0.6983 ± 0.0020	0.7672 ± 0.0026	0.6714 ± 0.0023
5 Solid Fuel Lumps	0.6995 ± 0.0024	0.7620 ± 0.0028	0.6723 ± 0.0022
Mixture Full Can Height	0.6917 ± 0.0021	0.7592 ± 0.0024	0.8669 ± 0.0022
Mixture Half Can Height	0.6932 ± 0.0021	0.7582 ± 0.0025	0.7226 ± 0.0022
Mixture Full Can Height, 50 % mass	0.6807 ± 0.0022	0.7606 ± 0.0025	0.7416 ± 0.0021

Table 6.4.6-6   Sealed Can Preferential Flooding and Partial Loading Reactivity
Evaluations for TRIGA Fuel Rod Clusters, Poisoned Basket

Description	$k_{eff} \pm \sigma$ Dry Cask/Dry Can	$k_{eff} \pm \sigma$ Wet Cask/Wet Can	$k_{eff} \pm \sigma$ Dry Cask/Wet Can
1 Solid Fuel Lump	0.6957 ± 0.0022	0.7937 ± 0.0025	0.6662 ± 0.0020
2 Solid Fuel Lumps	0.6704 ± 0.0021	0.7942 ± 0.0026	0.6405 ± 0.0022
3 Solid Fuel Lumps	0.6610 ± 0.0020	0.7959 ± 0.0026	0.6389 ± 0.0019
4 Solid Fuel Lumps	0.6592 ± 0.0020	0.7986 ± 0.0025	0.6389 ± 0.0022
5 Solid Fuel Lumps	0.6561 ± 0.0019	0.8001 ± 0.0023	0.6409 ± 0.0020
Mixture Full Can Height	0.6507 ± 0.0019	0.7993 ±0.0025	0.8384 ± 0.0021
Mixture Half Can Height	0.6575 ± 0.0019	0.8045 ± 0.0029	0.6741 ± 0.0022
Mixture Full Can Height, 50 % mass	0.6422 ± 0.0019	0.7992 ± 0.0027	0.6957 ± 0.0020

Table 6.4.6-7   Summary of Most Reactive Configurations, TRIGA Fuel Cluster Rods,
Nonpoisoned Basket

	Wet	Dry	Preferential
Intact Fuel	0.7682 ± 0.0026	0.8129 ± 0.0021	-
Sealed Fuel Cans[1]	0.7672 ± 0.0026	0.7184 ± 0.0025	0.8669 ± 0.0022

Note:

[1]   Remainder of baskets filled with intact fuel.

Table 6.4.6-8   Summary of Most Reactive Configurations, TRIGA Fuel Cluster Rods,
Poisoned Basket

	Wet	Dry	Preferential
Intact Fuel	0.8025 ± 0.0025	0.7518 ± 0.0018	-
Sealed Fuel Cans[1]	0.8045 ± 0.0029	0.6957 ± 0.0022	0.8384 ± 0.0021

Note:

[1]   Remainder of baskets filled with intact fuel.

Table 6.4.6-9   Reactivity Results for TRIGA Fuel Cluster Rods, Sealed Cans, Normal
Conditions, Nonpoisoned Basket

Moderator SG	Casks Touching ($k_{eff} \pm \sigma$)	8 Foot Center-To-Center ($k_{eff} \pm \sigma$)
Dry Exterior, Vary Internal Density		
0.00000	0.7292 ± 0.0023	0.7270 ± 0.0025
0.00100	0.7294 ± 0.0024	0.7258 ± 0.0026
0.00178	0.7262 ± 0.0025	0.7312 ± 0.0025
0.00316	0.7267 ± 0.0024	0.7316 ± 0.0024
0.00562	0.7277 ± 0.0024	0.7294 ± 0.0024
0.01000	0.7240 ± 0.0024	0.7312 ± 0.0023
0.01780	0.7249 ± 0.0025	0.7279 ± 0.0025
0.03160	0.7307 ± 0.0026	0.7322 ± 0.0025
0.05620	0.7392 ± 0.0024	0.7333 ± 0.0024
0.10000	0.7345 ± 0.0024	0.7349 ± 0.0025
0.17800	0.7354 ± 0.0025	0.7339 ± 0.0024
0.31600	0.7298 ± 0.0025	0.7285 ± 0.0025
0.56200	0.7074 ± 0.0024	0.7100 ± 0.0026
0.70000	0.7064 ± 0.0022	0.7055 ± 0.0026
0.80000	0.7140 ± 0.0027	0.7083 ± 0.0024
0.90000	0.7137 ± 0.0026	0.7201 ± 0.0024
1.00000	0.7168 ± 0.0026	0.7216 ± 0.0027
Optimally Moderated Cask Interior (SG = 0.05620), Vary External Density		
0.00000	0.7292 ± 0.0023	0.7270 ± 0.0025
0.00100	0.7354 ± 0.0024	0.7352 ± 0.0028
0.00178	0.7351 ± 0.0025	0.7360 ± 0.0026
0.00316	0.7347 ± 0.0024	0.7347 ± 0.0023
0.00562	0.7329 ± 0.0025	0.7372 ± 0.0025
0.01000	0.7303 ± 0.0023	0.7316 ± 0.0024
0.01780	0.7306 ± 0.0024	0.7296 ± 0.0027
0.03160	0.7296 ± 0.0025	0.7339 ± 0.0024
0.05620	0.7321 ± 0.0023	0.7324 ± 0.0022
0.10000	0.7369 ± 0.0023	0.7305 ± 0.0021
0.17800	0.7325 ± 0.0024	0.7343 ± 0.0025
0.31600	0.7307 ± 0.0026	0.7324 ± 0.0024
0.56200	0.7297 ± 0.0028	0.7359 ± 0.0025
0.70000	0.7341 ± 0.0021	0.7300 ± 0.0022
0.80000	0.7316 ± 0.0024	0.7359 ± 0.0024
0.90000	0.7334 ± 0.0025	0.7313 ± 0.0026
1.00000	0.7308 ± 0.0025	0.7318 ± 0.0023
Vary Internal and External Density Simultaneously		
0.00000	0.7292 ± 0.0023	0.7270 ± 0.0025
0.00100	0.7291 ± 0.0023	0.7275 ± 0.0025
0.00178	0.7271 ± 0.0026	0.7309 ± 0.0024
0.00316	0.7316 ± 0.0025	0.7271 ± 0.0024
0.00562	0.7286 ± 0.0027	0.7277 ± 0.0023
0.01000	0.7288 ± 0.0025	0.7254 ± 0.0024
0.01780	0.7329 ± 0.0024	0.7296 ± 0.0024
0.03160	0.7309 ± 0.0026	0.7300 ± 0.0026
0.05620	0.7321 ± 0.0023	0.7313 ± 0.0026
0.10000	0.7364 ± 0.0024	0.7299 ± 0.0025
0.17800	0.7344 ± 0.0026	0.7335 ± 0.0023
0.31600	0.7299 ± 0.0024	0.7301 ± 0.0026
0.56200	0.7139 ± 0.0026	0.7118 ± 0.0025
0.70000	0.7024 ± 0.0025	0.7025 ± 0.0027
0.80000	0.7116 ± 0.0024	0.7029 ± 0.0023
0.90000	0.7177 ± 0.0028	0.7142 ± 0.0024
1.00000	0.7204 ± 0.0025	0.7187 ± 0.0026

Table 6.4.6-10   Reactivity Results for TRIGA Fuel Cluster Rods, Sealed Can, Accident Conditions, Nonpoisoned Basket

Moderator SG	Casks Touching ($k_{eff} \pm \sigma$)	8 Foot Center-To-Center ($k_{eff} \pm \sigma$)
Dry Exterior and Neutron Shield, Vary Internal Moderator		
0.00000	0.8669 ± 0.0022	0.8756 ± 0.0023
0.00100	0.8725 ± 0.0022	0.8687 ± 0.0022
0.00178	0.8737 ± 0.0022	0.8668 ± 0.0022
0.00316	0.8721 ± 0.0024	0.8744 ± 0.0024
0.00562	0.8703 ± 0.0022	0.8693 ± 0.0024
0.01000	0.8716 ± 0.0022	0.8646 ± 0.0021
0.01780	0.8658 ± 0.0022	0.8614 ± 0.0021
0.03160	0.8620 ± 0.0023	0.8620 ± 0.0021
0.05620	0.8536 ± 0.0022	0.8561 ± 0.0025
0.10000	0.8345 ± 0.0023	0.8373 ± 0.0023
0.17800	0.8138 ± 0.0022	0.8152 ± 0.0024
0.31600	0.7862 ± 0.0021	0.7830 ± 0.0024
0.56200	0.7570 ± 0.0025	0.7500 ± 0.0024
0.70000	0.7439 ± 0.0023	0.7424 ± 0.0027
0.80000	0.7383 ± 0.0025	0.7404 ± 0.0026
0.90000	0.7415 ± 0.0027	0.7391 ± 0.0025
1.00000	0.7398 ± 0.0026	0.7303 ± 0.0026
Optimally Moderated Internal (SG = 0.0), Vary Neutron Shield and Exterior		
0.00000	0.8669 ± 0.0022	0.8756 ± 0.0023
0.00100	0.8620 ± 0.0022	0.7950 ± 0.0023
0.00178	0.8488 ± 0.0022	0.7755 ± 0.0025
0.00316	0.8366 ± 0.0023	0.7509 ± 0.0024
0.00562	0.8209 ± 0.0022	0.7403 ± 0.0024
0.01000	0.7994 ± 0.0023	0.7341 ± 0.0024
0.01780	0.7795 ± 0.0022	0.7272 ± 0.0022
0.03160	0.7618 ± 0.0024	0.7270 ± 0.0025
0.05620	0.7497 ± 0.0025	0.7251 ± 0.0025
0.10000	0.7395 ± 0.0023	0.7238 ± 0.0025
0.17800	0.7300 ± 0.0023	0.7244 ± 0.0025
0.31600	0.7280 ± 0.0024	0.7285 ± 0.0022
0.56200	0.7311 ± 0.0025	0.7283 ± 0.0024
0.70000	0.7322 ± 0.0024	0.7243 ± 0.0025
0.80000	0.7305 ± 0.0025	0.7267 ± 0.0024
0.90000	0.7237 ± 0.0022	0.7324 ± 0.0023
1.00000	0.7286 ± 0.0024	0.7287 ± 0.0025
Vary Interior, Exterior and Neutron Shield Simultaneously		
0.00000	0.8669 ± 0.0022	0.8756 ± 0.0023
0.00100	0.8615 ± 0.0023	0.7989 ± 0.0022
0.00178	0.8550 ± 0.0023	0.7755 ± 0.0025
0.00316	0.8397 ± 0.0022	0.7520 ± 0.0024
0.00562	0.8268 ± 0.0022	0.7439 ± 0.0024
0.01000	0.7988 ± 0.0025	0.7333 ± 0.0025
0.01780	0.7788 ± 0.0024	0.7305 ± 0.0023
0.03160	0.7600 ± 0.0023	0.7259 ± 0.0024
0.05620	0.7510 ± 0.0024	0.7350 ± 0.0024
0.10000	0.7444 ± 0.0024	0.7349 ± 0.0024
0.17800	0.7397 ± 0.0025	0.7298 ± 0.0024
0.31600	0.7284 ± 0.0025	0.7297 ± 0.0024
0.56200	0.7106 ± 0.0022	0.7056 ± 0.0024
0.70000	0.7051 ± 0.0025	0.7004 ± 0.0025
0.80000	0.7146 ± 0.0025	0.7104 ± 0.0027
0.90000	0.7107 ± 0.0025	0.7195 ± 0.0026
1.00000	0.7204 ± 0.0025	0.7251 ± 0.0025

Table 6.4.6-11   Reactivity Results for TRIGA Fuel Cluster Rods, Sealed Cans, Normal
Conditions, Poisoned Basket

Moderator SG	Casks Touching ($k_{eff} \pm \sigma$)	8 Foot Center-To-Center ($k_{eff} \pm \sigma$)
Dry Exterior, Vary Internal Density		
0.00000	0.7274 ± 0.0026	0.7319 ± 0.0024
0.00100	0.7342 ± 0.0022	0.7283 ± 0.0023
0.00178	0.7296 ± 0.0024	0.7268 ± 0.0023
0.00316	0.7286 ± 0.0024	0.7328 ± 0.0024
0.00562	0.7294 ± 0.0023	0.7277 ± 0.0023
0.01000	0.7309 ± 0.0022	0.7338 ± 0.0024
0.01780	0.7319 ± 0.0023	0.7308 ± 0.0023
0.03160	0.7338 ± 0.0023	0.7334 ± 0.0023
0.05620	0.7349 ± 0.0024	0.7290 ± 0.0023
0.10000	0.7328 ± 0.0021	0.7339 ± 0.0026
0.17800	0.7346 ± 0.0024	0.7339 ± 0.0023
0.31600	0.7332 ± 0.0026	0.7315 ± 0.0023
0.56200	0.7324 ± 0.0024	0.7308 ± 0.0024
0.70000	0.7245 ± 0.0025	0.7304 ± 0.0023
0.80000	0.7401 ± 0.0025	0.7310 ± 0.0024
0.90000	0.7455 ± 0.0025	0.7375 ± 0.0028
1.00000	0.7573 ± 0.0027	0.7593 ± 0.0026
Optimally Moderated Cask Interior (SG = 1.0), Vary External Density		
0.00000	0.7274 ± 0.0026	0.7319 ± 0.0024
0.00100	0.7667 ± 0.0026	0.7623 ± 0.0026
0.00178	0.7635 ± 0.0024	0.7652 ± 0.0025
0.00316	0.7636 ± 0.0026	0.7596 ± 0.0027
0.00562	0.7675 ± 0.0028	0.7636 ± 0.0027
0.01000	0.7697 ± 0.0025	0.7661 ± 0.0026
0.01780	0.7634 ± 0.0025	0.7615 ± 0.0029
0.03160	0.7664 ± 0.0027	0.7641 ± 0.0024
0.05620	0.7635 ± 0.0030	0.7688 ± 0.0026
0.10000	0.7599 ± 0.0029	0.7676 ± 0.0024
0.17800	0.7622 ± 0.0024	0.7637 ± 0.0024
0.31600	0.7620 ± 0.0026	0.7690 ± 0.0023
0.56200	0.7685 ± 0.0030	0.7643 ± 0.0028
0.70000	0.7632 ± 0.0025	0.7684 ± 0.0028
0.80000	0.7645 ± 0.0028	0.7657 ± 0.0027
0.90000	0.7615 ± 0.0028	0.7624 ± 0.0027
1.00000	0.7641 ± 0.0028	0.7659 ± 0.0025
Vary Internal and External Density Simultaneously		
0.00000	0.7274 ± 0.0026	0.7319 ± 0.0024
0.00100	0.7328 ± 0.0022	0.7281 ± 0.0024
0.00178	0.7279 ± 0.0025	0.7297 ± 0.0024
0.00316	0.7306 ± 0.0023	0.7310 ± 0.0023
0.00562	0.7323 ± 0.0024	0.7331 ± 0.0025
0.01000	0.7291 ± 0.0026	0.7291 ± 0.0024
0.01780	0.7306 ± 0.0024	0.7309 ± 0.0024
0.03160	0.7291 ± 0.0022	0.7314 ± 0.0023
0.05620	0.7292 ± 0.0026	0.7299 ± 0.0024
0.10000	0.7302 ± 0.0026	0.7356 ± 0.0025
0.17800	0.7363 ± 0.0024	0.7288 ± 0.0023
0.31600	0.7366 ± 0.0025	0.7316 ± 0.0025
0.56200	0.7296 ± 0.0026	0.7300 ± 0.0025
0.70000	0.7318 ± 0.0023	0.7276 ± 0.0025
0.80000	0.7350 ± 0.0025	0.7385 ± 0.0024
0.90000	0.7423 ± 0.0027	0.7385 ± 0.0024
1.00000	0.7641 ± 0.0028	0.7659 ± 0.0029

Table 6.4.6-12   Reactivity Results for TRIGA Fuel Cluster Rods, Sealed Cans, Accident
Conditions, Poisoned Basket

Moderator SG	Casks Touching ($k_{eff} \pm \sigma$)	8 Foot Center-To-Center ($k_{eff} \pm \sigma$)
Dry Exterior and Neutron Shield, Vary Internal Moderator		
0.00000	0.8384 ± 0.0021	0.8375 ± 0.0023
0.00100	0.8394 ± 0.0022	0.8343 ± 0.0021
0.00178	0.8376 ± 0.0022	0.8316 ± 0.0022
0.00316	0.8373 ± 0.0022	0.8319 ± 0.0024
0.00562	0.8399 ± 0.0021	0.8336 ± 0.0025
0.01000	0.8356 ± 0.0022	0.8321 ± 0.0023
0.01780	0.8380 ± 0.0022	0.8314 ± 0.0022
0.03160	0.8302 ± 0.0025	0.8208 ± 0.0021
0.05620	0.8240 ± 0.0021	0.8188 ± 0.0024
0.10000	0.8127 ± 0.0023	0.8112 ± 0.0023
0.17800	0.7993 ± 0.0024	0.7936 ± 0.0022
0.31600	0.7773 ± 0.0024	0.7738 ± 0.0027
0.56200	0.7616 ± 0.0026	0.7559 ± 0.0023
0.70000	0.7570 ± 0.0025	0.7578 ± 0.0022
0.80000	0.7647 ± 0.0026	0.7589 ± 0.0025
0.90000	0.7728 ± 0.0028	0.7671 ± 0.0026
1.00000	0.7802 ± 0.0026	0.7803 ± 0.0026
Optimally Moderated Internal (SG = 0.0), Vary Neutron Shield and Exterior		
0.00000	0.8384 ± 0.0021	0.8375 ± 0.0023
0.00100	0.8282 ± 0.0022	0.7710 ± 0.0023
0.00178	0.8210 ± 0.0021	0.7593 ± 0.0024
0.00316	0.8150 ± 0.0022	0.7532 ± 0.0023
0.00562	0.7993 ± 0.0023	0.7398 ± 0.0024
0.01000	0.7882 ± 0.0024	0.7336 ± 0.0024
0.01780	0.7664 ± 0.0026	0.7326 ± 0.0024
0.03160	0.7546 ± 0.0024	0.7290 ± 0.0023
0.05620	0.7480 ± 0.0022	0.7285 ± 0.0023
0.10000	0.7387 ± 0.0022	0.7267 ± 0.0022
0.17800	0.7308 ± 0.0023	0.7265 ± 0.0026
0.31600	0.7324 ± 0.0023	0.7310 ± 0.0025
0.56200	0.7278 ± 0.0025	0.7291 ± 0.0022
0.70000	0.7320 ± 0.0023	0.7317 ± 0.0025
0.80000	0.7320 ± 0.0024	0.7268 ± 0.0026
0.90000	0.7313 ± 0.0025	0.7291 ± 0.0026
1.00000	0.7329 ± 0.0025	0.7329 ± 0.0025
Vary Interior, Exterior and Neutron Shield Simultaneously		
0.00000	0.8384 ± 0.0021	0.8375 ± 0.0023
0.00100	0.8269 ± 0.0024	0.7802 ± 0.0024
0.00178	0.8258 ± 0.0021	0.7625 ± 0.0022
0.00316	0.8089 ± 0.0022	0.7525 ± 0.0023
0.00562	0.7928 ± 0.0022	0.7409 ± 0.0025
0.01000	0.7825 ± 0.0023	0.7308 ± 0.0025
0.01780	0.7721 ± 0.0023	0.7305 ± 0.0026
0.03160	0.7552 ± 0.0023	0.7327 ± 0.0023
0.05620	0.7457 ± 0.0023	0.7283 ± 0.0025
0.10000	0.7420 ± 0.0024	0.7343 ± 0.0025
0.17800	0.7365 ± 0.0023	0.7322 ± 0.0026
0.31600	0.7379 ± 0.0024	0.7333 ± 0.0024
0.56200	0.7292 ± 0.0026	0.7333 ± 0.0022
0.70000	0.7286 ± 0.0023	0.7307 ± 0.0027
0.80000	0.7334 ± 0.0023	0.7292 ± 0.0023
0.90000	0.7516 ± 0.0026	0.7517 ± 0.0024
1.00000	0.7608 ± 0.0029	0.7608 ± 0.0029

Table 6.4.6-13   Single Package 10 CFR 71.55(b)(3) Evaluation k_{eff} Summary, TRIGA
Fuel Cluster Rod, Nonpoisoned Basket

Description	$k_{eff} \pm \sigma$	k_s
Single Cask / Inner Shell Reflected with H_2O	0.73003 ± 0.00254	0.75191
Single Cask / Inner Shell and Lead Reflected with H_2O	0.76100 ± 0.00243	0.78266
Single Cask / Inner Shell, Lead & Outer Shell Reflected with H_2O	0.76366 ± 0.00240	0.78526
Single Intact Cask Reflected with H_2O	0.76360 ± 0.00273	0.78586

Table 6.4.6-14   Single Package 10 CFR 71.55(b)(3) Evaluation k_{eff} Summary, TRIGA
Fuel Cluster Rod, Poison Basket

Description	$k_{eff} \pm \sigma$	k_s
Single Cask / Inner Shell Reflected with H_2O	0.76615 ± 0.00265	0.78825
Single Cask / Inner Shell and Lead Reflected with H_2O	0.80117 ± 0.00287	0.82371
Single Cask / Inner Shell, Lead & Outer Shell Reflected with H_2O	0.80106 ± 0.00250	0.82286
Single Intact Cask Reflected with H_2O	0.79815 ± 0.00228	0.81951

Table 6.4.6-15   Increased Fuel Dimensional Parameter k_{eff} Summary, TRIGA Fuel
Cluster Rod, Nonpoisoned Basket

Description	$k_{eff} \pm \sigma$	k_s
Base Case (Section 6.4.6.3)	0.8756 ± 0.0023	0.8970
22.5-inch Active Fuel Height 0.015-inch Cladding Thickness 0.52-inch Fuel Pellet Diameter	0.8793 ± 0.0024	0.9009
22.5-inch Active Fuel Height 0.015-inch Cladding Thickness 0.53-inch Fuel Pellet Diameter	0.8876 ± 0.0021	0.9086

Table 6.4.6-16   TRIGA Cluster Rod Reactivities – Accident Conditions

	HEU			LEU		
	Cask Cavity	k_{eff}	σ	Cask Cavity	k_{eff}	σ
Intact Fuel	Dry (0 g/cc)	0.86414	0.00112	Wet (0.9882 g/cc)	0.77727	0.00121
Damaged Fuel	Dry (0 g/cc)	0.91119	0.00117	Dry (0 g/cc)	0.84872	0.00109

Table 6.4.6-17   TRIGA Cluster Rod Reactivities – Normal Conditions

Description	k_{eff}	σ
HEU - Dry Normal Condition Array	0.56007	0.00114
HEU - Dry Cask Cavity - Preferential Flooded Can - Normal Condition Array	0.74210	0.00132
LEU - Dry Normal Condition Array	0.44760	0.00094
LEU - Dry Cask Cavity - Preferential Flooded Can - Normal Condition Array	0.71750	0.00123

Table 6.4.6-18   TRIGA Cluster Rod Reactivities – Single Cask with Containment Fully Water Reflected

Description	k_{eff}	σ
HEU - Dry Cask Cavity - Preferential Flooded Can	0.74059	0.00120
LEU - Dry Cask Cavity - Preferential Flooded Can	0.71063	0.00117

Table 6.4.6-19   Summary of TRIGA Cluster Rod Maximum Reactivity Configuration

Fuel Material Configuration	HEU			LEU		
	k_{eff}	σ	k_s	k_{eff}	σ	k_s
Accident Array – Preferentially Flooded	0.91119	0.00117	0.93033	0.84872	0.00109	0.86770
Normal Array – Preferentially Flooded	0.74210	0.00132	0.76154	0.71750	0.00123	0.73676
Normal Array – Dry	0.56007	0.00114	0.57915	0.44760	0.00094	0.46628
Single Cask Fully (Water) Reflected	0.74059	0.00120	0.75979	0.71063	0.00117	0.72977

Table 6.4.6-20   Licensing Parameters for TRIGA Cluster Rods

Parameter	Value
Fuel Form	U-ZrH$_x$
Number of Rods Per Basket Opening	16
Clad Material	Incoloy
HEU Max. Enrichment (wt % ^{235}U)	95
HEU Min. U in Fuel Meat (wt %)	9.5[1]
HEU Max ^{235}U Per Rod (g)	46.5
LEU Max. Enrichment (wt % ^{235}U)	20
LEU Min. U in Fuel Meat (wt %)	43[2]
LEU Max ^{235}U Per Rod (g)	55
Maximum Hydrogen to Zirconium Ratio	1.70
Maximum Pellet Diameter (inch)	0.53
Minimum Clad Thickness (inch)	0.015
Maximum Active Fuel Length (inch)	22.5

---

[1] Equivalent to 457 grams zirconium

[2] Equivalent to 357 grams zirconium

6.4.7   DIDO Fuel Assemblies

This section presents the criticality analyses for the NAC-LWT cask with the DIDO fuel assembly and basket configuration. Criticality analyses of the seven assembly arrangement with the most limiting assembly type is performed to satisfy the criticality safety requirements of 10 CFR Parts 71.55 and 71.59, as well as IAEA Transportation Safety Standards (TS-R-1). In this analysis, the bounding DIDO fuel assembly type is determined, and infinite and finite arrays of NAC-LWT casks loaded with the design basis DIDO fuel are studied for criticality under normal and accident conditions. Moderator density in the cavity, neutron shield tank and outside is varied to determine the maximum k_{eff}. The analyses demonstrate that, including all calculational and mechanical uncertainties, the NAC-LWT remains subcritical under normal and accident conditions for all DIDO fuel assemblies.

6.4.7.1   Maximum Reactivity DIDO Assembly

This evaluation determines the maximum reactivity based on LEU, MEU and HEU fuel assembly configurations. Assemblies and baskets are modeled at nominal characteristics under normal conditions (i.e., the neutron shield is assumed intact). The cask interior and exterior are flooded with full density water. Based on the thickness of the neutron shield little interaction between casks is expected resulting in minimal impact of exterior moderator density variations. The results in Table 6.4.7-1 show that the maximum reactivity is obtained from HEU assemblies. The HEU assembly is more reactive than the LEU and MEU assemblies due to reduced parasitic absorption by ^{238}U. The fuel assembly is modeled with uniform cylinder spacing, referred to as "loose fuel elements" in this section, which has reactivity significantly higher than the reactivity of the crimped fuel element.

As demonstrated, the reactivity for LEU and MEU fuel assemblies is significantly lower than that of the HEU assembly. Shipment of LEU, MEU and HEU assemblies in the same basket is therefore permissible.

6.4.7.2   Radial and Axial Assembly Shifting Under Normal Conditions

The reactivity result in Table 6.4.7-1 shows that fuel assemblies axially shifted towards the adjoining basket (i.e., three groups of two baskets) are more reactive than those placed at the top or bottom of the basket. Shifting fuel assemblies in adjoining baskets towards one another brings the maximum fissile material into its closest proximity.

Radial outward shifting of both crimped and loose fuel assemblies shows that system reactivity decreases when shifting the assembly radially out from the center of the cask. Patterns designated as "in" shift the six peripheral fuel assemblies towards the basket center with the

centered tube assembly pushed out to approach the +x axis assembly. The radial "out" pattern similarly pushes the six peripheral assemblies away from the basket center. The "custom" pattern indicated in the result table represents the "in" pattern with the center assembly shifted out at 45 degrees. The crimped pattern indicated as "single" corresponds to all assemblies being crimped in the same direction (for this evaluation at an angle of 45 degrees). For the loose fuel cylinder model, there appears to be no statistically significant reactivity difference between the centered or shifted radially in fuel assemblies. For the crimped pattern, crimping the fuel assembly radially out provides for a significant increase in reactivity in the radially shifted in assembly configuration. No significant difference in reactivity for modified crimp directions is shown in the radially out assembly configuration.

6.4.7.3   Radial Shifting and Exterior Moderator Density Changes Under Accident Conditions

The cask accident configuration is one where the material of the neutron shield is replaced by the cask exterior material definition. Both loose and crimped assemblies are evaluated at full density water in the cask interior and at a void exterior under various radial shift conditions. All cases are based on the alternate axial shifting of fuel shown in Section 6.4.7.2 to be the most reactive. Results of these analyses are shown in Table 6.4.7-2. As expected, the void exterior condition produces the maximum reactivity configuration. Reactivity increases due to increased interaction between individual casks in the array.

In addition to the shifted standard "in" configuration, the inward shifted configuration with a centered middle assembly is also evaluated (designated as InC in the result table). This configuration is slightly more reactive than the configuration with all assemblies centered, but it is within the statistical uncertainty band (2 sigma) of the Monte Carlo base result. Mechanical perturbation and uncertainty results are therefore evaluated with the all assemblies centered configuration.

Table 6.4.7-3 displays results for test cases based on modifying the material of the aluminum shell surrounding the basket and the heat transfer shunts in the center of the basket. The base case for this analysis is the radially centered, fully moderated interior, dry exterior configuration. Replacing the shell material by water or steel in the accident model inhibits interaction between packages and produces lower reactivities in the infinite array of casks. Modeling the heat transfer shunts as all water increases reactivity slightly. This supports modeling the shunts as a set of three small rods with a smaller cross-section area.

6.4.7.4   Basket Manufacturing Tolerance Evaluation

In this evaluation, set basket tolerances are applied to the criticality evaluation. The base case
for this evaluation is the cask accident model (i.e, neutron shield replaced by exterior moderator
which in this case is void) with centered fuel assembly. As shown in Table 6.4.7-4, basket
tolerances do not produce a significant reactivity increase. Note that the tube wall thickness
minimum tolerance is set to a zero percent change. The minimum tube wall case is, therefore,
identical to the base case. All further analysis is, therefore, set to nominal basket parameters.

6.4.7.5   Fuel Assembly Tolerance Evaluation

This evaluation contains the fuel assembly perturbation studies. Each of the parameters is
evaluated independently with the results compared to the cask accident condition base case. For
fuel cylinder pitch, two studies are performed. The first fixes the inner plate (cylinder) and
varies the outer three cylinders and is noted as "IF." The second fixes the outer plate and is noted
as "OF." Per the reactivity results in Table 6.4.7-5, tolerances that produce an increase in
reactivity are:

- Minimum plate thickness (increases moderator between plates)

- Minimum clad thickness

- Maximum plate pitch (outer diameter fixed; increasing the outer diameter will
  decrease the amount of moderator between assemblies)

- Minimum active fuel height (reduces the space between fissile material in the
  alternating shifted model)

- Minimum element height (reduces the space between fissile material in the
  alternating shifted model)

- Maximum fissile mass

- Maximum uranium weight percent (minimum impact but is added to the final
  reactivity models)

6.4.7.6   Maximum Reactivity Configuration

The parameters shown in Section 6.4.7.5 to increase system reactivity are combined to form a
worst case cask payload configuration. The limiting fuel assembly description based on the
critical fuel assembly parameters is shown in Table 6.4.7-12. Table 6.4.7-6 displays the
evaluation results of the worst case configured DIDO NAC-LWT. Since the radially in
configuration with a centered basket middle assembly was statistically the same as the all
centered configuration (see Table 6.4.7-2), both configurations are evaluated with the toleranced
fuel parameters. The most reactive configuration for the DIDO assembly in the infinite array
configuration is above 0.95. To remain below 0.95 under all conditions, a finite array of 8 casks

in close pitch configuration is modeled. The array is reflected by a water boundary condition and is evaluated with a flooded cask interior and void cask exterior. Both eight cask array configurations result in maximum k_s below 0.95. The CSI for the eight cask accident configuration is 12.5. Based on the normal to accident condition reactivity difference of 0.04 Δk, versus the 0.01 Δk that 0.95 was exceeded for the infinite array, the CSI for normal condition is 0 (infinite array is acceptable).

6.4.7.7   Moderator Density Variation Reactivity Configuration

Table 6.4.7-7 contains a cask interior and exterior moderator density variation study for the HEU fuel assembly in the accident configuration. All basket and fuel parameters are set to nominal conditions and an infinite array of casks is evaluated. The basket shows a relatively constant reactivity between cask interior densities of 1.0 g/cm^3 and 0.9 g/cm^3. While reactivity increases above the two sigma (95/95) uncertainty band typically applied in this calculation as statistically significant, the results are within the three sigma (99% confidence) band and are considered constant for the purposes of this calculation (Note that the maximum reactivity of the 8-cask array is below 0.92). At lower interior water densities the reactivity begins to decrease significantly. The exterior density study demonstrates that any significant amount of cask exterior moderator density will reduce the interaction between casks in the array.

6.4.7.8   Single Package Criticality Evaluation

To satisfy 10 CFR 71.55(b)(3), an analysis of the reflection of the containment system (inner shell) by water is performed on a single wet cask. Successive replacement of the cask radial shields with water reflection is also evaluated. A significant decrease in reactivity occurs when the lead gamma shield is replaced by water. The results from this evaluation can be seen in Table 6.4.7-8.

6.4.7.9   Reduced Clad Thickness Evaluations

This section documents the reactivity change due to a reduction in the DIDO element minimum clad thickness to 0.025 cm. The analysis in the previous sections is for a minimum clad thickness of 0.0325 cm.

The effect of the reduced clad thickness on system reactivity is determined by repeating cases from Section 6.4.7.5 and Section 6.4.7.6. Table 6.4.7-9 repeats the Section 6.4.7.5 minimum clad thickness case for the reduced value and compares it to the main section results. As expected, the reduced minimum clad thickness yields a proportional increase in k_{eff}. Table 6.4.7-10 show the results for the worst-case tolerance combination with the reduced clad thickness for the cases discussed in Section 6.4.7.6. The maximum k_{eff} is based on an eight-cask

array with a void exterior. All cases show a slight increase in reactivity due to the reduced clad thickness.

6.4.7.10   Expanded Inner and Outer Shell Diameter Evaluations

Based on the fuel assembly tolerance and moderator studies, a combination of a reduced inner diameter fuel tube ID (Tube 1) with a maximized outer fuel tube ID (Tube 4) is expected to maximize system reactivity (i.e., fuel plates are under-moderated with the previously evaluated conditions and increased pitch will increase system reactivity). Based on tolerances previously applied, the minimum Tube 1 ID is 5.88 cm and the maximum Tube 4 OD is 9.52 cm. This range is evaluated by fixing the Tube 1 ID at minimum and evaluating the nominal, minimum and maximum Tube 4 OD according to the values in the following list.

Tube Number	Min OD (cm)	Nom OD (cm)	Max OD (cm)
1	6.01	6.01	6.01
2	7.05	7.11	7.18
3	8.08	8.22	8.35
4	9.12	9.32	9.52

For this study, the tube pitch is a calculated variable and is larger than the maximum pitch considered in the previous calculation sections.

Table 6.4.7-11 documents the results of the tube diameter study. Based on the trend of increasing reactivity with increasing outer tube OD, the system remains under-moderated. The maximum k_s for the system is 0.9304 for an eight-cask array. Note that significant margin exists in these results, as the basket tube material is modeled as aluminum rather than stainless steel. System reactivity for the steel tube basket at the specified maximum reactivity configuration is < 0. 8.

6.4.7.11   Code Bias and Code Bias Uncertainty Adjustments

A calculation of k_s under normal and accident conditions can now be made based on the previous results and based on the KENO-Va validation statistics presented in Section 6.5.2 for high enriched uranium fuel. The value k_s is calculated based on the KENO-Va Monte Carlo average plus any biases and uncertainties associated with the methods and the modeling, i.e.:

$$k_s = k_{eff} + \Delta k_{Bias} + \Delta k_{BU} + 2\sigma_{MC} \leq 0.95$$

In the validation presented in Section 6.5.2, a bias of -0.0044 (allowance for overprediction of k_{eff}) and a 95/95 method uncertainty of $\pm$ 0.0181 was determined. For added conservatism, the -

0.0044 bias correction is neglected. With these biases and uncertainties, the equation for k_s becomes:

$$k_s = k_{eff} + 0.0181 + 2\sigma_{MC}$$

k_s values for the relevant analysis are included in Table 6.4.7-1 through Table 6.4.7-11. The maximum k_s, 0.9304, for the DIDO shipment results from the eight-cask array accident configuration model.

For both normal and accident conditions, the calculated k_{eff} values, after correction for biases and uncertainties, are well below the 0.95 limit. The analyses demonstrate that, including all calculational and mechanical uncertainties, an infinite array of NAC-LWT casks with DIDO fuel remains subcritical under normal and accident conditions.

Table 6.4.7-1   Normal Condition HEU, LEU, MEU DIDO Evaluation

Fuel Type	Fuel Configuration	Crimp Pattern	Radial Shift Pattern	Axial Shift Pattern	k_{eff}	σ	$k_{eff}+2\sigma$	k_s	Δk	$\Delta k_{eff}/\sigma$
LEU	Loose	N/A	Centered	Down	0.82771	0.00067	0.82905	0.84715	-0.03689	-55.1
LEU	Loose	N/A	Centered	Alternating	0.83842	0.00070	0.83982	0.85792	-0.02612	-37.3
LEU	Crimped	Single	Centered	Down	0.81887	0.00069	0.82025	0.83835	-0.04569	-66.2
LEU	Crimped	Single	Centered	Alternating	0.83112	0.00068	0.83248	0.85058	-0.03346	-49.2
MEU	Loose	N/A	Centered	Down	0.84006	0.00070	0.84146	0.85956	-0.02448	-35.0
MEU	Loose	N/A	Centered	Alternating	0.85333	0.00072	0.85477	0.87287	-0.01117	-15.5
MEU	Crimped	Single	Centered	Down	0.83259	0.00070	0.83399	0.85209	-0.03195	-45.6
MEU	Crimped	Single	Centered	Alternating	0.84336	0.00069	0.84474	0.86284	-0.02120	-30.7
HEU	Loose	N/A	Centered	Down	0.85243	0.00070	0.85383	0.87193	-0.01211	-17.3
HEU	Loose	N/A	Centered	Alternating	0.86462	0.00066	0.86594	0.88404	--	--
HEU	Loose	N/A	Centered	Up	0.85275	0.00071	0.85417	0.87227	-0.01177	-16.6
HEU	Loose	N/A	In	Alternating	0.86361	0.00071	0.86503	0.88313	-0.00091	-1.3
HEU	Loose	N/A	Out	Alternating	0.85625	0.00070	0.85765	0.87575	-0.00829	-11.8
HEU	Loose	N/A	Custom	Alternating	0.86562	0.00072	0.86706	0.88516	0.00112	1.6
HEU	Crimped	Single	Centered	Down	0.84084	0.00072	0.84228	0.86038	-0.02366	-32.9
HEU	Crimped	Single	Centered	Alternating	0.85512	0.00069	0.85650	0.87460	-0.00944	-13.7
HEU	Crimped	Single	Centered	Up	0.84075	0.00070	0.84215	0.86025	-0.02379	-34.0
HEU	Crimped	Single	In	Alternating	0.85628	0.00072	0.85772	0.87582	-0.00822	-11.4
HEU	Crimped	Single	Out	Alternating	0.84484	0.00072	0.84628	0.86438	-0.01966	-27.3
HEU	Crimped	Single	Custom	Alternating	0.85688	0.00069	0.85826	0.87636	-0.00768	-11.1
HEU	Crimped	In	In	Alternating	0.84841	0.00071	0.84983	0.86793	-0.01611	-22.7
HEU	Crimped	Out	Out	Alternating	0.84118	0.00072	0.84262	0.86072	-0.02332	-32.4
HEU	Crimped	In	Out	Alternating	0.84552	0.00067	0.84686	0.86496	-0.01908	-28.5
HEU	Crimped	Out	In	Alternating	0.85786	0.00074	0.85934	0.87744	-0.00660	-8.9

Table 6.4.7-2   HEU DIDO Accident Evaluation – Radial Shift and Exterior Moderator Density Variation

Fuel Configuration	Crimp Pattern	Radial Shift Pattern	Interior Moderator Density (g/cm³)	Exterior Moderator Density (g/cm³)	k_{eff}	σ	$k_{eff}+2\sigma$	k_s	Δk	$\Delta k_{eff}/\sigma$
Loose	N/A	Centered	0.9998	0.9998	0.86276	0.00070	0.86416	0.88226	--	--
Loose	N/A	In	0.9998	0.9998	0.86468	0.00070	0.86608	0.88418	0.00192	2.7
Crimped	Out	Centered	0.9998	0.9998	0.85355	0.00068	0.85491	0.87301	-0.00925	-13.6
Crimped	Out	In	0.9998	0.9998	0.85666	0.00069	0.85804	0.87614	-0.00612	-8.9
Loose	N/A	Centered	0.9998	0.0001	0.90900	0.00069	0.91038	0.92848	--	--
Loose	N/A	In	0.9998	0.0001	0.90808	0.00071	0.90950	0.92760	-0.00088	-1.2
Loose	N/A	InC	0.9998	0.0001	0.91011	0.00069	0.91149	0.92959	0.00111	1.6
Crimped	Out	Centered	0.9998	0.0001	0.89962	0.00071	0.90104	0.91914	-0.00934	-13.2
Crimped	Out	In	0.9998	0.0001	0.90116	0.00069	0.90254	0.92064	-0.00784	-11.4

Table 6.4.7-3   DIDO Heat Shunt and Aluminum Shell Evaluation Results

Case Description	k_{eff}	σ	$k_{eff}+2\sigma$	k_s	Δk	$\Delta k_{eff}/\sigma$
Shell modeled as steel	0.90100	0.00067	0.90234	0.92044	-0.00804	-12.0
Shell modeled as water	0.90382	0.00070	0.90522	0.92332	-0.00516	-7.4
Aluminum shunts modeled as water	0.91157	0.00067	0.91291	0.93101	0.00253	3.8

Table 6.4.7-4   DIDO Basket Geometric Tolerance Study Results

Fuel Tube Outer Diameter Tolerance	Fuel Tube Thickness Tolerance	Fuel Tube Height Tolerance	Fuel Basket Base Plate Tolerance	k_{eff}	σ	$k_{eff}+2\sigma$	k_s	Δk	$\Delta k_{eff}/\sigma$
Min	Nominal	Nominal	Nominal	0.90979	0.00070	0.91119	0.92929	0.00081	1.2
Max	Nominal	Nominal	Nominal	0.90959	0.00069	0.91097	0.92907	0.00059	0.9
Nominal	Min	Nominal	Nominal	0.90900	0.00069	0.91038	0.92848	--	--
Nominal	Max	Nominal	Nominal	0.90489	0.00071	0.90631	0.92441	-0.00407	-5.7
Nominal	Nominal	Min	Nominal	0.90954	0.00068	0.91090	0.92900	0.00052	0.8
Nominal	Nominal	Max	Nominal	0.90953	0.00069	0.91091	0.92901	0.00053	0.8
Nominal	Nominal	Nominal	Min	0.90922	0.00067	0.91056	0.92866	0.00018	0.3
Nominal	Nominal	Nominal	Max	0.90858	0.00068	0.90994	0.92804	-0.00044	-0.6

Table 6.4.7-5   DIDO Fuel Assembly Tolerance Study Results

Fuel Cylinder Diameter Tolerance	Fuel Plate Thickness Tolerance	Fuel Plate Clad Thickness Tolerance	Fuel Cylinder Pitch Tolerance	Active Fuel Length Tolerance	Fuel Assembly Height Tolerance	^{235}U Mass Tolerance	Uranium Weight Fraction Tolerance	k_{eff}	σ	$k_{eff}+2\sigma$	k_s	Δk	$\Delta k_{eff}/\sigma$
Min	--	--	--	--	--	--	--	0.91024	0.00069	0.91162	0.92972	0.00124	1.8
Max	--	--	--	--	--	--	--	0.90691	0.00067	0.90825	0.92635	-0.00213	-3.2
--	Min	--	--	--	--	--	--	0.91188	0.00067	0.91322	0.93132	0.00284	4.2
--	Max	--	--	--	--	--	--	0.90539	0.00068	0.90675	0.92485	-0.00363	-5.3
--	--	Min	--	--	--	--	--	0.91253	0.00069	0.91391	0.93201	0.00353	5.1
--	--	Max	--	--	--	--	--	0.90685	0.00069	0.90823	0.92633	-0.00215	-3.1
--	--	--	IF - Max	--	--	--	--	0.90993	0.00068	0.91129	0.92939	0.00091	1.3
--	--	--	IF - Min	--	--	--	--	0.90864	0.00071	0.91006	0.92816	-0.00032	-0.5
--	--	--	OF - Max	--	--	--	--	0.91175	0.00068	0.91311	0.93121	0.00273	4.0
--	--	--	OF - Min	--	--	--	--	0.90787	0.00065	0.90917	0.92727	-0.00121	-1.9
--	--	--	--	Min	--	--	--	0.91067	0.00071	0.91209	0.93019	0.00171	2.4
--	--	--	--	Max	--	--	--	0.90853	0.00068	0.90989	0.92799	-0.00049	-0.7
--	--	--	--	--	Min	--	--	0.91108	0.00066	0.91240	0.93050	0.00202	3.1
--	--	--	--	--	Max	--	--	0.90735	0.00069	0.90873	0.92683	-0.00165	-2.4
--	--	--	--	--	--	Min	--	0.89234	0.00070	0.89374	0.91184	-0.01664	-23.8
--	--	--	--	--	--	Max	--	0.92431	0.00068	0.92567	0.94377	0.01529	22.5
--	--	--	--	--	--	--	Min	0.90761	0.00068	0.90897	0.92707	-0.00141	-2.1
--	--	--	--	--	--	--	Max	0.91070	0.00070	0.91210	0.93020	0.00172	2.5

Table 6.4.7-6   DIDO Fuel Maximum Reactivity Combinations

Cask Array	Radial Shift Pattern	Fuel Cylinder Diameter Tolerance	Fuel Plate Thickness Tolerance	Fuel Plate Clad Thickness Tolerance	Fuel Cylinder Pitch Tolerance	Active Fuel Length Tolerance	Fuel Assembly Height Tolerance	^{235}U Mass Tolerance	Uranium Weight Fraction Tolerance	k_{eff}	σ	k_{eff}+2σ	k_s
Infinite	Centered	Nominal	Min	Min	OF-Max	Min	Min	Max	Max	0.93813	0.00070	0.93953	0.95763
Infinite	InC	Nominal	Min	Min	OF-Max	Min	Min	Max	Max	0.93639	0.00073	0.93785	0.95595
8 cask	Centered	Nominal	Min	Min	OF-Max	Min	Min	Max	Max	0.89310	0.00072	0.89454	0.91264
8 cask	InC	Nominal	Min	Min	OF-Max	Min	Min	Max	Max	0.89596	0.00070	0.89736	0.91546

Table 6.4.7-7   Moderator Density Study for the Infinite Array of Casks (Nominal Fuel and Basket Configuration)

Radial Shift Pattern	Interior Moderator Density (g/cm³)	Exterior Moderator Density (g/cm³)	k_{eff}	σ	$k_{eff}+2\sigma$	k_s	Δk	$\Delta k_{eff}/\sigma$
Exterior Moderator Density Study								
Centered	0.9998	0.9	0.86274	0.00066	0.86406	0.88216	-0.04632	-70.2
Centered	0.9998	0.8	0.86320	0.00071	0.86462	0.88272	-0.04576	-64.5
Centered	0.9998	0.6	0.86400	0.00070	0.86540	0.88350	-0.04498	-64.3
Centered	0.9998	0.4	0.86367	0.00073	0.86513	0.88323	-0.04525	-62.0
Centered	0.9998	0.2	0.86441	0.00070	0.86581	0.88391	-0.04457	-63.7
Centered	0.9998	0.1	0.86822	0.00073	0.86968	0.88778	-0.04070	-55.8
Interior Moderator Density Study								
Centered	0.975	0.0001	0.91103	0.00069	0.91241	0.93051	0.00203	2.9
Centered	0.95	0.0001	0.91097	0.00066	0.91229	0.93039	0.00191	2.9
Centered	0.925	0.0001	0.90942	0.00070	0.91082	0.92892	0.00044	0.6
Centered	0.9	0.0001	0.91079	0.00070	0.91219	0.93029	0.00181	2.6
Centered	0.875	0.0001	0.90928	0.00068	0.91064	0.92874	0.00026	0.4
Centered	0.85	0.0001	0.90869	0.00072	0.91013	0.92823	-0.00025	-0.3
Centered	0.8	0.0001	0.90563	0.00088	0.90739	0.92549	-0.00299	-3.4
Centered	0.6	0.0001	0.88126	0.00102	0.88330	0.90140	-0.02708	-26.5
Centered	0.4	0.0001	0.80903	0.00118	0.81139	0.82949	-0.09899	-83.9
Centered	0.2	0.0001	0.62941	0.00122	0.63185	0.64995	-0.27853	-228.3
Centered	0.0001	0.0001	0.13951	0.00043	0.14037	0.15847	-0.77001	-1790.7
InC	0.975	0.0001	0.90855	0.00067	0.90989	0.92799	-0.00049	-0.7
InC	0.95	0.0001	0.90809	0.00072	0.90953	0.92763	-0.00085	-1.2
InC	0.925	0.0001	0.90723	0.00072	0.90867	0.92677	-0.00171	-2.4
InC	0.9	0.0001	0.90644	0.00071	0.90786	0.92596	-0.00252	-3.5
InC	0.875	0.0001	0.90525	0.00067	0.90659	0.92469	-0.00379	-5.7
InC	0.85	0.0001	0.90377	0.00075	0.90527	0.92337	-0.00511	-6.8
InC	0.8	0.0001	0.90218	0.00070	0.90358	0.92168	-0.00680	-9.7
InC	0.0001	0.0001	0.87289	0.00073	0.87435	0.89245	-0.03603	-49.4

Table 6.4.7-8   DIDO Single Package 10 CFR 71.55(b)(3) Evaluation k_{eff} Summary

Description	$k_{eff} \pm \sigma$	k_s
Single Cask / Inner Shell Reflected with H_2O	0.83670±0.00075	0.85630
Single Cask / Inner Shell and Lead Reflected with H_2O	0.88638±0.00070	0.90588
Single Cask / Inner Shell, Lead & Outer Shell Reflected with H_2O	0.89275±0.00070	0.91225
Single Intact Cask Reflected with H_2O	0.89352±0.00070	0.91302

Table 6.4.7-9   DIDO Fuel Assembly Tolerance Study Results (Reduced Clad Thickness)

Clad Thickness	k_{eff}	σ	$k_{eff}+2\sigma$	k_s	Δk
0.0425 cm (Nominal)	0.90900	0.00069	0.91038	0.92848	--
0.0325 cm (Min)	0.91253	0.00069	0.91391	0.93201	0.00353
0.0250 cm (Revised Min)	0.91578	0.00069	0.91716	0.93526	0.00678

Table 6.4.7-10   DIDO Fuel Maximum Reactivity Combinations (Reduced Clad Thickness)

Cask Array	Radial Shift Pattern	k_{eff}	σ	$k_{eff}+2\sigma$	k_s
Infinite	Centered	0.93921	0.00071	0.94063	0.95873
Infinite	InC	0.93866	0.00072	0.94010	0.95820
8 cask	Centered	0.89293	0.00071	0.89435	0.91245
8 cask	InC	0.89762	0.00071	0.89904	0.91714

Note: Fuel and basket configuration as detailed in Table 6.4.7-6.

Table 6.4.7-11   DIDO Fuel Maximum Reactivity Combinations (Reduced Clad and Maximum Pitch)

Configuration	k_{eff}	σ	$k_{eff}+2\sigma$	k_s
Minimum outer diameter	0.90282	0.00070	0.90422	0.92232
Nominal outer diameter	0.90770	0.00072	0.90914	0.92724
Maximum outer diameter	0.91088	0.00070	0.91228	0.93038

Note: All cases include the minimum inner diameter and the maximum reactivity fuel and basket configuration in an 8-cask array as specified in Sections 6.4.7.6 and 6.4.7.9 as bounding.

Table 6.4.7-12   DIDO Bounding Configurations

Parameter	Value
Number of Fuel Cylinders	4
Plate thickness	≥ 0.130 cm
Clad thickness	≥ 0.025 cm
^{235}U content per Assembly	≤ 190 g
Enrichment wt % ^{235}U	≤ 94
Active Fuel Height	≥ 58.75 cm
Assembly Height[1]	≥ 61.5 cm
Min Tube ID	5.88 cm
Max. Tube OD	9.52 cm

Note:

[1] Assembly height provides for spacing of fissile material. An optional spacer may be used to maintain spacing if the assembly is cut to shorter than 61.5 cm.

6.4.8   General Atomics Irradiated Fuel Material

This section presents the criticality analyses for the NAC-LWT cask with GA IFM. Criticality analyses are performed to satisfy the criticality safety requirements of 10 CFR Parts 71.55 and 71.59, as well as IAEA Transportation Safety Standards (TS-R-1). All criticality evaluations performed herein use an axially infinite model. An analysis of the NAC-LWT with a payload of either RERTR or HTGR fuel material shows that the TRIGA elements in the RERTR enclosure are more reactive than the HTGR fuel matrix. A detailed study of the combined payload evaluates TRIGA pitch, TRIGA array type (square or rectangular), interior moderator density including preferential flooding, and exterior moderator density. A single cask evaluation is also performed to comply with 10 CFR 71.55(b)(3). The analyses demonstrate that, including all calculational and mechanical uncertainties, the NAC-LWT remains subcritical under normal and accident conditions for the two GA IFM packages (FHUs).

6.4.8.1   Payload Evaluation

The results of the payload evaluation are used to determine the largest contributor to system reactivity. Four models were executed, with the characteristics listed below:

- TRIGA elements on rectangular 4×5 1.40-cm pitch.

- Flooded and dry HTGR fuel matrix.

- Interior (TRIGA package and cask cavity) moderator density at 0.9982 g/cm^3.

- Exterior moderator density at 0.9982 g/cm^3.

Results are shown in Table 6.4.8-1. Since the TRIGA fuel is the dominant contributor to the system reactivity, the TRIGA bias will be applied in order to calculate the bias-adjusted k_s. The bias is discussed in further detail in Section 6.4.8.8.

6.4.8.2   TRIGA Pitch/Array Evaluation

The combined payload model is used to evaluate the TRIGA element pitch in either a 'Rectangular' or 'Square' array as defined in Section 6.3.7. The HTGR FHU is modeled as dry in this configuration with the remaining cask void spaces flooded. Rectangular and square array results are shown in Table 6.4.8-2 and Table 6.4.8-3, respectively. In the rectangular array, the pitch is limited to 1.65 cm before interferences are created in the model. A larger pitch is possible in the square array, with a value of 1.73 cm allowed by the modeled geometry. The maximum reactivity is calculated for the square array with a pitch of 1.73 cm. Thus, the 1.73-cm pitch is employed in the optimum moderator density studies.

6.4.8.3   Interior Moderator Density Evaluation

The combined payload model is used to vary the interior moderator density with intact TRIGA elements in a square array on a 1.73-cm pitch. Based on the results shown in Table 6.4.8-4, a full density water package interior maximizes system reactivity at full density water exterior moderation.

6.4.8.4   HTGR Matrix Moderator Density Evaluation

The combined payload model is used to vary water density in the HTGR fuel matrix using the fully flooded TRIGA elements in a square array on a 1.73 cm pitch. Based on the results shown in Table 6.4.8-4, a water density of 1.0 g/cc for water homogenized with the HTGR fuel matrix maximizes system reactivity. Note that this configuration is conservative in that the HTGR fuel occupies part of the homogenized volume and full density water cannot occupy the same volume.

6.4.8.5   Exterior Moderator Density Evaluation

The combined payload model is used to vary the exterior moderator density with intact TRIGA elements in a square array on a 1.73 cm pitch. Interior moderator in the FHUs is set to full moderation as indicated by the evaluations in Sections 6.4.8.3 and 6.4.8.4. The cavity exterior to the FHUs is also flooded. Based on the results shown in Table 6.4.8-6, no significant change in system reactivity is obtained if the exterior moderator density varies below full density water. The maximum reactivity change of 2.9 $\Delta k/\sigma$ was obtained at an exterior water density of 0.0001 g/cc. This change, while outside the 2 $\Delta k/\sigma$ typical threshold for a significant change in reactivity, is less than 2.2×10^{-3} Δk and, therefore, not significant.

Note that the material description of the water neutron shield and the exterior moderator are identical in these evaluations addressing accident condition concerns (loss of neutron shield).

6.4.8.6   Partial Flooding Evaluation

During accident conditions, the loss of neutron shielding has the potential to increase neutronic interaction between casks in the infinite array. Significant amounts of moderator outside the FHUs, but in the flooded cask cavity, serves to isolate casks under the accident condition of loss of neutron shield. To investigate the potential impact of preferential flooding, an additional model is created. The model preferentially floods the RERTR and HTGR FHUs, with a separate interior moderator material filling the balance of the NAC-LWT cavity.

A full set of studies evaluating the reactivity changes associated with varying cavity interior, FHU, and exterior moderator densities is summarized in Table 6.4.8-7 through Table 6.4.8-11.

The studies indicate that the most reactive configuration is for flooding of the RERTR and HTGR enclosures (FHUs) with interior and exterior void (loss of neutron shield). This configuration produces the maximum reactivity FHUs, while maximizing interaction between the FHUs within the cask and between casks.

6.4.8.7   Single Cask Evaluation

The 10 CFR 71.55(b)(3) requires an evaluation of the NAC-LWT with the containment system fully reflected by water. The containment for the NAC-LWT is the cask inner shell. While no operating condition results in a removal of the cask outer shell and lead gamma shield, each of the partial flooding cases at four combinations of interior and exterior moderator is reevaluated by removing the lead and outer shells (including neutron shield), and reflecting the system by water at full density on the X and Y faces (the z faces are mirrored to yield an axially infinite model). The results of this analysis are shown in Table 6.4.8-12 and demonstrate that the system reactivity decreases with the removal of the lead, outer shell and neutron shield reflectors.

6.4.8.8   Damaged TRIGA Fuel Evaluation

The combined payload model with a homogenized TRIGA fuel description is used to evaluate the system reactivity in the event that both the intact and sectioned fuel elements become damaged. Models are executed by varying the volume fraction of water in the TRIGA fuel mixture from zero to unity. The maximum volume fraction is 0.6816 based on the FHU cavity volume (7140 cm^3) and the total volume of TRIGA elements (2,273 cm^3), which does not consider the volume of the aluminum tubing within the FHU primary enclosure.

Based on the results summarized in Table 6.4.8-13, homogenized TRIGA elements are more reactive than intact TRIGA elements. Evaluation results documented in Table 6.4.8-13 are based on infinite cask array models. A single cask evaluation of the maximum water volume fraction case yielded a k_{eff} of 0.38885 ± 0.00066.

6.4.8.9   Code Bias and Code Bias Uncertainty Adjustments

As shown in Section 6.4.8.1, the TRIGA elements in the RERTR enclosure are more reactive than the HTGR fuel matrix in its enclosure. Therefore, code bias and code uncertainty adjustments are based on the TRIGA fuel element criticality benchmarks in Section 6.1.1.

A calculation of k_s under normal and accident conditions can now be made based on the previous results and based on the KENO-Va validation statistics presented in Section 6.1.1. The value k_s is calculated based on the KENO-Va Monte Carlo average plus any biases and uncertainties associated with the methods and the modeling, i.e.:

$$k_s = k_{eff} + \Delta k_{Bias} + \Delta k_{BU} + 2\sigma_{MC} \leq 0.95$$

In the validation presented in Section 6.5.3, a negative bias (allowance for overprediction of k_{eff}) and a 95/95 method uncertainty of ± 0.0168 was determined. The negative bias correction is neglected. Thus, the equation for k_s becomes:

$$k_s = k_{eff} + 0.0168 + 2\sigma_{MC}$$

The k_s values for the relevant analysis are included in Table 6.4.8-1 through Table 6.4.8-13. The maximum k_s, 0.74015, for the GA IFM shipment results from an infinite height model with an infinite number of casks.

For both normal and accident conditions, the calculated k_{eff} values, after correction for uncertainty, are well below the 0.95 limit. The analyses demonstrate that, including all calculational and mechanical uncertainties, an infinite array of NAC-LWT casks with GA IFM remains subcritical under normal and accident conditions.

Table 6.4.8-1   GA IFM Payload Evaluation Result Summary

Payload	Cavity Moderator Density [g/cm³]	HTGR Moderator Density [g/cm³]	RERTR Moderator Density [g/cm³]	Exterior Moderator Density [g/cm³]	TRIGA Pitch [cm]	TRIGA Array	$k_{eff} \pm \sigma$
Combined	0.9882	0	0.9882	0.9882	1.40	Rectangular	0.44192±0.00073
RERTR	0.9882	0	0.9882	0.9882	1.40	Rectangular	0.42870±0.00080
HTGR	0.9882	0	0.9882	0.9882	N/A	N/A	0.06611±0.00020
HTGR	0.9882	0.9882	0.9882	0.9882	N/A	N/A	0.36907±0.00053

Table 6.4.8-2   GA IFM TRIGA Rectangular Array Pitch Evaluation Result Summary

Cavity (g/cc)	HTGR (g/cc)	RERTR (g/cc)	Exterior (g/cc)	TRIGA Pitch (cm)	TRIGA Array	k_{eff}	σ	k_s	$k_{eff}+2\sigma$	Δk	$\Delta k/\sigma$
1	0	1	1	1.40	Rectangular	0.44192	0.00073	0.46018	0.44338	0.00000	0.0
1	0	1	1	1.50	Rectangular	0.45796	0.00078	0.47632	0.45952	0.01614	20.7
1	0	1	1	1.60	Rectangular	0.47647	0.00080	0.49487	0.47807	0.03469	43.4
1	0	1	1	1.65	Rectangular	0.48529	0.00079	0.50367	0.48687	0.04349	55.1

Table 6.4.8-3   GA IFM TRIGA Square Array Pitch Evaluation Result Summary

Cavity (g/cc)	HTGR (g/cc)	RERTR (g/cc)	Exterior (g/cc)	TRIGA Pitch (cm)	TRIGA Array	k_{eff}	σ	k_s	$k_{eff}+2\sigma$	Δk	$\Delta k/\sigma$
1	0	1	1	1.40	Square	0.44618	0.00073	0.46444	0.44764	0.00000	0.0
1	0	1	1	1.50	Square	0.46343	0.00080	0.48183	0.46503	0.01739	21.7
1	0	1	1	1.60	Square	0.48072	0.00078	0.49908	0.48228	0.03464	44.4
1	0	1	1	1.65	Square	0.49026	0.00078	0.50862	0.49182	0.04418	56.6
1	0	1	1	1.70	Square	0.49727	0.00077	0.51561	0.49881	0.05117	66.5
1	0	1	1	1.73	Square	0.50289	0.00079	0.52127	0.50447	0.05683	71.9

Table 6.4.8-4   GA IFM Interior Moderator Density Evaluation Result Summary

Cavity (g/cc)	HTGR (g/cc)	RERTR (g/cc)	Exterior (g/cc)	TRIGA Pitch (cm)	TRIGA Array	k_{eff}	σ	k_s	$k_{eff}+2\sigma$	Δk	$\Delta k/\sigma$
1.00	0	1.00	1	1.73	Square	0.50289	0.00079	0.52127	0.50447	0.00000	0.0
0.95	0	0.95	1	1.73	Square	0.48897	0.00077	0.50731	0.49051	-0.01396	-18.1
0.90	0	0.90	1	1.73	Square	0.47787	0.00079	0.49625	0.47945	-0.02502	-31.7
0.85	0	0.85	1	1.73	Square	0.46611	0.00076	0.48443	0.46763	-0.03684	-48.5
0.80	0	0.80	1	1.73	Square	0.45420	0.00077	0.47254	0.45574	-0.04873	-63.3
0.75	0	0.75	1	1.73	Square	0.44289	0.00073	0.46115	0.44435	-0.06012	-82.4
0.70	0	0.70	1	1.73	Square	0.42888	0.00071	0.44710	0.43030	-0.07417	-104.5
0.65	0	0.65	1	1.73	Square	0.41568	0.00073	0.43394	0.41714	-0.08733	-119.6
0.60	0	0.60	1	1.73	Square	0.40369	0.00069	0.42187	0.40507	-0.09940	-144.1
0.55	0	0.55	1	1.73	Square	0.39298	0.00069	0.41116	0.39436	-0.11011	-159.6
0.50	0	0.50	1	1.73	Square	0.38075	0.00069	0.39893	0.38213	-0.12234	-177.3
0.45	0	0.45	1	1.73	Square	0.36922	0.00069	0.38740	0.37060	-0.13387	-194.0
0.40	0	0.40	1	1.73	Square	0.35645	0.00067	0.37459	0.35779	-0.14668	-218.9
0.35	0	0.35	1	1.73	Square	0.34396	0.00064	0.36204	0.34524	-0.15923	-248.8
0.30	0	0.30	1	1.73	Square	0.33007	0.00064	0.34815	0.33135	-0.17312	-270.5
0.25	0	0.25	1	1.73	Square	0.31618	0.00059	0.33416	0.31736	-0.18711	-317.1
0.20	0	0.20	1	1.73	Square	0.29802	0.00056	0.31594	0.29914	-0.20533	-366.7
0.15	0	0.15	1	1.73	Square	0.27758	0.00057	0.29552	0.27872	-0.22575	-396.1
0.10	0	0.10	1	1.73	Square	0.24971	0.00052	0.26755	0.25075	-0.25372	-487.9
0.05	0	0.05	1	1.73	Square	0.21145	0.00048	0.22921	0.21241	-0.29206	-608.5

Table 6.4.8-5 GA IFM HTGR Matrix Moderator Density Evaluation Result Summary

Cavity (g/cc)	HTGR (g/cc)	RERTR (g/cc)	Exterior (g/cc)	TRIGA Pitch (cm)	TRIGA Array	k_{eff}	σ	k_s	$k_{eff}+2\sigma$	Δk	$\Delta k/\sigma$
1	0.00	1	1	1.73	Square	0.50289	0.00079	0.52127	0.50447	0.00000	0.0
1	0.05	1	1	1.73	Square	0.50363	0.00076	0.52195	0.50515	0.00068	0.9
1	0.10	1	1	1.73	Square	0.50425	0.00079	0.52263	0.50583	0.00136	1.7
1	0.15	1	1	1.73	Square	0.50570	0.00076	0.52402	0.50722	0.00275	3.6
1	0.20	1	1	1.73	Square	0.50755	0.00077	0.52589	0.50909	0.00462	6.0
1	0.25	1	1	1.73	Square	0.50701	0.00078	0.52537	0.50857	0.00410	5.3
1	0.30	1	1	1.73	Square	0.50888	0.00079	0.52726	0.51046	0.00599	7.6
1	0.35	1	1	1.73	Square	0.50994	0.00079	0.52832	0.51152	0.00705	8.9
1	0.40	1	1	1.73	Square	0.51168	0.00079	0.53006	0.51326	0.00879	11.1
1	0.45	1	1	1.73	Square	0.51327	0.00079	0.53165	0.51485	0.01038	13.1
1	0.50	1	1	1.73	Square	0.51492	0.00078	0.53328	0.51648	0.01201	15.4
1	0.55	1	1	1.73	Square	0.51524	0.00080	0.53364	0.51684	0.01237	15.5
1	0.60	1	1	1.73	Square	0.51628	0.00078	0.53464	0.51784	0.01337	17.1
1	0.65	1	1	1.73	Square	0.51911	0.00077	0.53745	0.52065	0.01618	21.0
1	0.70	1	1	1.73	Square	0.52034	0.00076	0.53866	0.52186	0.01739	22.9
1	0.75	1	1	1.73	Square	0.52100	0.00074	0.53928	0.52248	0.01801	24.3
1	0.80	1	1	1.73	Square	0.52193	0.00076	0.54025	0.52345	0.01898	25.0
1	0.85	1	1	1.73	Square	0.52120	0.00075	0.53950	0.52270	0.01823	24.3
1	0.90	1	1	1.73	Square	0.52407	0.00074	0.54235	0.52555	0.02108	28.5
1	0.95	1	1	1.73	Square	0.52482	0.00076	0.54314	0.52634	0.02187	28.8
1	1.00	1	1	1.73	Square	0.52764	0.00070	0.54584	0.52904	0.02457	35.1

Table 6.4.8-6   GA IFM Exterior Moderator Density Evaluation Result Summary

Cavity (g/cc)	HTGR (g/cc)	RERTR (g/cc)	Exterior (g/cc)	TRIGA Pitch (cm)	TRIGA Array	k_{eff}	σ	k_s	$k_{eff}+2σ$	Δk	Δk/σ
1	1	1	1.00	1.73	Square	0.52764	0.00070	0.54584	0.52904	0.00000	0.0
1	1	1	0.95	1.73	Square	0.52634	0.00073	0.54460	0.52780	-0.00124	-1.7
1	1	1	0.90	1.73	Square	0.52787	0.00077	0.54621	0.52941	0.00037	0.5
1	1	1	0.85	1.73	Square	0.52539	0.00073	0.54365	0.52685	-0.00219	-3.0
1	1	1	0.80	1.73	Square	0.52733	0.00075	0.54563	0.52883	-0.00021	-0.3
1	1	1	0.75	1.73	Square	0.52921	0.00079	0.54759	0.53079	0.00175	2.2
1	1	1	0.70	1.73	Square	0.52632	0.00071	0.54454	0.52774	-0.00130	-1.8
1	1	1	0.65	1.73	Square	0.52551	0.00073	0.54377	0.52697	-0.00207	-2.8
1	1	1	0.60	1.73	Square	0.52695	0.00079	0.54533	0.52853	-0.00051	-0.6
1	1	1	0.55	1.73	Square	0.52712	0.00078	0.54548	0.52868	-0.00036	-0.5
1	1	1	0.50	1.73	Square	0.52612	0.00077	0.54446	0.52766	-0.00138	-1.8
1	1	1	0.45	1.73	Square	0.52584	0.00076	0.54416	0.52736	-0.00168	-2.2
1	1	1	0.40	1.73	Square	0.52669	0.00076	0.54501	0.52821	-0.00083	-1.1
1	1	1	0.35	1.73	Square	0.52661	0.00076	0.54493	0.52813	-0.00091	-1.2
1	1	1	0.30	1.73	Square	0.52735	0.00078	0.54571	0.52891	-0.00013	-0.2
1	1	1	0.25	1.73	Square	0.52644	0.00076	0.54476	0.52796	-0.00108	-1.4
1	1	1	0.20	1.73	Square	0.52775	0.00080	0.54615	0.52935	0.00031	0.4
1	1	1	0.15	1.73	Square	0.52812	0.00075	0.54642	0.52962	0.00058	0.8
1	1	1	0.10	1.73	Square	0.52904	0.00073	0.54730	0.53050	0.00146	2.0
1	1	1	0.05	1.73	Square	0.52655	0.00072	0.54479	0.52799	-0.00105	-1.5
1	1	1	0.00	1.73	Square	0.52970	0.00073	0.54796	0.53116	0.00212	2.9

Table 6.4.8-7   GA IFM Partial Flooding Comparison Result Summary

Cavity (g/cc)	HTGR (g/cc)	RERTR (g/cc)	Exterior (g/cc)	TRIGA Pitch (cm)	TRIGA Array	k_{eff}	σ	k_s	$k_{eff}+2\sigma$	Δk	$\Delta k/\sigma$
0	1	0	0	1.73	Square	0.57362	0.00054	0.59150	0.57470	0.00000	0.0
0	1	1	0	1.73	Square	0.70197	0.00076	0.72029	0.70349	0.12879	169.5

Table 6.4.8-8   GA IFM Partial Flooding Interior Moderator Density, Void Exterior Result Summary

Cavity (g/cc)	HTGR (g/cc)	RERTR (g/cc)	Exterior (g/cc)	TRIGA Pitch (cm)	TRIGA Array	k_{eff}	σ	k_s	$k_{eff}+2\sigma$	Δk	$\Delta k/\sigma$
0.0	1	1	0	1.73	Square	0.70197	0.00076	0.72029	0.70349	0.00000	0.0
0.1	1	1	0	1.73	Square	0.63582	0.00076	0.65414	0.63734	-0.06615	-87.0
0.2	1	1	0	1.73	Square	0.59419	0.00074	0.61247	0.59567	-0.10782	-145.7
0.3	1	1	0	1.73	Square	0.57060	0.00078	0.58896	0.57216	-0.13133	-168.4
0.4	1	1	0	1.73	Square	0.55551	0.00073	0.57377	0.55697	-0.14652	-200.7
0.5	1	1	0	1.73	Square	0.54367	0.00074	0.56195	0.54515	-0.15834	-214.0
0.6	1	1	0	1.73	Square	0.53824	0.00074	0.55652	0.53972	-0.16377	-221.3
0.7	1	1	0	1.73	Square	0.53478	0.00075	0.55308	0.53628	-0.16721	-222.9
0.8	1	1	0	1.73	Square	0.53243	0.00074	0.55071	0.53391	-0.16958	-229.2
0.9	1	1	0	1.73	Square	0.53192	0.00075	0.55022	0.53342	-0.17007	-226.8
1.0	1	1	0	1.73	Square	0.52970	0.00073	0.54796	0.53116	-0.17233	-236.1

Table 6.4.8-9   GA IFM Partial Flooding Interior Moderator Density, Water Exterior Result Summary

Cavity (g/cc)	HTGR (g/cc)	RERTR (g/cc)	Exterior (g/cc)	TRIGA Pitch (cm)	TRIGA Array	k_{eff}	σ	k_s	$k_{eff}+2\sigma$	Δk	$\Delta k/\sigma$
0.0	1	1	1	1.73	Square	0.55598	0.00074	0.57426	0.55746	0.00000	0.0
0.1	1	1	1	1.73	Square	0.54649	0.00073	0.56475	0.54795	-0.00951	-13.0
0.2	1	1	1	1.73	Square	0.53804	0.00075	0.55634	0.53954	-0.01792	-23.9
0.3	1	1	1	1.73	Square	0.53458	0.00073	0.55284	0.53604	-0.02142	-29.3
0.4	1	1	1	1.73	Square	0.52971	0.00076	0.54803	0.53123	-0.02623	-34.5
0.5	1	1	1	1.73	Square	0.52610	0.00074	0.54438	0.52758	-0.02988	-40.4
0.6	1	1	1	1.73	Square	0.52725	0.00075	0.54555	0.52875	-0.02871	-38.3
0.7	1	1	1	1.73	Square	0.52668	0.00071	0.54490	0.52810	-0.02936	-41.4
0.8	1	1	1	1.73	Square	0.52630	0.00077	0.54464	0.52784	-0.02962	-38.5
0.9	1	1	1	1.73	Square	0.52711	0.00074	0.54539	0.52859	-0.02887	-39.0
1.0	1	1	1	1.73	Square	0.52764	0.00070	0.54584	0.52904	-0.02842	-40.6

Table 6.4.8-10   GA IFM Partial Flooding Exterior Moderator Density, Void Interior Result Summary

Cavity (g/cc)	HTGR (g/cc)	RERTR (g/cc)	Exterior (g/cc)	TRIGA Pitch (cm)	TRIGA Array	k_{eff}	σ	k_s	$k_{eff}+2\sigma$	Δk	$\Delta k/\sigma$
0	1	1	0.0	1.73	Square	0.70197	0.00076	0.72029	0.70349	0.00000	0.0
0	1	1	0.1	1.73	Square	0.56743	0.00075	0.58573	0.56893	-0.13456	-179.4
0	1	1	0.2	1.73	Square	0.55761	0.00075	0.57591	0.55911	-0.14438	-192.5
0	1	1	0.3	1.73	Square	0.55699	0.00076	0.57531	0.55851	-0.14498	-190.8
0	1	1	0.4	1.73	Square	0.55603	0.00072	0.57427	0.55747	-0.14602	-202.8
0	1	1	0.5	1.73	Square	0.55553	0.00071	0.57375	0.55695	-0.14654	-206.4
0	1	1	0.6	1.73	Square	0.55550	0.00073	0.57376	0.55696	-0.14653	-200.7
0	1	1	0.7	1.73	Square	0.55648	0.00075	0.57478	0.55798	-0.14551	-194.0
0	1	1	0.8	1.73	Square	0.55610	0.00075	0.57440	0.55760	-0.14589	-194.5
0	1	1	0.9	1.73	Square	0.55524	0.00075	0.57354	0.55674	-0.14675	-195.7
0	1	1	1.0	1.73	Square	0.55598	0.00074	0.57426	0.55746	-0.14603	-197.3

Table 6.4.8-11   GA IFM Partial Flooding Exterior Moderator Density, Water Interior Result Summary

Cavity (g/cc)	HTGR (g/cc)	RERTR (g/cc)	Exterior (g/cc)	TRIGA Pitch (cm)	TRIGA Array	k_{eff}	σ	k_s	$k_{eff}+2\sigma$	Δk	$\Delta k/\sigma$
1	1	1	0.0	1.73	Square	0.52970	0.00073	0.54796	0.53116	0.00000	0.0
1	1	1	0.1	1.73	Square	0.52904	0.00073	0.54730	0.53050	-0.00066	-0.9
1	1	1	0.2	1.73	Square	0.52775	0.00080	0.54615	0.52935	-0.00181	-2.3
1	1	1	0.3	1.73	Square	0.52735	0.00078	0.54571	0.52891	-0.00225	-2.9
1	1	1	0.4	1.73	Square	0.52669	0.00076	0.54501	0.52821	-0.00295	-3.9
1	1	1	0.5	1.73	Square	0.52612	0.00077	0.54446	0.52766	-0.00350	-4.5
1	1	1	0.6	1.73	Square	0.52695	0.00079	0.54533	0.52853	-0.00263	-3.3
1	1	1	0.7	1.73	Square	0.52632	0.00071	0.54454	0.52774	-0.00342	-4.8
1	1	1	0.8	1.73	Square	0.52733	0.00075	0.54563	0.52883	-0.00233	-3.1
1	1	1	0.9	1.73	Square	0.52787	0.00077	0.54621	0.52941	-0.00175	-2.3
1	1	1	1.0	1.73	Square	0.52764	0.00070	0.54584	0.52904	-0.00212	-3.0

Table 6.4.8-12   GA IFM Partial Flooding Single Cask Result Comparison

Cavity (g/cc)	HTGR (g/cc)	RERTR (g/cc)	Exterior (g/cc)	TRIGA Pitch (cm)	TRIGA Array	k_{eff}	σ	k_s	$k_{eff}+2\sigma$	Δk	$\Delta k/\sigma$
0	1	1	0	1.73	Square	0.70197	0.00076	0.72029	0.70349	0.00000	0.0
0	1	1	0	1.73	Square	0.42657	0.00066	0.44469	0.42789	-0.27560	-417.6
1	1	1	0	1.73	Square	0.52970	0.00073	0.54796	0.53116	0.00000	0.0
1	1	1	0	1.73	Square	0.52108	0.00074	0.53936	0.52256	-0.00860	-11.6
0	1	1	1	1.73	Square	0.55598	0.00074	0.57426	0.55746	0.00000	0.0
0	1	1	1	1.73	Square	0.45370	0.00074	0.47198	0.45518	-0.10228	-138.2
1	1	1	1	1.73	Square	0.52764	0.00070	0.54584	0.52904	0.00000	0.0
1	1	1	1	1.73	Square	0.52056	0.00076	0.53888	0.52208	-0.00696	-9.2

Table 6.4.8-13   GA IFM Damaged TRIGA Fuel Result Summary

Cavity (g/cc)	HTGR (g/cc)	Exterior (g/cc)	TRIGA Config.	TRIGA H$_2$O (g/cc)	k$_{eff}$	σ	k$_s$	k$_{eff}$+2σ	Δk	Δk/σ
0	1	0	Homog.	0.0001	0.53943	0.00055	0.55733	0.54053	-0.18282	-332.4
0	1	0	Homog.	0.1000	0.55711	0.00055	0.57501	0.55821	-0.16514	-300.3
0	1	0	Homog.	0.2000	0.57987	0.00054	0.59775	0.58095	-0.14240	-263.7
0	1	0	Homog.	0.3000	0.60672	0.00062	0.62476	0.60796	-0.11539	-186.1
0	1	0	Homog.	0.4000	0.63609	0.00062	0.65413	0.63733	-0.08602	-138.7
0	1	0	Homog.	0.5000	0.66661	0.00064	0.68469	0.66789	-0.05546	-86.7
0	1	0	Homog.	0.6000	0.69621	0.00067	0.71435	0.69755	-0.02580	-38.5
0	1	0	Homog.	0.6816	0.72199	0.00068	0.74015	0.72335	0.00000	0.0
0	1	0	Homog.	0.7000	0.72738	0.00069	0.74556	0.72876	0.00541	7.8
0	1	0	Homog.	0.8000	0.75724	0.00070	0.77544	0.75864	0.03529	50.4
0	1	0	Homog.	0.9000	0.78650	0.00071	0.80472	0.78792	0.06457	90.9
0	1	0	Homog.	1.0000	0.81239	0.00073	0.83065	0.81385	0.09050	124.0

6.4.9   PULSTAR Fuel Contents

This section presents the criticality analyses for the NAC-LWT cask with PULSTAR fuel contents. Criticality analyses are performed to satisfy the criticality safety requirements of 10 CFR Parts 71.55 and 71.59, as well as IAEA TS-R-1. All criticality evaluations performed herein use an axially finite cask model. An analysis of the NAC-LWT with each of the four postulated basket loadings shows that damaged PULSTAR fuel elements in a can are most reactive.

The maximum reactivity is based on the following model characteristics.

- 14 cans (25 elements per can) in the top and base modules
- 14 intact assemblies in the two intermediate modules
- Flooded cans
- Void cask cavity and exterior
- Loss of neutron shield

A single cask evaluation is also performed to comply with 10 CFR 71.55(b)(3). The analyses demonstrate that, including all calculational and mechanical uncertainties, the NAC-LWT remains subcritical under normal and accident conditions.

6.4.9.1   Intact Assembly Payload

An intact PULSTAR fuel assembly is placed in each of the 28 cells in the 28 MTR basket assembly. Results of the mechanical perturbation, axial and radial shift are shown in Table 6.4.9-1 through Table 6.4.9-3. Optimum moderator studies for the cask are shown in Figure 6.4.9-2. All intact fuel assembly runs are based on an infinite cask array model.

From a base model, which has the PULSTAR fuel assemblies centered in the module cell and touching the module base plates, various component shift and module plate thickness combinations are evaluated. Assembly shift results, shown in Table 6.4.9-1, indicate that a basket assembly with PULSTAR fuel assemblies in the "Xlong" alignment and axially alternated represents the most reactive scenario for intact fuel assemblies. The "modified" Ylong configuration represents a mix of rotations and is shown in Figure 6.4.9-1. Considering assembly shifts the maximum k_{eff} is 0.80517 ± 0.00083.

Mechanical perturbation results from a study of plate thickness and cell opening size are shown in Table 6.4.9-2. This study indicates that a maximum module cell width produces a slight increase in reactivity for a maximum k_{eff} of 0.80929 ± 0.00084.

Previous evaluations documented in this section are based on a flooded pellet to clad gap and fuel parameters producing the maximum lattice H/U ratio. Minimum H/U ratio and dry gap

cases are run to verify that the lattice is under moderated and that appropriate fuel parameters were chosen for the base analysis. The results of this analysis are listed in Table 6.4.9-3 and clearly demonstrate that the element lattice is under moderated and that the flooded pellet to clad gap and maximum H/U lattice model options are conservative for the analysis.

Graphical results of the optimum moderator density studies are shown in Figure 6.4.9-2. This study further confirms that the assembly is under moderated and that maximum system reactivity is obtained from a flooded cask cavity with a dry cask exterior and neutron shield.

The CSI for intact fuel assemblies is 0 as an infinite array of cask is modeled and maximum reactivity is well below the 0.95 licensing limit.

6.4.9.2   Intact Elements – Fuel Rod Insert

A single KENO-Va case is executed to demonstrate that a payload of 448 PULSTAR fuel elements (16 elements per 4×4 insert; 28 MTR basket cells) is significantly less reactive than the assembly model containing 28 intact assemblies (700 elements).

For a model with the insert radially centered within the cell, alternating axial shifting, full density water in the cavity, and a void exterior, the calculated k_{eff} is 0.70076 ± 0.00079. This reactivity is substantially lower than that of the intact assemblies. Therefore no further analysis is performed with the rod insert configuration.

6.4.9.3   Canned Elements

Intact or damaged (failed) PULSTAR fuel elements and nonfuel components of fuel assemblies may be placed into either of the PULSTAR cans. Each configuration is individually evaluated.

Intact Fuel Elements

Intact fuel element models place 25 rods into the can in a 0.66-inch square pitch. This pitch is the maximum allowed by the modeled can cavity width and is conservative as the elements were significantly under moderated at their smaller "in assembly" pitch. A can is placed into each of the 28 MTR basket assembly cells in an alternate axial shift configuration with the cask and canister cavity flooded. The alternate shift configuration was determined to be most reactive in the intact assembly analysis. For an infinite array of casks under accident condition (void exterior and neutron shield) a k_{eff} of 0.89919 ± 0.00083 is calculated. Results in Table 6.4.9-4 indicate that the preferential flooding of the canister cavity with a void cask cavity for the same physical configuration results in k_{eff} of 0.98516 ± 0.00076. Additional evaluations and limitations, are therefore, required to document an acceptable system configuration. KENO models with cans restricted to the top and base modules and intact fuel assemblies in the remaining two modules reduces system reactivity significantly as documented in Table 6.4.9-4.

Without the neutron shield (accident conditions) there is substantial neutronic coupling between casks in an array and limiting the number of casks produces a significant additional reactivity reduction. For the mixed loaded three-cask array, the calculated k_{eff} is 0.84910 ± 0.00079. A limit of a three-cask array produces a CSI of 33.4 under the accident conditions modeled. System reactivity for a normal condition infinite array of casks loaded with damaged fuel cans is low, $k_{eff} < 0.2$. The normal condition based CSI is therefore 0.

Damaged (Failed) Elements

Damaged elements are modeled as a homogenized fuel and water mixture within the can cavity. Analysis trends for the homogenized contents are similar to those for the intact elements in a can. Bias and uncertainty adjusted system reactivity of the damaged fuel elements is higher than allowed for a full cask load (28 cans), but restricting the cask array under accident condition to three casks and limiting each cask's contents to 14 damaged fuel cans, seven in each of the top and base basket modules, and intact fuel assemblies or rod holders in the intermediate basket modules, produces acceptable reactivities as shown in Table 6.4.9-5. For the 3-cask array, the maximum calculated k_{eff} is 0.86961 ± 0.00081.

6.4.9.4 Single Cask Evaluation

The 10 CFR 71.55(b)(3) requires an evaluation of the NAC-LWT with the containment system fully reflected by water. The containment for the NAC-LWT is the cask inner shell. While no operating condition results in a removal of the cask outer shell and lead gamma shield, each of the partial flooding cases at four combinations of interior and exterior moderator is reevaluated by removing the lead and outer shells (including neutron shield), and reflecting the system by water at full density on the X, Y, and Z faces. Using the maximum reactivity model from Section 6.4.9.3, the calculated k_{eff} is 0.72674 ± 0.00087.

6.4.9.5 Code Bias and Code Bias Uncertainty Adjustments

PULSTAR fuel elements are similar to LWR fuel rods with a shorter active fuel length and smaller assembly array. While the enrichment for PULSTAR fuel is outside the enrichment range validated for LWR fuel, Figure 6.5.1-2 shows no statistical trend in k_{eff} versus enrichment. Further, any trend that may be postulated from the criticality benchmarks indicates a higher predicted k_{eff} value at higher enrichments. Therefore, code bias and code uncertainty adjustments are based on the LWR fuel assembly criticality benchmarks in Section 6.5.1.

A calculation of k_s under normal and accident conditions can now be made based on the previous results and based on the KENO-Va validation statistics presented in Section 6.5.1. The value k_s is calculated based on the KENO-Va Monte Carlo average plus any biases and uncertainties associated with the methods and the modeling, i.e.:

$$k_s = k_{eff} + \Delta k_{Bias} + \Delta k_{BU} + 2\sigma_{MC} \leq 0.95$$

In the validation presented in Section 6.5.1, a bias of ± 0.0052 and a 95/95 method uncertainty of ± 0.0087 were determined. Thus, the equation for k_s becomes as follows.

$$k_s = k_{eff} + 0.0139 + 2\sigma_{MC}$$

The k_s values for each evaluated payload are summarized in Table 6.4.9-6. The maximum k_s, 0.88513, results from a mixed loading of intact assemblies and canned elements.

For both normal and accident conditions, the calculated k_{eff} values, after correction for uncertainty, are well below the 0.95 limit. The analyses demonstrate that, including all calculational and mechanical uncertainties, an array of NAC-LWT casks with PULSTAR fuel remains subcritical under normal and accident conditions.

6.4.9.6   Allowable Cask Loading

Based on the results of the previous sections, the following cask loadings are permissible. For intact elements, any combination of assemblies and 4×4 rod inserts may be loaded into any module cell. Up to 14 damaged fuel cans each containing up to 25 PULSTAR fuel elements may be loaded in the top and base modules only; module cells loaded without cans may contain any combination of intact assemblies or 4×4 rod inserts. Each can is allowed the equivalent fissile material content of 25 fuel elements in either intact or damaged (failed) form. Damaged fuel may include fuel debris.

Figure 6.4.9-1   PICTURE Schematic of Modified PULSTAR Fuel Assembly Alignment
Configuration
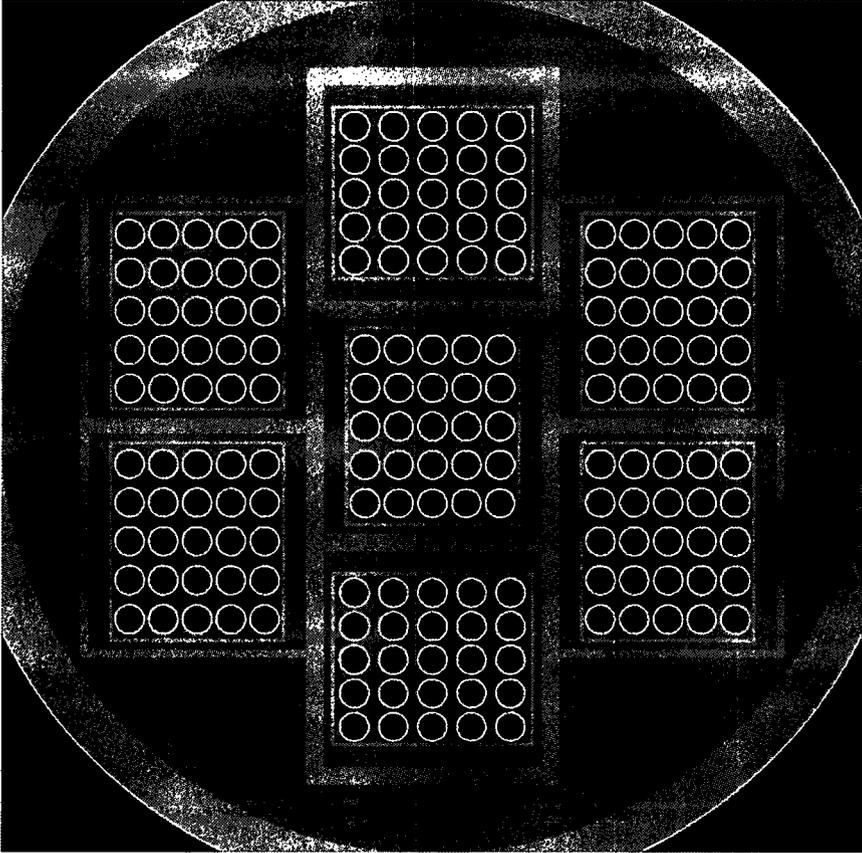
Figure 6.4.9-2   PULSTAR Intact Assembly Model Moderator Density Study Graphical Results
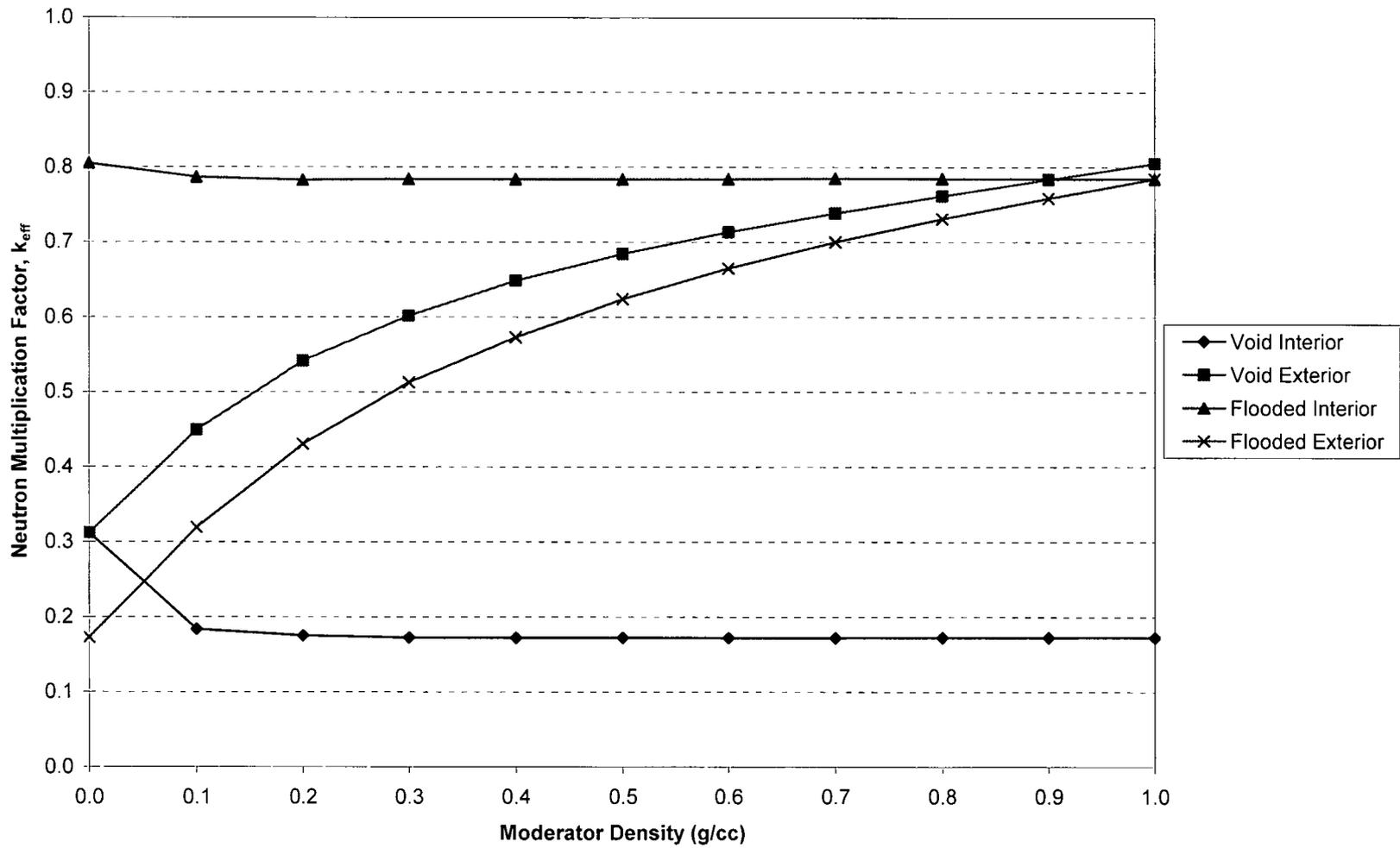
Table 6.4.9-1   PULSTAR Intact Assembly Shift Results

Alignment	Radial Shift	Axial Shift	k_{eff}	σ	$k_{eff}+2\sigma$	Δk	$\Delta k/\sigma$
Ylong	Centered	Centered	0.78916	0.00081	0.79078	--	--
Ylong	In	Centered	0.77268	0.00085	0.77438	-0.01648	-14.0
Ylong	Out	Centered	0.78773	0.00081	0.78935	-0.00143	-1.2
Xlong	Centered	Centered	0.79134	0.00083	0.79300	--	--
Xlong	In	Centered	0.77006	0.00080	0.77166	-0.02128	-18.5
Xlong	Out	Centered	0.78979	0.00080	0.79139	-0.00155	-1.3
Ylong	Centered	Alternating	0.80182	0.00084	0.80350	--	--
Ylong	In	Alternating	0.78767	0.00081	0.78929	-0.01415	-12.1
Ylong	Out	Alternating	0.80176	0.00081	0.80338	-0.00006	-0.1
Xlong	Centered	Alternating	0.80517	0.00083	0.80683	--	--
Xlong	In	Alternating	0.77968	0.00083	0.78134	-0.02549	-21.7
Xlong	Out	Alternating	0.80522	0.00080	0.80682	0.00005	0.0
Mod. Ylong	Centered	Alternating	0.80348	0.00087	0.80522	--	--
Mod. Ylong	In	Alternating	0.78247	0.00082	0.78411	-0.02101	-17.6
Mod. Ylong	Out	Alternating	0.80427	0.00081	0.80589	0.00079	0.7

Table 6.4.9-2   PULSTAR Intact Assembly Mechanical Perturbation Results

Alignment	Radial Shift	Axial Shift	Basket Cell Opening	Basket Plate Thickness	k_{eff}	σ	$k_{eff}+2\sigma$	Δk	$\Delta k/\sigma$
Xlong	Centered	Alternating	Min	Min	0.80517	0.00083	0.80683	--	--
Xlong	Centered	Alternating	Nominal	Nominal	0.80202	0.00084	0.80370	-0.00315	-2.7
Xlong	Centered	Alternating	Max	Max	0.78640	0.00081	0.78802	-0.01877	-16.2
Xlong	Centered	Alternating	Max	Min	0.80929	0.00084	0.81097	--	--
Xlong	In	Alternating	Max	Min	0.78826	0.00082	0.78990	-0.01691	-14.5
Xlong	Out	Alternating	Max	Min	0.80056	0.00081	0.80218	-0.00461	-4.0

Table 6.4.9-3   PULSTAR Intact Assembly Lattice Moderator Ratio Results

Alignment	Radial Shift	Axial Shift	Basket	Lattice H/U Ratio	Pellet to Clad Gap (g/cc)	Interior (g/cc)	Exterior (g/cc)	k_{eff}	σ	$k_{eff}+2\sigma$	Δk	$\Delta k/\sigma$
Xlong	Centered	Alternating	Min	Max	1	1	0	0.80517	0.00083	0.80683	--	--
Xlong	Centered	Alternating	Min	Max	1	1	0	0.79497	0.00080	0.79657	-0.01020	-8.8
Xlong	Centered	Alternating	Min	Max	1	1	0	0.80517	0.00083	0.80683	--	--
Xlong	Centered	Alternating	Min	Min	0	1	0	0.79541	0.00080	0.79701	-0.00976	-8.5

Table 6.4.9-4   PULSTAR Canned Intact Element Results

Cask Array	# Cans per Cask	Assembly Alignment	Interior (g/cc)	Exterior (g/cc)	Can (g/cc)	k_{eff}	σ	$k_{eff}+2\sigma$	Δk	$\Delta k/\sigma$
Infinite	28	--	1	0	1	0.89919	0.00083	0.90085	--	--
Infinite	28	--	0	0	1	0.98516	0.00076	0.98668	0.08597	76.4
Infinite	28	--	1	0	0	0.52383	0.00066	0.52515	-0.46133	-458.3
Infinite	14	Xlong	0	0	1	0.92654	0.00079	0.92812	--	--
Single	14	Xlong	0	0	1	0.84286	0.00083	0.84452	-0.08368	-73.0
3 Casks	14	Xlong	0	0	1	0.84910	0.00079	0.85068	-0.07744	-69.3
Infinite; Water Neutron Shield	14	Xlong	0	0	0	0.17042	0.00023	0.17088	-0.75612	-919.0

Table 6.4.9-5   PULSTAR Canned Homogenized Element Results

Cask Array	# Cans per Cask	Assembly Alignment	Interior (g/cc)	Exterior (g/cc)	Can (g/cc)	k$_{eff}$	σ	k$_{eff}$+2σ	Δk	Δk/σ
Infinite	28	--	1	0	1	0.92819	0.00079	0.92977	--	--
Infinite	28	--	0	0	1	1.01473	0.00075	1.01623	0.08654	79.4
Infinite	28	--	1	0	0	0.52684	0.00067	0.52818	-0.48789	-485.1
Infinite	14	Xlong	0	0	1	0.94917	0.00074	0.95065	--	--
Single	14	Xlong	0	0	1	0.86031	0.00081	0.86193	-0.08886	-81.0
3 Casks	14	Xlong	0	0	1	0.86961	0.00081	0.87123	-0.07956	-72.5
Infinite; Water Neutron Shield	14	Xlong	0	0	0	0.16471	0.00023	0.16517	-0.78446	-1012.3

Table 6.4.9-6   PULSTAR Maximum Reactivity Summary

Configuration	Cask Array	k$_{eff}$ + 2σ	k$_s$	CSI
28 Intact Assemblies	Infinite	0.81097	0.82487	0
28 16-Element Fuel Rod Inserts	Infinite	0.70234	0.71624	0
14 Intact Assemblies & 14 Cans w/Intact Elements	3	0.85068	0.86458	33.4
14 Intact Assemblies & 14 Cans w/Homogenized Elements	3	0.87123	0.88513	33.4

6.4.10   ANSTO Basket Payloads

This section presents the criticality analyses for the NAC-LWT cask with the spiral fuel assemblies and MOATA plate bundles in the ANSTO basket configuration. This evaluation meets the criticality safety requirements of 10 CFR Parts 71.55 and 71.59, as well as IAEA Transportation Safety Standards (TS-R-1). In this analysis, the bounding assembly characteristics are determined and infinite arrays of NAC-LWT casks are studied to determine bounding basket configurations for criticality under normal and accident conditions. Moderator density in the cavity, neutron shield tank and outside is varied to determine the maximum k_{eff}. The analyses demonstrate that, including all calculational and mechanical uncertainties, the NAC-LWT remains subcritical under normal and accident conditions for spiral fuel assemblies and MOATA plate bundles in the ANSTO basket configuration.

6.4.10.1   Spiral Fuel Assemblies

Initial evaluations document the reactivity of the fuel assembly in a nominal configuration basket. The cask model is set to accident conditions with neutron shield and cask exterior material voided. This base model is then modified to evaluate basket configuration and fuel material changes individually or in combination. For all evaluations, the ^{235}U enrichment percentage is set to its maximum value, as increased ^{235}U weight percent minimizes parasitic absorption in ^{238}U.

Reactivity results for the mechanical perturbation studies of the system and tolerances applied to the fuel material definition are included in Table 6.4.10-1. Manufacturing tolerance studies of the basket are listed in Table 6.4.10-2. Basket tolerance studies, as well as fuel studies shown later, rely on a base model containing maximum tolerance fissile material mass and uranium weight percent in the fuel meat.

The majority of evaluations presented in this section are based on a volume-conserving model with three fuel rings. This model requires a significant decrease in core thickness to conserve fuel meat volume, with only a minimal change to the plate thickness. As shown in Table 6.4.10-1, the model based on the original fuel plate dimension has a slightly higher reactivity. The increased reactivity in the plate-based model is the result of a smaller clad thickness than the one applied to the volume-conserving model. Evaluations performed later in this section reduce the clad to a minimum (0.01 cm) and, therefore, bound the as-manufactured plate configuration. Further calculations are, therefore, all based on a volume-conserving base model.

Maximum reactivity material, basket tolerances, and mechanical perturbation configurations are listed in the following bullets:

- Radial shift in – close approach active fuel

  There is no statistically significant difference between a shifted middle fuel element and a centered middle fuel element. The centered middle fuel element is chosen to continue the remaining evaluations.

- Axial alternating shift – close approach active fuel

- Maximum ^{235}U mass and maximum uranium weight percentage

  Within the range of uranium weight percentages evaluated, there is no effect on system reactivity. As documented in the MTR evaluation set, a large increase in uranium percentage (well beyond reasonable manufacturing limits) will increase reactivity. Therefore, maximum uranium percentage is retained for the remaining reactivity evaluations.

- Minimum fuel tube thickness

  For the tube specified, minimum tube thickness equals nominal thickness (tolerance is defined as -0%, +22%).

- No significant effect associated with other basket tolerances

  As reduced basket bottom plate and tube height removes absorber material from the system, the remaining reactivity evaluations set these variables to minimum.
  Fuel tube OD is set to maximum as it shows a slight, if not significant, reactivity increase. Increasing tube OD trades off raised moderation against increased absorber in the larger tube.

Next, fuel assembly dimensional effects are evaluated. The results of the fuel tolerance studies are documented in Table 6.4.10-3. The maximum system reactivity fuel configuration is itemized in the following bullets.

- Minimum plate thickness – increases moderator available between inner and outer assembly sleeves

- Minimum clad thickness

  Maximum reactivity obtained from a case where clad thickness is conservatively set to a minimum of 0.01 cm.

- Minimum active fuel height – reduces the space between fissile material in the alternating shifted model

- Minimum element height – reduces the space between fissile material in the alternating shifted model

  Set to active fuel height to remove variable as a potential licensing limit.

- Minimum sleeve (shell dimensions) – conservatively set to 0.01 cm thick

  Provides additional moderation in the system.

- Maximum plate pitch

  Plates were modeled as a set of three cylinders at various pitches. Maximum reactivity is obtained from a system with the middle cylinder centered between inner and outer aluminum assembly shells (sleeves) and the remaining cylinders pushed away from the center. This significantly increases the pitch between fuel materials above the 10 plate as-built assembly. Inner and outer sleeve (shell) dimensions were

conservatively set to a thickness of 0.01 cm. This was done to increase volume inside the annular region, maximizing the volume available for fuel and moderator.

Cask interior and exterior moderator density variation studies are included in Table 6.4.10-4. Moderator density variations are performed on the most-reactive basket and cask configuration under the accident condition (i.e., loss of neutron shield integrity). These studies demonstrate that for a fully moderated cask interior, any increase in cask exterior moderator density reduces reactivity by decoupling the casks in the array. This data is consistent with the lower reactivity obtained from the normal condition case, where the cask water neutron shield isolates casks in the infinite array. The reactivity curve for modified interior density demonstrates that within the statistical uncertainty of the evaluation, a fully moderated cask interior represents a bounding condition. No significant variations in reactivity occur for moderator densities above 0.9 g/cm^3. A plot of the interior density study is shown in Figure 6.4.10-1.

Results for a nominal condition infinite cask array, worst-case configuration accident condition (voided neutron shield) and normal conditions of operations (filled neutron shield) arrays, and for a single cask with a fully reflected containment boundary are included in Table 6.4.10-5. Maximum bias adjusted system reactivity is 0.746, well below the 0.95 safety limit for the system. As an infinite array of casks is subcritical under both normal and accident conditions, the criticality safety index (CSI) is 0.

The reactivity evaluation of the NAC-LWT cask containing up to 42 spiral fuel assemblies (elements), demonstrates that subcritical margin ($k_s \leq 0.95$) can be maintained under the following conditions:

Parameter	Value
Number of Fuel Plates	10
Plate Thickness	≥ 0.124 cm
Active Fuel Height	≥ 59.075 cm
^{235}U Content per Element	≤ 160
Enrichment wt % ^{235}U	≤ 95[1]

---

[1]　Section 6.4.10 is based on a maximum 85 wt % ^{235}U evaluation. The maximum 95 wt % ^{235}U content is justified in Section 6.4.11.6 for both ANSTO and combined basket configurations.

6.4.10.2   MOATA Plate Bundles

Initial evaluations document the reactivity of the plate bundle in a nominal configuration basket. The cask model is set to accident conditions with neutron shield and cask exterior material voided. This base model is then modified to evaluate basket configuration and fuel material changes individually or in combination. Results of these evaluations are documented in Table 6.4.10-6 and Table 6.4.10-7. Basket tolerance studies, as well as fuel studies shown later, rely on a base model containing maximum tolerance fissile material mass and uranium weight percent in the fuel meat. For all evaluations, the ^{235}U enrichment percentage is set to its maximum value as increased ^{235}U weight percent minimizes parasitic absorption in ^{238}U.

Maximum reactivity material, basket tolerances, and mechanical perturbation configurations are listed in the following bullets.

- Radial shift in – close approach active fuel
  No statistically significant difference between shifted middle fuel element and a centered middle fuel element. The centered middle fuel element is chosen to continue the remaining evaluations.

- Axial alternating shift – close approach active fuel

- Maximum ^{235}U mass and maximum uranium weight percentage

- Minimum fuel tube thickness
  For the tube specified, minimum tube thickness equals nominal thickness (tolerance is defined as -0%, +22%).

- No significant effect associated with other basket tolerances
  As reduced basket bottom plate and tube height removes absorber material from the system, the remaining reactivity evaluations set these variables to minimum.
  Fuel tube OD is retained at nominal as there is no significant effect on system reactivity for this variable, and offsetting neutronic effects occur for a change in tube size (e.g., increasing OD increases parasitic absorber and separates fissile material but provides additional moderator in the fuel region).

Next, fuel assembly dimensional and material effects are evaluated. The results of the fuel tolerance studies are documented in Table 6.4.10-8. Maximum system reactivity fuel configuration is itemized in the following bullets.

- Maximum active fuel width
  The tolerance applied to the active fuel width is one-half the distance between active fuel width and plate width. Applying this tolerance (0.3175 cm for the nominal plate width and 0.3366 cm for the maximum tolerance plate width) significantly increases system reactivity. Maximum allowed active fuel width by this analysis is 7.32 cm (conservatively rounded down from the 7.3266 cm evaluated).

- Maximum plate width
  Plate width variation taken independently has no effect on system reactivity.
  Analysis tied plate width to active fuel width. as no tolerance on the actual fuel width
  was available. Increasing plate width thereby increased the maximum active fuel
  width, which was shown to be bounding.

- Nominal plate thickness
  Plate bundle moderator to fuel ration (H/U) is controlled by the plate spacer thickness
  not plate thickness. Therefore, there is no significant effect of plate thickness on the
  bundle reactivity.

- Minimum clad thickness
  Maximum reactivity obtained from a case where clad thickness is conservatively set
  to a minimum of 0.01 cm.

- Nominal active fuel height
  Contrary to the spiral fuel and DIDO evaluation set, no significant effect of active
  fuel height was observed in the calculations.

- Minimum element height – reduces the space between fissile materials in the
  alternating shifted model
  Set to active fuel height to remove variable as a potential licensing limit. Note that
  the end-fitting structure of the plate bundle will assure significant separation between
  active fuel regions.

- Maximum plate spacer
  A conservative maximum spacer of 0.18 cm thickness was evaluated and shown to be
  bounding.

- Replacing aluminum side plates by water
  Provides additional moderation in the system.

Cask interior and exterior moderator density variation studies are included in Table 6.4.10-9.
These studies demonstrate that for a fully moderated cask interior, any increase in cask exterior
density reduces reactivity by decoupling the casks in the array. This data is consistent for
reduced reactivity obtained from the normal condition case where the cask water neutron shield
isolates casks in the infinite array modeled. The reactivity curve for modified interior density
demonstrates that within the statistical uncertainty of the evaluation, a fully moderated cask
interior represents a bounding condition. No significant variations in reactivity occur for
moderator densities above 0.95 g/cm^3. A plot of the interior density study is shown in Figure
6.4.10-2.

Results for a nominal condition infinite cask array, worst-case configuration accident condition
(voided neutron shield) and normal conditions of operation (filled neutron shield) arrays, and for
a single cask with a fully reflected containment boundary are included in Table 6.4.10-10.
Maximum bias adjusted system reactivity is 0.763, well below the 0.95 safety limit for the

system. As an infinite array of casks is subcritical under both normal and accident conditions, the criticality safety index (CSI) is 0.

The reactivity evaluation of the NAC-LWT cask containing up to 42 MOATA plate bundles demonstrates that subcritical margin ($k_s \leq 0.95$) can be maintained under the following conditions.

Parameter	MOATA Plate Bundle
Max. Number of Fuel Plates	14
Spacer Thickness	≤ 0.18 cm
Active Fuel Width	≤ 7.32 cm
235U Content per Plate	≤ 22.3
Enrichment wt % 235U	≤ 92

6.4.10.3   Mixed Basket Loading – Spiral Assemblies Basket and Plate Bundle Basket

The NAC-LWT may transport a combination of spiral elements and plate bundle elements. Given the low, and similar, reactivity of each payload, the combination of payloads is not expected to increase reactivity. A combination of three baskets of spiral elements and three baskets of plate bundles is evaluated to support the bounding statement. Casks are evaluated once with the top three baskets loaded with plate bundles and the bottom three baskets loaded with spiral elements, and once with an alternating spiral elements and plate bundles set. As shown in the following list, there is no increase in reactivity associated with mixed loading of plate bundles and spiral elements.

# Casks	Condition	Description	k_{eff}	σ	$k_{eff}+2\sigma$
Infinite Array	Accident	Nominal case of MOATA plate bundle load	0.68207	0.00078	0.68363
Infinite Array	Accident	Nominal case of spiral fuel	0.65957	0.00066	0.66089
Infinite Array	Accident	Alternating MOATA and spiral fuel load	0.67249	0.00068	0.67385
Infinite Array	Accident	Stack of 3 MOATA baskets and 3 spiral baskets	0.67403	0.00069	0.67541

Figure 6.4.10-1   Spiral Fuel – Moderator Density Plot
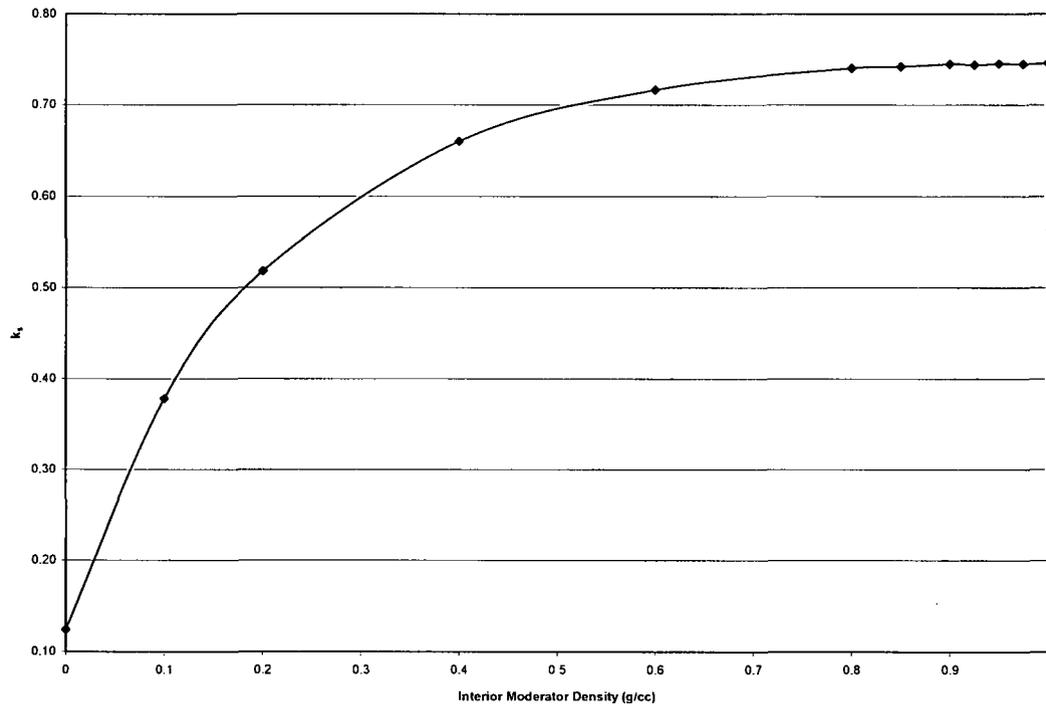
Figure 6.4.10-2   MOATA Plate Bundle – Moderator Density Plot
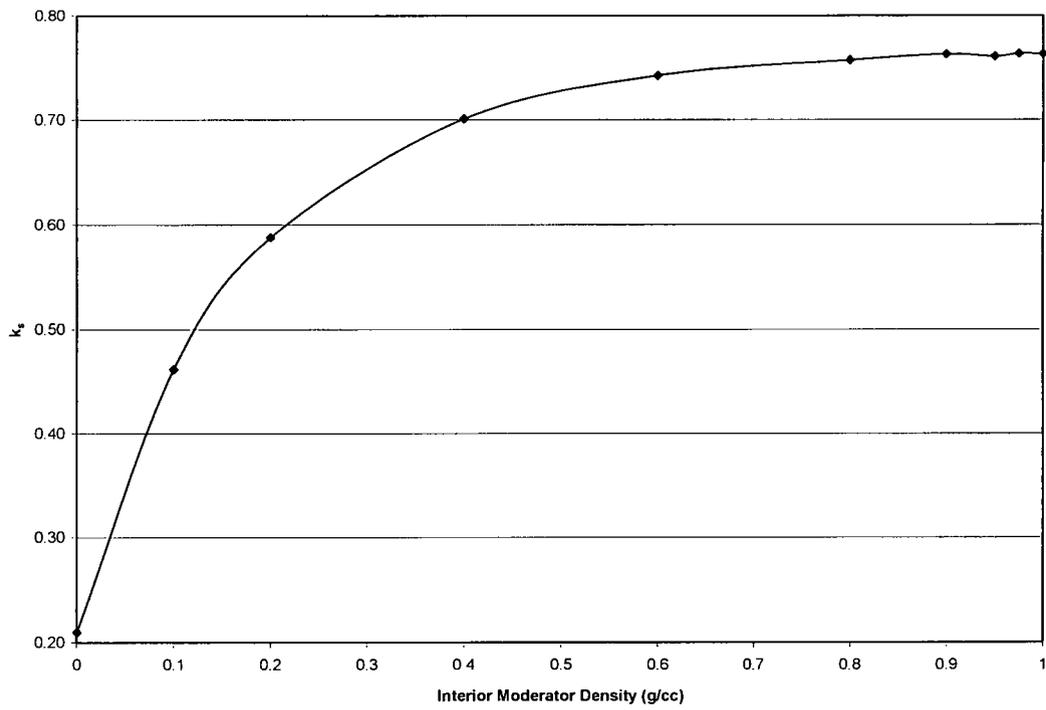
Table 6.4.10-1   Spiral Fuel Assembly – Base Data Comparisons

Base Data[1]	Cask Condition	Radial Shift Pattern	Axial Shift Pattern	^{235}U Mass Tolerance	Uranium Weight Fraction Tolerance	k_{eff}	σ	$k_{eff}+2\sigma$	k_s	Δk	$\Delta k_{eff}/\sigma$
Volume	Accident	CenteredC	Down	Nominal	Nominal	0.65222	0.00064	0.65350	0.67160	-0.00862	-13.5
Volume	Accident	CenteredC	Alternating	Nominal	Nominal	0.65957	0.00066	0.66089	0.67899	-0.00123	-1.9
Plate	Accident	CenteredC	Alternating	Nominal	Nominal	0.66084	0.00064	0.66212	0.68022	--	--
Volume	Accident	CenteredC	Alternating	Min	Nominal	0.63917	0.00067	0.64051	0.65861	-0.02161	-32.3
Volume	Accident	CenteredC	Alternating	Max	Nominal	0.68143	0.00065	0.68273	0.70083	0.02061	31.7
Volume	Accident	CenteredC	Alternating	Nominal	Min	0.65967	0.00066	0.66099	0.67909	-0.00113	-1.7
Volume	Accident	CenteredC	Alternating	Nominal	Max	0.66025	0.00065	0.66155	0.67965	-0.00057	-0.9
Volume	Accident	OutC	Alternating	Nominal	Nominal	0.65823	0.00062	0.65947	0.67757	-0.00265	-4.3
Volume	Accident	In	Alternating	Nominal	Nominal	0.66333	0.00063	0.66459	0.68269	0.00247	3.9
Volume	Accident	InC	Alternating	Nominal	Nominal	0.66273	0.00069	0.66411	0.68221	0.00199	2.9
Volume	Accident	InC	Alternating	Max	Nominal	0.68337	0.00066	0.68469	0.70279	0.02257	34.2

[1] Refers to cylindrical fuel approximation being based on the original plate dimension or on volume (i.e., H/U ratio) conserving model.

Table 6.4.10-2   Spiral Fuel Assembly – Basket Tolerance Evaluations

Fuel Tube Outer Diameter Tolerance	Fuel Tube Thickness Tolerance	Fuel Tube Height Tolerance	Fuel Basket Base Plate Tolerance	k_{eff}	σ	$k_{eff}+2\sigma$	k_s	Δk	$\Delta k_{eff}/\sigma$
Nominal	Nominal	Nominal	Nominal	0.68310	0.00069	0.68448	0.70258	--	--
Min	Nominal	Nominal	Nominal	0.68153	0.00066	0.68285	0.70095	-0.00163	-2.5
Max	Nominal	Nominal	Nominal	0.68410	0.00067	0.68544	0.70354	0.00096	1.4
Nominal	Min	Nominal	Nominal	0.68310	0.00069	0.68448	0.70258	--	--
Nominal	Max	Nominal	Nominal	0.65917	0.00067	0.66051	0.67861	-0.02397	-35.8
Nominal	Nominal	Min	Nominal	0.68368	0.00067	0.68502	0.70312	0.00054	0.8
Nominal	Nominal	Max	Nominal	0.68218	0.00065	0.68348	0.70158	-0.00100	-1.5
Nominal	Nominal	Nominal	Min	0.68341	0.00067	0.68475	0.70285	0.00027	0.4
Nominal	Nominal	Nominal	Max	0.68325	0.00064	0.68453	0.70263	0.00005	0.1
Min	Min	Min	Min	0.68254	0.00064	0.68382	0.70192	-0.00066	-1.0
Nominal	Min	Min	Min	0.68316	0.00068	0.68452	0.70262	0.00004	0.1
Max	Min	Min	Min	0.68434	0.00068	0.68570	0.70380	0.00122	1.8

Table 6.4.10-3   Spiral Fuel Assembly – Fuel Tolerance Evaluations

Fuel Plate Thickness Tolerance	Fuel Plate Clad Thickness Tolerance	Active Fuel Length Tolerance	Element Height Tolerance	H/U Study (Plate Location)	Inner & Outer Shells	k_{eff}	σ	$k_{eff}+2\sigma$	k_s	Δk	$\Delta k_{eff}/\sigma$
Nominal	Nominal	Nominal	Nominal	Nominal	Nominal	0.68310	0.00069	0.68448	0.70258	--	--
Min	Nominal	Nominal	Nominal	Nominal	Nominal	0.68643	0.00067	0.68777	0.70587	0.00329	4.9
Max	Nominal	Nominal	Nominal	Nominal	Nominal	0.68082	0.00067	0.68216	0.70026	-0.00232	-3.5
Nominal	No Clad	Nominal	Nominal	Nominal	Nominal	0.69059	0.00067	0.69193	0.71003	0.00745	11.1
Nominal	Min	Nominal	Nominal	Nominal	Nominal	0.68737	0.00066	0.68869	0.70679	0.00421	6.4
Nominal	Max	Nominal	Nominal	Nominal	Nominal	0.68003	0.00064	0.68131	0.69941	-0.00317	-5.0
Nominal	Nominal	Min	Nominal	Nominal	Nominal	0.68619	0.00067	0.68753	0.70563	0.00305	4.6
Nominal	Nominal	Max	Nominal	Nominal	Nominal	0.68111	0.00068	0.68247	0.70057	-0.00201	-3.0
Nominal	Nominal	Nominal	Fuel	Nominal	Nominal	0.68821	0.00065	0.68951	0.70761	0.00503	7.7
Nominal	Nominal	Nominal	Min	Nominal	Nominal	0.68512	0.00066	0.68644	0.70454	0.00196	3.0
Nominal	Nominal	Nominal	Max	Nominal	Nominal	0.68125	0.00068	0.68261	0.70071	-0.00187	-2.8
Nominal	Nominal	Nominal	Nominal	Min	Nominal	0.67318	0.00066	0.67450	0.69260	-0.00998	-15.1
Nominal	Nominal	Nominal	Nominal	Max	Nominal	0.69131	0.00066	0.69263	0.71073	0.00815	12.3
Nominal	Nominal	Nominal	Nominal	Min	Min	0.67580	0.00068	0.67716	0.69526	-0.00732	-10.8
Nominal	Nominal	Nominal	Nominal	Nominal	Min	0.69148	0.00067	0.69282	0.71092	0.00834	12.4
Nominal	Nominal	Nominal	Nominal	Max	Min	0.70408	0.00067	0.70542	0.72352	0.02094	31.3
Min	No_Clad	Min	Fuel	Max	Min	0.72459	0.00066	0.72591	0.74401	0.04143	62.8

Table 6.4.10-4   Spiral Fuel Assembly – Moderator Density Variations

Set	Interior Moderator Density (g/cm³)	Exterior Moderator Density (g/cm³)	k_{eff}	σ	$k_{eff}+2\sigma$	k_s
H1	0.9998	0.0001	0.72640	0.00067	0.72774	0.74584
	0.9998	0.1	0.69875	0.00066	0.70007	0.71817
	0.9998	0.5	0.69587	0.00067	0.69721	0.71531
	0.9998	0.9998	0.69661	0.00067	0.69795	0.71605
H2	0.9998	0.0001	0.72640	0.00067	0.72774	0.74584
	0.975	0.0001	0.72575	0.00066	0.72707	0.74517
	0.95	0.0001	0.72604	0.00066	0.72736	0.74546
	0.925	0.0001	0.72466	0.00068	0.72602	0.74412
	0.9	0.0001	0.72562	0.00066	0.72694	0.74504
	0.85	0.0001	0.72273	0.00067	0.72407	0.74217
	0.8	0.0001	0.72102	0.00069	0.72240	0.74050
	0.6	0.0001	0.69709	0.00068	0.69845	0.71655
	0.4	0.0001	0.63905	0.00150	0.64205	0.66015
	0.2	0.0001	0.49709	0.00138	0.49985	0.51795
	0.1	0.0001	0.35749	0.00125	0.35999	0.37809
	0.0001	0.0001	0.10524	0.00046	0.10616	0.12426

Table 6.4.10-5   Spiral Fuel Assembly – Maximum Reactivity Case Summary

# Casks	Condition	Description	k_{eff}	σ	$k_{eff}+2\sigma$	k_s
Infinite Array	Accident	Nominal configuration accident case	0.66084	0.00064	0.66212	0.68022
Infinite Array	Accident	Maximum reactivity material and shift case nominal fuel and basket configuration	0.68310	0.00069	0.68448	0.70258
Infinite Array	Accident	Maximum reactivity basket tolerance – nominal fuel configuration	0.68434	0.00068	0.68570	0.70380
Infinite Array	Accident	Maximum reactivity fuel tolerance – nominal basket configuration	0.72459	0.00066	0.72591	0.74401
Infinite Array	Accident	Combined maximum reactivity configuration case	0.72640	0.00067	0.72774	0.74584
Infinite Array	Normal	Combined maximum reactivity configuration case	0.69609	0.00069	0.69747	0.71557
Single Cask	N/A	Single cask / inner shell reflected with water - maximum reactivity configuration	0.65762	0.00067	0.65896	0.67706

Table 6.4.10-6   MOATA Plate Bundle – Base Data Comparisons

Cask Condition	Radial Shift Pattern	Axial Shift Pattern	235U Mass Tolerance	Uranium Weight Fraction Tolerance	k_{eff}	σ	$k_{eff}+2\sigma$	k_s	Δk	$\Delta k_{eff}/\sigma$
Accident	CenteredC	Down	Nominal	Nominal	0.67757	0.00074	0.67905	0.69715	-0.00458	-6.2
Accident	CenteredC	Alternating	Nominal	Nominal	0.68207	0.00078	0.68363	0.70173	--	--
Accident	CenteredC	Alternating	Nominal	Min	0.68113	0.00077	0.68267	0.70077	-0.00096	-1.2
Accident	CenteredC	Alternating	Nominal	Max	0.68367	0.00077	0.68521	0.70331	0.00158	2.1
Accident	CenteredC	Alternating	Min	Nominal	0.68163	0.00076	0.68315	0.70125	-0.00048	-0.6
Accident	CenteredC	Alternating	Max	Nominal	0.68624	0.00076	0.68776	0.70586	0.00413	5.4
Accident	OutC	Alternating	Max	Nominal	0.67948	0.00077	0.68102	0.69912	-0.00261	-3.4
Accident	In	Alternating	Max	Nominal	0.69075	0.00078	0.69231	0.71041	0.00868	11.1
Accident	InC	Alternating	Max	Nominal	0.69125	0.00080	0.69285	0.71095	0.00922	11.5
Accident	InC	Alternating	Max	Max	0.69234	0.00078	0.69390	0.71200	0.01027	13.2

Table 6.4.10-7   MOATA Plate Bundle – Basket Tolerance Evaluations

Fuel Tube Outer Diameter Tolerance	Fuel Tube Thickness Tolerance	Fuel Tube Height Tolerance	Fuel Basket Base Plate Tolerance	k_{eff}	σ	$k_{eff}+2\sigma$	k_s	Δk	$\Delta k_{eff}/\sigma$
Nominal	Nominal	Nominal	Nominal	0.69234	0.00078	0.69390	0.71200	--	--
Min	Nominal	Nominal	Nominal	0.68994	0.00077	0.69148	0.70958	-0.00242	-3.1
Max	Nominal	Nominal	Nominal	0.69108	0.00075	0.69258	0.71068	-0.00132	-1.8
Nominal	Min	Nominal	Nominal	0.69234	0.00078	0.69390	0.71200	--	--
Nominal	Max	Nominal	Nominal	0.67140	0.00077	0.67294	0.69104	-0.02096	-27.2
Nominal	Nominal	Min	Nominal	0.69146	0.00080	0.69306	0.71116	-0.00084	-1.0
Nominal	Nominal	Max	Nominal	0.69054	0.00079	0.69212	0.71022	-0.00178	-2.3
Nominal	Nominal	Nominal	Min	0.69152	0.00078	0.69308	0.71118	-0.00082	-1.1
Nominal	Nominal	Nominal	Max	0.69204	0.00079	0.69362	0.71172	-0.00028	-0.4
Max	Min	Min	Min	0.69326	0.00078	0.69482	0.71292	0.00092	1.2
Nominal	Min	Min	Min	0.69364	0.00077	0.69518	0.71328	0.00128	1.7
Min	Min	Min	Min	0.69024	0.00079	0.69182	0.70992	-0.00208	-2.6

Table 6.4.10-8   MOATA Plate Bundle – Fuel Tolerance Evaluations

Fuel Plate Width Tolerance	Fuel Plate Thickness Tolerance	Fuel Plate Clad Thickness Tolerance	Active Fuel Length Tolerance	Active Fuel Width Tolerance	Element Height Tolerance	Spacer Thickness Tolerance	Side Plate Thickness Tolerance	Side Plate Width Tolerance	k_{eff}	σ	$k_{eff}+2σ$	k_s	Δk	$Δk_{eff}/σ$
Nominal	Nominal	Nominal	Nominal	Nominal	Nominal	Nominal	Nominal	Nominal	0.69234	0.00078	0.69390	0.71200	--	--
Min	Nominal	Nominal	Nominal	Nominal	Nominal	Nominal	Nominal	Nominal	0.69017	0.00078	0.69173	0.70983	-0.00217	-2.8
Max	Nominal	Nominal	Nominal	Nominal	Nominal	Nominal	Nominal	Nominal	0.69105	0.00077	0.69259	0.71069	-0.00131	-1.7
Nominal	Min	Nominal	Nominal	Nominal	Nominal	Nominal	Nominal	Nominal	0.69190	0.00078	0.69346	0.71156	-0.00044	-0.6
Nominal	Max	Nominal	Nominal	Nominal	Nominal	Nominal	Nominal	Nominal	0.69192	0.00077	0.69346	0.71156	-0.00044	-0.6
Nominal	Nominal	Min	Nominal	Nominal	Nominal	Nominal	Nominal	Nominal	0.69424	0.00077	0.69578	0.71388	0.00188	2.4
Nominal	Nominal	Max	Nominal	Nominal	Nominal	Nominal	Nominal	Nominal	0.69150	0.00078	0.69306	0.71116	-0.00084	-1.1
Nominal	Nominal	Nominal	Min	Nominal	Nominal	Nominal	Nominal	Nominal	0.68998	0.00079	0.69156	0.70966	-0.00234	-3.0
Nominal	Nominal	Nominal	Max	Nominal	Nominal	Nominal	Nominal	Nominal	0.69153	0.00078	0.69309	0.71119	-0.00081	-1.0
Nominal	Nominal	Nominal	Nominal	Min	Nominal	Nominal	Nominal	Nominal	0.68240	0.00082	0.68404	0.70214	-0.00986	-12.0
Nominal	Nominal	Nominal	Nominal	Max	Nominal	Nominal	Nominal	Nominal	0.69920	0.00080	0.70080	0.71890	0.00690	8.6
Nominal	Nominal	Nominal	Nominal	Nominal	Fuel	Nominal	Nominal	Nominal	0.70756	0.00079	0.70914	0.72724	0.01524	19.3
Nominal	Nominal	Nominal	Nominal	Nominal	Min	Nominal	Nominal	Nominal	0.69029	0.00077	0.69183	0.70993	-0.00207	-2.7
Nominal	Nominal	Nominal	Nominal	Nominal	Max	Nominal	Nominal	Nominal	0.69220	0.00080	0.69380	0.71190	-0.00010	-0.1
Nominal	Nominal	Nominal	Nominal	Nominal	Nominal	Min	Nominal	Nominal	0.67080	0.00076	0.67232	0.69042	-0.02158	-28.4
Nominal	Nominal	Nominal	Nominal	Nominal	Nominal	Max	Nominal	Nominal	0.70952	0.00078	0.71108	0.72918	0.01718	22.0
Nominal	Nominal	Nominal	Nominal	Nominal	Nominal	Nominal	Water	Nominal	0.69518	0.00080	0.69678	0.71488	0.00288	3.6
Nominal	Nominal	Nominal	Nominal	Nominal	Nominal	Nominal	Min	Nominal	0.69087	0.00079	0.69245	0.71055	-0.00145	-1.8
Nominal	Nominal	Nominal	Nominal	Nominal	Nominal	Nominal	Max	Nominal	0.69185	0.00077	0.69339	0.71149	-0.00051	-0.7
Nominal	Nominal	Nominal	Nominal	Nominal	Nominal	Nominal	Nominal	Min	0.69203	0.00075	0.69353	0.71163	-0.00037	-0.5
Nominal	Nominal	Nominal	Nominal	Nominal	Nominal	Nominal	Nominal	Max	0.69179	0.00074	0.69327	0.71137	-0.00063	-0.9
Max	Nominal	Min	Nominal	Max	Fuel	Max	Nominal	Nominal	0.73925	0.00078	0.74081	0.75891	0.04691	60.1
Max	Nominal	Min	Nominal	Max	Fuel	Max	Water	Water	0.74205	0.00081	0.74367	0.76177	0.04977	61.4

Table 6.4.10-9   MOATA Plate Bundle – Moderator Density Variations

Set	Interior Moderator Density (g/cm³)	Exterior Moderator Density (g/cm³)	k_{eff}	σ	$k_{eff}+2\sigma$	k_s
H1	0.9998	0.0001	0.74285	0.00081	0.74447	0.76257
	0.9998	0.1	0.71116	0.00081	0.71278	0.73088
	0.9998	0.5	0.70785	0.00080	0.70945	0.72755
	0.9998	0.9998	0.70742	0.00081	0.70904	0.72714
H2	0.9998	0.0001	0.74285	0.00081	0.74447	0.76257
	0.975	0.0001	0.74337	0.00080	0.74497	0.76307
	0.95	0.0001	0.74073	0.00078	0.74229	0.76039
	0.9	0.0001	0.74275	0.00078	0.74431	0.76241
	0.8	0.0001	0.73741	0.00077	0.73895	0.75705
	0.6	0.0001	0.72186	0.00124	0.72434	0.74244
	0.4	0.0001	0.67919	0.00174	0.68267	0.70077
	0.2	0.0001	0.56690	0.00133	0.56956	0.58766
	0.1	0.0001	0.44132	0.00118	0.44368	0.46178
	0.0001	0.0001	0.19016	0.00057	0.19130	0.20940

Table 6.4.10-10   MOATA Plate Bundle – Maximum Reactivity Case Summary

# Casks	Condition	Description	k_{eff}	σ	$k_{eff}+2\sigma$	k_s
Infinite Array	Accident	Nominal configuration accident case	0.68207	0.00078	0.68363	0.70173
Infinite Array	Accident	Maximum reactivity material and shift case	0.69234	0.00078	0.69390	0.71200
Infinite Array	Accident	Maximum reactivity basket tolerance	0.69024	0.00079	0.69182	0.70992
Infinite Array	Accident	Maximum reactivity fuel tolerance	0.74205	0.00081	0.74367	0.76177
Infinite Array	Accident	Combined maximum reactivity configuration case	0.74285	0.00081	0.74447	0.76257
Infinite Array	Normal	Combined maximum reactivity configuration case	0.70622	0.00082	0.70786	0.72596
Single Cask	N/A	Single cask / inner shell reflected with water - maximum reactivity configuration	0.65594	0.00082	0.65758	0.67568

6.4.11   Combined DIDO-ANSTO Basket Payloads

This section presents the criticality analyses for the NAC-LWT cask with a stack of five DIDO baskets containing DIDO fuel, and an ANSTO top module that may contain DIDO, spiral fuel assemblies or MOATA plate bundles. ANSTO module contents may be placed in aluminum damaged fuel cans (DFCs). DFC contents may be complete fuel elements or individual fuel plates (potentially segmented). This evaluation meets the criticality safety requirements of 10 CFR Parts 71.55 and 71.59, as well as IAEA Transportation Safety Standards (TS-R-1). In this analysis, the bounding system characteristics are determined for an infinite array of NAC-LWT casks under normal and accident conditions. Cask cavity, neutron shield tank and outside moderator density effects were studied in the DIDO and ANSTO basket evaluation sections and demonstrated maximum reactivity for a dry cask exterior and fully flooded cask cavity. Optimum moderator density evaluations in this analysis section are, therefore, limited to the effect of canister preferential flooding. The analyses demonstrate that, including all calculational and mechanical uncertainties, the NAC-LWT cask remains subcritical under normal and accident conditions containing a combination of DIDO baskets and the ANSTO top basket module, where the top basket module may contain DIDO or ANSTO fuel.

The evaluation was performed in several analysis stages to move from existing DIDO and ANSTO analyses to a bounding mixed payload analysis, including DFCs. The first analysis set establishes an initial baseline reactivity model of the NAC-LWT cask loaded with a full set of DIDO basket modules and for a set of five DIDO basket modules with a DIDO payload inside an ANSTO (top) basket module. The next analysis stage inserts ANSTO specific payloads, i.e., Mark II MOATA plate and Mark III spiral fuel, into the top ANSTO module. Following this analysis stage, mixed payloads, canistered payloads, optimum moderator conditions and segmented plates are evaluated.

6.4.11.1   DIDO Basket and ANSTO Basket Substitution

The maximum reactivity DIDO case is modified to replace the aluminum fuel tubes by the stainless steel basket tubes specified by the component drawing. Next, the input file is revised to include an ANSTO top basket module containing a full load of the bounding DIDO fuel. Modifications for this geometry change involve a duplication of the basket and tube related KENO units corresponding to the larger ANSTO fuel tubes. To minimize model development, the ANSTO basket module geometry units were copied into a DIDO input file with appropriate units renumbered. Material compositions were similarly inserted and renumbered with resonance characteristics for the non-DIDO fuels being added using the "RES" and "DAN"

CSAS input variables. The resonance characteristics for the non-DIDO fuel had to be generated using stand-alone runs each time the fuel geometry was changed.

As seen in Table 6.4.11-1, there is no statistical difference between loading DIDO elements into a DIDO or ANSTO top basket module. Further, the analysis results for the insertion of ANSTO payloads demonstrate that system reactivity is controlled by the five DIDO basket stack. This result was expected as maximum reactivities (k_{eff}) for the plate and spiral basket assemblies are less than that of the DIDO basket assembly. Therefore, inserting a lower reactivity plate and spiral payload into the DIDO basket stack does not increase system reactivity.

6.4.11.2   Mixed Payloads

Within the ANSTO top basket module plate, spiral or DIDO fuel types are permitted to be loaded into any of the basket locations. To support this loading criterion, sample mixed payload variations are evaluated. Results are shown in Table 6.4.11-2 for various combinations of fuel types. The maximum reactivity full set of DIDO elements serves as the basis for this analysis. As expected, replacing higher reactivity DIDO fuel with spiral and plate assemblies has no statistically significant effect on maximum system reactivity as the five full DIDO basket modules control system reactivity. As the maximum reactivity payload is DIDO fuel, the analysis results in this section bound placement of the mixed payload top ANSTO basket module onto an ANSTO basket stack, loaded with MOATA plate and spiral elements.

6.4.11.3   Separated Fuel Plates

MOATA plate and spiral fuel assemblies may be disassembled prior to placement into a DFC. As typical plate material is undermoderated, the plates are evaluated at various pitch configurations from touching to the maximum pitch allowed by the basket tubes. For this analysis set, no credit is taken for the DFC. Each case in this set represents a system containing five DIDO modules (loaded with DIDO fuel) and a top ANSTO module with the specified fuel type. As demonstrated in Table 6.4.11-3, system reactivity increases for maximum plate separation with MOATA plates producing a higher system reactivity than the DIDO base case and the separated spiral case.

Previous plate evaluations (Section 6.4.3) have demonstrated that a reduction in the number of plates, allowing an increase in pitch, reduces system reactivity due to the removal of fissile material and is, therefore, not duplicated here.

6.4.11.4 Aluminum DFC

Fuel material in individual plates, including plates that may have clad defects or are segmented, are transported within an aluminum DFC. Only the radial shell of the DFC is modeled. This model is conservative since including DFC bottom/top plates in the model would separate fuel material axially and increase neutron leakage. Inserting the DFC into the model constricts the allowable space for fuel plate expansion and, therefore, reduces system reactivity. To demonstrate this effect, the maximum reactivity DIDO, MOATA plate and spiral models are modified to contain a DFC (with the resulting restriction in maximum plate pitch). Results of the DFC insertion analysis are shown in Table 6.4.11-4 and demonstrate that maximum reactivity is achieved in models containing no DFC.

DFCs contain screens to facilitate draining and drying of the system. Hypothetical preferential flooding scenarios are considered by modeling various combinations of full density water and void in the canister interior and cask cavity moderator combinations. Results of the evaluations for the Table 6.4.11-4 model of five DIDO baskets and one ANSTO basket containing maximum pitch MOATA plates are shown in Table 6.4.11-5. As seen in Table 6.4.11-5, the maximum reactivity moderator condition is represented by a dry cask with flooded DFCs in the top ANSTO module. A more detailed moderator density evaluation, displayed in Table 6.4.11-6, demonstrates that as the density of the water in the cask cavity is lowered, the reactivity of the system increases. This effect is due to the increased neutron interaction between DFCs and non-canistered fuel, while retaining water within the DFC fuel lattice.

6.4.11.5 Segmented Fuel Plates

In addition to complete fuel plates, the canister may also contain segmented fuel plates. Segmenting the plates decreases the distance between fuel in adjacent baskets, but also displaces moderator. Table 6.4.11-7 contains results for reactivity evaluations of the ANSTO top basket module MOATA plate payload with each plate cut in half (i.e, 28 half-height plates in the array). System reactivity decreases as moderator is displaced in the plate array. This demonstrates that the model based on complete plates at maximum pitch is bounding.

6.4.11.6 Conclusions and Recommendations

The maximum bias adjusted reactivity (k_s) for an NAC-LWT cask loaded with five DIDO baskets containing DIDO fuel elements and an ANSTO basket with any combination of DIDO elements, MOATA plate bundles, and HIFAR spiral fuel assemblies is 0.8291. Although the maximum reactivity is above that of an NAC-LWT cask completely loaded with steel DIDO baskets and DIDO fuel, it is significantly lower than the reactivity of the previously licensed NAC-LWT cask loaded with aluminum DIDO baskets and DIDO fuel that has a maximum

reactivity of 0.93. The reactivity of the mixed basket stack bounds that of an ANSTO stack containing DFCs. This reactivity is well within the safety limit ($k_s < 0.95$). Single cask and normal condition evaluations are not performed in this calculation, as DIDO and ANSTO analyses have previously demonstrated that the accident condition array bounds (maximum reactivity) results. The criticality safety index (CSI) for the shipment is 0, as it was modeled as an infinite array of casks.

Table 6.4.11-1   DIDO/ANSTO Basket Module Replacement

Top Basket Module		k_{eff}	σ	k_s	Δk	$\Delta k / \sigma$
Type	Content					
DIDO[1]	DIDO	0.7709	0.0007	0.7904	--	--
ANSTO	DIDO	0.7696	0.0007	0.7891	-0.0013	-1.9
ANSTO	MOATA	0.7703	0.0007	0.7898	-0.0006	-0.9
ANSTO	Spiral	0.7691	0.0007	0.7886	-0.0018	-2.6

Note: [1] The aluminum tube DIDO basket assembly model produced a maximum k_s of 0.9304.

Table 6.4.11-2   DIDO/ANSTO Mixed Payload Analysis Results

ANSTO Module		k_{eff}	σ	k_s	Δk	$\Delta k / \sigma$
Interior	Exterior					
D	6D	0.7709	0.0007	0.7904	--	--
D	3D/3S	0.7697	0.0007	0.7892	-0.0012	-1.7
D	3D/3M	0.7695	0.0007	0.7890	-0.0014	-2.0
D	2D/2M/2S	0.7697	0.0007	0.7892	-0.0012	-1.7
S	2D/2M/2S	0.7705	0.0007	0.7900	-0.0004	-0.6
M	2D/2M/2S	0.7702	0.0007	0.7897	-0.0007	-1.0

Note: Abbreviated names are (M) for MOATA plate, (S) for Spiral and (D) for DIDO.

Table 6.4.11-3   DIDO/ANSTO Basket Plate Separation Evaluation

ANSTO Module		k_{eff}	σ	k_s	Δk	$\Delta k / \sigma$
Fuel Type	Plate Pitch (cm)					
Spiral	As Built	0.7691	0.0007	0.7886	--	--
Spiral	Touch	0.7678	0.0007	0.7873	-0.0013	-1.9
Spiral	0.3055	0.7677	0.0007	0.7872	-0.0014	-2.0
Spiral	0.4634	0.7678	0.0007	0.7873	-0.0013	-1.9
Spiral	0.6212	0.7677	0.0007	0.7872	-0.0014	-2.0
Spiral	0.7791	0.7676	0.0007	0.7871	-0.0015	-2.1
Spiral	0.8500	0.7695	0.0007	0.7890	0.0004	0.6
Spiral	*0.9370	0.7695	0.0007	0.7890	0.0004	0.6
MOATA	As Built	0.7703	0.0007	0.7898	--	--
MOATA	Touch	0.7680	0.0007	0.7875	-0.0023	-3.3
MOATA	0.2696	0.7684	0.0007	0.7879	-0.0019	-2.7
MOATA	0.3353	0.7678	0.0007	0.7873	-0.002	-3.6
MOATA	0.4011	0.7724	0.0007	0.7919	0.002	3.0
MOATA	0.4668	0.7852	0.0007	0.8047	0.015	21.3
MOATA	*0.5326	0.8096	0.0007	0.8291	0.0393	56.1

*Maximum Pitch Allowable by Tube

Table 6.4.11-4   DIDO/ANSTO Basket DFC Addition

ANSTO Module Payload	DFC	k_{eff}	σ	k_s	Δk	$\Delta k / \sigma$
DIDO	No	0.7709	0.0007	0.7904	--	--
DIDO	Yes	0.7690	0.0007	0.7885	-0.0019	-2.7
Spiral	No	0.7695	0.0007	0.7890	--	--
Spiral	Yes	0.7703	0.0007	0.7898	0.0008	1.1
Plate	No	0.8096	0.0007	0.8291	--	--
Plate	Yes	0.7782	0.0007	0.7977	-0.0314	-44.9

Table 6.4.11-5   DIDO/ANSTO Basket Preferential Flood Analysis

Moderator Density (g/cc)		k_{eff}	σ	k_s	Δk	$\Delta k/\sigma$
Cask	Can					
1.0	1.0	0.7782	0.0007	0.7977	--	--
1.0	0.0	0.7674	0.0007	0.7869	-0.0108	-15.4
0.0	1.0	0.7992	0.0007	0.8187	0.0210	30.0
0.0	0.0	0.1440	0.0002	0.1625	-0.6352	-3176.0

Table 6.4.11-6   DIDO/ANSTO Basket Cask Cavity Moderator Density Study

Moderator Density (g/cc)		k_{eff}	σ	k_s	Δk	$\Delta k/\sigma$
Cask	DFC					
1.0	1.0	0.7782	0.0007	0.7977	--	--
0.9	1.0	0.7796	0.0007	0.7991	0.0014	2.0
0.8	1.0	0.7827	0.0007	0.8022	0.0045	6.4
0.7	1.0	0.7844	0.0007	0.8039	0.0062	8.9
0.6	1.0	0.7885	0.0007	0.808	0.0103	14.7
0.5	1.0	0.7896	0.0007	0.8091	0.0114	16.3
0.4	1.0	0.7941	0.0007	0.8136	0.0159	22.7
0.3	1.0	0.7970	0.0007	0.8165	0.0188	26.9
0.2	1.0	0.7989	0.0008	0.8186	0.0209	26.1
0.1	1.0	0.7992	0.0008	0.8189	0.0212	26.5
0.0	1.0	0.7992	0.0007	0.8187	0.0210	30.0

Table 6.4.11-7   DIDO/ANSTO Basket Segmented Plate Study

Plate Configuration	k_{eff}	σ	k_s	Δk	$\Delta k/\sigma$
Complete	0.7782	0.0007	0.7977	--	--
Segmented	0.7697	0.0007	0.7892	-0.0085	-12.1

6.5 Criticality Benchmarks

The results of the criticality analyses presented in this chapter are corrected for bias and uncertainty resulting from the method using information obtained from the analysis of criticality benchmark experimental data.

6.5.1 CSAS25 Criticality Benchmark for LEU LWR Oxide Fuel

This section provides the validation of the CSAS25 criticality analysis sequence contained in Version 4.3 of the SCALE package. This validation is required by the criticality safety standards ANSI/ANS-8.1. The section describes the method, computer program and cross-section libraries used, experimental data, areas of applicability, and bias and margins of safety.

ANSI/ANS-8.17 prescribes the criterion to establish subcriticality safety margins. This criterion is as follows:

$$k_s \leq k_c - \Delta k_s - \Delta k_c - \Delta k_m \qquad (1)$$

where:

k_s = calculated allowable maximum multiplication factor, k_{eff}, of system being evaluated for all normal or credible abnormal conditions or events.

k_c = mean k_{eff} that results from calculation of benchmark criticality experiments using particular calculational method. If calculated k_{eff} values for criticality experiments exhibit trend with parameter, then k_c shall be determined by extrapolation based on best fit to calculated values. Criticality experiments used as benchmarks in computing k_c should have physical compositions, configurations, and nuclear characteristics (including reflectors) similar to those of system being evaluated.

Δk_s = allowance for:

    a.   statistical or convergence uncertainties, or both, in computation of k_s,

    b.   material and fabrication tolerances, and

    c.   geometric or material representations used in computational method.

Δk_c = margin for uncertainty in k_c which includes allowance for:

    a.   uncertainties in critical experiments,

    b.   statistical or convergence uncertainties, or both, in computation of k_c,

    c.   uncertainties resulting from extrapolation of k_c outside range of experimental data, and

        d.   uncertainties resulting from limitations in geometrical of material representations used in computational method.

Δk_m= arbitrary margin to ensure subcriticality of k_s.

The various uncertainties are combined statistically if they are independent. Correlated uncertainties are combined additively.

Equation 1 can be rewritten as:

$$k_s \leq 1 - \Delta k_m - \Delta k_s - (1 - k_c) - \Delta k_c \qquad (2)$$

Noting that the NRC requires a 5% subcriticality margin ($\Delta k_m = 0.05$) and the definition of the bias ($\Delta k_{Bias} = 1 - k_c$), the Equation 2 can then be written as:

$$k_s \leq 0.95 - \Delta k_s - \Delta k_{Bias} - \Delta k_{BU} \qquad (3)$$

where $\Delta k_{BU} = \Delta k_c$. Thus, the k_s (the maximum allowable value for k_{eff}) must be below 0.95 minus the bias, uncertainties in the bias, and uncertainties in the system being analyzed (i.e., Monte Carlo, mechanical, and modeling). This is an upper safety limit criteria often used in the DOE criticality safety community.

Alternatively, Equation 3 can be rewritten applying the bias and uncertainties to the k_{eff} of the system being analyzed as:

$$k_s \equiv k_{eff} + \Delta k_s + \Delta k_{Bias} + \Delta k_{BU} \leq 0.95 \qquad (4)$$

In Equation 4, k_{eff} replaces k_s, and k_s has been redefined as the effective multiplication factor of the system being analyzed, including the method bias and all uncertainties. This is a maximum calculated k_{eff} criteria often used in LWR spent fuel storage and transport analyses.

For use in criticality evaluations of LWR fuel in storage and transport casks, both k_{Bias} and Δk_{Bias} are evaluated below for KENO-Va with the 27-group ENDF/B-IV library.

6.5.1.1   Benchmark Experiments and Applicability

The criticality safety method is CSAS embedded in SCALE version 4.3 for the PC. CSAS includes the SCALE Material Information Processor, BONAMI-S, NITAWL-S, and KENO-Va. The Material Information Processor generates number densities for standard compositions, prepares geometry data for resonance self-shielding, and creates data input files for the cross-section processing codes. The BONAMI-S and NITAWL-S codes are used to prepare a resonance-corrected cross-section library in AMPX working format. The KENO-Va code uses Monte Carlo techniques to calculate the model k_{eff}. The 27-group ENDF/B-IV neutron cross-section library is used in this validation.

6.5.1.1.1   Description of Experiments

The 63 critical experiments selected are as follows: 9 B&W 2.46 wt % ^{235}U fuel storage (Baldwin), 10 PNL 4.31 wt % ^{235}U lattice (Bierman and Clayton, July 1980), 21 PNL 2.35 and 4.31 wt % ^{235}U with metal reflectors (Bierman, April 1979 and August 1981), 12 PNL flux trap (Bierman, July 1980 and June 1988) and 11 VCML 4.74 wt % ^{235}U experiments, some involving moderator density variations (Manaranche). These experiments span a range of fuel enrichments, fuel rod pitches, neutron absorber sheet characteristics, shielding materials and geometries that are typical of LWR fuel in a cask.

To achieve accurate results, three-dimensional models, as close to the actual experiment as possible, are used to evaluate the experiments. Stochastic Monte Carlo error is kept within ±0.1% by executing at least 1,000 neutrons/generation for more than 400 generations.

6.5.1.1.2   Applicability of Experiments

All of the experiments chosen in this validation are applicable to either PWR or BWR fuel. Fuel enrichments have covered a range from 2.35 up to 4.74 wt % ^{235}U, typical of LWR fuel presently used. The experiment fuel rod and pitch characteristics are within the range of standard PWR or BWR fuel rods (i.e., pellet OD from 0.78 to 1.2 cm, rod OD from 0.95 to 1.88 cm, and pitch from 1.26 to 1.87 cm). This is particularly true of the VCML (PWR rod type) and B&W experiments (BWR rod type). The H/U volume ratios of the experimental fuel arrays are within the range of PWR fuel assemblies (1.6 to 2.32) and BWR fuel assemblies (1.6 to 1.9). The experiments addressed the influence of water and metal reflector regions, including steel and lead, such as that present in the NAC-LWT cask.

Confidence in predicting criticality, including bias and uncertainty, has been demonstrated for LWR fuel with enrichments up to 4.74 wt % ^{235}U and, based on the lack of a significant trend with increasing enrichment, confidence in extrapolating up to 5 wt % ^{235}U is still high. Confidence in predicting subcriticality has been demonstrated for arrays in which critical controls consist of flux trap or single neutron absorber sheets or simple spacing. Confidence in predicting subcriticality has also been demonstrated for LWR fuel arrays next to water and metal reflector regions.

6.5.1.2   Results of Benchmark Calculations

The k-effective results for the experiments are shown in Table 6.5.1-1 and a frequency plot is provided in Figure 6.5.1-1. Five sets of cases are presented: Set 1, B&W; Set 2, PNL lattice; Set 3, PNL reflector; Set 4, PNL flux trap, and Set 5,VCML critical experiments. Sixty-three results are reported.

The overall average and standard deviation of the 63 cases is 0.9948 ± 0.0044. The average Monte Carlo error (statistical convergence) is ± 0.0012 for the 63 cases. This uncertainty component is statistically subtracted from the uncertainties because it is previously included in the standard deviation. The KENO-Va models are three-dimensional, fully explicit representations (no homogenization) of the experimental geometry. Therefore, the uncertainty resulting from limitations of geometrical modeling is taken to be 0.0. The experiments modeled cover the range of fuel types, enrichments, and metal reflector effects so that no extrapolations are necessary outside the range of data, and the uncertainty resulting from extrapolation is also taken to be 0.0. On the basis of the reported experimental error for the B&W cases, the reported error of the critical size number of rods for the PNL cases and the reported error for the critical height in the VCML cases, the experimental error is conservatively taken to be ± 0.001. Criticality can then be represented as 1.000 ± 0.001. This uncertainty component is added to the sum of the other uncertainties.

Thus, the bias or average difference between code calculated and the critical condition is Δk_{Bias}=1-0.9948 = 0.0052. The uncertainty in the bias, accounting for the statistical convergence (Monte Carlo error) and the uncertainty in criticality is $(0.0044^2 - 0.0012^2 + 0.0010^2)^{1/2} = 0.0043$. For 63 samples of criticality, the 95/95 one-side tolerance factor is 2.012 (Owen, 1963). The result is a 95/95 one-sided uncertainty in the bias of $\Delta k_{BU} = 2.012 \times 0.0043 = 0.0087$. Equation 4 now becomes:

$k_{eff} + \Delta k_s + 0.0052 + 0.0087 \le 0.95$

Where Δk_s becomes the uncertainty in k_s resulting from Monte Carlo error, mechanical and material tolerances, and geometric or material representations. If the nominal representation of the system is evaluated for k_s, then the mechanical and material perturbations can be evaluated independently and can be combined statistically as the root sum of squares. If the worst-case mechanical and material tolerances are used in the analysis, then Δk_s becomes 0.0 and the Monte Carlo error, σ_{mc}, can be combined with the uncertainty in the bias as:

$k_{eff} + 2\sigma_{mc} + 0.0052 + 0.0087 \le 0.95$

6.5.1.3   Trends

Frequency distribution of k_{eff} values and scatter plots of k_{eff} versus wt % ^{235}U, rod pitch, H/U volume ratio, and average neutron group causing fission are shown in Figure 6.5.1-1 through Figure 6.5.1-5. Included in the scatter plots are linear regression lines with a corresponding correlation coefficient to statistically indicate any trend or lack thereof. In particular, the correlation coefficient is a measure of the linear relationship between k_{eff} and a critical experiment parameter. If r is +1, a perfect linear relationship with a positive slope is indicated, and if r is -1, a perfect linear relationship with a negative slope is indicated. When r is 0, no linear relationship is indicated. The largest correlation coefficient indicated in the plots is 0.1302 (k_{eff} versus enrichment) and the lowest is 0.0176 (k_{eff} versus Average Group of Fission). On the basis of the correlation coefficients, no statistically significant trends exist over the range of variables studied.

Figure 6.5.1-1   KENO-Va Validation—27 Group Library Results: Frequency Distribution of k_{eff} Values
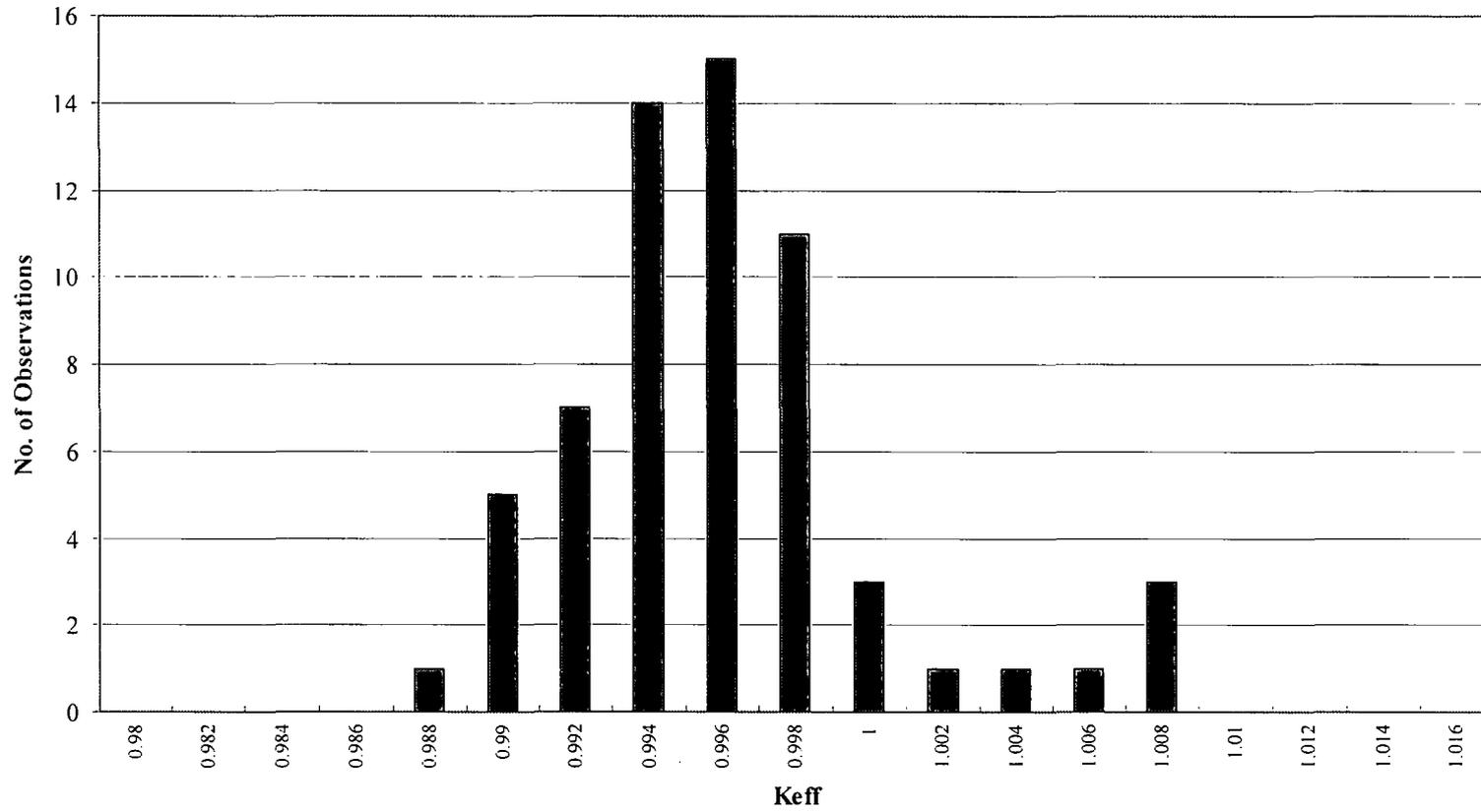
Figure 6.5.1-2   KENO-Va Validation—27-Group Library Results: k_{eff} versus Enrichment
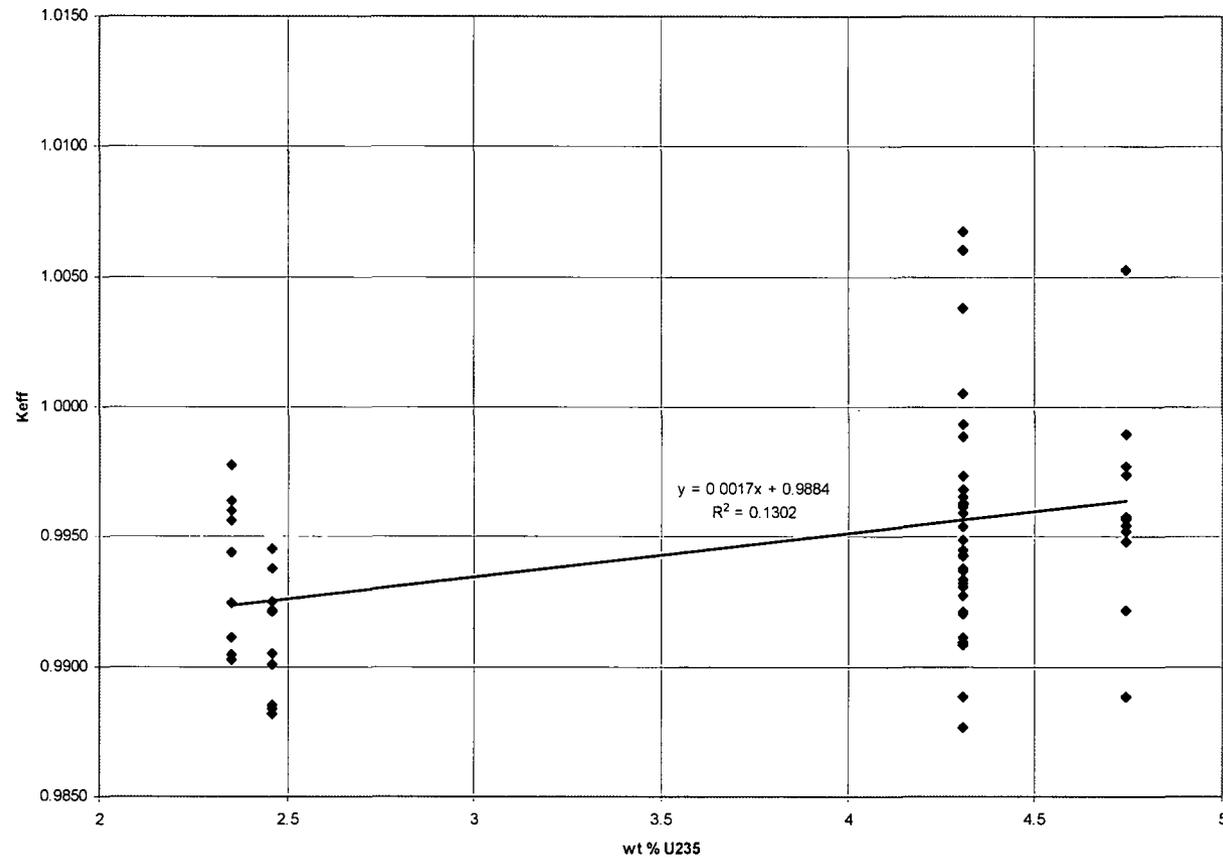
Figure 6.5.1-3   KENO-Va Validation—27-Group Library Results: k_{eff} versus Rod Pitch
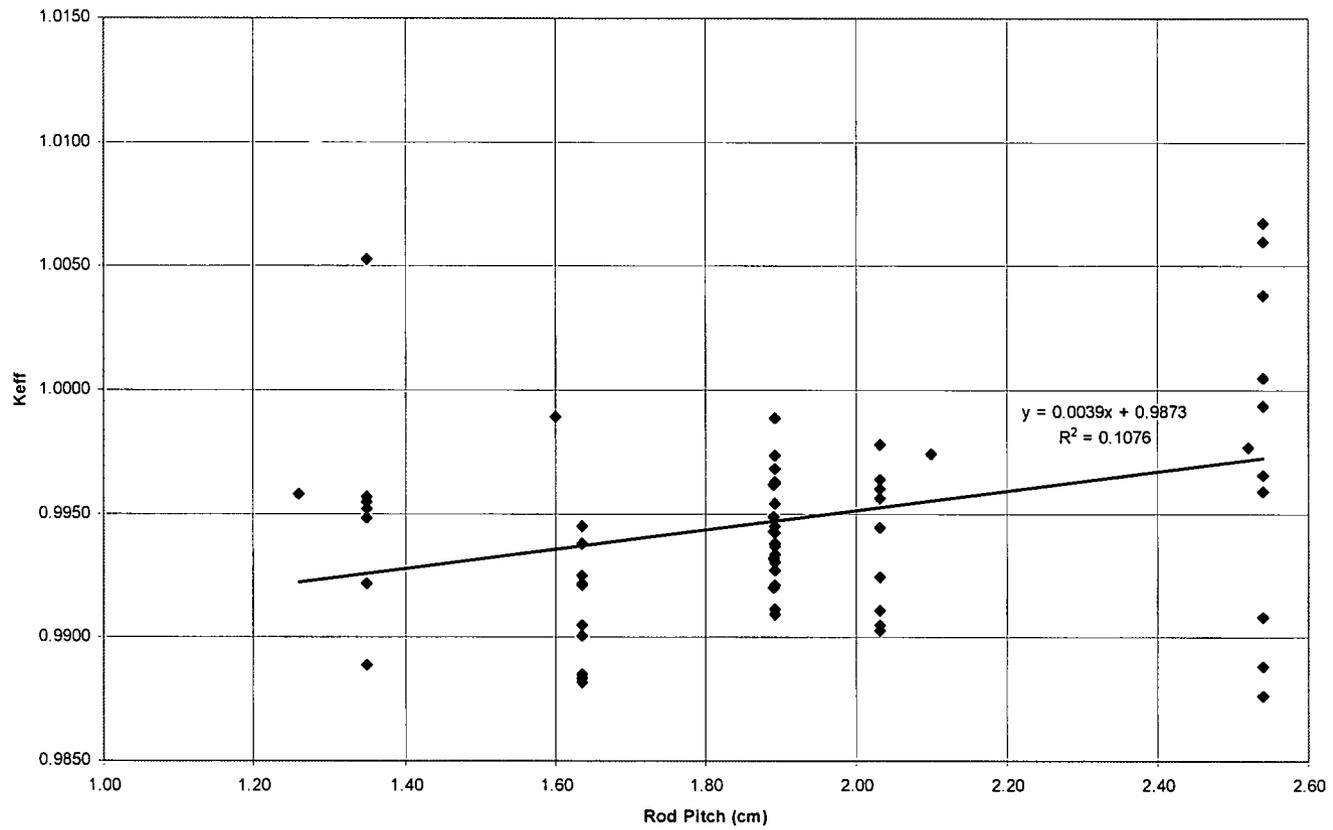
Figure 6.5.1-4   KENO-Va Validation—27-Group Library Results: k_{eff} versus H/U Volume Ratio
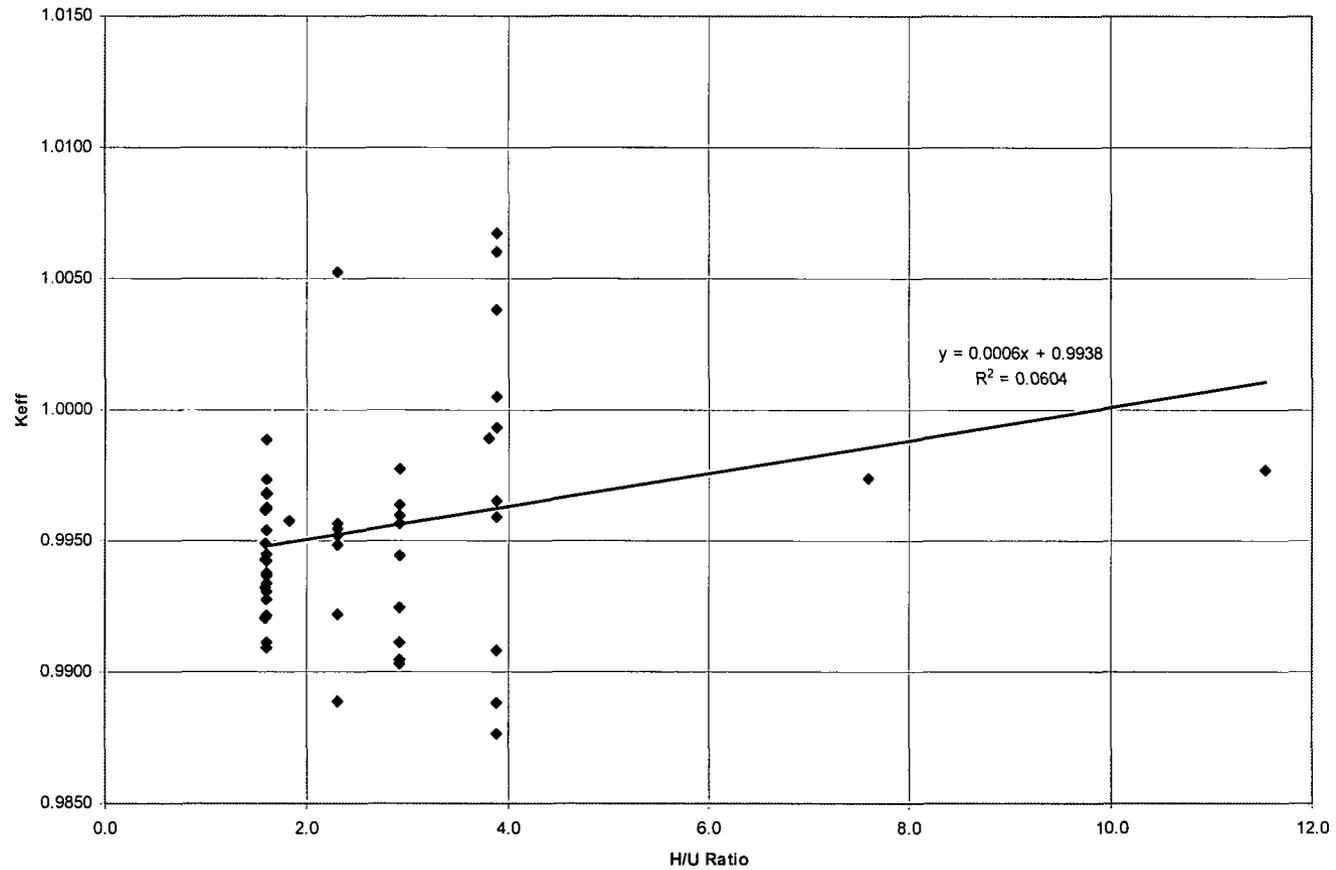
Figure 6.5.1-5   KENO-Va Validation—27-Group Library Results: k_{eff} versus Average Group of Fission
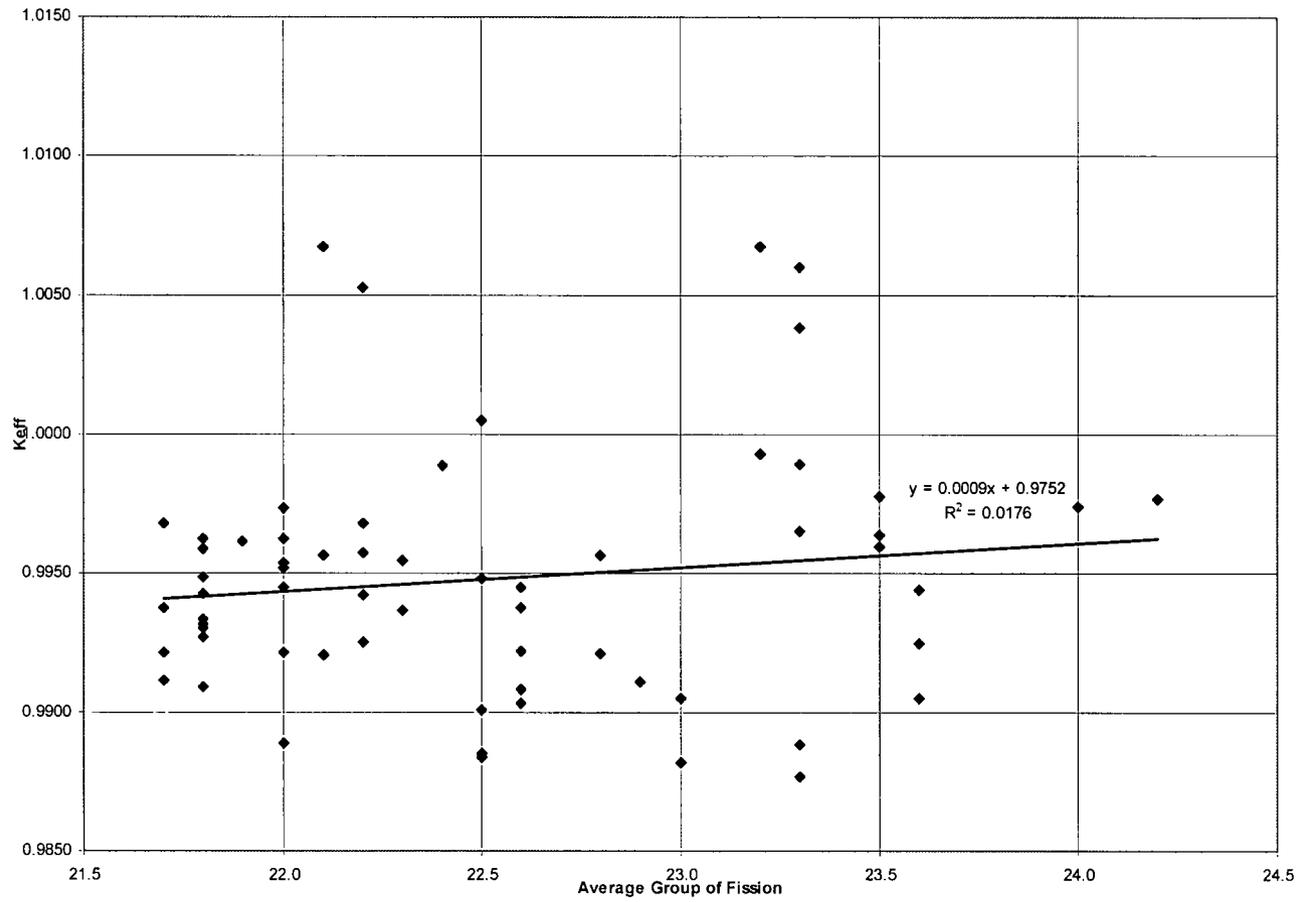
Table 6.5.1-1   KENO-Va and 27-Group Library Validation Statistics

Criticals	Configuration	wt % ^{235}U	Pitch (cm)	Pellet OD (cm)	Clad OD (cm)	H/U	Sol. B (ppm)	Poison	g ^{10}B/cm²	Gap(cm)	Gap Den.	Ave. Gfis	K$_{eff}$	k$_s$
Set 1										Gap				
B&W-I	Cylindrical	2.46	1.636	1.03	1.206	1.6	0	na	na	0		22.8	0.9921	0.0011
B&W-II	3X3-14X14	2.46	1.636	1.03	1.206	1.6	1037	na	na	0		22.2	0.9925	0.0009
B&W-III	3X3-14X14	2.46	1.636	1.03	1.206	1.6	764	na	na	1.636		22.6	0.9938	0.0009
B&W-IX	3X3-14X14	2.46	1.636	1.03	1.206	1.6	0	na	na	6.543		23	0.9905	0.0010
B&W-X	3X3-14X14	2.46	1.636	1.03	1.206	1.6	143	na	na	4.907		23	0.9882	0.0010
B&W-XI	3X3-14X14	2.46	1.636	1.03	1.206	1.6	514	Steel	0	1.636		22.6	0.9945	0.0010
B&W-XIII	3X3-14X14	2.46	1.636	1.03	1.206	1.6	15	B-Al	0.0052	1.636		22.6	0.9922	0.0010
B&W-XIV	3X3-14X14	2.46	1.636	1.03	1.206	1.6	92	B-Al	0.0040	1.636		22.5	0.9885	0.0010
B&W-XVII	3X3-14X14	2.46	1.636	1.03	1.206	1.6	487	B-Al	0.0008	1.636		22.5	0.9884	0.0010
B&W-XIX	3X3-14X14	2.46	1.636	1.03	1.206	1.6	634	B-Al	0.0003	1.636		22.5	0.9901	0.0009
												Average	0.9911	0.0023
Set 2										Gap				
PNL-043	17X13 Lattice	4.31	1.892	1.415	1.265	1.6	0	na	na	na	na	22.0	0.9954	0.0014
PNL-044	16X14 Lattice	4.31	1.892	1.415	1.265	1.6	0	na	na	na	na	22.0	0.9945	0.0013
PNL-045	14X16 Lattice	4.31	1.892	1.415	1.265	1.6	0	na	na	na	na	22.0	0.9974	0.0013
PNL-046	12x19 Lattice	4.31	1.892	1.415	1.265	1.6	0	na	na	na	na	22.0	0.9963	0.0013
PNL-087	4 11X14 Arrays	4.31	1.892	1.415	1.265	1.6	0	BORAL	0.066	2.83		21.8	0.9927	0.0012
PNL-079	4 11X14 Arrays	4.31	1.892	1.415	1.265	1.6	0	BORAL	0.030	2.83		21.8	0.9909	0.0012
PNL-093	4 11X14 Arrays	4.31	1.892	1.415	1.265	1.6	0	BORAL	0.026	2.83		21.8	0.9962	0.0012
PNL-115	4 9X12 Arrays	4.31	1.892	1.415	1.265	1.6	0	Aluminum	0	2.83		22.3	0.9937	0.0013
PNL-064	4 9X12 Arrays	4.31	1.892	1.415	1.265	1.6	0	Steel (.302)	0	2.83		22.2	0.9942	0.0012
PNL-071	4 9X12 Arrays	4.31	1.892	1.415	1.265	1.6	0	Steel (.485)	0	2.83		22.2	0.9968	0.0012
												Average	0.9948	0.0020

Table 6.5.1-1   KENO-Va and 27-Group Library Validation Statistics (Continued)

Criticals	Configuration	wt % 235U	Pitch (cm)	Pellet OD (cm)	Clad OD (cm)	H/U	Sol. B (ppm)	Poison	g 10B/cm²	Gap(cm)	Gap Den.	Ave. Gfis	Keff	ks
Set 3										Cluster	Wall/Cluster			
PNL-STA	3X1 St Refl.	2.35	2.032	1.1176	1.27	2.9	0	na	na	10.65	0.00	23.5	0.9964	0.0010
PNL-STB	3X1 St Refl.	2.35	2.032	1.1176	1.27	2.9	0	na	na	11.20	1.32	23.6	0.9944	0.0010
PNL-STC	3X1 St Refl.	2.35	2.032	1.1176	1.27	2.9	0	na	na	10.36	2.62	23.6	0.9905	0.0010
PNL-PBA	3X1 Pb Refl.	2.35	2.032	1.1176	1.27	2.9	0	na	na	13.84	0.00	23.5	0.9960	0.0011
PNL-PBB	3X1 Pb Refl.	2.35	2.032	1.1176	1.27	2.9	0	na	na	13.72	0.66	23.5	0.9978	0.0010
PNL_PBC	3X1 Pb Refl.	2.35	2.032	1.1176	1.27	2.9	0	na	na	11.25	2.62	23.6	0.9925	0.0010
PNL-DUA	3X1 DU Refl.	2.35	2.032	1.1176	1.27	2.9	0	na	na	11.83	0.00	22.6	0.9903	0.0009
PNL-DUB	3X1 DU Refl.	2.35	2.032	1.1176	1.27	2.9	0	na	na	14.11	1.96	22.8	0.9957	0.0010
PNL-DUC	3X1 DU Refl.	2.35	2.032	1.1176	1.27	2.9	0	na	na	13.70	2.62	22.9	0.9911	0.0010
PNL-H20	3X1 H2O Refl	4.31	2.54	1.265	1.415	3.9	0	na	na	8.24	inf	23.3	0.9877	0.0023
PNL-ST0	3X1 St Refl.	4.31	2.54	1.265	1.415	3.9	0	na	na	12.89	0	23.2	0.9993	0.0012
PNL-ST1	3X1 St Refl.	4.31	2.54	1.265	1.415	3.9	0	na	na	14.12	1.32	23.3	1.0060	0.0022
PNL-ST26	3X1 St Refl.	4.31	2.54	1.265	1.415	3.9	0	na	na	12.44	2.62	23.3	0.9965	0.0011
PNL-PB0	3X1 Pb Refl.	4.31	2.54	1.265	1.415	3.9	0	na	na	20.62	0	23.2	1.0068	0.0021
PNL-PB13	3X1 Pb Refl.	4.31	2.54	1.265	1.415	3.9	0	na	na	19.04	1.32	23.3	1.0038	0.0012
PNL-PB5	3X1 Pb Refl.	4.31	2.54	1.265	1.415	3.9	0	na	na	10.3	5.41	23.3	0.9889	0.0011
PNL-DU0	3X1 DU Refl.	4.31	2.54	1.265	1.415	3.9	0	na	na	15.38	0	21.8	0.9959	0.0011
PNL-DU13	3X1 DU Refl.	4.31	2.54	1.265	1.415	3.9	0	na	na	19.04	1.32	22.1	1.0067	0.0010
PNL-DU39	3X1 DU Refl.	4.31	2.54	1.265	1.415	3.9	0	na	na	18.05	3.91	22.5	1.0005	0.0011
PNL-DU54	3X1 DU Refl.	4.31	2.54	1.265	1.415	3.9	0	na	na	13.49	5.41	22.6	0.9908	0.0011
												Average	0.9964	0.0060

Table 6.5.1-1   KENO-Va and 27-Group Library Validation Statistics (Continued)

Criticals	Configuration	wt % 235U	Pitch (cm)	Pellet OD (cm)	Clad OD (cm)	H/U	Sol. B (ppm)	Poison	g 10B/cm²	Gap(cm)	Gap Den.	Ave. Gfis	Keff	ks
Set 4														
PNL-229	2x2 Flux Trap	4.31	1.89	1.265	1.415	1.6	0	Aluminum	0	3.81	0.9982	22.4	0.9989	0.0012
PNL-230	2x2 Flux Trap	4.31	1.89	1.265	1.415	1.6	0	BORAL	0.05	3.75	0.9982	21.7	0.9921	0.0012
PNL-228	2x2 Flux Trap	4.31	1.89	1.265	1.415	1.6	0	BORAL	0.13	3.73	0.9982	21.7	0.9911	0.0012
PNL-214	2x2 Flux Trap	4.31	1.89	1.265	1.415	1.6	0	BORAL	0.36	3.73	0.9982	21.7	0.9968	0.0013
PNL-231	2x2 Flux Trap	4.31	1.89	1.265	1.415	1.6	0	BORAL	0.45	3.71	0.9982	21.7	0.9938	0.0012
PNL-127	2x1 Flux Trap	4.31	1.89	1.265	1.415	1.6	0	BORAL	0.026	0.64	0.9982	21.8	0.9934	0.0010
PNL-126	2x1 Flux Trap	4.31	1.89	1.265	1.415	1.6	0	BORAL	0.026	1.54	0.9982	21.8	0.9931	0.0010
PNL-123	2x1 Flux Trap	4.31	1.89	1.265	1.415	1.6	0	BORAL	0.026	3.80	0.9982	21.8	0.9943	0.0010
PNL-125	2x1 Flux Trap	4.31	1.89	1.265	1.415	1.6	0	BORAL	0.026	5.16	0.9982	21.8	0.9932	0.0010
PNL-124	2x1 Flux Trap	4.31	1.89	1.265	1.415	1.6	0	BORAL	0.026	INF	0.9982	21.8	0.9949	0.0010
PNL-123-S	2x1 Flux Trap	4.31	1.89	1.265	1.415	1.6	0	Steel	0	3.80	0.9982	22.1	0.9920	0.0010
PNL-124-S	2x1 Flux Trap	4.31	1.89	1.265	1.415	1.6	0	Steel	0	INF	0.9982	21.9	0.9962	0.0010
												Average	0.9941	0.0022
Set 5										Gap(cm)	Gap Den.			
VCML	2x2 Water Gap	4.74	1.35	0.79	0.94	2.3	0	na	na	1.90	0	22.0	0.9922	0.0013
VCML	2x2 Water Gap	4.74	1.35	0.79	0.94	2.3	0	na	na	1.90	0.0323	22.0	0.9889	0.0013
VCML	2x2 Water Gap	4.74	1.35	0.79	0.94	2.3	0	na	na	1.90	0.2879	22.1	0.9957	0.0013
VCML	2x2 Water Gap	4.74	1.35	0.79	0.94	2.3	0	na	na	1.90	0.5540	22.2	1.0053	0.0011
VCML	2x2 Water Gap	4.74	1.35	0.79	0.94	2.3	0	na	na	2.50	0.9982	22.3	0.9955	0.0012
VCML	2x2 Water Gap	4.74	1.35	0.79	0.94	2.3	0	na	na	5.00	0.9982	22.5	0.9948	0.0013
VCML	Square Lattice	4.74	1.26	0.79	0.94	1.8	0	na	na	na	na	22.2	0.9958	0.0012
VCML	Square Lattice	4.74	1.35	0.79	0.94	2.3	0	na	na	na	na	22.0	0.9952	0.0012
VCML	Square Lattice	4.74	1.60	0.79	0.94	3.8	0	na	na	na	na	23.3	0.9989	0.0013
VCML	Square Lattice	4.74	2.10	0.79	0.94	7.6	0	na	na	na	na	24.0	0.9974	0.0012
VCML	Square Lattice	4.74	2.52	0.79	0.94	11.5	0	na	na	na	na	24.2	0.9977	0.0011
												Average	0.9961	0.0041

6.5.2 CSAS25 Criticality Benchmarks for Research Reactor Fuel Elements (MTR and DIDO)

In this section, the CSAS25 SCALE criticality analysis sequence is validated for use with high enrichment uranium (HEU), 80-90 wt % ^{235}U based, research reactor fuel. Not included in this validation section is Zirconium hydride based (TRIGA) fuel. This validation provides an estimate of the method bias and uncertainty to be applied in setting criticality safety limits for the NAC-LWT with MTR and DIDO fuel elements. Spiral type fuel and MOATA plate bundles are composed of MTR type fuel elements (flat or curved metallic plates with a uranium-aluminum alloy fuel meat within an aluminum clad). Bias established for the MTR and DIDO fuels is, therefore, applicable to the spiral fuel assemblies and plate bundles.

A subset of high enrichment critical experiments is selected from (Jordan) and (Johnson). (Johnson) contains detailed critical experiments with SPERT-D MTR plate fuel. The selected experiments are described in more detail below.

Five sets of critical experiments were selected from (Jordan). The first set included five experiments with various uranyl nitrate solutions in an unreflected cylindrical aluminum tank. Criticality was achieved by varying concentration, solution level or tank diameter. The second set included four experiments, which utilized the same solutions and tanks, but surrounded the tank with rectangular plexiglass reflector. The third set included seven experiments with various unreflected and reflected metal shapes. The fourth set included five experiments with various unreflected and reflected arrays of uranium metal cylinders in which criticality was achieved by spacing between arrays. The fifth set included four experiments with rectangular uranyl fluoride solution tanks made of aluminum in which criticality was achieved by adjusting tank spacing and solution height.

Five critical experiments were selected from (Johnson). The experiments selected were 4x4 arrays of MTR fuel plate type elements in which criticality was studied versus spacing between fuel elements. Criticality was achieved by setting up a 4x4 array with the given spacing and loading the outer row of fuel elements with a partial loading of fuel plates. The maximum loading of fuel plates in an element was 22. In order to preserve rectangular geometry, each partial element in a row contained the same number of fuel plates, ± 1 plate.

The results for the thirty cases executed on NAC's version of CSAS25 are shown in Table 6.5.1-1. The average, standard deviation, average Monte Carlo error, method bias and method uncertainty are evaluated as follows:

Average: $\bar{k} = \dfrac{1}{30}\sum_{I}^{30} k_i = 1.0044$

Raw Standard Deviation: $\sigma = \sqrt{\dfrac{1}{29}\sum_{I}^{30}(k_i - \bar{k})} = \pm\,0.0089$

Average Monte Carlo Error: $\sigma_{mc} = \sqrt{\dfrac{1}{30}\sum_{I}^{30}\sigma_i} = \pm\,0.0037$

Method Bias: $\Delta k_{bias} = 1 - \bar{k} = -0.0044$

Method Uncertainty: $\Delta k_{BU} = \sqrt{\sigma^2 - \sigma_{mc}^2} = \pm\,0.0081$

95/95 One Sided Factor for 30 Cases: 2.23 (Owen)
95/95 Method Uncertainty: 2.23 * 0.0081 = 0.0181

These statistical results lead to the following equation for calculating criticality safety limits:

$$k_s = k_{nom} - 0.0044 + 0.0181 + 2\sigma_{mc}$$

   where:

k_{nom} is the k_{eff} of the KENO-Va calculation

Δk_{BU} is the uncertainty associated with the benchmark calculations

σ_{mc} is the KENO-Va Monte Carlo Error associated with the calculated k_{eff} value

After conservatively neglecting the negative bias associated with the overprediction in k_{eff} produced by KENO-Va for these cases, the equation becomes:

$$k_s = k_{nom} + 0.0181 + 2\sigma_{mc}$$

No specific benchmarks are available for DIDO fuel assemblies. Since the fuel cylinders for the DIDO assembly are comprised of fuel plates similar in composition to those of the MTR element, the validation for the MTR element is considered to be applicable to the DIDO assembly.

Table 6.5.2-1   Criticality Results for High Enrichment Uranium Systems

Case	Geometry	Composition/ wt % ^{235}U	$k_{eff} \pm \sigma$
1	28 cm Cylindrical Tank 142.92 gU/l Solution	$UO_2(NO_3)_2$ 93.172	1.0238 ± 0.0042
2	28 cm Cylindrical Tank 357.71 gU/l Solution	$UO_2(NO_3)_2$ 93.172	1.0225 ± 0.0042
3	33 cm Cylindrical Tank 54.98 gU/l Solution	$UO_2(NO_3)_2$ 93.172	1.0037 ± 0.0034
4	33 cm Cylindrical Tank 137.4 gU/l Solution	$UO_2(NO_3)_2$ 93.172	1.0007 ± 0.0042
5	33 cm Cylindrical Tank 357.71 gU/l Solution	$UO_2(NO_3)_2$ 93.172	1.0031 ± 0.0040
6	28 cm Cyl. Plexi. Refl. 147.66 gU/l Solution	$UO_2(NO_3)_2$ 93.172	1.0114 ± 0.0043
7	28 cm Cyl. Plexi. Refl. 345.33 gU/l Solution	$UO_2(NO_3)_2$ 93.172	1.0094 ± 0.0040
8	33 cm Cyl. Plexi. Refl. 147.66 gU/l Solution	$UO_2(NO_3)_2$ 93.172	1.0082 ± 0.0038
9	33 cm Cyl. Plexi. Refl. 345.33 gU/l Solution	$UO_2(NO_3)_2$ 93.172	1.0090 ± 0.0048
10	17.4 cm Sphere	U Metal 93.8	1.0056 ± 0.0029
11	20.3 cm Cylinder Annulus	U-Mo Alloy 93.2	1.0048 ± 0.0026
12	70 cm Sphere	UO_2F_2 Solution 93.2	1.0016 ± 0.0021
13	64 cm Cylinder U/Graphite Annulus	U Metal/Graphite 93.2	1.0167 ± 0.0030
14	7.62 x 8.89 x 15.24 cm³ Cuboid, Nat U Refl.	U Metal 94	1.0088 ± 0.0038
15	12.7 cm Hemisphere H_2O Reflector	U Metal 93.5	1.0053 ± 0.0030
16	13 cm Sphere H_2O Reflector	U Metal 97.67	1.0002 ± 0.0033

Table 6.5.2-1   Criticality Results for High Enrichment Uranium Systems (Continued)

Case	Geometry	Composition/ wt % ^{235}U	$K_{eff} \pm \sigma$
17	11.5 cm Cylinders 4x4x4 Array	U Metal 93.2	0.9937 ± 0.0028
18	11.5 cm Cylinders 2x2x2 Array	U Metal 93.2	1.0038 ± 0.0029
19	9.1 cm Cylinders 2x2x2 Array Paraf Refl	U Metal 93.2	1.0072 ± 0.0035
20	11.5 cm Cylinders 2x2x2 Array Paraf Refl	U Metal 93.2	1.0047 ± 0.0027
21	11.5 cm Cylinders 2x2x2 Array Paraf Refl	U Metal 93.2	1.0134 ± 0.0030
22	U Sol. Slabs bet. Al 3x1x1 Array 0 Sep.	UO_2F_2 Solution 93.2	1.0055 ± 0.0037
23	U Sol. Slabs bet. Al 3x1x1 2.54 cm Sep.	UO_2F_2 Solution 93.2	0.9866 ± 0.0036
24	U Sol. Slabs bet. Al 3x1x1 7.62 cm Sep.	UO_2F_2 Solution 93.2	0.9806 ± 0.0040
25	U Sol. Slabs bet. Al 3x1x1 11.43 cm Sep.	UO_2F_2 Solution 93.2	0.9939 ± 0.0044
26	22 U-Al Plates 4x4 Array 0.0" Spacing	U-Al Metal 93.17	1.0049 ± 0.0042
27	22 U-Al Plates 4x4 Array .25" Spacing	U-Al Metal 93.17	0.9980 ± 0.0038
28	22 U-Al Plates 4x4 Array .50" Spacing	U-Al Metal 93.17	1.0060 ± 0.0045
29	22 U-Al Plates 4x4 Array .75" Spacing	U-Al Metal 93.17	0.9979 ± 0.0041
30	22 U-Al Plates 4x4 Array 1.00" Spacing	U-Al Metal 93.17	1.0024 ± 0.0044

6.5.3   CSAS25 Criticality Benchmarks for TRIGA Fuel Elements

Three core configurations presented in the TRIGA MARK II Benchmark (Mele) were modeled with KENO-Va and the 27 Group ENDF/B-IV neutron cross section library to establish the KENO-Va. bias as part of the SCALE 4.3 package for use on TRIGA fuel elements. The core analyzed is an LEU (low enriched fuel, 20%) fueled core. Due to the relatively high ^{235}U density in the fuel element, the trend of this analysis is expected to be similar for the HEU (high enriched uranium, 70 wt% ^{235}U) elements. The results are summarized below.

Configuration	keff $\pm$ σ
Core 132	1.01892 $\pm$ 0.00126
Core 133	1.02206 $\pm$ 0.00125
Core 134	1.01774 $\pm$ 0.00129
Average $\pm$ σ	1.0196 $\pm$ 0.0022

Thus, the bias for these critical experiments is an approximate 2% over-prediction. This over-prediction will be conservatively ignored in the k_s calculations. The 95/95 Uncertainty Factor from [Owen] for 3 data points is 7.656. Therefore, the uncertainty factory to be applied in the k_s calculation is the standard deviation from the critical experiments multiplied by the 95/95 factor for 3 data points, or 7.656 × 0.0022 = 0.0168.

A review of the calculations performed for the benchmark experiments shows that the average energy causing fission is approximately 0.05 eV. The average energy causing fission for the wet base case is 0.0999 eV, while for the dry base case it is 0.415 eV. Because the benchmark calculation and TRIGA 24 fissions occur at energies below 1 eV, it is reasonable to assume that the benchmarks are applicable to these cases.

In the case of the TRIGA fuel criticality evaluations, the basic form for the application of bias and uncertainty is:

$$k_s = k_{mc} + \Delta k_{Meth\,Bias} + \Delta k_{Benchmark\,Uncertainty} + \Delta k_{Basket\,Tolerances} + 2\sigma_{mc}$$

where:

k_{mc} - CSAS reported reactivity

$\Delta k_{Meth\,Bias}$ - Method bias for TRIGA Fuel from benchmark calculations

$\Delta k_{Benchmark\,Uncertainty}$ - Uncertainty associated with the TRIGA benchmark calculations

$\Delta k_{Basket\,Tolerances}$ - Mechanical biases associated with the basket and fuel configuration

σ_{mc} - Uncertainty associated with the CSAS reported reactivity

Based on benchmark information, the k_s equation is written as follows:

$$k_s = k_{mc} + 0.0 + 0.0168 + \Delta k_{Basket\,Tolerances} + 2\sigma_{mc}$$

If the worst case fuel element and basket configuration are used, the above equation reduces to:

$$k_s = k_{mc} + 0.0168 + 2\sigma_{mc}$$

6.5.4   MCNP Criticality Benchmarks LEU Oxide and MOX LWR Fuels

The results of the criticality analyses presented in this chapter must be compared to the upper subcritical limit (USL). The USL accounts for bias and uncertainty resulting from the method using information obtained from the analysis of criticality benchmark experimental data.

Criticality code validation is performed for the Monte Carlo evaluation code and neutron cross-section libraries. Criticality validation is required by the criticality safety standard ANSI/ANS-8.1.

6.5.4.1   Benchmark Experiments and Applicability Discussion

NUREG/CR-6361, "Criticality Benchmark Guide for Light-Water-Reactor Fuel in Transportation and Storage Packages" (NUREG), provides a guide to LWR criticality benchmark calculations and the determination of bias and subcritical limits in critical safety evaluations. In Section 2 of the NUREG, a series of LWR critical experiments is described in sufficient detail for independent modeling. In Section 3, the critical experiments are modeled, and the results (k_{eff} values) are presented. The method utilized in the NUREG is KENO-Va with the 44-group ENDF/B-V cross-section library embedded in SCALE 4.3. In Section 4, a guide for the determination of bias and subcritical safety limits is provided based on ANSI/ANS-8.1 and statistical analysis of the trending in the bias. Finally, guidelines for experiment selection and applicability are presented in Section 5. The approach outlined in Section 4 of the NUREG is described in detail herein and is implemented for MCNP5 with continuous energy ENDF/B-VII cross-sections.

NUREG/CR-6361 implements ANSI/ANS-8.1 criticality safety criterion as follows.

$$k_s \leq k_c - \Delta k_s - \Delta k_c - \Delta k_m \quad \text{(Equation 1)}$$

where:

k_s = calculated allowable maximum multiplication factor, k_{eff}, of the system being evaluated for all normal or credible abnormal conditions or events.

k_c = mean k_{eff} that results from a calculation of benchmark criticality experiments using a particular calculation method. If the calculated k_{eff} values for the criticality experiments exhibit a trend with an independent parameter, then k_c shall be determined by extrapolation based on best fit to calculated values. Criticality experiments used as benchmarks in computing k_c should have physical compositions, configurations and nuclear characteristics (including reflectors) similar to those of the system being evaluated.

Δk_s = allowance for the following:

- statistical or convergence uncertainties, or both, in computation of k_s

- material and fabrication tolerances
- geometric or material representations used in computational method

Δk_c = margin for uncertainty in kc, which includes allowance for the following:

- uncertainties in critical experiments
- statistical or convergence uncertainties, or both, in computation of k_c
- uncertainties resulting from extrapolation of k_c outside range of experimental data
- uncertainties resulting from limitations in geometrical or material representations used in the computational method

Δk_m = arbitrary administrative margin to ensure subcriticality of ks

The various uncertainties are combined statistically if they are independent. Correlated uncertainties are combined by addition.

Equation 1 can be rewritten as shown.

$$k_s \leq 1 - \Delta k_m - \Delta k_s - (1 - k_c) - \Delta k_c \quad \text{(Equation 2)}$$

Noting that the definition of the bias is $\beta = 1 - k_c$, Equation 2 can be written as shown.

$$k_s + \Delta k_s \leq 1 - \Delta k_m - \beta - \Delta\beta \quad \text{(Equation 3)}$$

where:

$$\Delta\beta = \Delta k_c$$

Thus, the maximum allowable value for k_{eff} plus uncertainties in the system being analyzed must be below 1 minus an administrative margin (typically 0.05), which includes the bias and the uncertainty in the bias. This can also be written as shown.

$$k_s + \Delta k_s \leq \text{Upper Subcritical Limit (USL)} \quad \text{(Equation 4)}$$

where:

$$USL \equiv 1 - \Delta k_m - \beta - \Delta\beta \quad \text{(Equation 5)}$$

This is the USL criterion as described in Section 4 of NUREG/CR-6361. Two methods are prescribed for the statistical determination of the USL. The "Confidence Band with Administrative Margin (USL-1)" approach is implemented here and is referred to generically as USL. A $\Delta k_m = 0.05$ and a lower confidence band are specified based on a linear regression of k_{eff} as a function of some system parameter. As recommended in NUREG/CR-6361, a simple linear regression is performed on each system parameter, and the line with the greatest correlation is used to functionalize β.

Application specific sections (e.g., low enriched uranium, MOX) contains the list of criticality benchmarks employed in the validation of MCNP with its continuous energy neutron cross-

section libraries and the processing of the experimental results into the USL. Included in the subsequent sections are linear fits of reactivity (k_{eff}) to each of the system parameters. Experiments were chosen to reflect the fuel geometry and materials as closely as available.

6.5.4.2   LEU (Maximum 5 wt % ^{235}U in UO$_2$) Results of Benchmark Calculations

The range of parameters included in the low enriched uranium (LEU) benchmarks is shown in Table 6.5.4-1. Experiments are chosen to reflect the fuel evaluated for shipment. This includes the use of arrays of low enriched uranium oxide fuel rods with light water moderation. To cover potential borated water conditions within spent fuel pools or absorbers placed into the basket experiments with criticality control by spacing, borated moderator and/or borated absorber panels and tubes are included in the benchmarks effort. Trending in k_{eff} was evaluated for the following independent variables: wt % ^{235}U, rod pitch, H/U volume ratio, energy of the average neutron lethargy causing fission (EALCF), ^{10}B loading of the absorber sheet, and soluble boron loading. No statistically significant trends were found for any of the system parameters. USLs are, therefore, generated for each of the independent variables. A minimum USL covering the range of applicability of the benchmark set is determined.

To evaluate the relative importance of the trend analysis to the upper subcritical limits, correlation coefficients are required for all independent parameters. The linear correlation coefficient, R, is calculated by taking the square root of the R^2 value. In particular, the correlation coefficient, R, is a measure of the linear relationship between k_{eff} and a critical experiment parameter. If R is +1, a perfect linear relationship with a positive slope is indicated. If R is -1, a perfect linear relationship with a negative slope is indicated. When R is 0, no linear relationship is indicated.

Table 6.5.4-2 contains the correlation coefficient, R, for each linear fit of k_{eff} versus experimental parameter. Linear fits and correlation constants are based on the 183 data-point evaluation sets plotted in Section 6.5.4.3. The cluster gap plot is limited to the 137 data points for experiments containing multiple fuel rod clusters. Single fuel rod cluster experiments documented in LEU-COMP-THERM sets 06, 14, 35 and 50, in addition to LEU-COMP-THERM experiments 01-01, 02-01 to -03, and 08-01 to -15, were, therefore, excluded from the cluster gap study. The 183 data points evaluated for the remaining parameters represent the complete set of experiments listed in Section 6.5.4.3 minus the three high energy lethargy experiments above 0.35 eV (Experiments LEU-COMP-THERM 14-05, -06 and -07). The addition of these points, while not resulting in a significant linear fit, produces a noticeable slope to the USL correlation not representative of the remaining data fits. As this increased slope results in a higher USL, it is acceptable to discard these data points. The three higher energy points are removed from all independent variables for consistency.

As there is no significant correlation to any of the independent variables, the USL for each independent variable is calculated and shown with its range of applicability in Table 6.5.4-2. A sample output for EALCF is shown in Figure 6.5.4-1. Uncertainties included in the USLSTATS evaluation are the Monte Carlo uncertainty associated with the reactivity calculation and experimental uncertainty that was provided in the literature for each of the cases.

Based on all the independent variable correlations, a lower limit constant USL of 0.9376 may be applied. The range of applicability (area of applicability) of this limit may be extended to 5 wt % enriched fuel, as the correlation shows no significant trend with enrichment between 2.35 and 4.74 wt %, and that the limited trending observed increases the USL. Extending the range of applicability for the average neutron lethargy is based on a minimal, but positive, trend of the USL versus EALCF. Studies, including additional data points up to 0.7722 eV, indicate that the trending continues to the higher energy levels.

Figure 6.5.4-1   LEU USLSTATS Output for EALCF

```
++++++++++++++++++++++++++++++++++++++++++++++++++++++++++++++++++++++++++++
                  Version 1.4, April 23, 2003
                  Oak Ridge National Laboratory
++++++++++++++++++++++++++++++++++++++++++++++++++++++++++++++++++++++++++++
    Input to statistical treatment from file:enrich-183.in
Title: keff vs enrichment
    Proportion of the population = .995
    Confidence of fit          = .950
    Confidence on proportion   = .950
    Number of observations     = 183
    Minimum value of closed band =   0.00
    Maximum value of closed band =   0.00
    Administrative margin        =   0.05
```

independent variable - x	dependent variable - y	deviation in y	independent variable - x	dependent variable - y	deviation in y
2.35000E+00	9.94910E-01	3.42000E-03	2.35000E+00	9.95090E-01	3.46000E-03
2.35000E+00	9.92830E-01	3.38000E-03	2.35000E+00	9.92520E-01	3.47000E-03
2.35000E+00	9.98060E-01	3.38000E-03	2.35000E+00	9.95620E-01	3.50000E-03
2.35000E+00	9.96550E-01	3.42000E-03	2.35000E+00	9.93130E-01	3.55000E-03
2.35000E+00	9.89310E-01	3.44000E-03	2.35000E+00	9.98130E-01	3.58000E-03
2.35000E+00	9.95340E-01	3.41000E-03	2.35000E+00	9.96700E-01	3.56000E-03
2.35000E+00	9.93880E-01	3.44000E-03	2.35000E+00	9.93830E-01	3.55000E-03
2.35000E+00	9.89690E-01	3.36000E-03	2.35000E+00	9.92770E-01	3.47000E-03
4.30600E+00	9.95160E-01	2.79000E-03	2.35000E+00	9.92920E-01	3.50000E-03
4.30600E+00	9.93670E-01	2.54000E-03	2.35000E+00	9.96410E-01	3.46000E-03
4.30600E+00	9.96340E-01	2.76000E-03	2.35000E+00	9.93060E-01	3.49000E-03
4.30600E+00	9.93110E-01	2.64000E-03	2.35000E+00	9.96500E-01	3.45000E-03
4.30600E+00	9.93000E-01	2.49000E-03	2.35000E+00	9.94680E-01	3.50000E-03
2.59600E+00	9.92680E-01	2.10000E-03	2.35000E+00	9.93300E-01	3.47000E-03
2.59600E+00	9.93190E-01	2.14000E-03	2.35000E+00	9.91810E-01	3.46000E-03
2.59600E+00	9.92990E-01	2.13000E-03	2.35000E+00	9.93920E-01	3.47000E-03
2.59600E+00	9.94790E-01	2.13000E-03	2.35000E+00	9.95560E-01	3.55000E-03
2.59600E+00	9.93100E-01	2.13000E-03	2.35000E+00	9.94540E-01	3.51000E-03
2.59600E+00	9.93240E-01	2.13000E-03	2.35000E+00	9.94490E-01	3.47000E-03
2.59600E+00	9.91990E-01	2.12000E-03	2.35000E+00	9.91300E-01	3.52000E-03
2.59600E+00	9.93820E-01	2.12000E-03	2.35000E+00	9.94800E-01	3.47000E-03
2.59600E+00	9.94450E-01	2.12000E-03	2.35000E+00	9.93500E-01	3.60000E-03
2.59600E+00	9.95440E-01	2.13000E-03	2.35000E+00	9.94000E-01	3.45000E-03
2.59600E+00	9.94410E-01	2.12000E-03	2.35000E+00	9.96280E-01	3.53000E-03
2.59600E+00	9.93930E-01	2.15000E-03	2.35000E+00	9.92620E-01	3.45000E-03
2.59600E+00	9.95090E-01	2.14000E-03	2.35000E+00	9.94100E-01	3.53000E-03
2.59600E+00	9.93780E-01	2.12000E-03	2.35000E+00	9.96470E-01	3.52000E-03
2.59600E+00	9.95040E-01	2.14000E-03	2.35000E+00	9.93600E-01	3.47000E-03
2.59600E+00	9.94380E-01	2.11000E-03	2.35000E+00	9.97020E-01	3.49000E-03
2.59600E+00	9.95730E-01	2.12000E-03	2.35000E+00	9.94970E-01	3.50000E-03
2.59600E+00	9.94270E-01	2.14000E-03	2.35000E+00	9.91950E-01	3.55000E-03
2.45900E+00	9.98350E-01	1.34000E-03	2.59600E+00	9.93410E-01	1.93000E-03
2.45900E+00	9.96860E-01	1.36000E-03	2.59600E+00	9.91310E-01	2.05000E-03
2.45900E+00	9.99310E-01	1.24000E-03	4.73800E+00	9.95860E-01	4.36000E-03
2.45900E+00	9.97950E-01	1.36000E-03	4.73800E+00	9.93580E-01	4.53000E-03
2.45900E+00	9.97650E-01	1.38000E-03	4.73800E+00	9.95390E-01	4.58000E-03
2.45900E+00	9.96990E-01	1.35000E-03	4.73800E+00	9.92370E-01	4.54000E-03
2.45900E+00	9.97230E-01	1.37000E-03	4.73800E+00	9.91440E-01	4.62000E-03
2.45900E+00	9.96590E-01	1.40000E-03	4.73800E+00	9.98780E-01	4.82000E-03
2.45900E+00	9.95260E-01	1.40000E-03	4.73800E+00	9.94180E-01	4.94000E-03
2.45900E+00	9.97450E-01	1.36000E-03	4.73800E+00	9.92400E-01	4.90000E-03
2.45900E+00	9.97590E-01	1.38000E-03	4.73800E+00	9.96930E-01	4.98000E-03
2.45900E+00	9.97650E-01	1.36000E-03	4.73800E+00	9.91370E-01	5.05000E-03
2.45900E+00	9.98850E-01	1.39000E-03	2.35000E+00	9.92500E-01	2.34000E-03
2.45900E+00	9.97350E-01	1.37000E-03	2.35000E+00	9.95140E-01	2.43000E-03
2.45900E+00	9.97580E-01	1.39000E-03	2.35000E+00	9.92190E-01	2.33000E-03
2.45900E+00	9.97720E-01	1.39000E-03	2.35000E+00	9.94760E-01	2.40000E-03
2.45900E+00	9.96910E-01	1.35000E-03	2.35000E+00	9.94690E-01	3.67000E-03
4.30600E+00	9.95480E-01	2.84000E-03	2.35000E+00	9.94340E-01	2.49000E-03
4.30600E+00	9.93430E-01	2.78000E-03	2.35000E+00	9.93190E-01	2.39000E-03
4.30600E+00	9.93300E-01	2.81000E-03	4.73800E+00	9.93300E-01	1.28000E-03
4.30600E+00	9.93710E-01	2.85000E-03	4.73800E+00	9.93400E-01	1.23000E-03
4.30600E+00	9.95930E-01	2.73000E-03	4.73800E+00	9.94890E-01	1.25000E-03
4.30600E+00	9.92950E-01	2.85000E-03	4.73800E+00	9.93190E-01	1.25000E-03
4.30600E+00	9.96160E-01	2.89000E-03	4.73800E+00	9.93060E-01	1.28000E-03
4.30600E+00	9.93890E-01	2.73000E-03	2.45900E+00	9.91330E-01	2.03000E-03
4.30600E+00	9.95710E-01	2.96000E-03	2.45900E+00	9.95970E-01	2.43000E-03
4.30600E+00	9.93190E-01	2.60000E-03	2.45900E+00	9.95550E-01	2.42000E-03
4.30600E+00	9.93780E-01	2.75000E-03	2.45900E+00	9.94860E-01	2.42000E-03
4.30600E+00	9.92630E-01	2.84000E-03	2.45900E+00	9.95040E-01	2.42000E-03
4.30600E+00	9.95660E-01	2.75000E-03	2.45900E+00	9.95420E-01	2.42000E-03
4.30600E+00	9.94310E-01	2.82000E-03	2.45900E+00	9.95300E-01	2.42000E-03

Figure 6.5.4-1   LEU USLSTATS Output for EALCF (cont'd)

```
4.30600E+00    9.96390E-01    2.95000E-03         2.45900E+00    9.95070E-01    2.42000E-03
4.30600E+00    9.96860E-01    2.79000E-03         2.45900E+00    9.93680E-01    1.93000E-03
4.30600E+00    9.97160E-01    2.68000E-03         2.45900E+00    9.92100E-01    1.93000E-03
4.30600E+00    9.92370E-01    2.86000E-03         2.45900E+00    9.94470E-01    1.93000E-03
4.30600E+00    9.97190E-01    2.81000E-03         2.45900E+00    9.90730E-01    1.93000E-03
4.30600E+00    9.94340E-01    2.76000E-03         2.45900E+00    9.86520E-01    2.23000E-03
4.30600E+00    9.96920E-01    2.79000E-03         2.45900E+00    9.86340E-01    1.93000E-03
4.30600E+00    9.96060E-01    2.83000E-03         2.45900E+00    9.90420E-01    2.42000E-03
4.30600E+00    9.97400E-01    2.94000E-03         2.45900E+00    9.89740E-01    2.03000E-03
4.30600E+00    9.92810E-01    2.69000E-03         2.45900E+00    9.91520E-01    2.72000E-03
4.30600E+00    9.92560E-01    2.88000E-03         2.45900E+00    9.90290E-01    2.13000E-03
4.30600E+00    9.93650E-01    2.88000E-03         2.45900E+00    9.89270E-01    1.93000E-03
4.30600E+00    9.94970E-01    2.85000E-03         2.60000E+00    9.95710E-01    1.42000E-03
2.45900E+00    9.94820E-01    3.21000E-03         2.60000E+00    9.96180E-01    1.42000E-03
2.45900E+00    9.94940E-01    3.21000E-03         2.60000E+00    9.95340E-01    1.52000E-03
2.45900E+00    9.95140E-01    3.21000E-03         2.60000E+00    9.95470E-01    1.52000E-03
2.45900E+00    9.95640E-01    3.21000E-03         2.60000E+00    9.96910E-01    1.42000E-03
2.45900E+00    9.95080E-01    3.21000E-03         2.60000E+00    9.96140E-01    1.42000E-03
2.45900E+00    9.95260E-01    3.21000E-03         2.60000E+00    9.95890E-01    1.42000E-03
2.45900E+00    9.95200E-01    3.21000E-03         2.60000E+00    9.96240E-01    1.62000E-03
4.30600E+00    9.94020E-01    1.92000E-03         2.60000E+00    9.96670E-01    1.52000E-03
4.30600E+00    9.94460E-01    1.91000E-03         2.60000E+00    9.96760E-01    1.62000E-03
4.30600E+00    9.93550E-01    1.91000E-03         2.60000E+00    9.96370E-01    1.62000E-03
4.30600E+00    9.94010E-01    1.91000E-03         2.60000E+00    9.96430E-01    1.72000E-03
4.30600E+00    9.92810E-01    3.27000E-03         2.60000E+00    9.97010E-01    1.62000E-03
4.30600E+00    9.94960E-01    1.91000E-03         2.60000E+00    9.96500E-01    1.62000E-03
4.30600E+00    9.93780E-01    1.90000E-03         2.60000E+00    9.96340E-01    1.62000E-03
4.30600E+00    9.96680E-01    1.95000E-03         2.60000E+00    9.96580E-01    1.71000E-03
4.30600E+00    9.85950E-01    7.71000E-03         2.60000E+00    9.96450E-01    1.62000E-03
2.35000E+00    9.94940E-01    3.54000E-03
chi =  2.5464 (upper bound = 9.49). The data tests normal.
        Output from statistical treatment
keff vs enrichment
 Number of data points (n)                      183
 Linear regression, k(X)                        0.9950 + (-1.5719E-04)*X
 Confidence on fit (1-gamma) [input]            95.0%
 Confidence on proportion (alpha) [input]       95.0%
 Proportion of population falling above
 lower tolerance interval (rho) [input]         99.5%
 Minimum value of X                             2.3500E+00
 Maximum value of X                             4.7380E+00
 Average value of X                             3.0597E+00
 Average value of k                              0.99453
 Minimum value of k                              0.98595
 Variance of fit, s(k,X)^2                      5.0408E-06
 Within variance, s(w)^2                        7.8633E-06
 Pooled variance, s(p)^2                        1.2904E-05
 Pooled std. deviation, s(p)                    3.5922E-03
 C(alpha,rho)*s(p)                              1.5554E-02
 student-t @ (n-2,1-gamma)                      1.64500E+00
 Confidence band width, W                       5.9793E-03
 Minimum margin of subcriticality, C*s(p)-W     9.5746E-03

 Upper subcritical limits: (  2.3500     <= X <=    4.7380    )
 +++++ +++++++++++ ++++++
 USL Method 1 (Confidence Band with
 Administrative Margin)          USL1 = 0.9390 + (-1.5719E-04)*X
 USL Method 2 (Single-Sided Uniform
 Width Closed Interval Approach)  USL2 = 0.9795 + (-1.5719E-04)*X
 USLs Evaluated Over Range of Parameter X:
 +++++ +++++++++ ++++ ++++++ ++ +++++++++ ++


 X:  2.35E+0  2.69E+0  3.03E+0  3.37E+0  3.71E+0  4.06E+0  4.40E+0  4.74E+0
     -----------------------------------------------------------------------
USL-1:  0.9387   0.9386   0.9386   0.9385   0.9385   0.9384   0.9383   0.9383
USL-2:  0.9791   0.9790   0.9790   0.9789   0.9789   0.9788   0.9788   0.9787
     -----------------------------------------------------------------------
```

Table 6.5.4-1   LEU Range of Applicability for Complete Set of 186 Benchmark
Experiments

Parameter	Minimum	Maximum
Enrichment (wt % ^{235}U)	2.350%	4.738%
Fuel rod pitch (cm)	1.30	2.54
Fuel pellet outer diameter (cm)	0.790	1.265
Fuel rod diameter (cm)	0.9400	1.4172
H/^{235}U atom ratio	72.7	403.9
Soluble boron (ppm by weight)	0	4986
Cluster gap (cm)	1.206	13.750
Boron (^{10}B) plate loading (g/cm^2)	0.0000	0.0670
Energy of average neutron lethargy causing fission (eV)	0.09781	0.77219

Table 6.5.4-2   LEU Correlation Coefficients and USLs for Benchmark Experiments

Variable	R^2	R	Range of Applicability	USLSTATS Correlation	USL Low	USL High
Enrichment (wt % ^{235}U)	0.00410	0.064	2.35<=X<=4.738	0.9390-1.57E-04X	0.9382	0.9386
Fuel rod pitch (cm)	0.00150	0.039	1.3<=X<=2.54	0.9380+2.64E-04X	0.9383	0.9386
Fuel pellet outer diameter (cm)	0.00260	0.051	0.79<=X<=1.265	0.9376+8.25E-04X	0.9382	0.9386
Fuel rod diameter (cm)	0.00380	0.062	0.94<=X<=1.4172	0.9372+1.01E-03X	0.9381	0.9386
H/^{235}U atom ratio	3.00E-06	0.002	106.2<=X<=403.9	0.9386-4.74E-08X	0.9385	0.9385
Soluble boron (ppm by weight)	0.01730	0.132	0<=X<=4986	0.9379+3.96E-07X	0.9379	0.9398
Cluster gap (cm)	0.01940	0.139	1.2<=X<=13.8	0.9375+9.82E-05X	0.9376	0.9388
Boron (^{10}B) plate loading (g/cm^2)	0.00006	0.008	0<=X<=0.067	0.9382-1.37E-03X	0.9381	0.9382
Energy of average neutron lethargy causing fission (eV)	0.00900	0.095	0.09781<=X<=0.3447	0.9379+3.45E-03X	0.9382	0.9390

6.5.4.3   LEU (Maximum 5 wt % ^{235}U in UO$_2$) Criticality Benchmarks

From the International Handbook of Evaluated Criticality Safety Benchmark Experiments, 186 experiments are selected as the basis of the MCNP benchmarking. Experiments were selected for compatibility of materials and geometry with the spent fuel casks. Of particular interest are benchmarks with arrays of low enriched uranium oxide fuel rods.

MCNP benchmark cases represent a collection of files composed of inputs directly obtained from references (with cross-section sets adjusted to those used in the cask analysis), NAC modified input files representing unique geometries based on reference input files, and input files constructed from the experimental material and geometry information. All cases were reviewed on a "preparer/checker" principle for modeling consistency with the cask models and the choice of code options. Due to large variations in the benchmark complexities, not all options employed in the cask models are reflected in each of the benchmarks (e.g., UNIVERSE structure). A review of the criticality results did not indicate any result trend due to particular modeling choices (e.g., using the UNIVERSE structure versus a single universe, or employing KSRC versus SDEF sampling).

Key system parameters, the experimental uncertainty, and calculated k_{eff} and σ for each experiment are shown in Table 6.5.4-3. Stochastic Monte Carlo error is kept within ±0.2% and each output is checked to assure that the MCNP built-in statistical checks on the results are passed and that all fissile material is sampled.

Scatter plots of k_{eff} versus system parameters for 183 data point sets (full set minus three high lethargy points above 0.35 eV) are created (see Figure 6.5.4-2 through Figure 6.5.4-10). Included in these scatter plots are linear regression lines with a corresponding correlation coefficient (R^2) to statistically indicate any trend or lack thereof. Scatter plates are created for k_{eff} versus the following.

- Enrichment in ^{235}U (wt % ^{235}U)
- Fuel rod pitch (cm)
- Fuel pellet outer diameter (cm)
- Fuel rod outer diameter (cm)
- Hydrogen/uranium (^{235}U) atom ratio
- Soluble boron (ppm by weight)
- Cluster gap spacing (spacing between assemblies in cm)
- Boron (^{10}B) plate loading (g/cm^2)
- Energy of average neutron lethargy causing fission (eV)

Figure 6.5.4-2   k_eff versus Fuel Enrichment (LEU)
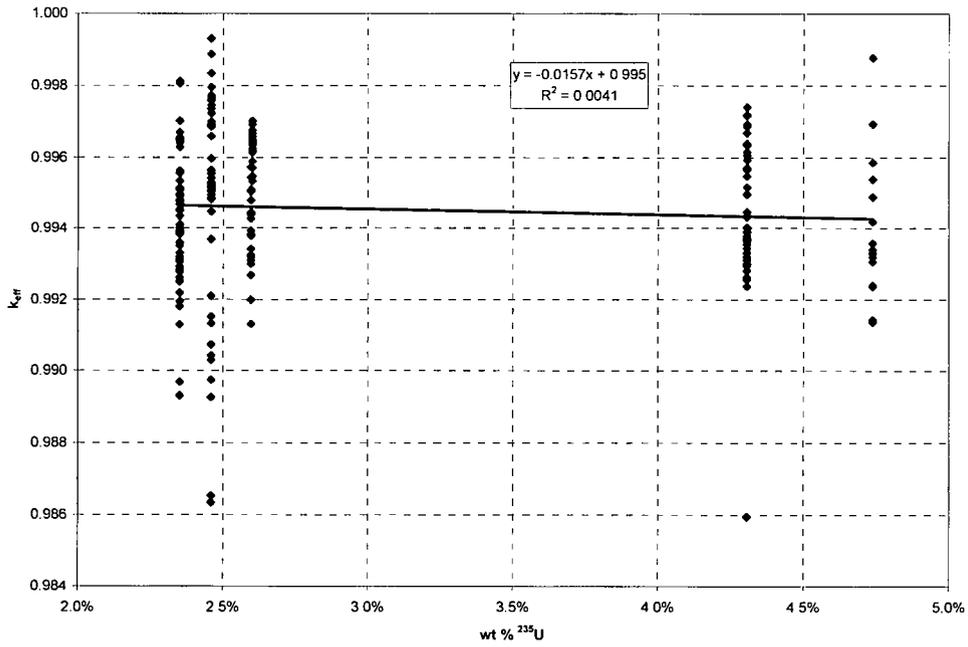
Figure 6.5.4-3   k_eff versus Rod Pitch (LEU)
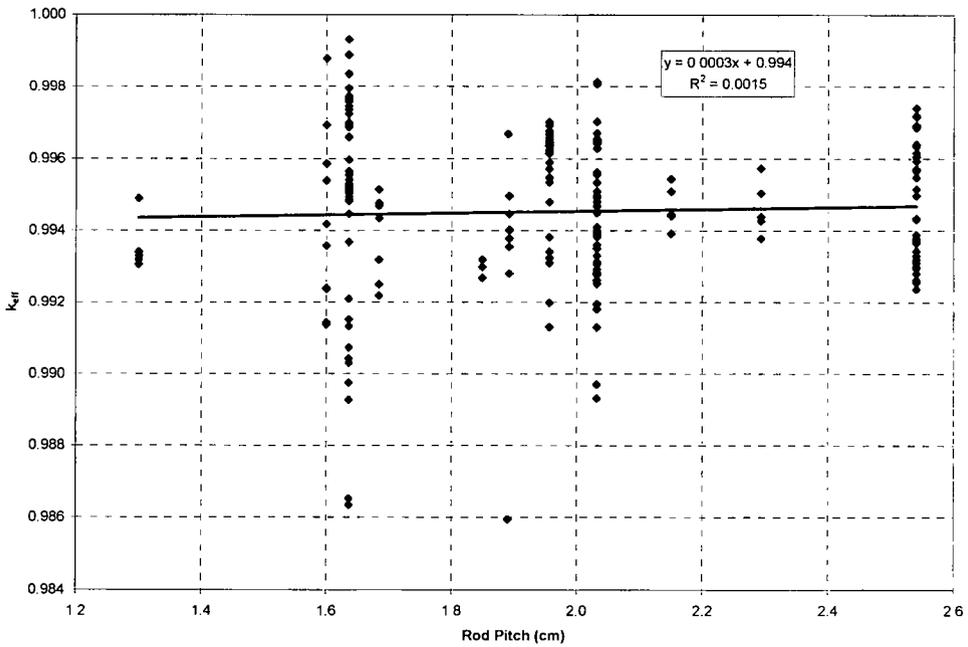
Figure 6.5.4-4   k_eff versus Fuel Pellet Diameter (LEU)
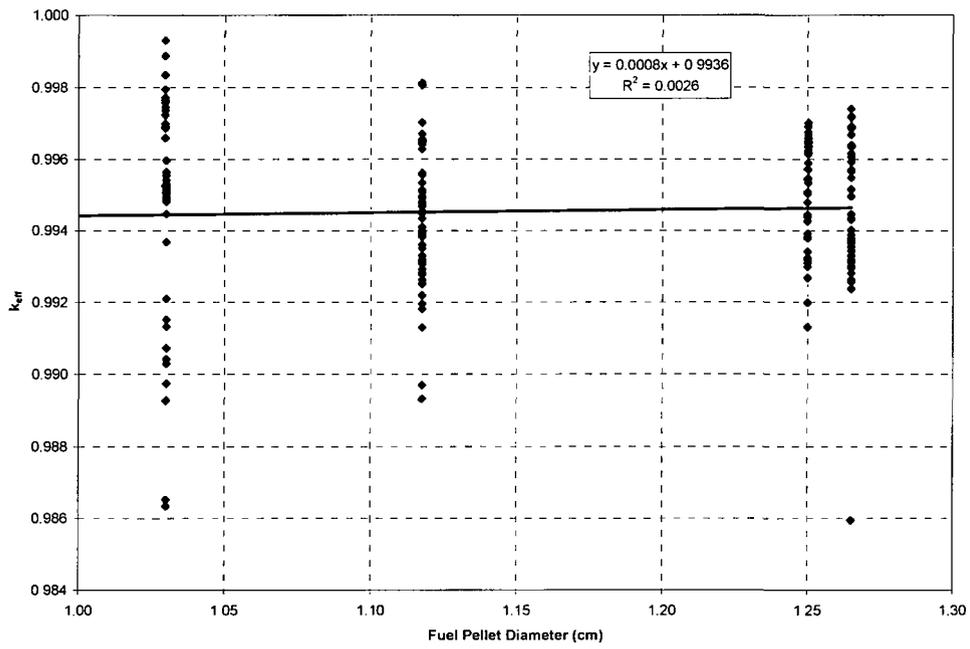
Figure 6.5.4-5   k_eff versus Fuel Rod Outside Diameter (LEU)
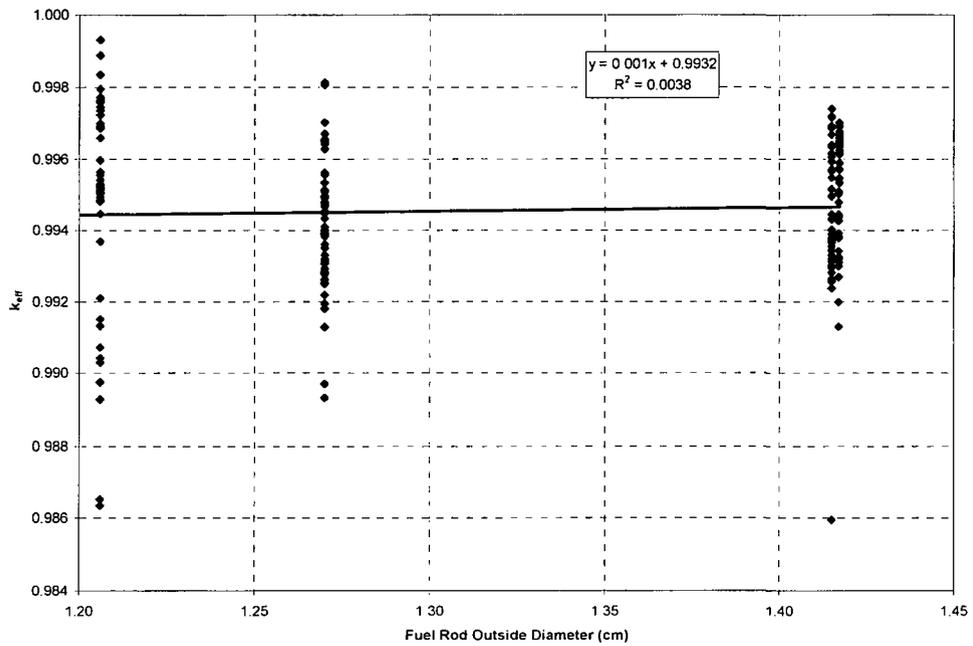
Figure 6.5.4-6 k_{eff} versus Hydrogen/^{235}U Atom Ratio (LEU)
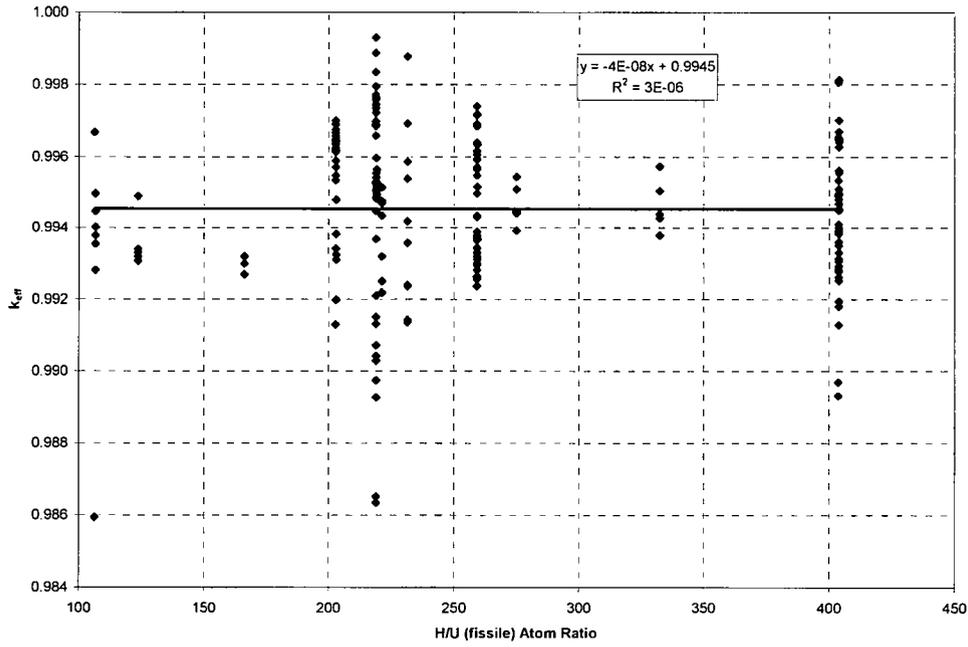
Figure 6.5.4-7 k_{eff} versus Soluble Boron Concentration (LEU)
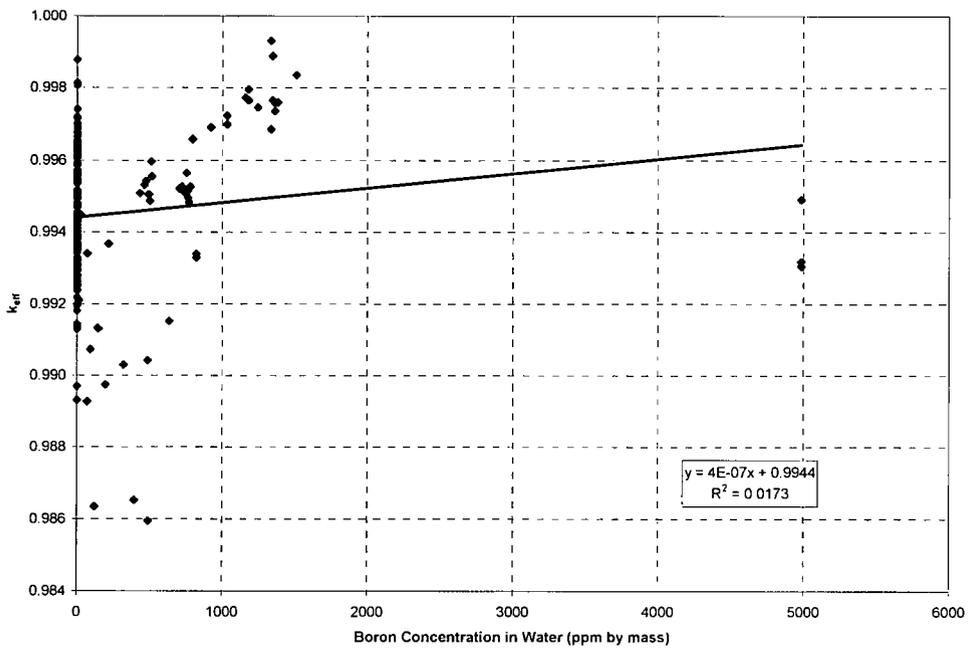
Figure 6.5.4-8 k_{eff} versus Cluster Gap Thickness (LEU)
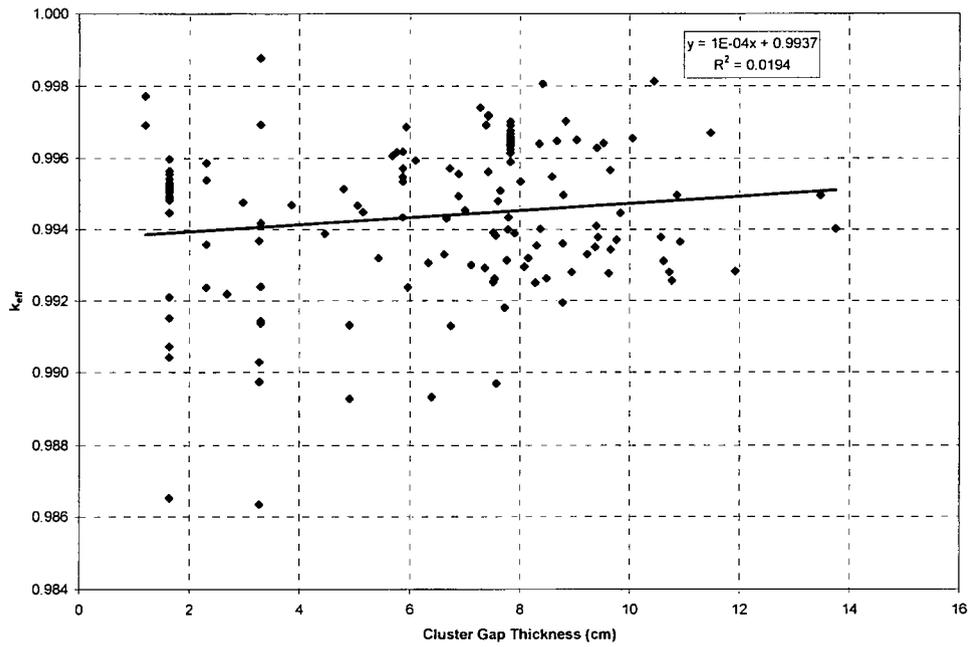
Figure 6.5.4-9 k_{eff} versus ^{10}B Plate Loading (LEU)
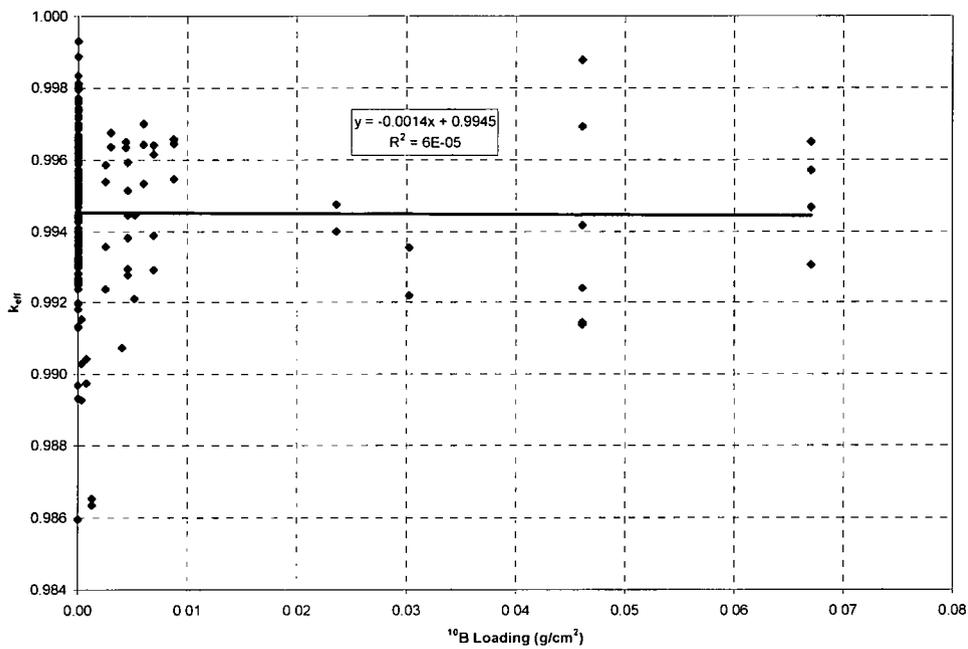
Figure 6.5.4-10   k$_{eff}$ versus Energy of Average Neutron Lethargy Causing Fission (LEU)
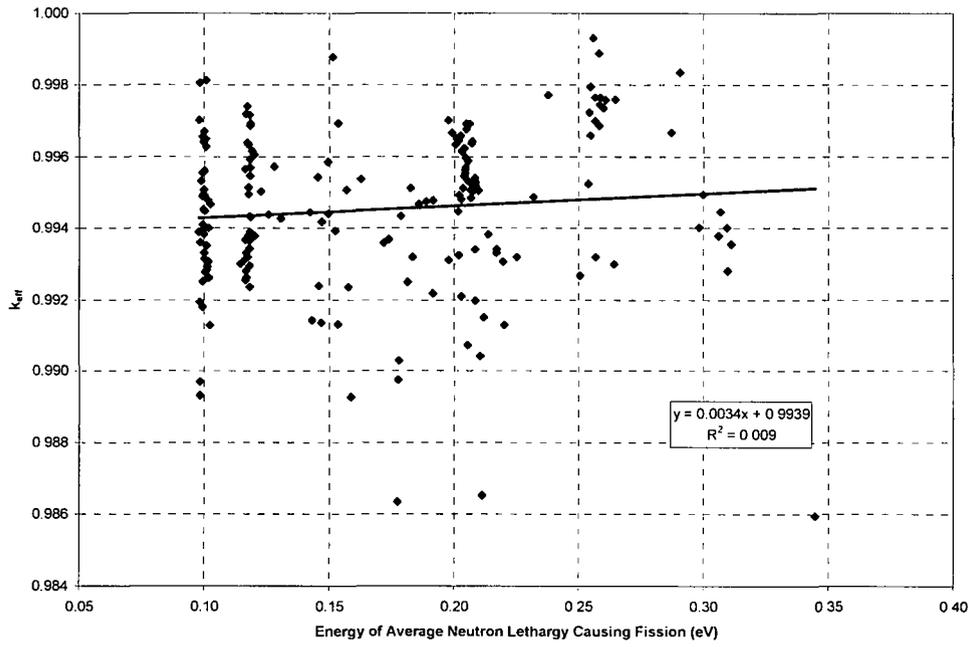
Table 6.5.4-3   LEU MCNP Validation Statistics

Case	1.01	1.02	1.03	1.04	1.05	1.06	1.07	1.08
Clusters	1	3	3	3	3	3	3	3
Enrichment (wt % ^{235}U)	2.35%	2.35%	2.35%	2.35%	2.35%	2.35%	2.35%	2.35%
Pitch (cm)	2.032	2.032	2.032	2.032	2.032	2.032	2.032	2.032
Fuel OD (cm)	1.118	1.118	1.118	1.118	1.118	1.118	1.118	1.118
Clad OD (cm)	1.270	1.270	1.270	1.270	1.270	1.270	1.270	1.270
Clad Material	Al	Al	Al	Al	Al	Al	Al	Al
H/U (fissile)	404	404	404	404	404	404	404	404
Soluble B (ppm)	--	--	--	--	--	--	--	--
Absorber Type	--	--	--	--	--	--	--	--
Cluster Gap (cm)	--	11.9	8.4	10.1	6.4	8.0	4.5	7.6
Reflector	H_2O	H_2O	H_2O	H_2O	H_2O	H_2O	H_2O	H_2O
Plate Loading (g ^{10}B/cm^2)	--	--	--	--	--	--	--	--
EALCF (MeV)	9.916E-8	1.010E-7	9.838E-8	9.933E-8	9.837E-8	9.874E-8	9.781E-8	9.826E-8
Exp. σ	0.0030	0.0030	0.0030	0.0030	0.0030	0.0030	0.0031	0.0030
k_{eff}	0.99491	0.99283	0.99806	0.99655	0.98931	0.99534	0.99388	0.98969
σ	0.00165	0.00155	0.00155	0.00165	0.00169	0.00162	0.00150	0.00152

Table 6.5.4-3   LEU MCNP Validation Statistics (cont'd)

Case	2.01	2.02	2.03	2.04	2.05
Clusters	1	1	1	3	3
Enrichment (wt % ^{235}U)	4.31%	4.31%	4.31%	4.31%	4.31%
Pitch (cm)	2.540	2.540	2.540	2.540	2.540
Fuel OD (cm)	1.265	1.265	1.265	1.265	1.265
Clad OD (cm)	1.415	1.415	1.415	1.415	1.415
Clad Material	Al	Al	Al	Al	Al
H/U (fissile)	259	259	259	259	259
Soluble B (ppm)	--	--	--	--	--
Absorber Type	--	--	--	--	--
Cluster Gap (cm)	--	--	--	10.6	7.1
Reflector	H_2O	H_2O	H_2O	H_2O	H_2O
Plate Loading (g ^{10}B/cm^2)	--	--	--	--	--
EALCF (MeV)	1.177E-7	1.164E-7	1.175E-7	1.161E-7	1.146E-7
Exp. σ	0.0020	0.0020	0.0020	0.0018	0.0019
k_{eff}	0.99516	0.99367	0.99634	0.99311	0.99300
σ	0.00195	0.00157	0.00190	0.00193	0.00161

Table 6.5.4-3   LEU MCNP Validation Statistics (cont'd)

Case	6.01	6.02	6.03	6.04	6.05	6.06	6.07	6.08	6.09
Clusters	1	1	1	1	1	1	1	1	1
Enrichment (wt % ^{235}U)	2.60%	2.60%	2.60%	2.60%	2.60%	2.60%	2.60%	2.60%	2.60%
Pitch (cm)	1.849	1.849	1.849	1.956	1.956	1.956	1.956	1.956	2.150
Fuel OD (cm)	1.250	1.250	1.250	1.250	1.250	1.250	1.250	1.250	1.250
Clad OD (cm)	1.417	1.417	1.417	1.417	1.417	1.417	1.417	1.417	1.417
Clad Material	Al	Al	Al	Al	Al	Al	Al	Al	Al
H/U (fissile)	166	166	166	203	203	203	203	203	275
Soluble B (ppm)	--	--	--	--	--	--	--	--	--
Absorber Type	--	--	--	--	--	--	--	--	--
Cluster Gap (cm)	--	--	--	--	--	--	--	--	--
Reflector	H_2O	H_2O	H_2O	H_2O	H_2O	H_2O	H_2O	H_2O	H_2O
Plate Loading (g ^{10}B/cm^2)	--	--	--	--	--	--	--	--	--
EALCF (MeV)	2.506E-7	2.568E-7	2.642E-7	1.915E-7	1.978E-7	2.018E-7	2.085E-7	2.136E-7	1.422E-7
Exp. σ	0.0020	0.0020	0.0020	0.0020	0.0020	0.0020	0.0020	0.0020	0.0020
k_{eff}	0.99268	0.99319	0.99299	0.99479	0.99310	0.99324	0.99199	0.99382	0.99445
σ	0.00065	0.00076	0.00074	0.00074	0.00069	0.00070	0.00071	0.00071	0.00069

Table 6.5.4-3   LEU MCNP Validation Statistics (cont'd)

Case	6.10	6.11	6.12	6.13	6.14	6.15	6.16	6.17	6.18
Clusters	1	1	1	1	1	1	1	1	1
Enrichment (wt % ^{235}U)	2.60%	2.60%	2.60%	2.60%	2.60%	2.60%	2.60%	2.60%	2.60%
Pitch (cm)	2.150	2.150	2.150	2.150	2.293	2.293	2.293	2.293	2.293
Fuel OD (cm)	1.250	1.250	1.250	1.250	1.250	1.250	1.250	1.250	1.250
Clad OD (cm)	1.417	1.417	1.417	1.417	1.417	1.417	1.417	1.417	1.417
Clad Material	Al	Al	Al	Al	Al	Al	Al	Al	Al
H/U (fissile)	275	275	275	275	332	332	332	332	332
Soluble B (ppm)	--	--	--	--	--	--	--	--	--
Absorber Type	--	--	--	--	--	--	--	--	--
Cluster Gap (cm)	--	--	--	--	--	--	--	--	--
Reflector	H_2O	H_2O	H_2O	H_2O	H_2O	H_2O	H_2O	H_2O	H_2O
Plate Loading (g ^{10}B/cm^2)	--	--	--	--	--	--	--	--	--
EALCF (MeV)	1.453E-7	1.496E-7	1.523E-7	1.568E-7	1.202E-7	1.227E-7	1.257E-7	1.280E-7	1.306E-7
Exp. σ	0.0020	0.0020	0.0020	0.0020	0.0020	0.0020	0.0020	0.0020	0.0020
k$_{eff}$	0.99544	0.99441	0.99392	0.99509	0.99378	0.99504	0.99438	0.99573	0.99427
σ	0.00073	0.00071	0.00078	0.00076	0.00070	0.00075	0.00067	0.00070	0.00076

Table 6.5.4-3   LEU MCNP Validation Statistics (cont'd)

Case	8.01	8.02	8.03	8.04	8.05	8.06	8.07	8.08
Clusters	3 x 3	3 x 3	3 x 3	3 x 3	3 x 3	3 x 3	3 x 3	3 x 3
Enrichment (wt % ^{235}U)	2.46%	2.46%	2.46%	2.46%	2.46%	2.46%	2.46%	2.46%
Pitch (cm)	1.636	1.636	1.636	1.636	1.636	1.636	1.636	1.636
Fuel OD (cm)	1.030	1.030	1.030	1.030	1.030	1.030	1.030	1.030
Clad OD (cm)	1.206	1.206	1.206	1.206	1.206	1.206	1.206	1.206
Clad Material	Al	Al	Al	Al	Al	Al	Al	Al
H/U (fissile)	219	219	219	219	219	219	219	219
Soluble B (ppm)	1511	1336	1336	1182	1182	1033	1033	794
Absorber Type	--	--	--	--	--	--	--	--
Cluster Gap (cm)	--	--	--	--	--	--	--	--
Reflector	H_2O	H_2O	H_2O	H_2O	H_2O	H_2O	H_2O	H_2O
Plate Loading (g ^{10}B/cm^2)	--	--	--	--	--	--	--	--
EALCF (MeV)	2.907E-7	2.583E-7	2.559E-7	2.548E-7	2.566E-7	2.568E-7	2.544E-7	2.548E-7
Exp. σ	0.0012	0.0012	0.0012	0.0012	0.0012	0.0012	0.0012	0.0012
k_{eff}	0.99835	0.99686	0.99931	0.99795	0.99765	0.99699	0.99723	0.99659
σ	0.00060	0.00063	0.00032	0.00063	0.00069	0.00061	0.00066	0.00073

Table 6.5.4-3   LEU MCNP Validation Statistics (cont'd)

Case	8.09	8.10	8.11	8.12	8.13	8.14	8.15	8.16	8.17
Clusters	3 x 3	3 x 3	3 x 3	3 x 3	3 x 3	3 x 3	3 x 3	5	5 x 5
Enrichment (wt % ^{235}U)	2.46%	2.46%	2.46%	2.46%	2.46%	2.46%	2.46%	2.46%	2.46%
Pitch (cm)	1.636	1.636	1.636	1.636	1.636	1.636	1.636	1.636	1.636
Fuel OD (cm)	1.030	1.030	1.030	1.030	1.030	1.030	1.030	1.030	1.030
Clad OD (cm)	1.206	1.206	1.206	1.206	1.206	1.206	1.206	1.206	1.206
Clad Material	Al	Al	Al	Al	Al	Al	Al	Al	Al
H/U (fissile)	219	219	219	219	219	219	219	219	219
Soluble B (ppm)	779	1245	1384	1348	1348	1363	1363	1158	921
Absorber Type	--	--	--	--	--	--	--	--	--
Cluster Gap (cm)	-	-	-	-	-	-	-	1.2	1.2
Reflector	H_2O	H_2O	H_2O	H_2O	H_2O	H_2O	H_2O	H_2O	H_2O
Plate Loading (g ^{10}B/cm^2)	--	--	--	--	--	--	--	--	--
EALCF (MeV)	2.538E-7	2.586E-7	2.647E-7	2.587E-7	2.582E-7	2.600E-7	2.609E-7	2.379E-7	2.063E-7
Exp. σ	0.0012	0.0012	0.0012	0.0012	0.0012	0.0012	0.0012	0.0012	0.0012
k_{eff}	0.99526	0.99745	0.99759	0.99765	0.99888	0.99735	0.99758	0.99772	0.99691
σ	0.00072	0.00065	0.00068	0.00065	0.00070	0.00067	0.00071	0.00070	0.00062

Table 6.5.4-3   LEU MCNP Validation Statistics (cont'd)

Case	9.01	9.02	9.03	9.04	9.05	9.06	9.07	9.08	9.09	9.10	9.11	9.12	9.13
Clusters	3	3	3	3	3	3	3	3	3	3	3	3	3
Enrichment (wt % ^{235}U)	4.31%	4.31%	4.31%	4.31%	4.31%	4.31%	4.31%	4.31%	4.31%	4.31%	4.31%	4.31%	4.31%
Pitch (cm)	2.540	2.540	2.540	2.540	2.540	2.540	2.540	2.540	2.540	2.540	2.540	2.540	2.540
Fuel OD (cm)	1.265	1.265	1.265	1.265	1.265	1.265	1.265	1.265	1.265	1.265	1.265	1.265	1.265
Clad OD (cm)	1.415	1.415	1.415	1.415	1.415	1.415	1.415	1.415	1.415	1.415	1.415	1.415	1.415
Clad Material	Al	Al	Al	Al	Al	Al	Al	Al	Al	Al	Al	Al	Al
H/U (fissile)	259	259	259	259	259	259	259	259	259	259	259	259	259
Soluble B (ppm)	-	-	-	-	-	-	-	-	-	-	-	-	-
Absorber Type	304L SS (no B)	304L SS (no B)	304L SS (no B)	304L SS (no B)	304L SS (1.05% B)	304L SS (1.05% B)	304L SS (1.62% B)	304L SS (1.62% B)	Boral	Cu	Cu	Cu	Cu
Cluster Gap (cm)	8.6	9.7	9.2	9.8	6.1	8.1	5.8	7.9	6.7	8.2	9.4	8.5	9.6
Reflector	H_2O	H_2O	H_2O	H_2O	H_2O	H_2O	H_2O	H_2O	H_2O	H_2O	H_2O	H_2O	H_2O
Plate Loading (g ^{10}B/cm^2)	0.00000	0.00000	0.00000	0.00000	0.00455	0.00455	0.00690	0.00690	0.06704	-	-	-	-
EALCF(MeV)	1.183E-7	1.181E-7	1.168E-7	1.179E-7	1.182E-7	1.182E-7	1.191E-7	1.182E-7	1.183E-7	1.173E-7	1.176E-7	1.169E-7	1.163E-7
Exp. σ	0.0021	0.0021	0.0021	0.0021	0.0021	0.0021	0.0021	0.0021	0.0021	0.0021	0.0021	0.0021	0.0021
k_{eff}	0.99548	0.99343	0.99330	0.99371	0.99593	0.99295	0.99616	0.99389	0.99571	0.99319	0.99378	0.99263	0.99566
σ	0.00191	0.00182	0.00187	0.00192	0.00174	0.00193	0.00198	0.00175	0.00209	0.00153	0.00178	0.00191	0.00177

Table 6.5.4-3   LEU MCNP Validation Statistics (cont'd)

Case	9.14	9.15	9.16	9.17	9.18	9.19	9.20	9.21	9.22	9.23	9.24	9.25	9.26	9.27
Clusters	3	3	3	3	3	3	3	3	3	3	3	3	3	3
Enrichment (wt % ^{235}U)	4.31%	4.31%	4.31%	4.31%	4.31%	4.31%	4.31%	4.31%	4.31%	4.31%	4.31%	4.31%	4.31%	4.31%
Pitch (cm)	2.540	2.540	2.540	2.540	2.540	2.540	2.540	2.540	2.540	2.540	2.540	2.540	2.540	2.540
Fuel OD (cm)	1.265	1.265	1.265	1.265	1.265	1.265	1.265	1.265	1.265	1.265	1.265	1.265	1.265	1.265
Clad OD (cm)	1.415	1.415	1.415	1.415	1.415	1.415	1.415	1.415	1.415	1.415	1.415	1.415	1.415	1.415
Clad Material	Al	Al	Al	Al	Al	Al	Al	Al	Al	Al	Al	Al	Al	Al
H/U (fissile)	259	259	259	259	259	259	259	259	259	259	259	259	259	259
Soluble B (ppm)	--	--	--	--	--	--	--	--	--	--	--	--	--	--
Absorber Type	Cu (0.989 wt % Cd)	Cu (0.989 wt % Cd)	Cd	Cd	Cd	Cd	Cd	Cd	Cd	Cd	Al (no B)	Al (no B)	Zircaloy-4	Zircaloy-4
Cluster Gap (cm)	6.7	8.4	5.9	7.4	6.0	7.4	5.9	7.4	5.7	7.3	10.7	10.8	10.9	10.9
Reflector	H_2O	H_2O	H_2O	H_2O	H_2O	H_2O	H_2O	H_2O	H_2O	H_2O	H_2O	H_2O	H_2O	H_2O
Plate Loading (g ^{10}B/cm^2)	--	--	--	--	--	--	--	--	--	--	0.00000	0.00000	--	--
EALCF(MeV)	1.186E-7	1.171E-7	1.186E-7	1.183E-7	1.183E-7	1.168E-7	1.182E-7	1.187E-7	1.199E-7	1.173E-7	1.167E-7	1.165E-7	1.181E-7	1.177E-7
Exp. σ	0.0021	0.0021	0.0021	0.0021	0.0021	0.0021	0.0021	0.0021	0.0021	0.0021	0.0021	0.0021	0.0021	0.0021
k_{eff}	0.99431	0.99639	0.99686	0.99716	0.99237	0.99719	0.99434	0.99692	0.99606	0.99740	0.99281	0.99256	0.99365	0.99497
σ	0.00188	0.00207	0.00183	0.00166	0.00194	0.00187	0.00179	0.00183	0.00189	0.00206	0.00168	0.00197	0.00197	0.00193

Table 6.5.4-3   LEU MCNP Validation Statistics (cont'd)

Case	11.03	11.04	11.05	11.06	11.07	11.08	11.09
Clusters	3	3	3	3	3	3	3
Enrichment (wt % ^{235}U)	2.46%	2.46%	2.46%	2.46%	2.46%	2.46%	2.46%
Pitch (cm)	1.636	1.636	1.636	1.636	1.636	1.636	1.636
Fuel OD (cm)	1.030	1.030	1.030	1.030	1.030	1.030	1.030
Clad OD (cm)	1.206	1.206	1.206	1.206	1.206	1.206	1.206
Clad Material	Al	Al	Al	Al	Al	Al	Al
H/U (fissile)	219	219	219	219	219	219	219
Soluble B (ppm)	769	764	762	753	739	721	702
Absorber Type	--	--	--	--	--	--	--
Cluster Gap (cm)	1.6	1.6	1.6	1.6	1.6	1.6	1.6
Reflector	H_2O	H_2O	H_2O	H_2O	H_2O	H_2O	H_2O
Plate Loading (g ^{10}B/cm^2)	--	--	--	--	--	--	--
EALCF [MeV]	2.027E-7	2.020E-7	2.035E-7	2.044E-7	2.065E-7	2.068E-7	2.085E-7
Exp. σ	0.0032	0.0032	0.0032	0.0032	0.0032	0.0032	0.0032
k_{eff}	0.99482	0.99494	0.99514	0.99564	0.99508	0.99526	0.99520
σ	0.00031	0.00030	0.00030	0.00030	0.00031	0.00030	0.00031

Table 6.5.4-3   LEU MCNP Validation Statistics (cont'd)

Case	13.01	13.02	13.03	13.04	13.05	13.06	13.07
Clusters	3	3	3	3	3	3	3
Enrichment (wt % ^{235}U)	4.31%	4.31%	4.31%	4.31%	4.31%	4.31%	4.31%
Pitch (cm)	1.892	1.892	1.892	1.892	1.892	1.892	1.892
Fuel OD (cm)	1.265	1.265	1.265	1.265	1.265	1.265	1.265
Clad OD (cm)	1.415	1.415	1.415	1.415	1.415	1.415	1.415
Clad Material	Al	Al	Al	Al	Al	Al	Al
H/U (fissile)	107	107	107	107	107	107	107
Soluble B (ppm)	--	--	--	--	--	--	--
Absorber Type	304L SS (no B)	304L SS (1.05% B)	Boral B	Boroflex	Cd	Cu	Cu (0.989 wt % Cd)
Cluster Gap (cm)	13.8	9.8	8.3	8.4	8.9	13.5	10.6
Reflector	Steel	Steel	Steel	Steel	Steel	Steel	Steel
Plate Loading (g ^{10}B/cm^2)	0.00000	0.00455	0.03022	0.02361	--	--	--
EALCF (MeV)	2.982E-7	3.068E-7	3.111E-7	3.094E-7	3.097E-7	2.998E-7	3.061E-7
Exp. σ	0.0018	0.0018	0.0018	0.0018	0.0032	0.0018	0.0018
k_{eff}	0.99402	0.99446	0.99355	0.99401	0.99281	0.99496	0.99378
σ	0.00068	0.00064	0.00064	0.00064	0.00066	0.00063	0.00062

Table 6.5.4-3   LEU MCNP Validation Statistics (cont'd)

Case	14.01	14.02	14.05	14.06	14.07
Clusters	1	1	1	1	1
Enrichment (wt % ^{235}U)	4.31%	4.31%	4.31%	4.31%	4.31%
Pitch (cm)	1.890	1.890	1.890	1.715	1.715
Fuel OD (cm)	1.265	1.265	1.265	1.265	1.265
Clad OD (cm)	1.415	1.415	1.415	1.415	1.415
Clad Material	Al	Al	Al	Al	Al
H/U (fissile)	106	106	106	73	73
Soluble B (ppm)	0	491	2539	0	1030
Absorber Type	--	--	--	--	--
Cluster Gap (cm)	--	--	--	--	--
Reflector	H_2O	H_2O	H_2O	H_2O	H_2O
Plate Loading (g ^{10}B/cm^2)	--	--	--	--	--
EALCF (MeV)	2.873E-7	3.447E-7	6.003E-7	5.175E-7	7.722E-7
Exp. σ	0.0019	0.0077	0.0069	0.0033	0.0051
k_{eff}	0.99668	0.98595	1.00221	1.00245	0.99973
σ	0.00044	0.00045	0.00043	0.00045	0.00044

Table 6.5.4-3   LEU MCNP Validation Statistics (cont'd)

Case	16.01	16.02	16.03	16.04	16.05	16.06	16.07	16.08	16.09	16.10
Clusters	3	3	3	3	3	3	3	3	3	3
Enrichment (wt % ^{235}U)	2.35%	2.35%	2.35%	2.35%	2.35%	2.35%	2.35%	2.35%	2.35%	2.35%
Pitch (cm)	2.032	2.032	2.032	2.032	2.032	2.032	2.032	2.032	2.032	2.032
Fuel OD (cm)	1.118	1.118	1.118	1.118	1.118	1.118	1.118	1.118	1.118	1.118
Clad OD (cm)	1.270	1.270	1.270	1.270	1.270	1.270	1.270	1.270	1.270	1.270
Clad Material	Al	Al	Al	Al	Al	Al	Al	Al	Al	Al
H/U (fissile)	404	404	404	404	404	404	404	404	404	404
Soluble B (ppm)	--	--	--	--	--	--	--	--	--	--
Absorber Type	304L SS (no B)	304L SS (no B)	304L SS (no B)	304L SS (no B)	304L SS (no B)	304L SS (no B)	304L SS (no B)	304L SS (1.05% B)	304L SS (1.05% B)	304L SS (1.62% B)
Cluster Gap (cm)	6.9	7.6	7.5	7.4	7.8	10.4	11.5	7.6	9.6	7.4
Reflector	H_2O	H_2O	H_2O	H_2O	H_2O	H_2O	H_2O	H_2O	H_2O	H_2O
Plate Loading (g ^{10}B/cm^2)	0.00000	0.00000	0.00000	0.00000	0.00000	0.00000	0.00000	0.00455	0.00455	0.00690
EALCF (MeV)	1.000E-7	9.983E-8	9.947E-8	1.001E-7	1.002E-7	1.009E-7	1.001E-7	9.993E-8	1.004E-7	1.012E-7
Exp. σ	0.0031	0.0031	0.0031	0.0031	0.0031	0.0031	0.0031	0.0031	0.0031	0.0031
k_{eff}	0.99494	0.99509	0.99252	0.99562	0.99313	0.99813	0.99670	0.99383	0.99277	0.99292
σ	0.00171	0.00153	0.00157	0.00162	0.00173	0.00179	0.00175	0.00172	0.00157	0.00162

Table 6.5.4-3   LEU MCNP Validation Statistics (cont'd)

Case	16.11	16.12	16.13	16.14	16.15	16.16	16.17	16.18	16.19	16.20	16.21	16.22
Clusters	3	3	3	3	3	3	3	3	3	3	3	3
Enrichment (wt % ^{235}U)	2.35%	2.35%	2.35%	2.35%	2.35%	2.35%	2.35%	2.35%	2.35%	2.35%	2.35%	2.35%
Pitch(cm)	2.032	2.032	2.032	2.032	2.032	2.032	2.032	2.032	2.032	2.032	2.032	2.032
Fuel OD (cm)	1.118	1.118	1.118	1.118	1.118	1.118	1.118	1.118	1.118	1.118	1.118	1.118
Clad OD (cm)	1.270	1.270	1.270	1.270	1.270	1.270	1.270	1.270	1.270	1.270	1.270	1.270
Clad Material	Al	Al	Al	Al	Al	Al	Al	Al	Al	Al	Al	Al
H/U (fissile)	404	404	404	404	404	404	404	404	404	404	404	404
Soluble B (ppm)	--	--	--	--	--	--	--	--	--	--	--	--
Absorber Type	304L SS (1.62% B)	Boral	Boral	Boral	Cu	Cu	Cu	Cu	Cu	Cu (0.989 wt % Cd)	Cd	Cd
Cluster Gap (cm)	9.5	6.3	9.0	5.1	6.6	7.7	7.5	6.9	7.0	5.2	6.7	7.6
Reflector	H_2O	H_2O	H_2O	H_2O	H_2O	H_2O	H_2O	H_2O	H_2O	H_2O	H_2O	H_2O
Plate Loading (g ^{10}B/cm^2)	0.00690	0.06704	0.06704	0.06704	--	--	--	--	--	--	--	--
EALCF (MeV)	9.962E-8	1.016E-7	1.006E-7	1.025E-7	1.000E-7	9.944E-8	9.904E-8	9.919E-8	9.971E-8	1.001E-7	1.024E-7	1.014E-7
Exp. σ	0.0031	0.0031	0.0031	0.0031	0.0031	0.0031	0.0031	0.0031	0.0031	0.0031	0.0031	0.0031
k_{eff}	0.99641	0.99306	0.99650	0.99468	0.99330	0.99181	0.99392	0.99556	0.99454	0.99449	0.99130	0.99480
σ	0.00154	0.00161	0.00152	0.00162	0.00157	0.00153	0.00155	0.00172	0.00165	0.00155	0.00166	0.00157

Table 6.5.4-3   LEU MCNP Validation Statistics (cont'd)

Case	16.23	16.24	16.25	16.26	16.27	16.28	16.29	16.30	16.31	16.32
Clusters	3	3	3	3	3	3	3	3	3	3
Enrichment (wt % ^{235}U)	2.35%	2.35%	2.35%	2.35%	2.35%	2.35%	2.35%	2.35%	2.35%	2.35%
Pitch(cm)	2.032	2.032	2.032	2.032	2.032	2.032	2.032	2.032	2.032	2.032
Fuel OD (cm)	1.118	1.118	1.118	1.118	1.118	1.118	1.118	1.118	1.118	1.118
Clad OD (cm)	1.270	1.270	1.270	1.270	1.270	1.270	1.270	1.270	1.270	1.270
Clad Material	Al	Al	Al	Al	Al	Al	Al	Al	Al	Al
H/U (fissile)	404	404	404	404	404	404	404	404	404	404
Soluble B (ppm)	--	--	--	--	--	--	--	--	--	--
Absorber Type	Cd	Cd	Cd	Cd	Cd	Al (no B)	Al (no B)	Al (no B)	Zircaloy-4	Zircaloy-4
Cluster Gap cm)	9.4	7.8	9.4	7.5	9.4	8.7	8.8	8.8	8.8	8.8
Reflector	H_2O	H_2O	H_2O	H_2O	H_2O	H_2O	H_2O	H_2O	H_2O	H_2O
Plate Loading (g ^{10}B/cm^2)	--	--	--	--	--	0.00000	0.00000	0.00000	--	--
EALCF (MeV)	1.010E-7	1.018E-7	1.006E-7	1.019E-7	9.948E-8	9.991E-8	9.843E-8	9.807E-8	9.964E-8	9.834E-8
Exp. σ	0.0031	0.0031	0.0031	0.0031	0.0031	0.0031	0.0031	0.0031	0.0031	0.0031
k_{eff}	0.99350	0.99400	0.99628	0.99262	0.99410	0.99647	0.99360	0.99702	0.99497	0.99195
σ	0.00184	0.00152	0.00169	0.00151	0.00168	0.00166	0.00157	0.00160	0.00163	0.00172

Table 6.5.4-3   LEU MCNP Validation Statistics (cont'd)

Case	35.01	35.02	40.01	40.02	40.03	40.04	40.05	40.06	40.07	40.08	40.09	40.10
Clusters	1	1	4	4	4	4	4	4	4	4	4	4
Enrichment (wt % ^{235}U)	2.60%	2.60%	4.74%	4.74%	4.74%	4.74%	4.74%	4.74%	4.74%	4.74%	4.74%	4.74%
Pitch (cm)	1.956	1.956	1.600	1.600	1.600	1.600	1.600	1.600	1.600	1.600	1.600	1.600
Fuel OD (cm)	1.250	1.250	0.790	0.790	0.790	0.790	0.790	0.790	0.790	0.790	0.790	0.790
Clad OD (cm)	1.417	1.417	0.940	0.940	0.940	0.940	0.940	0.940	0.940	0.940	0.940	0.940
Clad Material	Al	Al	Al alloy	Al alloy	Al alloy	Al alloy	Al alloy	Al alloy	Al alloy	Al alloy	Al alloy	Al alloy
H/U (fissile)	203	203	231	231	231	231	231	231	231	231	231	231
Soluble B (ppm)	70	148	--	--	--	--	--	--	--	--	--	--
Absorber Type	--	--	Z2 CN18/10 SS (1.10% B)	Z2 CN18/10 SS (1.10% B)	Z2 CN18/10 SS (1.10% B)	Z2 CN18/10 SS (1.10% B)	Boral	Boral	Boral	Boral	Boral	Boral
Cluster Gap (cm)	--	--	2.3	2.3	2.3	2.3	3.3	3.3	3.3	3.3	3.3	3.3
Reflector	H_2O	H_2O	H_2O	Lead	Lead	Lead	H_2O	Lead	Lead	Lead	Steel	Steel
Plate Loading (g ^{10}B/cm^2)	--	--	0.00252	0.00252	0.00252	0.00252	0.04608	0.04608	0.04608	0.04608	0.04608	0.04608
EALCF (MeV)	2.170E-7	2.202E-7	1.493E-7	1.717E-7	1.625E-7	1.576E-7	1.432E-7	1.515E-7	1.470E-7	1.459E-7	1.537E-7	1.469E-7
Exp. σ	0.0018	0.0019	0.0039	0.0041	0.0041	0.0041	0.0042	0.0044	0.0044	0.0044	0.0046	0.0046
k_{eff}	0.99341	0.99131	0.99586	0.99358	0.99539	0.99237	0.99144	0.99878	0.99418	0.99240	0.99693	0.99137
σ	0.00070	0.00078	0.00195	0.00192	0.00203	0.00194	0.00193	0.00196	0.00224	0.00216	0.00190	0.00208

Table 6.5.4-3   LEU MCNP Validation Statistics (cont'd)

Case	42.01	42.02	42.03	42.04	42.05	42.06	42.07
Clusters	3	3	3	3	3	3	3
Enrichment (wt % ^{235}U)	2.35%	2.35%	2.35%	2.35%	2.35%	2.35%	2.35%
Pitch (cm)	1.684	1.684	1.684	1.684	1.684	1.684	1.684
Fuel OD (cm)	1.118	1.118	1.118	1.118	1.118	1.118	1.118
Clad OD (cm)	1.270	1.270	1.270	1.270	1.270	1.270	1.270
Clad Material	Al	Al	Al	Al	Al	Al	Al
H/U (fissile)	221	221	221	221	221	221	221
Soluble B (ppm)	--	--	--	--	--	--	--
Absorber Type	304L SS (no B)	304L SS (1.05% B)	Boral B	Boroflex	Cd	Cu	Cu-Cd
Cluster Gap (cm)	8.3	4.8	2.7	3.0	3.9	7.8	5.4
Reflector	Steel	Steel	Steel	Steel	Steel	Steel	Steel
Plate Loading (g ^{10}B/cm^2)	0.00000	0.00455	0.03022	0.02361	--	--	--
EALCF (MeV)	1.813E-7	1.824E-7	1.915E-7	1.887E-7	1.857E-7	1.786E-7	1.833E-7
Exp. σ	0.0016	0.0016	0.0016	0.0017	0.0033	0.0016	0.0018
k_{eff}	0.99250	0.99514	0.99219	0.99476	0.99469	0.99434	0.99319
σ	0.00171	0.00183	0.00169	0.00169	0.00161	0.00191	0.00157

Table 6.5.4-3   LEU MCNP Validation Statistics (cont'd)

Case	50.03	50.03	50.03	50.03	50.03
Clusters	1	1	1	1	1
Enrichment (wt % ^{235}U)	4.74%	4.74%	4.74%	4.74%	4.74%
Pitch (cm)	1.300	1.300	1.300	1.300	1.300
Fuel OD (cm)	0.790	0.790	0.790	0.790	0.790
Clad OD (cm)	0.940	0.940	0.940	0.940	0.940
Clad Material	Al alloy	Al alloy	Al alloy	Al alloy	Al alloy
H/U (fissile)	124	124	124	124	124
Soluble B (ppm)	821	821	4986	4986	4986
Absorber Type	--	--	--	--	--
Cluster Gap (cm)	--	--	--	--	--
Reflector	Borated H$_2$O	Borated H$_2$O	Borated H$_2$O	Borated H$_2$O	Borated H$_2$O
Plate Loading (g ^{10}B/cm^2)	--	--	--	--	--
EALCF (MeV)	2.170E-7	2.083E-7	2.318E-7	2.252E-7	2.195E-7
Exp. σ	0.0010	0.0010	0.0010	0.0010	0.0010
k$_{eff}$	0.99330	0.99340	0.99489	0.99319	0.99306
σ	0.00080	0.00071	0.00075	0.00075	0.00080

Table 6.5.4-3   LEU MCNP Validation Statistics (cont'd)

Case	51.01	51.02	51.03	51.04	51.05	51.06	51.07	51.08	51.09
Clusters	9	9	9	9	9	9	9	9	9
Enrichment (wt % ^{235}U)	2.46%	2.46%	2.46%	2.46%	2.46%	2.46%	2.46%	2.46%	2.46%
Pitch (cm)	1.636	1.636	1.636	1.636	1.636	1.636	1.636	1.636	1.636
Fuel OD (cm)	1.030	1.030	1.030	1.030	1.030	1.030	1.030	1.030	1.030
Clad OD (cm)	1.206	1.206	1.206	1.206	1.206	1.206	1.206	1.206	1.206
Clad Material	Al	Al	Al	Al	Al	Al	Al	Al	Al
H/U (fissile)	219	219	219	219	219	219	219	219	219
Soluble B (ppm)	143	510	514	501	493	474	462	432	217
Absorber Type	none	SS	SS	SS	SS	SS	SS	SS	SS
Cluster Gap (cm)	4.9	1.6	1.6	1.6	1.6	1.6	1.6	1.6	3.3
Reflector	Borated H$_2$O	Borated H$_2$O	Borated H$_2$O	Borated H$_2$O	Borated H$_2$O	Borated H$_2$O	Borated H$_2$O	Borated H$_2$O	Borated H$_2$O
Plate Loading (g ^{10}B/cm^2)	0.00000	--	--	--	--	--	--	--	--
EALCF (MeV)	1.535E-7	2.045E-7	2.043E-7	2.067E-7	2.074E-7	2.083E-7	2.085E-7	2.098E-7	1.737E-7
Exp. σ	0.0020	0.0024	0.0024	0.0024	0.0024	0.0024	0.0024	0.0024	0.0019
k$_{eff}$	0.99133	0.99597	0.99555	0.99486	0.99504	0.99542	0.99530	0.99507	0.99368
σ	0.00033	0.00035	0.00033	0.00034	0.00034	0.00034	0.00034	0.00034	0.00033

Table 6.5.4-3   LEU MCNP Validation Statistics (cont'd)

Case	51.10	51.11	51.12	51.13	51.14	51.15	51.16	51.17	51.18	51.19
Clusters	9	9	9	9	9	9	9	9	9	9
Enrichment (wt % ^{235}U)	2.46%	2.46%	2.46%	2.46%	2.46%	2.46%	2.46%	2.46%	2.46%	2.46%
Pitch (cm)	1.636	1.636	1.636	1.636	1.636	1.636	1.636	1.636	1.636	1.636
Fuel OD (cm)	1.030	1.030	1.030	1.030	1.030	1.030	1.030	1.030	1.030	1.030
Clad OD (cm)	1.206	1.206	1.206	1.206	1.206	1.206	1.206	1.206	1.206	1.206
Clad Material	Al	Al	Al	Al	Al	Al	Al	Al	Al	Al
H/U (fissile)	219	219	219	219	219	219	219	219	219	219
Soluble B (ppm)	15	28	92	395	121	487	197	634	320	72
Absorber Type	B/Al Set 5	B/Al Set 5A	B/Al Set 4	B/Al Set 3	B/Al Set 3	B/Al Set 2	B/Al Set 2	B/Al Set 1	B/Al Set 1	B/Al Set 1
Cluster Gap (cm)	1.6	1.6	1.6	1.6	3.3	1.6	3.3	1.6	3.3	4.9
Reflector	Borated H$_2$O	Borated H$_2$O	Borated H$_2$O	Borated H$_2$O	Borated H$_2$O	Borated H$_2$O	Borated H$_2$O	Borated H$_2$O	Borated H$_2$O	Borated H$_2$O
Plate Loading (g ^{10}B/cm^2)	0.00517	0.00519	0.00403	0.00128	0.00128	0.00078	0.00078	0.00032	0.00032	0.00032
EALCF (MeV)	2.029E-7	2.015E-7	2.056E-7	2.112E-7	1.773E-7	2.106E-7	1.775E-7	2.119E-7	1.780E-7	1.587E-7
p. σ	0.0019	0.0019	0.0019	0.0022	0.0019	0.0024	0.0020	0.0027	0.0021	0.0019
k$_{eff}$	0.99210	0.99447	0.99073	0.98652	0.98634	0.99042	0.98974	0.99152	0.99029	0.98927
σ	0.00034	0.00034	0.00034	0.00034	0.00034	0.00034	0.00034	0.00034	0.00035	0.00035

Table 6.5.4-3   LEU MCNP Validation Statistics (cont'd)

Case	65.01	65.02	65.03	65.04	65.05	65.06	65.07	65.08
Clusters	2	2	2	2	2	2	2	2
Enrichment (wt % ^{235}U)	2.60%	2.60%	2.60%	2.60%	2.60%	2.60%	2.60%	2.60%
Pitch (cm)	1.956	1.956	1.956	1.956	1.956	1.956	1.956	1.956
Fuel OD (cm)	1.250	1.250	1.250	1.250	1.250	1.250	1.250	1.250
Clad OD (cm)	1.417	1.417	1.417	1.417	1.417	1.417	1.417	1.417
Clad Material	Al	Al	Al	Al	Al	Al	Al	Al
H/U (fissile)	203	203	203	203	203	203	203	203
Soluble B (ppm)	--	--	--	--	--	--	--	--
Absorber Type	none	304L SS (No B)	304L SS (0.67% B)	304L SS (0.98% B)	none	304L SS (No B)	304L SS (No B)	304L SS (No B)
Cluster Gap (cm)	5.9	5.9	5.9	5.9	7.8	7.8	7.8	7.8
Reflector	H_2O	H_2O	H_2O	H_2O	H_2O	H_2O	H_2O	H_2O
Plate Loading (g ^{10}B/cm^2)	--	0.00000	0.00599	0.00875	--	0.00000	0.00000	0.00000
EALCF [MeV]	2.045E-7	2.030E-7	2.054E-7	2.038E-7	2.049E-7	2.030E-7	2.055E-7	2.040E-7
Exp. σ	0.0014	0.0014	0.0015	0.0015	0.0014	0.0014	0.0014	0.0016
k$_{eff}$	0.99571	0.99618	0.99534	0.99547	0.99691	0.99614	0.99589	0.99624
σ	0.00023	0.00022	0.00023	0.00023	0.00023	0.00023	0.00023	0.00023

Table 6.5.4-3   LEU MCNP Validation Statistics (cont'd)

Case	65.09	65.10	65.11	65.12	65.13	65.14	65.15	65.16	65.17
Clusters	2	2	2	2	2	2	2	2	2
Enrichment (wt % ^{235}U)	2.60%	2.60%	2.60%	2.60%	2.60%	2.60%	2.60%	2.60%	2.60%
Pitch (cm)	1.956	1.956	1.956	1.956	1.956	1.956	1.956	1.956	1.956
Fuel OD (cm)	1.250	1.250	1.250	1.250	1.250	1.250	1.250	1.250	1.250
Clad OD (cm)	1.417	1.417	1.417	1.417	1.417	1.417	1.417	1.417	1.417
Clad Material	Al	Al	Al	Al	Al	Al	Al	Al	Al
H/U (fissile)	203	203	203	203	203	203	203	203	203
Soluble B (ppm)	--	--	--	--	--	--	--	--	--
Absorber Type	304L SS (No B)	304L SS (0.67% B)	304L SS (0.67% B)	304L SS (0.67% B)	304L SS (0.67% B)	304L SS (0.98% B)	304L SS (0.98% B)	304L SS (0.98% B)	304L SS (0.98% B)
Cluster Gap (cm)	7.8	7.8	7.8	7.8	7.8	7.8	7.8	7.8	7.8
Reflector	H_2O	H_2O	H_2O	H_2O	H_2O	H_2O	H_2O	H_2O	H_2O
Plate Loading (g ^{10}B/cm^2)	0.00000	0.00299	0.00299	0.00599	0.00599	0.00438	0.00438	0.00875	0.00875
EALCF [MeV]	1.993E-7	2.050E-7	2.069E-7	2.072E-7	1.977E-7	2.010E-7	2.004E-7	2.027E-7	2.017E-7
Exp. σ	0.0015	0.0016	0.0016	0.0017	0.0016	0.0016	0.0016	0.0017	0.0016
k_{eff}	0.99667	0.99676	0.99637	0.99643	0.99701	0.99650	0.99634	0.99658	0.99645
σ	0.00022	0.00022	0.00023	0.00023	0.00022	0.00023	0.00023	0.00022	0.00023

6.5.4.4   MOX (Plutonium Oxide/Uranium Oxide Mix) Results of Benchmark Calculations

The range of parameters included in the MOX benchmarks is shown in Table 6.5.4-4. Experiments are chosen to reflect the fuel evaluated for shipment. This includes the use of arrays of MOX rods (<10 wt % Pu) with light water moderation. Trending in k_{eff} was evaluated for the following independent variables: isotope weight percent as a function of ^{238}U fraction, moderator to fuel volume ratio, and energy of the average neutron lethargy causing fission (EALCF). No statistically significant trends were found for any of the system parameters. USLs are, therefore, generated for each of the independent variables. A minimum USL covering the range of applicability of the benchmark set is determined.

To evaluate the relative importance of the trend analysis to the upper subcritical limits, correlation coefficients are required for all independent parameters. The linear correlation coefficient, R, is calculated by taking the square root of the R^2 value. In particular, the correlation coefficient, R, is a measure of the linear relationship between k_{eff} and a critical experiment parameter. If R is +1, a perfect linear relationship with a positive slope is indicated. If R is -1, a perfect linear relationship with a negative slope is indicated. When R is 0, no linear relationship is indicated.

Table 6.5.4-5 contains the correlation coefficient, R, for each linear fit of k_{eff} versus experimental parameter. Linear fits and correlation constants are based on the 59 data-point evaluation sets plotted in Section 6.5.4.5.

As there is no significant correlation to any of the independent variables, the USL for each independent variable is calculated and shown with its range of applicability in Table 6.5.4-2. A sample output for EALCF is shown in Figure 6.5.4-11. Uncertainties included in the USLSTATS evaluation are the Monte Carlo uncertainty associated with the reactivity calculation and experimental uncertainty that was provided in the literature for each of the cases.

The $^{242}Pu/^{238}U$ ratio had the strongest correlation and the water-to-fuel volume ratio produced the minimum USL for all the independent variables correlated. Upper subcritical limits (USLs) are generated based on minimum margins of subcriticality (MMS), also referred to as administrative margin of 5%. The resulting minimum USLSTATS derived USL is 0.9331.

Figure 6.5.4-11 PWR MOX USLSTATS Output for Water to Fuel Volume Ratio

```
            uslstats: a utility to calculate upper subcritical
                   limits for criticality safety applications

    ++++++++++++++++++++++++++++++++++++++++++++++++++++++++++++++++++++++
                         Version 1.4, April 23, 2003
                         Oak Ridge National Laboratory
    ++++++++++++++++++++++++++++++++++++++++++++++++++++++++++++++++++++++


       Input to statistical treatment from file:w2fvr5.in

   Title: keff vs Water-to-Fuel Volume Ratio

       Proportion of the population =  .995
       Confidence of fit            =  .950
       Confidence on proportion     =  .950
       Number of observations       =  59
       Minimum value of closed band =   0.00
       Maximum value of closed band =   0.00
       Administrative margin        =   0.05


    independent   dependent    deviation     independent   dependent    deviation
    variable - x  variable - y  in y         variable - x  variable - y  in y

     1.19000E+00  9.91550E-01  5.96000E-03    1.52000E+00  9.88170E-01  5.14000E-03
     1.19000E+00  9.95580E-01  4.59000E-03    2.49000E+00  9.93450E-01  3.65000E-03
     2.52000E+00  9.93540E-01  3.02000E-03    3.52000E+00  9.87870E-01  3.65000E-03
     2.52000E+00  1.00039E+00  2.26000E-03    4.40000E+00  9.93650E-01  4.44000E-03
     3.64000E+00  9.93960E-01  2.34000E-03    6.28000E+00  9.96480E-01  5.43000E-03
     3.64000E+00  1.00264E+00  2.53000E-03    7.05000E+00  9.93170E-01  5.13000E-03
     1.68000E+00  9.93170E-01  7.16000E-03    2.49000E+00  9.96100E-01  3.53000E-03
     2.16000E+00  9.91940E-01  5.77000E-03    3.52000E+00  9.91630E-01  3.93000E-03
     2.16000E+00  9.96120E-01  5.28000E-03    4.40000E+00  9.94460E-01  4.62000E-03
     4.71000E+00  9.94700E-01  2.95000E-03    6.28000E+00  9.95150E-01  5.72000E-03
     5.67000E+00  9.94430E-01  2.56000E-03    7.05000E+00  9.91400E-01  6.11000E-03
     1.08000E+01  9.99990E-01  2.16000E-03    1.52000E+00  9.90720E-01  3.27000E-03
     2.42000E+00  9.90540E-01  4.71000E-03    2.49000E+00  9.91190E-01  3.05000E-03
     2.42000E+00  9.95620E-01  4.72000E-03    3.52000E+00  9.91770E-01  3.84000E-03
     2.42000E+00  1.00016E+00  4.72000E-03    4.40000E+00  9.97310E-01  4.73000E-03
     2.98000E+00  9.92510E-01  4.05000E-03    6.28000E+00  9.97440E-01  5.62000E-03
     2.98000E+00  9.95970E-01  4.02000E-03    7.05000E+00  9.96110E-01  6.52000E-03
     2.98000E+00  1.00453E+00  4.02000E-03    1.10000E+00  9.93110E-01  5.43000E-03
     4.24000E+00  9.94610E-01  4.12000E-03    1.56000E+00  9.89370E-01  4.93000E-03
     4.24000E+00  9.98940E-01  4.14000E-03    2.71000E+00  9.88960E-01  5.03000E-03
     4.24000E+00  9.99980E-01  4.12000E-03    3.79000E+00  9.89000E-01  6.22000E-03
     5.55000E+00  9.94400E-01  5.18000E-03    5.14000E+00  9.89770E-01  7.42000E-03
     5.55000E+00  9.97870E-01  5.19000E-03    5.58000E+00  9.90580E-01  8.01000E-03
     1.93000E+00  9.93380E-01  2.27000E-03    1.14000E+01  9.99200E-01  2.48000E-03
     2.56000E+00  9.92740E-01  2.67000E-03    1.14000E+01  9.98350E-01  2.47000E-03
     3.62000E+00  9.99510E-01  2.96000E-03    1.14000E+01  9.99230E-01  2.58000E-03
     4.53000E+00  9.96420E-01  2.86000E-03    2.07000E+01  1.00066E+00  1.89000E-03
     7.27000E+00  9.98140E-01  3.63000E-03    2.07000E+01  9.97920E-01  1.71000E-03
     1.01000E+01  9.97360E-01  4.23000E-03    2.07000E+01  9.97870E-01  1.70000E-03
     1.16000E+01  9.99430E-01  4.23000E-03

   chi =  1.2542 (upper bound = 9.49). The data tests normal.



        Output from statistical treatment

   keff vs Water-to-Fuel Volume Ratio

   Number of data points (n)                        59
   Linear regression, k(X)                          0.9932 + ( 3.5528E-04)*X
   Confidence on fit (1-gamma) [input]              95.0%
   Confidence on proportion (alpha) [input]         95.0%
   Proportion of population falling above
   lower tolerance interval (rho) [input]           99.5%
   Minimum value of X                               1.1000E+00
   Maximum value of X                               2.0700E+01
   Average value of X                               5.3212E+00
   Average value of k                               0.99509
```

Figure 6.5.4-11   PWR MOX USLSTATS Output for Water to Fuel Volume Ratio (cont'd)

```
Minimum value of k                              0.98787
Variance of fit, s(k,X)^2                        1.2095E-05


Within variance, s(w)^2                          1.9626E-05
Pooled variance, s(p)^2                          3.1721E-05
Pooled std. deviation, s(p)                       5.6322E-03
C(alpha,rho)*s(p)                                 2.2969E-02
student-t @ (n-2,1-gamma)                        1.67295E+00
Confidence band width, W                          1.0388E-02
Minimum margin of subcriticality, C*s(p)-W        1.2582E-02


Upper subcritical limits: (  1.1000    <= X <=   20.700    )
***** *********** *******


USL Method 1 (Confidence Band with
Administrative Margin)         USL1 = 0.9328 + ( 3.5528E-04)*X (X <    19.146   )
                                    = 0.9396                   (X >=   19.146   )


USL Method 2 (Single-Sided Uniform
Width Closed Interval Approach)  USL2 = 0.9702 + ( 3.5528E-04)*X (X <  1.91462E+01)
                                      = 0.9770                   (X >= 1.91462E+01)



USLs Evaluated Over Range of Parameter X:
**** ********* **** ***** ** ********* **


X:   1.10E+0  3.90E+0  6.70E+0  9.50E+0  1.23E+1  1.51E+1  1.79E+1  2.07E+1
     -------------------------------------------------------------------
USL-1:  0.9332   0.9342   0.9352   0.9362   0.9372   0.9382   0.9392   0.9396
USL-2:  0.9706   0.9716   0.9726   0.9736   0.9746   0.9756   0.9766   0.9770
     -------------------------------------------------------------------


**************************************************************************
```

Table 6.5.4-4   PWR MOX Range of Applicability for Complete Set of 59 Benchmark
Experiments

Parameter	Minimum	Maximum
Energy of average neutron lethargy causing fission (eV)	8.10E-02	8.99E-01
Uranium-235/Uranium-238 Ratio	1.58E-03	1.51E+00
Plutonium-238/Uranium-238 Ratio	1.88E-06	1.54E-04
Plutonium-239/Uranium-238 Ratio	1.39E-02	7.77E-01
Plutonium-240/Uranium-238 Ratio	1.20E-03	8.48E-02
Plutonium-241/Uranium-238 Ratio	7.90E-05	7.59E-03
Plutonium-242/Uranium-238 Ratio	4.63E-06	6.38E-04
Water-to-fuel volume ratio	1.10E+00	2.07E+01

Table 6.5.4-5   PWR MOX Correlation Coefficients and USLs for Benchmark
Experiments

Variable	R^2	R	Range of Applicability	USLSTATS Correlation	USL Low	USL High
Energy of average. neutron lethargy causing fission (eV)	0.0046	0.068	8.10E-02<=X<=8.99E-01	0.9372+-1.3542E-03X	0.9359	0.9370
U-235/U-238 Ratio	0.1148	0.339	1.58E-03<=X<=1.51E+00	0.9343+2.8147E-03X	0.9343	0.9385
Pu-238/U-238 Ratio	0.1030	0.321	1.88E-06<=X<=1.54E-04	0.9343+1.8044E+01X	0.9343	0.9370
Pu-239/U-238 Ratio	0.1202	0.347	1.39E-02<=X<=7.77E-01	0.9342+5.7481E-03X	0.9342	0.9386
Pu-240/U-238 Ratio	0.1409	0.375	1.20E-03<=X<=8.48E-02	0.9341+5.8088E-02X	0.9341	0.9390
Pu-241/U-238 Ratio	0.2160	0.465	7.90E-05<=X<=7.59E-03	0.9338+8.0681E-01X	0.9338	0.9399
Pu-242/U-238 Ratio	0.2440	0.494	4.63E-06<=X<=6.38E-04	0.9338+6.7569E+00X	0.9338	0.9381
Water-to-fuel volume ratio	0.1787	0.423	1.10E+00<=X<=2.07E+01	0.9328+3.5528E-04X	0.9331	0.9401

6.5.4.5   MOX (Plutonium Oxide/Uranium Oxide Mix) Criticality Benchmarks

From the International Handbook of Evaluated Criticality Safety Benchmark Experiments, 59 experiments are selected as the basis of the MCNP benchmarking. Experiments were selected for compatibility with LWR MOX rods evaluated for shipment. Of particular interest are benchmarks with rectangular arrays of MOX rods with plutonium weight percent less than 10%.

MCNP benchmark cases represent a collection of files composed of inputs directly obtained from references (with cross-section sets adjusted to those used in the cask analysis), NAC modified input files representing unique geometries based on reference input files, and input files constructed from the experimental material and geometry information. All cases were reviewed on a "preparer/checker" principle for modeling consistency with the cask models and the choice of code options. Due to large variations in the benchmark complexities, not all options employed in the cask models are reflected in each of the benchmarks (e.g., UNIVERSE structure). A review of the criticality results did not indicate any result trend due to particular modeling choices (e.g., using the UNIVERSE structure versus a single universe, or employing KSRC versus SDEF sampling).

Identifiers for the experiment, uncertainty and calculated k_{eff} and σ for each experiment are shown in Table 6.5.4-6. Stochastic Monte Carlo error is kept within ±0.2% and each output is checked to assure that the MCNP built-in statistical checks on the results are passed and that all fissile material is sampled.

Scatter plots of k_{eff} versus system parameters for 59 data point sets (see Figure 6.5.4-12 through Figure 6.5.4-19). Included in these scatter plots are linear regression lines with a corresponding correlation coefficient (R^2) to statistically indicate any trend or lack thereof. Scatter plots are created for k_{eff} versus the following.

- Energy of average neutron lethargy causing fission
- $^{235}U/^{238}U$ ratio
- $^{238}Pu/^{238}U$ ratio
- $^{239}Pu/^{238}U$ ratio
- $^{240}Pu/^{238}U$ ratio
- $^{241}Pu/^{238}U$ ratio
- $^{242}Pu/^{238}U$ ratio
- Water-to-fuel volume ratio

Figure 6.5.4-12   Adjusted k_{eff} vs. Energy of Average Neutron Lethargy Causing Fission
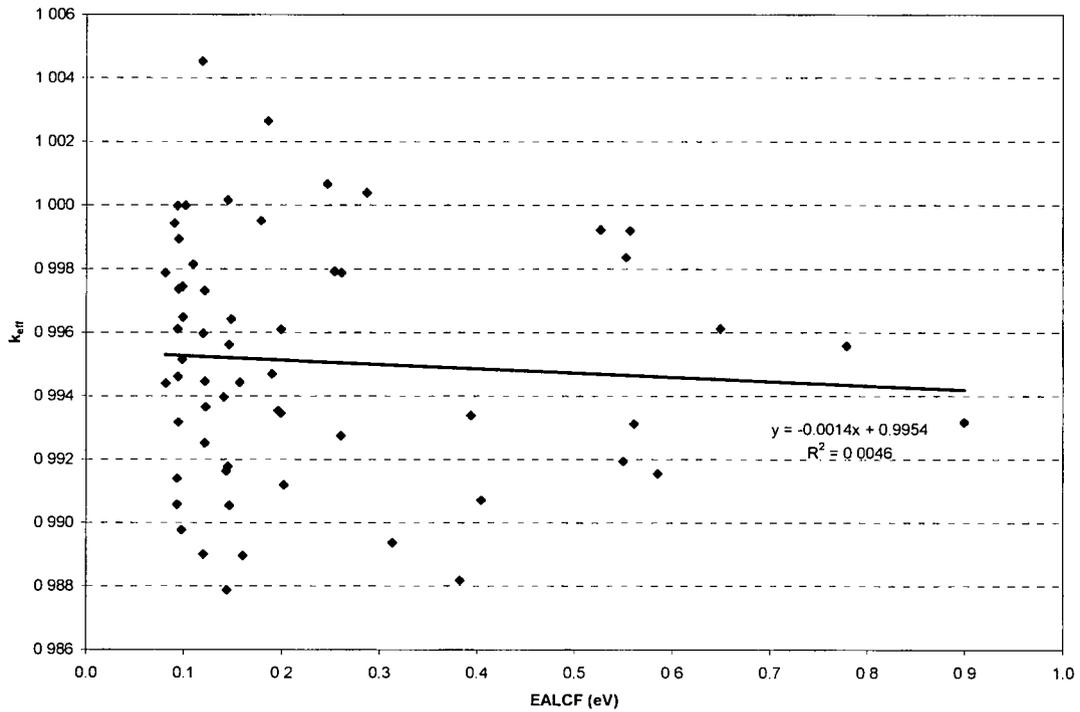
Figure 6.5.4-13   Adjusted k_{eff} vs. $^{235}U/^{238}U$ Ratio
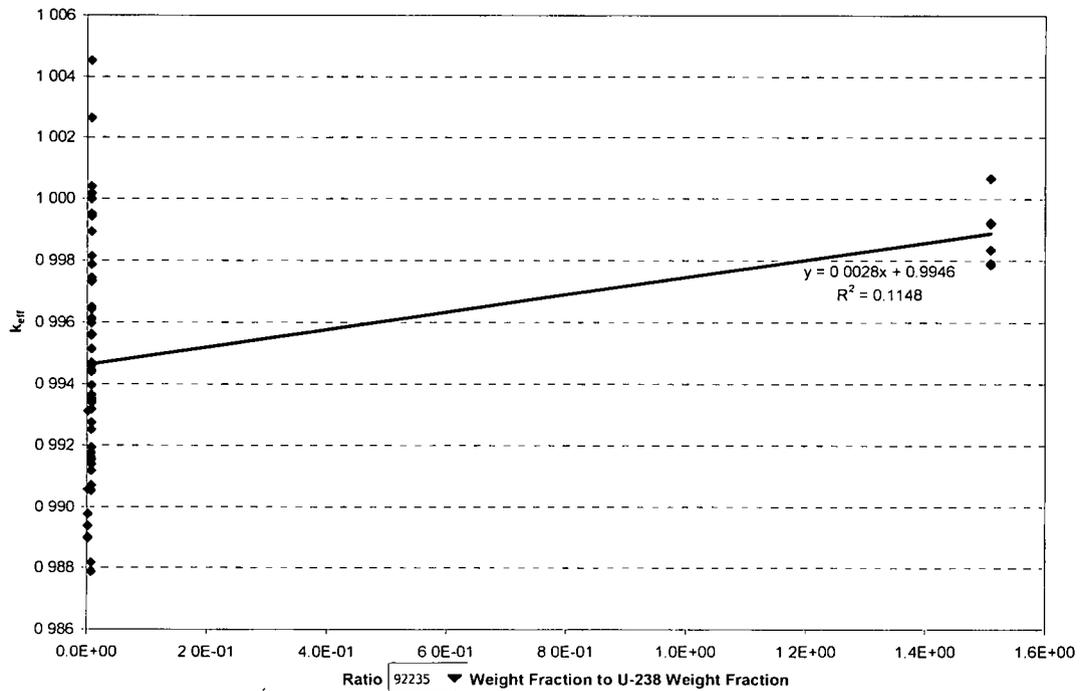
Figure 6.5.4-14   Adjusted k_{eff} vs. $^{238}Pu/^{238}U$ Ratio
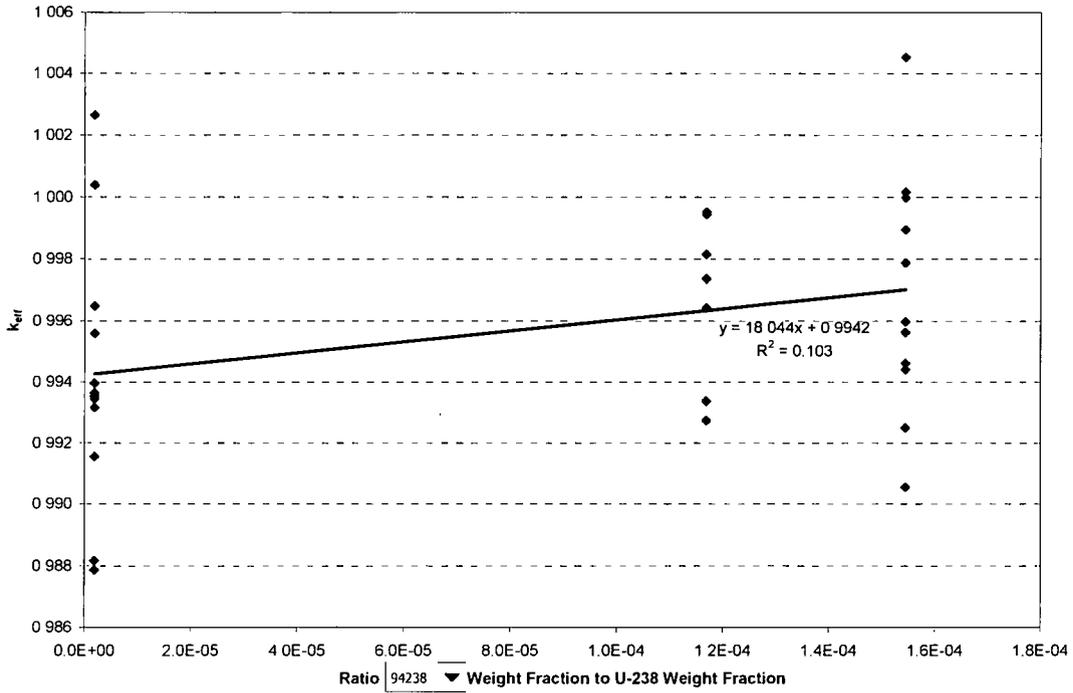
Figure 6.5.4-15   Adjusted k_{eff} vs. $^{239}Pu/^{238}U$ Ratio
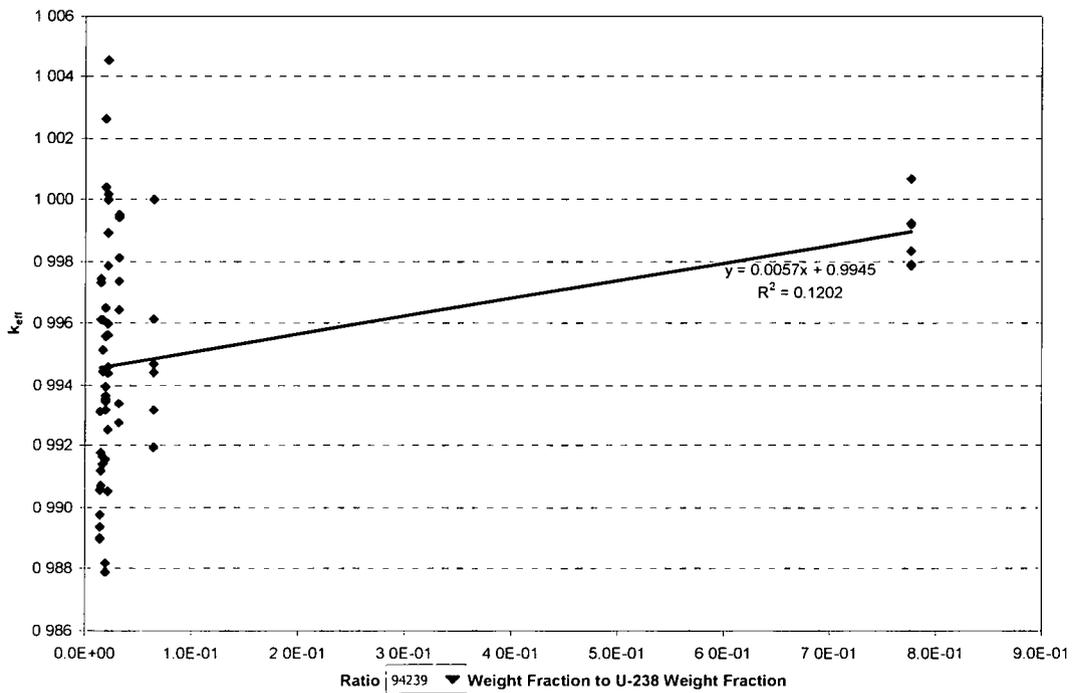
Figure 6.5.4-16   Adjusted k_{eff} vs. ^{240}Pu/^{238}U Ratio
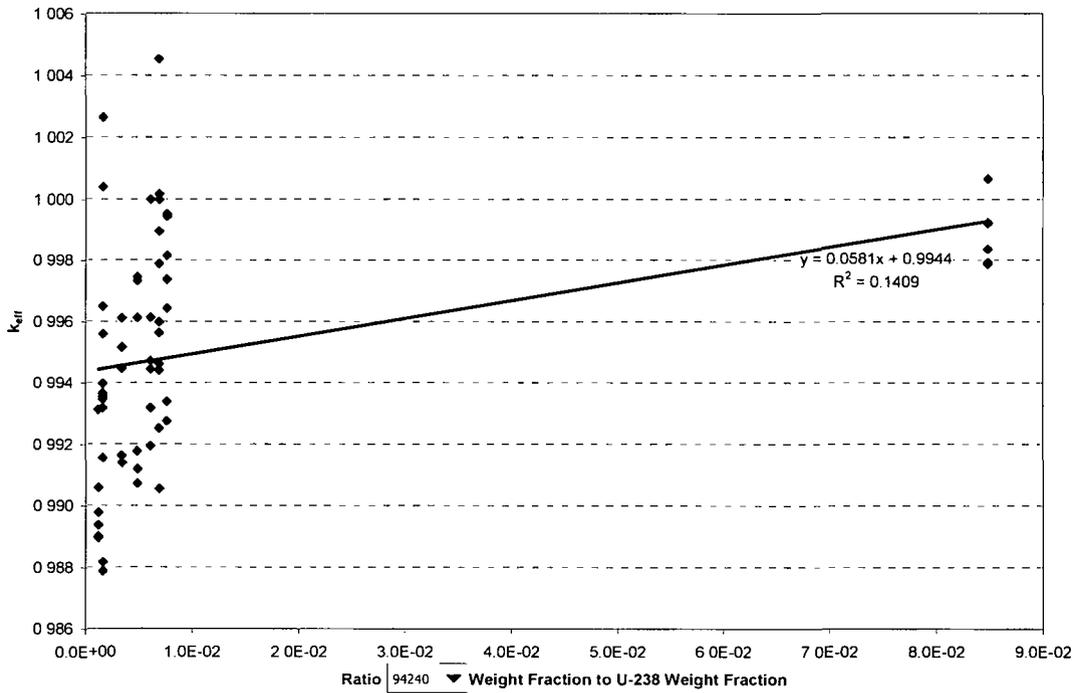
Figure 6.5.4-17   Adjusted k_{eff} vs. ^{241}Pu/^{238}U Ratio
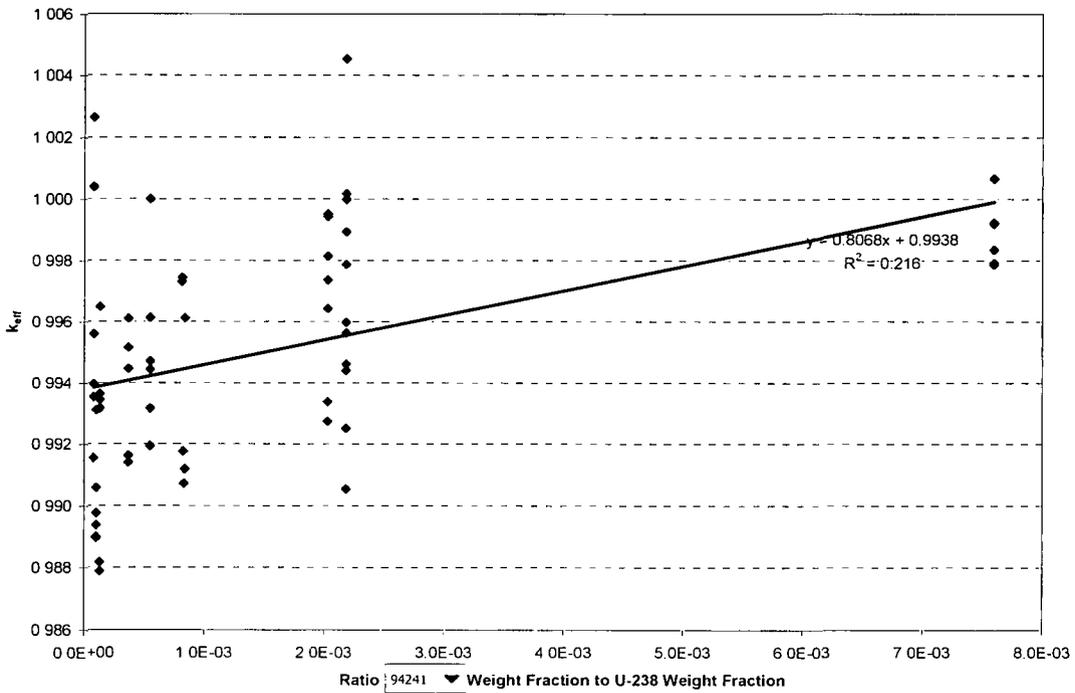
Figure 6.5.4-18   Adjusted k_{eff} vs. $^{242}Pu/^{238}U$ Ratio
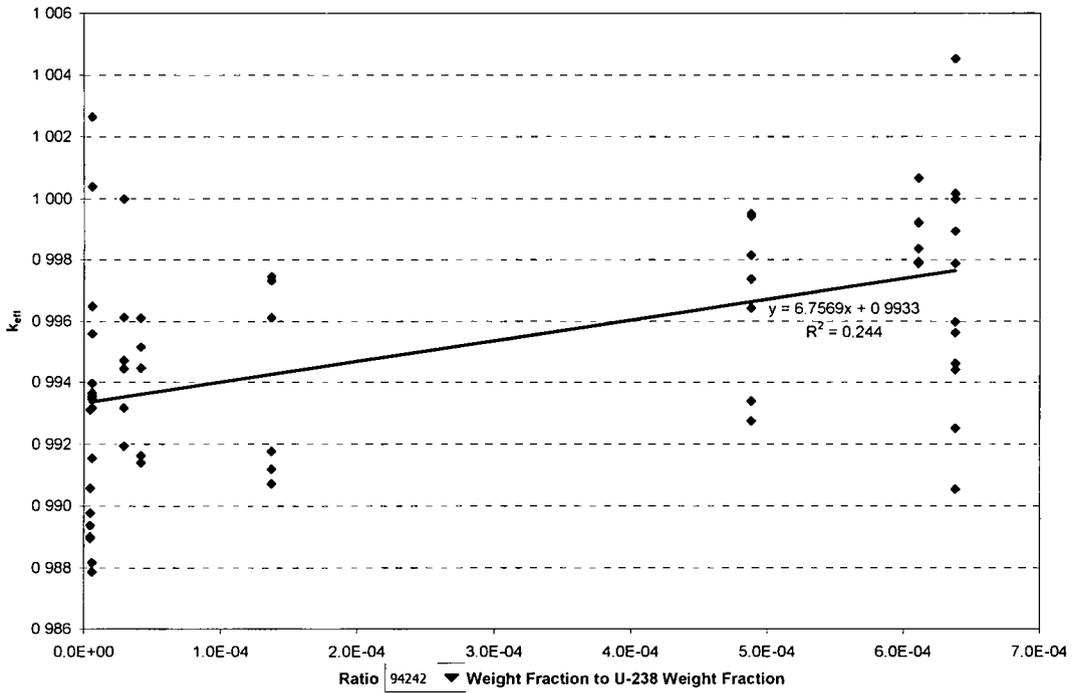
Figure 6.5.4-19   Adjusted k_{eff} vs. Water-to-Fuel Volume Ratio
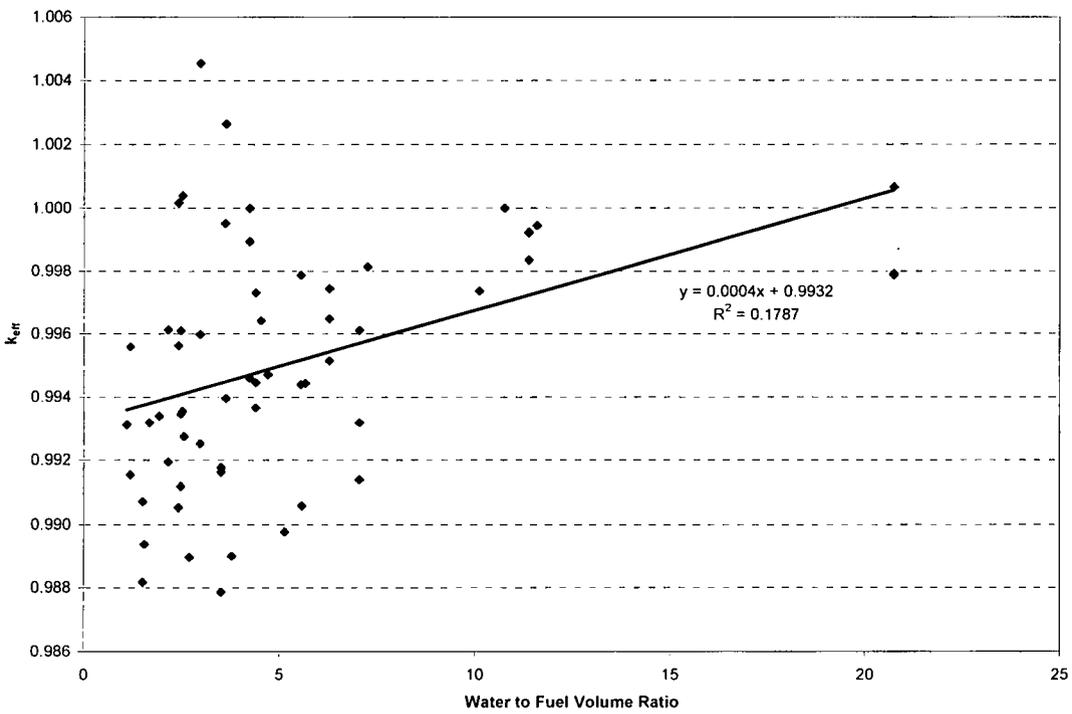
Table 6.5.4-6   MCNP Validation Statistics

Identification	Water-to-Fuel Ratio	Benchmark			MCNP5 v1.30			EALCF (eV)
		k_{eff}	σ	Δk	k_{eff}	σ	Adj. k_{eff}	
MIXCT-002-01	1.2	1.0010	0.0059	-0.0010	0.99255	0.00082	0.99155	0.58526
MIXCT-002-02	1.2	1.0009	0.0045	-0.0009	0.99648	0.00088	0.99558	0.77857
MIXCT-002-03	2.5	1.0024	0.0029	-0.0024	0.99594	0.00083	0.99354	0.19618
MIXCT-002-04	2.5	1.0024	0.0021	-0.0024	1.00279	0.00083	1.00039	0.28661
MIXCT-002-05	3.6	1.0038	0.0022	-0.0038	0.99776	0.00081	0.99396	0.14069
MIXCT-002-06	3.6	1.0029	0.0024	-0.0029	1.00554	0.00080	1.00264	0.18588
MIXCT-003-01	1.7	1.0000	0.0071	0.0000	0.99317	0.00092	0.99317	0.89937
MIXCT-003-02	2.2	1.0000	0.0057	0.0000	0.99194	0.00090	0.99194	0.54987
MIXCT-003-03	2.2	1.0000	0.0052	0.0000	0.99612	0.00093	0.99612	0.64918
MIXCT-003-04	4.7	1.0000	0.0028	0.0000	0.99470	0.00092	0.99470	0.18983
MIXCT-003-05	5.7	1.0000	0.0024	0.0000	0.99443	0.00088	0.99443	0.15707
MIXCT-003-06	10.8	1.0000	0.0020	0.0000	0.99999	0.00082	0.99999	0.10167
MIXCT-004-01	2.4	1.0000	0.0046	0.0000	0.99054	0.00099	0.99054	0.14647
MIXCT-004-02	2.4	1.0000	0.0046	0.0000	0.99562	0.00106	0.99562	0.14615
MIXCT-004-03	2.4	1.0000	0.0046	0.0000	1.00016	0.00107	1.00016	0.14470
MIXCT-004-04	3.0	1.0000	0.0039	0.0000	0.99251	0.00111	0.99251	0.12146
MIXCT-004-05	3.0	1.0000	0.0039	0.0000	0.99597	0.00098	0.99597	0.11971
MIXCT-004-06	3.0	1.0000	0.0039	0.0000	1.00453	0.00097	1.00453	0.11898
MIXCT-004-07	4.2	1.0000	0.0040	0.0000	0.99461	0.00100	0.99461	0.09396
MIXCT-004-08	4.2	1.0000	0.0040	0.0000	0.99894	0.00106	0.99894	0.09454
MIXCT-004-09	4.2	1.0000	0.0040	0.0000	0.99998	0.00097	0.99998	0.09350
MIXCT-004-10	5.6	1.0000	0.0051	0.0000	0.99440	0.00092	0.99440	0.08152
MIXCT-004-11	5.6	1.0000	0.0051	0.0000	0.99787	0.00094	0.99787	0.08098
MIXCT-005-01	1.9	1.0008	0.0022	-0.0008	0.99418	0.00057	0.99338	0.39380
MIXCT-005-02	2.6	1.0011	0.0026	-0.0011	0.99384	0.00059	0.99274	0.26049
MIXCT-005-03	3.6	1.0016	0.0029	-0.0016	1.00111	0.00058	0.99951	0.17856
MIXCT-005-04	4.5	1.0021	0.0028	-0.0021	0.99852	0.00057	0.99642	0.14820
MIXCT-005-05	7.3	1.0026	0.0036	-0.0026	1.00074	0.00049	0.99814	0.10925
MIXCT-005-06	10.1	1.0033	0.0042	-0.0033	1.00066	0.00048	0.99736	0.09455
MIXCT-005-07	11.6	1.0035	0.0042	-0.0035	1.00293	0.00046	0.99943	0.09019

Table 6.5.4-6   MCNP Validation Statistics (cont'd)

Identification	Water-to-Fuel Ratio	Benchmark			MCNP5 v1.30			EALCF (eV)
		k_{eff}	σ	Δk	k_{eff}	σ	Adj. k_{eff}	
MIXCT-006-01	1.5	1.0016	0.0051	-0.0016	0.98977	0.00060	0.98817	0.38252
MIXCT-006-02	2.5	1.0017	0.0036	-0.0017	0.99515	0.00061	0.99345	0.19894
MIXCT-006-03	3.5	1.0026	0.0036	-0.0026	0.99047	0.00059	0.98787	0.14393
MIXCT-006-04	4.4	1.0051	0.0044	-0.0051	0.99875	0.00058	0.99365	0.12231
MIXCT-006-05	6.3	1.0040	0.0054	-0.0040	1.00048	0.00055	0.99648	0.09904
MIXCT-006-06	7.1	1.0055	0.0051	-0.0055	0.99867	0.00052	0.99317	0.09438
MIXCT-007-01	2.5	1.0023	0.0035	-0.0023	0.99840	0.00049	0.99610	0.19918
MIXCT-007-02	3.5	1.0024	0.0039	-0.0024	0.99403	0.00050	0.99163	0.14313
MIXCT-007-03	4.4	1.0036	0.0046	-0.0036	0.99806	0.00048	0.99446	0.12122
MIXCT-007-04	6.3	1.0037	0.0057	-0.0037	0.99885	0.00043	0.99515	0.09818
MIXCT-007-05	7.1	1.0044	0.0061	-0.0044	0.99580	0.00042	0.99140	0.09330
MIXCT-008-01	1.5	0.9997	0.0032	0.0003	0.99042	0.00066	0.99072	0.40443
MIXCT-008-02	2.5	1.0008	0.0030	-0.0008	0.99199	0.00057	0.99119	0.20199
MIXCT-008-03	3.5	1.0023	0.0038	-0.0023	0.99407	0.00056	0.99177	0.14500
MIXCT-008-04	4.4	1.0015	0.0047	-0.0015	0.99881	0.00057	0.99731	0.12108
MIXCT-008-05	6.3	1.0022	0.0056	-0.0022	0.99964	0.00050	0.99744	0.09872
MIXCT-008-06	7.1	1.0028	0.0065	-0.0028	0.99891	0.00049	0.99611	0.09362
MIXCT-009-01	1.1	1.0003	0.0054	-0.0003	0.99341	0.00059	0.99311	0.56093
MIXCT-009-02	1.6	1.0020	0.0049	-0.0020	0.99137	0.00058	0.98937	0.31308
MIXCT-009-03	2.7	1.0035	0.0050	-0.0035	0.99246	0.00056	0.98896	0.16022
MIXCT-009-04	3.8	1.0046	0.0062	-0.0046	0.99360	0.00054	0.98900	0.11987
MIXCT-009-05	5.1	1.0059	0.0074	-0.0059	0.99567	0.00049	0.98977	0.09776
MIXCT-009-06	5.6	1.0067	0.0080	-0.0067	0.99728	0.00047	0.99058	0.09313
MIXCT-011-01	11.4	1.0000	0.0024	0.0000	0.99920	0.00063	0.99920	0.55670
MIXCT-011-02	11.4	1.0000	0.0024	0.0000	0.99835	0.00060	0.99835	0.55254
MIXCT-011-03	11.4	1.0000	0.0025	0.0000	0.99923	0.00062	0.99923	0.52644
MIXCT-011-04	20.7	1.0000	0.0018	0.0000	1.00066	0.00056	1.00066	0.24638
MIXCT-011-05	20.7	1.0000	0.0016	0.0000	0.99792	0.00059	0.99792	0.25390
MIXCT-011-06	20.7	1.0000	0.0016	0.0000	0.99787	0.00058	0.99787	0.26082

6.5.5   MCNP Criticality Benchmarks for Research Reactor Fuels

The results of the criticality analyses presented in this chapter must be compared to the upper subcritical limit (USL). The USL accounts for bias and uncertainty resulting from the method using information obtained from the analysis of criticality benchmark experimental data. Code bias calculated in this section is applicable to research reactor fuel (e.g., MTR, DIDO, SLOWPOKE, and NRU/NRX) with the exception of TRIGA (U-ZrH) elements.

Criticality code validation is performed for the Monte Carlo evaluation code and neutron cross-section libraries. Criticality validation is required by the criticality safety standard ANSI/ANS-8.1.

6.5.5.1   Benchmark Experiments and Applicability Discussion

NUREG/CR-6361, "Criticality Benchmark Guide for Light-Water-Reactor Fuel in Transportation and Storage Packages," provides a guide to LWR criticality benchmark calculations and the determination of bias and subcritical limits in criticality safety evaluations. In Section 2 of the NUREG, a series of LWR criticality experiments is described in sufficient detail for independent modeling. In Section 3, the criticality experiments are modeled, and the results (k_{eff} values) are presented. The method utilized in the NUREG is KENO-Va with the 44-group ENDF/B-V cross-section library embedded in SCALE 4.3. In Section 4, a guide for the determination of bias and subcritical safety limits is provided based on ANSI/ANS-8.1 and statistical analysis of the trending in the bias. Finally, guidelines for experiment selection and applicability are presented in Section 5. The approach outlined in Section 4 of the NUREG is described in detail herein and is implemented for MCNP5 with continuous energy ENDF/B-VI cross-sections.

NUREG/CR-6361 implements ANSI/ANS-8.1 criticality safety criterion as follows.

$$k_s \leq k_c - \Delta k_s - \Delta k_c - \Delta k_m \qquad \text{(Equation 1)}$$

   where:

   k_s = calculated allowable maximum multiplication factor, k_{eff}, of the system being evaluated for all normal or credible abnormal conditions or events.

   k_c = mean k_{eff} that results from a calculation of benchmark criticality experiments using a particular calculation method. If the calculated k_{eff} values for the criticality experiments exhibit a trend with an independent parameter, then k_c shall be determined by extrapolation based on best fit to calculated values. Criticality experiments used as benchmarks in computing k_c should have physical compositions, configurations and nuclear characteristics (including reflectors) similar to those of the system being evaluated.

Δk_s = allowance for the following:

- statistical or convergence uncertainties, or both, in computation of k_s
- material and fabrication tolerances
- geometric or material representations used in computational method

Δk_c = margin for uncertainty in k_c, which includes allowance for the following:

- uncertainties in criticality experiments
- statistical or convergence uncertainties, or both, in computation of k_c
- uncertainties resulting from extrapolation of k_c outside range of experimental data
- uncertainties resulting from limitations in geometrical or material representations used in the computational method

Δk_m = arbitrary administrative margin to ensure subcriticality of k_s

The various uncertainties are combined statistically if they are independent. Correlated uncertainties are combined by addition.

Equation 1 can be rewritten as shown.

$$k_s \leq 1 - \Delta k_m - \Delta k_s - (1 - k_c) - \Delta k_c \quad \text{(Equation 2)}$$

Noting that the definition of the bias is $\beta = 1 - k_c$, Equation 2 can be written as shown.

$$k_s + \Delta k_s \leq 1 - \Delta km - \beta - \Delta\beta \quad \text{(Equation 3)}$$

where:

$$\Delta\beta = \Delta k_c$$

Thus, the maximum allowable value for k_{eff} plus uncertainties in the system being analyzed must be below 1 minus an administrative margin (typically 0.05), which includes the bias and the uncertainty in the bias. This can also be written as shown.

$$k_s + \Delta k_s \leq \text{Upper Subcritical Limit (USL)} \quad \text{(Equation 4)}$$

where:

$$USL \equiv 1 - \Delta k_m - \beta - \Delta\beta \quad \text{(Equation 5)}$$

This is the USL criterion as described in Section 4 of NUREG/CR-6361. Two methods are prescribed for the statistical determination of the USL. The "Confidence Band with Administrative Margin (USL-1)" approach is implemented here and is referred to generically as USL. A $\Delta k_m = 0.05$ and a lower confidence band are specified based on a linear regression of k_{eff} as a function of some system parameter.

Subsequent sections contain the list of critical benchmarks employed in the validation of MCNP with its continuous energy neutron cross-section libraries and the processing of the experimental results into the USL. Also included are linear fits of reactivity (k_{eff}) to each of the system

parameters evaluated. Experiments were chosen to reflect the in-cask fuel geometry and materials as closely as available.

6.5.5.2   HEU and IEU Criticality Benchmarks

From the International Handbook of Evaluated Criticality Safety Benchmark Experiments, intermediate and high enriched thermal neutron experiments are selected as the basis of the MCNP benchmarking. Materials selected were compounds and metallic fuels. Experiments were selected for compatibility of materials and geometry with the spent fuel casks. As such, experiments containing significant neutron absorber in the form of plates, rods, or soluble poison are eliminated. Also removed are experiments containing non light water moderator. Further review eliminated experiments if they did not contain a primarily thermal neutron spectrum causing fission.

All cases were reviewed on a "preparer/checker" principle for modeling consistency with the cask models and the choice of code options. Case inputs from the handbook where modified as necessary to match experimental data or to correct modeling errors. Due to large variations in the benchmark complexities, not all options employed in the cask models are reflected in each of the benchmarks (e.g., UNIVERSE structure). A review of the criticality results did not indicate any result trend due to particular modeling choices (e.g., using the UNIVERSE structure versus a single universe, or employing KSRC versus SDEF sampling).

Key system parameters for the experiments are listed in Table 6.5.5-1. Table 6.5.5-2 lists the benchmark k_{eff} and experimental uncertainty. The NAC calculated MCNP k_{eff}s and Monte Carlo uncertainties are shown in Table 6.5.5-3. Stochastic Monte Carlo error is kept within ±0.2% and each output is checked to assure that the MCNP built-in statistical checks on the results are passed and that all fissile material is sampled. Also included in the table are the combined Monte Carlo and experimental uncertainty and the results of the initial processing of the data indicating the minimum and average bias of each experiment.

Scatter plots of k_{eff} versus enrichment and average lethargy of neutrons causing fission are shown in Figure 6.5.5-1 and Figure 6.5.5-2. Included in these scatter plots are linear regression lines with a corresponding correlation coefficient (R^2) to statistically indicate any trend or lack thereof.

6.5.5.3   Results of MCNP Research Reactor Benchmark Calculations

Trending in k_{eff} was evaluated for wt% ^{235}U and energy of the average neutron lethargy causing fission (EALCF), the two parameters most likely to show cross section effects. No statistically significant trends were found for any of the system parameters. USLs are generated for each of

the independent variables. A minimum USL covering the range of applicability of the benchmark set is determined.

To evaluate the relative importance of the trend analysis to the upper subcritical limits, correlation coefficients are required for all independent parameters. The linear correlation coefficient, R, is calculated by taking the square root of the R^2 value. In particular, the correlation coefficient, R, is a measure of the linear relationship between k_{eff} and a critical experiment parameter. If R is +1, a perfect linear relationship with a positive slope is indicated. If R is -1, a perfect linear relationship with a negative slope is indicated. When R is 0, no linear relationship is indicated.

Table 6.5.5-4 contains the correlation coefficient, R, for each linear fit of k_{eff} versus experimental parameter. Linear fits and correlation constants are based on full 54 data-point evaluation sets plotted in the previous section.

The USL for each independent variable is calculated and shown with its range of applicability in Table 6.5.5-5. The USLSTATS output of k_{eff} versus EALCF and enrichment are shown in Figure 6.5.5-3 and Figure 6.5.5-4. Uncertainties included in the USLSTATS evaluation are the Monte Carlo uncertainty associated with the reactivity calculation, and the experimental uncertainty that was provided in the literature for each of the cases.

Based on all the independent variable correlations, a lower limit constant USL of 0.9171 may be applied. The range of applicability (area of applicability) of this limit may be extended to lower enrichment as the correlation shows an increase in USL as a function of reduced enrichment.

Figure 6.5.5-1 k_{eff} versus Fuel Enrichment (MCNP – Research Reactor Fuel)
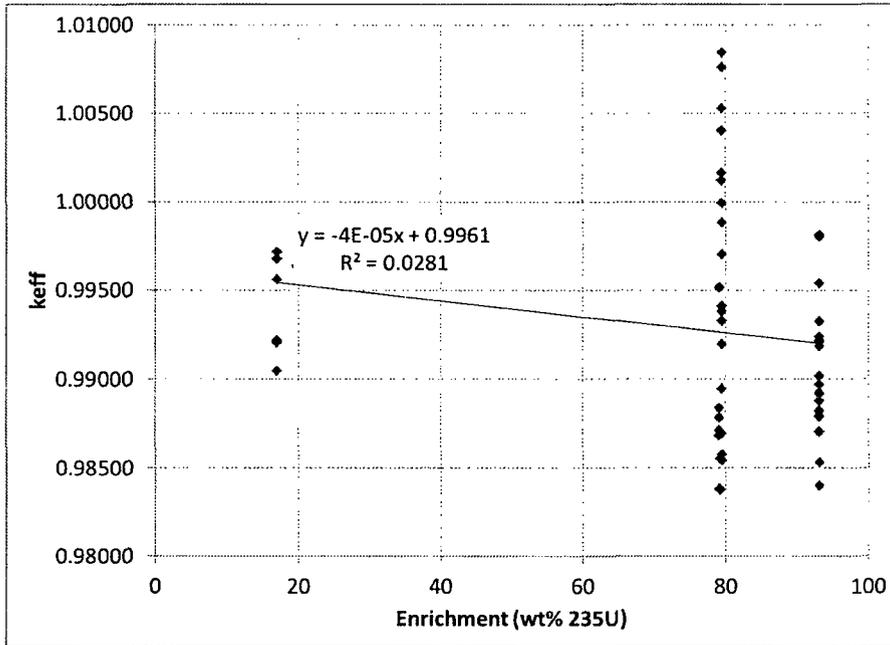
Figure 6.5.5-2 k_{eff} versus Energy of Average Neutron Lethargy Causing Fission
(MCNP – Research Reactor Fuel)
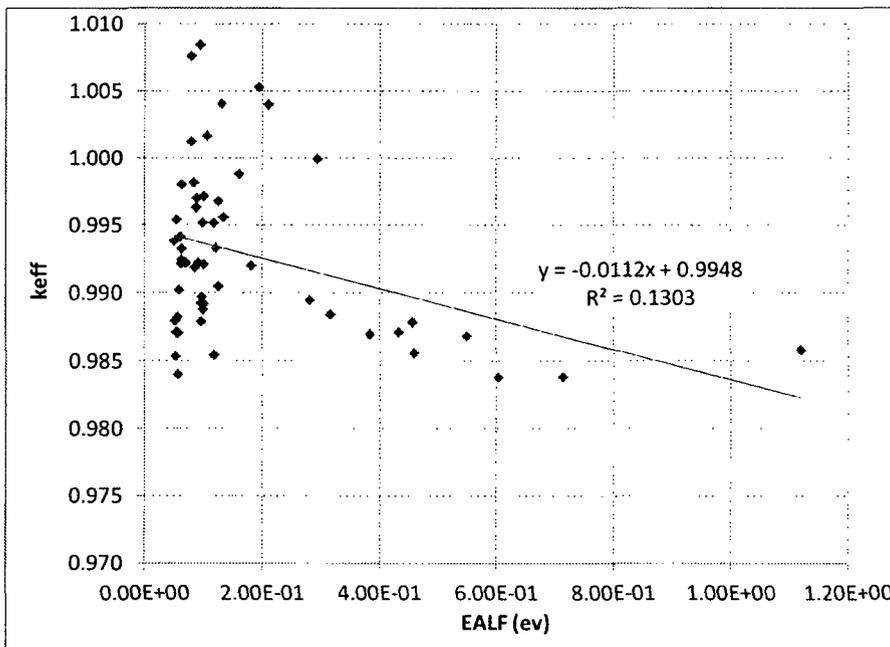
Figure 6.5.5-3   MCNP Research Reactor Fuel USLSTATS Output for EALCF

```
Proportion of the population = .995
Confidence of fit           = .950
Confidence on proportion    = .950
Number of observations      =   54
Minimum value of closed band =  0.00
Maximum value of closed band =  0.00
Administrative margin        =  0.05


independent   dependent    deviation          independent   dependent    deviation
variable - x  variable - y  in y              variable - x  variable - y  in y

3.83770E-01   9.86960E-01  4.65000E-03        9.65800E-02   9.89240E-01  8.11000E-03
2.81040E-01   9.89440E-01  4.68000E-03        9.82040E-02   9.89700E-01  8.11000E-03
1.81510E-01   9.91990E-01  4.66000E-03        9.95040E-02   9.88780E-01  8.11000E-03
1.21140E-01   9.93300E-01  4.62000E-03        1.00600E-01   9.89170E-01  8.11000E-03
8.96800E-02   9.96990E-01  4.62000E-03        9.66350E-02   9.87890E-01  8.11000E-03
2.93880E-01   9.99910E-01  4.65000E-03        8.57350E-02   9.91880E-01  4.49000E-03
2.10270E-01   1.00396E+00  4.66000E-03        7.12960E-02   9.92190E-01  4.09000E-03
1.94070E-01   1.00527E+00  4.62000E-03        6.39970E-02   9.98000E-01  4.08000E-03
1.31260E-01   1.00402E+00  4.61000E-03        6.25290E-02   9.92120E-01  4.08000E-03
9.46680E-02   1.00843E+00  4.66000E-03        5.91670E-02   9.90210E-01  4.07000E-03
7.99520E-02   1.00758E+00  4.63000E-03        5.67170E-02   9.88230E-01  4.08000E-03
1.18230E-01   9.85420E-01  4.62000E-03        5.50180E-02   9.87090E-01  4.06000E-03
6.12710E-02   9.94110E-01  4.60000E-03        5.30120E-02   9.85340E-01  4.06000E-03
1.61160E-01   9.98810E-01  4.64000E-03        5.27070E-02   9.87930E-01  4.06000E-03
7.97960E-02   1.00119E+00  4.56000E-03        8.34310E-02   9.98130E-01  4.10000E-03
1.11980E+00   9.85800E-01  5.96000E-03        6.31130E-02   9.93270E-01  4.08000E-03
1.05990E-01   1.00162E+00  2.35000E-03        5.49410E-02   9.95360E-01  4.06000E-03
5.02850E-02   9.93820E-01  4.89000E-03        5.78770E-02   9.87070E-01  4.07000E-03
7.15000E-01   9.83810E-01  4.29000E-03        5.71950E-02   9.83980E-01  4.07000E-03
5.50720E-01   9.86840E-01  4.31000E-03        6.37490E-02   9.92430E-01  4.08000E-03
4.34030E-01   9.87120E-01  4.29000E-03        9.13040E-02   9.92190E-01  3.96000E-03
6.03930E-01   9.83750E-01  3.34000E-03        1.34700E-01   9.95590E-01  4.07000E-03
4.58840E-01   9.85560E-01  3.49000E-03        1.00680E-01   9.97130E-01  4.46000E-03
4.57170E-01   9.87850E-01  4.30000E-03        1.25750E-01   9.96750E-01  4.46000E-03
3.16220E-01   9.88370E-01  4.39000E-03        1.00650E-01   9.92110E-01  4.36000E-03
1.18400E-01   9.95140E-01  4.88000E-03        1.25740E-01   9.90480E-01  4.47000E-03
9.84130E-02   9.95140E-01  4.97000E-03        8.78000E-02   9.96310E-01  1.40000E-03

chi = 0.6296 (upper bound = 9.49). The data tests normal.

     Output from statistical treatment

keff vs EALCF

Number of data points (n)                      54
Linear regression, k(X)                        0.9948 + (-1.1154E-02)*X
Confidence on fit (1-gamma) [input]            95.0%
Confidence on proportion (alpha) [input]       95.0%
Proportion of population falling above
lower tolerance interval (rho) [input]         99.5%
Minimum value of X                             5.0285E-02
Maximum value of X                             1.1198E+00
Average value of X                             1.7980E-01
Average value of k                             0.99279
Minimum value of k                             0.98375
Variance of fit, s(k,X)^2                      3.4489E-05
Within variance, s(w)^2                        2.3078E-05
Pooled variance, s(p)^2                        5.7567E-05
Pooled std. deviation, s(p)                    7.5873E-03
C(alpha,rho)*s(p)                              3.4132E-02
student-t @ (n-2,1-gamma)                      1.67620E+00
Confidence band width, W                       1.5195E-02
Minimum margin of subcriticality, C*s(p)-W     1.8937E-02


Upper subcritical limits: ( 5.02850E-02 <= X <= 1.1198    )
*****  ***********  *******


USL Method 1 (Confidence Band with
Administrative Margin)           USL1 = 0.9296 + (-1.1154E-02)*X

USL Method 2 (Single-Sided Uniform
Width Closed Interval Approach)   USL2 = 0.9607 + (-1.1154E-02)*X

USLs Evaluated Over Range of Parameter X:
****  *********  ****  *****  **  *********  **

X:  5.03E-2  2.03E-1  3.56E-1  5.09E-1  6.61E-1  8.14E-1  9.67E-1  1.12E+0
     -------------------------------------------------------------------
USL-1:  0.9290   0.9273   0.9256   0.9239   0.9222   0.9205   0.9188   0.9171
USL-2:  0.9601   0.9584   0.9567   0.9550   0.9533   0.9516   0.9499   0.9482
```

Figure 6.5.5-4 MCNP Research Reactor Fuel USLSTATS Output for wt% ^{235}U

```
Proportion of the population = .995
    Confidence of fit          = .950
    Confidence on proportion   = .950
    Number of observations     =    54
    Minimum value of closed band =   0.00
    Maximum value of closed band =   0.00
    Administrative margin      =   0.05
```

independent variable - x	dependent variable - y	deviation in y	independent variable - x	dependent variable - y	deviation in y
7.94700E+01	9.86960E-01	4.65000E-03	9.32000E+01	9.89240E-01	8.11000E-03
7.94700E+01	9.89440E-01	4.68000E-03	9.32000E+01	9.89700E-01	8.11000E-03
7.94700E+01	9.91990E-01	4.66000E-03	9.32000E+01	9.88730E-01	8.11000E-03
7.94700E+01	9.93300E-01	4.62000E-03	9.32000E+01	9.89170E-01	8.11000E-03
7.94700E+01	9.96990E-01	4.62000E-03	9.32000E+01	9.87890E-01	8.11000E-03
7.94700E+01	9.99910E-01	4.65000E-03	9.31700E+01	9.91880E-01	4.49000E-03
7.94700E+01	1.00396E+00	4.66000E-03	9.31700E+01	9.92190E-01	4.09000E-03
7.94700E+01	1.00527E+00	4.62000E-03	9.31700E+01	9.98000E-01	4.08000E-03
7.94700E+01	1.00402E+00	4.61000E-03	9.31700E+01	9.92120E-01	4.08000E-03
7.94700E+01	1.00843E+00	4.66000E-03	9.31700E+01	9.90210E-01	4.07000E-03
7.94700E+01	1.00758E+00	4.63000E-03	9.31700E+01	9.88230E-01	4.08000E-03
7.94700E+01	9.85420E-01	4.62000E-03	9.31700E+01	9.87090E-01	4.06000E-03
7.94700E+01	9.94110E-01	4.60000E-03	9.31700E+01	9.85340E-01	4.06000E-03
7.94700E+01	9.98810E-01	4.64000E-03	9.31700E+01	9.87930E-01	4.06000E-03
7.94700E+01	1.00119E+00	4.56000E-03	9.31700E+01	9.98130E-01	4.10000E-03
7.94700E+01	9.85800E-01	5.96000E-03	9.31700E+01	9.93270E-01	4.08000E-03
7.94700E+01	1.00162E+00	2.35000E-03	9.31700E+01	9.95360E-01	4.06000E-03
7.94700E+01	9.93820E-01	4.89000E-03	9.31700E+01	9.87070E-01	4.07000E-03
7.91900E+01	9.83810E-01	4.29000E-03	9.31700E+01	9.83980E-01	4.07000E-03
7.91900E+01	9.86840E-01	4.31000E-03	9.31700E+01	9.92430E-01	4.08000E-03
7.91900E+01	9.87120E-01	4.29000E-03	1.70000E+01	9.92190E-01	3.96000E-03
7.92400E+01	9.83750E-01	3.34000E-03	1.70000E+01	9.95580E-01	4.07000E-03
7.92400E+01	9.85560E-01	3.49000E-03	1.70000E+01	9.97130E-01	4.46000E-03
7.91900E+01	9.87850E-01	4.30000E-03	1.70000E+01	9.96750E-01	4.46000E-03
7.91900E+01	9.88370E-01	4.39000E-03	1.70000E+01	9.92110E-01	4.36000E-03
7.91900E+01	9.95140E-01	4.88000E-03	1.70000E+01	9.90480E-01	4.47000E-03
7.91900E+01	9.95140E-01	4.97000E-03	1.97700E+01	9.96310E-01	1.40000E-03

```
chi = 0.6296 (upper bound = 9.49). The data tests normal.

        Output from statistical treatment

keff vs enrichment

    Number of data points (n)                         54
    Linear regression, k(X)                           0.9961 + (-4.3735E-05)*X
    Confidence on fit (1-gamma) [input]               95.0%
    Confidence on proportion (alpha) [input]          95.0%
    Proportion of population falling above
    lower tolerance interval (rho) [input]            99.5%
    Minimum value of X                                1.7000E+01
    Maximum value of X                                9.3200E+01
    Average value of X                                7.6455E+01
    Average value of k                                0.99279
    Minimum value of k                                0.98375
    Variance of fit, s(k,X)^2                         3.8545E-05
    Within variance, s(w)^2                           2.3078E-05
    Pooled variance, s(p)^2                           6.1623E-05
    Pooled std. deviation, s(p)                       7.8500E-03
    C(alpha,rho)*s(p)                                 3.0787E-02
    student-t @ (n-2,1-gamma)                         1.67620E+00
    Confidence band width, W                          1.4021E-02
    Minimum margin of subcriticality, C*s(p)-W        1.6767E-02

    Upper subcritical limits: ( 17.000    <= X <=   93.200    )
    +++++ ++++++++++++ +++++++

    USL Method 1 (Confidence Band with
    Administrative Margin)              USL1 = 0.9321 + (-4.3735E-05)*X

    USL Method 2 (Single-Sided Uniform
    Width Closed Interval Approach)    USL2 = 0.9653 + (-4.3735E-05)*X

    USLs Evaluated Over Range of Parameter X:
    ++++ +++++++++ ++++ +++++ ++ +++++++++ ++

    USLs Evaluated Over Range of Parameter X:
    ++++ +++++++++ ++++ +++++ ++ +++++++++ ++

    X:  1.70E+1  2.79E+1  3.88E+1  4.97E+1  6.05E+1  7.14E+1  8.23E+1  9.32E+1
    ----------------------------------------------------------------------
    USL-1:  0.9314   0.9309   0.9304   0.9299   0.9295   0.9290   0.9285   0.9280
    USL-2:  0.9646   0.9641   0.9637   0.9632   0.9627   0.9622   0.9617   0.9613
```

Table 6.5.5-1   MCNP Benchmark Configurations for Research Reactor Fuel Benchmarks

Identification	%U235	Clusters	Config.	Lattice	Fuel Elements	Fuel Shape	Pitch (cm)	Fuel OD (cm)	Clad OD (cm)	Fuel Mat'l	Clad Mat'l
HCT-003-01	79.47	1	--	hex	1409	cross	1.22/0.61	0.475 side to side	varies, 0.2 on sides	UO$_2$+Cu	SS
HCT-003-02	79.47	1	--	hex	1243	cross	1.22/0.61	0.475 side to side	varies, 0.2 on sides	UO$_2$+Cu	SS
HCT-003-03	79.47	1	--	hex	1018	cross	1.22/0.61	0.475 side to side	varies, 0.2 on sides	UO$_2$+Cu	SS
HCT-003-04	79.47	1	--	hex	776	cross	1.22/0.61	0.475 side to side	varies, 0.2 on sides	UO$_2$+Cu	SS
HCT-003-05	79.47	1	--	hex	596	cross	1.22/0.61	0.475 side to side	varies, 0.2 on sides	UO$_2$+Cu	SS
HCT-003-06	79.47	1	--	hex	1266	cross	0.61/1.22	0.475 side to side	varies, 0.2 on sides	UO$_2$+Cu	SS
HCT-003-07	79.47	1	--	hex	1043	cross	0.61/1.22	0.475 side to side	varies, 0.2 on sides	UO$_2$+Cu	SS
HCT-003-08	79.47	1	--	hex	1006	cross	0.61/1.22	0.475 side to side	varies, 0.2 on sides	UO$_2$+Cu	SS
HCT-003-09	79.47	1	--	hex	764	cross	0.61/1.22	0.475 side to side	varies, 0.2 on sides	UO$_2$+Cu	SS
HCT-003-10	79.47	1	--	hex	589	cross	0.61/1.22	0.475 side to side	varies, 0.2 on sides	UO$_2$+Cu	SS
HCT-003-11	79.47	1	--	hex	500	cross	0.61/1.22	0.475 side to side	varies, 0.2 on sides	UO$_2$+Cu	SS
HCT-003-12	79.47	1	--	hex	1106	cross	1.83/0.61	0.475 side to side	varies, 0.2 on sides	UO$_2$+Cu	SS
HCT-003-13	79.47	1	--	hex	727	cross	1.83/0.61	0.475 side to side	varies, 0.2 on sides	UO$_2$+Cu	SS
HCT-003-14	79.47	1	--	hex	949	cross	0.61/1.82	0.475 side to side	varies, 0.2 on sides	UO$_2$+Cu	SS
HCT-003-15	79.47	1	--	hex	662	cross	0.61/1.83	0.475 side to side	varies, 0.2 on sides	UO$_2$+Cu	SS
HCT-006-01	79.47	1	--	hex	1819	cross	0.56	0.475 side to side	varies, 0.2 on sides	UO$_2$+Cu	SS
HCT-006-02	79.47	1	--	hex	457	cross	1	0.475 side to side	varies, 0.2 on sides	UO$_2$+Cu	SS
HCT-006-03	79.47	1	--	hex	554	cross	2.113	0.475 side to side	varies, 0.2 on sides	UO$_2$+Cu	SS

Note: Some wt%U235 values were converted from atom fractions

NAC International   6.5.5-8

Table 6.5.5-1   MCNP Benchmark Configurations for Research Reactor Fuel Benchmarks (cont'd)

Identification	%U235	Clusters	Config.	Lattice	Fuel Elements	Fuel Shape	Pitch (cm)	Fuel OD (cm)	Clad OD (cm)	Fuel Mat'l	Clad Mat'l
HCT-011-01	79.19	1	21x21	square	1764	cylinder	1.4	0.7	1 (0.05 thick)	UO_2+Al	SS
HCT-011-02	79.19	1	21x21	square	1764	cylinder	1.4	0.7	1 (0.05 thick)	UO_2+Al	SS
HCT-011-03	79.19	1	21x21	square	1764	cylinder	1.4	0.7	1 (0.05 thick)	UO_2+Al	SS
HCT-012-01	79.24	4	18x18	square	1296	cylinder	1.4	0.7	1 (0.05 thick)	UO_2+Al	SS
HCT-012-02	79.24	4	18x18	square	1296	cylinder	1.4	0.7	1 (0.05 thick)	UO_2+Al	SS
HCT-013-01	79.19	9	14x14	square	1764	cylinder	1.4	0.7	1 (0.05thick)	UO_2+Al	SS
HCT-013-02	79.19	9	14x14	square	1764	cylinder	1.4	0.7	1 (0.05 thick)	UO_2+Al	SS
HCT-014-01	79.19	9	10x10	square	900	cylinder	1.4√2	0.7	1 (0.05 thick)	UO_2+Al	SS
HCT-014-02	79.19	9	10x10	square	900	cylinder	1.4√2	0.7	1 (0.05thick)	UO_2+Al	SS
HCT-022-01	93.2	13	4/5/4	square	494	plate	0.40132	.0508 thick	0.0762 thick	UO_2+SS	SS
HCT-022-02	93.2	14	5/5/4	square	532	plate	0.40132	.0508 thick	0.0762 thick	UO_2+SS	SS
HCT-022-03	93.2	15	5x3	square	570	plate	0.40132	.0508 thick	0.0762 thick	UO_2+SS	SS
HCT-022-04	93.2	15	5x3	square	570	plate	0.40132	.0508 thick	0.0762 thick	UO_2+SS	SS
HCT-022-05	93.2	24	4x3&4x3	square	912	plate	0.40132	.0508 thick	0.0762 thick	UO_2+SS	SS

Note: Some wt%U235 values were converted from atom fractions

Table 6.5.5-1   MCNP Benchmark Configurations for Research Reactor Fuel Benchmarks (cont'd)

Identification	%U235	Clusters	Config.	Lattice	Fuel Elements	Fuel Shape	Pitch (cm)	Fuel OD (cm)	Clad OD (cm)	Fuel Mat'l	Clad Mat'l
HMT-006-01	93.17	1	4x4	square	194	plate	0.316411	.0508 thick	0.1524	U+Al	AL
HMT-006-02	93.17	1	4x4	square	188	plate	0.316411	.0508 thick	0.1524	U+Al	AL
HMT-006-03	93.17	1	4x4	square	221	plate	0.316411	.0508 thick	0.1524	U+Al	AL
HMT-006-04	93.17	1	4x4	square	255	plate	0.316411	.0508 thick	0.1524	U+Al	AL
HMT-006-05	93.17	1	4x4	square	520	plate	0.316411	.0508 thick	0.1524	U+Al	AL
HMT-006-06	93.17	1	4x4	square	286	plate	0.316411	.0508 thick	0.1524	U+Al	AL
HMT-006-07	93.17	1	5x5	square	233	plate	0.316411	.0508 thick	0.1524	U+Al	AL
HMT-006-08	93.17	1	6x6	square	232	plate	0.316411	.0508 thick	0.1524	U+Al	AL
HMT-006-09	93.17	1	7x7	square	296	plate	0.316411	.0508 thick	0.1524	U+Al	AL
HMT-006-10	93.17	1	4x4	square	365	plate	0.316411	.0508 thick	0.1524	U+Al	AL
HMT-006-11	93.17	1	3x4	square	1487	plate	0.316411	.0508 thick	0.1524	U+Al	AL
HMT-006-12	93.17	1	4x4	square	829	plate	0.316411	.0508 thick	0.1524	U+Al	AL
HMT-006-14	93.17	1	16x3	square	420	plate	0.316411	.0508 thick	0.1524	U+Al	AL
HMT-006-15	93.17	1	16x4	square	452	plate	0.316411	.0508 thick	0.1524	U+Al	AL
HMT-006-16	93.17	2	16x4	square	488	plate	0.316411	.0508 thick	0.1524	U+Al	AL

Note: Some wt%U235 values were converted from atom fractions

Table 6.5.5-1   MCNP Benchmark Configurations for Research Reactor Fuel Benchmarks (cont'd)

Identification	%U235	Clusters	Config.	Lattice	Fuel Elements	Fuel Shape	Pitch (cm)	Fuel OD (cm)	Clad OD (cm)	Fuel Mat'l	Clad Mat'l
ICT-002-01	17	1	--	hex	34	tube	6.8	4.18	4.12	UO_2	SS
ICT-002-02	17	1	--	hex	34	tube	6.8	4.18	4.12	UO_2	SS
ICT-002-03	17	1	--	hex	74	tube	6.8	4.18	4.12	UO_2	SS
ICT-002-04	17	1	--	hex	74	tube	6.8	4.18	4.12	UO_2	SS
ICT-002-05	17	1	--	hex	68	tube	6.8	4.18	4.12	UO_2	SS
ICT-002-06	17	1	--	hex	68	tube	6.8	4.18	4.12	UO_2	SS
ICT-014	19.77	1	2/1-c-1-c-1/5/1-c-1-c-1/3	square	360	plate	3.21	0.05066	0.04917	U_3Si_2	Al

Note: Some wt%U235 values were converted from atom fractions

Table 6.5.5-2   Research Reactor Fuel Benchmark K_eff's and Uncertainties

Identification	k_{eff}	σ	Identification	k_{eff}	σ
HCT-003-01	1.0000	0.0044	HCT-022-01	1.0000	0.0081
HCT-003-02	1.0000	0.0044	HCT-022-02	1.0000	0.0081
HCT-003-03	1.0000	0.0044	HCT-022-03	1.0000	0.0081
HCT-003-04	1.0000	0.0044	HCT-022-04	1.0000	0.0081
HCT-003-05	1.0000	0.0044	HCT-022-05	1.0000	0.0081
HCT-003-06	1.0000	0.0044	HMT-006-01	1.0000	0.0044
HCT-003-07	1.0000	0.0044	HMT-006-02	1.0000	0.0040
HCT-003-08	1.0000	0.0044	HMT-006-03	1.0000	0.0040
HCT-003-09	1.0000	0.0044	HMT-006-04	1.0000	0.0040
HCT-003-10	1.0000	0.0044	HMT-006-05	1.0000	0.0040
HCT-003-11	1.0000	0.0044	HMT-006-06	1.0000	0.0040
HCT-003-12	1.0000	0.0044	HMT-006-07	1.0000	0.0040
HCT-003-13	1.0000	0.0044	HMT-006-08	1.0000	0.0040
HCT-003-14	1.0000	0.0044	HMT-006-09	1.0000	0.0040
HCT-003-15	1.0000	0.0044	HMT-006-10	1.0000	0.0040
HCT-006-01	1.0000	0.0058	HMT-006-11	1.0000	0.0040
HCT-006-02	1.0000	0.0020	HMT-006-12	1.0000	0.0040
HCT-006-03	1.0000	0.0048	HMT-006-14	1.0000	0.0040
HCT-011-01	0.9988	0.0042	HMT-006-15	1.0000	0.0040
HCT-011-02	0.9988	0.0042	HMT-006-16	1.0000	0.0040
HCT-011-03	0.9988	0.0042	ICT-002-01	1.0014	0.0039
HCT-012-01	0.9987	0.0032	ICT-002-02	1.0019	0.0040
HCT-012-02	0.9987	0.0034	ICT-002-03	1.0017	0.0044
HCT-013-01	0.9988	0.0042	ICT-002-04	1.0019	0.0044
HCT-013-02	0.9988	0.0043	ICT-002-05	1.0014	0.0043
HCT-014-01	0.9986	0.0048	ICT-002-06	1.0016	0.0044
HCT-014-02	0.9986	0.0049	ICT-014	1.0016	0.0014

Table 6.5.5-3   MCNP Criticality Results Research Reactor Fuel Benchmarks

Identification	MCNP5 v1.30			EALCF (eV)	Total σ	Bias		
	k_{eff}	σ	Adj. k_{eff}			Δk		
HCT-003-01	0.98696	0.00151	0.98696	0.38377	0.0047	-0.01304		
HCT-003-02	0.98944	0.00159	0.98944	0.28104	0.0047	-0.01056		
HCT-003-03	0.99199	0.00153	0.99199	0.18151	0.0047	-0.00801		
HCT-003-04	0.99330	0.00141	0.99330	0.12114	0.0046	-0.00670		
HCT-003-05	0.99699	0.00142	0.99699	0.08968	0.0046	-0.00301		
HCT-003-06	0.99991	0.00149	0.99991	0.29388	0.0046	-0.00009		
HCT-003-07	1.00396	0.00153	1.00396	0.21027	0.0047	0.00396		
HCT-003-08	1.00527	0.00140	1.00527	0.19407	0.0046	0.00527		
HCT-003-09	1.00402	0.00136	1.00402	0.13126	0.0046	0.00402		
HCT-003-10	1.00843	0.00152	1.00843	0.09467	0.0047	0.00843		
HCT-003-11	1.00758	0.00145	1.00758	0.07995	0.0046	0.00758		
HCT-003-12	0.98542	0.00141	0.98542	0.11823	0.0046	-0.01458		
HCT-003-13	0.99411	0.00133	0.99411	0.06127	0.0046	-0.00589		
HCT-003-14	0.99881	0.00147	0.99881	0.16116	0.0046	-0.00119	average	-0.00217
HCT-003-15	1.00119	0.00118	1.00119	0.07980	0.0046	0.00119	min	-0.01458
HCT-006-01	0.98580	0.00136	0.98580	1.11980	0.0060	-0.01420		
HCT-006-02	1.00162	0.00124	1.00162	0.10599	0.0024	0.00162	average	-0.00625
HCT-006-03	0.99382	0.00095	0.99382	0.05029	0.0049	-0.00618	min	-0.0142
HCT-011-01	0.98261	0.00088	0.98381	0.71500	0.0043	-0.01619		
HCT-011-02	0.98564	0.00095	0.98684	0.55072	0.0043	-0.01316	average	-0.01408
HCT-011-03	0.98592	0.00085	0.98712	0.43403	0.0043	-0.01288	min	-0.01619
HCT-012-01	0.98245	0.00094	0.98375	0.60393	0.0033	-0.01625	average	-0.01535
HCT-012-02	0.98426	0.00080	0.98556	0.45884	0.0035	-0.01444	min	-0.01625
HCT-013-01	0.98665	0.00092	0.98785	0.45717	0.0043	-0.01215	average	-0.01189
HCT-013-02	0.98717	0.00090	0.98837	0.31622	0.0044	-0.01163	min	-0.01215
HCT-014-01	0.99374	0.00086	0.99514	0.11840	0.0049	-0.00486	average	-0.00486
HCT-014-02	0.99374	0.00081	0.99514	0.09841	0.0050	-0.00486	min	-0.00486
HCT-022-01	0.98924	0.00030	0.98924	0.09658	0.0081	-0.01076		
HCT-022-02	0.98970	0.00031	0.98970	0.09820	0.0081	-0.01030		
HCT-022-03	0.98878	0.00031	0.98878	0.09950	0.0081	-0.01122		
HCT-022-04	0.98917	0.00031	0.98917	0.10060	0.0081	-0.01083	average	-0.01104
HCT-022-05	0.98789	0.00030	0.98789	0.09664	0.0081	-0.01211	min	-0.01211

Table 6.5.5-3   MCNP Criticality Results Research Reactor Fuel Benchmarks (cont'd)

Identification	MCNP5 v1.30			EALCF (eV)	Total σ	Bias		
	k$_{eff}$	σ	Adj. k$_{eff}$			Δk		
HMT-006-01	0.99188	0.00087	0.99188	0.08574	0.0045	-0.00812		
HMT-006-02	0.99219	0.00087	0.99219	0.07130	0.0041	-0.00781		
HMT-006-03	0.99800	0.00081	0.99800	0.06400	0.0041	-0.00200		
HMT-006-04	0.99212	0.00082	0.99212	0.06253	0.0041	-0.00788		
HMT-006-05	0.99021	0.00077	0.99021	0.05917	0.0041	-0.00979		
HMT-006-06	0.98823	0.00079	0.98823	0.05672	0.0041	-0.01177		
HMT-006-07	0.98709	0.00072	0.98709	0.05502	0.0041	-0.01291		
HMT-006-08	0.98534	0.00068	0.98534	0.05301	0.0041	-0.01466		
HMT-006-09	0.98793	0.00068	0.98793	0.05271	0.0041	-0.01207		
HMT-006-10	0.99813	0.00088	0.99813	0.08343	0.0041	-0.00187		
HMT-006-11	0.99327	0.00078	0.99327	0.06311	0.0041	-0.00673		
HMT-006-12	0.99536	0.00069	0.99536	0.05494	0.0041	-0.00464		
HMT-006-14	0.98707	0.00077	0.98707	0.05788	0.0041	-0.01293		
HMT-006-15	0.98398	0.00077	0.98398	0.05720	0.0041	-0.01602	average	**-0.00912**
HMT-006-16	0.99243	0.00078	0.99243	0.06375	0.0041	-0.00757	min	-0.01602
ICT-002-01	0.99359	0.00070	0.99219	0.09130	0.0040	-0.00781		
ICT-002-02	0.99748	0.00077	0.99558	0.13470	0.0041	-0.00442		
ICT-002-03	0.99883	0.00074	0.99713	0.10068	0.0045	-0.00287		
ICT-002-04	0.99865	0.00074	0.99675	0.12575	0.0045	-0.00325		
ICT-002-05	0.99351	0.00072	0.99211	0.10065	0.0044	-0.00789	average	**-0.00596**
ICT-002-06	0.99208	0.00076	0.99048	0.12574	0.0045	-0.00952	min	-0.00952
ICT-014	0.99791	0.00009	0.99631	0.08780	0.0014	-0.00369		

Table 6.5.5-4   Range of Applicability and Excel Generated Correlation Coefficients of
Research Reactor Fuel Benchmarks

Correlation	R^2	Minimum	Maximum
Enrichment (wt% ^{235}U)	0.0281	17	93.2
Energy of average neutron lethargy causing fission (eV)	0.1303	0.0503	1.12

Table 6.5.5-5   MCNP Research Reactor Fuel USLSTATS Generated USLs for
Benchmark Experiments

Variable	Enrichment (wt% ^{235}U)	EALCF (eV)
# Points	54	54
AOA Range	$17 \leq X \leq 93.2$	$0.050285 \leq X \leq 1.1198$
USL Limit	0.9321 -4.3735E-05 X	0.9296 -1.1154E-02 X
USL Low	0.9280	0.9171
USL High	0.9314	0.9290

Note: USL increases as a function of decreasing enrichment. The USL determined from this data may therefore be applied to low enriched research reactor fuels (<17 wt% ^{235}U).

6.5.6   MCNP5 Version 1.60 Criticality Benchmarks for Research Reactor Fuels

The results of the criticality analyses presented in this chapter must be compared to the upper subcritical limit (USL). The USL accounts for bias and uncertainty resulting from the method using information obtained from the analysis of criticality benchmark experimental data. Code bias calculated in this section is applicable to research reactor fuel (e.g., MTR, DIDO, SLOWPOKE, and NRU/NRX) with the exception of TRIGA (U-ZrH) elements.

Criticality code validation is performed for the Monte Carlo evaluation code and neutron cross-section libraries. Criticality validation is required by the criticality safety standard ANSI/ANS-8.1.

6.5.6.1   Benchmark Experiments and Applicability Discussion

NUREG/CR-6361, "Criticality Benchmark Guide for Light-Water-Reactor Fuel in Transportation and Storage Packages," provides a guide to LWR criticality benchmark calculations and the determination of bias and subcritical limits in criticality safety evaluations. In Section 2 of the NUREG, a series of LWR criticality experiments is described in sufficient detail for independent modeling. In Section 3, the criticality experiments are modeled, and the results (k_{eff} values) are presented. The method utilized in the NUREG is KENO-Va with the 44-group ENDF/B-V cross-section library embedded in SCALE 4.3. In Section 4, a guide for the determination of bias and subcritical safety limits is provided based on ANSI/ANS-8.1 and statistical analysis of the trending in the bias. Finally, guidelines for experiment selection and applicability are presented in Section 5. The approach outlined in Section 4 of the NUREG is described in detail herein and is implemented for MCNP5 with continuous energy ENDF/B-VI cross-sections.

NUREG/CR-6361 implements ANSI/ANS-8.1 criticality safety criterion as follows.

$$k_s \leq k_c - \Delta k_s - \Delta k_c - \Delta k_m \qquad \text{(Equation 1)}$$

where:

k_s = calculated allowable maximum multiplication factor, k_{eff}, of the system being evaluated for all normal or credible abnormal conditions or events.

k_c = mean k_{eff} that results from a calculation of benchmark criticality experiments using a particular calculation method. If the calculated k_{eff} values for the criticality experiments exhibit a trend with an independent parameter, then k_c shall be determined by extrapolation based on best fit to calculated values. Criticality experiments used as benchmarks in computing k_c should have physical compositions, configurations and nuclear characteristics (including reflectors) similar to those of the system being evaluated.

Δk_s = allowance for the following:

- statistical or convergence uncertainties, or both, in computation of k_s
- material and fabrication tolerances
- geometric or material representations used in computational method

Δk_c = margin for uncertainty in k_c, which includes allowance for the following:

- uncertainties in criticality experiments
- statistical or convergence uncertainties, or both, in computation of k_c
- uncertainties resulting from extrapolation of k_c outside range of experimental data
- uncertainties resulting from limitations in geometrical or material representations used in the computational method

Δk_m = arbitrary administrative margin to ensure subcriticality of k_s

The various uncertainties are combined statistically if they are independent. Correlated uncertainties are combined by addition.

Equation 1 can be rewritten as shown.

$$k_s \leq 1 - \Delta k_m - \Delta k_s - (1 - k_c) - \Delta k_c \quad \text{(Equation 2)}$$

Noting that the definition of the bias is $\beta = 1 - k_c$, Equation 2 can be written as shown.

$$k_s + \Delta k_s \leq 1 - \Delta km - \beta - \Delta\beta \quad \text{(Equation 3)}$$

where:

$$\Delta\beta = \Delta k_c$$

Thus, the maximum allowable value for k_{eff} plus uncertainties in the system being analyzed must be below 1 minus an administrative margin (typically 0.05), which includes the bias and the uncertainty in the bias. This can also be written as shown.

$$k_s + \Delta k_s \leq \text{Upper Subcritical Limit (USL)} \quad \text{(Equation 4)}$$

where:

$$USL \equiv 1 - \Delta k_m - \beta - \Delta\beta \quad \text{(Equation 5)}$$

This is the USL criterion as described in Section 4 of NUREG/CR-6361. Two methods are prescribed for the statistical determination of the USL. The "Confidence Band with Administrative Margin (USL-1)" approach is implemented here and is referred to generically as USL. A $\Delta k_m = 0.05$ and a lower confidence band are specified based on a linear regression of k_{eff} as a function of some system parameter.

Subsequent sections contain the list of critical benchmarks employed in the validation of MCNP with its continuous energy neutron cross-section libraries and the processing of the experimental results into the USL. Also included are linear fits of reactivity (k_{eff}) to each of the system

parameters evaluated. Experiments were chosen to reflect the in-cask fuel geometry and materials as closely as available.

6.5.6.2   HEU and IEU Criticality Benchmarks

From the International Handbook of Evaluated Criticality Safety Benchmark Experiments, intermediate and high enriched thermal neutron experiments are selected as the basis of the MCNP benchmarking. Materials selected were compounds and metallic fuels. Experiments were selected for compatibility of materials and geometry with the spent fuel casks. As such, experiments containing significant neutron absorber in the form of plates, rods, or soluble poison are eliminated. Also removed are experiments containing non light water moderator. Further review eliminated experiments if they did not contain a primarily thermal neutron spectrum causing fission.

All cases were reviewed on a "preparer/checker" principle for modeling consistency with the cask models and the choice of code options. Case inputs from the handbook where modified as necessary to match experimental data or to correct modeling errors. Due to large variations in the benchmark complexities, not all options employed in the cask models are reflected in each of the benchmarks (e.g., UNIVERSE structure). A review of the criticality results did not indicate any result trend due to particular modeling choices (e.g., using the UNIVERSE structure versus a single universe, or employing KSRC versus SDEF sampling).

Key system parameters for the experiments are listed in Table 6.5.6-1. Table 6.5.6-2 lists the benchmark k_{eff} and experimental uncertainty. The NAC calculated MCNP k_{eff}'s and Monte Carlo uncertainties are shown in Table 6.5.6-3. Stochastic Monte Carlo error is kept within ±0.2% and each output is checked to assure that the MCNP built-in statistical checks on the results are passed and that all fissile material is sampled. Also included in the table are the combined Monte Carlo and experimental uncertainty and the results of the initial processing of the data indicating the minimum and average bias of each experiment.

NAC-LWT maximum reactivity cases are typically at thermal energy lines with EALCF (energy average lethargy causing fission) below 0.2 eV. A limited number of benchmark cases (i.e., HEU-COMP-THERM-011, HEU-COMP-THERM-012, HEU-COMP-THERM-006 Case 1, and HEU-COMP-THERM-013 Case 1) have an EALCF above 0.4. The area of applicability for this evaluation is restricted to an EALCF below 0.4 and cases above this level are removed from plotting and USL calculations but are included in the MCNP result summary.

Scatter plots of k_{eff} versus enrichment and average lethargy of neutrons causing fission are shown in Figure 6.5.6-1 and Figure 6.5.6-2. Included in these scatter plots are linear regression lines with a corresponding correlation coefficient (R^2) to statistically indicate any trend or lack thereof.

6.5.6.3   Results of MCNP Research Reactor Benchmark Calculations

Trending in k_{eff} was evaluated for wt% ^{235}U and energy of the average neutron lethargy causing fission (EALCF), the two parameters most likely to show cross section effects. No statistically significant trends were found for any of the system parameters. USLs are generated for each of the independent variables. A minimum USL covering the range of applicability of the benchmark set is determined.

To evaluate the relative importance of the trend analysis to the upper subcritical limits, correlation coefficients are required for all independent parameters. The linear correlation coefficient, R, is calculated by taking the square root of the R^2 value. In particular, the correlation coefficient, R, is a measure of the linear relationship between k_{eff} and a critical experiment parameter. If R is +1, a perfect linear relationship with a positive slope is indicated. If R is -1, a perfect linear relationship with a negative slope is indicated. When R is 0, no linear relationship is indicated.

Table 6.5.6-4 contains the correlation coefficient, R^2, for each linear fit of k_{eff} versus experimental parameter. Linear fits and correlation constants are based on full 54 data-point evaluation sets plotted in the previous section.

The USL for each independent variable is calculated and shown with its range of applicability in Table 6.5.6-5. The USLSTATS output of k_{eff} versus EALCF and enrichment are shown in Figure 6.5.6-3 and Figure 6.5.6-4. Uncertainties included in the USLSTATS evaluation are the Monte Carlo uncertainty associated with the reactivity calculation and experimental uncertainty that was provided in the literature for each of the cases.

Based on all the independent variable correlations, a lower limit constant USL of 0.9270 may be applied. The range of applicability (area of applicability) of this limit may be extended to lower enrichment as the correlation shows an increase in USL as a function of reduced enrichment. The range may be extended up to fully enriched (100% ^{235}U) as the USL is only very weakly correlated to enrichment and that an extrapolated USL based on the enrichment correlation results in a higher predicted USL value than the EALCF derived 0.9270.

Figure 6.5.6-1 k_{eff} versus Fuel Enrichment (MCNP5 v1.60– Research Reactor Fuel)
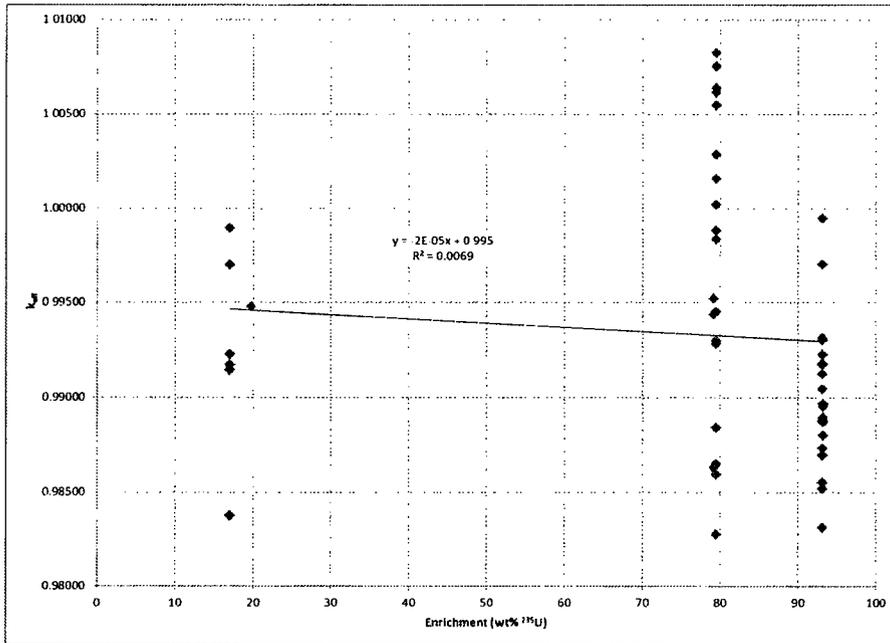
Figure 6.5.6-2 k_{eff} versus Energy of Average Neutron Lethargy Causing Fission
(MCNP5 v1.60– Research Reactor Fuel)
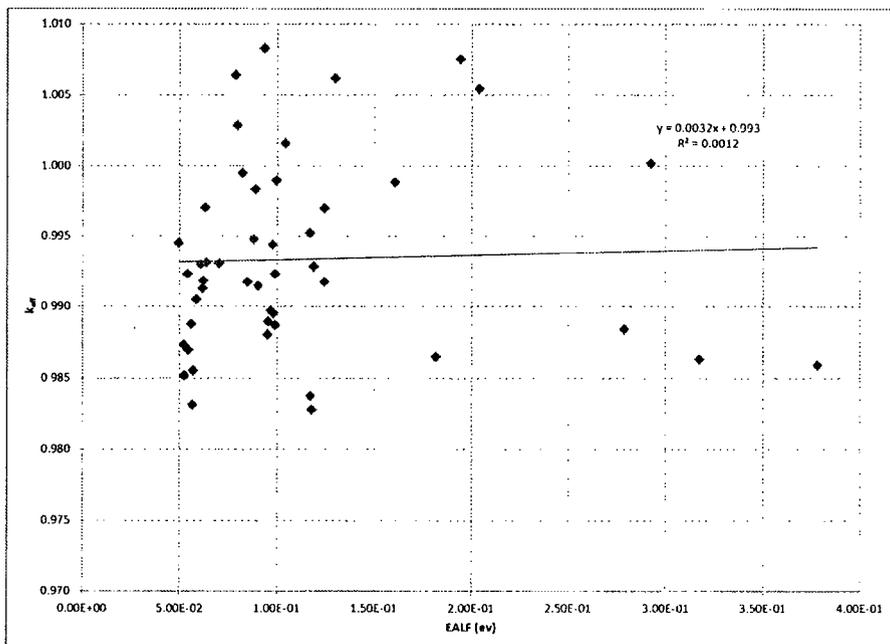
Figure 6.5.6-3   MCNP Research Reactor Fuel USLSTATS Output for EALCF

```
Proportion of the population = .995
Confidence of fit           = .950
Confidence on proportion    = .950
Number of observations      =   47
Minimum value of closed band =   0.00
Maximum value of closed band =   0.00
Administrative margin       =   0.05


independent     dependent     deviation          independent     dependent     deviation
variable - x    variable - y    in y             variable - x    variable - y    in y

  4.96000E-02   9.94500E-01   4.90000E-03          9.55000E-02   9.88940E-01   8.11000E-03
  5.21000E-02   9.87320E-01   4.06000E-03          9.68000E-02   9.89660E-01   8.11000E-03
  5.24000E-02   9.85170E-01   4.06000E-03          9.78000E-02   9.94370E-01   4.97000E-03
  5.43000E-02   9.92270E-01   4.06000E-03          9.81000E-02   9.89520E-01   8.11000E-03
  5.43000E-02   9.86960E-01   4.07000E-03          9.92000E-02   9.88690E-01   8.11000E-03
  5.61000E-02   9.88760E-01   4.07000E-03          9.92000E-02   9.92260E-01   4.36000E-03
  5.68000E-02   9.83120E-01   4.07000E-03          9.96000E-02   9.98940E-01   4.46000E-03
  5.71000E-02   9.85510E-01   4.07000E-03          1.04000E-01   1.00156E+00   2.41000E-03
  5.86000E-02   9.90450E-01   4.09000E-03          1.17000E-01   9.95200E-01   4.87000E-03
  6.09000E-02   9.92990E-01   4.57000E-03          1.17000E-01   9.83730E-01   4.06000E-03
  6.20000E-02   9.91250E-01   4.09000E-03          1.18000E-01   9.82760E-01   4.61000E-03
  6.22000E-02   9.91780E-01   4.09000E-03          1.19000E-01   9.92810E-01   4.66000E-03
  6.31000E-02   9.97010E-01   4.07000E-03          1.24000E-01   9.91690E-01   4.47000E-03
  6.37000E-02   9.93120E-01   4.08000E-03          1.24000E-01   9.96950E-01   4.46000E-03
  7.03000E-02   9.93020E-01   4.09000E-03          1.30000E-01   1.00615E+00   4.66000E-03
  7.86000E-02   1.00637E+00   4.64000E-03          1.61000E-01   9.98800E-01   4.62000E-03
  7.98000E-02   1.00294E+00   4.55000E-03          1.82000E-01   9.86500E-01   4.67000E-03
  8.24000E-02   9.99460E-01   4.09000E-03          1.94000E-01   1.00751E+00   4.65000E-03
  8.48000E-02   9.91720E-01   4.49000E-03          2.04000E-01   1.00544E+00   4.67000E-03
  9.82000E-02   9.94770E-01   1.40000E-03          2.79000E-01   9.88410E-01   4.65000E-03
  8.90000E-02   9.98340E-01   4.64000E-03          2.92000E-01   1.00018E+00   4.66000E-03
  9.04000E-02   9.91430E-01   3.97000E-03          3.17000E-01   9.86290E-01   4.41000E-03
  9.36000E-02   1.00626E+00   4.64000E-03          3.78000E-01   9.85930E-01   4.64000E-03
  9.51000E-02   9.98000E-01   8.11000E-03

chi =  2.0426 (upper bound = 9.49). The data tests normal.



        Output from statistical treatment

keff vs EALCF

    Number of data points (n)                    47
    Linear regression, k(X)                      0.9930 + ( 3.2033E-03)*X
    Confidence on fit (1-gamma) [input]          95.0%
    Confidence on proportion (alpha) [input]     95.0%
    Proportion of population falling above
    lower tolerance interval (rho) [input]       99.5%
    Minimum value of X                           4.9600E-02
    Maximum value of X                           3.7800E-01
    Average value of X                           1.1280E-01
    Average value of k                           0.99333
    Minimum value of k                           0.98276
    Variance of fit, s(k,X)^2                    4.6641E-05
    Within variance, s(w)^2                      2.3714E-05
    Pooled variance, s(p)^2                      7.0355E-05
    Pooled std. deviation, s(p)                  8.3878E-03
    C(alpha,rho)*s(p)                            3.6520E-02
    student-t @ (n-2,1-gamma)                    1.68075E+00
    Confidence band width, W                     1.6108E-02
    Minimum margin of subcriticality, C*s(p)-W   2.0412E-02

    Upper subcritical limits: ( 4.96000E-02 <= X <=  0.37800    )
    ***** *********** *******


    USL Method 1 (Confidence Band with
    Administrative Margin)          USL1 = 0.9269 + ( 3.2033E-03)*X

    USL Method 2 (Single-Sided Uniform
    Width Closed Interval Approach)  USL2 = 0.9565 + ( 3.2033E-03)*X



    USLs Evaluated Over Range of Parameter X:
    **** ********* **** ***** ** ********* **

    X:  4.96E-2  9.65E-2  1.43E-1  1.90E-1  2.37E-1  2.84E-1  3.31E-1  3.78E-1
    -----------------------------------------------------------------------
USL-1:  0.9270   0.9272   0.9273   0.9275   0.9276   0.9278   0.9279   0.9281
USL-2:  0.9566   0.9568   0.9569   0.9571   0.9572   0.9574   0.9575   0.9577
    -----------------------------------------------------------------------
```

Figure 6.5.6-4 MCNP Research Reactor Fuel USLSTATS Output for wt% ^{235}U

```
Proportion of the population = .995
Confidence of fit            = .950
Confidence on proportion     = .950
Number of observations       =   47
Minimum value of closed band =   0.00
Maximum value of closed band =   0.00
Administrative margin        =   0.05


independent   dependent    deviation        independent   dependent    deviation
variable - x  variable - y  in y            variable - x  variable - y   in y

7.95000E+01   9.85930E-01  4.64000E-03      9.32000E+01   9.88000E-01  8.11000E-03
7.95000E+01   9.88410E-01  4.65000E-03      9.32000E+01   9.91720E-01  4.49000E-03
7.95000E+01   9.86500E-01  4.67000E-03      9.32000E+01   9.93020E-01  4.09000E-03
7.95000E+01   9.92810E-01  4.66000E-03      9.32000E+01   9.97010E-01  4.07000E-03
7.95000E+01   9.98340E-01  4.64000E-03      9.32000E+01   9.91250E-01  4.09000E-03
7.95000E+01   1.00018E+00  4.66000E-03      9.32000E+01   9.90450E-01  4.09000E-03
7.95000E+01   1.00544E+00  4.67000E-03      9.32000E+01   9.88760E-01  4.07000E-03
7.95000E+01   1.00751E+00  4.65000E-03      9.32000E+01   9.86960E-01  4.07000E-03
7.95000E+01   1.00615E+00  4.66000E-03      9.32000E+01   9.85170E-01  4.06000E-03
7.95000E+01   1.00826E+00  4.64000E-03      9.32000E+01   9.87320E-01  4.06000E-03
7.95000E+01   1.00637E+00  4.64000E-03      9.32000E+01   9.99460E-01  4.09000E-03
7.95000E+01   9.82760E-01  4.61000E-03      9.32000E+01   9.91780E-01  4.09000E-03
7.95000E+01   9.92990E-01  4.57000E-03      9.32000E+01   9.92270E-01  4.06000E-03
7.95000E+01   9.98800E-01  4.62000E-03      9.32000E+01   9.85510E-01  4.07000E-03
7.95000E+01   1.00284E+00  4.55000E-03      9.32000E+01   9.83120E-01  4.07000E-03
7.95000E+01   1.00156E+00  2.41000E-03      9.32000E+01   9.93120E-01  4.08000E-03
7.95000E+01   9.94500E-01  4.90000E-03      1.70000E+01   9.91430E-01  3.97000E-03
7.92000E+01   9.86290E-01  4.41000E-03      1.70000E+01   9.83730E-01  4.06000E-03
7.92000E+01   9.95200E-01  4.87000E-03      1.70000E+01   9.98940E-01  4.46000E-03
7.92000E+01   9.94370E-01  4.97000E-03      1.70000E+01   9.96950E-01  4.46000E-03
9.32000E+01   9.88940E-01  8.11000E-03      1.70000E+01   9.92260E-01  4.36000E-03
9.32000E+01   9.89660E-01  8.11000E-03      1.70000E+01   9.91690E-01  4.47000E-03
9.32000E+01   9.89520E-01  8.11000E-03      1.98000E+01   9.94770E-01  1.40000E-03
9.32000E+01   9.88690E-01  8.11000E-03

chi = 2.0426 (upper bound = 9.49). The data tests normal.



     Output from statistical treatment

keff vs enrichment

Number of data points (n)                    47
Linear regression, k(X)               0.9950 + (-2.1904E-05)*X
Confidence on fit (1-gamma) [input]          95.0%
Confidence on proportion (alpha) [input]     95.0%
Proportion of population falling above
lower tolerance interval (rho) [input]       99.5%
Minimum value of X                     1.7000E+01
Maximum value of X                     9.3200E+01
Average value of X                     7.6062E+01
Average value of k                     0.99333
Minimum value of k                     0.98276
Variance of fit, s(k,X)^2              4.6375E-05
Within variance, s(w)^2                2.3714E-05
Pooled variance, s(p)^2                7.0089E-05
Pooled std. deviation, s(p)            8.3719E-03
C(alpha,rho)*s(p)                      3.3389E-02
student-t @ (n-2,1-gamma)              1.68075E+00
Confidence band width, W               1.5003E-02
Minimum margin of subcriticality, C*s(p)-W   1.8386E-02


Upper subcritical limits: (   17.000     <= X <=   93.200    )
***** ********** *******


USL Method 1 (Confidence Band with
Administrative Margin)            USL1 = 0.9300 + (-2.1904E-05)*X

USL Method 2 (Single-Sided Uniform
Width Closed Interval Approach)   USL2 = 0.9616 + (-2.1904E-05)*X



USLs Evaluated Over Range of Parameter X:
**** ********** **** ***** ** ********** **

 X:  1.70E+1  2.79E+1  3.88E+1  4.97E+1  6.05E+1  7.14E+1  8.23E+1  9.32E+1
--------------------------------------------------------------------------
USL-1:  0.9296   0.9294   0.9291   0.9289   0.9287   0.9284   0.9282   0.9280
USL-2:  0.9612   0.9610   0.9608   0.9605   0.9603   0.9600   0.9598   0.9596
--------------------------------------------------------------------------
```

Table 6.5.6-1   MCNP5 v1.60 Benchmark Configurations for Research Reactor Fuel Benchmarks

Identification	%U235	Clusters	Config.	Lattice	Fuel Elements	Fuel Shape	Pitch (cm)	Fuel OD (cm)	Clad OD (cm)	Fuel Mat'l	Clad Mat'l
HCT-003-01	79.47	1	--	hex	1409	cross	1.22/0.61	0.475 side to side	varies, 0.2 on sides	UO₂+Cu	SS
HCT-003-02	79.47	1	--	hex	1243	cross	1.22/0.61	0.475 side to side	varies, 0.2 on sides	UO₂+Cu	SS
HCT-003-03	79.47	1	--	hex	1018	cross	1.22/0.61	0.475 side to side	varies, 0.2 on sides	UO₂+Cu	SS
HCT-003-04	79.47	1	--	hex	776	cross	1.22/0.61	0.475 side to side	varies, 0.2 on sides	UO₂+Cu	SS
HCT-003-05	79.47	1	--	hex	596	cross	1.22/0.61	0.475 side to side	varies, 0.2 on sides	UO₂+Cu	SS
HCT-003-06	79.47	1	--	hex	1266	cross	0.61/1.22	0.475 side to side	varies, 0.2 on sides	UO₂+Cu	SS
HCT-003-07	79.47	1	--	hex	1043	cross	0.61/1.22	0.475 side to side	varies, 0.2 on sides	UO₂+Cu	SS
HCT-003-08	79.47	1	--	hex	1006	cross	0.61/1.22	0.475 side to side	varies, 0.2 on sides	UO₂+Cu	SS
HCT-003-09	79.47	1	--	hex	764	cross	0.61/1.22	0.475 side to side	varies, 0.2 on sides	UO₂+Cu	SS
HCT-003-10	79.47	1	--	hex	589	cross	0.61/1.22	0.475 side to side	varies, 0.2 on sides	UO₂+Cu	SS
HCT-003-11	79.47	1	--	hex	500	cross	0.61/1.22	0.475 side to side	varies, 0.2 on sides	UO₂+Cu	SS
HCT-003-12	79.47	1	--	hex	1106	cross	1.83/0.61	0.475 side to side	varies, 0.2 on sides	UO₂+Cu	SS
HCT-003-13	79.47	1	--	hex	727	cross	1.83/0.61	0.475 side to side	varies, 0.2 on sides	UO₂+Cu	SS
HCT-003-14	79.47	1	--	hex	949	cross	0.61/1.82	0.475 side to side	varies, 0.2 on sides	UO₂+Cu	SS
HCT-003-15	79.47	1	--	hex	662	cross	0.61/1.83	0.475 side to side	varies, 0.2 on sides	UO₂+Cu	SS
HCT-006-01	79.47	1	--	hex	1819	cross	0.56	0.475 side to side	varies, 0.2 on sides	UO₂+Cu	SS
HCT-006-02	79.47	1	--	hex	457	cross	1	0.475 side to side	varies, 0.2 on sides	UO₂+Cu	SS
HCT-006-03	79.47	1	--	hex	554	cross	2.113	0.475 side to side	varies, 0.2 on sides	UO₂+Cu	SS

Note: Some wt%U235 values were converted from atom fractions

Table 6.5.6-1   MCNP v1.60Benchmark Configurations for Research Reactor Fuel Benchmarks (cont'd)

Identification	%U235	Clusters	Config.	Lattice	Fuel Elements	Fuel Shape	Pitch (cm)	Fuel OD (cm)	Clad OD (cm)	Fuel Mat'l	Clad Mat'l
HCT-011-01	79.19	1	21x21	square	1764	cylinder	1.4	0.7	1 (0.05 thick)	UO₂+Al	SS
HCT-011-02	79.19	1	21x21	square	1764	cylinder	1.4	0.7	1 (0.05 thick)	UO₂+Al	SS
HCT-011-03	79.19	1	21x21	square	1764	cylinder	1.4	0.7	1 (0.05 thick)	UO₂+Al	SS
HCT-012-01	79.24	4	18x18	square	1296	cylinder	1.4	0.7	1 (0.05 thick)	UO₂+Al	SS
HCT-012-02	79.24	4	18x18	square	1296	cylinder	1.4	0.7	1 (0.05 thick)	UO₂+Al	SS
HCT-013-01	79.19	9	14x14	square	1764	cylinder	1.4	0.7	1 (0.05thick)	UO₂+Al	SS
HCT-013-02	79.19	9	14x14	square	1764	cylinder	1.4	0.7	1 (0.05 thick)	UO₂+Al	SS
HCT-014-01	79.19	9	10x10	square	900	cylinder	1.4√2	0.7	1 (0.05 thick)	UO₂+Al	SS
HCT-014-02	79.19	9	10x10	square	900	cylinder	1.4√2	0.7	1 (0.05thick)	UO₂+Al	SS
HCT-022-01	93.2	13	4/5/4	square	494	plate	0.40132	.0508 thick	0.0762 thick	UO₂+SS	SS
HCT-022-02	93.2	14	5/5/4	square	532	plate	0.40132	.0508 thick	0.0762 thick	UO₂+SS	SS
HCT-022-03	93.2	15	5x3	square	570	plate	0.40132	.0508 thick	0.0762 thick	UO₂+SS	SS
HCT-022-04	93.2	15	5x3	square	570	plate	0.40132	.0508 thick	0.0762 thick	UO₂+SS	SS
HCT-022-05	93.2	24	4x3&4x3	square	912	plate	0.40132	.0508 thick	0.0762 thick	UO₂+SS	SS

Note: Some wt%U235 values were converted from atom fractions

Table 6.5.6-1   MCNP5 v1.60 Benchmark Configurations for Research Reactor Fuel Benchmarks (cont'd)

Identification	%U235	Clusters	Config.	Lattice	Fuel Elements	Fuel Shape	Pitch (cm)	Fuel OD (cm)	Clad OD (cm)	Fuel Mat'l	Clad Mat'l
HMT-006-01	93.17	1	4x4	square	194	plate	0.316411	.0508 thick	0.1524	U+Al	AL
HMT-006-02	93.17	1	4x4	square	188	plate	0.316411	.0508 thick	0.1524	U+Al	AL
HMT-006-03	93.17	1	4x4	square	221	plate	0.316411	.0508 thick	0.1524	U+Al	AL
HMT-006-04	93.17	1	4x4	square	255	plate	0.316411	.0508 thick	0.1524	U+Al	AL
HMT-006-05	93.17	1	4x4	square	520	plate	0.316411	.0508 thick	0.1524	U+Al	AL
HMT-006-06	93.17	1	4x4	square	286	plate	0.316411	.0508 thick	0.1524	U+Al	AL
HMT-006-07	93.17	1	5x5	square	233	plate	0.316411	.0508 thick	0.1524	U+Al	AL
HMT-006-08	93.17	1	6x6	square	232	plate	0.316411	.0508 thick	0.1524	U+Al	AL
HMT-006-09	93.17	1	7x7	square	296	plate	0.316411	.0508 thick	0.1524	U+Al	AL
HMT-006-10	93.17	1	4x4	square	365	plate	0.316411	.0508 thick	0.1524	U+Al	AL
HMT-006-11	93.17	1	3x4	square	1487	plate	0.316411	.0508 thick	0.1524	U+Al	AL
HMT-006-12	93.17	1	4x4	square	829	plate	0.316411	.0508 thick	0.1524	U+Al	AL
HMT-006-14	93.17	1	16x3	square	420	plate	0.316411	.0508 thick	0.1524	U+Al	AL
HMT-006-15	93.17	1	16x4	square	452	plate	0.316411	.0508 thick	0.1524	U+Al	AL
HMT-006-16	93.17	2	16x4	square	488	plate	0.316411	.0508 thick	0.1524	U+Al	AL

Note: Some wt%U235 values were converted from atom fractions

Table 6.5.6-1 MCNP Benchmark Configurations for Research Reactor Fuel Benchmarks (cont'd)

Identification	%U235	Clusters	Config.	Lattice	Fuel Elements	Fuel Shape	Pitch (cm)	Fuel OD (cm)	Clad OD (cm)	Fuel Mat'l	Clad Mat'l
ICT-002-01	17	1	--	hex	34	tube	6.8	4.18	4.12	UO₂	SS
ICT-002-02	17	1	--	hex	34	tube	6.8	4.18	4.12	UO₂	SS
ICT-002-03	17	1	--	hex	74	tube	6.8	4.18	4.12	UO₂	SS
ICT-002-04	17	1	--	hex	74	tube	6.8	4.18	4.12	UO₂	SS
ICT-002-05	17	1	--	hex	68	tube	6.8	4.18	4.12	UO₂	SS
ICT-002-06	17	1	--	hex	68	tube	6.8	4.18	4.12	UO₂	SS
ICT-014	19.77	1	2/1-c-1-c-1/5/1-c-1-c-1/3	square	360	plate	3.21	0.05066	0.04917	U₃Si₂	Al

Note: Some wt%U235 values were converted from atom fractions

Table 6.5.6-2   Research Reactor Fuel Benchmark K$_{eff}$'s and Uncertainties
(MCNP5 v1.60 Validation)

Identification	k$_{eff}$	σ	Identification	k$_{eff}$	σ
HCT-003-01	1.0000	0.0044	HCT-022-01	1.0000	0.0081
HCT-003-02	1.0000	0.0044	HCT-022-02	1.0000	0.0081
HCT-003-03	1.0000	0.0044	HCT-022-03	1.0000	0.0081
HCT-003-04	1.0000	0.0044	HCT-022-04	1.0000	0.0081
HCT-003-05	1.0000	0.0044	HCT-022-05	1.0000	0.0081
HCT-003-06	1.0000	0.0044	HMT-006-01	1.0000	0.0044
HCT-003-07	1.0000	0.0044	HMT-006-02	1.0000	0.0040
HCT-003-08	1.0000	0.0044	HMT-006-03	1.0000	0.0040
HCT-003-09	1.0000	0.0044	HMT-006-04	1.0000	0.0040
HCT-003-10	1.0000	0.0044	HMT-006-05	1.0000	0.0040
HCT-003-11	1.0000	0.0044	HMT-006-06	1.0000	0.0040
HCT-003-12	1.0000	0.0044	HMT-006-07	1.0000	0.0040
HCT-003-13	1.0000	0.0044	HMT-006-08	1.0000	0.0040
HCT-003-14	1.0000	0.0044	HMT-006-09	1.0000	0.0040
HCT-003-15	1.0000	0.0044	HMT-006-10	1.0000	0.0040
HCT-006-01	1.0000	0.0058	HMT-006-11	1.0000	0.0040
HCT-006-02	1.0000	0.0020	HMT-006-12	1.0000	0.0040
HCT-006-03	1.0000	0.0048	HMT-006-14	1.0000	0.0040
HCT-011-01	0.9988	0.0042	HMT-006-15	1.0000	0.0040
HCT-011-02	0.9988	0.0042	HMT-006-16	1.0000	0.0040
HCT-011-03	0.9988	0.0042	ICT-002-01	1.0014	0.0039
HCT-012-01	0.9987	0.0032	ICT-002-02	1.0019	0.0040
HCT-012-02	0.9987	0.0034	ICT-002-03	1.0017	0.0044
HCT-013-01	0.9988	0.0042	ICT-002-04	1.0019	0.0044
HCT-013-02	0.9988	0.0043	ICT-002-05	1.0014	0.0043
HCT-014-01	0.9986	0.0048	ICT-002-06	1.0016	0.0044
HCT-014-02	0.9986	0.0049	ICT-014	1.0016	0.0014

Table 6.5.6-3   MCNP5 v1.60 Criticality Results Research Reactor Fuel Benchmarks

| | MCNP5 v1.60 | | | | | Bias | |
Identification	k_{eff}	σ	Adj. k_{eff}	EALCF (eV)	Total σ	Δk	
HCT-003-01	0.98593	0.00147	0.98593	0.37808	0.0046	-0.01407	
HCT-003-02	0.98841	0.00149	0.98841	0.27888	0.0046	-0.01159	
HCT-003-03	0.98650	0.00156	0.98650	0.18180	0.0047	-0.01350	
HCT-003-04	0.99281	0.00152	0.99281	0.11899	0.0047	-0.00719	
HCT-003-05	0.99834	0.00146	0.99834	0.08900	0.0046	-0.00166	
HCT-003-06	1.00018	0.00153	1.00018	0.29235	0.0047	0.00018	
HCT-003-07	1.00544	0.00155	1.00544	0.20411	0.0047	0.00544	
HCT-003-08	1.00751	0.00150	1.00751	0.19431	0.0046	0.00751	
HCT-003-09	1.00615	0.00154	1.00615	0.12977	0.0047	0.00615	
HCT-003-10	1.00826	0.00148	1.00826	0.09363	0.0046	0.00826	
HCT-003-11	1.00637	0.00146	1.00637	0.07857	0.0046	0.00637	
HCT-003-12	0.98276	0.00137	0.98276	0.11795	0.0046	-0.01724	
HCT-003-13	0.99299	0.00122	0.99299	0.06087	0.0046	-0.00701	
HCT-003-14	0.99880	0.00140	0.99880	0.16052	0.0046	-0.00120	average	-0.00245
HCT-003-15	1.00284	0.00116	1.00284	0.07978	0.0046	0.00284	min	-0.01724
HCT-006-01	0.98477	0.00121	0.98338	1.09170	0.0059	-0.01553		
HCT-006-02	1.00156	0.00134	1.00156	0.10438	0.0024	0.00156	average	-0.00197
HCT-006-03	0.99450	0.00099	0.99450	0.04956	0.0049	-0.00550	min	-0.0055
HCT-011-01	0.98218	0.00092	0.98338	0.71067	0.0043	-0.01662		
HCT-011-02	0.98592	0.00085	0.98712	0.54510	0.0043	-0.01288	average	-0.01404
HCT-011-03	0.98618	0.00088	0.98738	0.43018	0.0043	-0.01262	min	-0.01662
HCT-012-01	0.98085	0.00091	0.98215	0.59930	0.0033	-0.01785	average	-0.01578
HCT-012-02	0.98500	0.00088	0.98630	0.45307	0.0035	-0.01370	min	-0.01785
HCT-013-01	0.98574	0.00094	0.98694	0.45306	0.0043	-0.01306	average	-0.01339
HCT-013-02	0.98509	0.00099	0.98629	0.31739	0.0044	-0.01371	min	-0.01371
HCT-014-01	0.99380	0.00083	0.99520	0.11682	0.0049	-0.00480	average	-0.00522
HCT-014-02	0.99297	0.00086	0.99437	0.09777	0.0050	-0.00563	min	-0.00563
HCT-022-01	0.98894	0.00031	0.98894	0.09546	0.0081	-0.01106		
HCT-022-02	0.98966	0.00030	0.98966	0.09677	0.0081	-0.01034		
HCT-022-03	0.98952	0.00031	0.98952	0.09809	0.0081	-0.01048		
HCT-022-04	0.98869	0.00031	0.98869	0.09917	0.0081	-0.01131	average	-0.01104
HCT-022-05	0.98800	0.00029	0.98800	0.09515	0.0081	-0.01200	min	-0.01200

Table 6.5.6-3   MCNP5 V1.60 Criticality Results Research Reactor Fuel Benchmarks
(cont'd)

| Identification | MCNP5 v1.30 | | | EALCF (eV) | Total σ | Bias | | |
	k_{eff}	σ	Adj. k_{eff}			Δk		
HMT-006-01	0.99172	0.00089	0.99172	0.08482	0.0045	-0.00828		
HMT-006-02	0.99302	0.00087	0.99302	0.07027	0.0041	-0.00698		
HMT-006-03	0.99701	0.00077	0.99701	0.06314	0.0041	-0.00299		
HMT-006-04	0.99125	0.00084	0.99125	0.06200	0.0041	-0.00875		
HMT-006-05	0.99045	0.00083	0.99045	0.05857	0.0041	-0.00955		
HMT-006-06	0.98876	0.00073	0.98876	0.05606	0.0041	-0.01124		
HMT-006-07	0.98696	0.00073	0.98696	0.05431	0.0041	-0.01304		
HMT-006-08	0.98517	0.00072	0.98517	0.05243	0.0041	-0.01483		
HMT-006-09	0.98732	0.00069	0.98732	0.05215	0.0041	-0.01268		
HMT-006-10	0.99946	0.00087	0.99946	0.08235	0.0041	-0.00054		
HMT-006-11	0.99178	0.00083	0.99178	0.06224	0.0041	-0.00822		
HMT-006-12	0.99227	0.00072	0.99227	0.05427	0.0041	-0.00773		
HMT-006-14	0.98551	0.00077	0.98551	0.05713	0.0041	-0.01449		
HMT-006-15	0.98312	0.00074	0.98312	0.05684	0.0041	-0.01688	average	**-0.00954**
HMT-006-16	0.99312	0.00081	0.99312	0.06366	0.0041	-0.00688	min	-0.01688
ICT-002-01	0.99283	0.00075	0.99143	0.09038	0.0040	-0.00857		
ICT-002-02	0.98563	0.00071	0.98373	0.11721	0.0041	-0.01627		
ICT-002-03	1.00064	0.00074	0.99894	0.09964	0.0045	-0.00106		
ICT-002-04	0.99885	0.00072	0.99695	0.12447	0.0045	-0.00305		
ICT-002-05	0.99366	0.00069	0.99226	0.09923	0.0044	-0.00774	average	**-0.00750**
ICT-002-06	0.99329	0.00076	0.99169	0.12423	0.0045	-0.00831	min	-0.01627
ICT-014	0.99637	0.00009	0.99477	0.08816	0.0014	-0.00523		

Table 6.5.6-4   Range of Applicability and Excel Generated Correlation Coefficients of
Research Reactor Fuel Benchmarks

Correlation	R^2	Minimum	Maximum
Enrichment (wt% ^{235}U)	0.0069	17	93.2
Energy of average neutron lethargy causing fission (eV)	0.0012	0.0496	0.378

Table 6.5.6-5   MCNP Research Reactor Fuel USLSTATS Generated USLs for
Benchmark Experiments

Variable	Enrichment (wt% ^{235}U)	EALCF (eV)
# Points	47	47
AOA Range	$17 \le X \le 93.2$	$0.0496 \le X \le 0.378$
USL Limit	0.9300 - 2.1904E-05 X	0.9269 + 3.2033E-03 X
USL Low	0.928	0.927
USL High	0.9296	0.9281

Note: USL increases as a function of decreasing enrichment. The USL determined from this data may therefore be applied to low enriched research reactor fuels (<17 wt% ^{235}U).

6.5.7   MCNP Criticality Benchmarks for Uranyl Nitrates

The results of the criticality analyses presented in this chapter must be compared to the upper subcritical limit (USL). The USL accounts for bias and uncertainty resulting from the method using information obtained from the analysis of criticality benchmark experimental data. Code bias calculated in this section is applicable to uranyl nitrates (e.g., HEUNL).

Criticality code validation is performed for the Monte Carlo evaluation code and neutron cross-section libraries. Criticality validation is required by the criticality safety standard ANSI/ANS-8.1.

6.5.7.1   Benchmark Experiments and Applicability Discussion

NUREG/CR-6361, "Criticality Benchmark Guide for Light-Water-Reactor Fuel in Transportation and Storage Packages," provides a guide to LWR criticality benchmark calculations and the determination of bias and subcritical limits in criticality safety evaluations. In Section 2 of the NUREG, a series of LWR criticality experiments is described in sufficient detail for independent modeling. In Section 3, the criticality experiments are modeled, and the results (k_{eff} values) are presented. The method utilized in the NUREG is KENO-Va with the 44-group ENDF/B-V cross-section library embedded in SCALE 4.3. In Section 4, a guide for the determination of bias and subcritical safety limits is provided based on ANSI/ANS-8.1 and statistical analysis of the trending in the bias. Finally, guidelines for experiment selection and applicability are presented in Section 5. The approach outlined in Section 4 of the NUREG is described in detail herein and is implemented for MCNP5 with continuous energy ENDF/B-VII cross-sections.

NUREG/CR-6361 implements ANSI/ANS-8.1 criticality safety criterion as follows.

$$k_s \leq k_c - \Delta k_s - \Delta k_c - \Delta k_m \quad \text{(Equation 1)}$$

where:

k_s = Calculated allowable maximum multiplication factor, k_{eff}, of the system being evaluated for all normal or credible abnormal conditions or events.

k_c = Mean k_{eff} that results from a calculation of benchmark criticality experiments using a particular calculation method. If the calculated k_{eff} values for the criticality experiments exhibit a trend with an independent parameter, then k_c shall be determined by extrapolation based on best fit to calculated values. Criticality experiments used as benchmarks in computing k_c should have physical compositions, configurations and nuclear characteristics (including reflectors) similar to those of the system being evaluated.

Δk_s = allowance for the following:

- statistical or convergence uncertainties, or both, in computation of k_s
- material and fabrication tolerances
- geometric or material representations used in computational method

Δk_c = margin for uncertainty in k_c, which includes allowance for the following:

- uncertainties in criticality experiments
- statistical or convergence uncertainties, or both, in computation of k_c
- uncertainties resulting from extrapolation of k_c outside range of experimental data
- uncertainties resulting from limitations in geometrical or material representations used in the computational method

Δk_m = arbitrary administrative margin to ensure subcriticality of k_s

The various uncertainties are combined statistically if they are independent. Correlated uncertainties are combined by addition.

Equation 1 can be rewritten as shown.

$$k_s \leq 1 - \Delta k_m - \Delta k_s - (1 - k_c) - \Delta k_c \quad \text{(Equation 2)}$$

Noting that the definition of the bias is $\beta = 1 - k_c$, Equation 2 can be written as shown.

$$k_s + \Delta k_s \leq 1 - \Delta k_m - \beta - \Delta\beta \quad \text{(Equation 3)}$$

where:

$$\Delta\beta = \Delta k_c$$

Thus, the maximum allowable value for k_{eff} plus uncertainties in the system being analyzed must be below 1 minus an administrative margin (typically 0.05), which includes the bias and the uncertainty in the bias. This can also be written as shown.

$$k_s + \Delta k_s \leq \text{Upper Subcritical Limit (USL)} \quad \text{(Equation 4)}$$

where:

$$\text{USL} \equiv 1 - \Delta k_m - \beta - \Delta\beta \quad \text{(Equation 5)}$$

This is the USL criterion as described in Section 4 of NUREG/CR-6361. Two methods are prescribed for the statistical determination of the USL. The "Confidence Band with Administrative Margin (USL-1)" approach is implemented here and is referred to generically as USL. A $\Delta k_m = 0.05$ and a lower confidence band are specified based on a linear regression of k_{eff} as a function of some system parameter.

Subsequent sections contain the list of critical benchmarks employed in the validation of MCNP with its continuous energy neutron cross-section libraries and the processing of the experimental results into the USL. Also included are linear fits of reactivity (k_{eff}) to each of the system parameters evaluated. Experiments were chosen to reflect the in-cask fuel geometry and materials as closely as available.

6.5.7.2   Highly Enriched Uranyl Nitrates Criticality Benchmarks

From the International Handbook of Evaluated Criticality Safety Benchmark Experiments, highly enriched uranyl nitrates are selected as the basis of the MCNP benchmarking. Materials selected were solutions of uranyl nitrate. Experiments were selected for compatibility of materials and geometry with the spent fuel casks. As such, experiments containing significant neutron absorber in the form of plates, rods, or soluble poison are eliminated. Also removed are experiments containing non light water moderator. Further review eliminated experiments if they did not contain a primarily thermal neutron spectrum causing fission.

All cases were reviewed on a "preparer/checker" principle for modeling consistency with the cask models and the choice of code options. Case inputs from the handbook where modified to the ENDF/B-VII library to maintain a consistent set. The validated cross-section libraries are listed in Table 6.5.7-6. For isotopes without an ENDF/B-VII library, the latest and most applicable library set was used (i.e. ENDF/B-VI, ENDF/B-V, etc.).

Table 6.5.7-1 lists the benchmark k_{eff} and experimental uncertainty. The NAC calculated MCNP k_{eff}s and Monte Carlo uncertainties are shown in Table 6.5.7-2. Stochastic Monte Carlo error is kept within ±0.3% and each output is checked to assure that the MCNP built-in statistical checks on the results are passed and that all fissile material is sampled. Also included in the table are the combined Monte Carlo and experimental uncertainty and the results of the initial processing of the data indicating the minimum and average bias of each experiment.

Scatter plots of k_{eff} versus enrichment and average lethargy of neutrons causing fission are shown in Figure 6.5.7-1 and Figure 6.5.7-2. Included in these scatter plots are linear regression lines with a corresponding correlation coefficient (R^2) to statistically indicate any trend or lack thereof.

Table 6.5.7-1   Highly Enriched Uranyl Nitrates Benchmark K$_{eff}$'s and Uncertainties

Identification	k$_{eff}$	σ	wt% ^{235}U
HST-001-01	1.00040	0.00600	93.172 ± 0.060
HST-001-02	1.00210	0.00720	93.172 ± 0.060
HST-001-03	1.00030	0.00350	93.172 ± 0.060
HST-001-04	1.00080	0.00530	93.172 ± 0.060
HST-001-05	1.00010	0.00490	93.172 ± 0.060
HST-001-06	1.00020	0.00460	93.172 ± 0.060
HST-001-07	1.00080	0.00400	93.172 ± 0.060
HST-001-08	0.99980	0.00380	93.172 ± 0.060
HST-001-09	1.00030	0.00540	93.172 ± 0.060
HST-001-10	0.99930	0.00540	93.172 ± 0.060
HST-002-01	1.00250	0.00580	93.172 ± 0.060
HST-002-02	1.00280	0.00580	93.172 ± 0.060
HST-002-03	1.00330	0.00680	93.172 ± 0.060
HST-002-04	1.00340	0.00690	93.172 ± 0.060
HST-002-05	1.00180	0.00440	93.172 ± 0.060
HST-002-06	1.00230	0.00410	93.172 ± 0.060
HST-002-07	1.00250	0.00500	93.172 ± 0.060
HST-002-08	1.00300	0.00550	93.172 ± 0.060
HST-002-09	1.00120	0.00460	93.172 ± 0.060
HST-002-10	1.00240	0.00500	93.172 ± 0.060
HST-002-11	1.00170	0.00380	93.172 ± 0.060
HST-002-12	1.00270	0.00500	93.172 ± 0.060
HST-002-13	1.00250	0.00550	93.172 ± 0.060
HST-002-14	1.00310	0.00660	93.172 ± 0.060

Table 6.5.7-1   Highly Enriched Uranyl Nitrates Benchmark K$_{eff}$'s and Uncertainties
(cont'd)

Identification	k$_{eff}$	σ	wt% ^{235}U
HST-003-1	1.00160	0.00560	93.172 ± 0.060
HST-003-2	1.00160	0.00570	93.172 ± 0.060
HST-003-3	1.00140	0.00560	93.172 ± 0.060
HST-003-4	1.00090	0.00570	93.172 ± 0.060
HST-003-5	1.00210	0.00680	93.172 ± 0.060
HST-003-6	1.00130	0.00700	93.172 ± 0.060
HST-003-7	1.00060	0.00460	93.172 ± 0.060
HST-003-8	1.00030	0.00330	93.172 ± 0.060
HST-003-9	0.99960	0.00350	93.172 ± 0.060
HST-003-10	1.00110	0.00500	93.172 ± 0.060
HST-003-11	0.99970	0.00520	93.172 ± 0.060
HST-003-12	1.00060	0.00470	93.172 ± 0.060
HST-003-13	1.00040	0.00590	93.172 ± 0.060
HST-003-14	1.00050	0.00470	93.172 ± 0.060
HST-003-15	1.00000	0.00450	93.172 ± 0.060
HST-003-16	1.00020	0.00370	93.172 ± 0.060
HST-003-17	0.99940	0.00420	93.172 ± 0.060
HST-003-18	1.00090	0.00500	93.172 ± 0.060
HST-003-19	0.99910	0.00590	93.172 ± 0.060
HST-007-01	1.00000	0.00350	93.172 ± 0.060
HST-007-02	1.00000	0.00500	93.172 ± 0.060
HST-007-03	1.00000	0.00350	93.172 ± 0.060
HST-007-04	1.00000	0.00350	93.172 ± 0.060
HST-007-05	1.00000	0.00350	93.172 ± 0.060
HST-007-06	1.00000	0.00350	93.172 ± 0.060
HST-007-07	1.00000	0.00350	93.172 ± 0.060
HST-007-08	1.00000	0.00350	93.172 ± 0.060
HST-007-09	1.00000	0.00350	93.172 ± 0.060
HST-007-10	1.00000	0.00350	93.172 ± 0.060
HST-007-11	1.00000	0.00350	93.172 ± 0.060
HST-007-12	1.00000	0.00350	93.172 ± 0.060
HST-007-13	1.00000	0.00350	93.172 ± 0.060
HST-007-14	1.00000	0.00350	93.172 ± 0.060
HST-007-15	1.00000	0.00350	93.172 ± 0.060
HST-007-16	1.00000	0.00350	93.172 ± 0.060
HST-007-17	1.00000	0.00350	93.172 ± 0.060

Table 6.5.7-1   Highly Enriched Uranyl Nitrates Benchmark K_{eff}'s and Uncertainties (cont'd)

Identification	k_{eff}	σ	wt% ^{235}U
HST-008-01	1.00000	0.00300	93.172 ± 0.060
HST-008-02	1.00000	0.00300	93.172 ± 0.060
HST-008-03	1.00000	0.00300	93.172 ± 0.060
HST-008-04	1.00000	0.00300	93.172 ± 0.060
HST-008-05	1.00000	0.00300	93.172 ± 0.060
HST-008-06	1.00000	0.00300	93.172 ± 0.060
HST-008-07	1.00000	0.00300	93.172 ± 0.060
HST-008-08	1.00000	0.00300	93.172 ± 0.060
HST-008-09	1.00000	0.00300	93.172 ± 0.060
HST-008-10	1.00000	0.00300	93.172 ± 0.060
HST-008-11	1.00000	0.00300	93.172 ± 0.060
HST-008-12	1.00000	0.00300	93.172 ± 0.060
HST-008-13	1.00000	0.00300	93.172 ± 0.060
HST-008-14	1.00000	0.00300	93.172 ± 0.060
HST-013-01	1.00120	0.00260	93.18
HST-032-01	1.0015	0.0026	93.21
HST-033-02A	1.00000	0.01110	93.219 ± 0.037
HST-033-02B	1.00000	0.01080	93.219 ± 0.037
HST-033-02C	1.00000	0.00650	93.219 ± 0.037
HST-033-011A	1.00000	0.01110	93.219 ± 0.037
HST-033-011B	1.00000	0.01080	93.219 ± 0.037

Table 6.5.7-1   Highly Enriched Uranyl Nitrates Benchmark K$_{eff}$'s and Uncertainties (cont'd)

Identification	k$_{eff}$	σ	wt% ^{235}U
HST-040-01	0.99570	0.00630	93.17
HST-040-02	0.99200	0.00700	93.17
HST-040-03	0.99290	0.00830	93.17
HST-040-04	0.99110	0.00810	93.17
HST-040-05	0.99220	0.00820	93.17
HST-040-06	0.99260	0.00720	93.17
HST-040-07	0.99140	0.00690	93.17
HST-040-08	0.99320	0.00780	93.17
HST-040-09	0.99380	0.00670	93.17
HST-040-10	0.99340	0.00660	93.17
HST-040-11	0.99410	0.00660	93.17
HST-040-12	0.99530	0.00730	93.17
HST-040-13	0.99750	0.00690	93.17
HST-040-14	0.99680	0.00680	93.17
HST-040-15	0.99310	0.00620	93.17
HST-040-16	0.99530	0.00600	93.17
HST-040-17	0.99620	0.00770	93.17
HST-042-01	0.99570	0.00390	93.22
HST-042-02	0.99650	0.00360	93.03
HST-042-03	0.99940	0.00280	93.12
HST-042-04	1.00000	0.00340	93.11
HST-042-05	1.00000	0.00340	93.01
HST-042-06	1.00000	0.00370	92.79
HST-042-07	1.00000	0.00360	92.78
HST-042-08	1.00000	0.00350	92.82

Table 6.5.7-2   MCNP Criticality Results Highly Enriched Uranyl Nitrates Benchmarks

Case Description		MCNP	v1.60	Results			Bias
Evaluation ID	Case ID	k_{eff}	σ	Adj. k_{eff}	EALCF (eV)	Total σ	Δk
HEU-SOL-THERM-001	Case_1	0.99705	0.00202	0.99665	0.08107	0.00633	-0.00335
HEU-SOL-THERM-001	Case_2	0.99421	0.00218	0.99211	0.27340	0.00752	-0.00789
HEU-SOL-THERM-001	Case_3	0.99759	0.00197	0.99729	0.07909	0.00402	-0.00271
HEU-SOL-THERM-001	Case_4	0.99505	0.00212	0.99425	0.29374	0.00571	-0.00575
HEU-SOL-THERM-001	Case_5	0.99593	0.00167	0.99583	0.04279	0.00518	-0.00417
HEU-SOL-THERM-001	Case_6	0.99925	0.00185	0.99905	0.04431	0.00496	-0.00095
HEU-SOL-THERM-001	Case_7	0.99820	0.00220	0.99740	0.07644	0.00457	-0.00260
HEU-SOL-THERM-001	Case_8	0.99980	0.00191	1.00000	0.08110	0.00425	0.00000
HEU-SOL-THERM-001	Case_9	0.99108	0.00229	0.99078	0.29289	0.00587	-0.00922
HEU-SOL-THERM-001	Case_10	0.99370	0.00175	0.99440	0.04600	0.00568	-0.00560
HEU-SOL-THERM-002	Case_1	0.99925	0.00224	0.99675	0.07931	0.00622	-0.00325
HEU-SOL-THERM-002	Case_2	1.00403	0.00224	1.00123	0.07843	0.00622	0.00123
HEU-SOL-THERM-002	Case_3	0.99997	0.00234	0.99667	0.24636	0.00719	-0.00333
HEU-SOL-THERM-002	Case_4	1.00422	0.00206	1.00082	0.23755	0.00720	0.00082
HEU-SOL-THERM-002	Case_5	1.00221	0.00234	1.00041	0.07952	0.00498	0.00041
HEU-SOL-THERM-002	Case_6	1.00599	0.00231	1.00369	0.07795	0.00471	0.00369
HEU-SOL-THERM-002	Case_7	1.00093	0.00232	0.99843	0.24417	0.00551	-0.00157
HEU-SOL-THERM-002	Case_8	1.00439	0.00220	1.00139	0.22955	0.00592	0.00139
HEU-SOL-THERM-002	Case_9	1.00156	0.00183	1.00036	0.04403	0.00495	0.00036
HEU-SOL-THERM-002	Case_10	1.00132	0.00198	0.99892	0.04415	0.00538	-0.00108
HEU-SOL-THERM-002	Case_11	1.00209	0.00225	1.00039	0.07914	0.00442	0.00039
HEU-SOL-THERM-002	Case_12	1.00378	0.00216	1.00108	0.07703	0.00545	0.00108
HEU-SOL-THERM-002	Case_13	0.99403	0.00240	0.99153	0.24669	0.00600	-0.00847
HEU-SOL-THERM-002	Case_14	1.00448	0.00229	1.00138	0.23036	0.00699	0.00138

Table 6.5.7-2   MCNP Criticality Results Highly Enriched Uranyl Nitrates Benchmarks (cont'd)

Case Description		MCNP	v1.60	Results			Bias
Evaluation ID	Case ID	k_{eff}	σ	Adj. k_{eff}	EALCF (eV)	Total σ	Δk
HEU-SOL-THERM-003	Case_1	1.00039	0.00186	0.99879	0.04389	0.00590	-0.00121
HEU-SOL-THERM-003	Case_2	1.00253	0.00213	1.00093	0.04429	0.00608	0.00093
HEU-SOL-THERM-003	Case_3	1.00114	0.00230	0.99974	0.07958	0.00605	-0.00026
HEU-SOL-THERM-003	Case_4	1.00280	0.00215	1.00190	0.07856	0.00609	0.00190
HEU-SOL-THERM-003	Case_5	0.99335	0.00253	0.99125	0.25934	0.00726	-0.00875
HEU-SOL-THERM-003	Case_6	1.00005	0.00251	0.99875	0.23639	0.00744	-0.00125
HEU-SOL-THERM-003	Case_7	1.00284	0.00191	1.00224	0.04358	0.00498	0.00224
HEU-SOL-THERM-003	Case_8	0.99867	0.00243	0.99837	0.08022	0.00410	-0.00163
HEU-SOL-THERM-003	Case_9	1.00727	0.00224	1.00767	0.07656	0.00416	0.00767
HEU-SOL-THERM-003	Case_10	0.98970	0.00221	0.98860	0.25778	0.00547	-0.01140
HEU-SOL-THERM-003	Case_11	0.99732	0.00256	0.99762	0.22161	0.00580	-0.00238
HEU-SOL-THERM-003	Case_12	0.99650	0.00207	0.99590	0.04416	0.00514	-0.00410
HEU-SOL-THERM-003	Case_13	0.99655	0.00188	0.99615	0.04314	0.00619	-0.00385
HEU-SOL-THERM-003	Case_14	1.00098	0.00210	1.00048	0.04390	0.00515	0.00048
HEU-SOL-THERM-003	Case_15	0.99555	0.00193	0.99555	0.04557	0.00490	-0.00445
HEU-SOL-THERM-003	Case_16	1.00086	0.00231	1.00066	0.08083	0.00436	0.00066
HEU-SOL-THERM-003	Case_17	1.00177	0.00216	1.00237	0.07554	0.00472	0.00237
HEU-SOL-THERM-003	Case_18	0.99632	0.00233	0.99542	0.25768	0.00552	-0.00458
HEU-SOL-THERM-003	Case_19	1.00703	0.00229	1.00793	0.21600	0.00633	0.00793
HEU-SOL-THERM-007	Case_1	1.01057	0.00189	1.01057	0.04681	0.00398	0.01057
HEU-SOL-THERM-007	Case_2	1.01134	0.00195	1.01134	0.25994	0.00537	0.01134
HEU-SOL-THERM-007	Case_3	1.00513	0.00198	1.00513	0.04619	0.00402	0.00513
HEU-SOL-THERM-007	Case_4	1.00912	0.00205	1.00912	0.23635	0.00406	0.00912
HEU-SOL-THERM-007	Case_5	1.00390	0.00198	1.00390	0.05067	0.00402	0.00390
HEU-SOL-THERM-007	Case_6	0.99989	0.00219	0.99989	0.26827	0.00546	-0.00011
HEU-SOL-THERM-007	Case_7	1.00719	0.00178	1.00719	0.04946	0.00393	0.00719
HEU-SOL-THERM-007	Case_8	0.99721	0.00225	0.99721	0.26604	0.00416	-0.00279
HEU-SOL-THERM-007	Case_9	1.00206	0.00204	1.00206	0.05135	0.00405	0.00206
HEU-SOL-THERM-007	Case_10	1.00815	0.00183	1.00815	0.05291	0.00395	0.00815
HEU-SOL-THERM-007	Case_11	1.00414	0.00208	1.00414	0.24960	0.00407	0.00414
HEU-SOL-THERM-007	Case_12	1.00792	0.00191	1.00792	0.05092	0.00399	0.00792
HEU-SOL-THERM-007	Case_13	1.00564	0.00213	1.00564	0.22987	0.00410	0.00564
HEU-SOL-THERM-007	Case_14	1.00676	0.00209	1.00676	0.23822	0.00408	0.00676
HEU-SOL-THERM-007	Case_15	1.00528	0.00225	1.00528	0.23761	0.00416	0.00528
HEU-SOL-THERM-007	Case_16	1.00839	0.00221	1.00839	0.25063	0.00414	0.00839
HEU-SOL-THERM-007	Case_17	1.00913	0.00208	1.00913	0.23465	0.00407	0.00913

Table 6.5.7-2   MCNP Criticality Results Highly Enriched Uranyl Nitrates Benchmarks
(cont'd)

Case Description		MCNP	v1.60	Results			Bias
Evaluation ID	Case ID	k_{eff}	σ	Adj. k_{eff}	EALCF (eV)	Total σ	Δk
HEU-SOL-THERM-008	Case_1	0.99891	0.00138	0.99891	0.04401	0.00330	-0.00109
HEU-SOL-THERM-008	Case_2	1.00709	0.00177	1.00709	0.22300	0.00348	0.00709
HEU-SOL-THERM-008	Case_3	0.99541	0.00185	0.99541	0.04315	0.00352	-0.00459
HEU-SOL-THERM-008	Case_4	1.00375	0.00214	1.00375	0.19991	0.00369	0.00375
HEU-SOL-THERM-008	Case_5	0.99828	0.00170	0.99828	0.04439	0.00345	-0.00172
HEU-SOL-THERM-008	Case_6	1.00609	0.00231	1.00609	0.24895	0.00379	0.00609
HEU-SOL-THERM-008	Case_7	0.99646	0.00184	0.99646	0.04330	0.00352	-0.00354
HEU-SOL-THERM-008	Case_8	1.00136	0.00234	1.00136	0.23821	0.00380	0.00136
HEU-SOL-THERM-008	Case_9	1.00012	0.00135	1.00012	0.04365	0.00329	0.00012
HEU-SOL-THERM-008	Case_10	1.00456	0.00226	1.00456	0.22348	0.00376	0.00456
HEU-SOL-THERM-008	Case_11	1.00000	0.00205	1.00000	0.04225	0.00363	0.00000
HEU-SOL-THERM-008	Case_12	1.00539	0.00216	1.00539	0.19416	0.00370	0.00539
HEU-SOL-THERM-008	Case_13	1.00075	0.00221	1.00075	0.22342	0.00373	0.00075
HEU-SOL-THERM-008	Case_14	1.00182	0.00198	1.00182	0.20513	0.00359	0.00182
HEU-SOL-THERM-013	Case1	0.99853	0.00041	0.99733	0.03240	0.00263	-0.00267
HEU-SOL-THERM-032	Case1	1.00029	0.00038	0.99879	0.031016	0.00263	-0.00121
HEU-SOL-THERM-033	CASE_02A	0.99825	0.00114	0.99825	0.30523	0.01116	-0.00175
HEU-SOL-THERM-033	CASE_02B	0.99586	0.00110	0.99586	0.31372	0.01086	-0.00414
HEU-SOL-THERM-033	CASE_02C	0.99639	0.00114	0.99639	0.31663	0.00660	-0.00361
HEU-SOL-THERM-033	CASE_11A	1.00322	0.00117	1.00322	0.28409	0.01116	0.00322
HEU-SOL-THERM-033	CASE_11B	1.00039	0.00111	1.00039	0.27909	0.01086	0.00039

Table 6.5.7-2   MCNP Criticality Results Highly Enriched Uranyl Nitrates Benchmarks
(cont'd)

Case Description		MCNP	v1.60	Results			Bias
Evaluation ID	Case ID	k_{eff}	σ	Adj. k_{eff}	EALCF (eV)	Total σ	Δk
HEU-SOL-THERM-040	Case1	0.99627	0.00050	1.00057	0.51504	0.00632	0.00057
HEU-SOL-THERM-040	Case2	0.98707	0.00049	0.99507	0.52411	0.00702	-0.00493
HEU-SOL-THERM-040	Case3	0.99802	0.00051	1.00512	0.52172	0.00832	0.00512
HEU-SOL-THERM-040	Case4	0.99229	0.00050	1.00119	0.52295	0.00812	0.00119
HEU-SOL-THERM-040	Case5	0.98982	0.00050	0.99762	0.52378	0.00822	-0.00238
HEU-SOL-THERM-040	Case6	0.99268	0.00050	1.00008	0.52375	0.00722	0.00008
HEU-SOL-THERM-040	Case7	0.99078	0.00052	0.99938	0.52266	0.00692	-0.00062
HEU-SOL-THERM-040	Case8	0.98911	0.00050	0.99591	0.52553	0.00782	-0.00409
HEU-SOL-THERM-040	Case9	0.99228	0.00051	0.99848	0.52431	0.00672	-0.00152
HEU-SOL-THERM-040	Case10	0.99932	0.00049	1.00592	0.51729	0.00662	0.00592
HEU-SOL-THERM-040	Case11	1.00217	0.00049	1.00807	0.51839	0.00662	0.00807
HEU-SOL-THERM-040	Case12	0.99763	0.00052	1.00233	0.51138	0.00732	0.00233
HEU-SOL-THERM-040	Case13	0.98865	0.00050	0.99115	0.51283	0.00692	-0.00885
HEU-SOL-THERM-040	Case14	1.00101	0.00051	1.00421	0.51565	0.00682	0.00421
HEU-SOL-THERM-040	Case15	0.98555	0.00051	0.99245	0.52099	0.00622	-0.00755
HEU-SOL-THERM-040	Case16	0.98671	0.00051	0.99141	0.52054	0.00602	-0.00859
HEU-SOL-THERM-040	Case17	0.98845	0.00051	0.99225	0.51188	0.00772	-0.00775
HEU-SOL-THERM-042	Case_1	0.99719	0.00027	1.00149	0.03165	0.00391	0.00149
HEU-SOL-THERM-042	Case_2	0.99695	0.00026	1.00045	0.03155	0.00361	0.00045
HEU-SOL-THERM-042	Case_3	1.00082	0.00022	1.00142	0.03103	0.00281	0.00142
HEU-SOL-THERM-042	Case_4	1.00209	0.00020	1.00209	0.03087	0.00341	0.00209
HEU-SOL-THERM-042	Case_5	0.99997	0.00017	0.99997	0.03072	0.00340	-0.00003
HEU-SOL-THERM-042	Case_6	1.00107	0.00018	1.00107	0.03084	0.00370	0.00107
HEU-SOL-THERM-042	Case_7	1.00133	0.00016	1.00133	0.03071	0.00360	0.00133
HEU-SOL-THERM-042	Case_8	1.00189	0.00015	1.00189	0.03060	0.00350	0.00189

Figure 6.5.7-1   K$_{eff}$ versus Fuel Enrichment (MCNP – Highly Enriched Uranyl Nitrates)
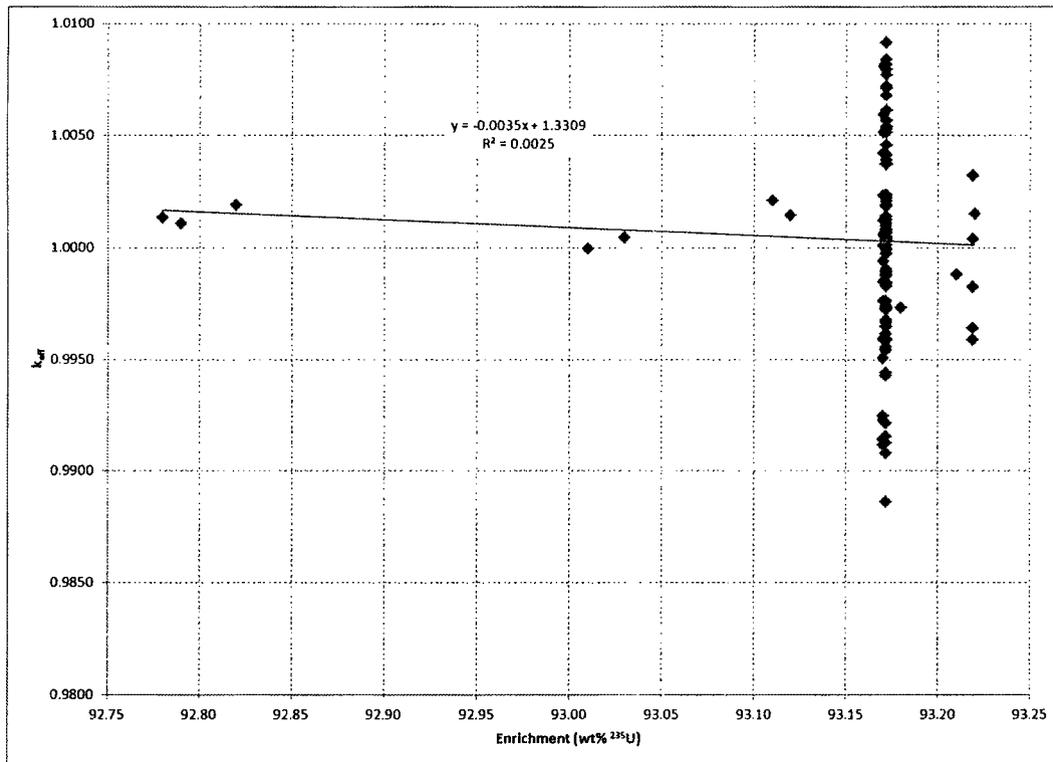
Figure 6.5.7-2 K_{eff} versus Energy of Average Neutron Lethargy Causing Fission
(MCNP – Highly Enriched Uranyl Nitrates)
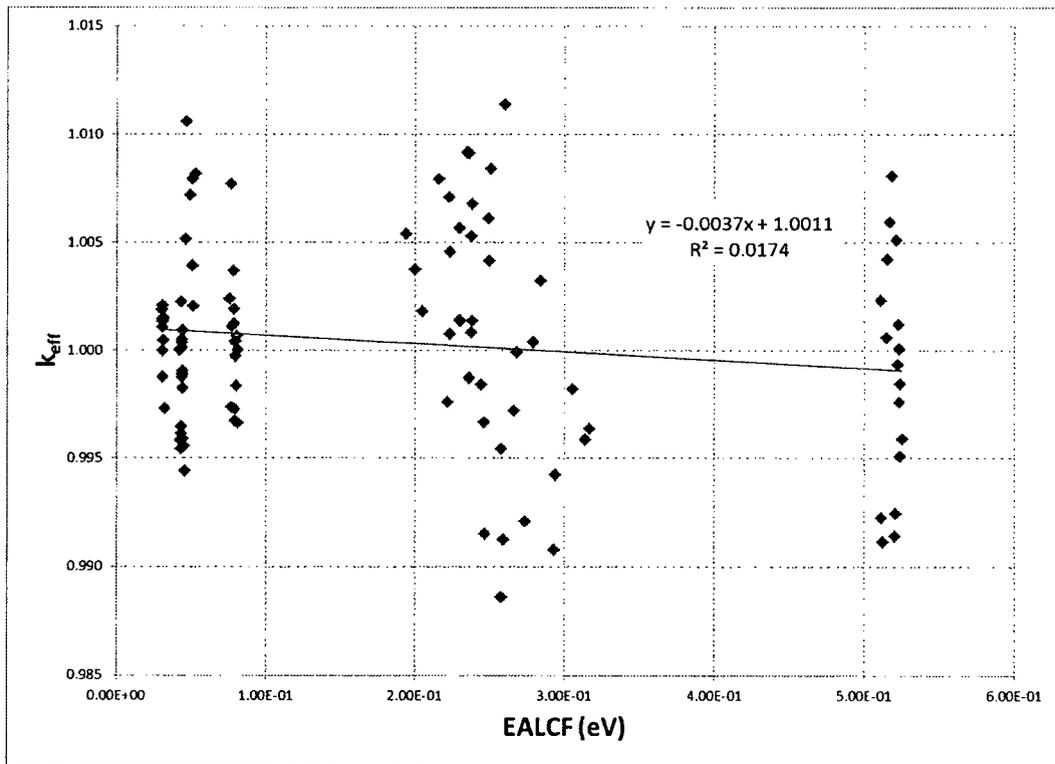
6.5.7.3 Results of MCNP Highly Enriched Uranyl Nitrates Benchmark Calculations

Trending in k_{eff} was considered for wt % ^{235}U and energy of the average neutron lethargy causing fission (EALCF), the two parameters most likely to show cross section effects.

To evaluate the relative importance of the trend analysis to the upper subcritical limits, correlation coefficients are required for all independent parameters. The linear correlation coefficient, R, is calculated by taking the square root of the R^2 value. In particular, the correlation coefficient, R, is a measure of the linear relationship between k_{eff} and a critical experiment parameter. If R is +1, a perfect linear relationship with a positive slope is indicated. If R is -1, a perfect linear relationship with a negative slope is indicated. When R is 0, no linear relationship is indicated.

Table 6.5.7-3 contains the correlation coefficient, R, for each linear fit of k_{eff} versus experimental parameter. Linear fits and correlation constants are based on 106 data-point evaluation sets plotted in the previous section. No statistically significant trends were found for either parameter. As all experiments contain primarily ^{235}U (92.78 wt% to 93.22 wt%) with minor impurities, the consistent attribute to trend analysis is the EALCF.

The USL for the EALCF is calculated and shown in Table 6.5.7-4. The USLSTATS output of k_{eff} versus EALCF is shown in Figure 6.5.7-3. Uncertainties included in the USLSTATS evaluation are the Monte Carlo uncertainty associated with the reactivity calculation and experimental uncertainty that was provided in the literature for each of the cases.

Based on all the independent variable correlations, a lower limit constant USL of 0.9366 may be applied. This validation and bias calculation is applicable to the critical configurations and parameters described in Table 6.5.7-5.

Figure 6.5.7-3   MCNP Highly Enriched Uranyl Nitrates USLSTATS Output for EALCF

```
Input to statistical treatment from file:ealcf.in

Title: keff vs EALCF

  Proportion of the population = .995
  Confidence of fit          = .950
  Confidence on proportion   = .950
  Number of observations     = 106
  Minimum value of closed band =   0.00
  Maximum value of closed band =   0.00
  Administrative margin      =   0.05
```

independent variable - x	dependent variable - y	deviation in y	independent variable - x	dependent variable - y	deviation in y
8.11000E-02	9.96650E-01	6.33000E-03	2.50000E-01	1.00414E+00	4.07000E-03
2.73000E-01	9.92110E-01	7.52000E-03	5.09000E-02	1.00792E+00	3.99000E-03
7.91000E-02	9.97290E-01	4.02000E-03	2.30000E-01	1.00564E+00	4.10000E-03
2.94000E-01	9.94250E-01	5.71000E-03	2.38000E-01	1.00676E+00	4.08000E-03
4.28000E-02	9.95830E-01	5.18000E-03	2.38000E-01	1.00528E+00	4.16000E-03
4.43000E-02	9.99050E-01	4.96000E-03	2.51000E-01	1.00839E+00	4.14000E-03
7.64000E-02	9.97400E-01	4.57000E-03	2.35000E-01	1.00913E+00	4.07000E-03
8.11000E-02	1.00000E+00	4.25000E-03	4.40000E-02	9.98910E-01	3.30000E-03
2.93000E-01	9.90780E-01	5.87000E-03	2.23000E-01	1.00709E+00	3.48000E-03
4.60000E-02	9.94400E-01	5.68000E-03	4.32000E-02	9.95410E-01	3.52000E-03
7.93000E-02	9.96750E-01	6.22000E-03	2.00000E-01	1.00375E+00	3.69000E-03
7.84000E-02	1.00123E+00	6.22000E-03	4.44000E-02	9.98280E-01	3.45000E-03
2.46000E-01	9.96670E-01	7.19000E-03	2.49000E-01	1.00609E+00	3.79000E-03
2.38000E-01	1.00082E+00	7.20000E-03	4.33000E-02	9.96460E-01	3.52000E-03
7.95000E-02	1.00041E+00	4.98000E-03	2.38000E-01	1.00136E+00	3.80000E-03
7.80000E-02	1.00369E+00	4.71000E-03	4.36000E-02	1.00012E+00	3.29000E-03
2.44000E-01	9.98430E-01	5.51000E-03	2.23000E-01	1.00456E+00	3.76000E-03
2.30000E-01	1.00139E+00	5.92000E-03	4.23000E-02	1.00000E+00	3.63000E-03
4.40000E-02	1.00036E+00	4.95000E-03	1.94000E-01	1.00539E+00	3.70000E-03
4.42000E-02	9.98920E-01	5.38000E-03	2.23000E-01	1.00075E+00	3.73000E-03
7.91000E-02	1.00039E+00	4.42000E-03	2.05000E-01	1.00182E+00	3.59000E-03
7.70000E-02	1.00108E+00	5.45000E-03	3.24000E-02	9.97330E-01	2.63000E-03
2.47000E-01	9.91530E-01	6.00000E-03	3.10000E-02	9.98790E-01	2.63000E-03
2.30000E-01	1.00138E+00	6.99000E-03	3.05000E-01	9.98250E-01	1.11000E-02
4.39000E-02	9.98790E-01	5.90000E-03	3.14000E-01	9.95860E-01	1.08600E-02
4.43000E-02	1.00093E+00	6.08000E-03	3.17000E-01	9.96390E-01	6.60000E-03
7.96000E-02	9.99740E-01	6.05000E-03	2.84000E-01	1.00322E+00	1.11600E-02
7.86000E-02	1.00190E+00	6.09000E-03	2.79000E-01	1.00039E+00	1.08600E-02
2.59000E-01	9.91250E-01	7.26000E-03	5.15000E-01	1.00057E+00	6.32000E-03
2.36000E-01	9.98750E-01	7.44000E-03	5.24000E-01	9.95070E-01	7.02000E-03
4.36000E-02	1.00224E+00	4.98000E-03	5.22000E-01	1.00512E+00	8.32000E-03
8.02000E-02	9.98370E-01	4.10000E-03	5.23000E-01	1.00119E+00	8.12000E-03
7.66000E-02	1.00767E+00	4.16000E-03	5.24000E-01	9.97620E-01	8.22000E-03
2.58000E-01	9.88600E-01	5.47000E-03	5.24000E-01	1.00008E+00	7.22000E-03
2.22000E-01	9.97620E-01	5.80000E-03	5.23000E-01	9.99380E-01	6.92000E-03
4.42000E-02	9.95900E-01	5.14000E-03	5.26000E-01	9.95910E-01	7.82000E-03
4.31000E-02	9.96150E-01	6.19000E-03	5.24000E-01	9.98480E-01	6.72000E-03
4.39000E-02	1.00048E+00	5.15000E-03	5.17000E-01	1.00592E+00	6.62000E-03
4.56000E-02	9.95550E-01	4.90000E-03	5.18000E-01	1.00807E+00	6.62000E-03
8.08000E-02	1.00066E+00	4.36000E-03	5.11000E-01	1.00233E+00	7.32000E-03
7.55000E-02	1.00237E+00	4.72000E-03	5.13000E-01	9.91150E-01	6.92000E-03
2.58000E-01	9.95420E-01	5.52000E-03	5.16000E-01	1.00421E+00	6.82000E-03
2.16000E-01	1.00793E+00	6.33000E-03	5.21000E-01	9.92450E-01	6.22000E-03
4.68000E-02	1.01057E+00	3.98000E-03	5.21000E-01	9.91410E-01	6.02000E-03
2.60000E-01	1.01134E+00	5.37000E-03	5.12000E-01	9.92250E-01	7.72000E-03
4.62000E-02	1.00513E+00	4.02000E-03	3.16000E-02	1.00149E+00	3.91000E-03
2.36000E-01	1.00912E+00	4.06000E-03	3.15000E-02	1.00045E+00	3.61000E-03
5.07000E-02	1.00390E+00	4.02000E-03	3.10000E-02	1.00142E+00	2.81000E-03
2.68000E-01	9.99890E-01	5.46000E-03	3.09000E-02	1.00209E+00	3.41000E-03
4.95000E-02	1.00719E+00	3.93000E-03	3.07000E-02	9.99970E-01	3.40000E-03
2.66000E-01	9.97210E-01	4.16000E-03	3.08000E-02	1.00107E+00	3.70000E-03
5.14000E-02	1.00206E+00	4.05000E-03	3.07000E-02	1.00133E+00	3.60000E-03
5.29000E-02	1.00815E+00	3.95000E-03	3.06000E-02	1.00189E+00	3.50000E-03

```
chi = 5.4151 (upper bound = 9.49). The data tests normal.
```

Figure 6.5.7-3   MCNP Highly Enriched Uranyl Nitrates USLSTATS Output for EALCF (cont'd)

```
        Output from statistical treatment

keff vs EALCF

  Number of data points (n)                 106
  Linear regression, k(X)                   1.0011 + (-3.7159E-03)*X
  Confidence on fit (1-gamma) [input]       95.0%
  Confidence on proportion (alpha) [input]  95.0%
  Proportion of population falling above
  lower tolerance interval (rho) [input]    99.5%
  Minimum value of X                        3.0600E-02
  Maximum value of X                        5.2600E-01
  Average value of X                        1.9825E-01
  Average value of k                        1.00032
  Minimum value of k                        0.98860
  Variance of fit, s(k,X)^2                 2.2267E-05
  Within variance, s(w)^2                   3.1899E-05
  Pooled variance, s(p)^2                   5.4166E-05
  Pooled std. deviation, s(p)               7.3597E-03
  C(alpha,rho)*s(p)                         2.5589E-02
  student-t @ (n-2,1-gamma)                 1.66147E+00
  Confidence band width, W                  1.2503E-02
  Minimum margin of subcriticality, C*s(p)-W 1.3086E-02

  Upper subcritical limits: ( 3.06000E-02 <= X <= 0.52600    )
  ***** ************* *******


  USL Method 1 (Confidence Band with
  Administrative Margin)       USL1 = 0.9386 + (-3.7159E-03)*X (X >  0.28480   )
                                    = 0.9375                   (X <= 0.28480   )


  USL Method 2 (Single-Sided Uniform
  Width Closed Interval Approach)  USL2 = 0.9755 + (-3.7159E-03)*X (X > 2.84799E-01)
                                       = 0.9744                   (X <= 2.84799E-01)



  USLs Evaluated Over Range of Parameter X:
  **** ********* **** ***** ** ********* **

  X:   3.06E-2  1.01E-1  1.72E-1  2.43E-1  3.14E-1  3.84E-1  4.55E-1  5.26E-1
  --------------------------------------------------------------------------
USL-1:  0.9375   0.9375   0.9375   0.9375   0.9374   0.9371   0.9369   0.9366
USL-2:  0.9744   0.9744   0.9744   0.9744   0.9743   0.9740   0.9738   0.9735
  --------------------------------------------------------------------------
```

Table 6.5.7-3   Range of Parameters and Correlation Coefficients for Highly Enriched
Uranyl Nitrates Benchmarks

Correlation	R^2	R	Minimum	Maximum
wt% ^{235}U	2.55E-03	0.0505	92.78%	93.22%
EALCF (eV)	1.74E-02	0.132	3.06E-02	5.26E-01

Table 6.5.7-4   MCNP Highly Enriched Uranyl Nitrates – USLSTATS Generated USLs
for Benchmark Experiments

Variable	EALCF
File Name	ealcf.out
# Points	106
AOA Range	$0.0306 \text{ eV} \leq X \leq 0.5260 \text{ eV}$
Administrative Margin	0.05
USL	0.9366

Table 6.5.7-5   MCNP Highly Enriched Uranyl Nitrates – Area of Applicability for
Benchmark Experiments

Fissile Form	Nitrate Solutions
Geometry	Spheres, Rods (Cylinders)
Moderator	Light Water, Tap Water, or None
H/U Ratio	51.010 to 2050
EALCF (eV)	3.06E-02 to 5.26E-01

Table 6.5.7-6   Highly Enriched Uranyl Nitrates Validated Cross-Section Libraries

1001.70c	14000.60c	24052.70c	28058.70c	92233.70c
1002.70c	15031.70c	24053.70c	28060.70c	92234.70c
5010.70c	16000.62c	24054.70c	28061.70c	92235.70c
6000.70c	16032.70c	25055.50c	28062.70c	92236.70c
6012.50c	17000.66c	26000.55c	28064.70c	92238.70c
7014.70c	19000.62c	26054.70c	29000.50c	lwtr.10t
7015.70c	20000.62c	26056.70c	29063.70c	
8016.70c	22000.62c	26057.70c	29065.70c	
11023.70c	23000.70c	26058.70c	42000.66c	
12000.62c	24000.50c	27059.70c	48000.51c	
13027.70c	24050.70c	28000.50c	73181.70c	

6.7   Payload Specific Details

This section contains NAC-LWT cask payload specific evaluation detail.

6.7.1   PWR Mixed Oxide Fuel Rods

This section includes input, analysis method, results, and criticality benchmark evaluations for the NAC-LWT cask containing a payload of up to 16 PWR rods. The PWR rods may be composed of uranium oxide fuel pellets or mixed oxide fuel pellets (depleted or natural uranium oxide with plutonium oxide contributing the primary quantity of fissile material).

6.7.1.1   Package Fuel Loading

The NAC-LWT cask may transport up to 16 undamaged PWR fuel rods in a fuel rod holder. To bound all PWR MOX rods that may be transported in the NAC-LWT cask, UO_2 rods are evaluated with enrichments up to 5.0 wt % ^{235}U, while MOX rods were evaluated up to 7 wt % fissile plutonium. Characteristics of the design basis PWR rods are presented in Table 6.7.1-12 and Table 6.7.1-13. Given a fixed fissile material density, defined by a maximum UO_2 enrichment or fissile plutonium weight percent, the most reactive rod has the greatest fissile mass, i.e., the rod with the largest pellet radius. Therefore, the CE 14×14 pellet diameter of 0.3765 inch is chosen as the base radius for the most reactive PWR fuel rod evaluated here. A conservative maximum fissile material length of 153.5 inches is also applied. As a maximum reactivity fuel pitch is established, and the zirconium alloy is essentially transparent to neutrons, the clad thickness has no significant effect on the analysis.

6.7.1.2   Criticality Model Specifications

This section describes the models that are used in the criticality analyses for the NAC-LWT cask containing up to 16 PWR rods. PWR rods are either low enriched uranium oxide (maximum 5 wt % ^{235}U) fueled or MOX fueled. The models are analyzed separately under normal conditions and hypothetical accident conditions to ensure that all possible configurations are subcritical.

The model uses the MCNP5 code package with the ENDF/B-VI cross-section set. No cross-section pre-processing is required prior to MCNP implementation. MCNP uses the Monte Carlo technique to calculate the k_{eff} of a system. In these analyses, approximately 530 cycles with 1,000 neutron histories per cycle are tracked through the system.

Description of Calculational Models

The MCNP model of the NAC-LWT cask with 16 undamaged PWR rods includes triangular and square lattice formation of design basis rods centered in the cask cavity. No credit is taken for

geometry control provided by the rod holder. The fuel rods, cask cavity and radial shields are explicitly modeled as shown in the Figure 6.7.1-1 model sketch.

The model of the NAC-LWT cask takes advantage of the universe structure of MCNP. Each universe defines an infinite space, bounded after its insertion into a containing cell. Four universes are employed herein. The "0" universe defines the cask universe. The remaining universes are discussed in the following sections. Each universe is developed independently as surfaces and cells. Fuel rod array surfaces and cells are configured to place the rods in either a rectangular (square) pitch array or a hex (triangular) pitch array. The rod pitch is a variable input into the model and is modified to achieve a maximum reactivity configuration. In the basket universe, the rod array is placed into a square (RPP) body that allows the moderator density outside the rod array to be adjusted independently.

The modeled accident condition completely removes the neutron shielding, the neutron shield tank and the cask impact limiters. In the normal conditions model, the impact limiter diameter is modeled as identical to the neutron shield tank diameter. This allows for closer packing for the cask array than physically possible.

VISED sketches of the assembled geometry are shown in Figure 6.7.1-2 through Figure 6.7.1-4. The cask outer surface is surrounded by a rectangular body with reflecting boundary conditions. The boundary conditions are imposed on the sides, top and bottom, which simulates an infinite array of casks.

Package Regional Densities

The composition densities (g/cc) and nuclide number densities (atm/b-cm) used in the subsequent criticality analyses are shown in Table 6.7.1-1. The various isotope weight compositions used in the MOX/UO$_2$ rod analysis are listed in Table 6.7.1-2.

Figure 6.7.1-1   **MCNP Model Sketch of the NAC-LWT Cask with PWR MOX/UO$_2$ Rods**

(Dimensions in centimeters)
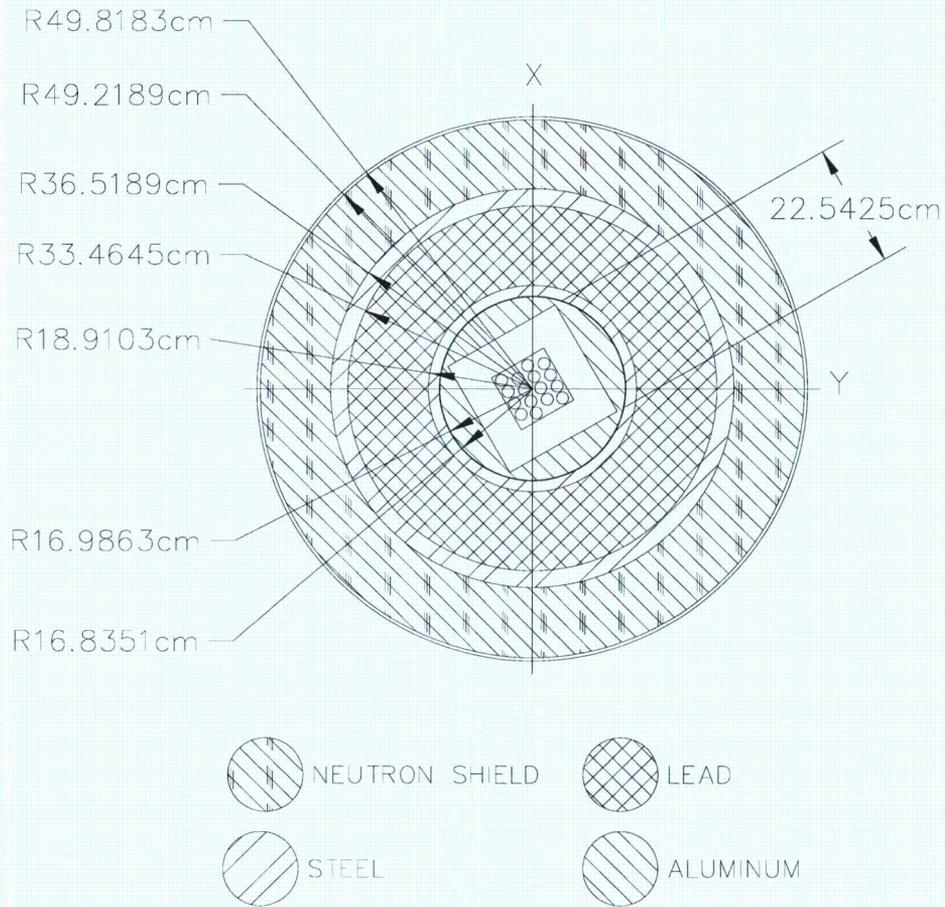
Figure 6.7.1-2   VISED Sketch of LWT Radial View – Hex Rod Array– Normal
Conditions
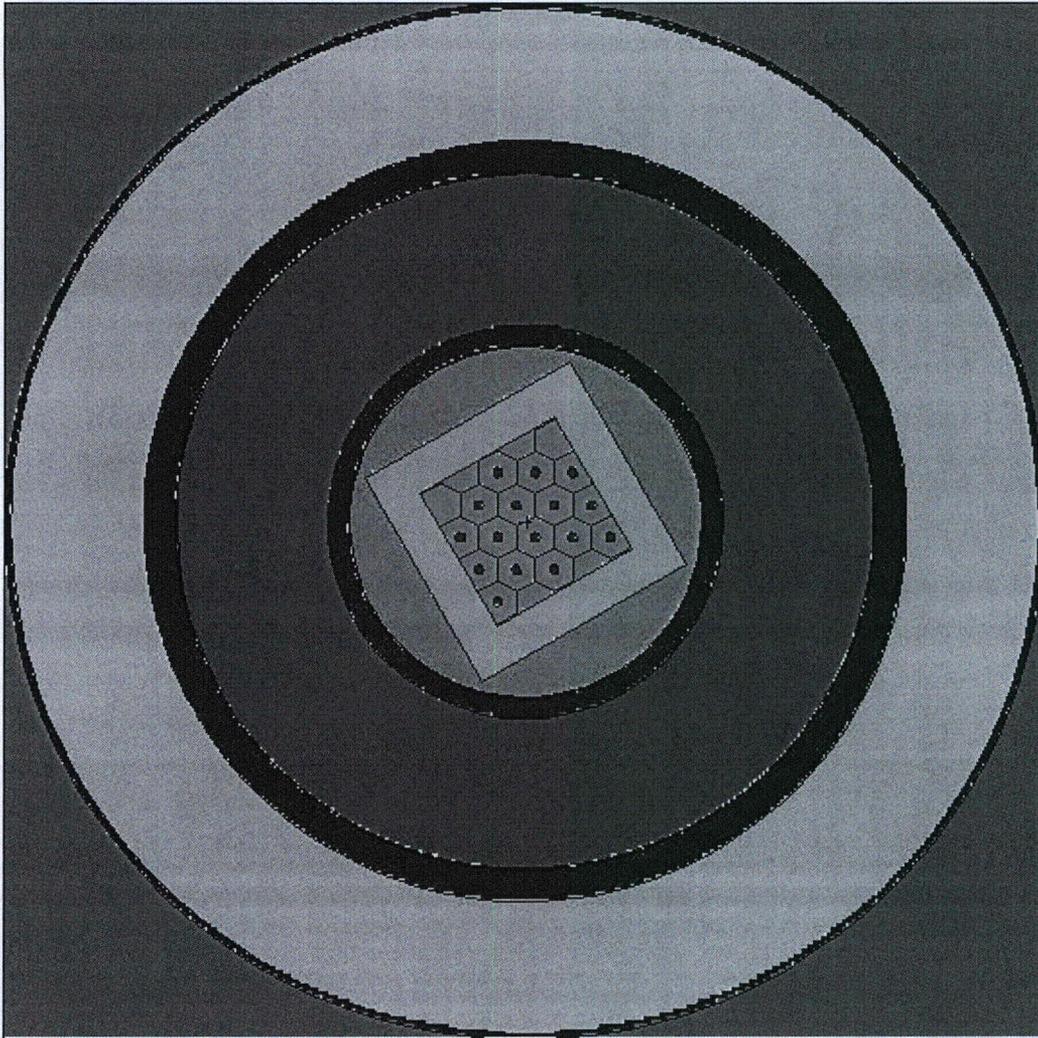
Figure 6.7.1-3   VISED Sketch of LWT Radial View – Square Rod Pitch –
Accident Conditions
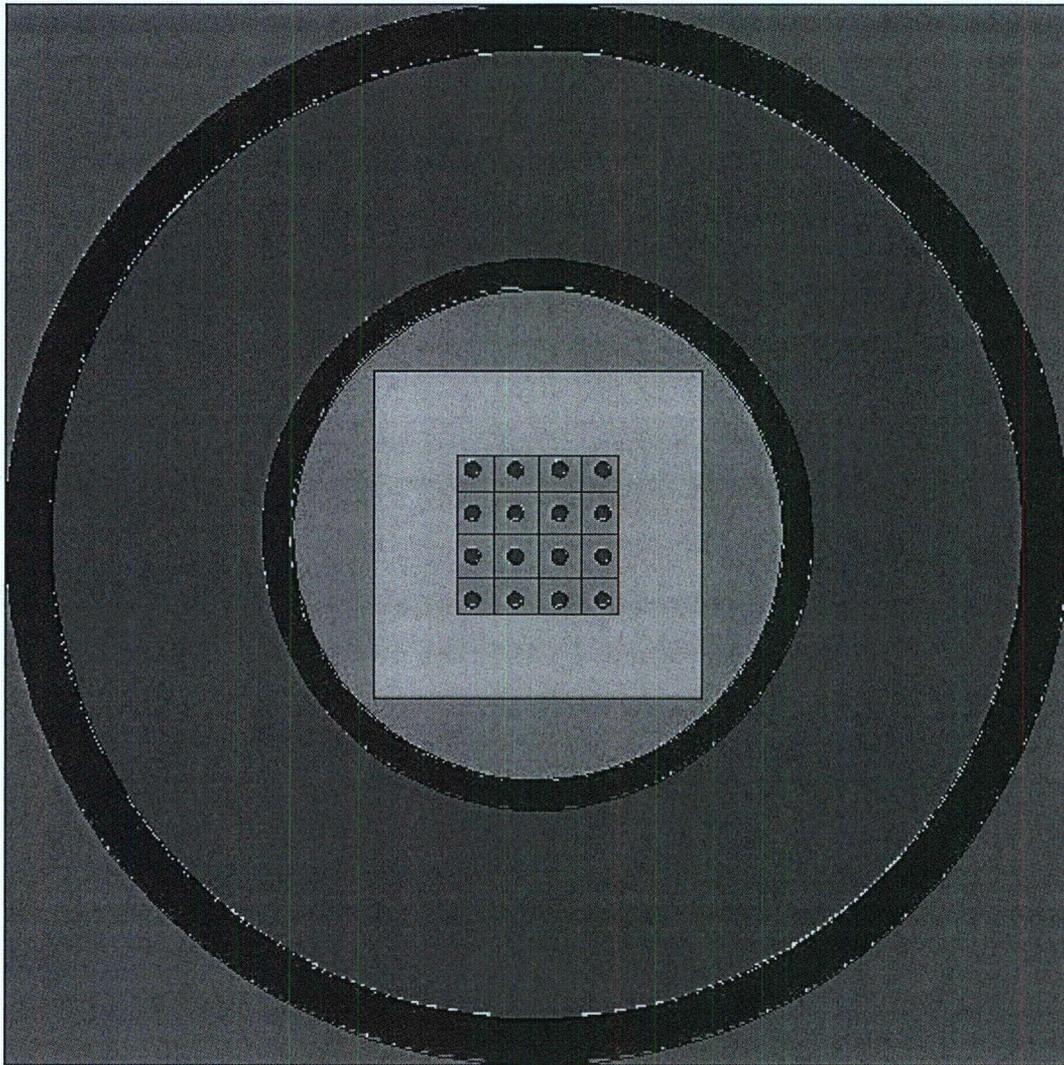
Figure 6.7.1-4   VISED Sketch of LWT Axial View – Accident Conditions
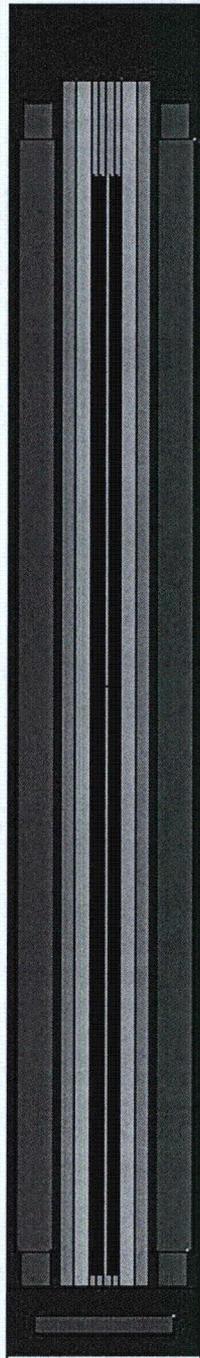
Table 6.7.1-1   PWR MOX Fuel Analysis Compositions and Number Densities

Material	5.0% Enriched UO₂	Weapons Grade (7 wt % Fissile Pu)[1]	Zirconium Alloy	H₂O	304 Stainless Steel	Pb	Al
Density, g/cc	10.522	10.556	6.56	0.9982	7.920	11.344	2.702
Density	atoms/b-cm						
Uranium-235	1.19E-03	1.54E-04					
Uranium-238	2.23E-02	2.16E-02					
Plutonium-238		9.15E-07					
Plutonium-239		1.70E-03					
Plutonium-240		1.09E-04					
Plutonium-241		7.23E-06					
Plutonium-242		9.00E-07					
Oxygen	4.70E-02	4.70E-02		3.338E-2			
Hydrogen				6.677E-2			
Zirconium Alloy			4.331E-2				
Iron					5.936E-2		
Chromium					1.743E-2		
Nickel					7.721E-3		
Manganese					1.736E-3		
Lead						3.297E-2	
Aluminum							6.031E-2

Table 6.7.1-2   PWR MOX Fuel Analysis Isotope Weight Fraction[2]

Isotope	UO₂	Weapon Grade	Fuel Grade	Power Grade	MOX Services
²³⁵U	5	0.7	0.7	0.7	0.7
²³⁸U	95	99.3	99.3	99.3	99.3
²³⁸Pu	0	0.05	0.1	1	0.05
²³⁹Pu	0	93.5	86.1	62	95
²⁴⁰Pu	0	6	12	22	4.5
²⁴¹Pu	0	0.4	1.6	12	0.4
²⁴²Pu	0	0.05	0.2	3	0.05

---

[1] Sample composition.

[2] Typical fresh fuel MOX material is composed of depleted uranium at 0.2 to 0.3 wt % ²³⁵U. A bounding natural uranium enrichment of 0.7 wt % ²³⁵U is used in the criticality evaluations.

6.7.1.3 Criticality Calculations

This section presents the criticality analysis for the NAC-LWT cask with up to 16 PWR UO_2 or MOX rods. UO_2 rods are enriched up to 5.0 wt % ^{235}U initial enrichment, while MOX rods contain up to 7 wt % fissile plutonium. No credit is taken for geometry control that is provided by the rod holder and no rod positions are specified for the rods in the lattice. Since various fuel rod arrangements may be shipped, the criticality of the PWR MOX rods in the NAC-LWT cask cavity is studied to determine the optimum pitch and, therefore, the maximum k_{eff} for the cask.

Criticality results are divided into individual sets of analyses.

- Evaluate the NAC-LWT accident configuration to demonstrate that, at a fixed fissile plutonium content, the maximum fissile percentage material (MOX Services definition) produces the maximum reactivity configuration.

- Determine the maximum reactivity pitch of the most reactive fuel material.

- Run the optimum moderator density evaluation.

- Evaluate normal condition and single cask "containment reflected" cases.

Included in all analyses are hypothetical plutonium compositions solely to justify the removal of the plutonium compositions as a licensing limit.

Rod Geometry and Material Composition Studies

Each of the material compositions is evaluated for the maximum fissile material mass rod. Fissile material in the uranium oxide rods is limited by the 5 wt % ^{235}U enrichment constraint, while the MOX material is limited by the 7 wt % fissile plutonium input. In addition to the physically realistic MOX material descriptions, three hypothetical MOX materials are evaluated: one containing all fissile plutonium (adding into ^{241}Pu the remaining plutonium weight fractions), an all ^{239}Pu material and an all ^{241}Pu material. The following nomenclature is used to describe the various plutonium fuel materials.

Abbreviation	Material
PG	Power grade plutonium isotopic distribution
FG	Fuel grade plutonium isotopic distribution
WG	Weapons grade plutonium isotopic distribution
MS	MOX Services "WG type" material
FP	Plutonium is modeled as all fissile plutonium
P9	Plutonium is modeled as all ^{239}Pu
P1	Plutonium is modeled as all ^{241}Pu

All cases are evaluated at a hexagonal pitch of 3.0 and 3.6 cm. Based on scoping evaluations, as validated in the following section, these fuel rod pitches approximate maximum reactivity configurations over a range of material composition.

As shown in later moderator density studies, maximum reactivity moderation is achieved by a preferentially flooded lattice with a void gap to the cask cavity. Fuel material and pitch studies are based on a flooded cask cavity. As these studies primarily rely on the interaction between rods in the lattice, rather than between casks, applying the results of the flooded cavity to the dry cavity/wet lattice is acceptable.

As seen in Table 6.7.1-3, maximum reactivity for physically realistic plutonium compositions is achieved by the MOX Services material. This result was expected as the MOX Services composition model contains the maximum fissile material within the plutonium oxide matrix. For the hypothetical compositions, the all ^{241}Pu case produces maximum reactivity. As the ^{241}Pu isotope has the highest fission cross-section, this result is to be expected.

Maximum Reactivity Rod Pitch Evaluation

The maximum fissile mass rod configuration is evaluated with uranium oxide, MOX Services (95 wt % ^{239}Pu in Pu), and 100% ^{241}Pu at a range of rod pitches to determine the maximum (optimum) pitch for a flooded cask cavity. This evaluation takes no credit for the actual pitch of the encapsulating stainless steel rod (11/16 inch at 1.75 cm OD) structure into which the rods are placed. As seen in Figure 6.7.1-5 and Table 6.7.1-4, the maximum reactivity pitch is approximately 3.4 to 3.6 cm for the MOX rods and around 3 cm for the uranium oxide rods, with a "flat" peak extending approximately 0.4 to 0.6 cm in width depending on material and configuration. Based on a three sigma uncertainty band, maximum reactivities do not statistically differ between hexagonal and square pitch configurations. The base case for the optimum moderator density studies will be the 3.6 cm hexagonal pitch for the MOX rods and the 3.0 cm hexagonal pitch for the UO$_2$ rods.

Optimum Moderator Density Evaluation

The maximum fissile mass rod is evaluated at various internal and external moderator densities, including preferential flooding of the fuel region. For the preferential flooding scenarios, the square container containing the rod array will be evaluated at a moderator density independent of that in the remainder of the cask cavity. Figure 6.7.1-6 through Figure 6.7.1-8 contain the moderator density plots of the uranium oxide, MOX Services, and all ^{241}Pu material configurations. All results produce identical trends in that maximum reactivity is achieved by a preferentially flooded fuel region and void cavity and cask exterior. This result was to be

expected as it provides maximum neutronic coupling within the reflective boundary (infinite array) model.

Maximum system reactivities are summarized in Table 6.7.1-5 for the UO_2 fuel composition, the MOX Services defined fuel composition, and the hypothetical fissile material composition (100% [241]Pu) at the bounding fissile configuration—a maximum fuel material rod (0.3765-in pellet OD, 153.5-in active fuel length).

Single Cask Containment (Fully Reflected) and Normal Condition Array Evaluations

A single cask evaluation is performed to comply with 10 CFR 71.55(b)(3).

The containment for the NAC-LWT is the cask inner shell. While no operating condition results in a removal of the cask outer shell and lead gamma shield, the most reactive preferential flooded and fully flooded cases are reevaluated by removing the lead and outer shells (including neutron shield), and reflecting the system by 20 cm water at full density on the X, Y, and Z faces. Single cask, containment fully reflected reactivities are summarized in Table 6.7.1-6.

A normal condition infinite cask array is also evaluated. As indicated by the evaluations of the accident conditions array, including the radial neutron shield reduces system reactivity by eliminating neutronic interaction between casks. Normal condition cask array results are summarized in Table 6.7.1-7.

Maximum Reactivities and Comparison to USL

The maximum $k_{eff} + 2\sigma$ results for three primary analysis groups (single cask, normal array and accident array) are summarized in Table 6.7.1-8. Two normal condition array cases are included as the cask remains dry through all operating conditions, while 10 CFR 71 requires a normal condition maximum reactivity moderator density case. The listed values represent the maximum system reactivity adjusted for Monte Carlo run uncertainty and are significantly below the lower of system USL.

No benchmarks for mixed heterogeneous UO_2 and MOX rod systems are publically available. Therefore, individual benchmarks are established for UO_2 and MOX systems. The more limiting USL is applied to the results of the MOX/UO_2 rod calculations. Per Section 6.7.3, the USL for an array of UO_2 rods is 0.9376 and 0.9331 for an array of MOX rods for a Δk of 0.0045 between the two fuel types. The evaluations demonstrated that MCNP, with its associated cross-sections, accurately predicts system reactivities containing either fuel rod type.

The focus of the evaluations is a wet (flooded) system, as no reasonable extrapolation of the data provided would indicate a safety concern for a dry system at the requested fissile material levels. While it is recognized that code performance and bias are potentially affected by the difference

in the energy level of neutron causing fission, the benchmarks accounted for the basic phenomena, and the computer code is capable of tracking particles at their relevant energy levels.

Analyses have demonstrated that the UO_2 rod payload, calculated to be at maximum reactivity flooded with an EALCF of 0.13 eV (3.0 cm pitch study UO_2 case), are significantly lower in reactivity than the MOX payload with an EALCF of 0.13 eV (note systems have identical EALCF at optimum pitch). Insertion of the lower reactivity UO_2 rods and corresponding replacement of higher reactivity MOX rods will reduce system reactivity.

Given the significant margin (Δk of 0.13) between maximum calculated reactivity for a hypothetical fuel material (all ^{241}Pu) at maximum reactivity pitch, without inclusion of the tube insert that retains the rods in a fixed position, the evaluations demonstrate that the system meets regulatory requirements. No mixed fuel evaluations are, therefore, performed and no mixed bias is discussed.

Table 6.7.1-9 compares the physical and hypothetical rod/material combinations to the area of applicability for the MOX material and maximum reactivity ^{241}Pu material. The MOX Services fuel material is within the area of applicability. No pure ^{241}Pu benchmark exists; therefore, the hypothetical configuration is significantly outside the area of applicability of the benchmark calculation. Compliance with regulatory limits is assured, as there is no significant reactivity trend versus plutonium isotopic composition. There is a significant margin to limits (0.13 Δk) versus a typical code bias in the 1-2% range, and the results are obtained from a hypothetical (conservative) isotope composition (all ^{241}Pu).

As the shipment includes uranium oxide rods, the maximum reactivity uranium oxide rod configuration characteristics are compared to the area of applicability in Table 6.7.1-10. The USL for UO_2 evaluations is 0.9372. Exceeding the area of applicability for enrichment and fuel to moderator ratios (expressed as rod pitch and H/U ratio) in the UO_2 benchmark cases is acceptable as neither function has a trend that is statistically significant and the margin to limits is large (> 0.4). A similar argument is applied to slightly lower fission energy for the maximum reactivity case than covered by the benchmark analysis. There is no statistically significant trend of reactivity versus energy, and any relative changes in USL postulated from the extrapolation is not significant versus the subcritical margin of the UO_2 rod shipment.

Evaluations of a mixed shipment of enriched UO_2 rods and MOX rods are not required, as the reactivity of the evaluated MOX rods are significantly higher than those of the UO_2 rods. Mixed shipments are, therefore, permitted.

Table 6.7.1-11 lists the bounding characteristics for the MOX/UO_2 PWR fuel rods evaluated in this section.

Figure 6.7.1-5   PWR MOX Rod Shipment – Reactivity versus Rod Pitch
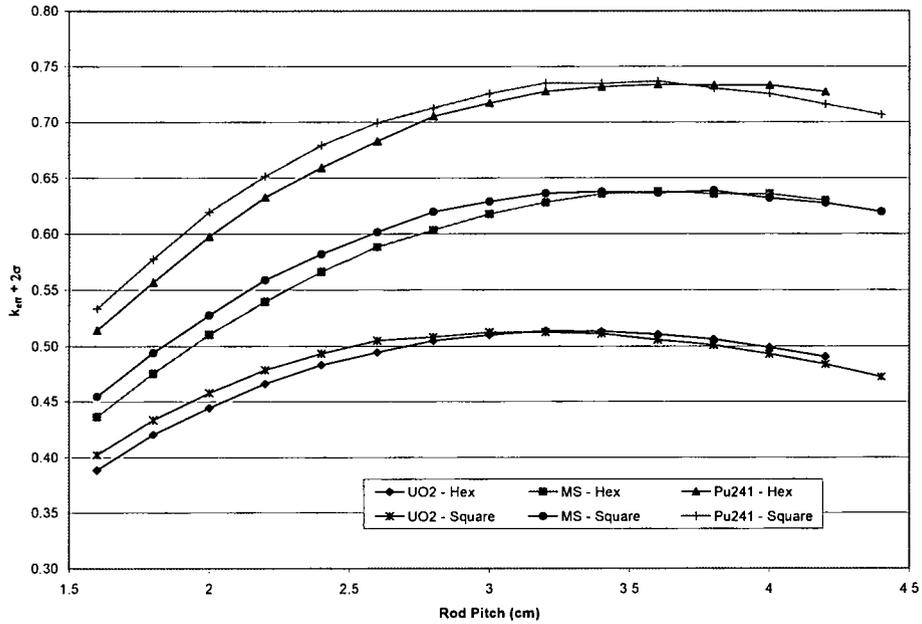
Figure 6.7.1-6   Moderator Density Study – UO₂ Fuel Material – 3.0 cm Rod Pitch
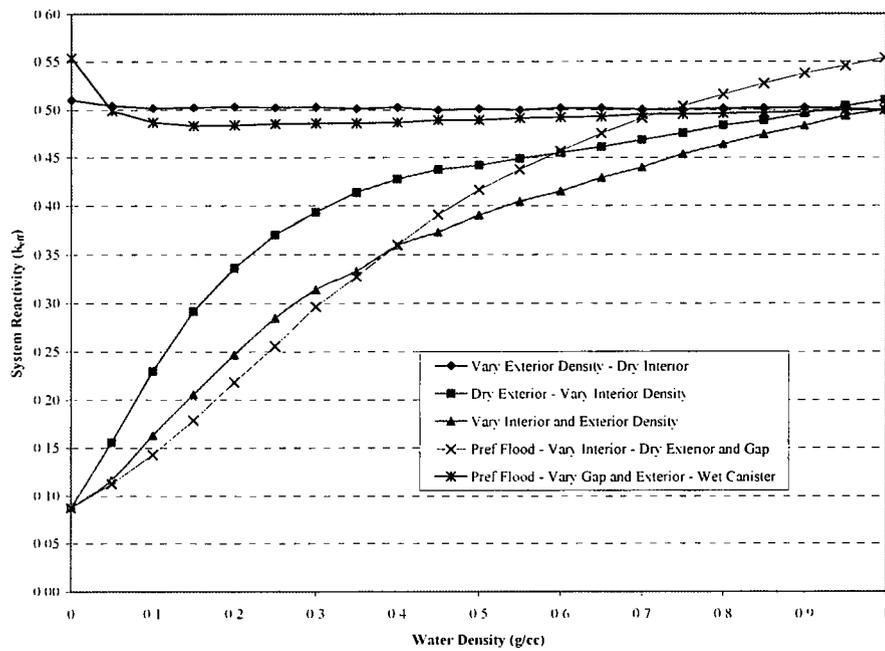
Figure 6.7.1-7   Moderator Density Study – MS Fuel Material – 3.6 cm Rod Pitch
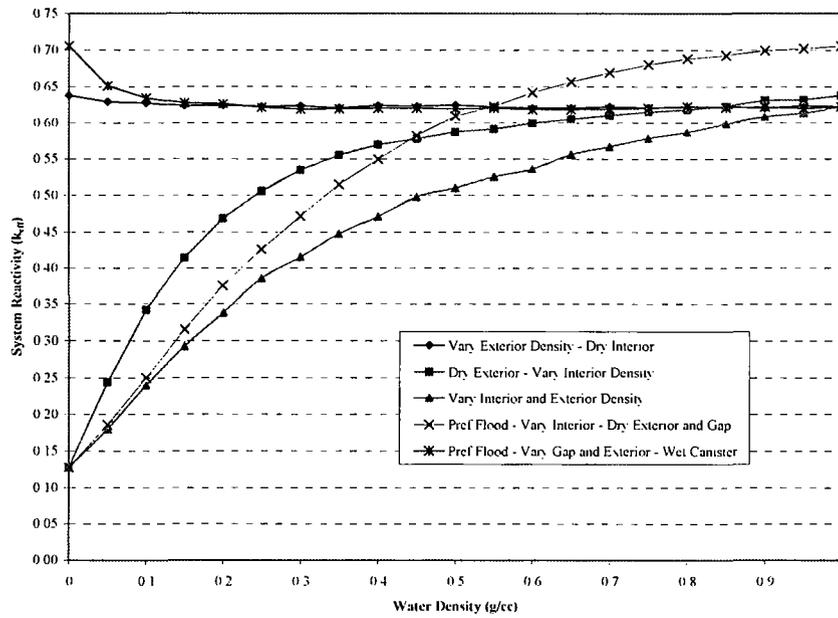
Figure 6.7.1-8   Moderator Density Study – PWR MOX ^{241}Pu Fuel Material –
3.6 cm Rod Pitch
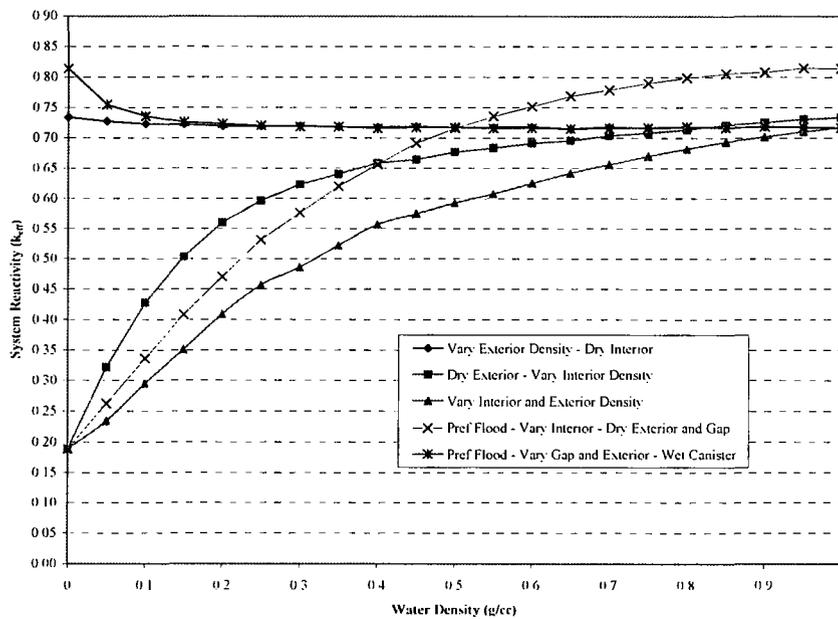
Table 6.7.1-3   PWR MOX Rod Shipment – Reactivity as a Function of Geometry and Material

Fuel Material	Rod Pitch	k_{eff}	σ	$k_{eff}+2\sigma$	vs. MS or P1 Composition	
					Δk_{eff}	$\Delta k_{eff}/\sigma$
UO$_2$	3.0	0.50837	0.00087	0.51011	-0.10728	-81.4
WG	3.0	0.61442	0.00106	0.61654	-0.00123	-0.8
FG	3.0	0.60516	0.00097	0.60710	-0.01049	-7.6
PG	3.0	0.59390	0.00104	0.59598	-0.02175	-15.1
MS	3.0	0.61565	0.00099	0.61763	--	--
FP	3.0	0.63359	0.00107	0.63573	-0.08132	-51.8
P9	3.0	0.62715	0.00111	0.62937	-0.08776	-54.9
P1	3.0	0.71491	0.00115	0.71721	--	--
UO$_2$	3.6	0.50911	0.00084	0.51079	-0.12688	-96.0
WG	3.6	0.63252	0.00098	0.63448	-0.00347	-2.5
FG	3.6	0.62282	0.00099	0.62480	-0.01317	-9.3
PG	3.6	0.61299	0.00105	0.61509	-0.02300	-15.7
MS	3.6	0.63599	0.00102	0.63803	--	--
FP	3.6	0.65225	0.00100	0.65425	-0.07909	-50.1
P9	3.6	0.64517	0.00107	0.64731	-0.08617	-53.1
P1	3.6	0.73134	0.00122	0.73378	--	--

Table 6.7.1-4   PWR MOX Fuel Shipment – Fuel Rod Pitch Study

Rod Pitch	Pitch Config	Fuel Material	k_{eff}	Fuel Material	k_{eff}	Fuel Material	k_{eff}
1.8	Hexagonal	UO_2	0.41843	MS	0.47357	^{241}Pu	0.55466
2.0	Hexagonal	UO_2	0.44262	MS	0.50841	^{241}Pu	0.59542
2.2	Hexagonal	UO_2	0.46448	MS	0.53761	^{241}Pu	0.63030
2.4	Hexagonal	UO_2	0.48147	MS	0.56403	^{241}Pu	0.65675
2.6	Hexagonal	UO_2	0.49260	MS	0.58626	^{241}Pu	0.68060
2.8	Hexagonal	UO_2	0.50325	MS	0.60145	^{241}Pu	0.70293
3.0	Hexagonal	UO_2	0.50837	MS	0.61565	^{241}Pu	0.71491
3.2	Hexagonal	UO_2	0.51224	MS	0.62593	^{241}Pu	0.72528
3.4	Hexagonal	UO_2	0.51156	MS	0.63376	^{241}Pu	0.72957
3.6	Hexagonal	UO_2	0.50911	MS	0.63599	^{241}Pu	0.73134
3.8	Hexagonal	UO_2	0.50464	MS	0.63360	^{241}Pu	0.73067
4.0	Hexagonal	UO_2	0.49718	MS	0.63359	^{241}Pu	0.73097
4.2	Hexagonal	UO_2	0.48894	MS	0.62789	^{241}Pu	0.72504
1.8	Square	UO_2	0.43146	MS	0.49220	^{241}Pu	0.57531
2.0	Square	UO_2	0.45613	MS	0.52574	^{241}Pu	0.61729
2.2	Square	UO_2	0.47678	MS	0.55687	^{241}Pu	0.64902
2.4	Square	UO_2	0.49150	MS	0.57989	^{241}Pu	0.67677
2.6	Square	UO_2	0.50343	MS	0.59949	^{241}Pu	0.69695
2.8	Square	UO_2	0.50669	MS	0.61768	^{241}Pu	0.71049
3.0	Square	UO_2	0.51090	MS	0.62688	^{241}Pu	0.72343
3.2	Square	UO_2	0.51089	MS	0.63415	^{241}Pu	0.73285
3.4	Square	UO_2	0.50965	MS	0.63544	^{241}Pu	0.73257
3.6	Square	UO_2	0.50429	MS	0.63440	^{241}Pu	0.73463
3.8	Square	UO_2	0.49939	MS	0.63658	^{241}Pu	0.72833
4.0	Square	UO_2	0.49120	MS	0.63003	^{241}Pu	0.72326
4.2	Square	UO_2	0.48232	MS	0.62576	^{241}Pu	0.71403

Table 6.7.1-5   PWR MOX Fuel Shipment – Optimum Moderator Study Maximum Reactivity Summary

Fuel Material	$k_{eff} + 2\sigma$
UO_2	0.55404
MOX Services	0.70523
^{241}Pu	0.81451

Table 6.7.1-6   PWR MOX Fuel Shipment Reactivity Summary for Single Cask
Containment Fully Reflected Cases

Fuel Mat'l	Rod Gap (g/cc)	Array (g/cc)	Cavity (g/cc)	Exterior (g/cc)	k_{eff}	σ	$k_{eff} + 2\sigma$
UO$_2$	0.0001	0.0001	0.0001	0.9982	0.03394	0.00018	0.03430
UO$_2$	0.9982	0.9982	0.9982	0.9982	0.49629	0.00085	0.49799
UO$_2$	0.9982	0.9982	0.0001	0.9982	0.43536	0.00091	0.43718
MS	0.0001	0.0001	0.0001	0.9982	0.04527	0.00028	0.04583
MS	0.9982	0.9982	0.9982	0.9982	0.61686	0.00100	0.61886
MS	0.9982	0.9982	0.0001	0.9982	0.58689	0.00102	0.58893
^{241}Pu	0.0001	0.0001	0.0001	0.9982	0.04895	0.00036	0.04967
^{241}Pu	0.9982	0.9982	0.9982	0.9982	0.71168	0.00115	0.71398
^{241}Pu	0.9982	0.9982	0.0001	0.9982	0.67957	0.00121	0.68199

Table 6.7.1-7   PWR MOX Fuel Shipment Reactivity Summary for Normal Condition
Array Cases

Fuel Mat'l	Rod Gap (g/cc)	Array (g/cc)	Cavity (g/cc)	Exterior (g/cc)	k_{eff}	σ	$k_{eff} + 2\sigma$
UO$_2$	0.0001	0.0001	0.0001	0.0001	0.03393	0.00016	0.03425
UO$_2$	0.9982	0.9982	0.9982	0.9982	0.49757	0.00089	0.49935
UO$_2$	0.9982	0.9982	0.9982	0.0001	0.49624	0.00092	0.49808
UO$_2$	0.9982	0.9982	0.0001	0.0001	0.43382	0.00087	0.43556
MS	0.0001	0.0001	0.0001	0.0001	0.04576	0.00025	0.04626
MS	0.9982	0.9982	0.9982	0.9982	0.61761	0.00101	0.61963
MS	0.9982	0.9982	0.9982	0.0001	0.61581	0.00102	0.61785
MS	0.9982	0.9982	0.0001	0.0001	0.58588	0.00099	0.58786
^{241}Pu	0.0001	0.0001	0.0001	0.0001	0.04905	0.00032	0.04969
^{241}Pu	0.9982	0.9982	0.9982	0.9982	0.71149	0.00112	0.71373
^{241}Pu	0.9982	0.9982	0.9982	0.0001	0.71256	0.0012	0.71496
^{241}Pu	0.9982	0.9982	0.0001	0.0001	0.68189	0.00118	0.68425

Table 6.7.1-8   PWR MOX Fuel Shipments – Summary of Maximum Reactivity
Configurations

Fuel Material	Result	Accident Array – Preferentially Flooded	Normal Array – Preferentially Flooded	Normal Array – Dry	Single Cask Fully (Water) Reflected
UO$_2$	$k_{eff} + 2\sigma$	0.55404	0.49808	0.03425	0.49799
	EALCF (eV)	9.79E-02	8.83E-02	2.95E+05	8.81E-02
MS	$k_{eff} + 2\sigma$	0.70523	0.61963	0.04626	0.61886
	EALCF (eV)	1.25E-01	1.17E-01	2.14E+05	1.17E-01
^{241}Pu	$k_{eff} + 2\sigma$	0.81386	0.71496	0.04969	0.71398
	EALCF (eV)	1.33E-01	1.21E-01	8.72E+04	1.22E-01

Table 6.7.1-9   PWR MOX Fuel Shipments – PWR MOX Comparison to Area of
Applicability

Parameter	Min	Max	MOX Services Materials	^{241}Pu Materials
EALCF (eV)	8.10E-02	8.99E-01	0.13	0.13
^{235}U/^{238}U Weight Ratio	1.58E-03	1.51E+00	7.05E-03	7.05E-03
^{238}Pu/^{238}U Weight Ratio	1.88E-06	1.54E-04	4.17E-05	0.0
^{239}Pu/ ^{238}U Weight Ratio	1.39E-02	7.77E-01	7.92E-02	0.0
^{240}Pu/^{238}U Weight Ratio	1.20E-03	8.48E-02	3.75E-03	0.0
^{241}Pu /^{238}U Weight Ratio	7.90E-05	7.59E-03	3.34E-04	7.94E-02
^{242} Pu /^{238}U Weight Ratio	4.63E-06	6.38E-04	4.17E-05	0.0
Water to Fuel Volume Ratio	1.10E+00	2.07E+01	1.43E+01	

Table 6.7.1-10   PWR MOX Fuel Shipments – UO₂ Comparison to Area of Applicability

Parameter	Min	Max	UO₂ Case
Enrichment (wt % ^{235}U)	2.35	4.738	5.0
Fuel rod pitch (cm)	1.3	2.54	3.0
Fuel pellet outer diameter (cm)	0.79	1.265	0.85/0.96
Fuel rod diameter (cm)	0.94	1.4172	0.93/1.12

Parameter	Min	Max	UO₂ Case
H/^{235}U atom ratio	106.2	403.9	627 to 2140[1]
EALCF (eV)	0.09781	0.3447	0.0874

Table 6.7.1-11   Bounding Parameters for PWR MOX/UO₂ Rod Shipments

Parameter	Value
Fuel Form	Clad UO₂ or MOX rod
Number of Rods	16[2]
Clad Material	Zirconium Alloy
UO₂ Rods – Max. Enrichment (wt % ^{235}U)	5
MOX Rods – Max. Fissile Pu Content (wt %)	7[3]
Maximum Heavy Metal Content Per Rod (kg)	2.60
Maximum Pellet Diameter (inch)	0.3765
Maximum Active Fuel Length (inch)	153.5

---

[1] Dependent on pitch configuration (square or hexagonal).

[2] Mixture of UO₂ and MOX rods is permitted.

[3] Sum of ^{239}Pu and ^{241}Pu.

Table 6.7.1-12   B&W, CE and Westinghouse PWR Fuel Assembly Data

Fuel Type/ Parameter	B&W 15×15 Mark B4	B&W 17×17 Mark C	CE 14×14	CE 16×16 SYS 80	WE 14×14 Std	WE 14×14 OFA	WE 15×15	WE 17×17	WE 17×17 OFA
Fuel Rod Data									
Rod Dia. (in)	0.43	0.379	0.44	0.382	0.422	0.4	0.422	0.374	0.36
Clad Thick. (in)	0.0265	0.024	0.028	0.025	0.0225	0.0243	0.0242	0.0225	0.0225
Clad Mat.	Zirc	Zirc	Zirc	Zirc	Zirc	Zirc	Zirc	Zirc	Zirc
Pellet Dia. (in)	0.3686	0.3232	0.3765	0.325	0.3674	0.3444	0.3659	0.3225	0.3088
Act. Length (in)	144	143	137	150	145.2	144	144	144	144

Table 6.7.1-13   Exxon/ANF PWR Fuel Assembly Data

Fuel Type/ Parameter	WE Ex/ANF 14×14	WE Ex/ANF 15×15	WE Ex/ANF 17×17	CE Ex/ANF 14×14
Fuel Rod Data				
# Rods	179	204	264	176
Pin Pitch (in)	0.556	0.563	0.496	0.58
Rod Dia. (in)	0.424	0.424	0.36	0.44
Clad Thick. (in)	0.03	0.03	0.025	0.031
Clad Mat.	Zirc	Zirc	Zirc	Zirc
Pellet Dia. (in)	0.3505	0.3565	0.303	0.37
Act. Length (in)	142	144	144	134

6.7.2   SLOWPOKE Fuel Rods

This section includes input, analysis method, results, and criticality benchmark evaluations for the NAC-LWT cask containing a payload of up to 800 SLOWPOKE rods. SLOWPOKE rods contain highly enriched uranium in an aluminum matrix material.

6.7.2.1   Package Fuel Loading

The NAC-LWT cask may transport up to 800 undamaged or its equivalent in damaged fuel rods in fuel canisters. The canisters are screened to prevent the release of gross particulate (note that based on the aluminum metal fuel material no significant release of fuel material from the rods is expected even under severe clad damage conditions). Characteristics of the design basis SLOWPOKE rods are presented in Table 6.7.2-1. Bounding characteristics applied to the model are listed in Table 6.7.2-2. The two characteristics most controlling in system reactivity are increased enrichment and ^{235}U mass per rod. This provides maximum fissile material mass while reducing parasitic absorption in ^{238}U.

6.7.2.2   Criticality Model Specifications

This section describes the models that are used in the criticality analyses for the NAC-LWT cask containing up to 800 SLOWPOKE rods. The models are analyzed separately under normal conditions and hypothetical accident conditions to ensure that all possible configurations are subcritical.

Each model uses the MCNP5 code package with the ENDF/B-VI cross-section set. No cross-section pre-processing is required prior to MCNP implementation. MCNP uses the Monte Carlo technique to calculate the k_{eff} of a system.

Description of Calculational Models

The base MCNP model of the NAC-LWT cask for the analysis of the SLOWPOKE payload is built based on the canister containing an axial stack of four canister inserts each containing a 5x5 fuel tube array (100 rods per canister). The canister is placed into the outer four openings of the NAC-LWT MTR-28 basket configuration. Only the top two baskets are loaded with the bottom two baskets acting as spacers. This allows the loading of up to 800 SLOWPOKE rods (or the equivalent material). Only the 5x5 array is evaluated. The 4x4 array, while allowing increased moderation, removes 36% of the fissile material from the system and will therefore be substantially less reactive. The SLOWPOKE fuel rod is depicted in Figure 6.7.2-1. The fuel rods, cask cavity, and radial shields are explicitly modeled as shown in Figure 6.7.2-2 model sketch.

The model of the NAC-LWT cask takes advantage of the universe structure of MCNP. Each universe defines an infinite space, bounded after its insertion into a containing cell. Four universes are employed herein. The "0" universe defines the cask universe. The remaining universes are discussed in the following sections. Each universe is developed independently as surfaces and cells. The canister interior material is defined separately from the cask cavity material to allow preferential flooding to be evaluated (i.e., different density water in the cask and canister cavity). This option is also exercised when modeling damaged fuel in which the distinct fuel rods are replaced and the canister cavity filled by a homogenized water/fuel mixture.

The modeled accident condition completely removes the neutron shielding, the neutron shield tank, and the cask impact limiters. In the normal conditions model, the impact limiter diameter is modeled as identical to the neutron shield tank diameter. This allows for closer packing for the cask array than physically possible.

VISED sketches of the assembled geometry are shown in Figure 6.7.2-3 through Figure 6.7.2-4. The cask outer surface is surrounded by a cylindrical body with the option of applying reflecting boundary conditions. The reflecting boundary conditions are imposed on the sides, top and bottom, which simulates an infinite array of casks. For single cask analysis (10 CFR 71.55), the cask is surrounded by 20 cm of water to apply full water reflection.

Package Regional Densities

The composition densities (g/cc) and nuclide number densities (atm/b-cm) used in the subsequent criticality analyses are shown in Table 6.7.2-3.

Figure 6.7.2-1   SLOWPOKE Fuel Element
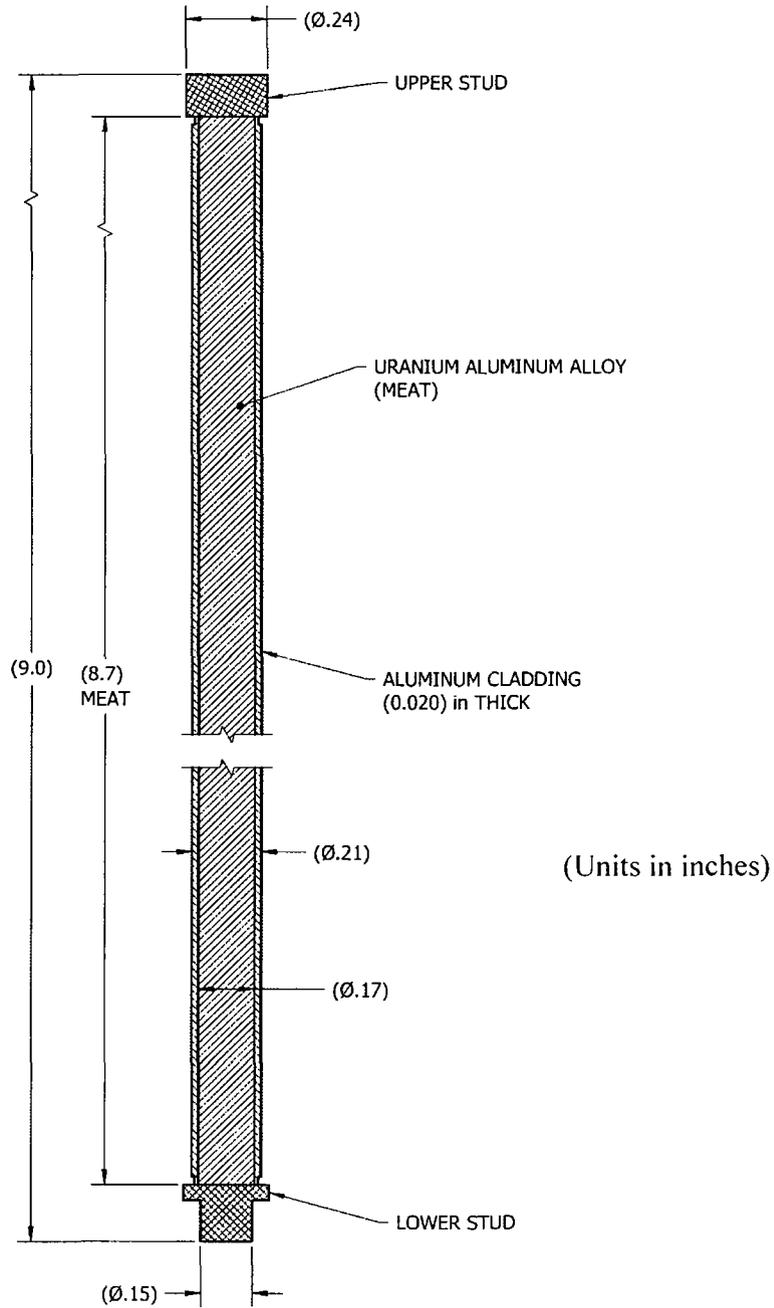
(Units in inches)

Figure 6.7.2-2   MCNP Model Sketch of the NAC-LWT Cask with SLOWPOKE Fuel
Rods

(Dimensions in inches)
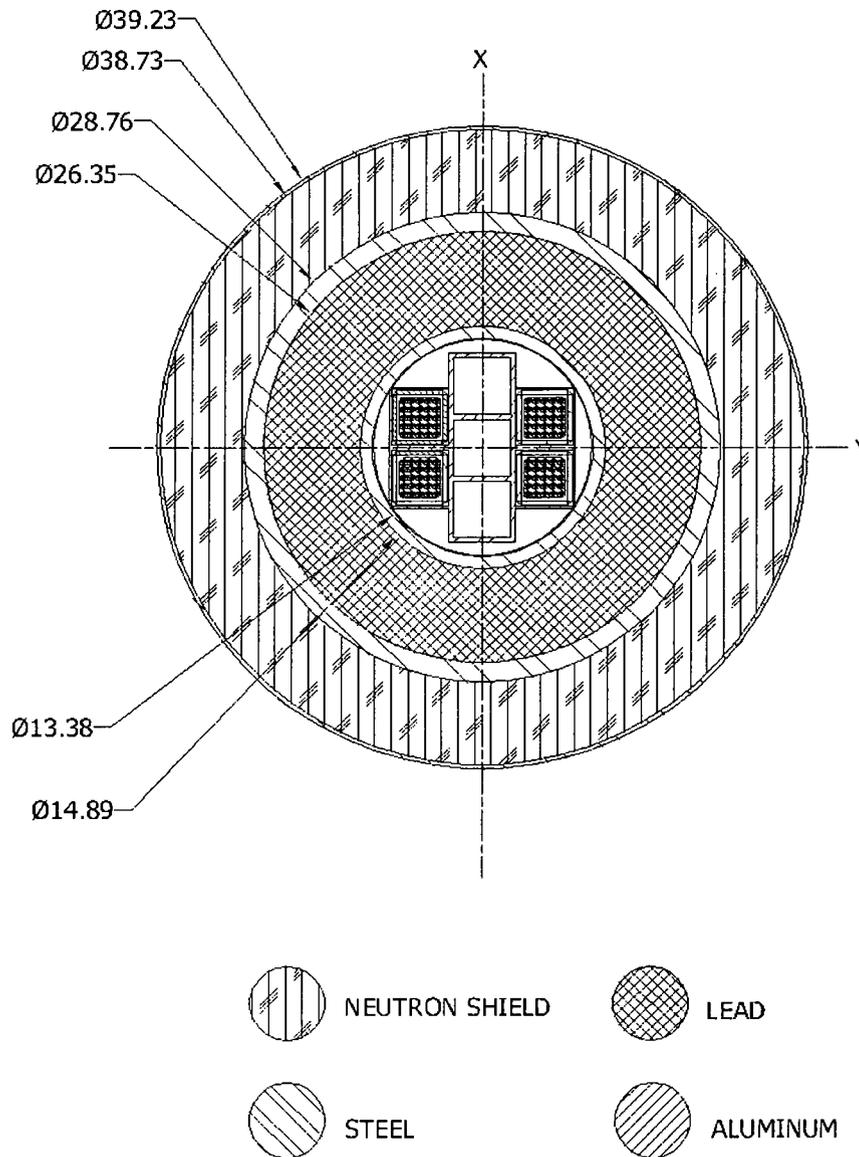
Figure 6.7.2-3   VISED Sketch of LWT Radial View – Undamaged Fuel
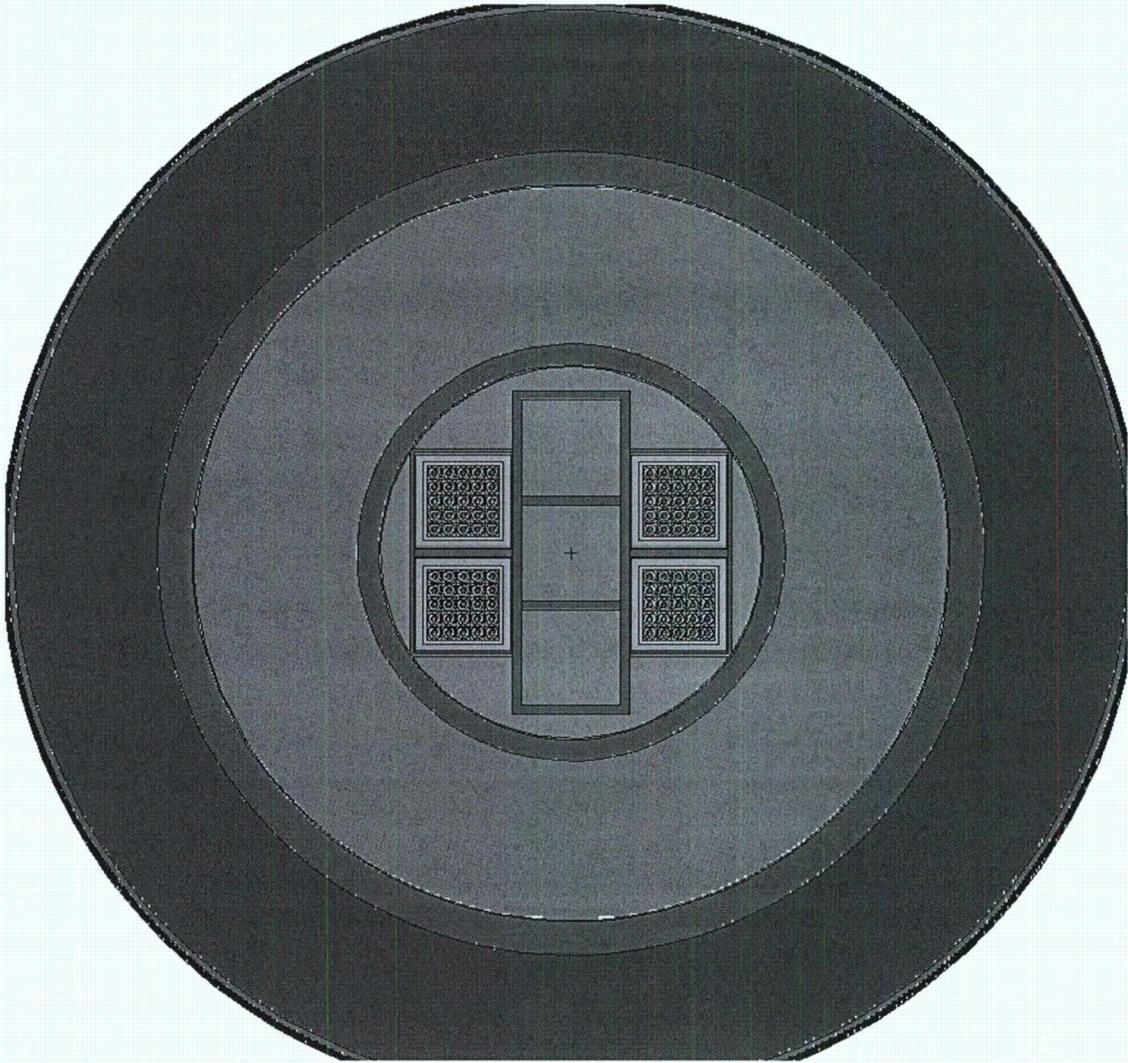
Figure 6.7.2-4   VISED Sketch of LWT Axial View – Undamaged Fuel – Normal Conditions
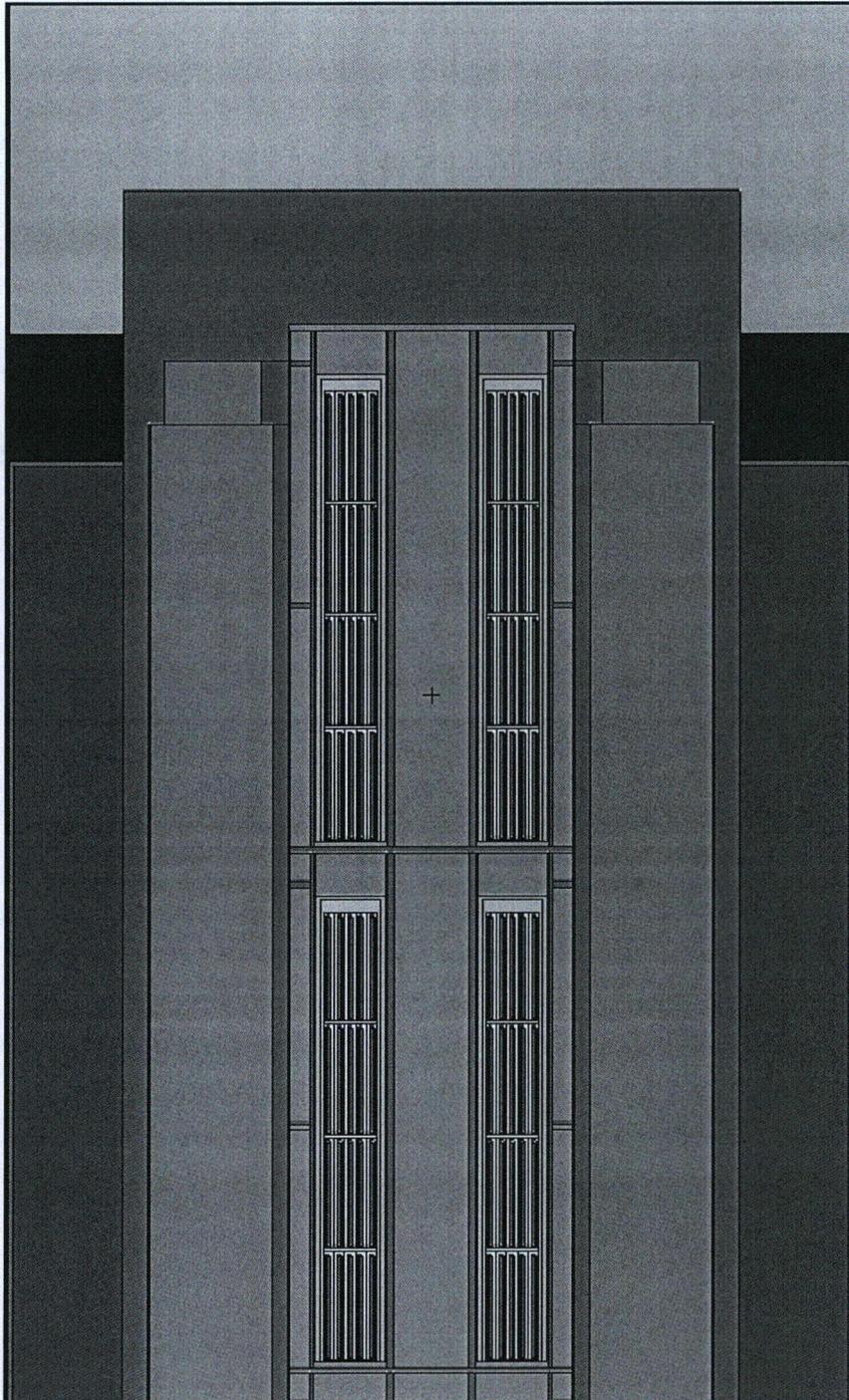
Note: Model extent shown is limited to loaded baskets. All four baskets modeled.

Table 6.7.2-1   SLOWPOKE Fuel Configuration

Parameter	Value
Fuel Matrix	U-Al Alloy
Clad Material	Al
Clad Thickness, cm	0.051
Fuel Thickness or Diameter, cm	0.422
Rod Length, cm	22.83
Active Fuel Length, cm	22.0
U-235 Enrichment, %	93
U-235 per Rod, g	2.79
U per Rod, g	2.99
Aluminum per Rod (Fuel), g	7.688
Total weight of Fuel per Rod, g	10.678
Rod End Cap Diameter, cm	0.61

Table 6.7.2-2   Modeled SLOWPOKE Fuel Configuration

Parameter	Value
U-235 Enrichment, %	95
U-235 per Rod, g	2.800
U per Rod, g	2.947
Aluminum per Rod (Fuel), g	7.688
Total Weight of Fuel per Rod, g	10.635
Active Fuel Length, cm	22.0
Fuel Thickness or Diameter, cm	0.422
Active Fuel Volume, cc	3.077
Rod Length, cm	22.83
Clad Thickness, cm	0.051
Clad Diameter, cm	0.5240
Rod End Cap Diameter, cm	0.61
Rod End Cap Height, cm	0.4150
Fuel Meat Density, g/cc (calculated)	3.457

Table 6.7.2-3   SLOWPOKE Analysis Compositions and Number Densities

Material	U-Al	H₂O	304 Stainless Steel	Pb	Al
Density, g/cc	3.457	0.9982	7.920	11.344	2.702
Density	atoms/b-cm				
Uranium-235	2.34E-03				
Uranium-238	1.14E-04				
Oxygen		3.338E-2			
Hydrogen		6.677E-2			
Zirconium Alloy					
Iron			5.936E-2		
Chromium			1.743E-2		
Nickel			7.721E-3		
Manganese			1.736E-3		
Lead				3.297E-2	
Aluminum	5.58E-02				6.031E-2

6.7.2.3   Criticality Calculations

The maximum reactivity configuration is determined by performing a series of studies. Based on preliminary calculations and results of other MTR basket payloads, it is initially assumed that accident conditions with close pitch and flooding of the canister interior provide the maximum reactivity configuration. Close pitch (surface reflected) models an infinite array of casks with void (no moderation/absorption) between cask surfaces. Other options for reflection include a cask separation of 40 cm (20 cm reflective surface from cask boundary) or no reflection modeled (single cask with 20-cm boundary at cask exterior conditions). Results of a preliminary study of reactivity versus flooding / configuration are shown in Table 6.7.2-4. A reflective condition of "none" and "wet" cask exterior conditions models a single cask that is fully water reflected. The cask condition of canister interior flooded with dry cask interior and exterior models a hypothetical preferential flooding configuration. The reactivity (k_{eff} + 2σ) of undamaged fuel is maximized for the preferential flooded configuration at a value of 0.5159 as seen in Table 6.7.2-4.

The maximum reactivity geometry and moderation studies will be based on the maximum reactivity preliminary case:

- Cask accident conditions
- Close pitch (cask surface reflected)
- Canister flooded, cask interior and exterior dry (preferential flooding)
- Nominal tolerances and no geometry perturbations
- Undamaged fuel

6.7.2.3.1   Geometric Perturbation Study

To observe potential geometry perturbations, the reactivity changes due to fuel and canister shifts were calculated. The base configuration was applied for the perturbation study. The fuel rods were shifted inside their individual tubes towards or away from the center of the 5x5 tube array. The canisters were also shifted towards or away from the center of the MTR-28 basket module. The reactivity results are shown in Table 6.7.2-5. The fuel shifted away from the center of the 5x5 array and canisters shifted toward the center produced a statistical increase (defined as $\Delta k_{eff}/\sigma > 3$). The more reactive outward fuel shift is due to the 5x5 array being under-moderated as is discussed in later sections. The more reactive inward canister shift allows for more neutron interaction between 5x5 arrays (other canisters).

6.7.2.3.2   Material Tolerance Study

The primary purpose of the material tolerance study is to observe the absorption/scatter effects of materials. It is expected that the aluminum of the canister will have no significant effect on the reactivity. The tolerance for the steel plates in the basket has a range from a low negative and to a

large positive. Parasitic absorption for stainless steel is expected to reduce system reactivity at the plus tolerances. The low negative tolerances are expected to have no significant effect. To observe potential tolerance effects in the basket and canister, the densities of the basket and canister materials were modified. A -5% and +25% density changes reflect potential tolerance thickness effects in the basket components. Density changes of ±50% for the aluminum canister are assumed. The reactivity results are shown in Table 6.7.2-6. The -5% density reduction for the toleranced basket produces a statistically negligible effect on reactivity. The increase in modeled steel density (equivalent to plate thickness increase) significantly reduces reactivity. The aluminum canister material variations have no statistical effect on the reactivity results.

6.7.2.3.3   Moderator Density Study (Including Preferential Flooding)

A moderator density study was performed to determine the moderator conditions that result in the most reactive system. The base configuration was changed from close pitch (surface reflected) to a 20-cm reflection surface to observe the variable exterior moderator conditions. Included in the moderator density study is preferential flooding. Preferential flooding includes the hypothetical flooding of the canister, interior, or exterior simultaneously.

The canister interior flooded condition with void in the cask exterior and interior remained the bounding condition (as was assumed in the base configuration). This condition allows moderation within the tube arrays and neutronic coupling of the canisters and casks. The results are tabulated in Table 6.7.2-7 and plotted in Figure 6.7.2-5.

6.7.2.3.4   Maximum Reactivity Configuration for Undamaged Fuel

Based on the previous analyses, the following conditions are bounding for the maximum reactivity configuration:

- Accident conditions
- Close pitch (surface reflected)
- Canister flooded, interior and exterior dry
- Canister shifted toward the center of basket
- Fuel shifted away from the center of 5x5 array

Toleranced components were not included as the reactivity effects were statistically negligible.

6.7.2.3.5   Undamaged Fuel Case Matrix to Conform to 10 CFR 71.55 and 10 CFR 71.59 Requirements

Compliance with the NRC Code of Federal Regulations (CFRs) for the transport of fissile material packages is evaluated. 10 CFR 71.55 general requirements are satisfied by evaluating the following configurations for both normal and accident conditions:

- Single Cask (no MCNP modeled reflective surfaces)

- Close full reflection of the containment system by water on all sides (cask exterior flooded up to 20 cm boundary, fully water reflected)

- Most reactive credible configuration:
  - o Canister shifted toward the center of basket
  - o Fuel shifted away from the center of 5x5 array
  - o Canister interior flooded, cask interior dry

10 CFR 71.59 standards are satisfied by evaluating the maximum reactivity configuration for both normal and accident conditions for an infinite array of casks at close pitch. These requirements are satisfied by modifying the cask and cask exterior configuration of the maximum reactivity configuration established by the preceding studies. Satisfying 10 CFR 71.59 under an infinite array allows the CSI designation of 0 for the transport package. Both CFR requirements are satisfied and transport of the undamaged fuel is acceptable. The results for the configurations stipulated in the CFR requirements are shown in Table 6.7.2-8 for undamaged fuel. The maximum reactivity configuration produced a reactivity of 0.5222. Satisfying 10 CFR 71.59 under an infinite array allows the CSI designation of 0 for the transport package.

6.7.2.3.6   Damaged Fuel Case Matrix to Conform to 10 CFR 71.55 and 10 CFR 71.59 Requirements

In addition to undamaged fuel, the canister is designed to contain gross fuel material from damaged fuel. The undamaged fuel analysis demonstrated that a significantly higher reactivity is obtained from a dry cask cavity, flooded canister interior, configuration as this configuration allows neutronic interaction between the basket locations (which is reduced by the approximately 3.5 inches of water between the two sets of two canisters), between baskets, and between casks in the infinite array. This configuration is therefore adopted for the damaged fuel analysis. Also adopted is the shifted in-canister configuration which minimizes distance between fissile material components. As fuel rods are replaced by a water/fuel mixture the fuel rod shift configuration is not applicable to damaged fuel. A fuel/water mixture is analyzed for compliance with 10 CFR 71.55 and 10 CFR 71.59. The results are shown in Table 6.7.2-9. The damaged fuel resulted in a maximum reactivity increase of approximately 10% from 0.5222 to 0.5706. Both CFR requirements are satisfied and transport of the damaged fuel is acceptable. As an infinite cask array is evaluated the CSI for damaged fuel is 0.

The maximum reactivity EALCF of 0.08eV is within the area of applicability of the research reactor benchmark. The enrichment of the maximum reactivity case is slightly above the benchmark at 95 wt% versus 93.2 wt% in the critical set. The USL of 0.9171 (per Section 6.5.5) is determined

using the range of applicability for the EALCF. If the enrichment range of applicability for the USL determination was increased from 93.2wt% to 95wt%, the expected USL decrease determined by applying the enrichment trend functions would be from 0.9280 to 0.9279. The applied USL of 0.9171 based on the EALCF bounds this limit and is therefore acceptable.

Figure 6.7.2-5   SLOWPOKE Moderator Density Study (Percent Full Density Water)
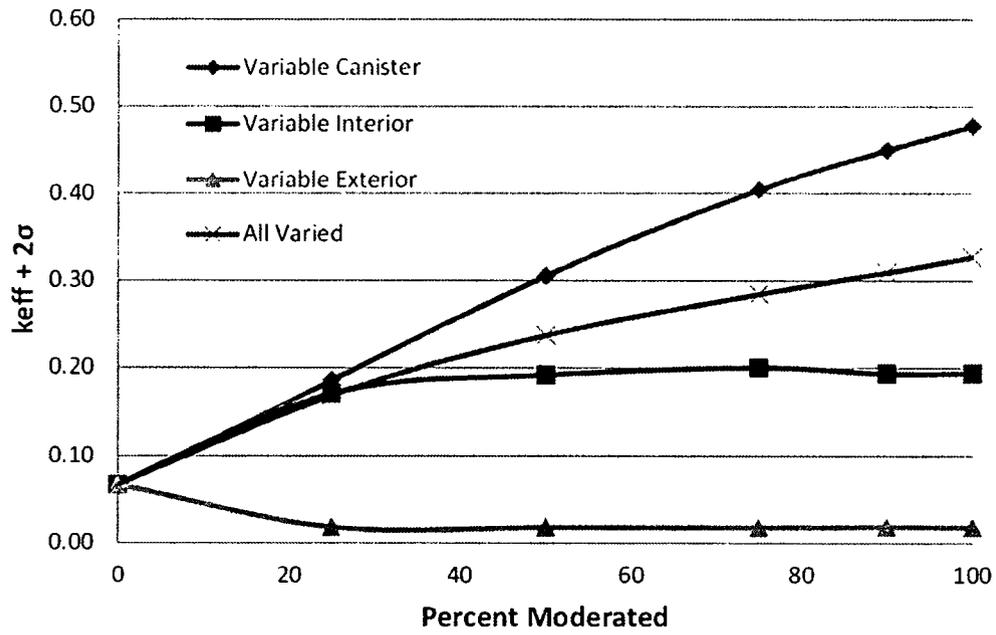
Table 6.7.2-4   Preliminary Reactivity Results for Undamaged SLOWPOKE Fuel

Condition	1	2	3	4
Canister Interior	Wet	Wet	Wet	Wet
Cask Interior	Wet	Dry	Dry	Dry
Cask Exterior	N/A	N/A	Dry	Wet
Reflected	Surface	Surface	20cm	None
k_{eff}+2σ	0.3502	0.5159	0.4774	0.3482

Table 6.7.2-5   SLOWPOKE Component Shift Reactivity Study Results

Parameter		k_{eff}	σ	k_{eff}+2σ	Δk_{eff}	$\Delta k_{eff}/\sigma$
Fuel	None	0.5146	0.0007	0.5159	--	--
Shift	In	0.5041	0.0007	0.5055	-0.0104	-11.1
	Out	0.5181	0.0006	0.5193	0.0034	3.8
Can	None	0.5146	0.0007	0.5159	--	--
Shift	In	0.5173	0.0007	0.5186	0.0028	3.0
	Out	0.5122	0.0006	0.5135	-0.0024	-2.7

Table 6.7.2-6   SLOWPOKE Component Tolerance Reactivity Study Results

Parameter	Δ%	k_{eff}	σ	k_{eff}+2σ	Δk_{eff}	$\Delta k_{eff}/\sigma$
Basket Tolerance	0%	0.5146	0.0007	0.5159	--	--
	-5%	0.5159	0.0006	0.5171	0.0013	1.37
	+25%	0.5078	0.0006	0.5091	-0.0068	-7.39
Canister Shell Tolerance	0%	0.5146	0.0007	0.5159	--	--
	-50%	0.5128	0.0006	0.5141	-0.0018	-2.00
	50%	0.5141	0.0006	0.5154	-0.0005	-0.53

Table 6.7.2-7   SLOWPOKE Moderator Density Study

Percent Moderated			Density [g/cc]	k_{eff}	σ	$k_{eff} + 2\sigma$
Canister Interior	Cask Interior	Cask Exterior				
0	0	0	0.00	0.0657	0.0004	0.0666
25	0	0	0.25	0.1837	0.0011	0.1859
50	0	0	0.50	0.3031	0.0010	0.3051
75	0	0	0.75	0.4030	0.0006	0.4041
90	0	0	0.90	0.4486	0.0006	0.4498
100	0	0	0.9982	0.4762	0.0006	0.4774
0	0	0	0.00	0.0657	0.0004	0.0666
0	25	0	0.25	0.1683	0.0016	0.1714
0	50	0	0.50	0.1884	0.0019	0.1921
0	75	0	0.75	0.1969	0.0018	0.2004
0	90	0	0.90	0.1898	0.0019	0.1936
0	100	0	0.9982	0.1903	0.0019	0.1940
0	0	0	0.00	0.0657	0.0004	0.0666
0	0	25	0.25	0.0177	0.0002	0.0182
0	0	50	0.50	0.0175	0.0002	0.0179
0	0	75	0.75	0.0175	0.0002	0.0179
0	0	90	0.90	0.0179	0.0003	0.0184
0	0	100	0.9982	0.0176	0.0003	0.0181
0	0	0	0.00	0.0657	0.0004	0.0666
25	25	25	0.25	0.1667	0.0012	0.1691
50	50	50	0.50	0.2345	0.0012	0.2369
75	75	75	0.75	0.2835	0.0005	0.2846
90	90	90	0.90	0.3079	0.0006	0.3091
100	100	100	0.9982	0.3250	0.0006	0.3262
100	100	0	0.9982	0.3418	0.0006	0.3430
100	0	100	0.9982	0.3485	0.0006	0.3498
0	100	100	0.9982	0.1741	0.0015	0.1771

Table 6.7.2-8   SLOWPOKE Undamaged Fuel Maximum Reactivity Results

Parameter		Cask	Pitch	Moderator			Shift		Toleranced		Reactivity Results		
				Canister	Interior	Exterior	Can	Fuel	Basket	Canister	k_{eff}	σ	$k_{eff}+2\sigma$
CFR 71.59	Accident	Acc	Close	Wet	Dry	Dry	In	Out	No	No	0.5209	0.0006	0.5222
	Normal	Nrm	Close	Wet	Dry	Dry	In	Out	No	No	0.3559	0.0006	0.3571
CFR 71.55	Accident	Acc	Single	Wet	Dry	Wet	In	Out	No	No	0.3529	0.0006	0.3542
	Normal	Nrm	Single	Wet	Dry	Wet	In	Out	No	No	0.3529	0.0006	0.3541

Table 6.7.2-9   SLOWPOKE Damaged Fuel Maximum Reactivity Results

Parameter		Cask	Pitch	Moderator			Shift		Toleranced		Reactivity Results		
				Canister	Interior	Exterior	Can	Fuel	Basket	Canister	k_{eff}	σ	$k_{eff}+2\sigma$
CFR 71.59	Accident	Acc	Close	Wet	Dry	Dry	In	N/A	No	No	0.5694	0.0006	0.5706
	Normal	Nrm	Close	Wet	Dry	Dry	In	N/A	No	No	0.3832	0.0005	0.3842
CFR 71.55	Accident	Acc	Single	Wet	Dry	Wet	In	N/A	No	No	0.3803	0.0006	0.3814
	Normal	Nrm	Single	Wet	Dry	Wet	In	N/A	No	No	0.3807	0.0006	0.3818

6.7.3   NRU and NRX Fuel Assemblies

This section includes input, analysis method, results, and criticality benchmark evaluations for the NAC-LWT cask containing a payload of up to 18 NRU or NRX fuel assemblies. NRU assemblies are built with either highly enriched uranium (HEU) or low enriched uranium (LEU) rods and NRX assemblies contain all highly enriched uranium rods. The uranium fuel meat is composed of an aluminum matrix material.

6.7.3.1   Package Fuel Loading

Up to eighteen NRU or NRX fuel assemblies may be loaded into the NAC-LWT. NRU and NRX rods may be loaded as either loose rods or fuel assemblies. NRU and NRX fuel rods are aluminum clad uranium-aluminum alloy with aluminum end plugs. The NRX fuel assemblies are analyzed at 94 wt% ^{235}U. The NRU fuel is analyzed at 94 and 21 wt% ^{235}U. The NRU assemblies are made up of 12 rods while the NRX assemblies contain 7 rods. NRU and NRX fuel rods contain fins attached to the rod clad. NRU assemblies also contain five spacer disks assuring the rods retain their in-core configurations. Both NRU and NRX assemblies are encased in an aluminum flow tube during in-core operations but NRU assemblies will have their flow tube removed before loading. NRU and NRX fuel assemblies may be cropped before loading into the NAC-LWT. NRX fuel assemblies/rods must be placed into a caddy. NRU fuel assemblies/rods may be placed into a caddy. The caddy has been structurally evaluated to retain its shape through all transport conditions.

Up to 18 NRU or NRX undamaged fuel assemblies may be loaded into the NAC-LWT. Undamaged fuel may include loose fuel rods as the assemblies will be cropped and may have the flow tube removed before loading in the NAC-LWT. Undamaged fuel includes rods with clad damage, provided structural integrity is maintained. Although the aluminum based fuel rods are expected to survive all transport conditions and are not subject to fuel debris formation, such as oxide pellets would be, a damaged fuel composition of fractured rod segments is evaluated.

NRU/NRX fuel rod and assembly characteristics are summarized in Table 6.7.3-1. A sketch of a NRU fuel assembly is shown in Figure 6.7.3-1 and a NRX fuel assembly is shown in Figure 6.7.3-2.

6.7.3.2   Criticality Model Specifications

This section describes the models that are used in the criticality analyses for the NAC-LWT cask containing up to 18 NRU or NRX fuel assemblies. The models are analyzed separately under normal conditions and hypothetical accident conditions to ensure that all possible configurations are subcritical.

Each model uses the MCNP5 (Version 1.60) code package with the ENDF/B-VI cross-section set. No cross-section pre-processing is required prior to MCNP implementation. MCNP uses the Monte Carlo technique to calculate the k_{eff} of a system.

Description of Calculational Models

NRU and NRX fuel are modeled in the NAC-LWT. Fuel parameters in Table 6.7.3-2 are employed for the evaluations of HEU and LEU types and are based on the data presented in Table 6.7.3-1. As the fuel will be cropped before loading the end fittings are not modeled in the evaluation.

Evaluations are performed for fuel at in-core conditions, loose fuel rods, and fractured rod sections (broken rods). The NAC-LWT has potential for significant neutron interaction when placed into an array configuration, while assuming a loss of the neutron shield. To eliminate this interaction all models, except the 10 CFR 71.59 normal condition array, employ a single cask, fully water reflected boundary. Normal condition analyses model the cask with the liquid neutron shield in place, while accident conditions remove the neutron shield and the neutron shield shell from the model. Accident conditions also remove the aluminum honeycomb impact limiters from the model. The NAC-LWT neutron shield contains soluble boron. Modeled neutron shield material, as listed in Table 6.7.3-4, does not include boron (removing a neutron absorber). For fully water-reflected single cask models, this produces similar reactivities (see Table 6.7.3-6) as radial cask model neutronic differences are limited to reflection by the ethyl glycol / water mixture and thin neutron shield shell versus reflection by water. The basket and cask models constructed for the NRU/NRX assemblies evaluations are based on the dimensions listed in Table 6.7.3-3. The caddy in the NRX model restricts component movement.

NRU and NRX rod sketches, including the radial fins attached to the clad, are illustrated in Figure 6.7.3-3 and Figure 6.7.3-4. The end plug contains a small section inserted into the fuel region. This region was modeled as fuel meat instead of an end plug. The minor quantity of additional fuel will not affect the conclusions of this analysis.

Figure 6.7.3-5 is a VISED cross-section of three basic configurations of NRU fuel evaluated. For the NRU fuel, these configurations are (a) fuel rods at a pitch identical to that of the rods during in-core configuration. The second configuration (b) represents the fuel with a maximum, most reactive pitch. The third configuration (c) represents a hypothetical condition where the rods are modeled as rod segments. Figure 6.7.3-6 is a VISED cross-section of three basic configurations of NRX fuel evaluated. For the NRX fuel, these configurations are (a) fuel rods at a pitch identical to that of the rods during in-core configuration; this includes the flow tube and fuel caddy. The second configuration (b) represents the fuel with a maximum, most reactive pitch. To achieve this pitch the flow tube is removed. The third configuration (c) represents a

hypothetical condition where the rods are modeled as rod segments. NRX models include the caddy.

The NRU/NRX fuel is placed into an 18-tube basket in the NAC-LWT. A bottom spacer is used to shift the NRU/NRX basket up in the NAC-LWT. A cross-section of the NRU/NRX basket loaded in the NAC-LWT is shown in Figure 6.7.3-7.

A radial sketch of the basket cross-section in the NAC-LWT is shown in Figure 6.7.3-8.

This model neglects the impact limiters and models the cask under accident conditions with the neutron shield voided.

Package Regional Densities

The composition densities (gm/cc) and nuclide number densities (atm/b-cm) evaluated in subsequent criticality analyses are shown in Table 6.7.3-4. Displayed are the NRU HEU, NRU LEU, and NRX HEU material densities for the fuel assemblies.

6.7.3.3   Criticality Calculations

This section presents the criticality analyses for the NAC-LWT cask with NRU and NRX fuel assemblies. Criticality analyses are performed to satisfy the criticality safety requirements of 10 CFR Parts 71.55 and 71.59, as well as IAEA TS-R-1. All criticality evaluations performed use a single cask model. An analysis of the NAC-LWT with each of the basket loadings shows that NRX and NRU fuel remain below the USL even when they are considered damaged (rod sections). The payload is most reactive under the following model characteristics.

- Maximum OD basket tubes and caddy (NRX only)
- Minimum basket tube and caddy (NRX only) thickness
- Flooded cask cavity and exterior
- Loss of neutron shield

A single cask containment water reflected evaluation is also performed to comply with 10 CFR 71.55(b)(3). The analyses demonstrate that, including all calculation and mechanical uncertainties, the NAC-LWT remains subcritical under normal and accident conditions.

6.7.3.4   NRU/NRX HEU Assembly (Undamaged Configuration)

An undamaged NRU or NRX fuel assembly is placed in each of the 18 tubes in the NRU/NRX basket assembly. Optimum moderator studies for the package are shown in Figure 6.7.3-10 for NRU fuel and Figure 6.7.3-11 for NRX fuel. The studies show that the tube moderator significantly influences system reactivity with cask interior density having a smaller effect on reactivity. The most reactive configuration for both fuel types is a system where the tube is fully flooded at maximum density water while the cask cavity is dry.

The next stage of analysis varies the fuel rod pitch. NRU fuel contains five axial rod spacer disks (disks containing openings for each rod) which prevent rod movement. For conservatism the disks are not credited in the prevention of rod movement. NRX fuel rods are located in a flow tube which fits tightly around the array and in conjunction with the fins attached to the clad to prevent rod movement. For conservatism, the flow tube is removed from the model. Results of the rod spacing studies are shown in Figure 6.7.3-12 for NRU fuel and Figure 6.7.3-13 for NRX fuel. The results from the models presented in Figures 6.7.3-5 and 6.7.3-6 are shown in Figures 6.7.3-12 and 6.7.3-13, respectively. The model figures are annotated to indicate outer ring fuel locations for NRU and NRX fuel and inner rod locations for the NRU fuel. In the context of the result figures, "nominal" refers to the "as-built/in-core" location of the rods. Maximum outer rod location indicates shift of the outer rods away from the tube center to the maximum permitted by the tube. Shift along the "x-axis" from 1 to 11 moves the referenced rod type (inner/outer) radially out from the center of the tube, with "1" indicating a close in (minimum radial location) shift and "11" indicating the maximum permitted shift (each shift direction is limited by either adjacent rods or tube/caddy). Both models indicate that moving fuel toward tube/caddy ID is most reactive. For NRU fuel, the interior rods are spaced approximately at the midpoint between the center of the tube and outer rods are most reactive. Changes in location of the interior rods have only a minor effect on system reactivity near this midpoint. As the NRX fuel is located in a caddy, the location of the caddy in the tube affects system reactivity. As indicated in the plots, a radial shift of the caddy toward the center of the cask is most reactive. The radial maximum shift of the outer rods is most reactive; therefore, no rod shifts require analysis. Note that both wet and dry cask cavities are evaluated in this section. Most reactive condition switches to a wet cask cavity for NRX fuel when considering a radial out fuel rod pitch. There is no statistical difference in reactivity for wet or dry cask cavity conditions for the NRU fuel type.

6.7.3.5   NRU/NRX Fuel in Hypothetical Damaged Condition (Rod Sections)

NRU/NRX fuel sections (broken rods) were evaluated in the NRU/NRX basket tubes. For the NRX rods, the caddy was assumed to retain the rod sections, as the space between the caddy and tube is smaller than a rod and the caddy runs essentially the full length of the basket tube.

Fuel mass is conserved by reducing active fuel height as the number or rod sections increases. Although reducing active fuel height reduces the H/U ratio, it also compacts the fuel region and produces a lower neutron leakage configuration.

Plots of system reactivity for NRU and NRX assemblies, based on a function of number of rod segments, are shown in Figure 6.7.3-14 and Figure 6.7.3-15, respectively. NRU studies were done at fully flooded (1 g/cm^3) interior cask cavity and tube moderator density; as Figure 6.7.3-16 demonstrates, this is the most reactive condition for fuel rod segments. The study demonstrates a

near flat reactivity curve as a function of cask cavity moderator density above 50% density. NRX moderator density studies (run with the maximum 15 rod segments feasible within the caddy) indicate small reactivity difference, wet or dry. Therefore, both were evaluated. The radial, in caddy, shift was also applied.

For both fuel types, maximum number of rod sections produced the maximum reactivity. These reactivities are well above those of the initial studies using full active fuel length rods. The k_{eff} of the NRU assembly is well above that of the NRX assembly, primarily due to the NRX fuel being restrained by the caddy. As the NRU fuel is more reactive than the NRX fuel, the effect of manufacturing tolerances on the fuel tube is only evaluated for the NRU elements.

The single cask maximum calculated $k_{eff} + 2\sigma$ is 0.92560, and is the result of a minimum tube wall thickness and maximum tube OD. There is no statistically significant effect of tube OD, as the effects of increased space for the rod shift are offset by increased separation of tube center to center and increased steel tube mass. Small tube wall thickness allows for increased moderator space and rod shift space and reduces the steel which absorbs neutrons while not affecting the tube to tube pitch.

The broken rod model is significantly higher in reactivity than the model of full length rods and, therefore, establishes the CSI. The CSI for accident conditions is 100. As a single cask model is applied, the cask accident model represents both 10 CFR 71.55 and 71.59 configurations.

To confirm that 10 CFR 71.55 required a single normal condition cask (i.e., with neutron shield and impact limiters) is not neutronically significantly different than that of the accident condition cask model, the "rod section" NRU HEU case that resulted in a $k_{eff} + 2\sigma$ of 0.92560 was evaluated with neutron shield and impact limiter on the cask. The result of a $k_{eff} + 2\sigma$ of 0.92525 demonstrates that the two configurations are not statistically different in the context of criticality analysis.

6.7.3.6   NRU LEU Fuel

All previous evaluations were at 94 wt% ^{235}U fuel assemblies. NRU assemblies were also made with an initial enrichment of 19.75 wt% ^{235}U. The enrichment was conservatively increased to 21 wt% ^{235}U and the most reactive configuration of rod sections was re-evaluated. The LEU NRU fuel results in a $k_{eff} + 2\sigma$ of 0.89508, compared to 0.92560 for the HEU fuel.

6.7.3.7   Single Cask Evaluation to Conform to 10 CFR 71.55 Requirements

The 10 CFR 71.55(b)(3) requires an evaluation of the NAC-LWT with the containment system fully reflected by water. The containment for the NAC-LWT is the cask inner shell. While no operating condition results in a removal of the cask outer shell and lead gamma shield, the most reactive normal condition case (i.e, the k_{eff} of 0.92525 case containing HEU NRU fuel with

broken fuel rod sections, fully moderated cask interior, described in Section 6.7.3.5) is reevaluated by removing the lead and outer shells (including neutron shield), and reflecting the system by 20 cm of water at full density on the X, Y, and Z faces. Using the maximum reactivity model from Section 6.7.3.5, the calculated $k_{eff} + 2\sigma$ is 0.85218.

6.7.3.8   Normal Condition Cask Array Evaluation to Conform to 10 CFR 71.59 Requirements

The 10 CFR 71.59 requires the evaluation of 5xN normal condition packages. Normal conditions are based on an infinite array of packages, square array / touching casks, with a dry cask interior with optimum moderator between casks. "Dry cask interior" applies dry conditions within the fuel tubes, between tubes, and any other void space in the cask cavity. Per NUREG-1617 Section 6.5.5.1, water in leakage need not be assumed during normal condition array analysis. Both full density moderator and void were evaluated between casks, and the maximum reactivity is achieved by the array having a dry exterior, resulting in a $k_{eff}+2\sigma$ of 0.07691. The resulting normal condition CSI for the infinite array is 0.

6.7.3.9   Code Bias and Upper Safety Limit (USL)

Critical benchmarks and USL are discussed in detail in Section 6.5.5. The following evaluates the applicability of the USL to the NRU/NRX fuel assemblies.

The EALCF of the most reactive case is 0.123 eV, and is within the area of applicability of the research reactor benchmark. At the thermal energy range of an EALCF at less 0.378 eV, the USL correlation derived in Section 6.5.5 provides a USL of 0.9270.

The LEU NRU assemblies are analyzed at an enrichment of 21 wt% ^{235}U, within the enrichment range of applicability for the USL. All evaluated LEU NRU fuel is below the EALCF USL, which is lower than the USL based on ^{235}U enrichment.

6.7.3.10   Allowable Cask Loading

Based on the results of the previous sections, any full loading of 18 undamaged NRU or NRX assemblies is allowed in the NAC-LWT. Undamaged fuel assemblies can include cropped fuel, loose fuel rods, or damaged fuel clad, provided the rod is structurally sound. NRU fuel may be placed into a caddy while NRX fuel must be placed into a caddy. Maximum reactivates are summarized in Table 6.7.3-6. Conditions at which the maximum reactivity cases occur are summarized in Table 6.7.3-7.

Figure 6.7.3-1   NRU Fuel Assembly
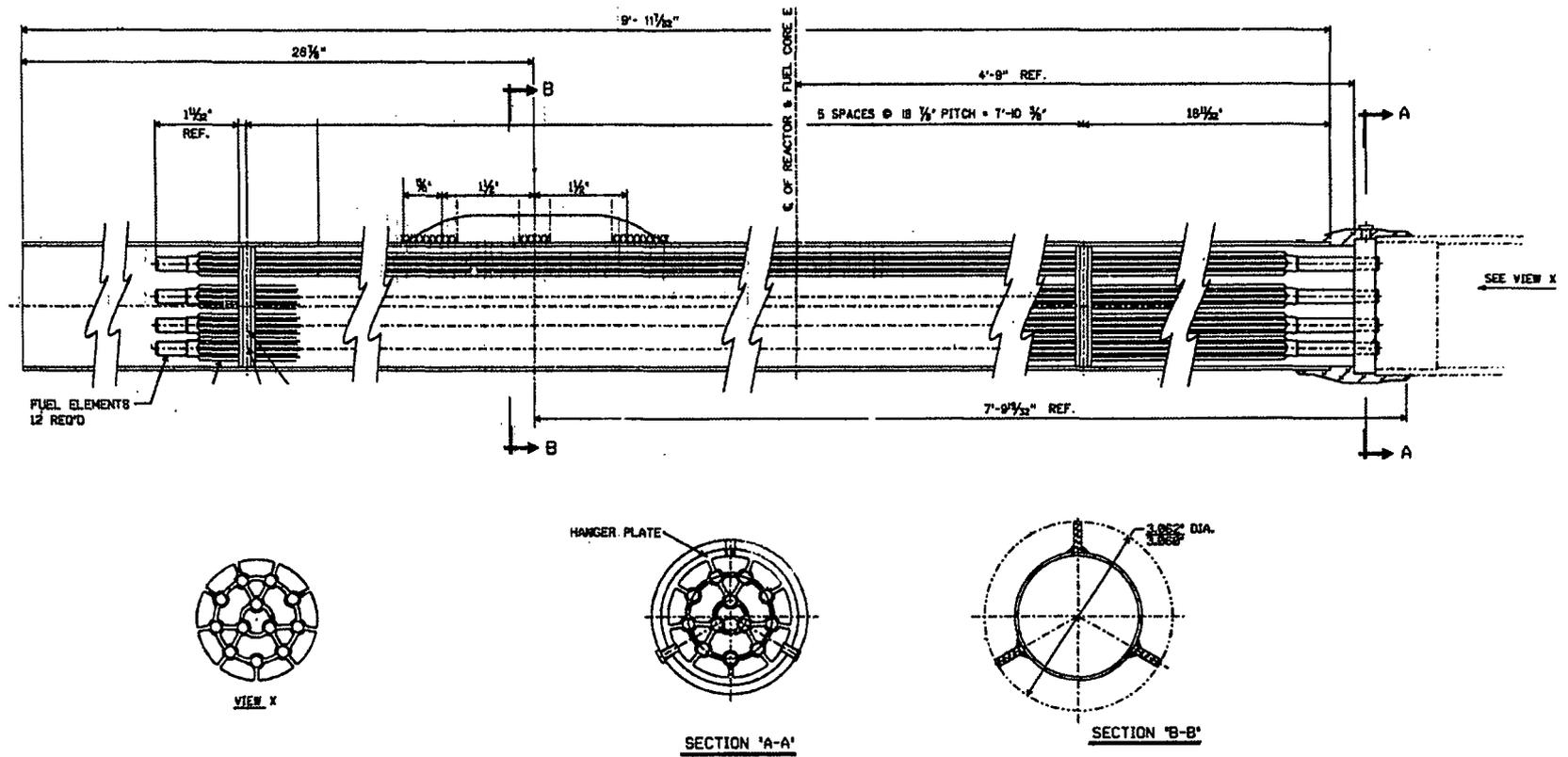
Figure 6.7.3-2   NRX Fuel Assembly
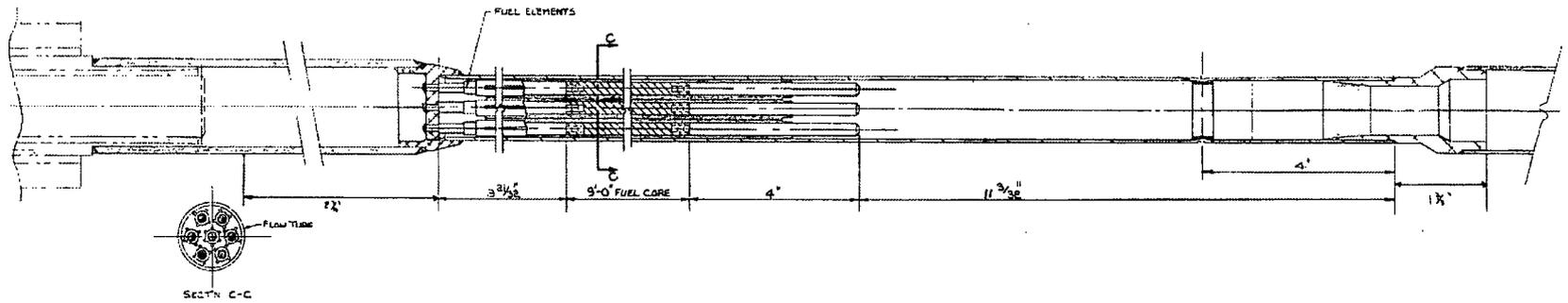
Figure 6.7.3-3   NRU Fuel Rod
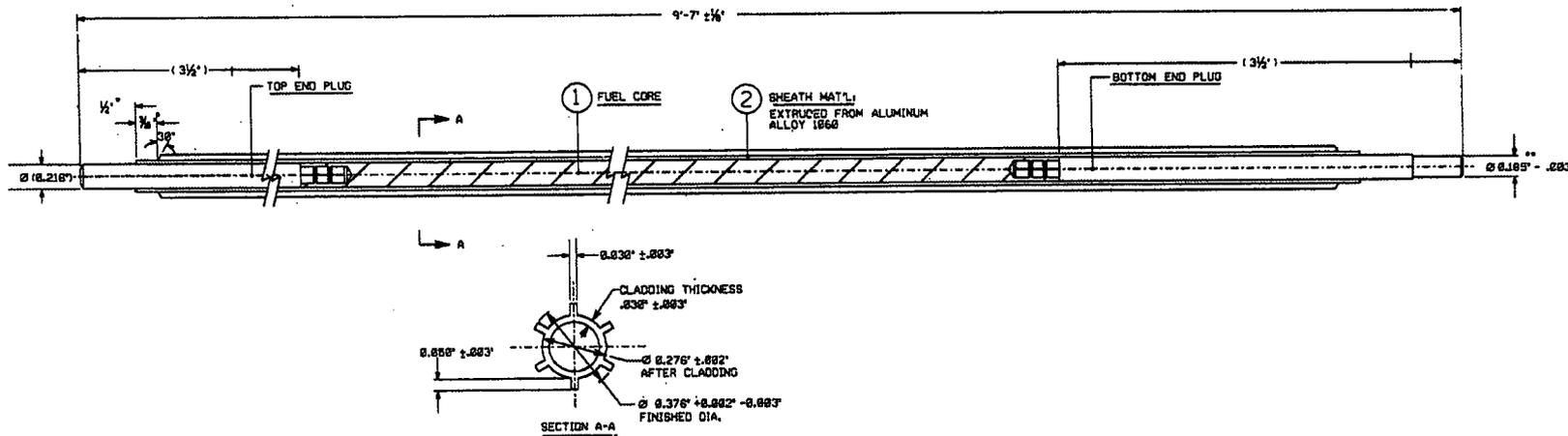
Figure 6.7.3-4   NRX Fuel Rod
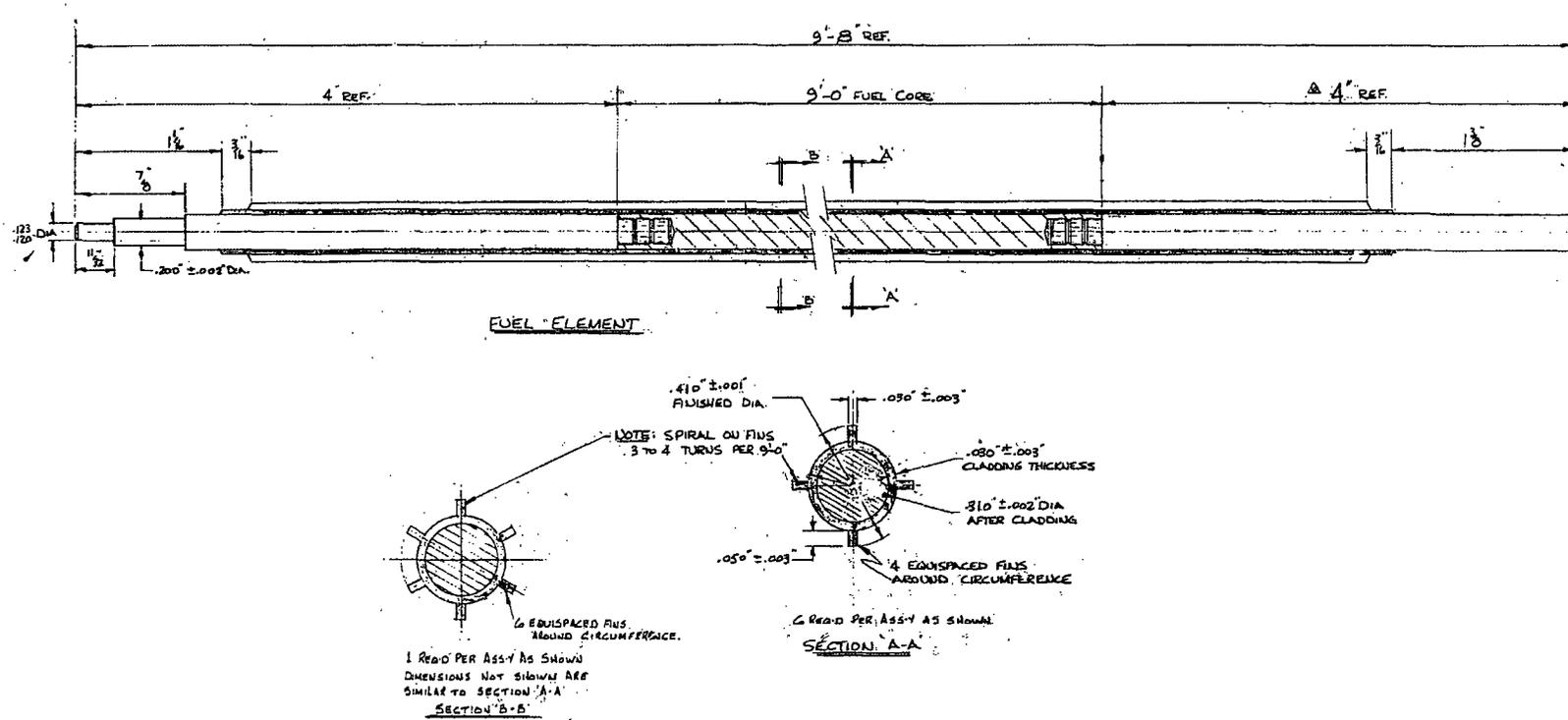
Figure 6.7.3-5   MCNP NRU Fuel in Fuel Tube Cross-Section (No Flow Tube)

Inner rods

Outer rods

Outer rods

Outer rods
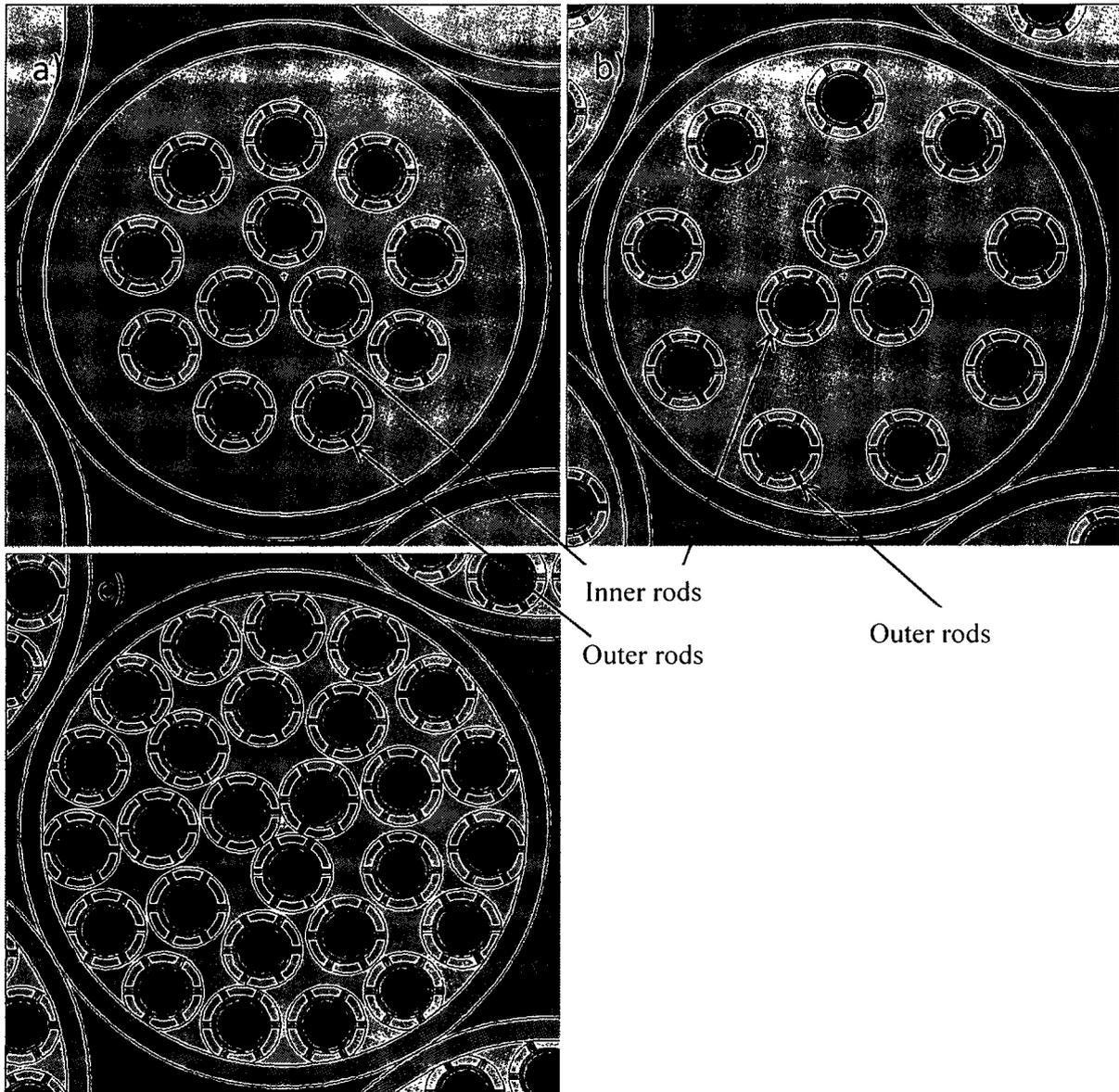
a) Fuel rods in the in-core configuration

b) Maximum reactivity rod pitch (space equivalent to flow tube thickness is retained at inner perimeter of fuel tube but fuel tube is not modeled)

c) Broken Rods – Maximum reactivity is achieved by maximum number of rod sections. Rod height reduced to conserve fuel mass

Figure 6.7.3-6   MCNP NRX Fuel in Fuel Tube Cross-Section (Caddy)

Outer rods
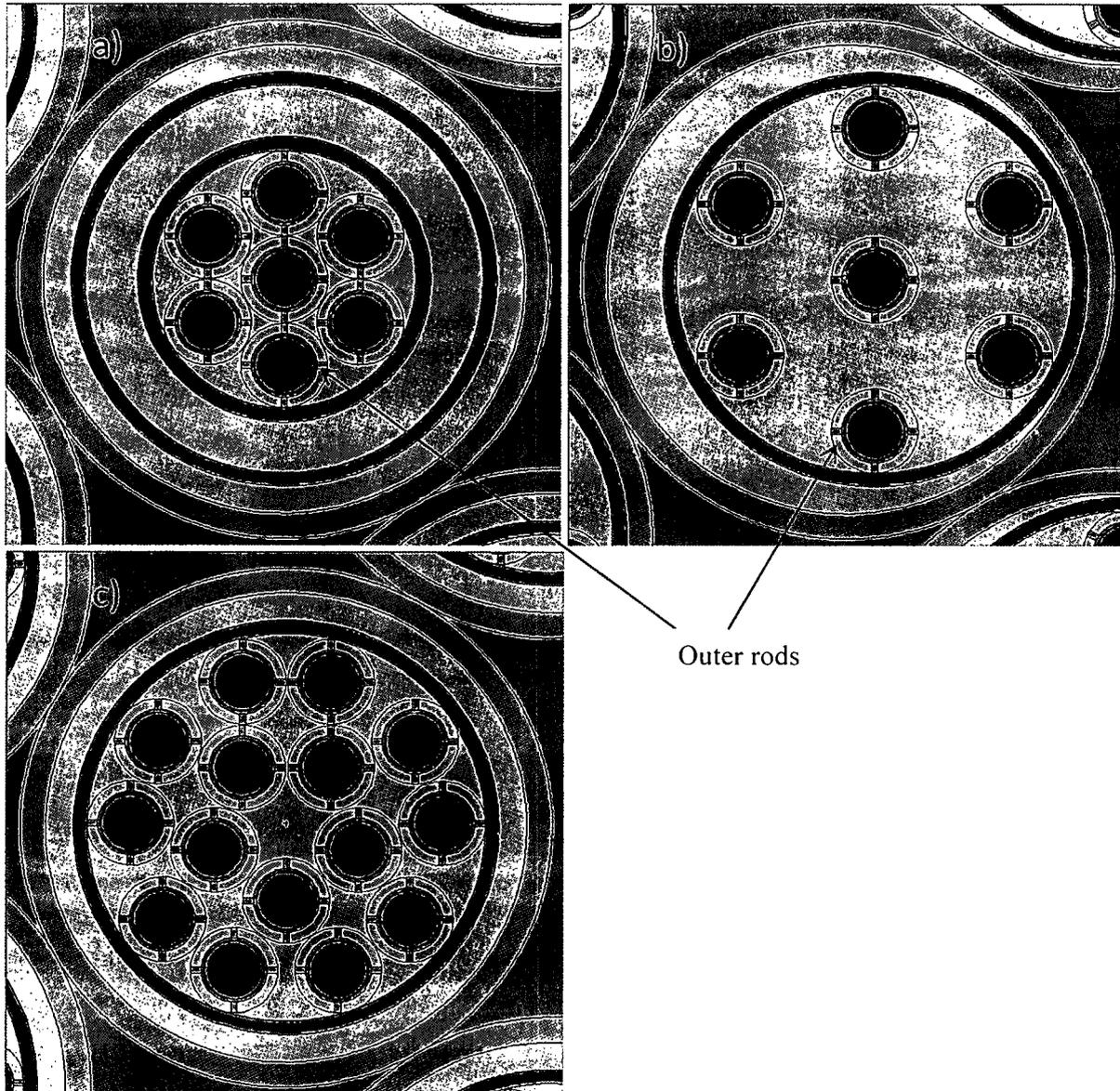
a) Fuel rods in the in-core configuration – with flow tube

b) Maximum reactivity rod pitch – Conservatively removed flow tube

c) Broken Rods – Maximum reactivity is achieved by maximum number of rod sections. Rod height reduced to conserve fuel mass

Figure 6.7.3-7   Sketch of NAC-LWT Cask Cross-Section with NRU/NRX Basket

—Neutron Shield O.D. ⌀39.23 in
—Neutron Shield O.D. ⌀38.73 in
—Cask Shell O.D. ⌀28.76 in
—Lead Outer O.D. ⌀26.35 in
—Cask Shell I.D. ⌀14.89 in
—Cavity ⌀13.38 in
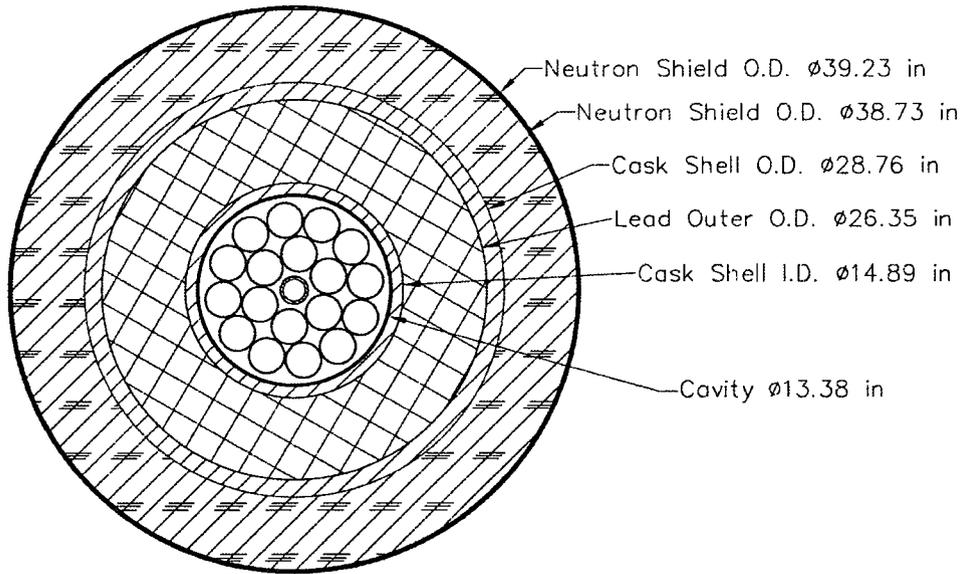
Steel

Lead

Liquid Neutron Shield

Figure 6.7.3-8   Full Length NAC-LWT Cask Sketch with NRU/NRX Basket
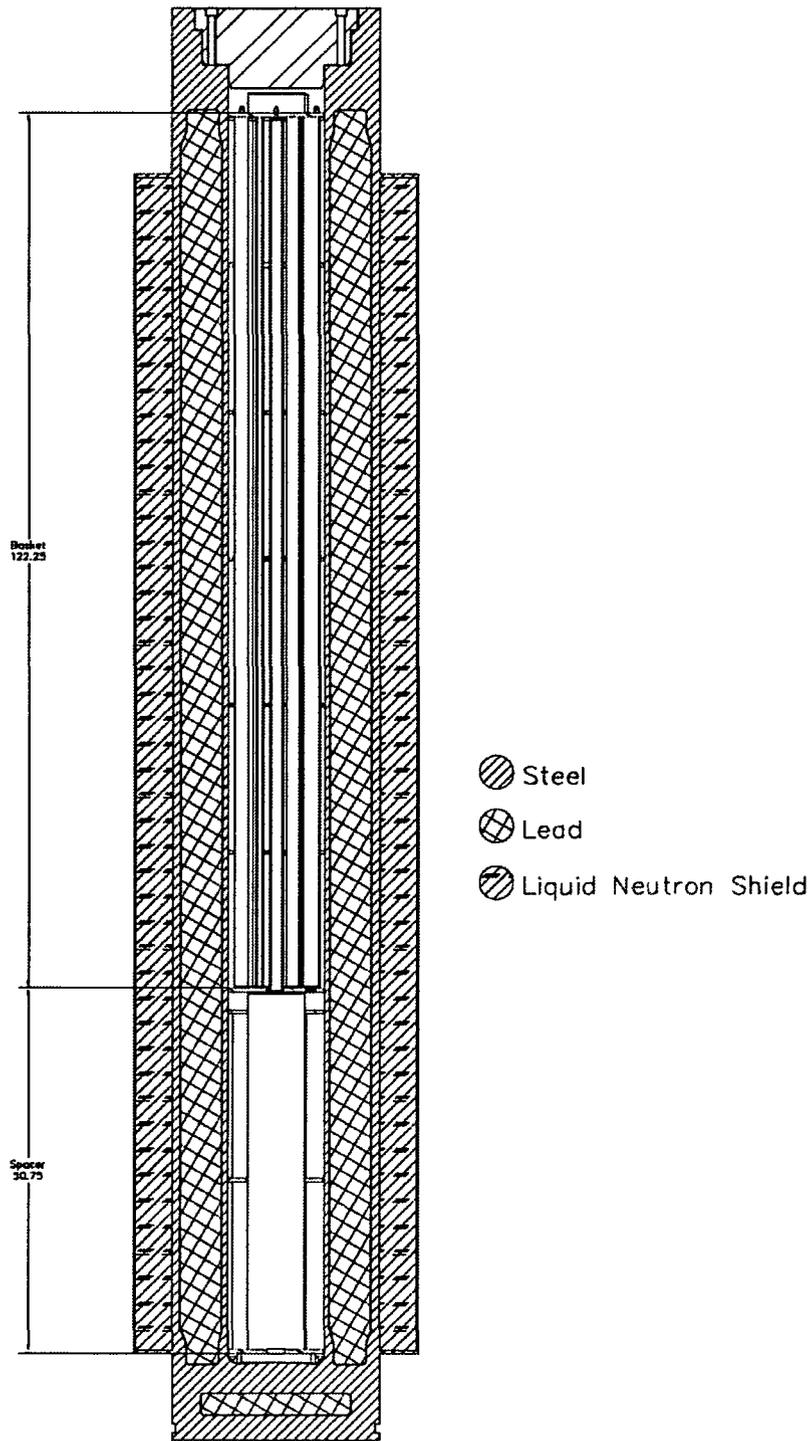
Figure 6.7.3-9　　VISED Maximum Reactivity NRU HEU Fuel (Rod Segments)
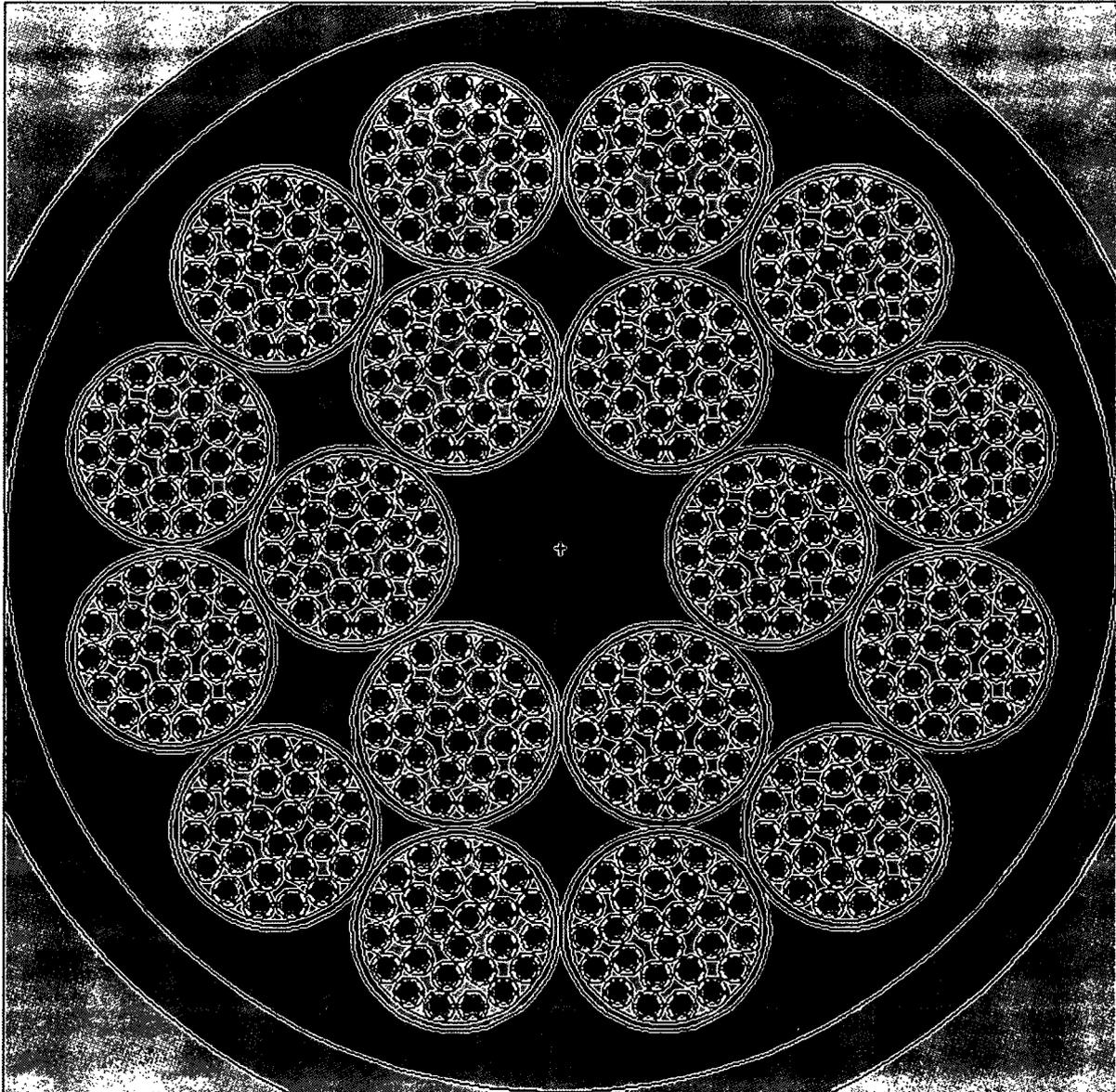
Figure 6.7.3-10   NRU HEU Assembly Moderator Density Study Graphical Results
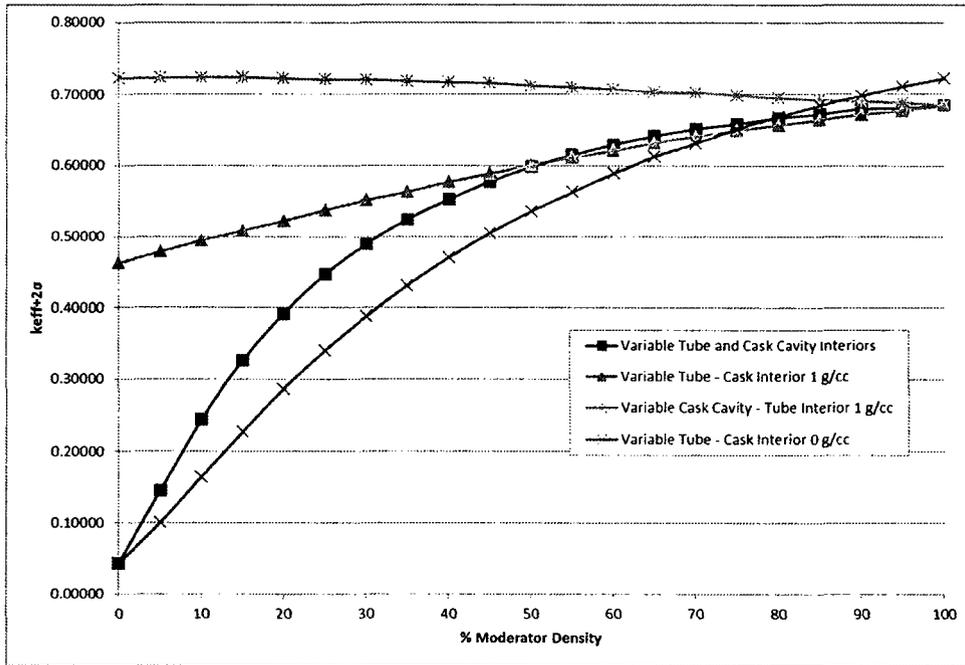
Figure 6.7.3-11   NRX HEU Assembly Moderator Density Study Graphical Results
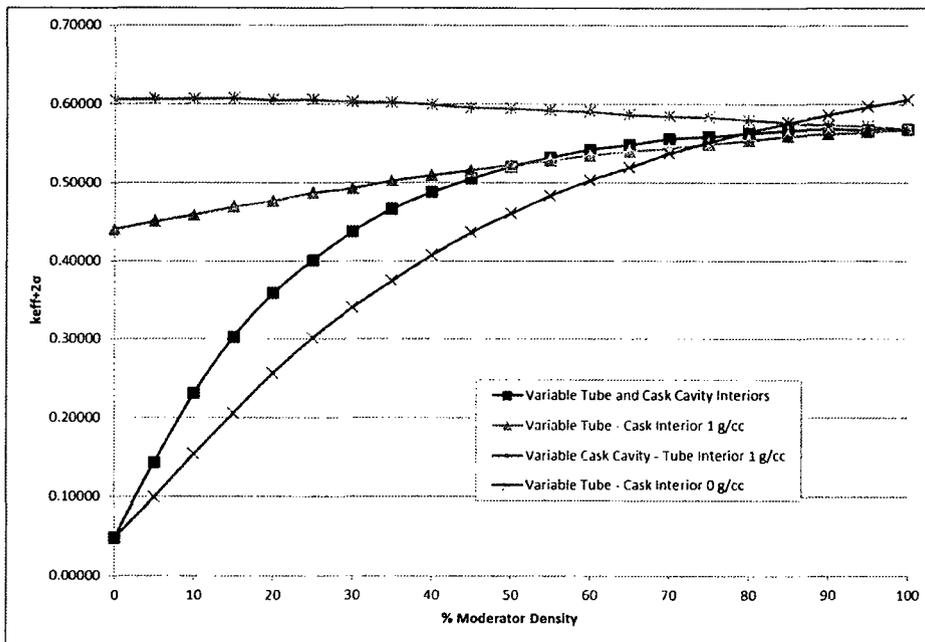
Figure 6.7.3-12   NRU HEU Fuel Rod Pitch Study Graphical Results
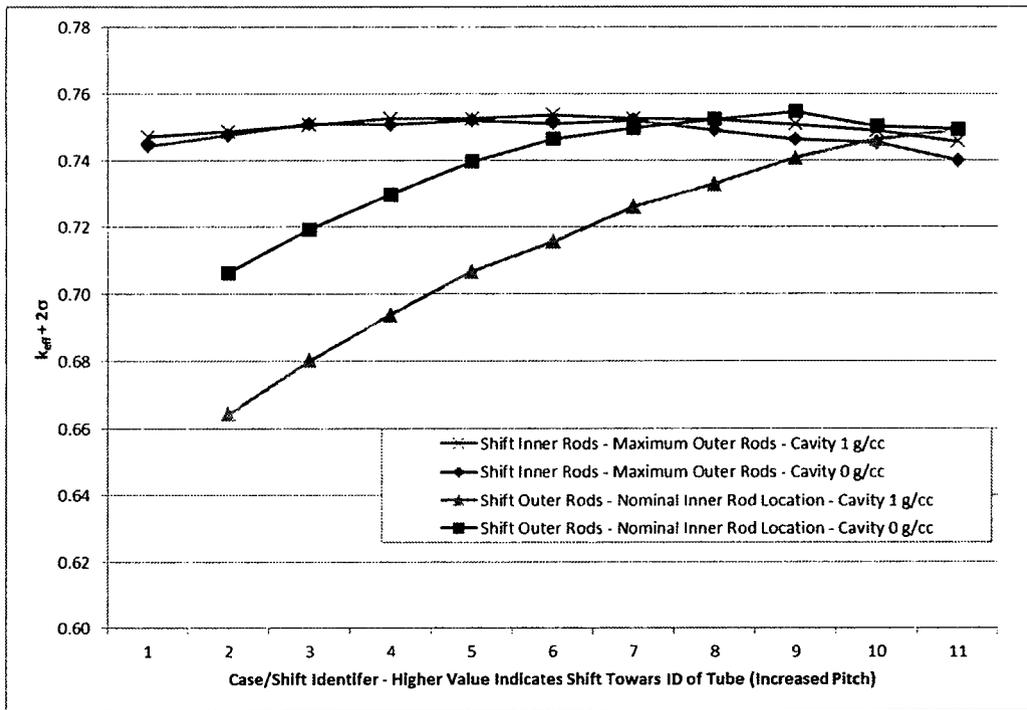
Figure 6.7.3-13   NRX HEU Fuel Rod Pitch Study Graphical Results
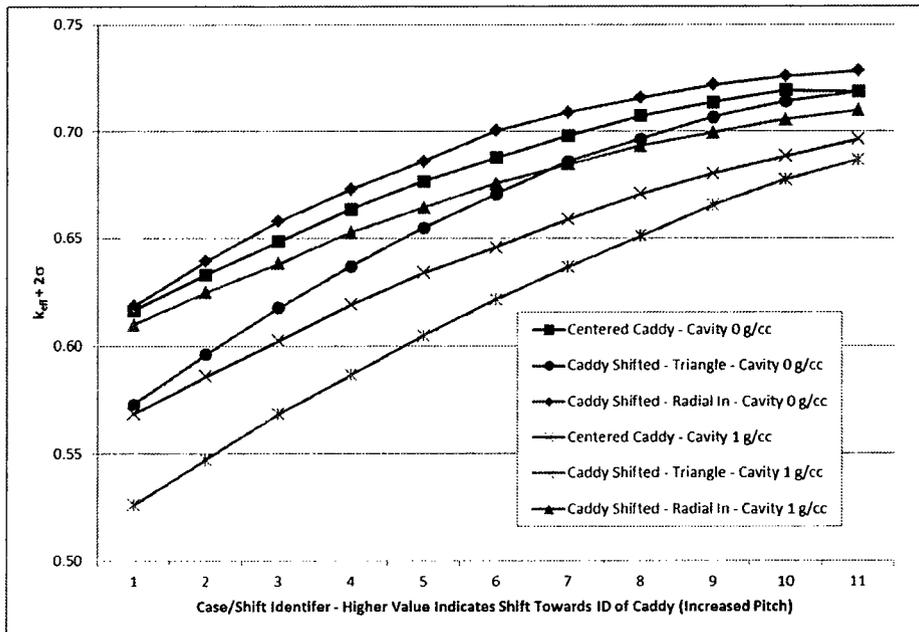
Figure 6.7.3-14   NRU HEU Number of Rod Sections (Broken Rods) Graphical Results
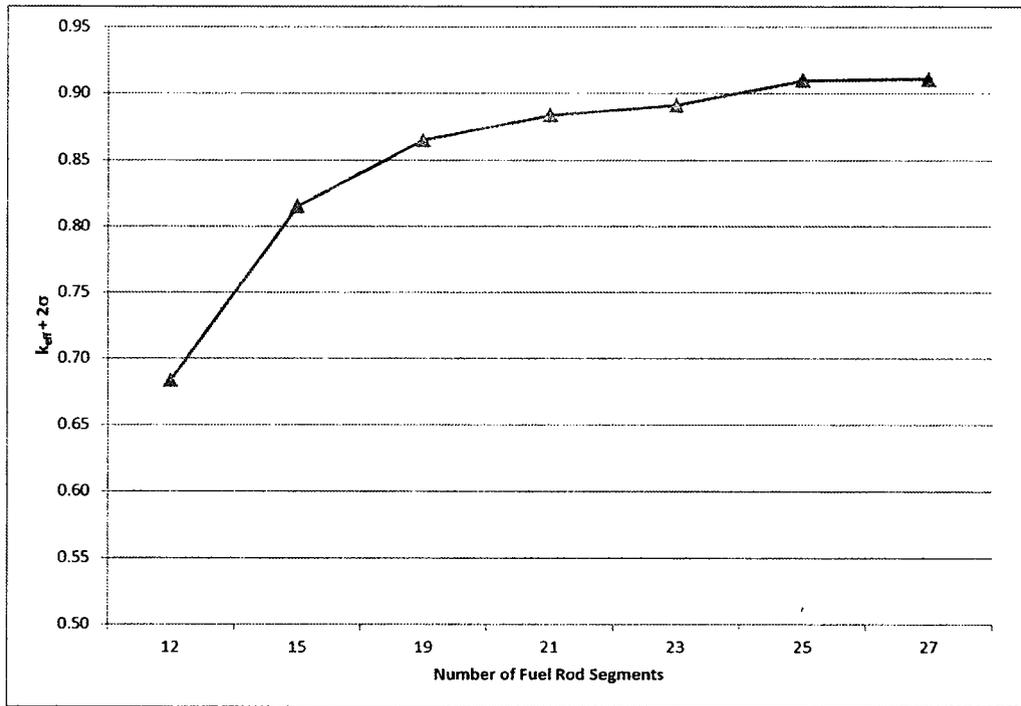
Figure 6.7.3-15   NRX HEU Number of Rod Sections (Broken Rods) Graphical Results

Figure 6.7.3-16   NRU HEU Rod Section (Broken Rods) Moderator Density Study
Graphical Results
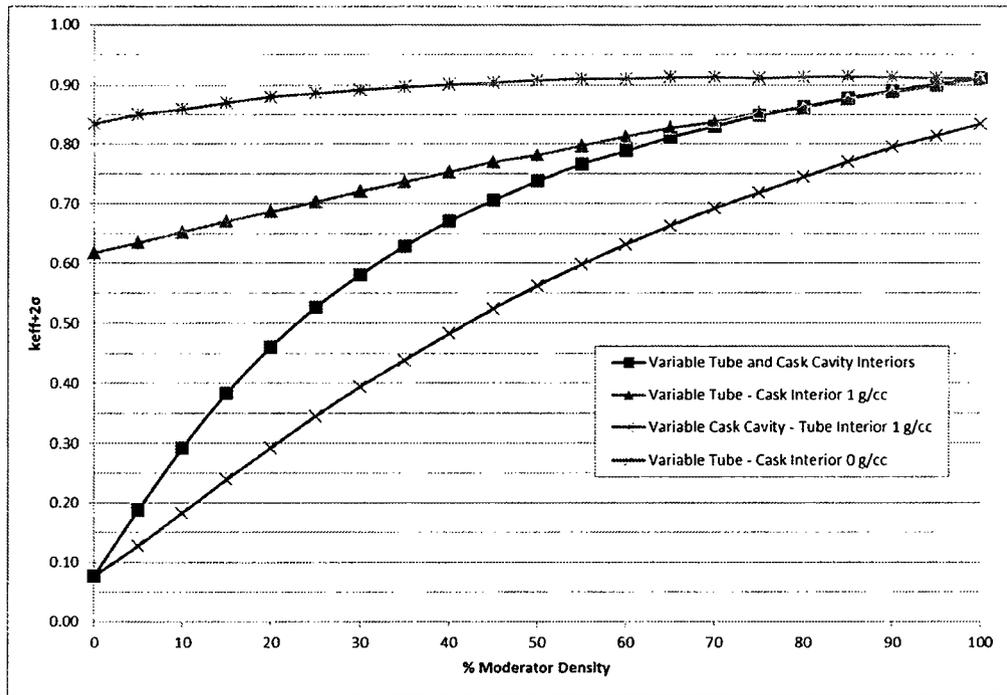
Figure 6.7.3-17   NRX HEU Rod Section (Broken Rods) Moderator Density Study
Graphical Results
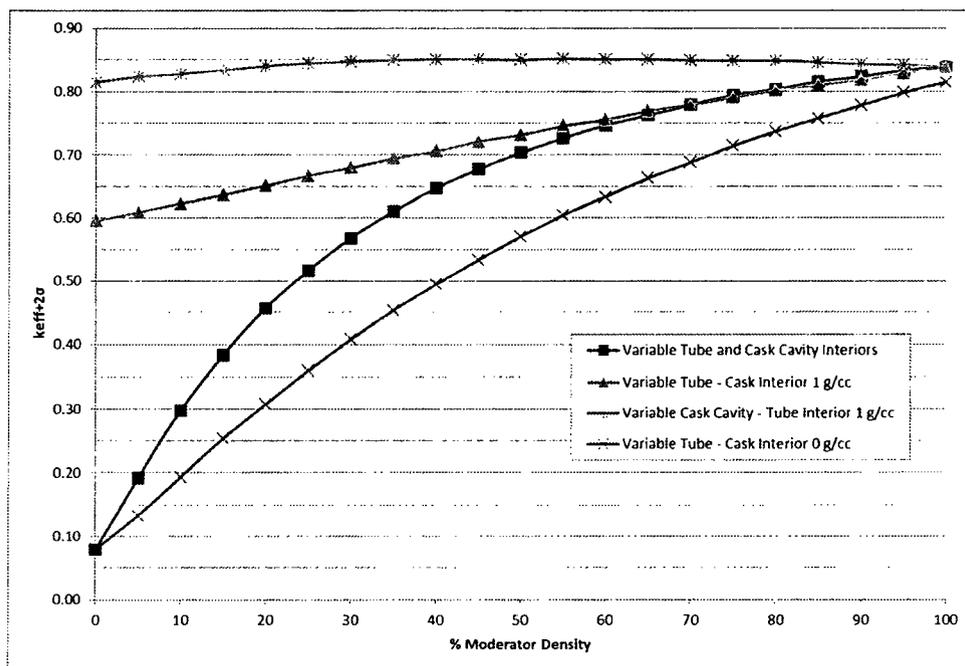
Figure 6.7.3-18   Sample NRX MCNP5 Input File for Normal Conditions

```
NAC-LWT Cask - Normal Transport Conditions
C NRX
C Fuel Rod Cells
1   2  -2.7020    -1          u=6      $ Bottom End Plug
2   1  -3.1889    -2          u=6      $ FuelMeat
3   2  -2.7020    -3 : -4 : -5         u=6      $ TopEndPlug
4   2  -2.7020    -6  #1 #2 #3          u=6      $ Sheath / Aluminum Clad
5   2  -2.7020    -7 +6      u=6      $ Clad Fins
6   2  -2.7020    -8 +6      u=6      $ Clad Fins
7   3  -0.0001    +1 +3 +4 +5 +6 +7 +8          u=6      $ Outside Fuel Rod
C Fuel Assembly Cells
11  3  -0.0001    -12  fill=6     trcl = ( 0.5365 0.7384 0.1600 )      u=5      $ Fuel Rod #1
12  like  11  but       trcl = ( -0.5365 0.7384 0.1600 )      u=5      $ Fuel Rod #2
13  like  11  but       trcl = ( -0.8681 -0.2821 0.1600 )      u=5      $ Fuel Rod #3
14  like  11  but       trcl = ( 0.0000 -0.9128 0.1600 )      u=5      $ Fuel Rod #4
15  like  11  but       trcl = ( 0.8681 -0.2821 0.1600 )      u=5      $ Fuel Rod #5
16  like  11  but       trcl = ( 0.5332 1.3001 0.1600 )      u=5      $ Fuel Rod #6
17  like  11  but       trcl = ( -0.5332 1.8001 0.1600 )      u=5      $ Fuel Rod #7
18  like  11  but       trcl = ( -1.5472 1.0634 0.1600 )      u=5      $ Fuel Rod #8
19  like  11  but       trcl = ( -1.8767 0.0491 0.1600 )      u=5      $ Fuel Rod #9
20  like  11  but       trcl = ( -1.4894 -1.1429 0.1600 )      u=5      $ Fuel Rod #10
21  like  11  but       trcl = ( -0.6267 -1.7697 0.1600 )      u=5      $ Fuel Rod #11
22  like  11  but       trcl = ( 0.6267 -1.7697 0.1600 )      u=5      $ Fuel Rod #12
23  like  11  but       trcl = ( 1.4894 -1.1429 0.1600 )      u=5      $ Fuel Rod #13
24  like  11  but       trcl = ( 1.8767 0.0491 0.1600 )      u=5      $ Fuel Rod #14
25  like  11  but       trcl = ( 1.5472 1.0634 0.1600 )      u=5      $ Fuel Rod #15
26  3  -0.0001       #11 #12 #13 #14 #15 #16 #17 #18 #19 #20
                     #21 #22
                     #23 #24 #25
                     u=5  $ Outside Fuel Rods
27  3  -0.0001       -15  -16  fill=5      u=4  $ Inside Caddy
28  2  -2.7020       -16  +15      u=4  $ Caddy
29  3  -0.0001       +16          u=4  $ Outside  Caddy
C Tube Cells
51  3  -0.0001    -51  fill=4    ( 0.3696 0.0000 0.6351 )      u=3  $ Tube Inside
52  5  -7.9200    -52  +51          u=3  $ Tube Shell
53  4  -0.0001    +52          u=3  $ Tube Exterior
C Cells - Basket
61  0             -69  fill=3  trcl=1        u=1  $ Basket Tube 1 (Inner Ring)
62  0             -69  fill=3  trcl=2        u=1  $ Basket Tube 2 (Inner Ring)
63  0             -69  fill=3  trcl=3        u=1  $ Basket Tube 3 (Inner Ring)
64  0             -69  fill=3  trcl=4        u=1  $ Basket Tube 4 (Inner Ring)
65  0             -69  fill=3  trcl=5        u=1  $ Basket Tube 5 (Inner Ring)
66  0             -69  fill=3  trcl=6        u=1  $ Basket Tube 6 (Inner Ring)
67  0             -69  fill=3  trcl=7        u=1  $ Basket Tube 7 (Inner Ring)
68  0             -69  fill=3  trcl=8        u=1  $ Basket Tube 8 (Outer Ring)
69  0             -69  fill=3  trcl=9        u=1  $ Basket Tube 9 (Outer Ring)
70  0             -69  fill=3  trcl=10       u=1  $ Basket Tube 10 (Outer Ring)
71  0             -69  fill=3  trcl=11       u=1  $ Basket Tube 11 (Outer Ring)
72  0             -69  fill=3  trcl=12       u=1  $ Basket Tube 12 (Outer Ring)
73  0             -69  fill=3  trcl=13       u=1  $ Basket Tube 13 (Outer Ring)
74  0             -69  fill=3  trcl=14       u=1  $ Basket Tube 14 (Outer Ring)
75  0             -69  fill=3  trcl=15       u=1  $ Basket Tube 15 (Outer Ring)
76  0             -69  fill=3  trcl=16       u=1  $ Basket Tube 16 (Outer Ring)
77  0             -69  fill=3  trcl=17       u=1  $ Basket Tube 17 (Outer Ring)
78  0             -69  fill=3  trcl=18       u=1  $ Basket Tube 19 (Outer Ring)
79  4  -0.0001    #61 #62 #63 #64 #65 #66 #67
                  #68 #69 #70 #71 #72 #73 #74 #75 #76 #77 #78
                  fill=2        u=1  $ Outside Outer Ring
80  5  -7.9200    -61          u=2  $ Bottom Disk
81  5  -7.9200    -62          u=2  $ Intermediate Disk
82  5  -7.9200    -63          u=2  $ Intermediate Disk
83  5  -7.9200    -64          u=2  $ Intermediate Disk
84  5  -7.9200    -65          u=2  $ Intermediate Disk
85  5  -7.9200    -66          u=2  $ Intermediate Disk
86  5  -7.9200    -67          u=2  $ Top Disk
87  4  -0.0001    #80 #81 #82 #83 #84 #85 #86          u=2  $ Outside Plates
C Cells - LWT Cask Normal Conditions
201  6  -11.344   -204          $ BotPb
202  4  -0.0001   -203  fill=1  (0 0 133.35 )      $ Cavity
203  5  -7.9200   -201  -202  +204          $ Bottom
204  5  -7.9200   -201  +202  +206  +209  +203      $ OuterShell
205  5  -7.9200   -205  +208  +203          $ InnerShellTaper
206  5  -7.9200   -207  +203          $ InnerShell
207  6  -11.344   -208  +207          $ Lead
208  6  -11.344   -206  +205  +208          $ LeadTaper
209  0            -209  +208          $ LeadGap
210  9  -0.9669   -211  +201          $ NeutronShield
211  5  -7.9200   -210  +201  +211          $ NSShell
212  7  -0.4997   -212  +201          $ UpperLimiter
213  7  -0.4997   -213  +201          $ LowerLimiter
214  8  -0.9982   -214  +201  +210  +212  +213      $ Container
215  8  -0.9982   214          $ Outside

C Fuel Rod Surfaces
1  RCC  0.0000  0.0000  0.0000  0.0000  0.0000  10.1600  0.3175      $ Bottom End Plug
2  RCC  0.0000  0.0000  10.1600  0.0000  0.0000  127.8667  0.3175      $ Fuel Meat
```
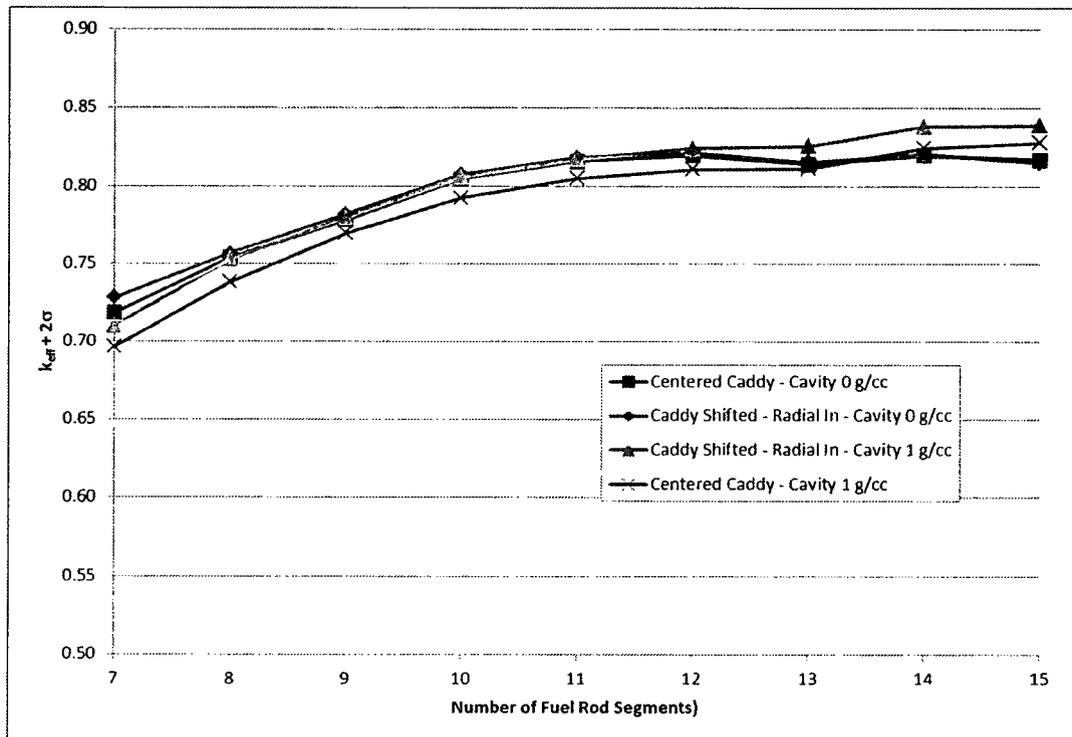
Figure 6.7.3-18   Sample NRX MCNP5 Input File for Normal Conditions (continued)

```
3   RCC   0.0000   0.0000   138.0267   0.0000   0.0000   7.9375   0.3175      $ Top End Plug Step 1
4   RCC   0.0000   0.0000   145.9642   0.0000   0.0000   1.3494   0.2540      $ Top End Plug Step 2
5   RCC   0.0000   0.0000   147.3135   0.0000   0.0000   0.8731   0.1562      $ Top End Plug Step 3
6   RCC   0.0000   0.0000   3.4925   0.0000   0.0000   144.6148   0.3937      $ Sheath / Aluminum Clad
7   RPP   -0.5207   0.5207   -0.0381   0.0381   3.4925   144.6148          $ Clad Fin
8   22  RPP   -0.5207   0.5207   -0.0381   0.0381   3.4925   144.6148      $ Clad Fin
C Fuel Assembly Surfaces
11   RCC   0.0000   0.0000   0.0001   0.0000   0.0000   292.9998   0.5206      $ Fuel Rod Container
12   CZ   0.5205                    $ Rod outer surface
13   CZ   1.5722                    $ Inner Flow Channel Surface (may not be used)
14   RCC   0.0000   0.0000   0.1600   0.0000   0.0000   293.0010   1.7500      $ Outer Flow Channel Surface (may not be used)
15   RCC   0.0000   0.0000   0.1600   0.0000   0.0000   309.0080   2.3914      $ Caddy Inner Surface (may not be used)
16   RCC   0.0000   0.0000   0.0000   0.0000   0.0000   308.0080   2.5464      $ Caddy Outer Surface (may not be used)
17   CZ   2.5932                    $ Surface accounting for flow tube and caddy
C Tube Surfaces
51   RCC   0.0000   0.0000   0.6350   0.0000   0.0000   308.6100   2.9159   $ Tube Inside
52   RCC   0.0000   0.0000   -0.0001   0.0000   0.0000   309.2452   3.1903   $ Tube Outside and Cap
C Surfaces - Basket
61   RCC   0.0000   0.0000   -1.2700   0.0000   0.0000   1.2699   16.8529      $ Bottom Disk
62   RCC   0.0000   0.0000   49.5300   0.0000   0.0000   1.2700   16.8529      $ Intermediate Disk 1
63   RCC   0.0000   0.0000   100.3300   0.0000   0.0000   1.2700   16.8529      $ Intermediate Disk 2
64   RCC   0.0000   0.0000   151.1300   0.0000   0.0000   1.2700   16.8529      $ Intermediate Disk 3
65   RCC   0.0000   0.0000   201.9300   0.0000   0.0000   1.2700   16.8529      $ Intermediate Disk 4
66   RCC   0.0000   0.0000   252.7300   0.0000   0.0000   1.2700   16.8529      $ Intermediate Disk 5
67   RCC   0.0000   0.0000   303.5300   0.0000   0.0000   1.2700   16.8529      $ Top Disk
68   RCC   0.0000   0.0000   -1.2701   0.0000   0.0000   310.5152   16.8530      $ Basket Outline
69   RCC   0.0000   0.0000   0.0000   0.0000   0.0000   309.2450   3.1902      $ Tube Outline
C Surfaces - LWT Cask Normal Conditions
201   RCC   0.0000   0.0000   -26.6700   0.0000   0.0000   507.3650   36.5189   $ Lwt
202   RCC   0.0000   0.0000   -26.6700   0.0000   0.0000   26.6700   36.5189   $ Bottom
203   RCC   0.0000   0.0000   0.0000   0.0000   0.0000   452.1200   16.9863   $ Cavity
204   RCC   0.0000   0.0000   -17.7800   0.0000   0.0000   7.6200   26.3525   $ Bottom gamma shield
205   RCC   0.0000   0.0000   0.0000   0.0000   0.0000   444.5000   20.1740   $ Lead id - taper
206   RCC   0.0000   0.0000   0.0000   0.0000   0.0000   444.5000   31.5976   $ Lead od - taper
207   RCC   0.0000   0.0000   13.8176   0.0000   0.0000   416.8648   18.9103   $ Lead id
208   RCC   0.0000   0.0000   13.8176   0.0000   0.0000   416.8648   33.3271   $ Lead od
209   RCC   0.0000   0.0000   13.8176   0.0000   0.0000   416.8648   33.4645   $ Lead gap
210   RCC   0.0000   0.0000   3.8100   0.0000   0.0000   419.1000   49.8183   $ Neutron shield shell
211   RCC   0.0000   0.0000   5.0800   0.0000   0.0000   416.5600   49.2189   $ Neutron shield
212   RCC   0.0000   0.0000   450.2150   0.0000   0.0000   70.5612   49.8183   $ Upper limiter
213   RCC   0.0000   0.0000   -68.0212   0.0000   0.0000   71.8312   49.8183   $ Lower limiter
214   RCC   0.0000   0.0000   -88.0212   0.0000   0.0000   628.7974   69.9183   $ Container - Gap To Reflector


C
C Materials List
C
C - wt%
m1   92235.69c   -2.8570E-01
       92238.69c   -1.8236E-02
       13027.62c   -6.9606E-01
C Aluminum
m2   13027.62c   -1.0
C Tube Cavity Water
m3   1001.62c   6.6667E-01   8016.62c   3.3333E-01
mt3   lwtr.60t
C Cask Cavity Water
m4   1001.62c   6.6667E-01   8016.62c   3.3333E-01
mt4   lwtr.60t
C Stainless Steel 304
m5   26000.55c   -0.695   24000.50c   -0.190   28000.50c   -0.095
       25055.62c   -0.020
C Lead
m6   82000.50c   -1.0
C Aluminum Honeycomb Impact Limiter
m7   13027.62c   -1.0
C Water/Glycol - Cask Neutron Shield
m9   1001.62c   -1.03651E-01   8016.62c   -6.75619E-01   6000.66c   -2.20730E-01
C Cask Exterior (Water at Various Densities)
m8   1001.62c   6.6667E-01   8016.62c   3.3333E-01
mt8   lwtr.60t
C
C Cell Importances
imp:n 1 69r 0
c
c Criticality Controls
c
kcode   2000   1.00   30   530
c
c Source Distribution for Initial Generation
SDEF   CEL=   202:D4:51:27:D5:2
       ERG=   D1
       POS=   0.0000   0.00   10.1600
       RAD=   D2
       AXS=   0.00   0.00   1.00
       EXT=   D3
C - Neutron Source Energy Source Distribution
#            SP1
       -3
C - Uniform Radial Distribution in Fuel Rod
#   SI2   SP2
```

Figure 6.7.3-18   Sample NRX MCNP5 Input File for Normal Conditions (continued)

```
        0.0000  -21
        0.3175   1
C - Axial Source Profile
#   SI3  SP3
        0   0.0
      274   1.0
C - 18 Tubes in Cask
#   SI4           SP4
        1              d
       61   1
       62   1
       63   1
       64   1
       65   1
       66   1
       67   1
       68   1
       69   1
       70   1
       71   1
       72   1
       73   1
       74   1
       75   1
       76   1
       77   1
       78   1
C - Rods Per Assembly
#   SI5           SP5
        1              d
       11   1
       12   1
       13   1
       14   1
       15   1
       16   1
       17   1
*TR1    6.3810  0.0000  0.0000  180  270  90  90  180  90  90  90  0
*TR2    3.1905  5.5261  0.0000  120  210  90  30  120  90  90  90  0
*TR3   -3.1905  5.5261  0.0000   60  150  90 -30   60  90  90  90  0
*TR4   -6.3810  0.0000  0.0000    0   90  90 -90    0  90  90  90  0
*TR5   -3.1905 -5.5261  0.0000  -60   30  90 -150  -60  90  90  90  0
*TR6    3.1905 -5.5261  0.0000 -120  -30  90 -210 -120  90  90  90  0
*TR7   11.9071  3.1905  0.0000  165  255  90  75  165  90  90  90  0
*TR8    8.7166  8.7166  0.0000  135  225  90  45  135  90  90  90  0
*TR9    3.1905 11.9071  0.0000  105  195  90  15  105  90  90  90  0
*TR10  -3.1905 11.9071  0.0000   75  165  90 -15   75  90  90  90  0
*TR11  -8.7166  8.7166  0.0000   45  135  90 -45   45  90  90  90  0
*TR12 -11.9071  3.1905  0.0000   15  105  90 -75   15  90  90  90  0
*TR13 -11.9071 -3.1905  0.0000  -15   75  90 -105  -15  90  90  90  0
*TR14  -8.7166 -8.7166  0.0000  -45   45  90 -135  -45  90  90  90  0
*TR15  -3.1905 -11.9071 0.0000  -75   15  90 -165  -75  90  90  90  0
*TR16   3.1905 -11.9071 0.0000 -105  -15  90 -195 -105  90  90  90  0
*TR17   8.7166 -8.7166  0.0000 -135  -45  90 -225 -135  90  90  90  0
*TR18  11.9071 -3.1905  0.0000 -165  -75  90 -255 -165  90  90  90  0
*TR21   0.0 0.0 0.0 60 150 90 -30 60 90 90 90 0    $ z-rotation 60 degrees
*TR22   0.0 0.0 0.0 90 180 90 0 90 90 90 90 0    $ z-rotation 90 degrees
*TR23   0.0 0.0 0.0 -60 30 90 -150 -60 90 90 90 0    $ z-rotation -60 degrees
C Print Control
prdmp  -30 -60 1 2
print
C Random Number Generator
rand  gen=2  seed=19073486328125  stride=152917  hist=1
```

Figure 6.7.3-19   Sample NRU MCNP5 Input File for Accident Conditions

```
NAC-LWT Cask - Accident Transport Conditions
C NRU
C Fuel Rod Cells
1   2  -2.7020    -1 : -2        u=5      $ Bottom End Plug
2   1  -3.2419    -3        u=5      $ FuelMeat
3   2  -2.7020    -4        u=5      $ TopEndPlug
4   2  -2.7020    -5 #1 #2 #3        u=5      $ Sheath / Aluminum Clad
5   2  -2.7020    -6 +5     u=5      $ Clad Fins
6   2  -2.7020    -7 +5     u=5      $ Clad Fins
7   2  -2.7020    -8 +5     u=5      $ Clad Fins
8   3  -0.9982    +1 +2 +4 +5 +6 +7 +8        u=5      $ Outside Fuel Rod
C Fuel Assembly Cells
11  3  -0.9982    -12    fill=5     trcl = ( 0.4224 0.3544 0.0000 )      u=4    $ Fuel Rod #1
12  like  11  but       trcl = ( -0.5181 0.1886 0.0000 )     u=4    $ Fuel Rod #2
13  like  11  but       trcl = ( 0.0957 -0.5430 0.0000 )     u=4    $ Fuel Rod #3
14  like  11  but       trcl = ( 1.4155 0.5152 0.0000 )      u=4    $ Fuel Rod #4
15  like  11  but       trcl = ( 0.7532 1.3046 0.0000 )      u=4    $ Fuel Rod #5
16  like  11  but       trcl = ( -0.2616 1.4835 0.0000 )     u=4    $ Fuel Rod #6
17  like  11  but       trcl = ( -1.1539 0.9683 0.0000 )     u=4    $ Fuel Rod #7
18  like  11  but       trcl = ( -1.5064 0.0000 0.0000 )     u=4    $ Fuel Rod #8
19  like  11  but       trcl = ( -1.1539 -0.9683 0.0000 )    u=4    $ Fuel Rod #9
20  like  11  but       trcl = ( -0.2616 -1.4835 0.0000 )    u=4    $ Fuel Rod #10
21  like  11  but       trcl = ( 0.7532 -1.3046 0.0000 )     u=4    $ Fuel Rod #11
22  like  11  but       trcl = ( 1.4155 -0.5152 0.0000 )     u=4    $ Fuel Rod #12
23  like  11  but       trcl = ( 2.3409 0.7606 0.0000 )      u=4    $ Fuel Rod #13
24  like  11  but       trcl = ( 1.8292 1.6470 0.0000 )      u=4    $ Fuel Rod #14
25  like  11  but       trcl = ( 1.0011 2.2486 0.0000 )      u=4    $ Fuel Rod #15
26  like  11  but       trcl = ( 0.0000 2.4614 0.0000 )      u=4    $ Fuel Rod #16
27  like  11  but       trcl = ( -1.0011 2.2486 0.0000 )     u=4    $ Fuel Rod #17
28  like  11  but       trcl = ( -1.8292 1.6470 0.0000 )     u=4    $ Fuel Rod #18
29  like  11  but       trcl = ( -2.3409 0.7606 0.0000 )     u=4    $ Fuel Rod #19
30  like  11  but       trcl = ( -2.4479 -0.2573 0.0000 )    u=4    $ Fuel Rod #20
31  like  11  but       trcl = ( -2.1316 -1.2307 0.0000 )    u=4    $ Fuel Rod #21
32  like  11  but       trcl = ( -1.4468 -1.9913 0.0000 )    u=4    $ Fuel Rod #22
33  like  11  but       trcl = ( -0.5117 -2.4076 0.0000 )    u=4    $ Fuel Rod #23
34  like  11  but       trcl = ( 0.5117 -2.4076 0.0000 )     u=4    $ Fuel Rod #24
35  like  11  but       trcl = ( 1.4468 -1.9913 0.0000 )     u=4    $ Fuel Rod #25
36  like  11  but       trcl = ( 2.1316 -1.2307 0.0000 )     u=4    $ Fuel Rod #26
37  like  11  but       trcl = ( 2.4479 -0.2573 0.0000 )     u=4    $ Fuel Rod #27
38  3  -0.9982        #11 #12 #13 #14 #15 #16 #17 #18 #19 #20
                 #21 #22
                 #23 #24 #25 #26 #27 #28 #29
                 #30 #31 #32 #33 #34 #35 #36 #37
                        u=4   $ Outside Fuel Rods
C Tube Cells
51  3  -0.9982   -51   fill=4  ( 0.0000 0.0000 0.6351 )     u=3  $ Tube Inside
52  5  -7.9200   -52 +51       u=3   $ Tube Shell
53  4  -0.9982   +52           u=3   $ Tube Exterior
C Cells - Basket
61  0            -69  fill=3   trcl=1       u=1  $ Basket Tube 1 (Inner Ring)
62  0            -69  fill=3   trcl=2       u=1  $ Basket Tube 2 (Inner Ring)
63  0            -69  fill=3   trcl=3       u=1  $ Basket Tube 3 (Inner Ring)
64  0            -69  fill=3   trcl=4       u=1  $ Basket Tube 4 (Inner Ring)
65  0            -69  fill=3   trcl=5       u=1  $ Basket Tube 5 (Inner Ring)
66  0            -69  fill=3   trcl=6       u=1  $ Basket Tube 6 (Inner Ring)
67  0            -69  fill=3   trcl=7       u=1  $ Basket Tube 7 (Inner Ring)
68  0            -69  fill=3   trcl=8       u=1  $ Basket Tube 8 (Outer Ring)
69  0            -69  fill=3   trcl=9       u=1  $ Basket Tube 9 (Outer Ring)
70  0            -69  fill=3   trcl=10      u=1  $ Basket Tube 10 (Outer Ring)
71  0            -69  fill=3   trcl=11      u=1  $ Basket Tube 11 (Outer Ring)
72  0            -69  fill=3   trcl=12      u=1  $ Basket Tube 12 (Outer Ring)
73  0            -69  fill=3   trcl=13      u=1  $ Basket Tube 13 (Outer Ring)
74  0            -69  fill=3   trcl=14      u=1  $ Basket Tube 14 (Outer Ring)
75  0            -69  fill=3   trcl=15      u=1  $ Basket Tube 15 (Outer Ring)
76  0            -69  fill=3   trcl=16      u=1  $ Basket Tube 16 (Outer Ring)
77  0            -69  fill=3   trcl=17      u=1  $ Basket Tube 17 (Outer Ring)
78  0            -69  fill=3   trcl=18      u=1  $ Basket Tube 18 (Outer Ring)
79  4  -0.9982   #61 #62 #63 #64 #65 #66 #67
                 #68 #69 #70 #71 #72 #73 #74 #75 #76 #77 #78
                        fill=2          u=1  $ Outside Outer Ring
80  5  -7.9200   -61           u=2  $ Bottom Disk
81  5  -7.9200   -62           u=2  $ Intermediate Disk
82  5  -7.9200   -63           u=2  $ Intermediate Disk
83  5  -7.9200   -64           u=2  $ Intermediate Disk
84  5  -7.9200   -65           u=2  $ Intermediate Disk
85  5  -7.9200   -66           u=2  $ Intermediate Disk
86  5  -7.9200   -67           u=2  $ Top Disk
87  4  -0.9982   #80 #81 #82 #83 #84 #85 #86        u=2  $ Outside Plates
C Cells - LWT Cask Accident Conditions
201  6  -11.344  -204           $ BotPb
202  4  -0.9982  -203   fill=1  (0 0 133.35 )       $ Cavity
203  5  -7.9200  -202 +204           $ Bottom
204  5  -7.9200  -201 +202 +206 +209 +203 #202   $ OuterShell
205  5  -7.9200  -205 +208 +203           $ InnerShellTaper
206  5  -7.9200  -207 +203           $ InnerShell
207  6  -11.344  -208 +207           $ Lead
209  6  -11.344  -206 +205 +208           $ LeadTaper
209  0           -209 +208           $ LeadGap
210  8  -0.9982  +201 -210           $ Gap To Reflector
```

Figure 6.7.3-19   Sample NRU MCNP5 Input File for Accident Conditions (continued)

```
211  0             210            $ Outside

C Fuel Rod Surfaces
1  RCC  0.0000  0.0000  0.0000  0.0000  0.0000  1.1100  0.2350    $ Bottom End Plug Step 1
2  RCC  0.0000  0.0000  1.1099  0.0000  0.0000  7.7800  0.2743    $ BottomEndPlugStep2
3  RCC  0.0000  0.0000  8.8899  0.0000  0.0000  121.7778  0.2743   $ Fuel Meat
4  RCC  0.0000  0.0000  130.6677  0.0000  0.0000  8.8900  0.2743   $ Top End Plug
5  RCC  0.0000  0.0000  2.3019  0.0000  0.0000  129.3977  0.3505   $ Sheath / Aluminum Clad
6  RPP  -0.4775  0.4775  -0.0381  0.0381  2.3019  129.3977        $ Clad Fin
7  21  RPP  -0.4775  0.4775  -0.0381  0.0381  2.3019  129.3977    $ Clad Fin
8  23  RPP  -0.4775  0.4775  -0.0381  0.0381  2.3019  129.3977    $ Clad Fin
C Fuel Assembly Surfaces
11  RCC  0.0000  0.0000  0.0001  0.0000  0.0000  290.9998  0.4774   $ Fuel Rod Container
12  CZ  0.4773                   $ Rod outer surface
13  CZ  2.3122                   $ Inner Flow Channel Surface (may not be used)
14  RCC  0.0000  0.0000  0.1600  0.0000  0.0000  291.0010  2.4900   $ Outer Flow Channel Surface (may not be used)
15  RCC  0.0000  0.0000  0.1600  0.0000  0.0000  309.0080  2.4143   $ Caddy Inner Surface (may not be used)
16  RCC  0.0000  0.0000  0.0000  0.0000  0.0000  308.0080  2.5591   $ Caddy Outer Surface (may not be used)
C Tube Surfaces
51  RCC  0.0000  0.0000  0.6350  0.0000  0.0000  308.6100  2.9159  $ Tube Inside
52  RCC  0.0000  0.0000  -0.0001  0.0000  0.0000  309.2452  3.1903  $ Tube Outside and Cap
C Surfaces - Basket
61  RCC  0.0000  0.0000  -1.2700  0.0000  0.0000  1.2699  16.8529   $ Bottom Disk
62  RCC  0.0000  0.0000  49.5300  0.0000  0.0000  1.2700  16.8529   $ Intermediate Disk 1
63  RCC  0.0000  0.0000  100.3300  0.0000  0.0000  1.2700  16.8529  $ Intermediate Disk 2
64  RCC  0.0000  0.0000  151.1300  0.0000  0.0000  1.2700  16.8529  $ Intermediate Disk 3
65  RCC  0.0000  0.0000  201.9300  0.0000  0.0000  1.2700  16.8529  $ Intermediate Disk 4
66  RCC  0.0000  0.0000  252.7300  0.0000  0.0000  1.2700  16.8529  $ Intermediate Disk 5
67  RCC  0.0000  0.0000  303.5300  0.0000  0.0000  1.2700  16.8529  $ Top Disk
68  RCC  0.0000  0.0000  -1.2701  0.0000  0.0000  310.5152  16.8530   $ Basket Outline
69  RCC  0.0000  0.0000  0.0000  0.0000  0.0000  309.2450  3.1902    $ Tube Outline
C Surfaces - LWT Cask Accident Conditions
201  RCC  0.0000  0.0000  -26.6700  0.0000  0.0000  507.3650  36.5189  $ Lwt
202  RCC  0.0000  0.0000  -26.6700  0.0000  0.0000  26.6700  36.5189  $ Bottom
203  RCC  0.0000  0.0000  0.0000  0.0000  0.0000  452.1200  16.9863  $ Cavity
204  RCC  0.0000  0.0000  -17.7800  0.0000  0.0000  7.6200  26.3525  $ Bottom gamma shield
205  RCC  0.0000  0.0000  0.0000  0.0000  0.0000  444.5000  20.1740  $ Lead id - taper
206  RCC  0.0000  0.0000  0.0000  0.0000  0.0000  444.5000  31.5976  $ Lead od - taper
207  RCC  0.0000  0.0000  13.8176  0.0000  0.0000  416.8648  18.9103  $ Lead id
208  RCC  0.0000  0.0000  13.8176  0.0000  0.0000  416.8648  33.3271  $ Lead od
209  RCC  0.0000  0.0000  13.8176  0.0000  0.0000  416.8648  33.4645  $ Lead gap
210  RCC  0.0000  0.0000  -46.6700  0.0000  0.0000  547.3650  56.5189  $ Container

C
C Materials List
C
C - wt%
m1  92235.69c  -2.0590E-01
    92238.69c  -1.3143E-02
    13027.62c  -7.8095E-01
C Aluminum
m2  13027.62c  -1.0
C Tube Cavity Water
m3  1001.62c  6.6667E-01  8016.62c  3.3333E-01
mt3  lwtr.60t
C Cask Cavity Water
m4  1001.62c  6.6667E-01  8016.62c  3.3333E-01
mt4  lwtr.60t
C Stainless Steel 304
m5  26000.55c  -0.695  24000.50c  -0.190  28000.50c  -0.095
    25055.62c  -0.020
C Lead
m6  82000.50c  -1.0
C Aluminum Honeycomb Impact Limiter
m7  13027.62c  -1.0
C Water/Glycol - Cask Neutron Shield
m9  1001.62c  -1.03651E-01  8016.62c  -6.75619E-01  6000.66c  -2.20730E-01
C Cask Exterior (Water at Various Densities)
m8  1001.62c  6.6667E-01  8016.62c  3.3333E-01
mt8  lwtr.60t
C
C Cell Importances
imp:n 1 75r 0
c
c Criticality Controls
c
kcode  2000  1.00  30  530
c
c Source Distribution for Initial Generation
SDEF  CEL= 202:D4:51:D5:2
      ERG= D1
      POS= 0.0000  0.00  8.8899
      RAD= D2
      AXS= 0.00  0.00  1.00
      EXT= D3
C - Neutron Source Energy Source Distribution
#          SP1
      -3
C - Uniform Radial Distribution in Fuel Rod
#  SI2  SP2
```

Figure 6.7.3 -19   Sample NRU MCNP5 Input File for Accident Conditions (continued)

```
          0.0000  -21
          0.2743   1
C - Axial Source Profile
#   SI3  SP3
          0   0.0
        274   1.0
C - 18 Tubes in Cask
#      SI4          SP4
          1            d
         61  1
         62  1
         63  1
         64  1
         65  1
         66  1
         67  1
         68  1
         69  1
         70  1
         71  1
         72  1
         73  1
         74  1
         75  1
         76  1
         77  1
         78  1
C - Rods Per Assembly
#      SI5          SP5
          1            d
         11  1
         12  1
         13  1
         14  1
         15  1
         16  1
         17  1
         18  1
         19  1
         20  1
         21  1
         22  1
*TR1    6.3810  0.0000  0.0000  0 90 90 -90 0 90 90 90 0
*TR2    3.1905  5.5261  0.0000  0 90 90 -90 0 90 90 90 0
*TR3   -3.1905  5.5261  0.0000  0 90 90 -90 0 90 90 90 0
*TR4   -6.3810  0.0000  0.0000  0 90 90 -90 0 90 90 90 0
*TR5   -3.1905 -5.5261  0.0000  0 90 90 -90 0 90 90 90 0
*TR6    3.1905 -5.5261  0.0000  0 90 90 -90 0 90 90 90 0
*TR7   11.9071  3.1905  0.0000  0 90 90 -90 0 90 90 90 0
*TR8    8.7166  8.7166  0.0000  0 90 90 -90 0 90 90 90 0
*TR9    3.1905 11.9071  0.0000  0 90 90 -90 0 90 90 90 0
*TR10  -3.1905 11.9071  0.0000  0 90 90 -90 0 90 90 90 0
*TR11  -8.7166  8.7166  0.0000  0 90 90 -90 0 90 90 90 0
*TR12 -11.9071  3.1905  0.0000  0 90 90 -90 0 90 90 90 0
*TR13 -11.9071 -3.1905  0.0000  0 90 90 -90 0 90 90 90 0
*TR14  -8.7166 -8.7166  0.0000  0 90 90 -90 0 90 90 90 0
*TR15  -3.1905 -11.9071 0.0000  0 90 90 -90 0 90 90 90 0
*TR16   3.1905 -11.9071 0.0000  0 90 90 -90 0 90 90 90 0
*TR17   8.7166 -8.7166  0.0000  0 90 90 -90 0 90 90 90 0
*TR18  11.9071 -3.1905  0.0000  0 90 90 -90 0 90 90 90 0
*TR21   0.0 0.0 0.0 60 150 90 -30 60 90 90 90 0    $ z-rotation 60 degrees
*TR22   0.0 0.0 0.0 90 180 90 0 90 90 90 90 0      $ z-rotation 90 degrees
*TR23   0.0 0.0 0.0 -60 30 90 -150 -60 90 90 90 0  $ z-rotation -60 degrees
C Print Control
prdmp   -30 -60 1 2
print
C Random Number Generator
rand  gen=2  seed=19073486328125  stride=152917  hist=1
```

Table 6.7.3-1   NRU/NRX Fuel Characteristics

Description		NRU [HEU]	NRX	NRU [LEU]
Fuel Rod Height	cm	291	293	291
Top End Plug Height	cm	9.6	11.1125	9.6
Bottom End Plug Height	cm	9.9	11.1125	9.9
End Plug OD	cm	0.5486	0.635	0.5486
Active Length	cm	274	274	274
Rod Diameter	cm	0.955	1.04	0.955
Clad Thickness	cm	0.0762	0.0762	0.0762
Fuel Meat Diameter	cm	0.5486	0.635	0.5486
Fuel Assembly Height	cm	291	321	291
Fuel Assembly OD	cm	4.98	3.5	4.98
Flow Tube Thickness	cm	0.1778	0.1778	0.1778
Number of Fuel Rods		12	7	12
Mass 235U [Rod]	g	41.36	78.68	43.68
Mass U [Rod]	g	44	83.7	208
Mass Fuel Meat [Rod]	g	210	276.7	
Clad Fin Thickness	cm	0.0762	0.0762	0.0762
Clad Fin Length	cm	0.1270	0.1270	0.1270

Table 6.7.3-2   NRU/NRX Evaluated Fuel Parameters

Description		NRU [HEU]	NRX	NRU [LEU]
Fuel Rod Height	cm	291	291	291
Top End Plug Height	cm	8.89	8.89	8.89
Bottom End Plug Height	cm	8.89	8.89	8.89
End Plug OD	cm	0.5486	0.635	0.5486
Active Length	cm	274	274	274
Rod Diameter	cm	0.955	1.04	0.955
Clad Thickness	cm	0.0762	0.0762	0.0762
Fuel Meat Diameter	cm	0.5486	0.635	0.5486
Fuel Assembly Height	cm	291	291	291
Fuel Assembly OD	cm	4.98	3.5	4.98
Flow Tube Thickness	cm	0.1778	0.1778	0.1778
Number of Fuel Rods		12	7	12
Mass 235U [Rod]	g	43.24	79.05	43.68
Mass U [Rod]	g	46	84.1	208
Mass Fuel Meat [Rod]	g	210	276.7	349.1

Table 6.7.3-3   NRU/NRX Basket and Cask Parameters

Description	Dimension [in]
Fuel tube outer diameter	2.5
Fuel tube wall thickness (stainless steel)	0.065
Fuel tube outer diameter tolerance	±0.012
Fuel tube thickness tolerance	±10%
Caddy Outer Diameter	2.0
Caddy Wall Thickness	0.065
Caddy Outer Diameter Tolerance	0.005
Caddy Wall Thickness Tolerance	0.004
Outer ring tube location diameter	9.78
Inner ring tube location diameter	5.06
Fuel basket outer diameter	13.27
Fuel basket disc thickness (stainless steel)	0.5
Cask cavity diameter	13.375
Lead shield inner diameter	14.89
Lead shield outer diameter	26.35
Lead shield outer diameter of taper	24.88
Cask outer diameter	28.755
Cask lid thickness	11.25
Bottom forging thickness	10.5
Bottom forging lead insert diameter	20.75
Bottom forging lead insert thickness	3
Offset bottom of cask to lead	3.5
Neutron shield thickness	5
Neutron shield tank skin	0.236

Table 6.7.3-4   Composition Densities Used in Criticality Analysis of NRU/NRX Fuel

Material	NRU HEU U-Al	NRX HEU U-Al	NRU LEU U-AlSi
Density, gm/cc	3.2419	3.1888	5.3899
Nuclide	Atoms/barn-cm		
Uranium 235	1.636E-3	2.323E-3	1.728E-3
Uranium 238	1.031E-4	1.464E-4	6.417E-3

Material	Al Clad	H_2O	304 Stainless Steel	Pb	H_2O/ Glycol
Density, gm/cc	2.702	0.998	7.920	11.344	0.9669
Nuclide	Atoms/barn-cm				
Aluminum	6.031E-2				
Oxygen		3.338E-2			2.459E-2
Hydrogen		6.675E-2			5.988E-2
Iron			5.936E-2		
Chromium			1.743E-2		
Nickel			7.721E-3		
Manganese			1.736E-3		
Lead				3.299E-2	
Carbon					1.070E-2

Table 6.7.3-5   NRU Manufacturing Tolerance Study

Tube Tolerance		k_{eff}	σ	$k_{eff} + 2\sigma$	$\Delta(k_{eff} + 2\sigma)/\sigma$
Thickness	OD				
Nom	Nom	0.90919	0.00080	0.91079	--
Nom	Min	0.90912	0.00077	0.91066	-0.1
Nom	Max	0.90981	0.00082	0.91145	0.6
Min	Nom	0.92474	0.00083	0.92640	13.5
Max	Nom	0.89374	0.00079	0.89532	-13.8
Min	Max	0.92398	0.00081	0.92560	13.0

Table 6.7.3-6   Maximum Reactivity Summary

Description	Cask Configuration (Single / Array)	$k_{eff} + 2\sigma$
10 CFR 71.55	Single Cask – Normal Conditions	0.92525
	Single Cask - Accident Conditions	0.92560
10 CFR 71.59	Infinite Array – Normal Conditions	0.07690
	Single Cask "Array" - Accident Condition	0.92560

Table 6.7.3-7   Cask Fuel Conditions for Maximum System Reactivity

	10 CFR 71.55		10 CFR 71.59	
Condition	Normal	Accident	Normal	Accident
Fuel Type	NRU HEU	NRU HEU	NRU HEU	NRU HEU
Fuel Enrichment	94wt% ^{235}U	94wt% ^{235}U	94wt% ^{235}U	94wt% ^{235}U
Fuel Condition	Broken Rods	Broken Rods	Broken Rods	Broken Rods
Cask/Array	Single Cask	Single Cask	Infinite Array	Single Cask
Neutron Reflection	20 cm Water	20 cm Water	N/A^2	20 cm Water
Neutron Shield	Yes	No	Yes^1	No
Cask Lead / Outer Steel Shell	Yes	Yes	Yes^1	Yes
Fuel Tube Interior Moderator	0.9982 g/cm^3	0.9982 g/cm^3	0 g/cm^3	0.9982 g/cm^3
Fuel Tube Exterior Moderator	0.9982 g/cm^3	0.9982 g/cm^3	0 g/cm^3	0.9982 g/cm^3
Cask Exterior Moderator	0.9982 g/cm^3	0.9982 g/cm^3	N/A^2	0.9982 g/cm^3

Notes:
1.) Section 6.7.3.7 demonstrates that removing cask material outside the containment boundary (cask inner shell) reduces system reactivity.
2.) MCNP reflective boundary condition is applied to the cask surface.

6.7.4   HEUNL

This section includes input, analysis method, and results for the NAC-LWT cask containing a payload of four HEUNL containers. The transport package is evaluated in compliance with 10 CFR 71.59 and 10 CFR 71.55. The evaluation considers an H/U study, shift study, moderator study, and container tolerance study.

6.7.4.1   Package Fuel Loading

Four HEUNL containers may be loaded into the NAC-LWT. The HEUNL material consists of uranyl nitrate, various other nitrates, and water. Composition of the HEUNL material is provided in Table 6.7.4-1. The evaluated nitrate contents are further detailed in Table 6.7.4-2. The HEUNL material density at 25°C is 1.30 g/cc.

The actual and modeled actinide concentrations are listed in Table 6.7.4-3. The HEUNL is conservatively modeled by increasing the ^{235}U partial density to 7.2 g/L. ^{234}U and ^{236}U are conservatively modeled as ^{238}U. ^{234}U ($\sigma_t = 116$ b) and ^{236}U ($\sigma_t = 14.1$ b) have higher absorption cross-sections than ^{238}U ($\sigma_t = 12.2$ b). Removing absorption from the criticality model is conservative. The evaluated ^{235}U partial density bounds all provided design input for the processed material. Additional analysis is performed for the target material initial enrichment. This additional analysis increases enrichment to 93.4 wt. % at a ^{235}U partial density of 7.40 g/L.

The HEUNL solution contains a negligible amount of ^{237}Np, ^{239}Pu, and ^{240}Pu. These isotopes are less than 0.001 wt. % of the solution and are therefore excluded from the MCNP model. Removal from the criticality evaluation will have a negligible effect.

The evaluated isotopic content for the HEUNL material is listed in Table 6.7.4-4. Critical properties for the HEUNL criticality evaluation are summarized in Table 6.7.4-5.

The water content of the solution is calculated using the solution density and nitrate inventory. The calculated water content is approximately 68 wt. %. The criticality analysis includes the uranyl nitrate at various geometries with water intrusion in the material lattice for optimal moderation. For the fissile material geometry study, a bounding container cavity volume of 17.0 gal (64.3 L) is applied. Due to void volume in the container that allows HEUNL thermal expansion, actual container capacity is less. For the initial nominal studies, a standard fill using the modeled container cavity volume is applied. The nominal case is bounded by the optimal fissile material geometry.

6.7.4.2   Criticality Model Specifications

This section describes the models that are used in the criticality analyses for the NAC-LWT cask containing four HEUNL containers. The models are analyzed separately under normal

conditions and hypothetical accident conditions to ensure that all possible configurations are subcritical.

Each model uses the MCNP5 v1.60 code package with the cross-section libraries validated for highly enriched uranyl nitrates (see Section 6.5.7). No cross-section pre-processing is required prior to MCNP use. MCNP uses the Monte Carlo technique to calculate the k_{eff} of a system.

Description of Calculational Models

Four HEUNL containers are modeled in the NAC-LWT. The containers and cask are modeled as described in the license drawings. Tube quick disconnect fittings, the bottom portion of the container outer shell that rests on the shoulder and axially overlaps the container and neck, and base plate are conservatively omitted from the shielding model. Removal of stainless steel, an absorption material, is conservative for the criticality evaluation.

Containers are shifted towards the top of the cask cavity. Axial location of the containers will have a negligible effect on the criticality evaluation. For all configurations, containers are modeled as touching to increase neutronic coupling. No evaluation of potential separation of containers with moderation is necessary as the optimal H/U ratio is established in the maximum reactivity configuration studies. Increased separation would only increase neutron leakage.
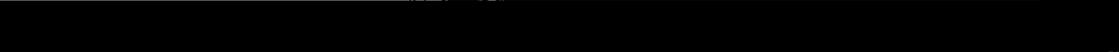
██ The flat configuration will have negligible effects on the criticality evaluation as a bounding container cavity volume is applied.

The criticality evaluation considers both normal and accident conditions. The accident conditions of transport include the loss of neutron shielding material, the neutron shield shell, and the impact limiters.

The geometric description of a MCNP model is based on the combinatorial geometry system embedded in the code. In this system, bodies such as cylinders and rectangular parallelepipeds and their logical intersections and unions are used to describe the extent of material zones.

Detailed model parameters used in creating the three-dimensional model are derived from the license drawings. Elevations associated with the three-dimensional features are established with respect to the center bottom of the NAC-LWT cask cavity for the MCNP combinatorial model.

The three-dimensional NAC-LWT MCNP models are shown in Figure 6.7.4-1 through Figure 6.7.4-3, while sketches are shown in Figure 6.7.4-4 through Figure 6.7.4-6. Select container dimensions critical to the MCNP model are listed in Table 6.7.4-6.

Package Regional Densities

The composition densities (g/cc) and nuclide number densities (atm/b-cm) evaluated in subsequent criticality analyses are shown in Table 6.7.4-7.

6.7.4.3   Criticality Calculations

This section presents the criticality analyses for the NAC-LWT cask with HEUNL containers. Criticality analyses are performed to satisfy the criticality safety requirements of 10 CFR Parts 71.55 and 71.59, as well as IAEA SSR-6.

The maximum reactivity configuration is determined by implementing a series of studies. The series of studies are designed to meet 10 CFR 71.55 (b) and (e) requirements on normal and accident condition single casks. The single cask analysis by regulation must consider a fully water reflected package and be at optimum physical configuration and moderation. Each study will retain the maximum reactivity configuration from the previous study.

After the single cask analysis is complete, cask array analysis is performed to meet 10 CFR 71.59 requirements. Per the standard review plan (NUREG-1617) the 10 CFR 71.59 requirements are met by evaluating a cask array with dry cask interior and cask exterior for normal condition and optimum interior and exterior moderated array for accident conditions (see Sections 6.5.5 and 6.5.6 in NUREG-1617). ████████████████████ As the HEUNL containing cask array is evaluated as an infinite array, the exterior to the array condition is not applicable.

10 CFR 71.55 Scoping Calculation

In compliance with 10 CFR 71.55 the scoping calculations are based on a single cask with a 20 cm boundary from the cask exterior dimensions. The space between cask and boundary is flooded with full density water to produce a fully water reflected system.

Initial scoping analysis evaluates cask interior flooding conditions. Due to the system containing little cavity volume for moderation, flooding conditions have negligible effects on reactivity. Normal and accident configuration casks are expected and are confirmed to be similar from a neutronics perspective. Geometry differences are limited to the presence/absence of the neutron shield. For a fully water reflected cask, differences in neutron tracking between the models are those associated with ethyl glycol/water in the first 5 inches of reflector and Monte Carlo differences for tracking through the additional reflector.

Table 6.7.4-8 contains a summary of the scoping results. Maximum reactivity is obtained by a void cask interior. Either normal or accident condition cask geometry can be chosen for the following evaluations without a statistically significant difference in result. For this calculation the accident condition cask geometry was chosen.

10 CFR 71.55 Uranyl Nitrate H/U Study

As shown in the scoping analysis, the nominal HEUNL solution k_{eff} is below limits. The nominal HEUNL solution is defined for this criticality evaluation as the loaded solution. The worst case configuration for the HEUNL includes all non-fissile nitrates precipitating out from the solution leaving only a uranyl nitrate-water mixture.
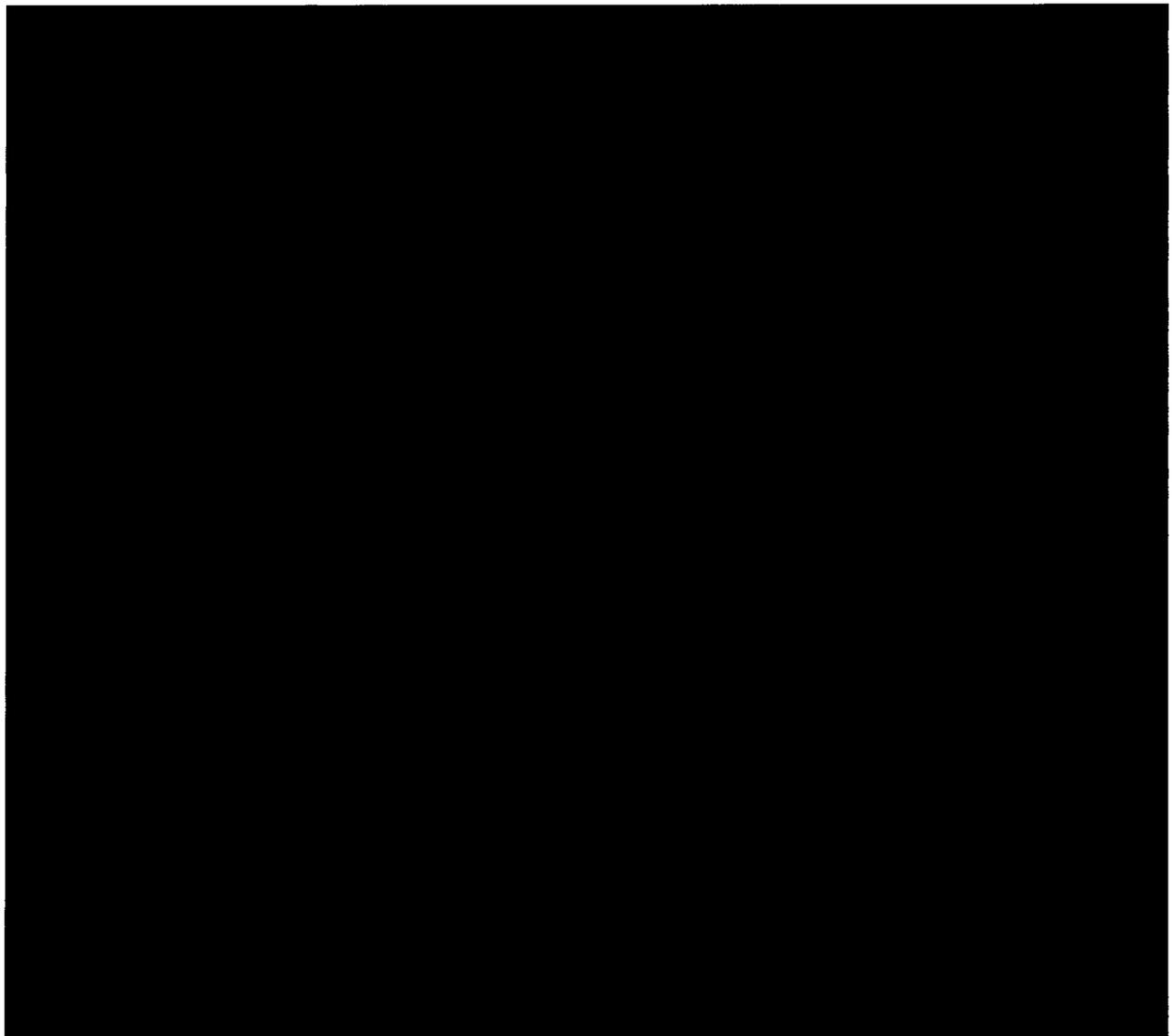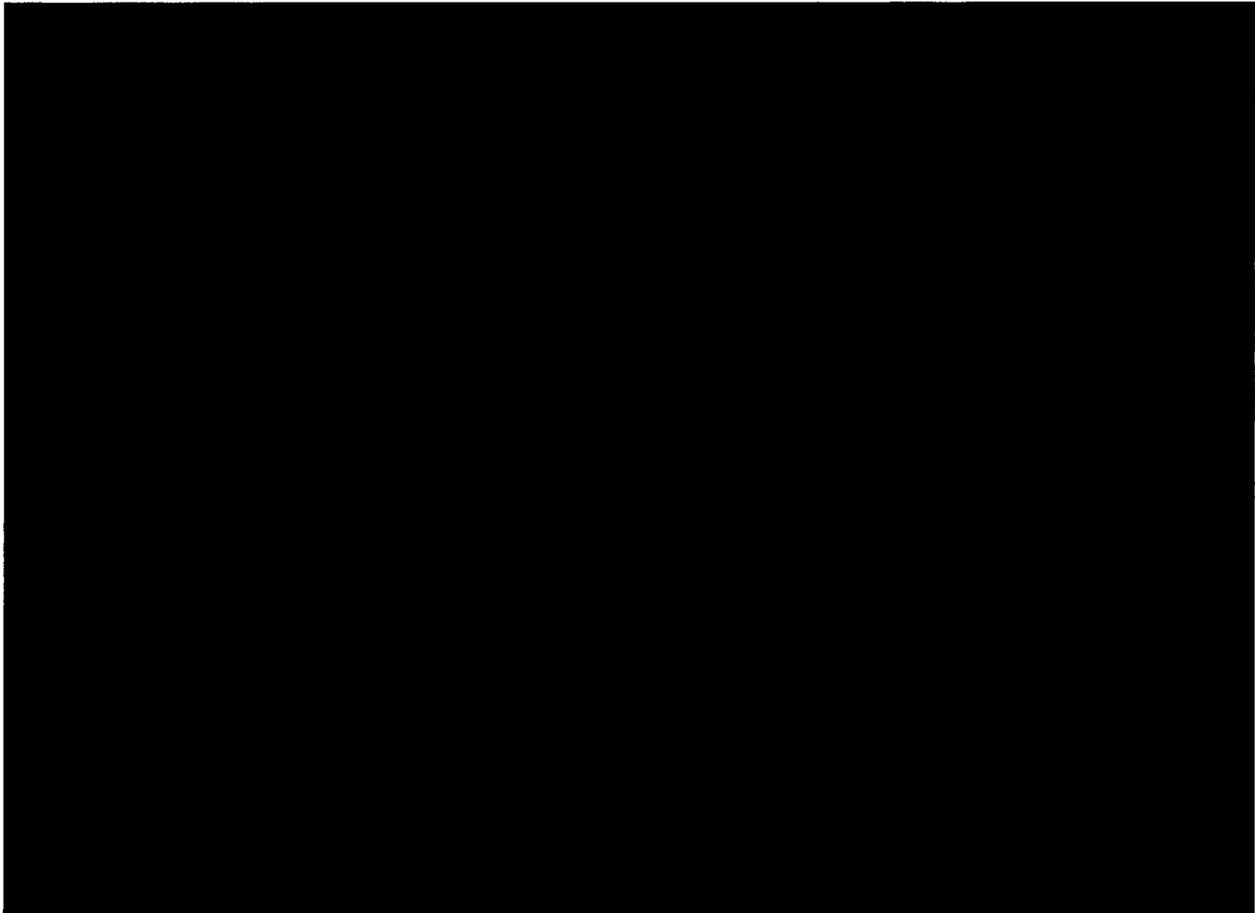
10 CFR 71.55 Uranyl Nitrate Shift and Cask Cavity Moderator Study
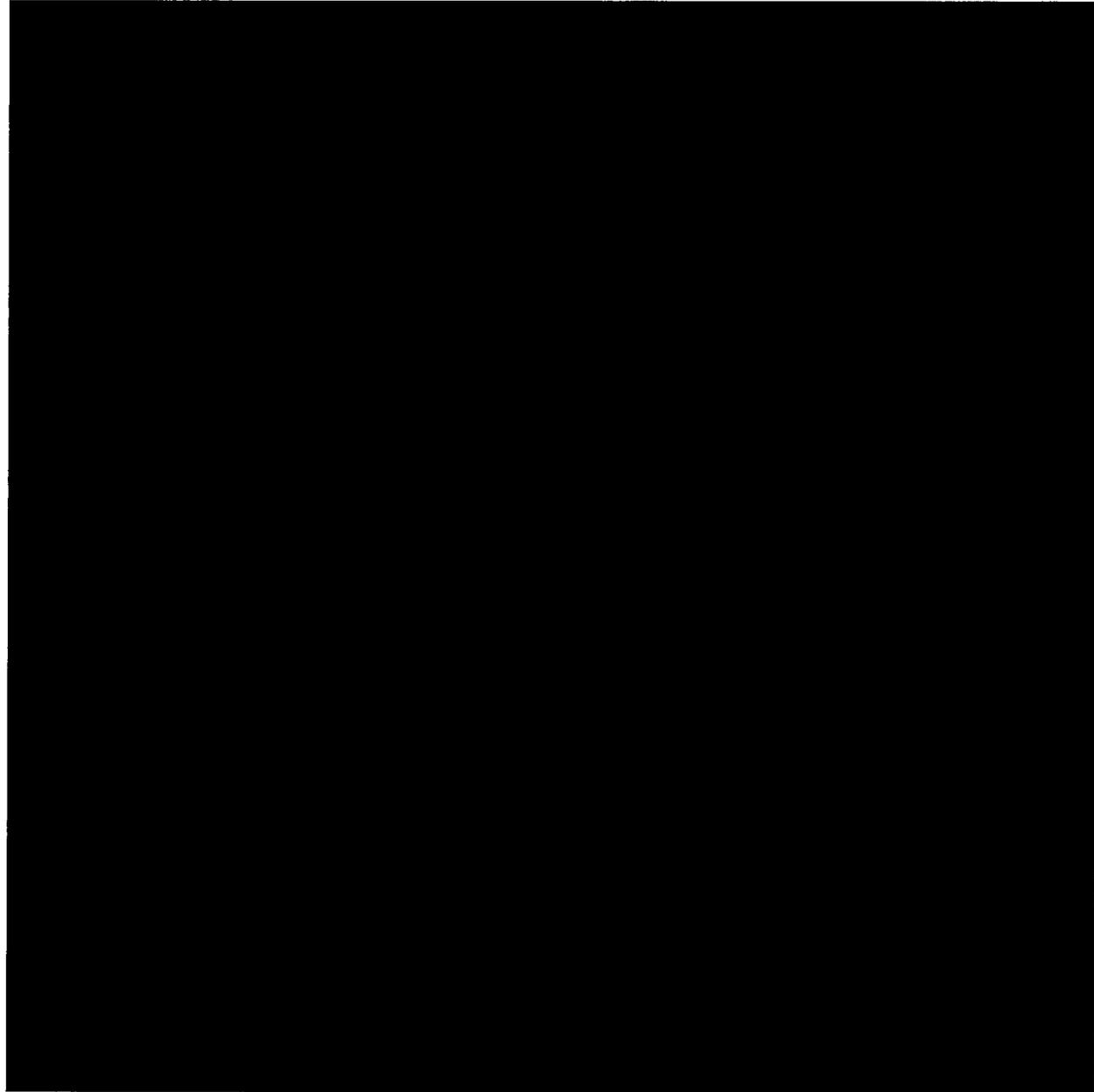
10 CFR 71.55 Optimum Tolerance Studies

Results for the tolerance study are shown in Table 6.7.4-14. The tolerance results show no statistically significant increase for any tolerance. Therefore, tolerances will not be applied in the maximum configuration.

MCNP Validated Libraries

The MCNP models use the cross-section libraries validated for highly enriched uranyl nitrates (see Section 6.5.7). The evaluated libraries are listed in Table 6.7.4-20.

The ZAID library for lead, 82000.50c, was not included in the MCNP validation highly enriched uranyl nitrates. Lead is used as a shield material in the NAC-LWT MCNP model. Exterior reflector material validation is not a significant issue for moderated systems where fuel region neutronic interaction, not reflection, is the primary reactivity driver.

The ZAID library for mercury, 80000.42c, was not included in the MCNP validation of highly enriched uranyl nitrates. Mercury is a strong absorber with capture cross section, σ_γ, of 376 b. Therefore, mercury is replaced in the MCNP model with aluminum ($\sigma_\gamma = 0.23$ b) to account for

the lack of validation for mercury. The previously established maximum reactivity configuration is retained for this study. As shown in Table 6.7.4-15, removal of mercury statistically increases system reactivity.

All other evaluated libraries are accounted for in the validation.

10 CFR 71.55 Maximum Reactivity Summary

Based on the previous studies, the following conditions are bounding for the maximum reactivity configuration:

- Uranyl nitrate – water mixture in ███████████████████
- Uranyl nitrate – water mixture optimally moderated
- Uranyl nitrate mixtures shifted in alternating configuration
- Dry cask cavity
- Mercury removed from model

Maximum system reactivities are determined with this maximum reactivity configuration under normal (neutron shield present) and accident (no neutron shield) conditions. As seen in Table 6.7.4-16, the maximum reactivity is 0.8952 and below the USL of 0.9366.

10 CFR 71.55 (b) (3) requires an evaluation of the NAC-LWT with the containment system fully reflected by water. The containment for the NAC-LWT is the cask inner shell. While no operating condition results in a removal of the cask outer shell and lead gamma shield, the most reactive case is re-evaluated by removing the lead and outer shells (including neutron shield), and reflecting the system by water at full density. Using the maximum reactivity configuration, the calculated $k_{eff}+2\sigma$ is 0.86235, which is significantly below that of the full cask water reflected model (i.e., neutron reflection produced by the lead gamma shield and outer steel cask shell produces a higher reactivity system than that produced by a water reflector.

10 CFR 71.59 Maximum Reactivity Summary

10 CFR 71.59 (a) (1) requires the evaluation of five times "N" normal condition packages. 10 CFR 71.59 (a) (2) requires the evaluation of two times "N" accident condition packages with optimum moderation. Both normal and accident conditions specified by the CFR are satisfied with the maximum reactivity configuration defined for the 10 CFR 71.55 evaluation. The model is modified by applying a reflecting surface at the cask exterior surface. This option produces an infinite array of casks. As seen in Table 6.7.4-17, while slightly increasing system reactivity above that of a single cask, both results are below the USL of 0.9366.

The resulting CSI for an infinite array of NAC-LWT casks with HEUNL is 0.

Water Reflector and Canister Dimensions

Increased Enrichment Evaluation

Previous analyses were based on measured uranium concentrations for the processed material. The analysis in this section applies the maximum initial enrichment of the target material, 93.4 wt. %. The partial density of ^{235}U is also increased from 7.20 g/L to 7.40 g/L. The modeled H/U ratio is slightly reduced from 547 to 533 for this model due to the changes in ^{235}U concentration (i.e., the sphere radius is held constant). All H/U ratios for the HEUNL evaluations and the validation in Section 6.5.7 for uranyl nitrates are in terms of moderator to fissile ratio (^{235}U). The evaluated HEUNL properties for the increased enrichment are provided in Table 6.7.4-21.

The 30 cm water reflector and increased container length are retained for this evaluation. Results for the 10 CFR 71.55 (b) and (e) evaluations are listed in Table 6.7.4-22. Results for the 10 CFR 71.59 (a) evaluations are listed in Table 6.7.4-23. For the 10 CFR 71.55 (b) (3) evaluation, the reactivity is calculated to be 0.8722. All results remain under the USL of 0.9366.

6.7.4.4   Code Validation and Area of Applicability

Critical benchmarks and USL are discussed in detail in Section 6.5.7. The following evaluates the applicability of the USL to HEUNL.

The area of applicability (AoA) for the validation is compared to the system parameters for the NAC-LWT with HEUNL most reactive case. The USL, 0.9366, used for this calculation is based on the energy of the average neutron lethargy causing fission (EALCF). Table 6.7.4-18 shows the validated range of EALCF. The USL for the validation is the minimum USL from the EALCF range. The EALCF for the most reactive HEUNL case is 0.04 eV and is within the validation range.

Exceeding the area of applicability for enrichment of the benchmark cases is acceptable as the parameter has a trend that is statistically insignificant (R = 0.05) and the difference outside the range is small (0.18 wt. %) relative to the margin to the USL (> 0.02).

6.7.4.5   Allowable Cask Loading

Based on the results of the previous sections, loading of 4 HEUNL containers is allowed in the NAC-LWT. Maximum content of the container is limited to 17 gallons of solution with a maximum 7.40 g ^{235}U per liter. The transport package has been found to be in compliance with 10 CFR 71.59 and 10 CFR 71.55. The maximum reactivity, including two sigma, of 0.9137 for the transport package is subcritical. This evaluation has considered an H/U study, shift study, moderator study, and container tolerance study. The transport package has been designated a CSI of 0.

Figure 6.7.4-1   VISED X-Z Cross-Section of NAC-LWT with HEUNL

Figure 6.7.4-2   VISED X-Z Cross-Section of HEUNL Container Detail

Figure 6.7.4-3   VISED X-Y Cross-Section of NAC-LWT with HEUNL
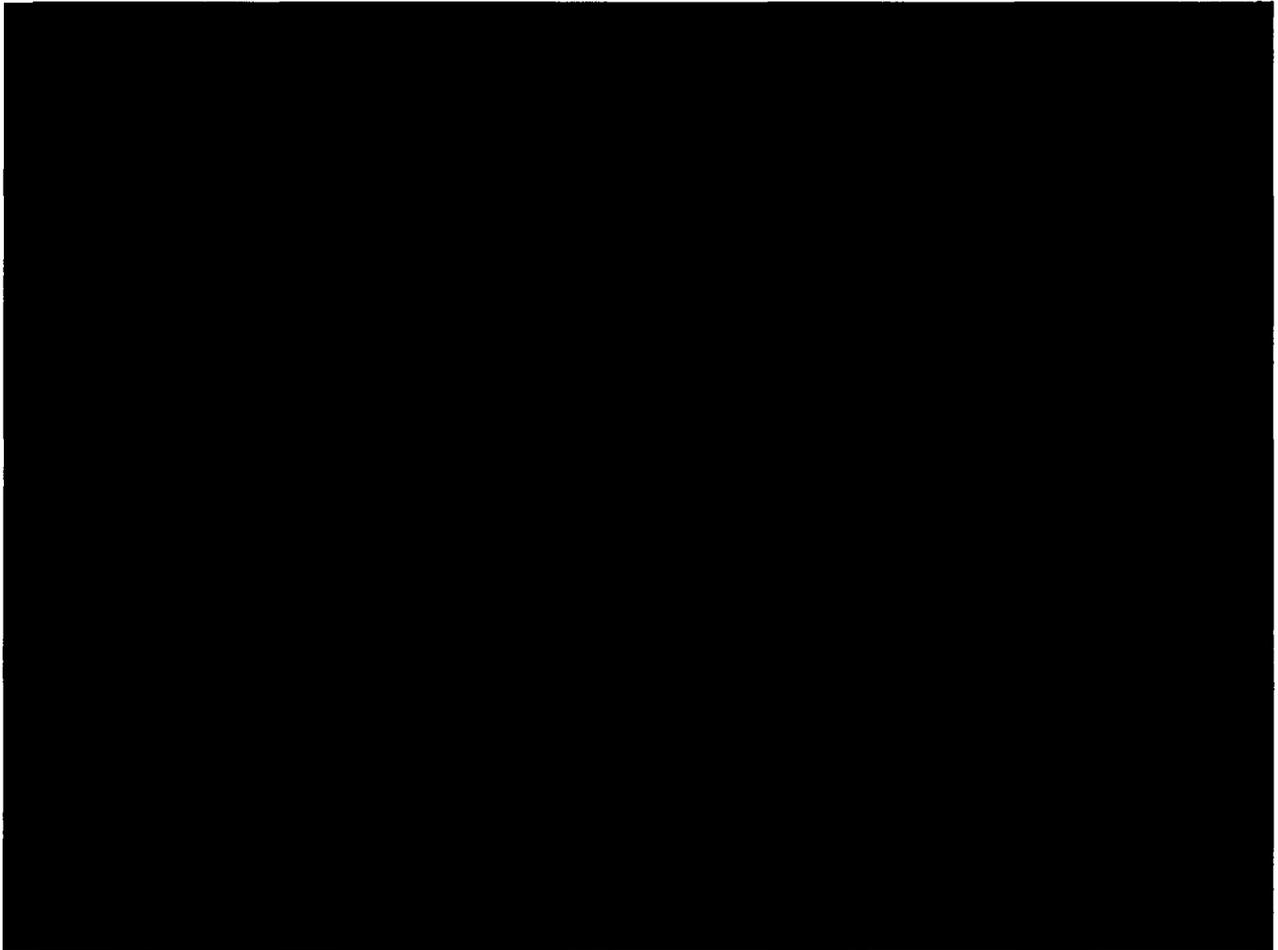
Figure 6.7.4-4   Axial Sketch of NAC-LWT with HEUNL
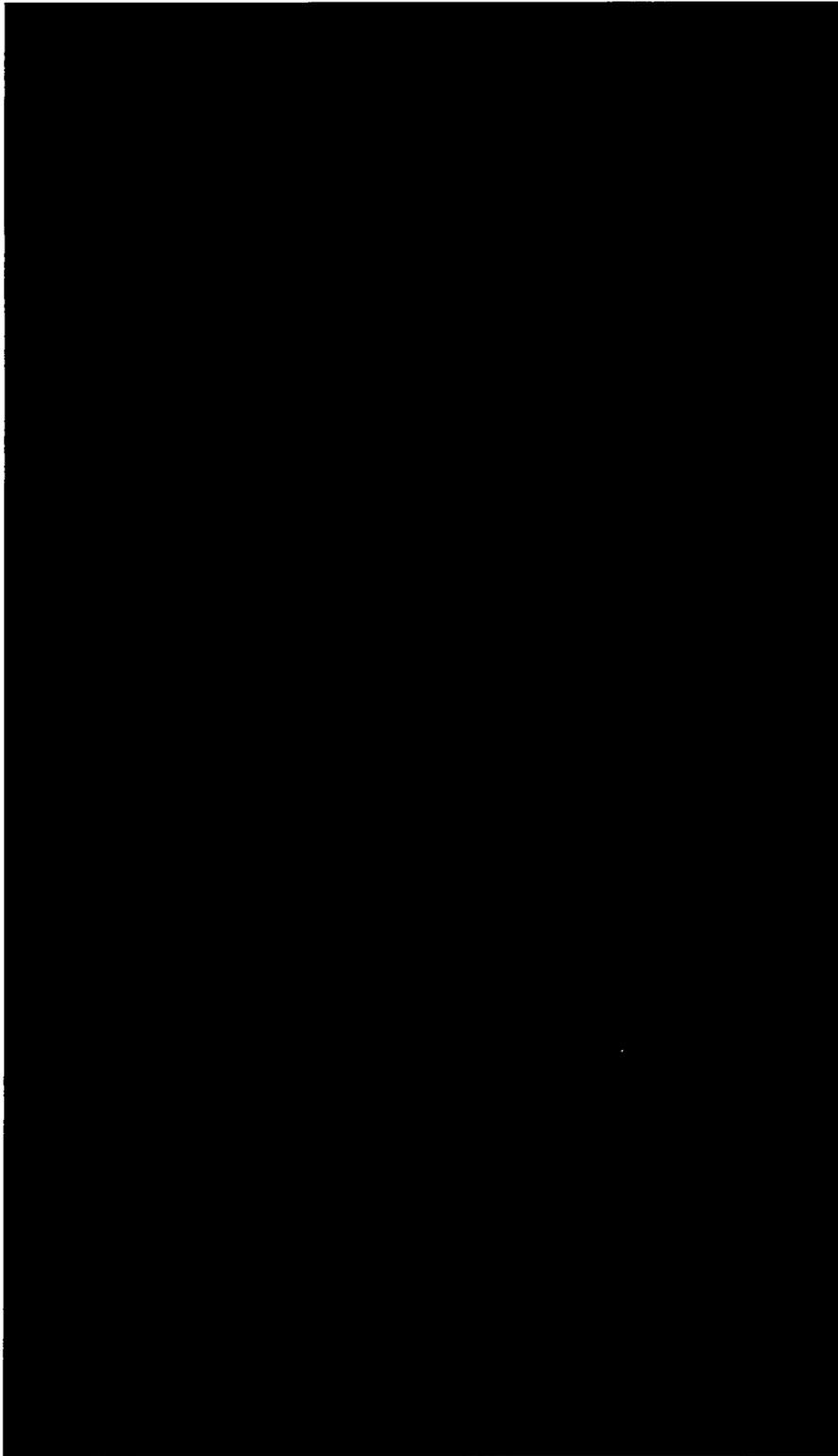
Figure 6.7.4-5   Radial Sketch of NAC-LWT with HEUNL

Figure 6.7.4-6   Axial Sketch of HEUNL Container
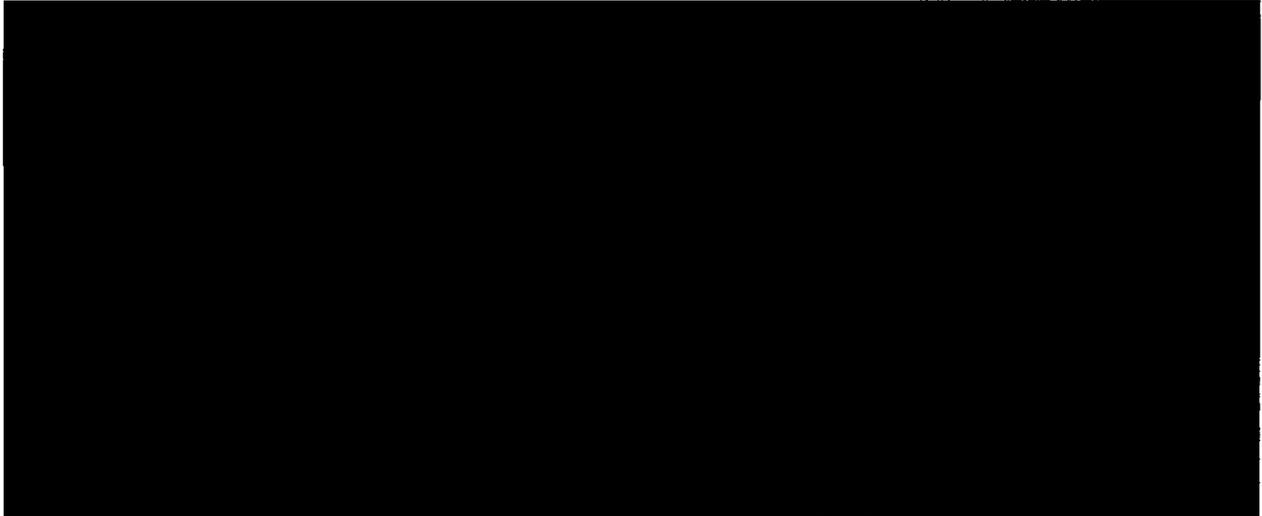
Figure 6.7.4-7   Reactivity Results by HEUNL ███████ H/U Ratio
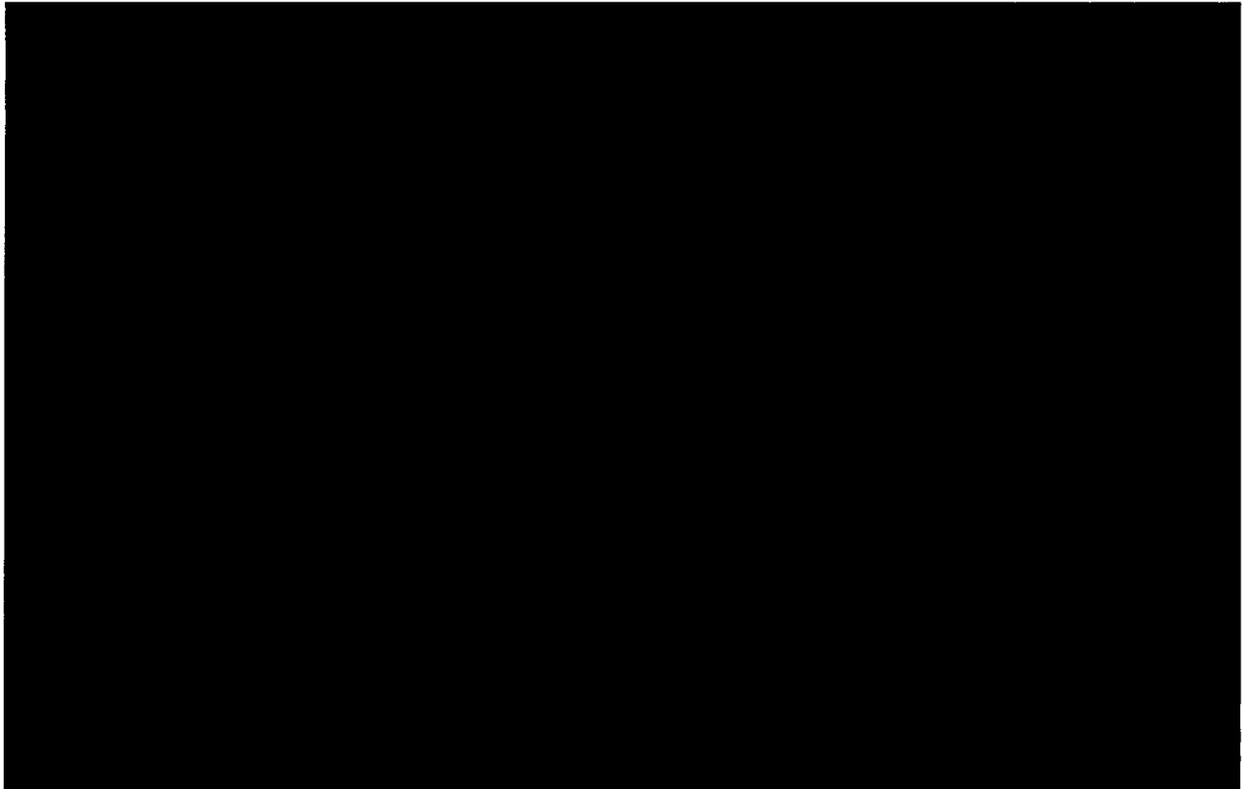
Figure 6.7.4-8   Reactivity Results by HEUNL ███████ H/U Ratio

Figure 6.7.4-9   VISED X-Z Cross-Section of HEUNL with Alternating Shift

Figure 6.7.4-10   VISED X-Z Cross-Section of HEUNL with Inward Shift
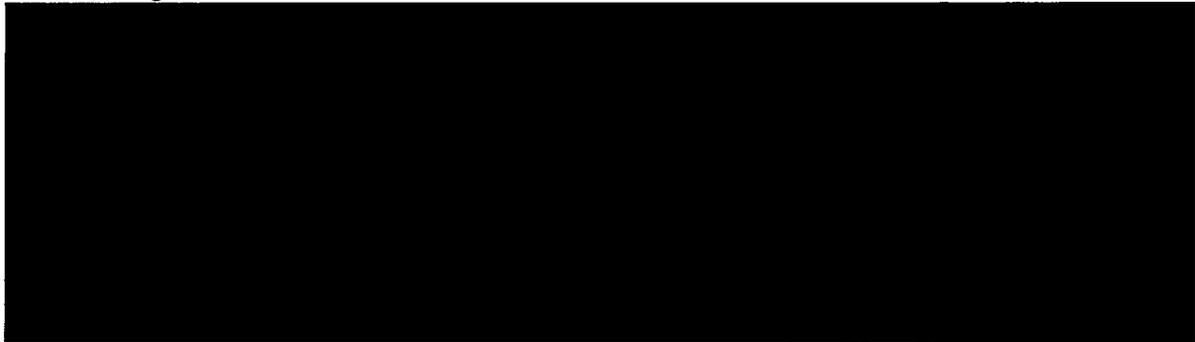
Figure 6.7.4-11   Cask Cavity Moderator Study Reactivity Results for HEUNL
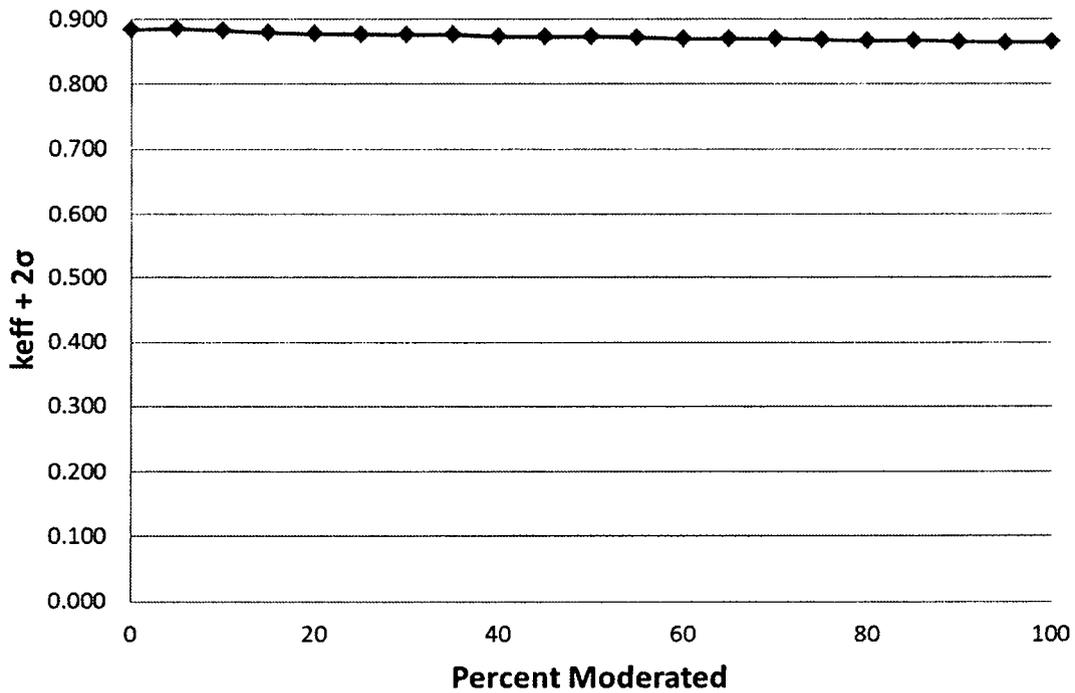
Table 6.7.4-1   Composition of HEUNL Solution

Chemical Compound	Concentration (mol/L)	Concentration of Metal Ion (g/L)
HNO_3	0.96	N/A
$Al(NO_3)_3$	1.5	40.5
$Hg(NO_3)_2$	0.053	10.6
$Fe(NO_3)_3$	0.019	1.06
$Cr(NO_3)_3$	0.005	0.26
$Ni(NO_3)_2$	0.003	0.18

Table 6.7.4-2   HEUNL Evaluated Model Composition

| Solution	Metal Ion	mol/L	A_r (metal)	Concentration (g/L)			
				Ion	N	O	Solution
HNO_3	H	0.96	1.00794	0.97	13.45	46.06	60.48
$Al(NO_3)_3$	Al	1.5	26.982	40.5	63.03	215.92	319.42
$Hg(NO_3)_2$	Hg	0.053	200.59	10.6	1.48	5.09	17.20
$Fe(NO_3)_3$	Fe	0.019	55.845	1.06	0.80	2.73	4.59
$Cr(NO_3)_3$	Cr	0.005	51.9961	0.26	0.21	0.72	1.19
$Ni(NO_3)_2$	Ni	0.003	58.6934	0.18	0.08	0.29	0.55
$UO_2(NO_3)_2$	U	0.0337	235.1738	7.925	0.94	4.31	13.18
			Total:		80.00	275.12	416.61

Table 6.7.4-3   HEUNL Actinide Concentration

Nuclide	DI Conc. (g/L)	Modeled Conc. (g/L)	Modeled wt. %
^{234}U	1.23E-01	--	--
^{235}U	7.00E+00	7.20E+00	90.85%
^{236}U	1.53E-01	--	--
^{238}U	4.49E-01	7.25E-01	9.15%

Table 6.7.4-4   Evaluated HEUNL Isotopic Composition

Element	Z	A	Conc. (g/L)	wt.%
H	1	1	9.676E-01	0.074%
Al	13	27	4.047E+01	3.113%
Hg	80	NA[1]	1.063E+01	0.818%
Fe	26	NA	1.061E+00	0.082%
Cr	24	NA	2.600E-01	0.020%
Ni	28	NA	1.761E-01	0.014%
N	7	14	8.000E+01	6.154%
O	8	16	2.751E+02	21.163%
U	92	234	1.230E-01	0.009%
	92	235	7.200E+00	0.554%
	92	236	1.530E-01	0.012%
	92	238	4.490E-01	0.035%
Np	93	237	1.720E-04	0.000%
Pu	94	239	5.630E-04	0.000%
	94	240	1.070E-05	0.000%
Total - Nitrates			4.166E+02	32.047%
Water Content				
H	1	1	9.815E+01	7.550%
O	8	16	7.852E+02	60.402%
Total - Water			8.834E+02	67.953%
Total - HEUNL			1.300E+03	100.0%

---

[1] Natural abundance

Table 6.7.4-5   Evaluated HEUNL Properties

Description	Value
HEUNL volume in cask (L / gal)	257 / 68.0
HEUNL volume in container (L / gal)	64.3 / 17.0
HEUNL mass in cask (kg)	334
HEUNL mass in container (kg)	83.5
Uranyl Nitrate mass in cask (kg)	3.39
Uranyl Nitrate mass in container (kg)	0.848
U concentration (g/L)	7.92
^{235}U concentration (g/L)	7.20
U mass in cask (kg)	2.04
U mass in container (kg)	0.509
^{235}U mass in cask (kg)	1.85
^{235}U mass in container (kg)	0.463

Table 6.7.4-6   HEUNL Container Design Parameters
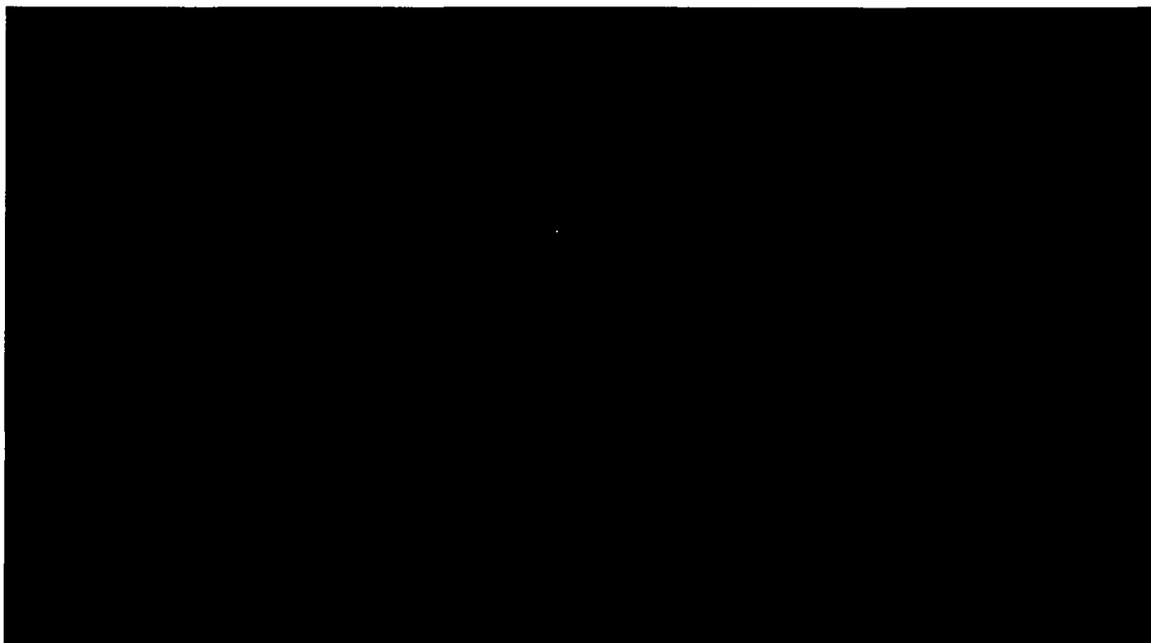
Table 6.7.4-7   HEUNL Analysis Compositions and Number Densities

Material	U-Al	H₂O	304 Stainless Steel	Pb	Al
Density, g/cc	1.300	0.9982	7.920	11.344	2.702
Density	atoms/b-cm				
Uranium-235	1.845E-05				
Uranium-238	1.834E-06				
Nitrogen	3.439E-03				
Oxygen	3.992E-02	3.340E-02			
Hydrogen	5.922E-02	6.679E-02			
Chromium	3.011E-06		1.747E-02		
Manganese			1.741E-03		
Iron	1.144E-05		5.854E-02		
Nickel	1.807E-06		7.739E-03		
Carbon			3.185E-04		
Silicon			1.702E-03		
Phosphorus			6.947E-05		
Lead				3.297E-02	
Aluminum	1.807E-06				6.030E-02

Table 6.7.4-8   HEUNL Scoping Reactivity Results

Condition	1	2	3	4
Interior Exterior Condition	Dry Wet Normal	Wet Wet Normal	Dry Wet Accident	Wet Wet Accident
$k_{eff}+2\sigma$	0.3359	0.3277	0.3359	0.3271

Table 6.7.4-9   Sample HEUNL Isotopic Composition for ▮▮▮▮ Uranyl Nitrate – Water Mixture

Element	Z	A	Conc. (g/L)	Mass (g/container)	wt.%
N	7	14	8.000E+01	6.074E+01	0.577%
O	8	16	2.751E+02	2.774E+02	2.636%
U	92	234	1.230E-01	7.914E+00	0.075%
	92	235	7.200E+00	4.633E+02	4.402%
	92	236	1.530E-01	9.845E+00	0.094%
	92	238	4.490E-01	2.889E+01	0.275%
Total - Nitrates			4.166E+02	8.482E+02	8.059%
Water Content					
H	1	1	9.815E+01	1.075E+03	10.216%
O	8	16	7.852E+02	8.601E+03	81.725%
Total - Water			8.834E+02	9.676E+03	91.941%
Total - HEUNL			1.300E+03	1.052E+04	100.0%

Table 6.7.4-10   HEUNL Reactivity Results for ███ of Uranyl Nitrate – Water Mixtures

███	H/U	$k_{eff}+2\sigma$
		0.3359
4.6	2	0.2329
6.0	29	0.3960
7.8	90	0.5985
9.8	201	0.7514
11.1	302	0.8158
11.6	347	0.8314
12.1	397	0.8437
12.6	451	0.8544
13.0	498	0.8570
13.4	547	0.8618
13.8	600	0.8605
14.2	655	0.8596
14.5	699	0.8560
14.8	745	0.8506
15.1	791	0.8443
15.5	855	0.8348
15.8	903	0.8244
16.4	1003	0.8076
17.5	1197	0.7713

Table 6.7.4-11   HEUNL Reactivity Results for ▉▉▉▉ of Uranyl Nitrate

Height (cm)	H/U	$k_{eff}+2\sigma$
		0.3359
0.7	3	0.3233
1.4	30	0.3761
3.0	90	0.4779
5.9	200	0.6212
8.5	300	0.7089
9.8	350	0.7405
11.1	400	0.7641
12.5	450	0.7848
13.8	500	0.7989
15.1	550	0.8114
16.4	600	0.8183
17.8	650	0.8229
19.1	700	0.8243
20.4	750	0.8251
21.7	800	0.8251
23.0	850	0.8223
24.4	900	0.8187
27.0	1000	0.8099
32.3	1200	0.7853

Table 6.7.4-12   HEUNL Reactivity Results for Fissile Material Shift Study

	Parameter		k_{eff}	σ	$k_{eff}+2\sigma$
Flooded Cask	▉▉▉▉	Nom	0.8530	0.0009	0.8548
		In	0.8614	0.0009	0.8631
		Alt	0.8628	0.0009	0.8647
		Nom	0.8226	0.0008	0.8243
		In	0.8412	0.0008	0.8429
		Alt	0.8388	0.0009	0.8405
Dry Cask	▉▉▉▉	Nom	0.8598	0.0010	0.8618
		In	0.8814	0.0009	0.8832
		Alt	0.8821	0.0009	0.8838
		Nom	0.8235	0.0008	0.8251
		In	0.8630	0.0009	0.8647
		Alt	0.8631	0.0008	0.8648

Table 6.7.4-13   HEUNL Reactivity Results for Cask Cavity Moderator Study

Density [g/cc]	k_{eff}	σ	$k_{eff} + 2\sigma$	Δk_{eff}/sigma
0.9982	0.8628	0.0009	0.8647	-15.0
0.9500	0.8627	0.0008	0.8644	-15.9
0.9000	0.8637	0.0009	0.8655	-14.2
0.8500	0.8655	0.0010	0.8674	-12.5
0.8000	0.8645	0.0009	0.8663	-13.9
0.7500	0.8667	0.0009	0.8684	-12.3
0.7000	0.8678	0.0009	0.8697	-10.9
0.6500	0.8681	0.0009	0.8698	-11.2
0.6000	0.8679	0.0008	0.8696	-11.7
0.5500	0.8704	0.0009	0.8723	-9.0
0.5000	0.8715	0.0009	0.8733	-8.2
0.4500	0.8711	0.0009	0.8730	-8.4
0.4000	0.8715	0.0009	0.8733	-8.4
0.3500	0.8746	0.0009	0.8763	-6.0
0.3000	0.8744	0.0009	0.8762	-5.9
0.2500	0.8752	0.0009	0.8769	-5.6
0.2000	0.8758	0.0010	0.8777	-4.7
0.1500	0.8774	0.0009	0.8792	-3.6
0.1000	0.8808	0.0009	0.8826	-1.0
0.0500	0.8834	0.0009	0.8852	1.1
0.00	0.8821	0.0009	0.8838	

Table 6.7.4-14   HEUNL Reactivity Results for Container Tolerance Study

Parameter		keff	σ	$k_{eff}+2\sigma$	Δk_{eff}	$\Delta k_{eff}/\sigma$
Container Bottom Thickness	Nom	0.8821	0.0009	0.8838	--	
	Min	0.8818	0.0009	0.8836	-0.0002	-0.2
	Max	0.8829	0.0009	0.8848	0.0010	0.7
Container Length	Nom	0.8821	0.0009	0.8838	--	
	Min	0.8840	0.0009	0.8859	0.0020	1.6
	Max	0.8805	0.0008	0.8821	-0.0017	-1.4
Container Top to Cavity Top Segment Length	Nom	0.8821	0.0009	0.8838	--	
	Min	0.8806	0.0009	0.8824	-0.0014	-1.1
	Max	0.8827	0.0009	0.8844	0.0006	0.4
Container Top to Bottom Plate Length	Nom	0.8821	0.0009	0.8838	--	
	Min	0.8805	0.0008	0.8821	-0.0017	-1.4
	Max	0.8822	0.0009	0.8840	0.0002	0.1

Table 6.7.4-15   HEUNL Reactivity Results for Mercury Removal

Parameter	k_{eff}	σ	$k_{eff}+2σ$	$Δk_{eff}$	$Δk_{eff}/σ$
Nom	0.8821	0.0009	0.8838	--	--
Removed	0.8932	0.0009	0.8950	0.0112	8.9

Table 6.7.4-16   HEUNL Maximum Reactivity per 10 CFR 71.55

Geometry	k_{eff}	σ	$k_{eff}+2σ$
Normal Conditions per 10 CFR 71.55 (b)	0.8935	0.0009	0.8952
Accident Conditions per 10 CFR 71.55 (e)	0.8932	0.0009	0.8950

Table 6.7.4-17   HEUNL Maximum Reactivity per 10 CFR 71.59

Geometry	k_{eff}	σ	$k_{eff}+2σ$	CSI
Normal Conditions per 10 CFR 71.59 (a) (1)	0.8947	0.0009	0.8965	0
Accident Conditions per 10 CFR 71.59 (a) (2)	0.9053	0.0009	0.9071	0

Table 6.7.4-18   Validation Area of Applicability Comparison with HEUNL Results

Parameter	Uranyl Nitrate Validation	HEUNL
Fissile Form	Nitrate Solutions	Uranyl Nitrate
Moderator	Light Water, Tap Water, or None	Light Water
H/U Ratio	51.010 to 2050	533
EALCF (eV)	3.06E-02 to 5.26E-01	0.04
Enrichment (wt%)	92.78 to 93.22	93.4

Table 6.7.4-19   HEUNL Reactivity Comparisons for Design Modification and Reflector Dimension Change

Geometry	Baseline Evaluation k_{eff}	Modified Design / Reflector 30 cm k_{eff}	Δk	$\Delta k/\sigma$
Normal Conditions per 10 CFR 71.55 (b)	0.8935	0.8940	0.0005	<1
Accident Conditions per 10 CFR 71.55 (e)	0.8932	0.8935	0.0003	<1
Normal Conditions per 10 CFR 71.59 (a) (1)	0.8947	0.8954	0.0007	<1
Accident Conditions per 10 CFR 71.59 (a) (2)	0.9053	0.9052	0.0001	<1

Table 6.7.4-20   HEUNL Evaluated Libraries

1001.70c	13027.70c	25055.50c	92238.70c
6000.70c	14000.60c	26000.55c	lwtr.10t
7014.70c	15031.70c	28000.50c	80000.42c
8016.70c	24000.50c	92235.70c	82000.50c

Table 6.7.4-21   Evaluated HEUNL Properties for Increased Enrichment

Description	Value
HEUNL volume in container (L / gal)	64.3 / 17.0
Enrichment (wt. %)	93.4
^{235}U concentration (g/L)	7.40
^{235}U mass in container (kg)	0.476

Table 6.7.4-22   HEUNL Maximum Reactivity per 10 CFR 71.55 for Increased Enrichment

Geometry	k_{eff}	σ	$k_{eff}+2\sigma$
Normal Conditions per 10 CFR 71.55 (b)	0.8997	0.0009	0.9014
Accident Conditions per 10 CFR 71.55 (e)	0.9016	0.0009	0.9035

Table 6.7.4-23   HEUNL Maximum Reactivity per 10 CFR 71.59 for Increased
Enrichment

Geometry	k_{eff}	σ	$k_{eff}+2\sigma$	CSI
Normal Conditions per 10 CFR 71.59 (a) (1)	0.9019	0.0009	0.9037	0
Accident Conditions per 10 CFR 71.59 (a) (2)	0.9120	0.0009	0.9137	0